

# Groundwater and Petroleum

Yousif Kharaka, Brian Hitchon  
and Jeffrey Hanor

# *Groundwater and Petroleum*

*The Groundwater Project*

The Groundwater Project relies on private funding for book production and management of the Project.

Please consider [making a donation to the Groundwater Project](#) ↗  
so books will continue to be freely available.

Thank you.

# *Yousif K. Kharaka*

*Research Geochemist Emeritus  
Water Resources Mission Area, US Geological Survey  
Menlo Park, California, USA*

# *Brian Hitchon*

*President  
Hitchon Geochemical Services Ltd.  
Edmonton, Alberta, Canada*

# *Jeffrey S. Hanor*

*Professor Emeritus  
Department of Geology and Geophysics, Louisiana State University  
Baton Rouge, Louisiana, USA*

## *Groundwater and Petroleum*

*The Groundwater Project  
Guelph, Ontario, Canada  
Version 3, August 2024*

This GW-Project original publication is not protected by copyright. Any part of this book may be reproduced in any form or by any means without permission in writing from the authors. However, commercial distribution and reproduction are strictly prohibited.

Note that most GW-Project books are copyrighted, and that it is not permissible to make GW-Project documents available on other websites nor to send copies of the documents directly to others. GW-Project works can be downloaded for free from [gw-project.org](http://gw-project.org). Anyone may use and share [gw-project.org](http://gw-project.org) links to GW-Project's work. Kindly honor this source of free knowledge that benefits you and all those who want to learn about groundwater.

Any use of trade, firm, or product names is for descriptive purposes only and does not imply endorsement by the U.S. Government.

Published by the Groundwater Project, Guelph, Ontario, Canada, 2023.

Kharaka, Yousif K.

Groundwater and Petroleum / Authors (Yousif K. Kharaka, Brian Hitchon, and Jeffrey S. Hanor) – Guelph, Ontario, Canada, 2023.

372 pages

ISBN: 978-1-77470-041-9

DOI: <https://doi.org/10.21083/978-1-77470-041-9>.

Please consider signing up for the GW-Project mailing list to stay informed about new book releases, events, and ways to participate in the GW-Project. When you sign up for our email list, it helps us build a global groundwater community. [Sign up](#).

APA (7th ed.) Citation: Kharaka, Y. K., Hitchon, B., & Hanor, J. S. (2023). [Groundwater and petroleum](#). The Groundwater Project. <https://doi.org/10.21083/978-1-77470-041-9>.



*Domain Editors:* Eileen Poeter and John Cherry.

*Board:* John Cherry, Paul Hsieh, Ineke Kalwij, Everton de Oliveira, and Eileen Poeter.

*Steering Committee:* John Cherry, Allan Freeze, Paul Hsieh, Ineke Kalwij, Douglas Mackay, Everton de Oliveira, Beth Parker, Eileen Poeter, Ying Fan, Warren Wood, and Yan Zheng.

*Cover Image:* Cross section from Kharaka and others (2007). Aerial photo courtesy of Ken Jewell, USEPA, Ada, Oklahoma (2005).

## Dedication

We dedicate this book to our extended families and to the scientists who inspired us to conduct in-depth investigations in geology and geochemistry including Robert M. Garrels, Donald E. White, Harold C. Helgeson, and Frederick A. F. Berry.

# Table of Contents

<b>DEDICATION</b> .....	<b>VI</b>
<b>TABLE OF CONTENTS</b> .....	<b>VII</b>
<b>THE GROUNDWATER PROJECT FOREWORD</b> .....	<b>VI</b>
<b>FOREWORD</b> .....	<b>VII</b>
<b>PREFACE</b> .....	<b>VIII</b>
<b>ACKNOWLEDGMENTS</b> .....	<b>X</b>
<b>1 INTRODUCTION</b> .....	<b>1</b>
1.1 TOPICS DISCUSSED IN THIS BOOK .....	5
1.2 EXERCISES PERTINENT TO SECTION 1.....	7
<b>2 A BRIEF HISTORY OF THE PETROLEUM INDUSTRY</b> .....	<b>8</b>
2.1 INTRODUCTION TO HISTORY OF THE PETROLEUM INDUSTRY.....	8
2.2 MODERN PETROLEUM INDUSTRY .....	9
2.3 2021 UN CLIMATE CHANGE SUMMIT: COP26, GLASGOW, SCOTLAND.....	13
2.4 EXERCISES PERTINENT TO SECTION 2.....	14
<b>3 DRILLING, COMPLETION, AND FLUID PRODUCTION FROM PETROLEUM WELLS</b> .....	<b>15</b>
3.1 INTRODUCTION TO DRILLING, COMPLETION AND PRODUCTION .....	15
3.2 WELL DRILLING.....	15
3.3 WELL COMPLETION .....	16
3.4 PETROLEUM PRODUCTION .....	17
3.5 WELL ABANDONMENT .....	18
<b>4 PRODUCED WATER FROM CONVENTIONAL PETROLEUM SOURCES OF ENERGY</b> .....	<b>20</b>
4.1 INTRODUCTION TO WATER FROM CONVENTIONAL SOURCES.....	20
4.2 HISTORICAL PERSPECTIVE ON THE VOLUME AND MANAGEMENT OF PRODUCED WATER .....	21
4.3 ENVIRONMENTAL QUALITY REGULATIONS.....	26
4.4 IRRIGATION WATER QUALITY CRITERIA.....	28
4.4.1 <i>Salinity Hazard</i> .....	29
4.4.2 <i>Sodium Hazard</i> .....	29
4.4.3 <i>pH and Alkalinity</i> .....	30
4.4.4 <i>Specific Ion Toxicity</i> .....	30
4.5 GOVERNMENT REGULATIONS TO PROTECT GROUNDWATER .....	31
4.6 EXERCISES PERTINENT TO SECTION 4.....	32
<b>5 FLUID PRODUCTION FROM UNCONVENTIONAL SOURCES OF ENERGY</b> .....	<b>33</b>
5.1 INTRODUCTION TO WATER FROM UNCONVENTIONAL SOURCES.....	33
5.2 VOLUME AND COMPOSITION OF FRACTURING FLUIDS .....	37
5.3 FLOWBACK WATER.....	38
5.4 PERMIAN BASIN: WATER CHALLENGES FOR UNCONVENTIONAL PRODUCTION.....	40
5.5 ENVIRONMENTAL IMPACTS: WATER USE AND WASTE-WATER DISPOSAL CHALLENGES.....	45
5.6 OIL SANDS.....	49
5.6.1 <i>Water Management</i> .....	50
5.7 EXERCISES PERTINENT TO SECTION 5.....	51
<b>6 INORGANIC CHEMICAL COMPOSITION OF PRODUCED WATER</b> .....	<b>52</b>
6.1 INTRODUCTION TO INORGANIC COMPOSITION OF PRODUCED WATER .....	52
6.2 FIELD AND LABORATORY METHODS AND PROCEDURES .....	57
6.3 PRODUCED WATER FROM GAS WELLS .....	63
6.4 INFORMATION FROM WIRE-LINE LOGS .....	64

6.5	GEOCHEMICAL DATA FROM THE SAME FORMATION USING FOUR SAMPLING METHODS .....	64
6.5.1	<i>Results and Discussion</i> .....	66
6.6	INORGANIC CHEMICAL COMPOSITION OF PRODUCED WATER: A BASIN AND COUNTRY-SCALE PERSPECTIVE .....	71
6.6.1	<i>Culling Criteria for Standard Formation Water</i> .....	72
6.6.2	<i>Statistical Classification of Elements in Produced Water</i> .....	74
6.6.3	<i>Salinity</i> .....	76
6.6.4	<i>Major Elements</i> .....	77
6.6.5	<i>Minor Elements</i> .....	85
6.6.6	<i>Trace Elements</i> .....	93
6.6.7	<i>Mineral Saturation Indices</i> .....	102
6.7	INORGANIC CHEMICAL COMPOSITION OF PRODUCED WATER: A FIELD SCALE PERSPECTIVE .....	104
6.7.1	<i>Water Salinity</i> .....	105
6.7.2	<i>Cations in Produced Water</i> .....	112
6.7.3	<i>Control of Cation Concentrations</i> .....	115
6.7.4	<i>Chemical Geothermometry and Barometry</i> .....	116
6.7.5	<i>Major Anions in Produced Water</i> .....	119
6.7.6	<i>Metal-Rich Brine</i> .....	123
6.7.7	<i>Geochemical Modeling of Ore Fluids</i> .....	125
6.8	THE INFLUENCE OF SHALE AND OTHER GEOLOGIC MEMBRANES .....	126
6.9	SECULAR VARIATIONS IN SEAWATER CHEMISTRY: IMPACT ON COMPOSITION OF BASINAL BRINE .....	128
6.10	EXERCISES PERTINENT TO SECTION 6 .....	128
<b>7</b>	<b>ORGANIC COMPOUNDS IN PRODUCED WATER .....</b>	<b>129</b>
7.1	INTRODUCTION TO ORGANIC COMPOSITION .....	129
7.2	MONOCARBOXYLIC ACID ANIONS .....	129
7.3	DICARBOXYLIC ACID ANIONS .....	132
7.4	OTHER REACTIVE ORGANIC SPECIES .....	133
7.5	ORIGIN OF MAJOR REACTIVE ORGANIC SPECIES .....	134
7.6	TOXICITY OF PRODUCED WATER AND CRUDE OIL RELEASES .....	134
7.6.1	<i>Toxicity Resulting from Crude Oil and Organic Chemicals</i> .....	135
7.6.2	<i>Toxicity Resulting from Inorganic Chemicals</i> .....	137
7.7	EXERCISES PERTINENT TO SECTION 7 .....	138
<b>8</b>	<b>ISOTOPIC COMPOSITION OF PRODUCED WATER .....</b>	<b>139</b>
8.1	INTRODUCTION TO ISOTOPIC COMPOSITION .....	139
8.2	WATER ISOTOPES .....	141
8.2.1	<i>Formation Water Derived from Holocene Meteoric Water</i> .....	142
8.2.2	<i>Formation Water Originating from "Old" Meteoric Water</i> .....	143
8.2.3	<i>Formation Water of Connate Marine Origin</i> .....	144
8.2.4	<i>Bittern Connate Water Associated with Evaporites</i> .....	147
8.2.5	<i>Brine of Mixed Origin</i> .....	149
8.3	ISOTOPIC COMPOSITION OF SOLUTES .....	150
8.3.1	<i>Boron Isotopes</i> .....	151
8.3.2	<i>Lithium Isotopes</i> .....	152
8.3.3	<i>Carbon Isotopes</i> .....	153
8.3.4	<i>Sulfur Isotopes</i> .....	153
8.3.5	<i>Chlorine Isotopes</i> .....	154
8.3.6	<i>Bromine Isotopes</i> .....	155
8.3.7	<i>Strontium Isotopes</i> .....	156

8.3.8	<i>Calcium Isotopes</i> .....	156
8.4	TRADITIONAL AND NONTRADITIONAL ISOTOPES .....	157
8.5	RADIOACTIVE ISOTOPES AND AGE DATING .....	158
8.6	EXERCISES PERTINENT TO SECTION 8.....	159
<b>9</b>	<b>GEOCHEMISTRY OF PRODUCED WATER IN BASINS WITH SALT DOMES .....</b>	<b>160</b>
9.1	INTRODUCTION TO WATER GEOCHEMISTRY NEAR SALT DOMES.....	160
9.2	GEOLOGIC SETTING OF THE GULF OF MEXICO BASIN .....	161
9.3	CHEMICAL COMPOSITION OF WATER ASSOCIATED WITH SALT DOMES.....	163
9.3.1	<i>Salt, Salinity, and Hydrogeology</i> .....	163
9.3.2	<i>Salt Dissolution: Bay Marchand Salt Dome</i> .....	164
9.3.3	<i>Salt Dissolution: Welsh Salt Dome</i> .....	166
9.3.4	<i>Regional Variations in Salinity</i> .....	167
9.4	GEOCHEMICAL COMPOSITION OF GULF OF MEXICO FORMATION WATER.....	168
9.4.1	<i>Chemical Composition of Formation Water at Individual Salt Structures</i> .....	170
9.4.2	<i>Effect of Salt Dissolution on Groundwater Resources</i> .....	173
9.5	EXERCISES PERTINENT TO SECTION 9.....	174
<b>10</b>	<b>FIELD STUDIES OF GROUNDWATER CONTAMINATION BY PRODUCED WATER AND PETROLEUM... 175</b>	
10.1	CASE STUDY 1: GROUNDWATER CONTAMINATION BY A CRUDE OIL SPILL .....	175
10.1.1	<i>Remediation at the Bemidji Site</i> .....	176
10.1.2	<i>Results and Discussion</i> .....	182
10.2	CASE STUDY 2: GROUNDWATER CONTAMINATION BY PRODUCED WATER AND PETROLEUM AT OSAGE SITES, OKLAHOMA .....	186
10.2.1	<i>Introduction</i> .....	186
10.2.2	<i>Site Investigations</i> .....	189
10.2.3	<i>Case Study 2A: Groundwater Contamination at an Active Oil Field</i> .....	191
10.2.4	<i>Case Study 2B: Groundwater Contamination at a Legacy Site</i> .....	202
10.3	CASE STUDY 3: POTENTIAL EFFECTS OF CATION EXCHANGE ON THE COMPOSITION AND MOBILITY OF PRODUCED WATER .....	212
10.3.1	<i>Site History</i> .....	212
10.3.2	<i>Field Techniques</i> .....	213
10.3.3	<i>Soil Data</i> .....	213
10.3.4	<i>Multicomponent Cation Exchange</i> .....	214
10.3.5	<i>Calculated Pore Water Compositions</i> .....	216
10.3.6	<i>Composition of Adsorbed Cations as a Function of Anionic Charge and Salinity</i> .....	217
10.3.7	<i>Discussion</i> .....	218
10.4	CASE STUDY 4: LIMITATIONS ON THE USE OF WATER LEVELS TO INFER DIRECTIONS OF FLUID FLOW IN VARIABLE-DENSITY GROUNDWATER SYSTEMS—A FIELD EXAMPLE .....	220
10.4.1	<i>Site Location and History</i> .....	220
10.4.2	<i>Site Geology</i> .....	220
10.4.3	<i>Extent of Saline Contamination near Pits</i> .....	221
10.4.4	<i>Total Lateral Extent of Saline Contamination</i> .....	222
10.4.5	<i>Site Hydrology: Constant Fluid Density Model</i> .....	223
10.4.6	<i>Site Hydrology: Variable Density Considerations</i> .....	225
10.4.7	<i>Site Hydrology: Conceptual Model for Site</i> .....	226
10.5	EXERCISES PERTINENT TO SECTION 10.....	227
<b>11</b>	<b>GEOLOGIC STORAGE OF CO<sub>2</sub>: ENVIRONMENTAL IMPACTS ON POTABLE GROUNDWATER .....</b>	<b>228</b>
11.1	INTRODUCTION .....	228
11.2	SEA LEVEL RISE FROM GLOBAL WARMING .....	230

11.3	CARBON CAPTURE AND STORAGE (CCS).....	235
11.3.1	<i>Concept of Hubs</i> .....	237
11.3.2	<i>Field Scale Demonstration Projects of Geologic Storage of CO<sub>2</sub></i> .....	240
11.4	CARBON DIOXIDE FOR EOR AND OTHER USES.....	245
11.5	MONITORING CO <sub>2</sub> AND BRINE LEAKAGE FROM STORAGE SITES.....	249
11.5.1	<i>Subsurface Monitoring at the Frio Site, Texas</i> .....	250
11.5.2	<i>Near Surface Monitoring at the ZERT Site, Bozeman, Montana</i> .....	252
11.5.3	<i>Dissolved Inorganic Chemicals</i> .....	255
11.5.4	<i>Carbon Isotopes</i> .....	260
11.6	POTENTIAL ENVIRONMENTAL IMPACTS AND HEALTH RISKS.....	261
11.6.1	<i>Environmental Impacts</i> .....	262
11.6.2	<i>Health and Safety Concerns</i> .....	263
11.7	EXERCISES PERTINENT TO SECTION 11.....	264
<b>12</b>	<b>SUMMARY AND WRAP UP.....</b>	<b>265</b>
12.1	SUMMARY OF THE THREE MAJOR PARTS OF THIS BOOK.....	266
12.2	THE IMPORTANCE OF PRODUCED WATER.....	267
12.2.1	<i>The Composition of Produced Water</i> .....	268
12.3	FUTURE RESEARCH.....	270
<b>13</b>	<b>EXERCISES.....</b>	<b>273</b>
	EXERCISE 1.....	273
	EXERCISE 2.....	273
	EXERCISE 3.....	273
	EXERCISE 4.....	274
	EXERCISE 5.....	274
	EXERCISE 6.....	274
	EXERCISE 7.....	275
	EXERCISE 8.....	275
	EXERCISE 9.....	275
	EXERCISE 10.....	276
	EXERCISE 11.....	276
	EXERCISE 12.....	276
	EXERCISE 13.....	276
	EXERCISE 14.....	277
	EXERCISE 15.....	277
	EXERCISE 16.....	277
	EXERCISE 17.....	277
	EXERCISE 18.....	278
	EXERCISE 19.....	278
	EXERCISE 20.....	278
	EXERCISE 21.....	278
	EXERCISE 22.....	279
	EXERCISE 23.....	279
	EXERCISE 24.....	279
	EXERCISE 25.....	280
	EXERCISE 26.....	280
<b>14</b>	<b>REFERENCES.....</b>	<b>281</b>
<b>15</b>	<b>BOXES.....</b>	<b>340</b>
	BOX 1 GLOSSARY.....	340

BOX 2 USA NATIONAL PRIMARY DRINKING WATER REGULATIONS ..... 344

BOX 3 USA NATIONAL SECONDARY DRINKING WATER REGULATIONS ..... 355

**16 EXERCISE SOLUTIONS ..... 356**

SOLUTION EXERCISE 1..... 356

SOLUTION EXERCISE 2..... 356

SOLUTION EXERCISE 3..... 357

SOLUTION EXERCISE 4..... 357

SOLUTION EXERCISE 5..... 357

SOLUTION EXERCISE 6..... 358

SOLUTION EXERCISE 7..... 358

SOLUTION EXERCISE 8..... 358

SOLUTION EXERCISE 9..... 359

SOLUTION EXERCISE 10..... 359

SOLUTION EXERCISE 11..... 360

SOLUTION EXERCISE 12..... 360

SOLUTION EXERCISE 13..... 361

SOLUTION EXERCISE 14..... 362

SOLUTION EXERCISE 15..... 363

SOLUTION EXERCISE 16..... 363

SOLUTION EXERCISE 17..... 364

SOLUTION EXERCISE 18..... 364

SOLUTION EXERCISE 19..... 365

SOLUTION EXERCISE 20..... 366

SOLUTION EXERCISE 21..... 367

SOLUTION EXERCISE 22..... 367

SOLUTION EXERCISE 23..... 367

SOLUTION EXERCISE 24..... 368

SOLUTION EXERCISE 25..... 368

SOLUTION EXERCISE 26..... 369

**17 ABOUT THE AUTHORS ..... 370**

**MODIFICATIONS TO ORIGINAL RELEASE ..... A**

## The Groundwater Project Foreword

At the United Nations (UN) Water Summit held on December 2022, delegates agreed that statements from all major groundwater-related events will be unified in 2023 into one comprehensive groundwater message. This message was released at the UN 2023 Water Conference, a landmark event that brought attention at the highest international level to the importance of groundwater for the future of humanity and ecosystems. This message clarified groundwater issues to advance understanding globally of the challenges faced and actions needed to resolve the world's groundwater problems. Groundwater education is key.

The 2023 World Water Day theme *Accelerating Change* is in sync with the goal of the Groundwater Project (GWA-Project). The GW-Project is a registered Canadian charity founded in 2018 and committed to the advancement of groundwater education as a means to accelerate action related to our essential groundwater resources. To this end, we create and disseminate knowledge through a unique approach: the democratization of groundwater knowledge. We act on this commitment through our website [gw-project.org/](http://gw-project.org/), a global platform, based on the following principle:

*“Knowledge should be free, and the best knowledge should be free knowledge.” Anonymous*

The mission of the GW-Project is to promote groundwater learning across the globe. This is accomplished by providing accessible, engaging, and high-quality educational materials—free-of-charge online and in many languages—to all who want to learn about groundwater. In short, the GW-Project provides essential knowledge and tools needed to develop groundwater sustainably for the future of humanity and ecosystems. This is a new type of global educational endeavor made possible through the contributions of a dedicated international group of volunteer professionals from diverse disciplines. Academics, consultants, and retirees contribute by writing and/or reviewing books aimed at diverse levels of readers from children to high school, undergraduate, and graduate students or professionals in the groundwater field. More than 1,000 dedicated volunteers from 127 countries and six continents are involved—and participation is growing.

Hundreds of books will be published online over the coming years, first in English and then in other languages. An important tenet of GW-Project books is a strong emphasis on visualization; with clear illustrations to stimulate spatial and critical thinking. In future, the publications will also include videos and other dynamic learning tools. Revised editions of the books are published from time to time. Users are invited to propose revisions.

We thank you for being part of the GW-Project-Community. We hope to hear from you about your experience with the project materials, and welcome ideas and volunteers!

The Groundwater Project Board of Directors, January 2023

## Foreword

Petroleum in the form of oil and gas has underpinned the large expansion of industrial economies and affluence across the globe for the past hundred years. This occurred as petroleum replaced coal to become the world's primary energy source. In the United States, five million oil and gas wells have been drilled, some as deep as five kilometers, and nearly a million are in operation today. The global number of wells is many times larger.

At each drilling location, the land surface is disturbed; some water coproduced with oil from great depth may be accidentally released onto the land surface. Typically, this water is saline and much of the released water infiltrates, contaminating the shallow fresh groundwater zone. In addition to the salt in this water, there are many other chemical elements including toxic organic compounds. Hence the contamination is chemically complex, involving many geochemical processes.

Human impacts on the environment and water resources come in many forms but contamination at oil and gas wellheads receives minimal public attention; most people remain unaware. This book focuses on this wellhead contamination with emphasis on conventional oil and gas wells. The book also covers other impacts of the petroleum industry including unconventional extraction such as hydraulic fracking and climate change related primarily to the industry's greenhouse gas emissions. A book with greater detail concerning the unconventional aspects of oil and gas production is in preparation for publication by the Groundwater Project.

Although this book uses examples from North America, it is unprecedented in its holistic coverage of the topic. It describes the wide spectrum of fluid chemical and isotopic compositions—and their geochemical origins—that occur in the intermediate and deep subsurface in many petroleum regions of the world, as well as their fate after they enter the shallow groundwater zone to form contaminant plumes.

The three authors of this book have long, distinguished careers studying the impacts of drilling and production of petroleum products on land and groundwater. They have been the primary contributors to scientific literature on the subject. Dr. Yousif Kharaka is a research scientist emeritus at the US Geological Survey (USGS), Menlo Park, California; Dr. Brian Hitchon is a research scientist emeritus at the Alberta Research Council and President of Hitchon Geochemical Services Ltd., Edmonton, Alberta; and Dr. Jeffrey Hanor is a professor emeritus of Louisiana State University, Baton Rouge, Louisiana. Together they convey a commanding story about the impacts of petroleum production on our groundwater resource.

John Cherry, The Groundwater Project Leader  
Guelph, Ontario, Canada, June 2023

## Preface

This book addresses the environmental impacts on groundwater that occur during exploration and production of oil and natural gas. These operations have had detrimental impacts on air, soils, surface water, groundwater, and ecosystems in the USA and throughout the world. For example, for every barrel of oil produced today in the USA, we also recover approximately ten barrels of high salinity (5,000 to 300,000 mg/L total dissolved solids) produced water with petroleum hydrocarbons and many toxic inorganic and organic chemicals that far exceed the quality criteria for drinking and irrigation water. These impacts have arisen primarily from the improper disposal of some of the large volumes of produced water recovered from petroleum well blowouts, accidental hydrocarbon and produced water releases, and wells that were “orphaned” and not correctly plugged.

The information in this book is presented in three major sections. The first section, an introduction to this volume, is followed by a summary introduction to the petroleum industry that describes how petroleum and produced water are brought to the surface with wells drilled into conventional and unconventional sources of energy. We include a brief history of the petroleum industry, starting before 1859 when the first commercial oil well (the Drake’s well) was drilled near Titusville, Pennsylvania.

We also provide a historical perspective on the volume and management of produced water. For close to a century, producers simply let their wastewater flow over natural channels into streams, rivers, and lakes with some percolating, thus contaminating potable groundwater. However, managing produced water to meet environmental quality regulations only started seriously in the 1970s following the creation of the US Environmental Protection Agency (EPA).

The second and largest section is a detailed description of the origin and evolution of the chemical and isotopic compositions of produced water and groundwater. We discuss the organic and inorganic chemicals and isotopes that are toxic to human health and the environment as well as those that provide the unique criteria for distinguishing contamination from petroleum sources.

The third and most important section details the various ways in which groundwater may be contaminated by produced water and petroleum. And it is here that we provide detailed field case studies of contaminated groundwater in active oil fields as well as in legacy sites. In the section before the summary and conclusions, we discuss global warming and its mitigation by carbon capture, utilization, and geological storage (CCUS).

Our main goals for the graduate students and professionals of hydrogeology, petroleum, geochemistry, and environmental sciences who will read this book are to

- understand the similarities and differences between the chemistry of groundwater and produced water as these differences may be applied to the potential contamination of groundwater, and
- develop the ability to sense when activities and accidents of the petroleum industry may have an impact on local groundwater and the environment, so as to ask pertinent questions based on an in-depth understanding of the geology, petroleum resources, and hydrogeochemistry of each individual situation.

Finally, if this knowledge helps the reader to be better able to protect groundwater and the environment, then we will have accomplished our primary goal of facilitating the many beneficial uses of hydrocarbon resources with minimal adverse impact on the environment.

## Acknowledgments

We are grateful to John Cherry, leader of the Groundwater Project, for inviting us to write this book and especially for his vision and ability to initiate and sustain this important project. The stated mission of the Groundwater Project is global promotion of groundwater learning—and we are delighted to be participants in such a profound goal.

We are also grateful to the following individuals for their thorough reviews and many useful contributions to our book.

- ❖ Pradeep Aggarwal, retired from the International Atomic Energy Agency, Vienna, Austria.
- ❖ William (Bill) Gunter, retired from the Alberta Research Council, Edmonton, Alberta, Canada.
- ❖ William (Bill) Herkelrath, Emeritus Hydrologist, Water Mission Area, USGS, Menlo Park, California, USA.
- ❖ Jean-Philippe Nicot, Senior Research Scientist, Bureau of Economic Geology, Jackson School of Geosciences, University of Texas, Austin, Texas, USA.

Our special thanks to Amanda Sills, Jamie Bain, Connie Bryson, Virginia McGowan, and Daniel Noble of the Groundwater Project for their oversight and copyediting of this book. We thank Eileen Poeter (Colorado School of Mines, Golden, Colorado, United States of America) for reviewing, editing, and producing this book.

We would also like to thank Atosa Abedini, Gil Ambats, Evangelos Kakouros, James Thordsen, Mark Huebner, and Matthias Kohler for helping with original figures, tables, and text formatting on this book and original reports by Kharaka. Much of Hanor's research on fluids in sedimentary basins has been supported by the National Science Foundation. The Frio and Cranfield projects were managed by Sue Hovorka (Bureau of Economic Geology, University of Texas, Austin), with financial support from the US Department of Energy (DOE) National Energy Technology Laboratory (NETL). The Zero Emission Research and Technology (ZERT) research was conducted within the ZERT project directed by Lee Spangler and managed by Laura Dobeck, Montana State University (MSU), Bozeman, MT. The ZERT research was funded primarily by the Electric Power Research Institute, EPRI, but funds were also provided by the EPA, DOE, Lawrence Berkeley National Laboratory, and the US Geological Survey (USGS).

Any use of trade, firm, or product names is for descriptive purposes only and does not imply endorsement by the US government.

# 1 Introduction

Water is an essential resource throughout the world and maintaining its quality is of utmost importance to safeguard the health of the public and the environment. The UN Water Data show that more than two billion people in the world currently live without adequate safe drinking water—and that number is likely to grow in the future due to increased population, poor water management, and climate change (UN, 2021).

Groundwater, which is water that exists underground in saturated zones beneath the land surface, comprises more than 95 percent of fresh water in the planet. It could play a major role in alleviating the current and future global water stress, but this requires science-based groundwater assessment, management, and protection from all sources of contamination. Approximately 50 percent of the world's population depends on groundwater for domestic use. The latest water data (Figure 1) available from the US Geological Survey (USGS) show that groundwater supplied  $31 \times 10^{10}$  L/d (liters/day or  $8.3 \times 10^{10}$  gallons/day) of fresh water in the USA in 2015. This is more than double the  $13 \times 10^{10}$  L/d supplied in 1950. In the USA in 2015, groundwater supplied the following:

- approximately 30 percent of all fresh water;
- almost all self-supplied domestic water;
- 40 percent of public water supply;
- over 40 percent of irrigation water; and
- more than half the water used for livestock (Dieter et al., 2018).

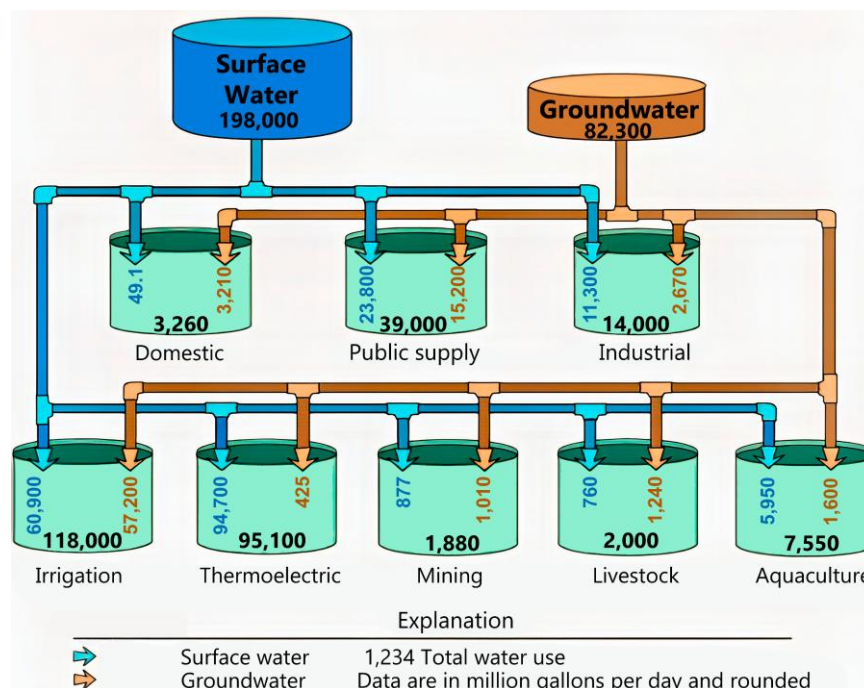


**Figure 1** - The source (groundwater or surface water) of fresh water and the purposes for which it was used in the USA in 2015. Data are reported in million gallons/d (M gal/d); 1 gal = 3.79 L (from Dieter et al., 2018).

Groundwater starts as precipitation that percolates through the soil and the unsaturated zone until it reaches the water table, adding to the existing supply. Groundwater is obtained from aquifers, which are sedimentary rocks or highly fractured igneous or metamorphic rocks with high porosity and permeability that are located close to the Earth's surface (Freeze & Cherry, 1979). Groundwater moves slowly—typically at rates in the range of 7 to 60 cm/d (centimeters/day) in an aquifer. As a result, water may remain in an aquifer for hundreds or thousands of years.

Aquifers may be confined when water collects—by gravity or fluid pressure—between two layers of impermeable strata; unconfined aquifers have no impermeable layer on top. Aquifers generally are shallow, with a water table less than 30 m (meters) deep, but some aquifers in deserts and arid regions may have water tables that are more than 1,500 m below the ground surface (Freeze & Cherry, 1979; Reilly et al., 2008). Detailed analyses of groundwater-levels in 170,000 monitoring wells and close to 1,700 aquifers in 40 countries by Jasechko and others (2024) showed rapid groundwater-level declines, >0.5 m per year, in the twenty first century, especially in dry regions with extensive croplands, like the Central Valley in California. They also showed that in the last four decades, groundwater-level declines accelerated in 30 percent of the world's regional aquifers. Their results, however, also showed reversal of declines in specific cases where aquifers were carefully managed.

Energy is also an essential commodity that powers the expanding global economy. Starting in the 1950s, oil and natural gas became the main sources of primary energy for the rapidly increasing world population and their dominance continues today (Kharaka & Otton, 2007; US Energy Information Administration (EIA), 2021). In 2019, oil was the source of 33 percent of global energy and natural gas was the source of 24 percent; coal contributed 27 percent; hydropower, six percent; renewables, five percent; and nuclear power, four percent (EIA, 2021). Projections by the EIA (2021) indicate that by 2050 nuclear power will not increase significantly from the 2019 level, natural gas will exceed coal, and renewable sources of energy will overtake liquid fuels, including biofuels, as the main source of global energy. However, oil and natural gas combined will continue to dominate the sources of global energy.

Oil and gas reservoirs, in contrast to aquifers, are generally located much deeper—up to 12,000 m below ground level—and deep wells drilled through one or more aquifers are required to produce the resource. Groundwater protection techniques have long played a crucial role in protecting environmental and human health during oil and gas drilling and production. Several layers of steel casing and cement (Figure 2) are used to prevent contamination of groundwater by leaks from oil or gas wells. Drilling fluids, consisting mainly of bentonite clay and water with dissolved potassium chloride (KCl) and small amounts of other chemicals and minerals, are used to lubricate drill bits, remove rock chips, and maintain pressure in the well during drilling.

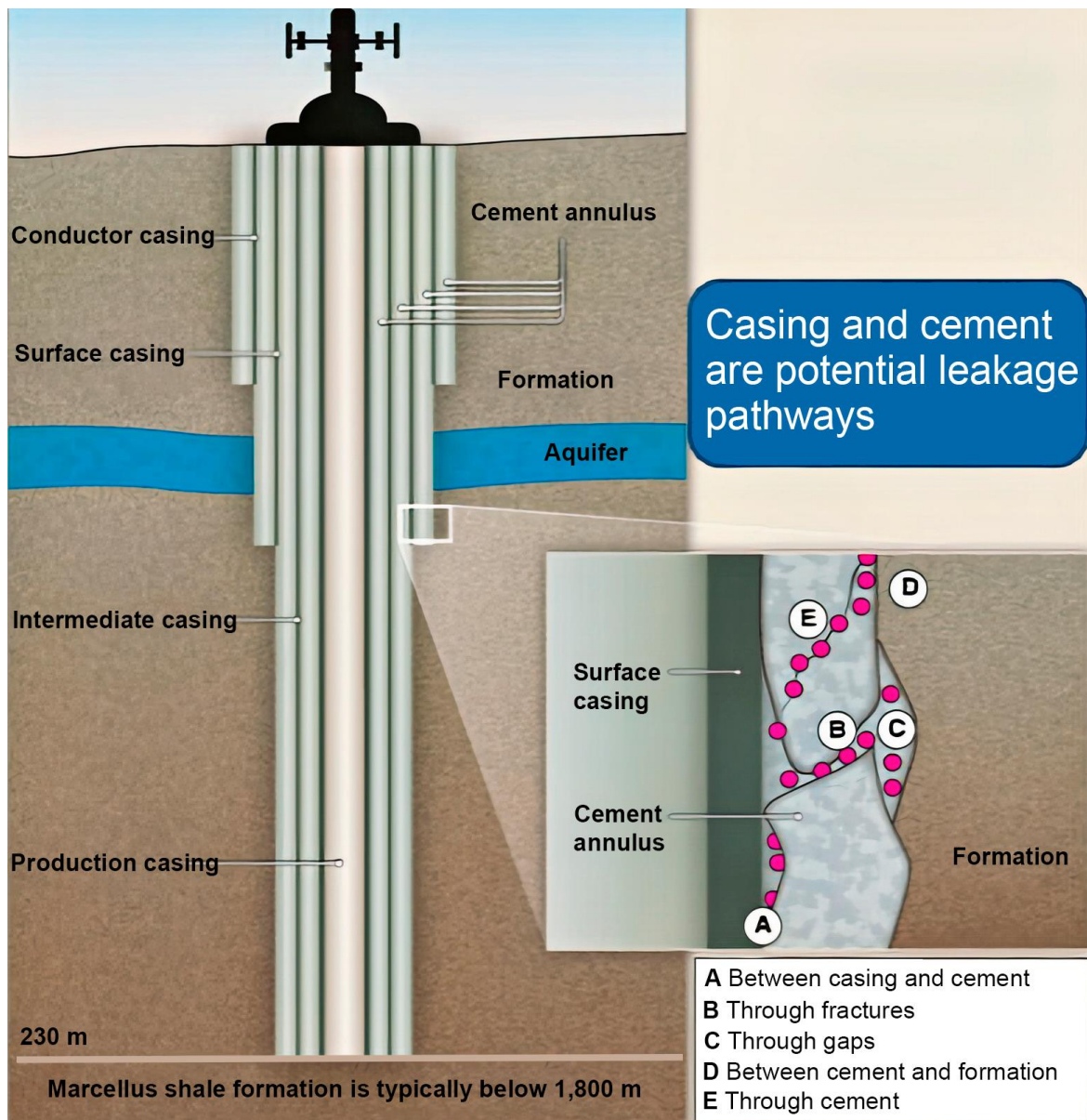


**Figure 2** - Several layers of steel casing and cement are used to prevent contamination of aquifers by leaks of produced water and petroleum. In a typical Marcellus well construction, (1) the conductor casing string, 12 m long, forms the outermost barrier closest to the surface; (2) the surface casing and the cement sheath surrounding it that extend to a minimum of 15 m below the lowest freshwater zone protects aquifers; (3) the annulus between the intermediate casing and the surface casing is filled with cement; and (4) the production string extends to the production zone (900 to 2,800 m) (modified from Vidic et al., 2013).

Most of the substances in drilling fluids are neither toxic nor harmful to the environment because regulators have imposed restrictions on additives that can be used when drilling through freshwater aquifers. However, there have been cases where unauthorized use of drilling fluid additives while drilling through freshwater aquifers has contaminated groundwater (Phillips, 2015). Leakage of drilling fluids, especially when mixed with saline formation water that enters the well from high pressure zones, can be harmful to freshwater aquifers.

The clear benefits of using hydrocarbons (coal, oil, and natural gas), however, carry major detrimental health and environmental impacts that may be local, regional, or global in scale (Everett et al., 2020; Kharaka & Otton, 2007; Meckel et al., 2021; Shaheen et al., 2022; EPA, 2019; Groundwater Protection Council, 2019). The local and regional impacts, including groundwater contamination related to petroleum operations, are discussed in detail in this book. Global impacts include air pollution and the interrelated global warming that results from continued addition of large and increasing amounts of carbon dioxide (CO<sub>2</sub>) to the atmosphere (40.1 billion tonnes CO<sub>2</sub>) were added in 2019, compared with 31 billion tonnes in 2011 and 20 billion tonnes in 1991), obtained largely from the burning of fossil fuels (Friedlingstein et al., 2020).

These impacts are briefly discussed but not addressed in detail here. We also do not cover in detail groundwater contamination from leaking underground storage tanks (USTs) or from large oil spills. USTs at homes and gas stations are the largest single threat to groundwater quality in the USA today. There are approximately 1.2 million USTs nationwide, many of which were installed prior to new regulations in 1988. These are of concern because older tanks corrode relatively quickly when buried unprotected in the soil (US Environmental Protection Agency (EPA), 2021).

Large oil spills have caused major environmental damage to occur in several different scenarios including the following:

- from international conflicts, such as the Iraq invasion of Kuwait in 1990 when Iraqi soldiers set 600 Kuwaiti oil wells on fire and released 11 million barrels (bbl) (1.49 million m<sup>3</sup>) of crude oil into the Persian Gulf (Michel, 2011)
- during ocean transport, such as the Exxon Valdez 1989 spill of 260,000 bbl (42,000 m<sup>3</sup>) of oil into Prince William Sound, Alaska; and
- from major well blowouts, such as the Lakeview Gusher #1, that erupted from a pressurized oil well in the Midway-Sunset Field in Kern County, California, in 1910–1911. This created the largest accidental oil spill in history, lasting 18 months and releasing 9.4 million bbl (1.5 million m<sup>3</sup>) of crude oil and produced water; less than half of the released crude was recovered. The rest evaporated or seeped into the ground, contaminating air, soil, and groundwater (Franks & Lambert, 1985). Similarly, the 4.9 million bbl (0.78 million m<sup>3</sup>) of crude oil and produced water released over an 87 day period in 2010 from the Deepwater Horizon well blowout in the Gulf of Mexico was the largest marine oil blowout in history (McNutt et al., 2012; Michel et al., 2013; National Oceanic and Atmospheric Agency (NOAA), 2020).

## 1.1 Topics Discussed in this Book

*Groundwater and Petroleum* is devoted primarily to environmental impacts on groundwater that occur during exploration for and production of oil and natural gas, including coal-bed natural gas (CBNG). These operations have caused detrimental impacts to air, soil, surface water, groundwater, and ecosystems in the thirty-six producing states in the USA and throughout the world (Kharaka & Dorsey, 2005; Kharaka & Hanor, 2014; Richter & Kreitler, 1993; Soeder & Kent, 2018). The detrimental impacts have arisen primarily from the accidental releases and improper disposal of some of the produced water, which are saline wastewater coproduced with oil and natural gas.

Currently in the USA, for every barrel of oil produced, approximately ten barrels of high salinity produced water is recovered for a high estimate of approximately 20 billion bbl/year (3.2 billion m<sup>3</sup>/year) (Kharaka et al., 1995; Kharaka & Otton, 2007; Solomon, 2021; Veil, 2020). In the last twenty years, production of oil and natural gas in the USA from shale and tight reservoirs that require the injection of large volumes of water with proppant (sand or ceramic particles) and chemicals at fluid pressures high enough to fracture the rocks has increased dramatically. In 2019, for example, 63 percent (7.7 million bbl/d or 1.2 million m<sup>3</sup>/d) of crude oil production and 87 percent of natural gas production in the USA came from shale and tight reservoirs (EIA, 2021). In later sections of this book, we discuss the chemistry of produced water derived from these unconventional sources of energy and the potential for groundwater contamination and induced seismicity associated with this important energy source.

Environmental impacts and ground surface disturbances on the order of a few hectares per well have arisen from related activities such as site clearance, construction of roads, tank batteries, brine pits and pipelines, and other land modifications necessary for the drilling of exploration and production wells and construction of production facilities. The cumulative impacts from these operations are high because approximately 5 million oil and gas wells have been drilled in the USA starting in 1859 when the first oil well, the Drake well, was drilled near Titusville, Pennsylvania. Currently, approximately 900,000 oil and gas wells are in production (Information Handling Services (IHS), 2018; Kharaka & Otton, 2007; Rostrom & Arkadakskiy, 2014; Veil, 2020).

For this book, we assume the readers have a basic knowledge of geology, hydrology, and chemistry but are less familiar with practices in the petroleum industry. A glossary of terms relevant to the topics in this book is provided in [Box 1](#) ↓. This book's content is presented in three major parts.

1. The first part includes introductory remarks followed by an introduction to the oil and natural gas industry describing how petroleum is brought to the surface with wells drilled into conventional and unconventional sources of energy, along with produced water, also known as formation water or oil field brine.

We summarize the history of petroleum production and the management of produced water in the USA. Although oil and natural gas contaminates groundwater in some places, we discuss contamination of groundwater by produced water in much more detail.

2. The second part is the largest as it describes the chemical and isotopic composition of produced water in detail through examination of literature that includes many publications authored or coauthored with one or more of us over the last fifty or more years of research in the field of water-rock-petroleum interactions. We emphasize two comprehensive geochemical data sets, one providing data for the Alberta sedimentary basin (Hitchon, 2023) and the second with data for several petroleum fields and basins in the USA (Blondes et al., 2019; Kharaka & Hanor, 2014). This information is compared and contrasted with chemical and isotopic data illustrating the average composition of precipitation, groundwater, and deep brine in sedimentary basins. This allows readers to appreciate how much shallow groundwater chemistry differs from produced water chemistry, which means produced water has potential to be a major contaminant. We discuss the organic and inorganic chemicals and isotopes that are toxic to human health and the environment as well as those that could provide the unique criteria for identifying contamination from petroleum sources.
3. The third part is arguably the most important because it describes the various ways in which groundwater may be contaminated by produced water and petroleum. We provide case studies of groundwater contaminated by produced water and petroleum in existing oil fields as well as in legacy sites where petroleum production ended many years ago (Hanor, 2007; Kharaka & Otton, 2007). We also discuss the Bemidji crude-oil spill, which has been the subject of major multidisciplinary research for more than thirty years. Approximately 10,000 barrels (1,590 m<sup>3</sup>) of crude oil spilled from a 34-inch broken pipeline near Bemidji, Minnesota, on August 20, 1979 (Delin et al., 1998). Petroleum seeped through the soil and is floating on the water table in the glacial-outwash aquifer. Remediation efforts have not succeeded in complete oil and toxic chemical recovery from the groundwater (Delin & Herkelrath, 2014; Delin et al., 2020). In the last section of the third part, we discuss the issues associated with, and the local, regional and global environmental impacts of, carbon capture, utilization, and geological storage (CCUS).

Our main goals for the readers of this book—who could be graduate students, petroleum geochemists, environmental, and other scientists and engineers interested in hydrogeology, geochemistry, and environmental sciences—are, first, to understand the similarities and differences between the chemistry of groundwater and produced water as

these differences may be applied to potential contamination of groundwater by produced water.

Second, to develop the ability to sense when activities and accidents of the petroleum industry may have an impact on local groundwater, so as to ask pertinent questions based on an in-depth understanding of the geology, petroleum resources and hydro-geochemistry of each individual situation.

And finally, for readers to improve their ability to protect groundwater and the environment. If readers enhance their knowledge in these ways, then we have accomplished our primary goal of facilitating beneficial use of hydrocarbon resources with minimal adverse impact on the environment.

## 1.2 Exercises Pertinent to Section 1

[Link to Exercise 1](#) ↓

## 2 A Brief History of the Petroleum Industry

### 2.1 Introduction to History of the Petroleum Industry

Petroleum has a long history: It was found in oil seeps and tar pits and used for illumination, medicine, and even warfare in antiquity. Its semisolid form, asphalt (bitumen), which is found naturally in large quantities near the Euphrates River in Iraq, was used according to Herodotus more than four thousand years ago in the pavement of streets and construction of the walls and towers of Babylon (Beloe, 1830). In China, one of the earliest Chinese writings cites the extraction and use of petroleum in the first century. In addition, the Chinese were the first to use petroleum as fuel as early as the fourth century BCE (Before the Current Era), according to Forbes (1958).

The earliest known oil wells were drilled in China around 347 CE (Current Era). They had depths of up to 800 feet (240 m) and were drilled using bits attached to bamboo poles. The oil was burned to evaporate brine and produce salt. By the tenth century, extensive bamboo pipelines connected oil wells with salt springs. The ancient records of China and Japan are said to contain many allusions to the use of natural gas for lighting and heating (Gorman, 1993).

The streets of Baghdad, Iraq, during its founding in 762 CE, were paved with tar obtained from petroleum from natural fields in the region. In the ninth century, oil fields were exploited in the area around modern Baku, Azerbaijan. These fields were described by Marco Polo in the thirteenth century, who estimated their output as hundreds of shiploads. The distillation of petroleum to produce fuel for kerosine lamps was described in detail by Persian and Arab chemists in the ninth century (Forbes, 1958). Arab and Persian chemists also distilled crude oil to produce flammable products for military purposes. Through Islamic Spain, distillation became available in western Europe by the twelfth century (Boverton, 1911).

The earliest mention of petroleum in the Americas occurs in Sir Walter Raleigh's 1595 account of the La Brea Pitch Lake in the contemporary Caribbean island of Trinidad, Republic of Trinidad and Tobago. Thirty-seven years later, the account of a visit of a Franciscan, Joseph de la Roche d'Allion, to the oil springs of New York was published in Gabriel Sagard's *Histoire du Canada*. The oil seeps of Pennsylvania were marked on a map by Peter Kalm in his work *Travels into North America* published first in 1753 (Boverton, 1911).

Oil sands were mined from 1745 in Merkwiller-Pechelbronn in the Alsace region of France. The Pechelbronn oil field was active until 1970 and was the birthplace of the Schlumberger family; their oilfield enterprise is now the world's largest offshore drilling contractor. The first modern refinery was built in Pechelbronn in 1857 (New York Times, 1880).

## 2.2 Modern Petroleum Industry

Oil and gas operations today are multibillion dollar industries that started modestly around 1850 when commercial wells were dug or drilled in several countries to obtain crude oil, primarily for kerosene and oil lamps. The question of where or when the first commercial oil well was drilled is difficult to answer, however.

Bibi-Heybat is an oil and gas-condensate field located on the west coast of the Caspian Sea in present day Azerbaijan, which was then part of the Russian Federation and was known as the *Land of Fire* for its ancient burning oil and gas seeps. In 1846, twelve years before oil was discovered in Oil Springs, Ontario, Canada, an oil well in the producing major oil field of Bibi-Heybat in the capital city of Baku laid the foundation for industrial production of “black gold” in Azerbaijan. By 1899, Azerbaijan led the world in the production and processing of oil and produced half of the world’s oil that year. From 1899 to 1901, the Russian oil industry in Baku was first in the world in total production, delivering 84.3 million barrels (13.4 million m<sup>3</sup>) of oil per year. At that time, production in the USA was about 66.7 million (10.6 million m<sup>3</sup>) barrels per year (Mir-Babayev, 2021).

However, Edwin L. Drake’s 1859 well—which initially produced 25 bbl/d (4 m<sup>3</sup>/d) of oil from a depth of 21 m (69 ft), in the Oil Creek Valley near Titusville, Pennsylvania, USA—is popularly considered the first modern well (Brice, 2009). There are several reasons why Drake’s well is singled out for this honor.

1. It was drilled, not dug by hand.
2. A steam engine was used to drill the well.
3. There was a company associated with it (the Seneca Oil Company with Drake as president).
4. It started a major oil boom, the first oil rush not only in Pennsylvania but throughout the USA.

Titusville and other towns on the banks of Oil Creek expanded rapidly as the number of oil wells and refineries increased dramatically across the region. In 1875, crude oil was discovered by David Beaty at his home in nearby Warren, Pennsylvania. This led to the opening of the Bradford Field, which by the 1880s produced 77 percent of the global oil supply. Oil quickly became one of the most valuable commodities in the USA and railroads expanded into western Pennsylvania to ship petroleum to the rest of the country and for export.

Annual output of crude oil in the USA increased rapidly from 2,000 bbl (318 m<sup>3</sup>) in 1859 to 4.2 million bbl (0.72 million m<sup>3</sup>) in 1869 and 20 million bbl (3.17 million m<sup>3</sup>) in 1879. During this time, the USA was by far the main oil producer in the world, its rapid expansion spurred by the ongoing industrial development of Europe. European, and especially British, factories began importing large quantities of cheap American oil during the 1860s. By the mid-1870s, the oil industry was well established, and the rush to drill wells and

control production was over. Pennsylvania oil production peaked in 1891 and was later surpassed by western states such as California, Texas, and Oklahoma, but some oil industry remains in Pennsylvania. By the end of the nineteenth century, the Russian Empire, particularly the Branobel company in Baku, Azerbaijan, had taken the lead in oil production (Mir-Babayev, 2021).

In 1908, Galician oilfields made the Austrian-Hungarian Empire the third largest oil producing country after the USA and the Russian Empire. By around 1910, major oil fields had been discovered and produced at commercial levels in many countries including the Dutch East Indies (1885, in Sumatra), Persia (1908, at Masjed Soleiman), Venezuela (1914, in the Maracaibo Basin), and Mexico (1901, Ebano Field). In the 1920s through 1940s, vast petroleum reserves were discovered and large amounts produced in Iraq, Iran, Saudi Arabia, and countries along the Persian Gulf. Significant oil fields were discovered in Alberta (Canada) beginning in 1947. Offshore oil drilling at Oil Rocks (Neft Daşlari) in the Caspian Sea off Azerbaijan eventually resulted in a city built on pylons in 1949.

Availability of oil—and access to it—became of great importance for military power before and after World War I, particularly for several national navies (e.g., USA, UK, Italy) as they changed from using coal to more efficient oil-fired boilers but also with the introduction of motor transport, tanks, and airplanes and as the base of many industrial chemicals (Fromkin, 1989). The importance of oil would continue in later conflicts of the twentieth century, including World War II, during which oil facilities were major strategic assets that were often targeted and damaged or destroyed (Baldwin, 1959).

In the 1950s and 1960s, the development of modern seismic technology allowed prospecting for oil and natural gas to be extended onto the continental shelves. Since the 1970s, an increasingly large share of international prospecting has taken place offshore, aided by improved seismic methods, advanced well-log technology, and powerful computers for data processing. Rising oil prices and new technology have made exploration financially attractive in areas that previously were of little interest, including in very deep water. High oil prices are also paying for enhanced hydrocarbon recovery from reservoirs including use of flooding with CO<sub>2</sub> (Bjørlykke, 2010).

Until the mid-1950s, coal was the world's primary energy source; oil and natural gas together have replaced coal since then and continue their dominance today. According to the *BP Statistical Review of World Energy 2020*, more than 95 million bbl/d (~15 million m<sup>3</sup>/d) of crude oil was produced globally during 2019—slightly above the level in 2018, but a 17 percent increase compared to 2009. Despite growing international momentum, especially following the Paris Accord of 2016, and behind policies to shift away from oil and other hydrocarbons as energy sources in response to concerns about global warming and related climate change, oil and natural gas remain for now the dominant ingredients of the world fuel supply.

The USA became the top global crude oil producer in 2017 and in 2019 produced 12.2 million bbl/d (1.94 million m<sup>3</sup>/d), which is equivalent to 18 percent of the global output. The USA surpassed Saudi Arabia because of major increases in oil and natural gas production from unconventional sources of energy: shale and tight reservoirs (this is discussed in more detail in Section 4). Production from unconventional sources resulted from the *fracking revolution* caused by recent developments in deep horizontal drilling, downhole telemetry, and massive multi-stage hydraulic fracturing of low permeability reservoirs using *slickwater* (water with chemicals added to increase flow).

Starting in 1991, but mainly after 2007, production of gas and oil from shale, siltstones, and other very low permeability (less than 0.1 mD; millidarcy) reservoirs increased dramatically in the USA (Arthur & Cole, 2014; Kharaka et al., 2020; EIA, 2018). Production of crude oil in the USA increased dramatically from 5.0 million bbl/d (0.80 million m<sup>3</sup>/d) in 2008 to 12.2 million bbl/d (1.94 million m<sup>3</sup>/d) in 2019, with 63 percent derived from unconventional sources. Natural gas production in the USA also increased rapidly—from 0.4 Tcf (trillion cubic feet) in 2000 to 34 Tcf in 2019; 87 percent was obtained from shale and tight reservoirs (EIA, 2021).

Production of oil and natural gas from unconventional sources, however, has its own set of environmental impacts, including groundwater and surface water contamination and seismicity, which are discussed in Section 5 (Patterson et al., 2017; Maloney et al., 2017; Bonetti et al., 2021; Groundwater Protection Council, 2023). Fracturing requires large volumes of fresh water that is an issue in USA's western states where water resources are scarce and needed for other uses. Gallegos and others (2015) calculated the median volumes of 15,000 m<sup>3</sup>/well and 19,000 m<sup>3</sup>/well were used to hydraulically fracture individual horizontal oil and gas wells, respectively.

Saudi Arabia is second in crude oil production, producing 11.8 million bbl/d (1.87 million m<sup>3</sup>/d), 12.4 percent of global output in 2019. Saudi Arabia is the world's biggest oil exporter and is the leader of the Organization of Petroleum Exporting Countries (OPEC), which attempts to control global oil production and oil price. Russia produced 12 percent of the world's oil supply in 2019 at 11.5 million bbl/d (1.82 million m<sup>3</sup>/d). Canada was fourth, producing 5.6 million bbl/d (0.89 million m<sup>3</sup>/d), about 6 percent of global output. After Venezuela and Saudi Arabia, Canada has the world's third-largest known oil reserves, mostly in oil sands in Alberta. Finally, Iraq, a founding member of OPEC, was fifth in oil production in 2019, producing 4.6 million bbl/d (0.73 million m<sup>3</sup>/d), close to 5 percent of total global output.

In 2019, the USA was also the top natural gas producer with 34 Tcf, followed by Russia, which produced 24 Tcf; Iran was third with 11.5 Tcf, followed by Qatar (6.3 Tcf) and Canada (5.8 Tcf). Total global natural gas production in 2019 reached a new high of 144 Tcf that was 3.3 percent higher than 2018.

Several oil crises in history have been brought about by national and international conflicts. The most serious oil crisis was in 1973–74 when the Arab members of OPEC proclaimed an oil embargo. The embargo was targeted at the USA but included the UK and other countries for their support of Israel during the Yom Kippur War (1973). By the end of the embargo in March 1974, the price of a barrel oil had risen nearly 300 percent: from \$3 USD to nearly \$12 USD globally (Black, 2012). The embargo caused an oil crisis, or “shock,” with many short- and long-term impacts on the global economy and politics (Maugeri, 2006).

Following the energy crises that resulted from the 1973–74 Arab oil embargo and 1979 Islamic revolution in Iran, there was significant discussion and concern on the subject of oil being a limited resource that will eventually run out, at least as an economically viable energy source. Although at the time the future supply predictions were quite dire, a period of increased production and reduced demand in the following years caused an oil glut, resulting in a significant drop in the price of oil in the 1980s. However, the glut did not last long and by the 2010s, concerns about peak oil had returned to the news. The petroleum glut cycle and reduced prices returned in 2016 following the use of new technology that allows the production of oil and natural gas from unconventional sources: shale and tight reservoirs. Also, the COVID-19 virus pandemic of 2020–21 lowered the use of fossil fuels globally by about 7 percent and caused the price of crude oil and gasoline to plummet.

The main concern about the use of coal, oil, and other fossil fuels today (in 2023) is related to global warming and associated climate issues that result from continual additions of large and increasing amounts of CO<sub>2</sub> in the atmosphere, obtained mainly from the burning of fossil fuels (Friedlingstein et al., 2020). The global temperature has already warmed 1.2 °C relative to pre-industrial times (1885 to 1900) and is predicted to increase to 2.7 °C by 2100. Potentially adverse impacts related to climate warming include the following:

1. sea-level rise from the melting of mountain glaciers and polar ice sheets and from ocean warming;
2. increased frequency and intensity of wildfires, floods, droughts, and tropical storms; and
3. changes in the amount, timing, and distribution of rain, snow, and runoff.

Rising CO<sub>2</sub> is also increasing the amount of CO<sub>2</sub> dissolved in ocean water, increasing its acidity (lowering its pH from 8.1 to 8.0), with potentially disruptive effects on coral reefs, marine plankton, and some marine ecosystems (International Panel on Climate Change (IPCC), 2022; Kharaka & Hanor, 2014; NRC, 2020; Sundquist et al., 2009).

To tackle climate change and its many negative global impacts, world leaders from 195 countries at the [UN Climate Change Conference \(COP21\)](#) in Paris reached the historic Paris Agreement on 12 December 2015. The parties pledged to substantially reduce their countries’ greenhouse gas emissions to limit the global temperature increase by 2100 to well

below 2 °C, and to pursue efforts to limit the temperature increase to 1.5 °C relative to pre-industrial times. The countries also pledged to review and strengthen their emission commitments every five years, thus providing a durable framework guiding the global effort for many decades (UN, 2015).

In 2021, the UN's IPCC released its first major assessment of human-caused global warming since 2013. The report shows a world that has starkly changed in eight years—warming by more than 0.3 °C to 1.2 °C above pre-industrial levels. Weather has grown more severe, sea levels are measurably higher, and mountain glaciers and polar ice shrank sharply. Future climate change will have a significant impact on the Earth's water cycle, and it is expected to exacerbate the intensity of both precipitation and droughts. These changes in turn influence other associated risks, such as the incidence of flooding and wildfires, all of which have major impacts on groundwater. Pushed by a concerned public and corporations, many countries have expressed willingness to curb their carbon emissions (IPCC, 2021, 2022).

### 2.3 2021 UN Climate Change Summit: COP26, Glasgow, Scotland

On 13 November 2021, diplomats from approximately 200 countries reached a major agreement aimed at intensifying efforts to fight climate change by calling on governments to return in 2022 with stronger plans to curb their planet-warming emissions. The summit urged wealthy nations—including the USA, Canada, Japan, and western Europe—to “at least double” funding by 2025 to protect the most vulnerable nations from the hazards of a hotter planet. The wealthy nations account for just 12 percent of the global population today but are responsible for 50 percent of all the planet-warming greenhouse gases released from fossil fuels and industry over the past 170 years (IPCC, 2021).

The top priority for the summit was to limit the rise in global temperatures to just 1.5 °C above pre-industrial levels. That is the threshold that scientists warned about, beyond which the risk of calamities like deadly heat waves, water shortages, and ecosystem collapses grow immensely (IPCC, 2021). The agreement established a clear consensus that all nations need to do much more, immediately, to prevent a catastrophic rise in global temperatures. The agreement outlines specific steps the world should take from slashing global CO<sub>2</sub> emissions nearly in half by 2030 to curbing emissions of methane, another potent greenhouse gas. And it sets up new rules to hold countries accountable for the progress they make or fail to make.

A major agreement was reached on how to regulate the fast-growing global market in carbon offsets, in which one company or country compensates for its own emissions by paying someone else to reduce theirs. One of the thorniest technical issues is how to properly account for these global trades so that any reductions in emissions are not overestimated or double-counted.

Other international agreements reached at the summit included the following.

- The USA and China announced a joint agreement to do more to cut emissions this decade, and China committed (for the first time) to develop a plan to reduce methane. The agreement was short on specifics and, while China agreed to 'phase down' coal starting in 2026, it did not specify by how much or over what period.
- Leaders of more than 100 countries (including Brazil, China, Russia, and the USA) vowed to end deforestation by 2030. The agreement covers about 85 percent of the world's forests, which are crucial to absorbing carbon dioxide and slowing the pace of global warming.
- More than 100 countries agreed to cut emissions of methane by 30 percent by the end of 2030. The pledge was part of a push by the USA's Biden administration, which also announced that the US EPA would limit the amount of methane coming from about one million oil and gas rigs across the USA.
- India joined the other nations pledging to reach "net zero" emissions, setting a 2070 deadline to stop adding greenhouse gases to the atmosphere. Other countries pledged net zero on or before 2050. India, one of the world's largest consumers of coal (55 percent of its total energy), also said that half of its energy would come from sources other than fossil fuels by 2030.

## 2.4 Exercises Pertinent to Section 2

[Link to Exercise 2](#) ↴

[Link to Exercise 3](#) ↴

## 3 Drilling, Completion, and Fluid Production from Petroleum Wells

### 3.1 Introduction to Drilling, Completion and Production

In the early days of the oil industry, petroleum wells were relatively simple, shallow, vertical boreholes similar to Drake's 1859 well in western Pennsylvania, which produced oil from a depth of 21 m. After 1859, oil wells were drilled onshore to greater depths and produced larger volumes of needed petroleum. Petroleum wells are now much more complex, including those drilled for production of oil and natural gas from conventional sources of energy such as high porosity and permeability sandstone and carbonate reservoirs. These sources of petroleum may be located on- or off-shore and penetrate to greater depths, thus producing from reservoirs at depths of up to 12,000 m.

In the early days of the petroleum industry, knowledge of local or regional geology was not required for exploration because oil wells were generally located in the vicinity of existing oil seeps and tar pits. It was soon discovered that oil and natural gas occur where sedimentary rock formations form anticlinal structures, and that a low permeability or seal layer had to be present to prevent the oil and gas from rising and escaping. Geological mapping of anticlines and salt domes became early important prospecting targets.

Much more sophisticated geological, geophysical, and geochemical investigations and detailed mapping and basin modeling came into practice in the early twenty first century before selecting a target reservoir for exploration and drilling. While these methods are beyond the scope of this book, they are covered in detail in several recent reports and petroleum geology books including Hunt (1996), Bjørlykke (2010), Selley and Sonnenberg (2014), Steelman and others (2017), and Stephens and others (2018).

### 3.2 Well Drilling

Once a target reservoir is chosen, the site selected for an oil well is leveled and cleared of vegetation, then a drilling "mud" pit is prepared (generally, a large tank that holds the mud that will be used as drilling fluid). The well is created by drilling a hole, 12 to 100 cm in diameter with a drilling rig that rotates a drill string with a bit attached. Several water and chemical tanks are installed before the well is spudded (i.e., drilling is initiated) above the target reservoir in the case of conventional wells.

After the hole is drilled 10 to 20 m deep, sections of steel pipe slightly smaller in diameter than the borehole are placed in the hole to form a conductor casing. Cement is then placed between the outside of the casing and the borehole—a space known as the annulus—to provide structural integrity to the newly drilled wellbore; this procedure also isolates shallow freshwater aquifers from contamination by the drilling operations. The well is then drilled deeper with a smaller bit and is cased with a smaller size casing. The

second casing, termed the surface casing, extends from ground surface to 150 to 500 m deep; it is intended to isolate deeper freshwater aquifers from contamination by the drilling operations as it reaches 10 to 60 m below underground sources of usable water (USUW). Modern wells often have two to five sets of subsequently smaller hole sizes drilled inside one another, each cemented with casing (Figure 2).

Drilling fluid (known as *drilling mud*) is pumped down the inside of the drill pipe and exits at the drill bit. The main components of drilling fluid are usually water and bentonite clay; however, it may also contain a complex mixture of fluids and solids, including barite, KCl, and other chemicals carefully selected to provide the correct physical and chemical characteristics required to drill the well safely and efficiently. The main functions of the drilling mud are cooling the bit, lifting rock cuttings to the surface, preventing damage of the rock wall in the wellbore, and overcoming the pressure of fluids inside the rock formation so these fluids do not invade the wellbore.

The drilling fluid with rock cuttings circulates back to the surface outside the drill pipe. The fluid then goes through *shakers* (vibrating sieves) that separate the cuttings from the drilling fluid, which is returned to the mud pit for reuse. The well operator examines the returning cuttings and drilling mud for any signs of hydrocarbons and for lost circulation, indicated by lower volume of returning drilling mud, because some drilling fluids in the well flow to the rock formation. The operator also watches for *kicks* (high pressure signals) that indicate formation water is entering the well because of contact with a rock formation with high fluid pressure. If such inflow is not controlled—initially by closing the blowout preventer valves and ultimately by increasing the density of the drilling fluid—then minor or large blowouts could occur that might contaminate the local soils and aquifers.

### 3.3 Well Completion

Following drilling and casing, the well is completed for production. Completion is carried out in cased holes by selecting the production zone and shooting charges to make 13 to 20 perforations per meter in the casing. These perforations allow the flow of oil or gas from the surrounding reservoir to the production tubing. In some wells, two or more production zones are perforated, and these may be separated by many meters of shale or other formations that do not contain hydrocarbons. In open hole completions, *sand screens* or a *gravel pack* (pea-sized gravel) is installed in the last drilled, uncased reservoir section. These maintain the structural integrity of the wellbore in the absence of casing, while still allowing flow from the reservoir into the wellbore.

After perforation, acids and fracturing fluids are often pumped into the well to fracture, clean, and stimulate the reservoir rock to optimally produce flow of hydrocarbons into the wellbore. Finally, the area above the reservoir section of the well is packed off inside the casing and connected to the surface via a smaller diameter pipe called tubing.

This arrangement provides a second barrier to leaks of hydrocarbons into overlying formations and aquifers.

In a new well, the natural fluid pressure in the reservoir is generally high enough for the oil or gas to flow to the surface. However, this is not always the case, especially in depleted fields where the pressures have been lowered by other producing wells, or in low permeability oil reservoirs. Installing a smaller diameter tubing may be enough to cause flow to the surface, but artificial lift methods may also be needed. Common solutions include downhole pumps, gas lift, or surface pump jacks.

### 3.4 Petroleum Production

The drilling rig and the smaller workover rigs used to drill and complete the well are removed from the site, and the top of the well is usually outfitted with a collection of valves called a *Christmas tree* or *production tree*. The production-tree valves regulate pressure, control flow, and allow access to the wellbore in the event that further completion work is needed. From the wellhead, oil and natural gas flow is connected to separation tanks, that allow the produced water to separate and accumulate at the bottom with oil at the top of the tank. Generally, water from several tanks is directed into an injection well and returned underground because most produced water cannot be allowed to contaminate surface water. Ultimately, oil and natural gas is directed to a distribution network of pipelines and tanks to supply the product to refineries, natural gas compressor stations, or oil export terminals.

In depleted reservoirs and older wells, in addition to artificial lift, workovers using service rigs are often necessary to improve production by adding a smaller diameter tubing, removing accumulated scale or paraffin from the well, using acid to enhance formation permeability, or even perforating and completing one or more new production zones.

The amount of petroleum recovered from a reservoir with natural flow and artificial lift, called *primary recovery*, is generally less than 30 percent of original oil-in-place. Improved recovery methods, using water flooding and pressure maintenance (termed *secondary recovery*) allow the recovery of up to 50 percent of oil-in-place. Finally, new *tertiary recovery* methods—using steam flooding and other heating methods, CO<sub>2</sub> or other gas injections, and sometimes microbial injections—may be used to increase reservoir pressure and provide a “sweep” effect to push hydrocarbons out of the reservoir. Such methods may result in recovering up to 80 percent of oil-in-place (Bjørlykke, 2010). However, care must be taken to ensure the increased reservoir pressures generated in these enhanced recovery methods do not cause leakage of hydrocarbons and formation water directly—or through the nearby old wells—into USUW.

### 3.5 Well Abandonment

A petroleum well may be abandoned for many reasons including, but not limited to, the price of oil and natural gas. At this stage, some abandoned wells are plugged and the site is reclaimed for other uses, but the cost is very high. Plugging the well means the tubing is removed and sections of the wellbore are filled with concrete to isolate the flow path between hydrocarbons and USUW zones from each other as well as from the surface. The surface around the wellhead is then excavated, the wellhead and casing are cut off, a cap is welded in place and then buried (US Environmental Protection Agency, 2019).

In the case of primary and secondary production wells, the bulk of the oil is still left in the reservoir at the time they reach their economic limit. It might be tempting to defer physical abandonment of such wells for an extended period in the hope that the price of oil will increase or that new recovery methods will allow additional economic recovery. In these cases, temporary plugs that may corrode are placed downhole and locks are attached to the wellhead to prevent tampering. There are many thousands of such abandoned wells throughout the USA. However, lease provisions, liability, and governmental regulations usually require quick abandonment (Hunt, 1996).

These abandoned wells are probably the main contaminants of freshwater aquifers in the USA and other oil-producing countries. Starting around 1930, oil producing states in the USA—and federal regulators by 1970—required oil field operators to cement abandoned wells above and below water-bearing formations to keep fluids from flowing between formations and contaminating USUW. However, not all operators followed the rules, and in older fields many wells were abandoned before regulatory agencies established adequate plugging procedures.

Some of these abandoned wells provided fluids with a path to flow between formations. An injection well, if located near a poorly plugged abandoned well, could force formation water up the abandoned hole, allowing it to move from one formation to another, and sometimes contaminating groundwater in the process (Figure 3). In addition, an injection well with corroded casing could provide its own path to other formations, including freshwater aquifers. Further, if a fault is present in the vicinity of an injection well, fluids may flow upward along that fault and contaminate USUW (Kharaka & Otton, 2007).

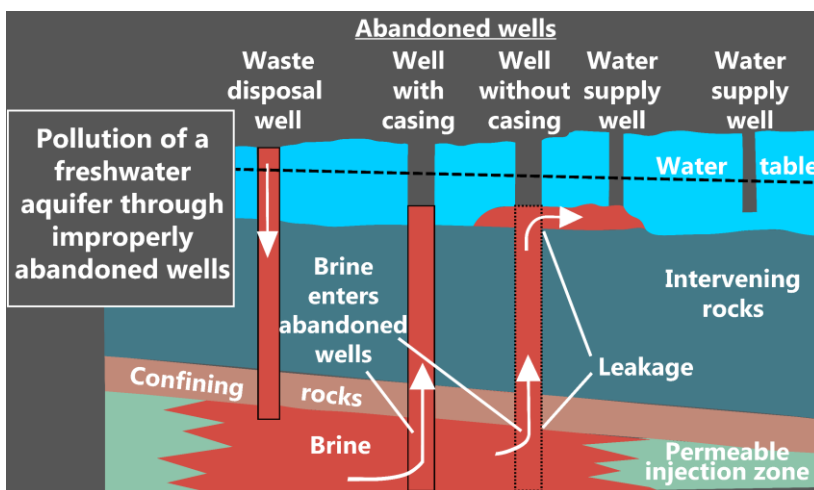


**Figure 3** - Contamination of groundwater by produced water injected into a disposal well near old and leaking abandoned oil or gas wells (unpublished figure used for presentations by Kharaka following Kharaka et al., 2005).

## 4 Produced Water from Conventional Petroleum Sources of Energy

### 4.1 Introduction to Water from Conventional Sources

Produced water (often called oil field brine, formation water, or petroleum wastewater) is saline water that is predominantly co-produced with oil and natural gas. In this book, the term produced water is used for all water obtained at ground level from wells drilled for the exploration and production of oil and natural gas. The bulk of produced water is generally that which is associated with oil and gas in the pores of reservoir rocks or in sedimentary rocks below or adjacent to the oil and natural gas. However, as the petroleum fields mature, modified fresh water, steam, seawater, or produced water with chemicals may be injected into the underlying water zone for pressure maintenance and improved production. Some of this injected fluid mixes with the pore water and is co-produced with oil and natural gas.

The chemical composition of produced water obtained from oil fields in the USA and other countries, which we discuss in detail in Section 5, is highly variable as it may have salinity ranging from about 3,000 to more than 400,000 mg/L total dissolved solids (TDS). It may contain a variety of toxic metals, organic and inorganic components, as well as  $^{226/228}\text{Ra}$  and other naturally occurring radioactive materials (NORMs).

The volume of produced water obtained with a given volume of oil (the W/O ratio) or natural gas from a conventional petroleum field also varies greatly, with the water/oil or water/gas ratios ranging from close to zero to more than 50, indicating that a given oil well is producing more than 98 percent water and the field is essentially depleted (Kharaka & Otton, 2007). Older oil fields produce much more water relative to oil even in the absence of water flooding for pressure maintenance and enhanced oil recovery. This is illustrated (Figure 4) in the volume of water and oil produced over time from the Prudhoe Bay Field, North Slope, Alaska, USA. In 1977, this field started producing about 0.7 million bbl/d (0.11 million m<sup>3</sup>/d) of crude oil, with essentially zero produced water. Oil production was from the Sadlerochit Group at a depth of about 2,750 m and continued to increase to approximately 1.6 million bbl/d (0.25 million m<sup>3</sup>/d), with produced water remaining very low. Produced water did not start to increase significantly until 1983 when modified seawater was first injected in the field for pressure maintenance and enhanced oil recovery (Kharaka et al., 1995). The water/oil (W/O) ratio reached 1.0 in approximately 1992, then increased as the oil production declined; the W/O ratio reached 4.3 in 2019 when 1.2 million bbl/d of water and 0.279 million bbl/d (0.044 million m<sup>3</sup>/d) of crude oil were produced. When oil production from wells in Prudhoe Bay or other oil fields is depleted, the W/O ratio may reach a value of 50, with oil making up 2 percent or less of the total fluid produced.

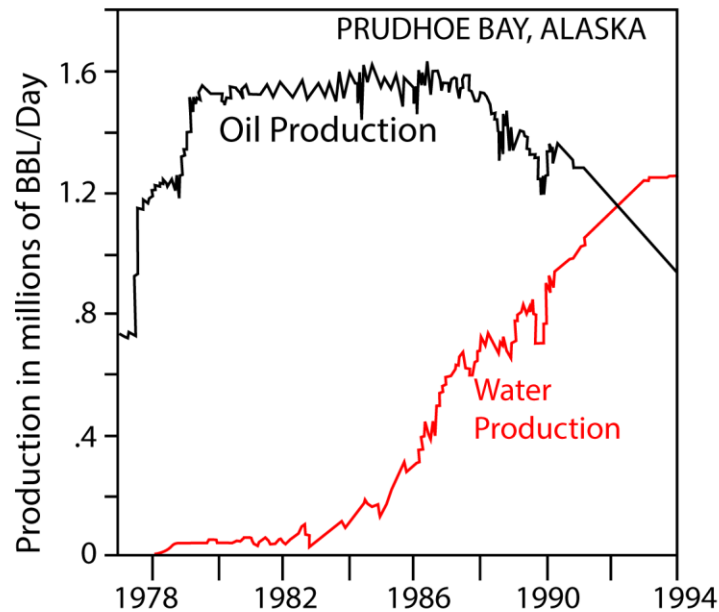


**Figure 4** - Oil and water production from Prudhoe Bay Field, Alaska, USA. Produced water volume is low at the beginning of production and increased as oil production decreased (Kharaka et al., 1995).

## 4.2 Historical Perspective on the Volume and Management of Produced Water

Oil producers in the USA have been separating and disposing of produced water since the time of Drake's well in 1859. However, neither the oil industry nor any state nor federal government agency paid much attention to this disposal activity for close to a century. Early producers simply let their saline wastewater run free over natural channels into streams, rivers, and lakes, with some wastewater percolating into and contaminating groundwater (Gorman, 1999).

In general, disposal of this saline water had not been a major concern in the early oil fields of western Pennsylvania because producers lifted relatively small amounts of oil and water and the wastewater had a relatively low TDS. Further, the heavy rains and fast-flowing streams that occurred there quickly diluted the released saline water to harmless concentrations. The total volume of produced water in the USA increased as oil production increased, so that by 1965 a total of 23 million bbl/d (3.65 million m<sup>3</sup>/d) were generated with 7.67 million bbl/d (1.22 million m<sup>3</sup>/d) oil, for a W/O ratio of 3.0 (Gorman, 1999). The W/O ratio in the USA today is not well known because the volume of produced water in many oil fields is neither carefully measured nor reported but is likely in the range 8 to 12. In an excellent review of the volume and management of produced water in the USA, Veil (2020) reports W/O ratios to be 9.4 and 7.4 in 2012 and 2017, respectively; the decrease in ratio in 2017 resulting mainly from increased production of oil from unconventional sources of energy.

The W/O ratio and the *water cut* (volume of water x 100/volume of water + oil) in petroleum fields in Saudi Arabia and other countries are generally much lower than the values in the USA because petroleum fields in those countries, for the most part, have not had as many years of production to deplete the reservoirs; the petroleum reservoirs generally have high porosity, permeability, and oil columns, with most wells shut-in when water production becomes high. Fakhru'l-Razi and others (2009) report on the global volume of produced water onshore and offshore from 1990 to 2015 (Figure 5). In 2015, the volume of produced water from global onshore and offshore operations was 310 million bbl/d (49.4 million m<sup>3</sup>/d) with concurrent crude oil production (including the USA) of 82 million bbl/d (13.0 million m<sup>3</sup>/d) (US Energy Information Administration, 2021). This is a low W/O ratio of 3.8.

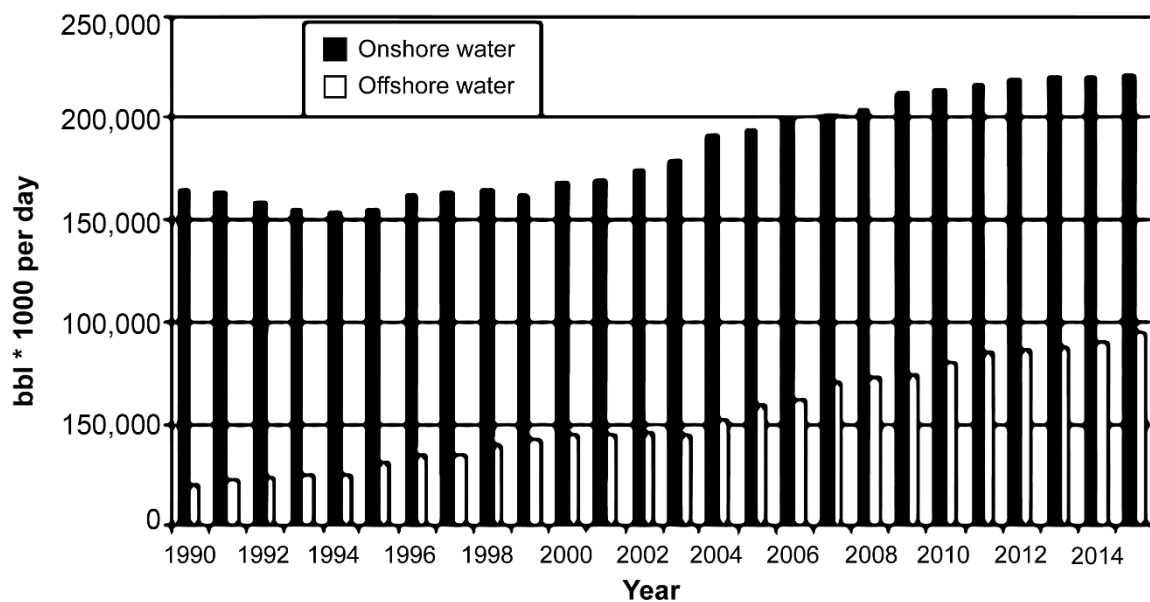


**Figure 5** - Global onshore and offshore produced water from 1990 to 2015 (from Fakhru'l-Razi et al., 2009).

In Saudi Arabia in 2009, the W/O ratio was 3. However, in the case of Saudi Arabia's Ghawar Field—the most productive onshore field in the world, producing continuously approximately 5 million bbl/d (37.7 m<sup>3</sup>/d) oil—the W/O ratios are much lower; in 1993, its water cut was only 25 percent. A decade later, the water cut was 33 percent (Figure 6), for very low W/O ratios of 0.25 and 0.33, respectively (Sorkhabi, 2010).

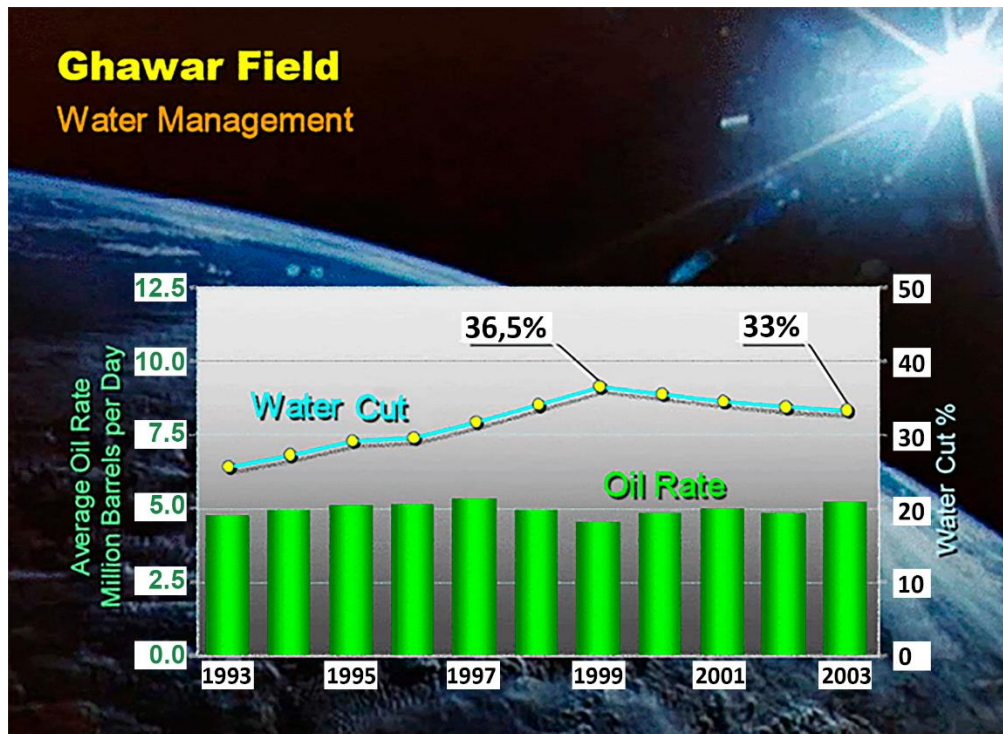


**Figure 6** - Production of oil and water from Saudi Arabia's Ghawar Field from 1993 to 2003. The field continuously produced approximately 5 million bbl/d (~0.8 million m<sup>3</sup>/d) oil, with very low W/O ratios of 0.25 to 0.33 (Reguly, 2019).

The W/O ratio in the USA is highly variable from state to state and even among fields in the same state. The highest W/O ratios are obtained in states with fields that have been producing petroleum for a long time and have limited unconventional petroleum production; for example, Kansas, which started oil production in 1892, has mainly conventional oil with high W/O ratios of 24.3 in 2012 and 33.6 in 2017. California, with notable production starting in 1865, had W/O ratios of 16 and 18 in 2012 and 2017, respectively (Gans et al., 2015; Groundwater Protection Council (GWPC), 2019; Kharaka et al., 2019; Veil, 2020). In 2017, Colorado produced 120 million bbl (~19.1 million m<sup>3</sup>) total oil, 308 million bbl (~49.0 million m<sup>3</sup>) total water, 290 billion ft<sup>3</sup> (8.2 billion m<sup>3</sup>) total coal bed natural gas (CBNG), and 1.71 trillion ft<sup>3</sup> (48.4 million m<sup>3</sup>) total gas (including CBNG). The W/O ratio in Colorado is low—only 2.34 for 2017—but was much higher (W/O = 7.26) in 2012.

The W/O ratio is much lower for oil and gas obtained from unconventional wells that generally produce much more crude oil and less water. Thus, the W/O ratio is only 0.47 for Weld County, Colorado, USA, with predominantly unconventional production but much higher (18.2) for Garfield County, also in Colorado (Piceance Basin), with no unconventional petroleum production (Kharaka et al., 2019).

Concern with petroleum wastes other than produced water was higher after World War I. For example, a rapid increase in the demand for motor fuel threatened to overwhelm the nation's supply of crude oil. Oil companies responded by drilling 64,000

new wells in a two-year period (Williamson et al., 1963). This rush solved the motor fuel shortages but led to a significant amount of oil loss and waste. The US Bureau of Mines, established in 1910, was tasked with identifying and eliminating waste in the petroleum industry. The Bureau had no regulatory power, but their scientists and engineers carried out research, wrote reports, and gave presentations and demonstrations, believing that education served as the best tool to eliminate inefficiency and waste from accidents and other sources.

These efforts resulted in less pollution for a given level of oil production, but the limit of this approach was reached by the late 1950s, when additional efforts to reduce pollution further were no longer reasonable in an economic sense. Furthermore, major increases in both oil production and use as well as in the toxicity of produced water caused the nation's air and water quality to decline with time. However, it took ten more years for the transition from *conservation* to *environment*, that is, from self-regulation based on the economics of efficiently using resources to government-enforced regulations based on specified criteria for environmental quality.

Serious brine disposal problems started being noticed after the 1920s when oil companies began producing significant quantities of brine with increased oil production in drier regions of the USA. The disposal problems usually grew worse over time because as more oil was produced, this led to more wastewater and to higher water/oil ratios. The streams, lakes, and soils that were contaminated by this wastewater gradually grew saltier, leading to complaints from farmers, ranchers, and the general public. Farmers and ranchers were quick to seek monetary compensation for their economic losses (Gorman, 1999).

Oil companies in California had the most direct solution for disposal of their produced water: They piped the brine to the Pacific Ocean. By 1930, California pipelines had the capacity to carry brine at a rate of 200,000 bbl/d (31,800 m<sup>3</sup>/d) to the ocean. In Kansas, however, ocean disposal was not a viable solution and producers used *evaporation ponds*—shallow pits surrounded by a brim of dirt—to dispose of their produced water. In parts of Texas, producers stored their produced water in tanks and reservoirs when streams were dry. They released this water only when rain turned those dry channels into fast-moving streams. A few oil companies in Texas had no disposal problem; their produced water had low salinity and farmers stored it in pools from which cattle could drink (Schmidt, 1928).

The use of evaporation ponds in Kansas and the controlled release of produced water from storage reservoirs and tanks in Texas did not solve the problem of brine disposal. In Kansas, evaporation ponds were not adequate for the volume of the brine produced. Also, evaporation resulted in the creation of a more concentrated brine and a great deal of that brine leaked through the underlying soils to reach and contaminate the shallow groundwater. The evaporation ponds became known as *percolation ponds*. By the 1930s, they had contaminated shallow aquifers throughout the oil-producing regions of

Kansas, forcing many farmers to relocate their freshwater wells and generate many cases of litigation against oil companies.

Produced water injection into petroleum formations was started first in Kansas, and by 1936 more than 300 wells were used for brine disposal. This not only solved the problem of brine disposal but also helped to maintain reservoir fluid pressures and increase the portion of available oil in the reservoir that could be produced.

Disposal of produced water was also a major problem in the East Texas Field—the second largest oil field in the USA (after Prudhoe Bay Field, Alaska), covering an area of 140,000 acres (57,000 ha): ~70 km long and 8 to 20 km wide. Approximately 6 billion barrels (0.95 billion m<sup>3</sup>) of oil have been produced to date from more than 30,000 historic and active wells in this field since its discovery in 1930.

Large volumes of produced water were obtained in the 1930s from the many wells in the East Texas Field, even after the volume of oil produced from each well was limited to 20 bbl/d (3.17 m<sup>3</sup>/d), because the wells in some sections of the field produced water at a rate of up to 300 bbl/d (47.7 m<sup>3</sup>/d), for a W/O ratio of 15. Initially, produced water was stored in tanks and pits and released during the rainy season, but to protect the Neches-Angelina watershed from salt contamination and to prevent reservoir pressures from dropping too rapidly, the newly formed East Texas Salt Water Disposal Corporation initiated well injection. By 1946, the corporation was injecting over 250,000 bbl/d (39,700 m<sup>3</sup>/d) of brine, an amount that doubled over the next two years (East Texas Salt Water Disposal Corporation, 1953). This brine injection solved the problem of produced water disposal, maintained reservoir fluid pressure, and initiated secondary recovery in the depleted parts of the field.

Throughout the 1940s, the US Bureau of Mines continued to promote injection systems as a way to dispose of waste brine, maintain reservoir pressure, and recover more oil from older fields, and this was adopted throughout the country. However, economic incentives associated with increasing efficiency began to diverge from efforts to reduce brine pollution in the 1950s. By then, it was becoming clear that while injection systems solved the most pressing brine disposal problems, they could not eliminate all water pollution caused by the petroleum industry's produced water. First, injection systems were not always economically viable. Many small-scale oil producers operating in marginal fields continued to depend on traditional disposal methods such as running their waste brine into streams or disposal pits. Second, even in oil fields where operators turned to injection systems, some contamination still occurred where poorly plugged abandoned wells or corroded injection wells allowed the salt water to flow between formations.

All states required oil field operators to cement abandoned wells above and below fluid-bearing formations to keep fluids from flowing between formations. However, in older fields, many wells had been abandoned before regulatory agencies established

adequate plugging procedures. Some of these abandoned wells provided fluids with a path to flow between formations, sometimes contaminating groundwater in the process. In addition, injection wells with corroded casing also provided a path to other formations, including freshwater aquifers.

Federal regulations or an agenda for controlling industrial pollution in general—and brine disposal problems in particular—did not exist until about the 1950s. The guiding principle at that time was self-regulation that focused on strictly economic factors not environmental quality. Unless a pollution control effort resulted in the recovery of oil or other valuable material or decreased the amount of money spent on damage and lawsuits, companies generally did not take direct action to reduce their emissions, effluents, leaks, spills, and other discharges. At the same time, many engineers and company managers assumed that as they made industrial operations more efficient and reduced the amount of material being discharged as waste, their efforts would also address pollution concerns.

In Texas, the state prohibited the disposal of produced water into pits in petroleum fields overlying the Ogallala Formation, the largest aquifer in the USA. This was triggered by increases in the salinity of groundwater withdrawn from this aquifer in the vicinity of oil fields. However, many operators responded to the “no pits over the Ogallala” order simply by injecting their saline wastewater into old wells, some of which had corroded casing and poor cement seals. In some of those wells, brine injected under pressure flowed behind the casing and found a path to the Ogallala aquifer (McMillion, 1965). Poorly plugged abandoned wells in the area also caused additional aquifer contamination.

Texas was not unique in having problems with produced water disposal. By the mid-1960s, oil field operators throughout the USA were lifting more than 23 million bbl (3.65 million m<sup>3</sup>) of oil field brine and 7.80 million bbl (1.24 million m<sup>3</sup>) of oil (W/O ratio of 3.0) each day. Approximately 71 percent of that wastewater was injected back into subsurface formations for pressure maintenance. Twelve percent of that water flowed into unlined disposal pits and another 5 percent flowed into streams and rivers. Newspapers and journals published articles about the contamination problem, but no good solutions were provided as to how oil companies could run a cost-effective secondary recovery operation and still verify they were not contaminating aquifers in the process (Payne, 1966). However, that was soon to change.

### 4.3 Environmental Quality Regulations

A new approach and guiding ethic framed explicitly in terms of environmental quality emerged in the late 1960s to address air and water pollution. In the early 1970s, efforts to manage environmental quality by placing explicit boundaries on industrial operations in the shared environment gathered momentum. Specifically, the National Environmental Policy Act (1969)—which created the US EPA in 1970 with rules, regulations, enforcement procedures, and legislation—empowered the EPA to use a new

approach to control industrial pollution, including disposal of oil field brine. The policy goal of the new approach was defining and enforcing clear rules associated with use of the shared environment; the goal then was to sustain environmental quality, not to improve economy by eliminating inefficiency.

Additional major federal regulations were instituted in the 1970s and later, including the Clean Air Act of 1970; the Federal Water Pollution Control Amendments of 1972; the Safe Drinking Water Act of 1974 and its amendments of 1984 and later; the Toxic Substances Control Act of 1976; the Resource Conservation and Recovery Act of 1976; and the Comprehensive Environmental Response, Compensation, and Liability Act of 1980.

Under the authority of the Safe Drinking Water Act in 1974, the EPA established a public drinking water system program. Under the Safe Drinking Water Act and the 1986 Amendments, the EPA set limits for contaminant levels in drinking water to ensure the safety of public drinking water as follows.

- Maximum Contaminant Levels (MCLs) as listed in [Box 2](#) ↓, were established for contaminants that, if present in drinking water, may cause adverse human health effects—MCLs are enforceable health-based standards (US EPA, 2017).
- Secondary Maximum Contaminant Levels (SMCLs) as listed in [Box 3](#) ↓, were established for contaminants that can adversely affect the taste, odor, or appearance of water and may result in discontinuation of use of the water—SMCLs are non-enforceable, generally non-health-based standards that are related to the aesthetics of water use.

National Secondary Drinking Water Regulations are non-enforceable guidelines regarding contaminants that may cause cosmetic effects (such as skin or tooth discoloration) or aesthetic effects (such as taste, odor, or color) in drinking water (Box 3). EPA recommends secondary standards for water systems but does not require systems to comply. However, some US states may choose to adopt them as enforceable standards.

Action levels are concentrations that determine whether treatment requirements may be necessary based on the maximum contaminant level goal (MCLG, as shown in the last column of Table Box 2-1), the level of a contaminant in drinking water below which there is no known or expected risk to health. Table Box 2-1 presents the water-quality criteria, standards, or recommended limits as well as the general significance of the physical properties and constituents discussed in this book.

The concentrations of constituents in any water are compared to drinking water standards set by the EPA. Although EPA standards apply only to public water supplies, households using water from private wells for domestic purposes may want to be aware of the potential health risks associated with drinking water that exceeds drinking-water standards. Drinking-water standards established by the EPA are based on total constituent concentrations: the combined concentrations of both dissolved and suspended phases of

the water sample. Results reported by the USGS and others as dissolved constituent concentrations may be less than those obtained for similar samples analyzed for total constituent concentrations.

The US EPA also provided concentration standards in water that are protective of aquatic life and the other specified beneficial uses. Streams and some wells are generally classified as for irrigation, fish and wildlife propagation, or stock watering. *Aquatic-life criteria* are estimates of the highest concentrations in surface water that aquatic life can be exposed to without a resulting unacceptable or harmful effect. *Chronic criteria* are based on concentrations that the aquatic life can be exposed to for an indefinite period without an unacceptable or harmful effect. *Acute criteria* are based on concentrations that the aquatic life can be exposed to for very short periods without an unacceptable or harmful effect. For several trace elements, aquatic criteria vary with stream hardness; generally, as hardness increases, the toxicity of the trace element decreases (US EPA, 2017). *Beneficial use criteria* are designed by the EPA to protect and ensure that a stream, a water well, or other sources of water can support the specified beneficial uses.

#### 4.4 Irrigation Water Quality Criteria

Irrigation water use includes water that is applied by an irrigation system to sustain plant growth in agricultural and horticultural practices. Irrigation also includes water that is used for chemical application, weed control, field preparation, harvesting, dust suppression, and leaching salts from the root zone (Miller et al., 2020). Estimates of irrigation withdrawals are generally accounted for at the point of diversion (wells, springs, streams, ponds) and include water that is lost in conveyance prior to application on fields, as well as water that may subsequently return to a surface-water body as runoff after application, water consumed as evapotranspiration from plants, water evaporated from the ground surface, and water that recharges aquifers as it seeps past the root zone. For 2015, the USGS estimated that total irrigation withdrawals were 118,000 million gallons/d (450 million m<sup>3</sup>/d), which accounted for 42 percent of total freshwater withdrawals. Withdrawals from surface water sources were 60,900 million gallons/d (230 million m<sup>3</sup>/d), which accounted for 52 percent of the total irrigation withdrawals. Groundwater withdrawals for 2015 were 57,200 million gallons/d (217 million m<sup>3</sup>/d) (Dieter et al., 2018).

Generally, water quality criteria developed for human health and aquatic life are sufficiently stringent to protect uses designated for agriculture and industry because those uses are generally less sensitive to water quality. Irrigation water quality is the most critical factor in predicting, managing, and reducing salt-affected soils. In addition to affecting crop yield and physical conditions of soil, irrigation water quality can affect crop fertility, irrigation system performance and longevity, and the water application method. Therefore, knowledge of irrigation water quality is critical to understanding what management changes are necessary for long-term agricultural productivity. Details about the impact of

irrigation water on crop yield and soil infiltration are provided by Ayers and Westcot (1976), Bauder and others (2014), and Fipps (2021).

Soil scientists use the following categories to describe irrigation water effects on crop production and soil quality, as discussed in subsequent sections.

- Salinity Hazard: total soluble salt content;
- Sodium Hazard: relative proportion of sodium to calcium and magnesium ions;
- pH: acidity;
- Alkalinity: carbonate and bicarbonate content; and
- Specific Ion Toxicity: chloride, sulfate, boron, and nitrate content.

#### 4.4.1 Salinity Hazard

Irrigation water salinity is the most important hazard to crop productivity. Because plants can only transpire “pure” water—and some of the soil water is fixed in hydration shells on dissolved ions—usable plant water in the soil decreases dramatically as salinity increases. Irrigation water with high salinity reduces crop yield to a degree that is directly related to the reduced amount of water transpired given the salinity level.

Crop yield reductions from irrigating with high salinity water varies substantially with crop type. For example, the yield for salinity-tolerant plants like barley is 100 percent if irrigation water salinity is < 4,250 mg/L but decreases to 50 percent for water salinity of approximately 10,000 mg/L. The yield for a sensitive crop like onions is 100 percent for salinity < 510 mg/L but decreases to 50 percent if irrigation water salinity is > 2,000 mg/L. The salinity of produced water can be higher than the threshold value for crops by a factor of 10 or 100, with a dramatic impact on yields.

#### 4.4.2 Sodium Hazard

Irrigation water high in Na (sodium) relative to Ca (calcium) and Mg (magnesium) can also impact plant growth in certain soil types by reduction of water infiltration. This condition (termed *sodicity*) results from excessive accumulation of sodium in the soil, which causes swelling and dispersion of soil clays, surface crusting, and pore plugging. This degraded soil structure condition in turn obstructs infiltration and may increase runoff. Sodicity causes a decrease in the downward movement of water into and through the soil, so that actively growing plant roots may not get adequate water, despite pooling of water on the soil surface after irrigation.

Sodicity in water and soil is assessed by the Sodium Adsorption Ratio (SAR) given by Equation (1) where the concentrations of Na, Ca, and Mg are given in meq/L (milliequivalents per liter).

$$\text{SAR} = \frac{\text{Na}^+}{\left[ \frac{\text{Ca}^{2+} + \text{Mg}^{2+}}{2} \right]^{0.5}} \quad (1)$$

Many factors (including soil texture, organic matter, irrigation system and its management) impact how sodium in irrigation water affects soils. Soils most likely to show reduced infiltration and crusting from water with elevated SAR ( $> 6$ ) are those containing more than 30 percent expansive clay (smectite) and include most soils in the clay loam, silty clay loam and finer textural classes, as well as some sandy clay loams.

#### 4.4.3 pH and Alkalinity

The normal pH range for irrigation water is 6.5 to 8.4. Abnormally low pH (acidic) water is generally not common but may cause accelerated corrosion of irrigation systems. High pH water ( $\text{pH} > 8.5$ ) is often caused by high concentrations of bicarbonate ( $\text{HCO}_3^-$ ) and carbonate ( $\text{CO}_3^{2-}$ ). High carbonates can cause calcium and magnesium ions to form insoluble carbonate minerals leaving sodium as the dominant ion in solution, causing infiltration problems and sodic soil conditions. Excessive amounts of bicarbonate can also be problematic for drip or micro-spray irrigation systems when calcite deposits (scale buildup) cause reduced flow rates through orifices or emitters. In these situations, injection of sulfuric or other acidic materials into the system may reduce the deposits.

#### 4.4.4 Specific Ion Toxicity

Toxicity problems occur if certain chemicals in the soil or water are taken up by the plant and accumulate to concentrations high enough to cause crop damage or reduced yields. Tree crops are the most sensitive. Damage often occurs at relatively low ion concentrations for sensitive crops. It is usually first evidenced by marginal leaf burn and interveinal chlorosis. If the accumulation is great enough, reduced yields result. The more tolerant annual crops are not sensitive at low concentrations but almost all crops will be damaged or killed if concentrations are sufficiently high.

The ions of primary concern are chloride, sodium, and boron. Although toxicity problems may occur even when these ions are at low concentrations, toxicity often accompanies and complicates a salinity or water infiltration problem. Damage results when the potentially toxic ions are absorbed in significant amounts along with water taken up by the roots. The absorbed ions are transported to the leaves where they accumulate during transpiration. The ions accumulate to the greatest extent in the areas where the water loss is greatest, usually the leaf tips and edges. Accumulation to toxic concentrations takes time and visual damage is often slow to be noticed. The degree of damage depends upon the duration of exposure, concentration of the toxic ion, crop sensitivity, and the volume of water transpired by the crop. In a hot climate or hot part of the year, accumulation is more rapid than if the same crop were grown in a cooler climate or cooler season, then it might show little or no damage.

The sulfate ion is commonly a major contributor to salinity in irrigation water. As with boron, sulfate in irrigation water has fertility benefits, and irrigation water often has enough sulfate for maximum production for most crops. Nitrogen in irrigation water is

largely a fertility issue, and nitrate-nitrogen ( $\text{NO}_3^- - \text{N}$ ) can be a significant nitrogen source in many areas. The nitrate ion often occurs at higher concentrations than the ammonium ion in irrigation water. Water high in nitrogen can cause quality problems in crops such as barley and sugar beets and excessive vegetative growth in some vegetables.

#### 4.5 Government Regulations to Protect Groundwater

While regulators in some US states dealt with salt contamination from past disposal practices and abandoned wells, officials with the EPA focused on preventing future contamination from new wells. The EPA proposed new design standards for injection wells that required three layers of protection to prevent groundwater contamination by fluid leakage. Producers could continue to inject produced water into existing wells with one and two layers of protection, but they had to test those wells every year and every three years, respectively (Stewart-Gordon, 1992). Although the regulations may be regarded by some as too strict and expensive, an editorial in *Oil and Gas Journal* (1993) points out that a small portion of injection and abandoned wells have caused groundwater contamination and the USA had 170,000 active injection wells and 2.2 million abandoned or inactive wells at the time the article was written. Those numbers have increased at the time of publication of this book.

Federal regulators, however, were more concerned about groundwater pollution, so the Safe Drinking Water Act of 1974 included provisions that explicitly ordered the EPA to protect underground sources of drinking water (USDW) from possible contamination by injection wells. The legislation divided injection wells into five categories, with Class II wells being those associated with oil field operations. A two-year EPA study in 1977 documented groundwater contamination from oil field brine in seventeen US states; the authors of the study concluded that existing state-level regulations did not sufficiently protect groundwater and determined that new regulations were necessary. The regulations proposed by the EPA required operators to monitor the integrity of all injection wells through regular pressure tests and to inspect their wells for mechanical integrity every five years. In addition, operators drilling new injection wells were required to search for and fix any leaky well located within one-quarter mile of the new injection well.

Major industry opposition to the EPA regulations followed with claims of high increased cost; however, with minor revisions, the regulations proposed by the EPA came into force in 1980, affecting 160,000 Class II injection wells in thirty-one oil-producing states. State agencies were given the primary responsibility (primacy) of designing programs to meet or exceed the criteria established by the EPA's underground injection program (UIC); implementation of the injection program was carried out by the EPA in a few states that did not accept primary responsibility for the program or failed to meet the EPA's UIC criteria.

In 1987, eight years after the well monitoring program was put in place, the General Accounting Office (GAO) conducted a study to evaluate the performance of US state agencies. It concluded that some agencies were lax in enforcing the new regulations. In that study, investigators checked the documentation for a random sample of injection wells in Texas, Oklahoma, Kansas, and New Mexico, and concluded that agencies in the first three states were not following the regulations as indicated by the issuing of permits without requiring evidence that operators had conducted the necessary pressure tests. In addition, the study discovered twenty-three cases of Class II injection wells that were contaminating USDW (Government Accounting Office (GAO), 1989).

Contamination of freshwater aquifers by petroleum brine was and continues to be a difficult problem to resolve. Contamination can only be detected by finding significant changes in the quality of water in existing freshwater wells in an area over time; in the chemistry section of this book, we discuss the organic and inorganic chemicals and isotopes that can be used to identify pollution from produced water sources. Identifying the source of contamination, of course, requires sampling and analyses of water from several groundwater and petroleum wells to obtain the required criteria. These types of time-consuming studies were deemed too expensive and of low priority by some oil companies. Generally, they were not conducted by the oil companies who more often than not lacked an adequate number of trained personnel to conduct such investigations.

However, by the 1980s, compliance with well-defined federal regulations was mostly accepted as a logical way to maintain the level of environmental quality desired by the US society. The resulting wave of pollution control legislation enacted in the 1970s left the efficiency-minded US Bureau of Mines with no meaningful function; it was dissolved in 1996, giving the EPA the authority to enforce pollution-control legislation. This empowerment of the EPA shifted the focus in the petroleum industry from efficiency to environmental quality, and this ethic continues today.

## 4.6 Exercises Pertinent to Section 4

[Link to Exercise 4](#) ↴

## 5 Fluid Production from Unconventional Sources of Energy

### 5.1 Introduction to Water from Unconventional Sources

In contrast to *conventional* sources of energy (crude oil, natural gas, and condensates discussed in the previous section) generally produced by drilling vertical wells into structural or stratigraphic traps, in this section we are concerned with unconventional sources such as shale or tight sandstone formations that are continuous and extend for 50 km or more (Figure 7). According to Zou (2017), *unconventional* (also known as *continuous*) sources of energy include

- shale natural gas and shale oil,
- tight sandstone oil and natural gas,
- heavy oil,
- tar sand (strictly bitumen sands), and
- coalbed methane (also referred to as coalbed natural gas).

However, the categories conventional and unconventional are not fixed; over time, as economic and technological conditions evolve, resources hitherto considered unconventional can migrate into the conventional category (International Energy Agency (IEA), 2013). Industry and governments across the globe are investing large amounts of funds in exploration for unconventional oil and natural gas resources due to the depletion of hydrocarbons in conventional petroleum fields and the increasing scarcity of conventional oil reserves.

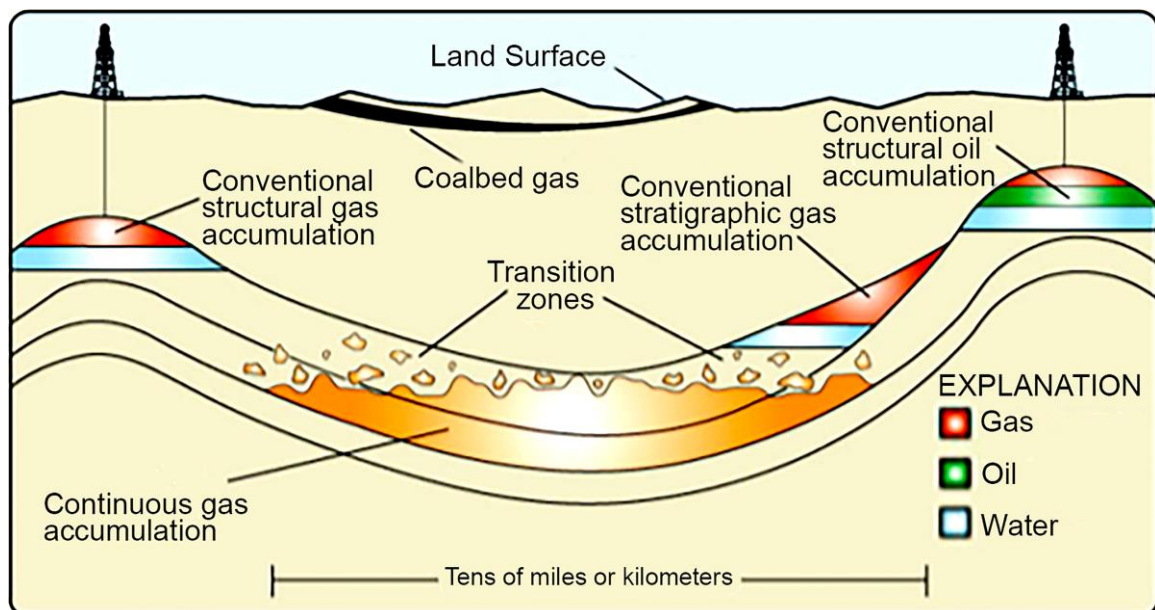


**Figure 7** - Schematic illustrating categories of natural gas occurrence, showing the relatively small conventional oil and natural gas accumulations compared to the much larger unconventional (continuous) energy resources of shale natural gas and tight oil reservoirs (from Schenk & Pollastro, 2001).

Starting in 1991, but mainly during the last fifteen years, production of gas and oil from shale, siltstones, and other very low permeability ( $< 0.1$  mD; millidarcy units) formations has increased dramatically in the USA due to recent technological developments in deep horizontal drilling (Figure 8), downhole telemetry, and massive multi-stage hydraulic fracturing using slickwater (Arthur & Cole, 2014; Healy et al., 2017; Kharaka et al., 2020; US Energy Information Administration, 2015). Production of natural gas in the USA from shale has increased rapidly, from 0.4 Tcf in 2000 to 34 Tcf in 2019; 87 percent was obtained from shale and tight reservoirs (US Energy Information Administration, 2021). Production of crude oil in the USA also increased dramatically from 5.0 million bbl/d in 2008 to 12.2 million bbl/d in 2019, with 63 percent obtained from unconventional sources (Scanlon et al., 2020a).

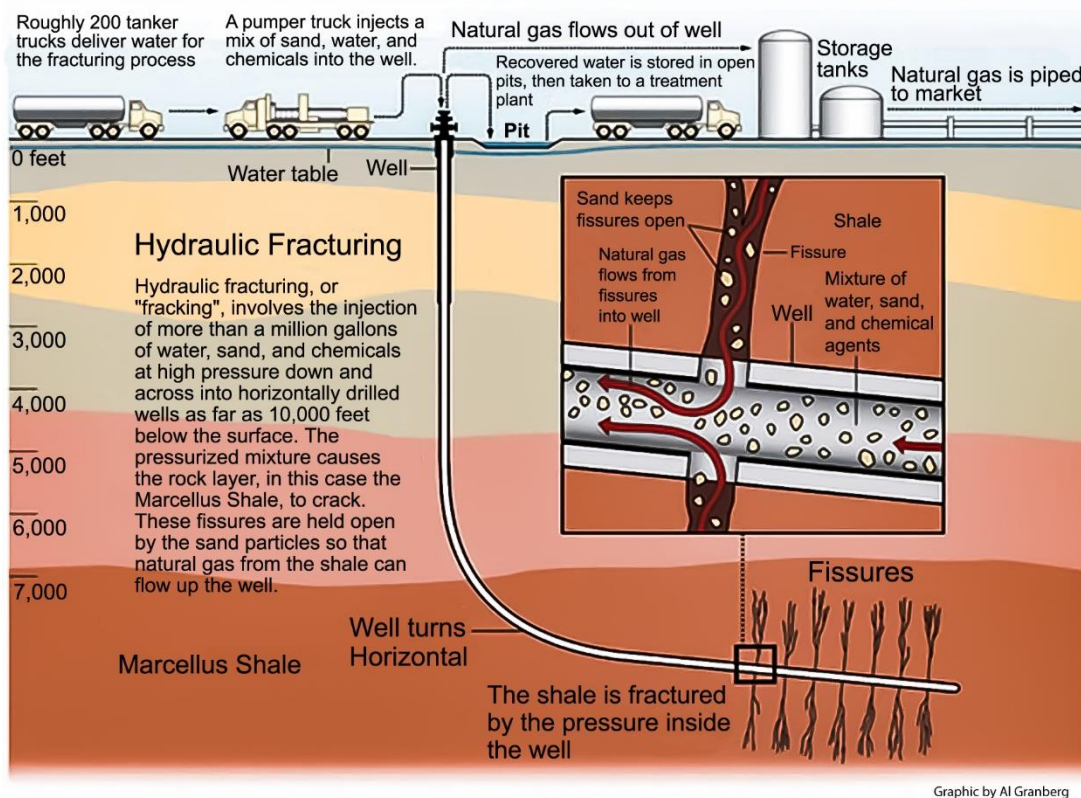


**Figure 8** - Schematic of recent technological developments in deep horizontal drilling, downhole telemetry, and massive multi-stage hydraulic fracturing using slickwater and proppant (graphic by Al Granberg, University of New Haven, 2011).

In the USA, shale oil and natural gas production is centered in eight major sedimentary basins: Anadarko, Appalachia, Bakken, Barnett, Eagle Ford, Haynesville, Niobrara, and the Permian (Nicot et al., 2017a, b, c; Groundwater Protection Council, 2019). The Permian Basin in southwest USA is the largest shale and tight oil basin in the USA in terms of both oil and gas production, with productions accelerating since early 2017 and reaching a record high of over 4.7 million bbl/d and 17 million cf/d (cubic feet per day) respectively in January 2020.

The Permian Basin province is one of the most productive areas for oil and gas in the entire USA (Nicot et al., 2020) and includes a series of sub-basins (e.g., Delaware sub-basin and Midland sub-basin) and other geologic formations in West Texas and southern New Mexico. According to the 2018 USGS assessment of unconventional undiscovered and technically recoverable resources, the Permian Basin contains very high volumes of oil and natural gas reserves in the Wolfcamp shale and overlying Bone Spring Formation in the Delaware sub-basin with B for Billion and T for Trillion: 46.3 B bbl (7.36 B m<sup>3</sup>) of oil, 281 Tcf (7.95 Tm<sup>3</sup>) of natural gas, and 20 B bbl (3.17 B m<sup>3</sup>) of natural gas liquids. The Wolfcamp shale in the Midland sub-basin was assessed separately by the USGS in 2016. At that time, it was the largest assessment of continuous oil conducted by the USGS. The Delaware sub-basin assessment of the Wolfcamp shale and Bone Spring Formation indicates they contain more than twice the reserves of the Midland sub-basin.

On the development and production front, new enhanced oil recovery approaches for tight shale reservoirs are being more widely implemented. Natural gas or CO<sub>2</sub> injection is currently being utilized in the Bakken Formation, Eagle Ford Formation, Anadarko Basin, and the Permian Basin to optimize injection sequences and boost recovery. Refracturing of existing wells to reduce drilling costs, improve production, and prolong the productive life of wells is now used more widely in developed petroleum fields (Birdwell et al., 2020). Worldwide, natural gas production is projected to increase from 342 B cf/d in 2015 to 554 B cf/d by 2040, with shale gas being the largest component of this increase. Shale gas is expected to account for 30 percent of world natural gas production by the end of 2040 (IEA, 2017).

Although in 2016 only four countries—the USA, Canada, China, and Argentina—had commercial shale gas production, technological improvements are expected to encourage development in other countries, primarily in Mexico and Algeria. Together, these six countries are projected to account for 70 percent of global shale production by 2040. Canada has been producing shale gas since 2008, reaching 4.1 B cf/d in 2015. Shale gas production in Canada is projected to continue increasing and will account for almost 30 percent of Canada's total natural gas production by 2040 (IEA, 2017).

South America's potential as a source of unconventional shale gas and oil lies mainly in Argentina and Brazil, where the production from the Neuquen Basin's tight shale of the Vaca Muerta Formation has been steadily increasing since 2016; however, only 4 percent of the shale resource has been developed thus far. According to the IEA's 2013 report, Globally, Brazil holds the ninth largest unconventional gas reserves. Brazil has shale oil and gas potential in the Parana, Solimoes, and Amazon basins and is actively producing from the oil shale unit of the Irati Formation. In 2019, the Brazilian energy ministry launched REATE 2020 to boost onshore investments that include the expectation of drilling an experimental unconventional well in the northeast region (Birdwell et al., 2020). Argentina's commercial shale gas production was just 0.07 B cf/d (cubic feet per day) at the

end of 2015, but foreign investment in shale gas production is increasing and shale production is projected to account for almost 75 percent of Argentina's total natural gas production by 2040 (IEA, 2017).

Algeria's production of both oil and natural gas has declined over the past decade, which prompted the government to begin revising investment laws that stipulate preferential treatment for national oil companies in favor of collaboration with international companies to develop shale resources. Algeria has begun a pilot shale gas well project and developed a twenty-year investment plan to produce shale gas commercially by 2020. Algerian shale production is projected to account for one-third of the country's total natural gas production by 2040.

Mexico is expected to gradually develop its shale resource basins after the recent opening of the upstream sector to foreign investors. At present, Mexico is expanding its pipeline capacity to import low-priced natural gas from the USA. Mexico is expected to begin producing shale gas commercially after 2030, with shale volumes projected to contribute more than 75 percent of total natural gas production by 2040 (IEA, 2017).

China was among the first countries outside of North America to develop shale resources. During the past five years, China drilled more than 700 shale gas wells, producing 0.6 B cf/d of shale gas in 2015. Shale gas is projected to account for more than 40 percent of the country's total natural gas production by 2040, which would make China the second-largest shale gas producer in the world (Ni et al., 2021). Over the past twenty-five years, China has attempted to develop its substantial CBNG (coalbed natural gas) resources, estimated by China's Ministry of Land and Resources at more than 1,000 Tcf. In 2015, about 20,000 wells produced a total of 0.36 B cf/d of CBNG in China. However, CBNG well productivity in China is significantly lower than in countries such as Australia and the USA. CBNG development in China has focused on the Ordos and Qinshui basins of Shanxi Province that, despite having China's best geologic conditions, have low well productivity (Ni et al., 2021).

The difficulties faced in expanding CBNG output have led China to increase its subsidies for the development of shale gas resources, estimated at 1,115 Tcf. Initial shale gas development has been focused on the Longmaxi Formation in the Sichuan Basin, which is estimated to hold technically recoverable volumes of 287 Tcf. Shale exploration has recently made a breakthrough in China with shale gas output in 2019 of 353 Bcf, 60 percent of which was produced from Sinopec's Fuling Shale Gas Field, located in the Sichuan Basin. As of 2018, lacustrine shale oil exploration has also been successful in the Sichuan and Ordos basins in central China, in the Junggar and Tarim basins in northwest China, the Songliao Basin in north China, and the Bohai Bay Basin in northeast China. Increasing shale gas output could eventually help to meet growing demand for natural gas in China and decrease the use of coal for energy production (Birdwell et al., 2020; Ni et al., 2021; Zou et al., 2018).

## 5.2 Volume and Composition of Fracturing Fluids

Fracturing is carried out by injecting large volumes of water with added proppant and disclosed and undisclosed organic and inorganic chemicals at pressures high enough to fracture the shale; fractures are kept open by the proppant particles (Arthur and Cole, 2014; Gregory et al., 2011; Harkness et al., 2017). Water volumes injected to hydraulically fracture over 260,000 oil and gas wells drilled in the USA between 2000 and 2014 were compiled and used to create the first comprehensive map of hydraulic fracturing water use in the USA (Gallegos et al., 2015). The median values of water volumes used to hydraulically fracture individual horizontal oil and gas wells in 2014 were 15,000 m<sup>3</sup>/well and 19,000 m<sup>3</sup>/well, respectively. At that time, about 40 percent of wells were either vertical or directional in 2014. These vertical or directional wells required much lower volumes of fracturing water, that is, less than 2,600 m<sup>3</sup>/well (Gallegos et al., 2015).

Water demand continues to increase in the Permian Basin as more wells are drilled and operators strive for longer laterals and improved completion efficacy (Valder et al., 2021). Scanlon and others (2020a) analyzed ten years of water data from 2005 to 2015, tracking the volume of water produced from conventional and unconventional wells and how it was managed, then compared those volumes to water use for hydraulic fracturing. They showed that the average volume of water needed per unconventional well increased by about ten times over the past decade, with a median value of 250,000 bbl (40,000 m<sup>3</sup>) per well of water used in the Midland Basin, Texas, in 2015. Volumes required per completion are an additional 50 percent higher now than in 2015: approximately 400,000 bbl (63,600 m<sup>3</sup>) per well in the Midland Wolfcamp (Villalobos, 2018). In this semi-arid region of the USA, the large volume of water used for drilling and fracking wells has serious negative effects on surface water for aquatic habitats and the availability of fresh water for farming and other uses.

Fracturing fluid is comprised of approximately 90.5 percent water, 9 percent proppant, and 0.5 percent organic and inorganic chemicals. Most of the water used in fracturing fluid is fresh surface or shallow groundwater, but in some cases, companies are now recycling produced water after diluting it with fresh water to a salinity of 50,000 mg/L (Nicot et al., 2014; Rowan et al., 2011, 2015). Petroleum companies also add a large number of disclosed and undisclosed chemicals including KCl, acids, bactericides, biocides, surfactants, friction reducers, as well as corrosion and scale inhibitors to the fracturing fluids to improve overall gas production (Table 1). Several states mandate the public disclosure of all chemicals used in fracturing fluids, but the US EPA does not mandate disclosure. Disclosure is now required for all federal and Tribal lands, and this makes it easier to investigate the nature, distribution, toxicity, interactions with natural fluids and rocks, fate, and environmental impacts of these added chemicals in these areas (Groundwater Protection Council, 2023; Groundwater Protection Council & ALL Consulting, 2009; Kharaka et al., 2020; McFeeley, 2012; Stringfellow et al., 2017).

**Table 1** - Selected list of chemical additives used in fracturing fluids (modified from FracFocus, 2021).<sup>1</sup>

Chemical Additive	Fluid composition (percent)	Function
<b>Gellant</b>	0.5	Thickens water to ensure the sand can keep the fractures open.
<b>Acid</b>	0.7	Helps dissolve minerals and initiate cracks in the rock.
<b>Corrosion Inhibitor</b>	0.05	Prevents corrosion of steel tubing, well casing tools, and tanks when acidic fluids are used.
<b>Friction Reducer</b>	0.5	Reduces the effects of friction in the pipe. It remains in the formation, where it can be broken down by high temperature and exposure to the breaker, which is a viscosity-reducing agent.
<b>Clay Control</b>	0.34	Reacts with clays in the formation, stabilizing and locking them down in the shale.
<b>Crosslinker</b>	0.32	A formula consisting primarily of borate salts that combine with the breaker and gel to break down gels and create salts that are returned in produced water. It also maintains viscosity as temperature increases.
<b>Scale Inhibitor</b>	0.23	Helps to prevent scale build up in the formation and in pipes by attaching itself to the formation.
<b>Breaker</b>	0.2	Makes it easier for fluid to flow through the borehole by creating a reaction with the crosslinker and gel, breaking down the gel.
<b>Iron Control</b>	0.004	Makes iron soluble in water to help prevent precipitation of metal oxides.
<b>Biocide</b>	0.001	Eliminates bacteria that can cause corrosive by-products by reacting with microorganisms that may be present in the treatment fluid and formation.

<sup>1</sup> Because fluid contents vary based on geologic and other factors, there is no "standard" formula for fracturing fluids. Most formulas consist of 10 to 20 chemicals that constitute about 0.5 to 2 percent chemical additives and 90 percent water and 8.5 percent proppant sand.

### 5.3 Flowback Water

Following the completion of hydraulic fracturing with high-pressure fluid, the fluid pressure in the well is lowered, causing the flowback brine (a variable mixture of fracturing fluid and formation water) to return to the surface through the well tubing. During the two to three weeks of the flowback period for a Marcellus Shale well, 10 to 30 percent of the fracturing fluid returns to the surface, and the portion of the returned fluid that is produced water increases to ~50 percent after a year of production (Rowan et al., 2015). For the Barnett Shale, Nicot and others (2014) report large variability in the ratios of returned-to-injected water: from < 20 percent to > 350 percent after four years of production. The rate of fluid return is initially high, being ~1,000 m<sup>3</sup>/d for Marcellus Shale but decreases rapidly to ~50 m<sup>3</sup>/d (Figure 9). This is followed by production of natural gas and produced water at a rate of approximately 2 to 8 m<sup>3</sup>/d per well (GWPC & ALL Consulting, 2009; Healy et al., 2017; Kharaka et al., 2020).

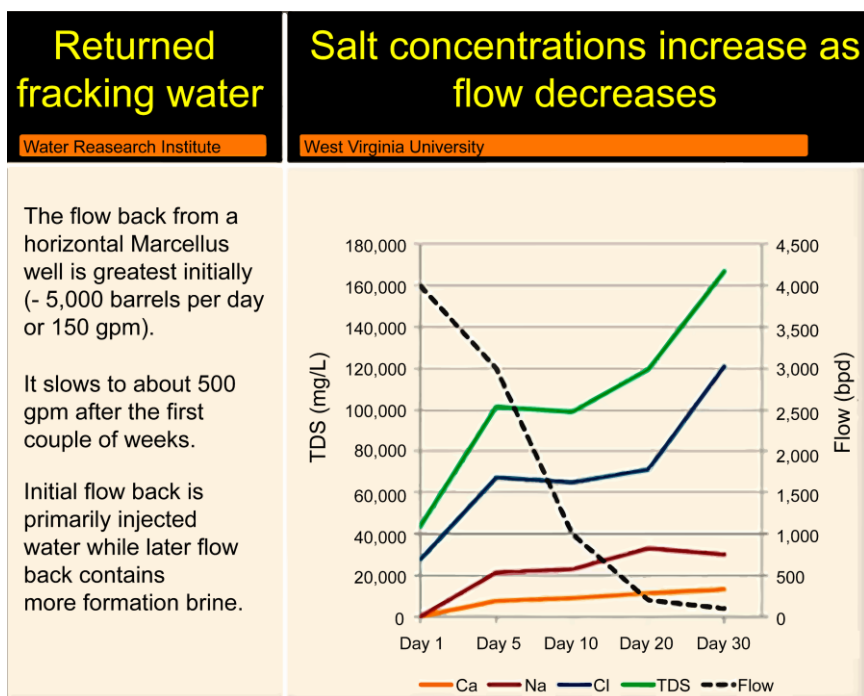


**Figure 9** - The rate of fluid production (flow) is initially high, being 4,000 bbl/d for the Marcellus Shale, decreasing rapidly to ~1000 bbl/d. This is followed by production of natural gas and produced water at a rate of approximately 50 bbl/d. The salinity of produced water increases from about 45,000 mg/L to more than 160,000 mg/L. The letters gpm represent gallons per minute; TDS is total dissolved solids (modified from Ziemkiewicz, 2012).

In the Bakken-Three Forks petroleum field of the Williston Basin, many oil wells that generally produced much oil with little produced water have become water wells that produce some oil because average oil production has remained constant while water production continues to increase. A complex interplay of reaching out beyond the main production zone to where water saturations are higher by using longer laterals, tighter spacing, to zones with higher relative permeability to water significantly increases the volume of produced water. Similar situations occur in the Permian and other basins. This is a serious threat for the unconventional oil and gas industry in the USA—for which managing produced water has come to cost \$34 billion per year—because it exposes operators to operational, environmental, and economic risks.

During hydraulic fracturing, a significant fraction of the injected water is imbibed by small pores in the shale; the imbibition process may continue over a period of weeks to months (Roychaudhuri et al., 2011). The salinity of the flowback and produced water from the Marcellus Shale in southwest Pennsylvania is initially moderate (45,000 mg/L TDS), reflecting the salinity of the fracturing water ( $50,000 \pm 20,000$  mg/L), but increases to ~170,000 mg/L and may reach 300,000 mg/L in north-central Pennsylvania. The concentrations of dissolved components may also increase with time of production, but variations are neither linear nor parallel (Figure 9) (GWPC & ALL Consulting, 2009; Haluszczak et al., 2013; Rowan et al., 2015).

The origin of saline water produced long-term (after one or more years of production) from the Marcellus Shale and other shale formations is controversial. The Marcellus Shale is considered by some to be a *dry* formation containing essentially no natural mobile water (Engelder, 2012; Striolo et al., 2012) that can be co-produced with gas. In this scenario, the natural formation water is immobile as it includes water retained in small pores by capillary pressure and the irreducible water layer bound to clay mineral surfaces by van der Waals forces (Passey, 2010). All the water co-produced with natural gas in this hypothesis is either drained from overlying or underlying formations via fractures or injected during hydraulic fracturing.

The higher salinity of produced water from the Marcellus Shale compared with the fracturing fluid (e.g., 200,000 versus 50,000 mg/L) is attributed by some to dissolution of lenses of halite, together with calcite and other minerals observed along bedding planes in core samples. It should be noted, however, that shale formations usually have several beds or lenses of siltstone and tight sandstones, and these could be the source of high salinity brine. This conclusion is supported by data from the Barnett Shale showing the ratios of returned to injection water in many wells to be > 350 percent after four years of production (Nicot et al., 2014).

#### 5.4 Permian Basin: Water Challenges for Unconventional Production

The Permian Basin, covering large areas (~400 km wide and 500 km long) of the USA in western Texas and southeastern New Mexico, includes the highly prolific Delaware and Midland sub-basins (Engle et al., 2014). It is one of the oldest and most prolific hydrocarbon-producing areas in the USA. The discovery well was drilled in the Midland sub-basin in July 1921; since that time, over 30 B bbl (4.76 B m<sup>3</sup>) of crude oil and 75 Tcf of natural gas have been produced from the total basin.

Production, initially from conventional vertical wells drilled in shallower zones like Grayburg, San Andreas, and Clear Fork, reached a peak in the 1970s during the Arab oil embargo, then steadily declined to a low after the 2008 recession (Figure 10). However, unconventional horizontal drilling and longer lateral wellbores have increased oil production, with the Permian Basin now producing more than 5 million bbl/d (~0.8 million m<sup>3</sup>/d) and accounting for approximately 30 percent of US oil production (Figure 10).

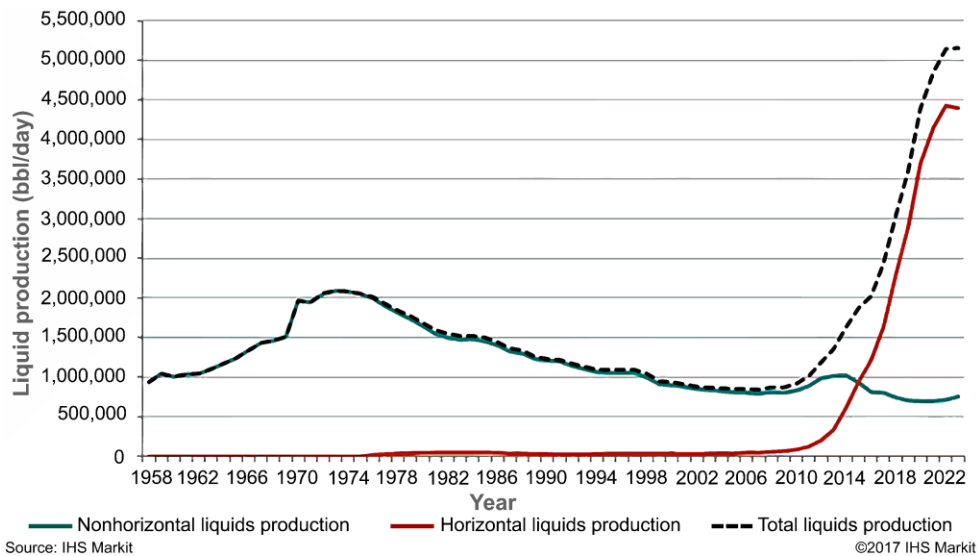


**Figure 10** - The Permian Basin reached a second production peak, eclipsing its 1973 record. Conventional (nonhorizontal) and unconventional (horizontal) oil production from the Permian Basin from 1958 to present. A huge increase in total production followed initiation of unconventional sources in the early 2000s (from IHS Markit, 2017).

While the Permian Basin produces oil at record levels, a large volume of produced water comes with that oil, which in 2018 comprised 47 percent of all the oil wastewater in the USA. The growing amount of produced water can be attributed to more well completions, longer horizontal sections (laterals generally ~2 km with a maximum 5.4 km), and the shift from crosslinker to slickwater as a fracturing fluid. In the last five years (starting in 2018), 4,620 wells per year were completed in the basin; the number increased to 550 wells per month in June 2019. Water demand continues to increase in the Permian Basin as more wells are drilled and operators strive to improve completion efficiency (Scanlon et al., 2020b).

Unconventional wells use much more water for drilling and completion than conventional wells (Gallegos et al., 2015). According to Gallegos and others' study, the average volume of water needed per well has increased by about ten times over the past decade, with a median value of 250,000 bbl (39,700 m<sup>3</sup>) per well of water used in the Midland Basin, Texas, USA, in 2015. Unconventional wells also generate much more produced water over time (Figure 11)—even though they produce oil with lower W/O ratios (3 versus 13 for conventional wells)—because the volume of oil obtained from unconventional wells is much higher (Figure 10). Volumes required per completion are an additional 50 percent higher now than in 2015, that is, approximately 400,000 bbl/well (63,600 m<sup>3</sup>) in the Midland Wolfcamp Formation. In general, volumes in the range of 300,000 (47,700 m<sup>3</sup>) to a million bbl/well (159,000 m<sup>3</sup>) are required per completion (Villalobos, 2018). In this semi-arid region of the USA, large volumes of water used for drilling and fracking wells has serious negative effects on surface water for aquatic habitats and the availability of fresh water for farming and other uses. The costs involved in sourcing, transporting, and storing water prior to hydraulic fracturing is substantial.

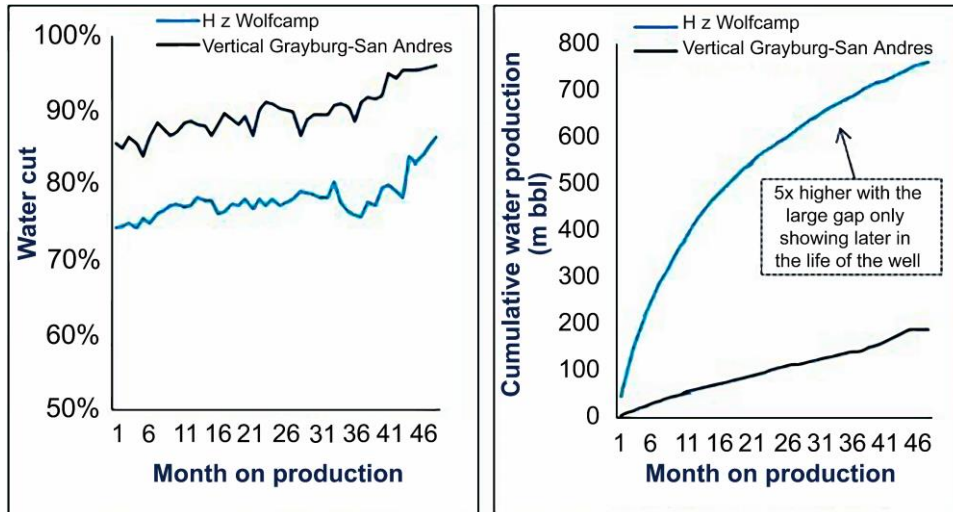
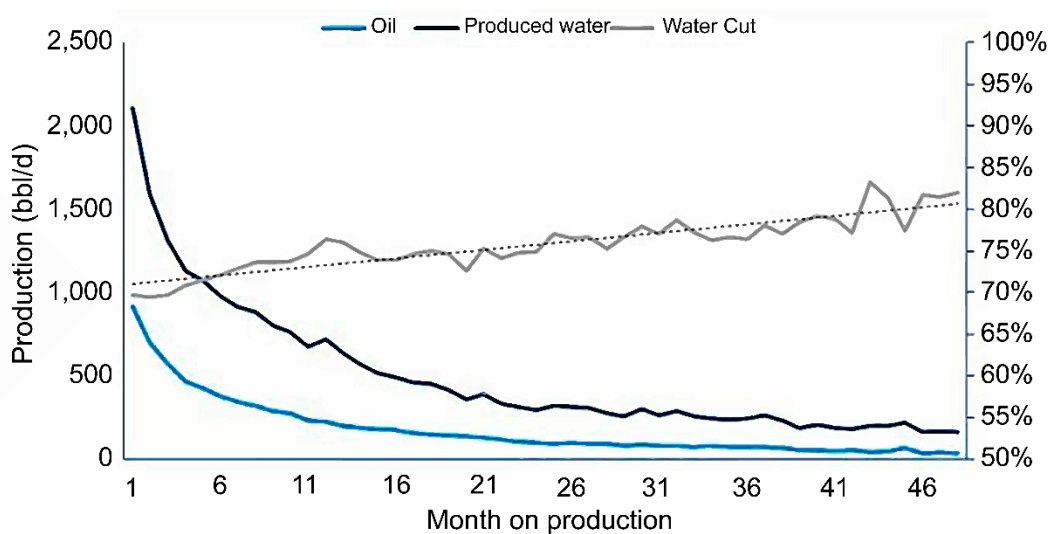


**Figure 11** - Total produced water and water cut obtained from unconventional (light blue line) and conventional (dark blue line) wells in the Permian Basin of Lea County, New Mexico, USA. Cumulative produced water is much higher from unconventional wells. The production units in the right graph are in thousands of barrels (from Wood Mackenzie North American Analysis Tool, 2019).

High water volume used for well completion, especially in the Delaware sub-basin, also result in a growing volume of produced water flowing back to the surface, because the Wolfcamp Formation has relatively high-water saturation and does not hold hydraulic fracturing fluids like the Marcellus Shale or other shale formations. Record drilling activity is compounded by water rising quickly in older horizontal wells when more water used in completions and water cuts from the targeted formations. This is of special concern because, in some cases, W/O ratios in the Delaware sub-basin can reach as high as 10:1 (Figure 12 and Figure 13) and as high as 15:1 in some areas of western Texas (Villalobos, 2018). Operators are simply unable to economically reinject all those volumes.



Source: Wood Mackenzie North American Well Analysis Tool

**Figure 12** - Production of oil and produced water (left axis) and water cut (right axis) over time in unconventional wells in the Permian Basin, USA (from Wood Mackenzie North American Analysis Tool, 2019).

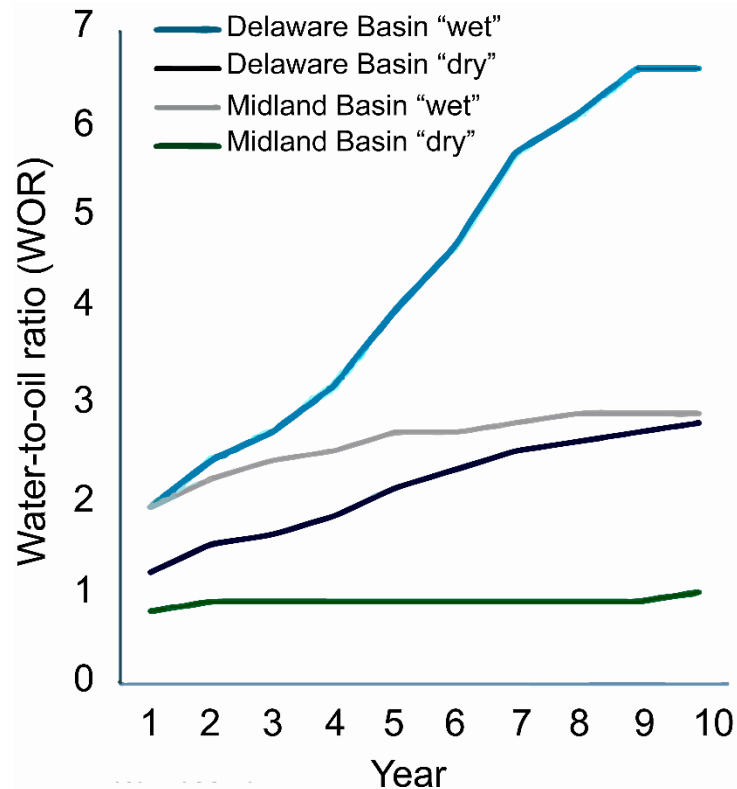


**Figure 13** – Water-to-oil ratios (W/O) from the dry and wet Midland and Delaware sub-basins of the Permian Basin, USA (from Wood Mackenzie North American Analysis Tool, 2019).

Because the cost of fluid injection into tight formations is very high, most of the produced water cannot be reinjected into shale or other tight formations for water floods or EOR, but must be injected into separate saltwater disposal (SWD) wells, recycled, or reused. Water handling is expensive and unit costs are expected to rise as simple solutions such as local shallow injection become exhausted. Multi-well pad development results in a higher concentration of produced water at a single location. This puts greater strain on nearby SWD wells and can cause sections of disposal formations to increase in pressure too quickly, limiting the injection rate and causing casing issues that may result in contamination of USDW in near the petroleum field (Hamlin, 2006).

High injection pressures at brine disposal wells, and high pressures during fracking operations, are triggering small earthquakes (Scanlon et al., 2019; Savvaidis et al., 2020). However, a moderate M5.0 earthquake occurred on Thursday, 26 March, 2020, near Mentone, Texas. The earthquake was the largest to occur for decades in the Permian Basin, and its cause has not been determined (Lund et al., 2020).

The challenging water management issues in the Permian Basin are being addressed as follows.

1. *The use of readily available brackish water (1,000 to 10,000 mg/L TDS), in addition to fresh water for drilling and hydraulic fracturing (Stanton et al., 2017). Reyes and others (2018) investigated the geochemistry and suitability for hydraulic*

fracturing of brackish groundwater within the Triassic Dockum Group that extends across the Midland Basin in Texas. Results indicated that the most groundwater in the basin is suitable for use with slickwater hydraulic fracturing fluids. Despite having lower salinity, however, the water in the down-gradient southern and eastern margins of the basin can have high  $\text{SO}_4$  (sulfate ion) concentrations that exceed acceptable limits for cross-linked gel fluids.

2. *Produced water recycling and reuse in drilling and fracturing operations (Scanlon, et al., 2020b), which is already practiced in the basin (Sharma, 2019) at the rate of at least 1.38 million bbl/d (0.28 million m<sup>3</sup>/d). Sharma's study also reported that 75 percent of water produced in the Permian Basin is disposed of in injection wells, with the remaining 25 percent being recycled for fracturing operations. The study also reported that water production in the Permian Basin leads the disposal volume by 5 million bbl/d (0.79 million m<sup>3</sup>/d), and the gap is expected to increase. According to their website, Chevron Oil used 99 percent recycled or brackish water (not fresh water) in their completion operations in 2017 and 2018 in the Permian Basin (Figure 14).*

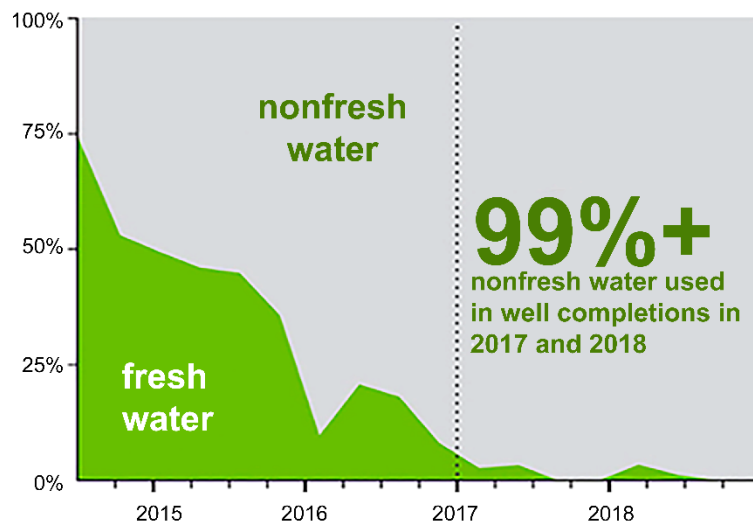


**Figure 14** - Percentage of non-freshwater used in well completions in the Chevron Oil operations in the Permian Basin, USA, increased with time reaching 99 percent in 2017 and 2018 (from <https://www.chevron.com/projects/permian>, accessed August 12, 2023).

Treating high salinity (120,000 to 140,000 mg/L) produced water for reuse in hydraulic fracturing of unconventional wells in the Permian Basin was investigated experimentally by Rodriguez and others (2020). Chemical coagulation using ferric chloride and aluminum sulfate as coagulants was compared with electrocoagulation (EC) with aluminum electrodes for removal of suspended contaminants. Results showed that aluminum sulfate was more efficient and cost-effective than ferric chloride for removing

turbidity from produced water. The EC treatment resulted in 74 percent removal of suspended solids and 53 to 78 percent removal of total organic carbon (TOC).

Fine particles and other contaminants remaining after coagulation were further treated in continuous-flow columns packed with different filter media. Biochar and granulated activated carbon showed the greatest removal of turbidity and TOC in produced water. Thus, the high salinity of produced water—up to 160,000 mg/L in the Permian Basin (Reyes et al., 2018)—may not be a limiting factor for reuse. The fluids were tested in a variety of water samples with salinity levels ranging from 43,000 to 350,000 mg/L from the Marcellus Shale and the Permian Basin; identical formulations of filter media showed improved performance as the salinity increased (Whitfield, 2017). Results demonstrate that such treatment technologies are effective for the removal of suspended constituents and iron and produce a clean brine for hydraulic fracturing (Macêdo-Júnior et al., 2020).

## 5.5 Environmental Impacts: Water Use and Waste-Water Disposal Challenges

Exploration for and production of shale gas causes major local surface land disturbance, air and noise pollution, habitat fragmentation, and other ecological impacts (Arthur & Cole, 2014; Darrah et al., 2014; Khan et al., 2016; Kharaka et al., 2020; Liu et al., 2020; Rowan & Kraemer, 2012; Skalak et al., 2014; US EPA, 2015; Vengosh et al., 2017; Warner et al., 2013). Potential contamination of surface water and groundwater are the major concerns, but communities in some impacted areas are also concerned about the possibility of induced seismicity (Bonetti et al., 2021; Chaudhary et al., 2019; Jackson et al., 2013; Plata et al., 2019; Vengosh et al., 2014; Vidic et al., 2013; Zhang et al., 2014).

Hydraulic fracturing does not generally cause earthquakes large enough to be felt ( $M > 3$ ) during the relatively short duration of hydraulic fracturing, but there have been exceptions. A study in Canada linked roughly 0.3 percent of hydraulically fractured wells to  $M > 3$  earthquakes. Although most of these earthquakes occur close to and at the same time as hydraulic fracturing operations, a small percentage of induced earthquakes may occur months later (Yaghoubi et al., 2022).

In Ohio, both Poland Township (2014) and Harrison County (2015) have experienced  $M3$  earthquakes caused by hydraulic fracturing. In Oklahoma, some small (mostly  $\leq M3$ ) earthquakes have been linked to hydraulic fracturing in a small percentage of hydraulically fractured wells. There is evidence that recent, moderately strong earthquakes ( $M 4$  to  $5.8$ ) that occurred in shale gas producing areas in Arkansas, Colorado, Ohio, Oklahoma, and Texas were induced by produced water disposal or other gas- and oil-related activities (Ellsworth, 2013; Ellsworth et al., 2012; National Academies of Sciences, Engineering, & Medicine, 2018; National Research Council, 2012; Rubinstein & Mahani, 2015).

In the Permian Basin, high fluid pressures associated with brine disposal wells as well as fracking operations are triggering small earthquakes that are related to oil operations (Savvaidis et al., 2020). The rate of earthquake occurrence increased sharply in the Delaware sub-basin beginning around 2009, with clusters of relatively small (mostly  $M < 4.0$ ) events occurring throughout Reeves and Pecos Counties. However, the moderate [M5 earthquake](#) that occurred on Thursday, 26 March, 2020, near Mentone, Texas, USA—shaking residents as far away as Midland and El Paso—was the largest to occur for decades in the Permian Basin and it was the most significant in the central and eastern USA since 2016. The cause of the earthquake has not been determined but was likely related to oil operations as two waste-water disposal wells and one injection well (potentially enhanced oil recovery) were active in the immediate area (Lund et al., 2020).

Shale gas is held in pore spaces and natural fractures or is adsorbed onto organic material (kerogen) and clay minerals in the formation. Shale total porosity (5 to 10 percent) is moderate, but the natural permeability of shale is extremely low (i.e., measured in nano Darcies), requiring horizontally completed wells (3,500 m and longer) and massive, multi-stage hydraulic fracturing to create pathways for the gas to flow into the well at economic rates.

Fracturing is carried out by injecting large volumes (up to 40,000 m<sup>3</sup> per well) of water containing proppant and organic and inorganic chemicals at pressures high enough to fracture the shale, with fractures kept open by the sand particles. Significant volumes of water—approximately 500 m<sup>3</sup> per well for the Marcellus Shale to 5,000 m<sup>3</sup> per well for the deeper Haynesville Shale—are also used for drilling gas wells. Because several hundred wells in the Fayetteville and Haynesville Shale and close to 1,000 wells in the Barnett and Marcellus Shale were completed during peak drilling years, the total volume of fresh water used for drilling and fracturing in some cases is high, approaching 10 million m<sup>3</sup>/year for the Barnett and Marcellus Shale (Groundwater Protection Council, 2019; Groundwater Protection Council & ALL Consulting, 2009).

Calculations show that the total water volume used for drilling and fracturing shale gas wells is relatively low compared to the total water (surface and groundwater) consumed by usage in wet regions. In Pennsylvania, for example, only 0.06 percent of water used for residential, commercial, and industrial applications is injected into the Marcellus Shale. However, it is much higher in arid regions (0.4 percent for the Barnett Shale and 0.8 percent for the Haynesville Shale) where water needed for shale gas could be a significant constraint for gas development because its use could affect the available water supply for domestic, irrigation, or other uses (GWPC & ALL Consulting, 2009; Nicot & Scanlon, 2012; Scanlon et al., 2022). The total water used for drilling and fracturing shale gas and tight reservoir wells compared to the consumptive total water usage is even higher for the semi-dry Permian Basin, as indicated by increasing oil production since 2011 (Figure

10), because of the higher number of unconventional wells drilled and wells with longer laterals.

Reclaiming produced water for reuse is rather expensive but possible where water salinity is relatively low ( $< 35,000$  mg/L) as was demonstrated at the Placerita Field in California (Kharaka et al., 1998; Kondash et al., 2020), but is extremely complicated and costly for produced and flowback water from Marcellus, Haynesville, and other shale where the salinity can be higher than 200,000 mg/L. The high concentrations of salt limits the use of membrane technology, but other treatment options—including distillation and crystallization—are being investigated (Clark & Viel, 2009; Igunnu & Chen, 2014; Macêdo-Júnior et al., 2020). Treating relatively high salinity (120,000 to 140,000 TDS) produced water for reuse in hydraulic fracturing of unconventional wells in the Permian Basin was demonstrated experimentally by Rodriguez and others (2020).

Unpublished data from Haynesville, east Texas, by the Kharaka group as well as published results (Rowan et al., 2015) show that produced water from Haynesville and the Marcellus Shale are Na-Ca-Cl brine with extremely high salinity ( $\geq 200,000$  mg/L), high NORMs (up to 10,000 picocuries/L for total Ra), and radon concentrations. Also, produced water from unconventional oil and oil wells will have additional chemicals including toxic inorganic and organic compounds reported in produced water from conventional petroleum. The concern in the case of organics is warranted as high concentrations of toxic organic compounds—including BTEX (up to 60 mg/L), phenols (up to 20 mg/L), and polycyclic aromatic hydrocarbons (PAHs, up to 10 mg/L)—have been reported in produced water (Akob et al., 2015; Kharaka & Hanor, 2014; Kharaka et al., 2020; McMahon et al., 2017; Orem et al., 2014).

In addition to the natural inorganic and organic chemicals, petroleum companies add a large number of disclosed and undisclosed chemicals (including potassium chloride, acids, bactericides, biocides, surfactants, friction reducers, and corrosion and scale inhibitors) to the fracturing fluids to improve overall gas production. Potential contamination of groundwater and surface water by the natural and added organic and inorganic chemicals and NORMs in flowback and produced water discussed above is the major concern associated with shale gas production (Kargbo et al., 2010; Osborn & McIntosh, 2010). The concern may be warranted as results of groundwater analyses by Osborn and others (2011) indicated that private water wells in parts of Pennsylvania and New York showed an association between shale gas operations and methane contamination of drinking water.

However, Molofsky and others (2011, 2016) analyzed groundwater samples from the same area of Pennsylvania and offered an alternative hypothesis: natural fractures, not shale gas operations, could be responsible for the stray methane detected in these wells. Using detailed geochemical evidence, Warner and others (2012, 2014) also invoked natural

fractures and pathways, and not recent drilling activities, to explain connections between some shallow groundwater and deep formation water from northeastern Pennsylvania.

Studies by Rozell and Reaven (2012) concluded that management of flowback and produced water, as is the case for conventional oil and gas operations (Kharaka and Dorsey, 2005), posed the greatest risk to groundwater and surface water quality. In the case of conventional oil and gas operations, significant local groundwater contamination has resulted mainly from the improper disposal of saline produced water, leaks through production and improperly sealed legacy wells, and from hydrocarbons and produced water discharging from malfunctioning equipment, or from vandalism and accidents (Kharaka & Otton, 2007; Veil, 2020). In the case of shale gas, the fracturing process, especially if accompanied by seismic events, may cause migration of fracturing fluids or formation brine through natural or artificial fissures or legacy wells connected to groundwater supplies (Kharaka et al., 2020).

It is important to emphasize that oil and gas (including shale gas) regulatory programs place great emphasis on protecting groundwater. Well construction requirements, consisting of installing multiple layers of protective steel casing and cement, are specifically designed to protect freshwater aquifers and ensure the producing zone is isolated from overlying formations. Despite these programs, however, a review of all oil and gas operations in Texas (1993–2008) and Ohio (1983–2007) by the Groundwater Protection Council (GWPC & ALL Consulting, 2009) reported 211 (Texas) and 183 (Ohio) groundwater contamination incidents primarily attributable to legacy wells, waste management and disposal, and leaks from tanks and flow lines. They reported no incidents caused by drilling, hydraulic fracturing, or production of shale gas.

Detailed site investigations are needed to better assess groundwater pollution at legacy and producing petroleum sites such as those conducted at the USGS OSPER sites in Oklahoma that included drilling and sampling monitoring wells in contaminated and background areas and using natural and added tracers to document leakages (Ball et al., 2019b; Kharaka & Otton, 2007). A similar study was conducted by the US EPA to investigate the potential effects of shale gas operations on drinking water at several sites (US EPA, 2011, 2015). Water quality monitoring before, during, and after hydraulic fracturing operations is planned at these sites and compared with similar measurements at comparable sites that do not experience hydraulic fracturing to provide some case-specific data for impacts on water quality. This and similar detailed studies from shale gas basins worldwide are needed to minimize all potential environmental impacts, especially groundwater contamination and induced seismicity, when producing these extremely important new sources of energy.

## 5.6 Oil Sands

Oil sands, also known as tar sands, bituminous sands, or extra-heavy oil sands, are a type of unconventional source of energy. Oil sands are either loose sands or partially consolidated sandstone containing bitumen, a form of petroleum with high density (API gravity  $\sim 8$ , thus heavier than water of 10) and extremely high viscosity (100 to 10,000 cP, where cP = centipoise). These attributes reflect the presence of up to 50 percent asphaltenes, very high molecular weight hydrocarbon molecules incorporating heteroatoms—mainly oxygen, nitrogen, and sulfur—in their lattices (Yen, 1984).

Almost all heavy oil and natural bitumen are alteration products of conventional oil (Head et al., 2003; Larter et al., 2006). Large bitumen deposits are reported in Canada, Venezuela, Kazakhstan, and Russia (Alberta Energy and Utilities Board, 2004), with estimated worldwide deposits of more than 2 trillion barrels (320 B m<sup>3</sup>). Proven reserves of bitumen contain approximately 100 B barrels; total natural bitumen reserves are estimated at 249 G bbl (40 G m<sup>3</sup>) worldwide (where G is a quadrillion: 10<sup>15</sup>), of which 177 G bbl (28 G m<sup>3</sup>), or 71 percent, are in Alberta, Canada (Meyer et al., 2007).

Crude bitumen is a thick, sticky form of crude oil, so viscous that it will not flow unless heated or diluted with lighter hydrocarbons such as light crude oil or natural-gas condensate. As a result of the high viscosity, bitumen cannot be produced by conventional methods, transported without heating or dilution with lighter hydrocarbons, or refined by older oil refineries without major modifications. Bitumen and heavy crude oils contain high concentrations of toxic compounds including sulfur, selenium, boron, and heavy metals, particularly nickel and vanadium, which interfere with refining processes (Harkness et al., 2018; Yen, 1984).

The Orinoco Belt in Venezuela is described as including oil sands, but these deposits are non-bituminous and are present at higher reservoir temperatures, falling instead into the category of heavy or extra-heavy oil (API  $< 8^\circ$ ) due to their lower viscosity. Natural bitumen and extra-heavy oil differ in the degree by which they have been degraded from the original conventional oils by bacteria (Dusseault, 2001; Head et al., 2003). The USGS (Schenk et al., 2010) estimated a mean volume of 513 B barrels (81.5 B m<sup>3</sup>) of technically recoverable heavy oil and a mean volume of associated dissolved-gas resource at 13 trillion cubic feet (0.36 trillion m<sup>3</sup>) of gas in the Orinoco heavy oil belt of eastern Venezuela. Venezuela thus contains one of the world's largest recoverable oil accumulations (Schenk et al., 2010). Oil production in Venezuela reached a peak of 3.5 million bbl/d (0.55 million m<sup>3</sup>/d) in 1997 but declined sharply due to political events (2.8 million bbl/d to 0.44 million m<sup>3</sup>/d) to a current amount of 0.5 million bbl/d to 0.08 million m<sup>3</sup>/d (US Energy Information Administration, 2021).

In 2019, oil sands accounted for 63 percent of Canadian oil production, with 2.95 million bbl/d (0.46 million m<sup>3</sup>/d); total production from onshore and offshore

conventional and tight reservoirs was 4.7 million bbl/d (0.75 million m<sup>3</sup>/d). Oil sands production has generally been increasing since 2006, peaking at 2.95 million bbl/d (0.46 million m<sup>3</sup>/d) in 2019 (Figure 15). Conventional crude oil, which is produced across Canada, production peaked in 2019 at 1.74 million bbl/d (0.28 million m<sup>3</sup>/d). With respect to the oil sands, the surface mining process (which can be used in formations of up to 75 m depth) represents half of current oil sands production and one-fifth of total oil sand resources. The surface area of Canadian oil sands deposits is 142,000 km<sup>2</sup>, all effectively located in Alberta. The total mineable area is 4,800 km<sup>2</sup>; the total area being mined is close to 1,000 km<sup>2</sup> (Government of Canada, 2020).

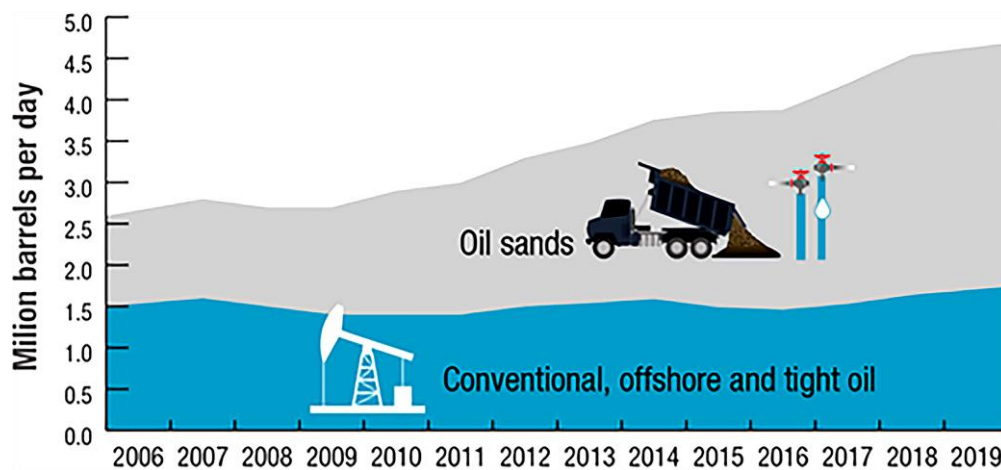


**Figure 15** - Oil sands production in Canada has generally been increasing since 2006, peaking at 2.95 million bbl/d in 2019. Conventional crude oil production also peaked in 2019 at 1.74 million bbl/d (Government of Canada, 2021).

### 5.6.1 Water Management

Water management is a key challenge for oil sands extraction (Government of Canada, 2020). Water requirements for oil sands production vary depending on the technology used for extraction. Oil sands surface mining uses 2.6 barrels of new water to produce one barrel of bitumen, while in situ processes (the remaining half of oil sands production) use an average of 0.2 barrels of fresh water for each barrel of oil produced. About 75 percent of water used in oil sands mining operations is recycled, compared to approximately 86 percent for in situ recovery.

However, some new water is required and comes from a variety of sources including on-site drainage, collected precipitation (rain and snow-melt), underground brackish aquifers, and local rivers. In situ projects rely largely on groundwater for their new water needs, with an increasing amount being non-potable, brackish water (1,000 to 10,000 mg/L TDS). Mining operations typically withdraw water from the Athabasca River. The Alberta government manages this water use by setting strict withdrawal limits (Government of Canada, 2021).

The governments of Canada and Alberta established a joint oil-sands monitoring program in early 2012. The program takes unprecedented steps to enhance the monitoring of air, land, water, and biodiversity to improve the ability to detect changes in the environment and in groundwater and to manage and improve cumulative impacts. The water monitoring component of the program has been designed to quantify and assess oil sands contaminants in the Athabasca River system, as well as their effects on groundwater and key aquatic ecosystem components (both within the oil sands development area and in downstream receiving environments). Water monitoring improvements include monitoring more sites to increase geographic coverage, as well as increasing the frequency of sampling and the number of different substances (water, soil, etc.) sampled. These steps provide an improved understanding of the long-term cumulative effects of oil sands development.

Surface mining operations of Canada's oil sand resources generate leftover material (tailings) after the bitumen is extracted. Oil sand tailings are a mixture of water, sand, fine silts, clay, residual bitumen and lighter hydrocarbons, inorganic salts, and water-soluble organic compounds. Tailings are stored in basins called *tailings ponds* that allow the solids in tailings to settle. The sand component settles out quickly, leaving the clay and silt to form fluid, fine- or small-sized tailings. Over the years, the fine solids also settle to form a suspension called mature fine tailings. Regulations require that the volume of fluid fine tailings be reduced and the ponds be ready for reclamation no longer than five years after they cease to be in service.

In addition to water issues, extracting oil from oil sands is difficult since the extraction process requires a great deal of capital, human power, and land. Another constraint is energy for heat and electricity generation, which currently comes from natural gas. A 2010 special report by (IHS) and Cambridge Energy Research Associates (CERA) estimated that production from Canada's oil sands emits "about 5–15 percent more carbon dioxide, over the well" (IHS CERA, 2010, p. 8). In 2014, Lattanzio reported that carbon dioxide emissions from oil sands are approximately 20 percent higher than average emissions from conventional oil. However, the emission intensity of oil sands operations dropped by approximately 36 percent from 2000 to 2018 as a result of technological and efficiency improvements, fewer venting emissions, and reductions in the percentage of crude bitumen being upgraded to synthetic crude oil (Government of Canada, 2021).

## 5.7 Exercises Pertinent to Section 5

[Link to Exercise 5](#) ↴

[Link to Exercise 6](#) ↴

## 6 Inorganic Chemical Composition of Produced Water

### 6.1 Introduction to Inorganic Composition of Produced Water

Approximately six million oil and natural gas wells have been drilled in the USA and Canada to date. We have detailed data for many of these wells, including locations, perforated depths, and types of reservoir rocks. Fewer data were collected on the inorganic and organic chemical and isotopic compositions of produced water during production of oil and natural gas or obtained from drill stem tests (Kharaka & Hanor, 2014; Kharaka et al., 2020). Comprehensive geochemical data for more than 120,000 oil and gas wells from the major sedimentary basins in the USA were obtained from published literature and received from oil companies and state oil and gas organizations. The data are listed in the updated USGS National Produced Waters Geochemical Database (Blondes et al., 2019).

As discussed by Kharaka and Hanor (2014) and Blondes and others (2016, 2019) for the USA basins and by Hitchon (2023) for the Alberta Basin, data sets obtained from oil companies are often incomplete, especially with regard to chemical and isotopic compositions of produced water. The lists in Blondes and others (2019) underwent initial culling, removing many wells that did not have data describing a specific location, a valid perforation zone, major cations and anions, and that had an anion cation charge balance >5 percent. Wells were also removed if the saturation state of calcite was > 1 kcal/mole and chemical geothermometer values were not concordant with reported subsurface temperature. Nonetheless, such data carry large uncertainties and require additional culling and analysis (Blondes et al., 2016, 2019).

Additional culling, as discussed further in the later part of this section and detailed in Hitchon (2023), was carried out for this book. The original USGS Geochemical Database (Blondes et al., 2019), however, is an important source of hydrogeochemical data for those interested in determining the geochemical nature of deep formation water, contamination sources of surface water and groundwater, and environmental impacts of hydraulic fracturing and other petroleum operations. The data may also be used beneficially to plan a more extensive and rigorous field sampling in a given petroleum field or a set of fields in a basin or region (Kharaka et al., 2020).

Approximately 90 percent of wells in the USGS database were drilled by conventional technologies; generally, these were vertical wells. More recently, geochemical data for produced water have also been obtained from production of gas and oil from unconventional energy sources that include shale and very low permeability (< 0.1 mD) sandstones as well as coalbed natural gas (CBNG) that accounted for approximately 3 percent of gas production in the USA in 2019 (US Energy Information Administration, 2021). Production of oil and gas from shale and tight reservoirs has increased dramatically

in the USA due to recent developments in deep horizontal drilling, downhole telemetry, and massive multi-stage hydraulic fracturing (Ilgen et al., 2017; Nicot, 2017; Kharaka et al., 2020; NRC, 2014; Rowan et al., 2015; Scanlon et al., 2020b, 2022). The current version (v2.3) of the USGS Geochemical Database (Blondes et al., 2019) contains geochemical data for ~15,000 wells that were drilled for shale gas, tight oil and gas, and CBNG (further discussion of CBNG is provided by Rice et al., 2000).

Natural gas production from shale started in 1991 with a well drilled in the Barnett Shale of Texas. From there, production of natural gas and oil from shale and tight reservoirs spread rapidly to other basins starting with the Appalachian Basin in 2005, which produces gas from the Marcellus Shale in Pennsylvania and Ohio. The Williston Basin, covering large areas in the USA and Canada, started producing oil from the Bakken Formation in 2007. The Permian Basin, located in western Texas and southeastern New Mexico, started production from unconventional sources in 2011. But production from this source accelerated since early 2017, hitting a record high of over 4.7 million bbl/d (0.75 million m<sup>3</sup>/d) oil (Figure 10) and 17 million cf/day natural gas in January 2020 (US Energy Information Administration, 2021).

Results from Blondes and others (2019, 2020) and Alley and others (2011) show an extremely wide range of produced water salinity (< 5,000 to > 400,000 mg/L) as illustrated in Figure 16 (Kharaka et al., 2020). The salinity is generally much higher in oil and natural gas wells in basins located in the southern and eastern parts of the USA compared with those in the Rocky Mountains and basins to the west. For example, produced water from shale gas and tight oil from the Marcellus Shale (Pennsylvania) and Bakken Formation (North Dakota) have salinity that exceeds 300,000 mg/L.

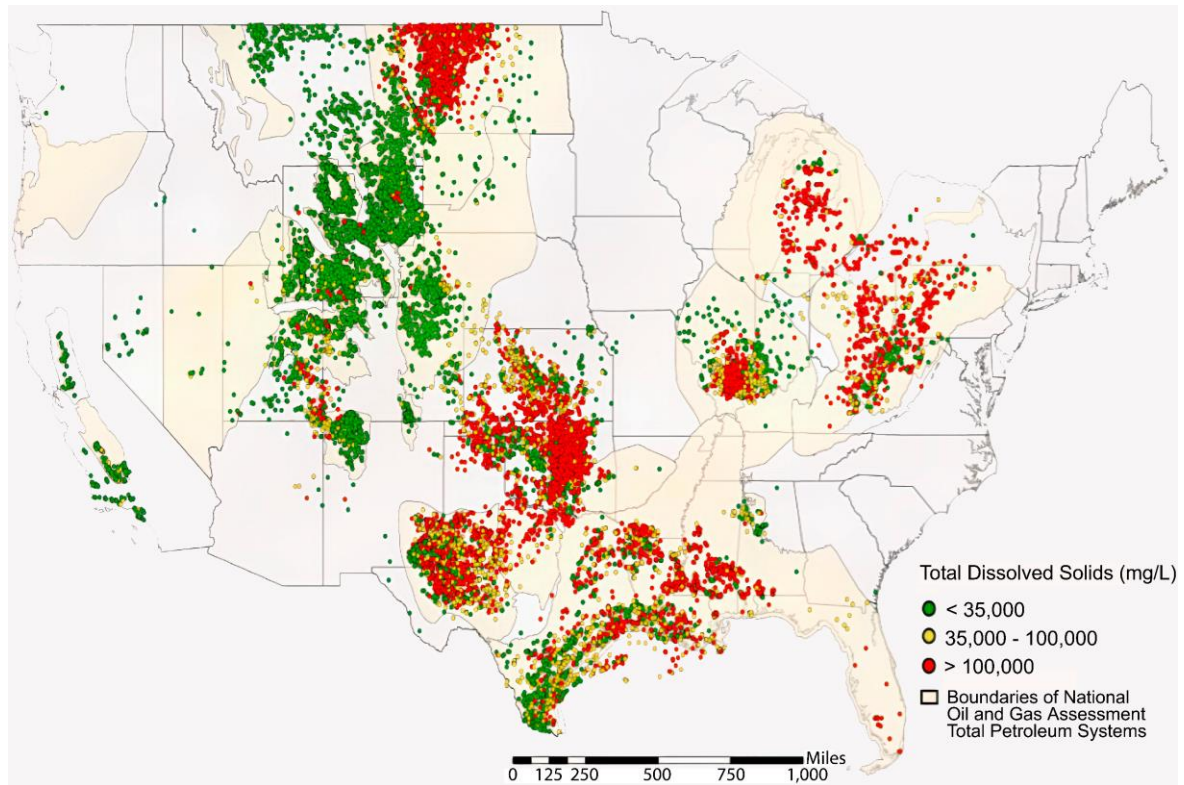


**Figure 16** - Salinity map of produced water from conventional and unconventional oil and gas wells from the major sedimentary basins in the USA. Data are from more than 150,000 points listed in the USGS National Produced Waters Geochemical Database (Blondes et al., 2019; figure from Kharaka et al., 2020).

However, produced water from oil and natural gas fields in California have lower salinity (Figure 17) that range from approximately 5,000 to 50,000 mg/L (Gans et al., 2015; Kharaka et al., 2019; McMahon et al., 2017). The concentrations of major, minor, and trace chemicals also vary widely between wells in the same field and from field to field in the same basin, depending on the origin of formation water and the water-mineral interactions that determine the chemical and isotopic composition of produced water.

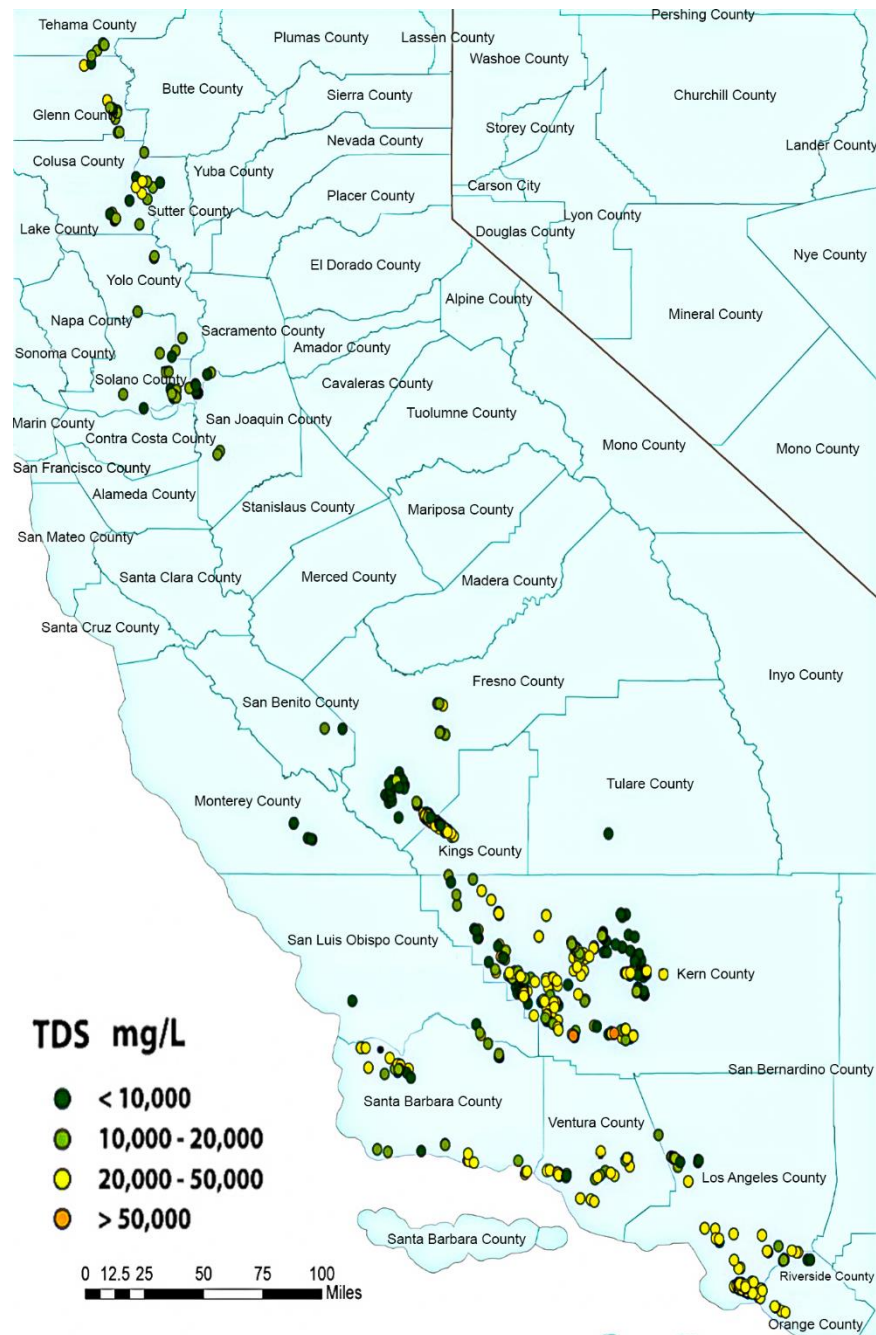


**Figure 17** - Salinity of produced water from California oil and gas fields. Salinity of produced water in California is relatively low compared with other USA basins such as the Gulf Coast (TDS = total dissolved solids) (modified from Gans et al., 2015).

Results from these geochemical studies including one or several petroleum fields in the same basin provide insights into a number of important processes that occur within petroleum fields and sedimentary basins, especially the following:

1. the generation, transport, accumulation, and production of petroleum;
2. chemical aspects of mineral diagenesis including dissolution, precipitation, and the alteration of sediment porosity and permeability;
3. transport and precipitation of copper, uranium, and especially lead and zinc in sediment-hosted Mississippi Valley-type ore deposits;

4. tectonic deformation;
5. transport of thermal energy for geothermal and geopressured-geothermal systems; and
6. interaction, movement, and ultimate fate of large quantities of liquid hazardous wastes injected into the subsurface (Hanor et al., 1988; Kharaka & Hanor, 2014; Kharaka & Thordsen, 1992).

Interest in the geochemistry of produced water has risen in the last thirty years for two main reasons. First, depleted petroleum fields and saline aquifers in sedimentary basins are being investigated as possible repositories for the storage of large amounts of anthropogenic CO<sub>2</sub> in the subsurface for thousands of years, to moderate the anticipated future increases in the concentration of atmospheric CO<sub>2</sub> and mitigate global warming, arguably the most important environmental issue facing the world today (Kharaka et al., 2006a; White et al., 2003). The success of such operations will depend largely on improved understanding of water–mineral–CO<sub>2</sub> interactions in the subsurface (Gunter et al., 2000; Hitchon, 1996a; Kharaka & Hanor, 2014; Shelton et al., 2020; Zuddas, 2010). Second, petroleum production, drilling operations, and improperly sealed abandoned wells have caused major contamination of the soil, surface water, and groundwater of energy-producing states in the USA and likely throughout the world (Kharaka & Dorsey, 2005; Kharaka et al., 1995; Richter & Kreitler, 1993).

Contamination results mainly from the improper disposal of large volumes, with 20 to 30 B bbl/year (3.18 to 7.78 B m<sup>3</sup>/year) of saline water produced with oil and natural gas from hydrocarbons and brine discharging from malfunctioning equipment, vandalism, and accidents. Prior to the institution of federal regulations in the USA in the 1970s, produced water was often discharged into streams, creeks, and unlined evaporation ponds. Because this water is highly saline and generally contains toxic metals, organic and inorganic components, and naturally occurring radioactive material including <sup>226</sup>Ra and <sup>228</sup>Ra, it has caused salt scars and surface and groundwater pollution (Kharaka et al., 1999, 2020; Otton et al., 2007; Vengosh et al., 2019).

Since the early 1970s, our knowledge and understanding of the properties, interactions, and origin of water in sedimentary basins has expanded substantially. This has come about as a result of four key developments:

1. improved sampling tools, including downhole samplers and the U-tube, and improved analytical methods that require only a small sample volume for the determination of multi-elements at very low concentrations (μg/L; Freifeld et al., 2005);
2. increased availability and utilization of data for a variety of stable and radioactive isotopes (Clark & Fritz, 2013; Faure, 1986; Faure & Mensing, 2005; Fritz & Fontes, 1986; Johnson et al., 2020; Kendall & McDonnell, 2012; Kraemer & Kharaka, 1986; Kraemer & Reid, 1984);

3. major improvements in the chemical thermodynamic data and procedures for applying them to brine and minerals (Helgeson et al., 1998; Shock, 1995;; Zhu & Anderson, 2002; Zuddas, 2010); and
4. development and application of detailed geochemical, hydrological, and solute transport codes (Bethke, 2015; Birkle et al., 2002; Hanor, 2001; Kharaka et al., 1988; Thorstenson & Parkhurst, 2004; Wolery, 1992; Xu et al., 2010).

We now know that water in sedimentary basins is more mobile and its interactions with rocks are more complex than previously realized. Also, the discovery of high concentrations (up to 10,000 mg/L) of reactive organic species in this water has led to a new field of organic–inorganic interactions and has developed bridges between the fields of aqueous fluids, organic matter, and petroleum (Crossey et al., 1985; Hanor & Workman, 1986; Kharaka et al., 2000; Willey et al., 1975).

## 6.2 Field and Laboratory Methods and Procedures

Before discussing water salinity and individual chemical components in produced water, it is important to emphasize that groundwater and produced water must be carefully sampled, preserved, and analyzed using the latest field and laboratory methods and protocols reported by the World Health Organization and by national government agencies that deal with water issues. In the USA, the appropriate federal agencies are the US Environmental Protection Agency (EPA) and the US Geological Survey (USGS). The USGS is generally accepted as the premier federal agency for collecting water quality data in the USA and as part of its mission, the USGS collects chemical and other data to assess the quality of surface water and groundwater resources. A high degree of reliability and standardization of these data are paramount to fulfilling this mission.

Documentation of nationally accepted methods used by the USGS personnel serves to maintain consistency and technical quality in data collection activities. These methods, procedures, protocols, and guidelines are documented and may be obtained from the USGS publication *National Field Manual for the Collection of Water-Quality Data* (NFM). This manual provides documented guidelines and protocols for USGS field personnel and others who collect water-quality data, as well as detailed, comprehensive, and citable procedures for monitoring the quality of surface water and groundwater. Topics included in the NFM are as follows:

- methods and protocols for sampling groundwater and surface water resources;
- methods for processing samples for analysis of water quality;
- methods for measuring field parameters, including pH, alkalinity, and dissolved O<sub>2</sub>; and
- specialized procedures such as sampling water for low levels of mercury and organic wastewater chemicals, measuring biological indicators, and sampling sediments for chemical and biological analysis.

NFM chapters that are of specific interest and importance for groundwater studies are Sandstrom and Wilde (2014), Wilde (2010), Wilde and others (2014), and the US Geological Survey (2018, 2020, 2021).

The US EPA was established in 1970 with rules, regulations, and enforcement procedures to control industrial pollution, including disposal of oil field brine. The policy goal was defining and enforcing clear rules associated with use of the shared environment and sustaining environmental quality. The EPA's web site has many reports that cover water issues including the National Primary and Secondary Drinking Water Regulations () that apply to public water systems in the USA. The reports also describe the acceptable treatment methods and techniques for contaminated water to protect public health by limiting the levels of contaminants in drinking water (US EPA, 2009).

The National Primary Drinking Water Regulations are legally enforceable primary standards and treatment techniques that apply to public water systems. The Maximum Contaminant Limits (MCL) values for contaminants as well as the Public Health Goal (sometimes listed as MCLG) are listed in Table Box 2-1. The contaminants listed together with their possible sources and adverse effects include:

- microorganisms,
- disinfectants,
- disinfection by-products,
- inorganic chemicals,
- organic chemicals, and
- radionuclides.

Samples of groundwater suspected of being contaminated may be collected and subjected to detailed chemical and isotope analyses, including the likely contaminants. The results may then be compared with the data in Table Box 2-1 to see if any inorganic or organic chemicals or radionuclides exceed the MCL or the MCLG values. Constituents that exceed these values are classed as contaminants.

The source of contamination may require additional investigation because it may be caused by natural sources (geogenic) like reactions of pristine groundwater with minerals in the aquifer. The main geogenic groundwater contaminants in the USA are Mn (manganese), As (arsenic), Ra (radium), Sr (strontium), and U (uranium) (DeSimone et al., 2014; Erickson et al., 2021). In Sections 6 through 8, we discuss in detail the concentrations of chemicals, stable isotopes, and radionuclides observed in produced water and uncontaminated groundwater. We also discuss the many diagnostic conservative chemicals (e.g., Cl, chlorine; Br, bromine; B, boron; PAHs) and isotopes that can conclusively distinguish contamination from petroleum operations.

Much of the detailed information generated on the composition of formation water in sedimentary basins has come from the analysis of aqueous fluids coproduced with crude oil and natural gas—here, called produced water. Of the approximately 5 million oil and

gas wells drilled in the USA since 1859, about 900,000 are currently in production. The remainder are abandoned or shut-in temporarily or permanently (Breit et al., 2001; Veil, 2020; Kharaka et al., 2020).

Most sampling takes place at the wellhead rather than downhole. The fluids are therefore subjected to major reductions in temperature and pressure, to gas loss, and exposure to oxidizing conditions during sampling. The special methods that must be used in sample collection, preservation, and field and laboratory determinations of chemical components and isotopes in formation water are detailed in Lico and others (1982), Kharaka and Hanor (2014, and references therein), Wolff-Boenisch and Evans (2014), and Conaway and others (2016).

Because of the importance of understanding water–rock–gas interactions in field experiments to investigate the potential for geologic storage of CO<sub>2</sub> in depleted petroleum fields and deep saline aquifers in sedimentary basins (Hovorka et al., 2006), a more rigorous sampling protocol was introduced. This protocol uses high temperature, pressure cleaned, and evacuated syringe-like downhole samplers (500 to 1,000 mL volume)—known as Kuster<sup>1</sup> samplers (Figure 18)—that can be lowered and opened at a specified depth to provide accurate data on water and gas compositions of the subsurface fluids (Kharaka et al., 2006a, 2009).

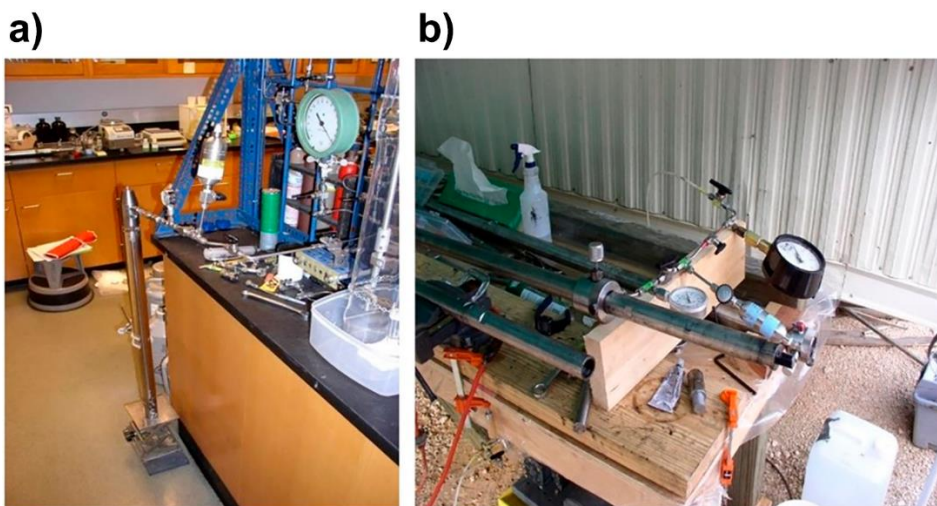


**Figure 18** - High temperature, pressure cleaned, and evacuated syringe-like downhole sampler (1,000 ml volume) that may be lowered into the wellbore and opened at a specified depth to provide accurate data on water and gas compositions of subsurface fluid. a) Obtaining brine and gas from the sampler in the USGS laboratory. b) Preparing the sampler for use at the Frio field test (Kharaka et al., 2006a, 2009).

During the CO<sub>2</sub> injection in the Frio Brine test—deep-seated salt domes south and southeast of Houston, Texas—intensive fluid sampling was obtained from an observation

<sup>1</sup> Any use of trade, firm, or product names is for descriptive purposes only and does not imply endorsement by the US Government.

well using a novel downhole U-tube system (Figure 19) designed for this experiment to track the arrival of CO<sub>2</sub> (Freifeld et al., 2005). The drilling and circulation fluids were tagged with Rhodamine WT, and fluorescein to allow for the identification of uncontaminated formation water (Kharaka et al., 2006b). Tracer gases, including SF<sub>6</sub> (sulfur hexafluoride), noble gases, tagged CH<sub>4</sub> (methane), and perfluorocarbon tracers (PFTs), were injected with the CO<sub>2</sub> to map its flow path in the reservoir sandstone and identify leakage into the overlying sandstones (Kharaka et al., 2009; Phelps et al., 2006).

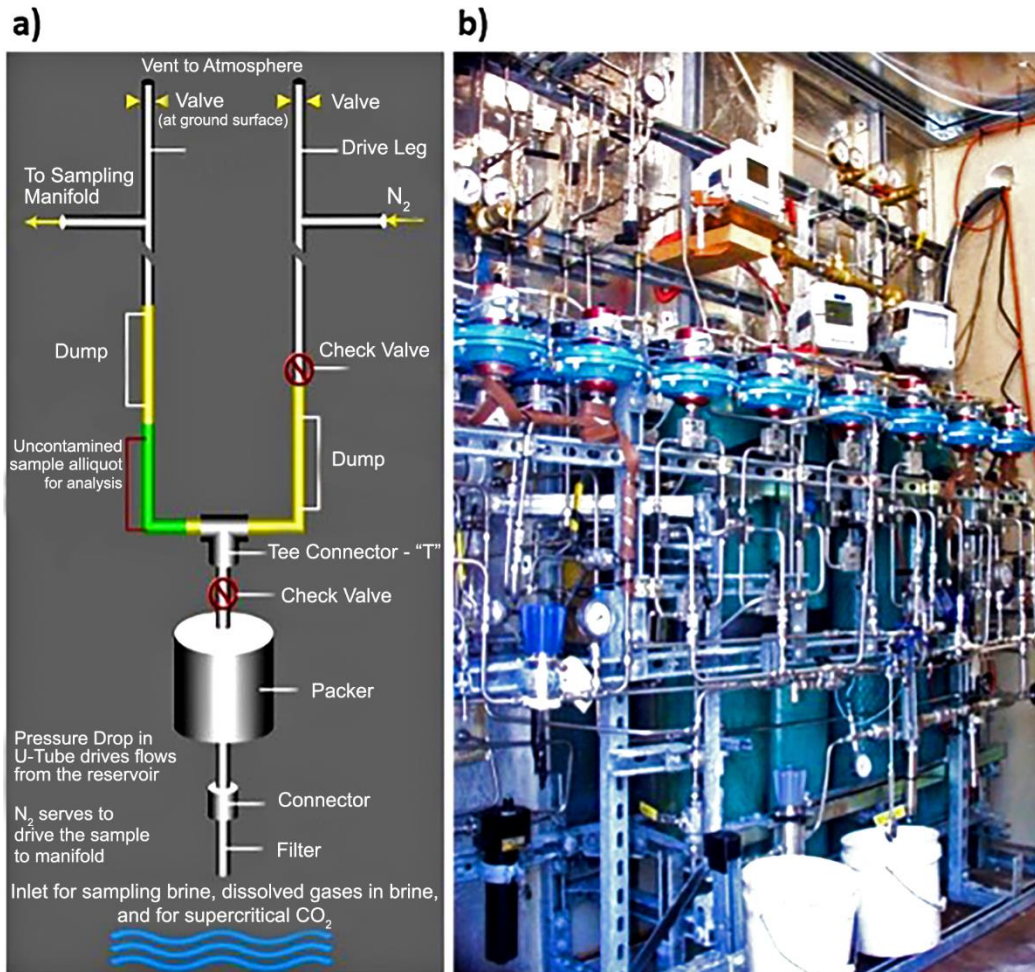


**Figure 19** - The U-tube tool used for sampling fluids in the Frio I and Frio II field tests. a) Schematic of the U-tube that is lowered into the well, with the packer placed just above the depth where fluids enter the well bore. Production fluids fill the U-tube, then nitrogen gas at high pressure is used in the drive-tubing leg to push the fluids for sampling in connections to the sampling manifold. b) Pressure and temperature gauges, pH, salinity, and other probes as well as sampling ports for brine and gases. A computer system is used to control the operations (modified from Freifeld et al., 2005).

To obtain accurate geochemical data for produced water, wells selected for sampling in a petroleum field must meet the following criteria:

1. have not been affected by water and CO<sub>2</sub> flooding or chemical treatment, including acidification;
2. have a single and narrow perforation zone;

3. produce large amounts of water relative to oil;
4. produce large amounts of water relative to natural gas,  $> 0.16 \text{ m}^3$  of water per  $3 \times 10^4 \text{ m}^3$  of gas (10 barrels of water per million  $\text{ft}^3$  of natural gas); and
5. have ports for sampling before the fluid enters a separator. In cases where the objective of the study is to determine disposal options for produced water, sampling from water disposal tanks may be appropriate to determine the physical and chemical properties of the mixture.

The fluids from petroleum wells are collected in prewashed and prerinsed 8 or 20 L carboys with a bottom spigot (Figure 20). Water and oil generally require from five minutes to several hours to separate, depending on the temperature, the proportion of water, and the composition of oil and water. In a few wells that produce fluids at low temperature, all that is produced is an oil-water emulsion that can only be separated by mild heating or high-speed centrifugation in the laboratory. Immediately after separation of water from oil, the water is passed through glass wool to remove solids and oil droplets before the samples are collected in separate 125 mL flint-glass bottles with polyseal caps for the field determination of conductance, pH, Eh (a measure of the redox state of solutes in a solution), alkalinity, and  $\text{H}_2\text{S}$  and for laboratory determination of the carbon isotopes (Lico et al., 1982; Conaway et al., 2016).

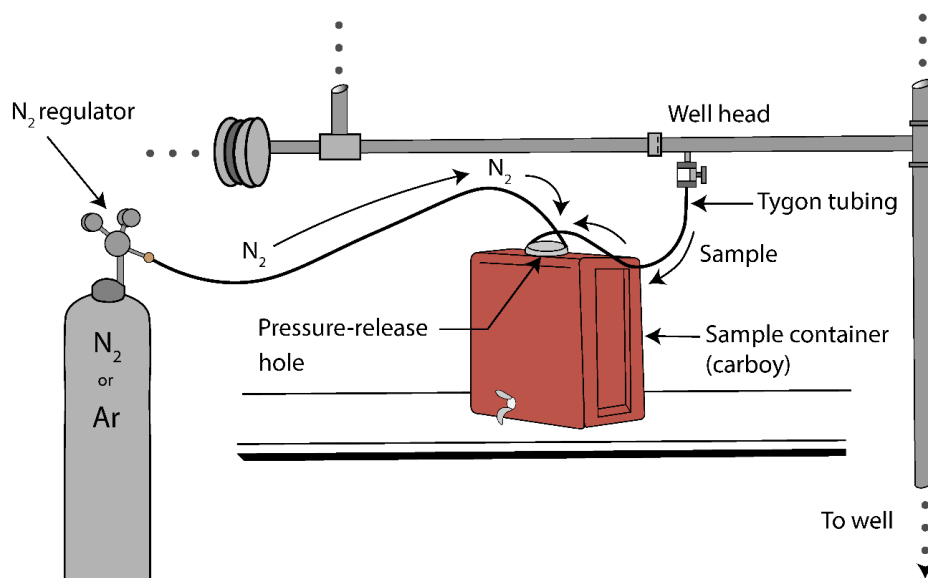


**Figure 20** - The fluids from petroleum wells are collected at the wellhead in prewashed and prerinsed 8 to 20 L carboys with a bottom spigot. Pure nitrogen or argon gas is used to displace oxygen in the carboy to prevent oxidation and precipitation of Fe, Mn, and other metals (from Lico et al., 1982).

Filtration and preservation of water samples immediately after collection (Figure 21) is important to prevent loss of constituents through precipitation and sorption. Filtration through a  $0.45 \mu\text{m}$  filter, using either compressed nitrogen or compressed air as the pressure source, is adequate for the determination of the major cations and all of the anions. However, filtration through a  $0.1 \mu\text{m}$  filter is required for aluminum, mercury, and

other trace metals because colloidal oxyhydroxides of iron and manganese and clay particles can pass through larger pores; these particles would then dissolve upon acidification, increasing the concentration of these trace metals (Kennedy et al., 1974; Kharaka et al., 1987, 2009). Filtration and field chemical determinations are better performed in a mobile laboratory equipped with pH meters, a spectrophotometer, filtration, titration, and other field equipment. Because of the presence of oil, the measurement of Eh is difficult for oil-field water, even when using flow-through cells (Kharaka et al., 1987, 2007b).

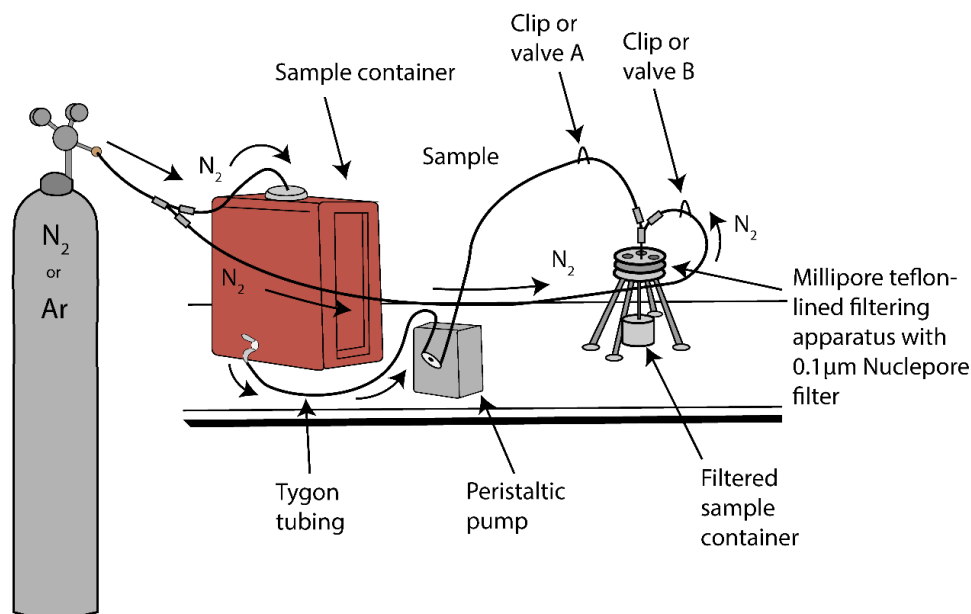


**Figure 21** – Field setup for the filtration and preservation of water samples. Filtration through a 0.45 µm filter, using compressed nitrogen or peristaltic pump, is adequate for the determination of the major cations and anions. However, filtration through a 0.1 µm filter is required for aluminum, mercury, and other trace metals (from Lico et al., 1982).

Samples collected for the determination of heavy and trace metals including iron, manganese, lead, zinc, and mercury require additional care to minimize contact with air during collection and filtration. This is required to prevent oxidation of metals (e.g., Fe<sup>2+</sup>) and their precipitation as oxyhydroxides, leading to coprecipitation and adsorption of other metals. Contact with air is minimized by taking the following steps:

1. flushing the air in the carboy with nitrogen or argon, or even natural gas;
2. inserting the tubing from the wellhead as far down in the carboy as possible through a hole drilled in the cap;
3. filling the carboy completely with fluid;
4. plugging the hole in the cap with a rubber stopper after the carboy is full;
5. minimizing the length of the Tygon tubing connecting the filtration unit to the carboy and filling it with formation water prior to filtration;
6. discarding the first 250 ml of the filtered sample; and

7. using the next liter of filtered water to rinse the collection bottles (Conaway et al., 2016; Kharaka et al., 1987).

Samples for the analysis of dissolved organic compounds are filtered through a 0.45 µm Teflon™ or silver filter and stored in amber bottles fitted with Teflon™ inserts in the caps. Stainless steel filtration units and copper or metal tubing are used for collection and filtration of these samples. Mercuric chloride (40 mg/L mercury) is added as a bactericide and the filtered samples are stored at 4 °C until analysis.

New methods for the laboratory analysis of cations and metals include the use of inductively coupled plasma emission spectrometry (ICP/ES) and the combination of ICP with mass spectrometry (ICP/MS) (Conaway et al., 2016; Harmon & Vannucci, 2006; Ivahnenko et al., 2001). The advantages of plasma techniques include

- a wide and linear dynamic concentration range,
- multi-element capability, and
- relative freedom from matrix interferences.

The use of ion chromatography (IC), gas chromatography (GC), and GC/MS has increased for the analysis of anions and dissolved organics (Barth, 1987; Ivahnenko et al., 2001; Kharaka & Thordsen, 1992).

Chemical data from drill stem and wire-line tests are always suspect because of likely contamination with drilling fluids and mixing with water from different production zones. Chemical analyses of water from carbonate reservoirs should be carefully examined for signs of contamination. These reservoirs are often stimulated by acid injection; the contaminating effects of the acid are noticeable for months after treatment. Properly evaluated, chemical data from producing wells may provide concentration values for a limited number of major cations and anions (Breit et al., 2001; Hitchon, 1996b). However, accurate concentrations of many of the dissolved constituents needed for evaluating water-rock interactions and mineral diagenesis—including field pH, dissolved silica, aluminum, and inorganic as opposed to total alkalinity—are not generally available (Kharaka & Thordsen, 1992).

### 6.3 Produced Water from Gas Wells

Chemical analyses of formation water from gas wells, especially those from reservoirs at temperatures higher than about 100 °C, may not represent the true chemical composition of formation water from the production zones because of dilution by mixing with condensed water vapor produced with natural gas. This is also a problem in oil wells from deep (high temperature) reservoirs with high gas content. The problem is particularly severe in wells that produce small volumes of water relative to the amount of natural gas: < 0.16 m<sup>3</sup> of water per 3×10<sup>4</sup> m<sup>3</sup> of gas (< 10 barrels of water per million ft<sup>3</sup>). In these wells, the produced water is a mixture of formation water and dilute water condensed because of the drop in temperature and pressure as the gases expand on entering the wellbore and the

separator. This problem, which can be corrected, is not generally recognized and is probably responsible for many of the reports of fresh or brackish water from petroleum reservoirs (Kharaka & Hanor 2014; Kharaka et al., 1985).

Deep wells that produce small volumes of water with high natural gas content should not be selected for water sampling if possible. In wells where fluids are split and directed to two separators, water and gas from both streams must be analyzed chemically and relative masses of the two streams measured to calculate the approximate downhole (reservoir) compositions.

## 6.4 Information from Wire-line Logs

The salinity of formation water is often calculated using electrical-resistivity and spontaneous-potential logs; the values obtained are reasonable, except in geopressured zones with high shale content (Gillespie et al., 2019; Hearst & Nelson, 1985; Rider, 1996). An alternative technique for calculating salinity of formation water in geopressured shaly sediments makes combined use of gamma ray, conductivity, and porosity logs (Revil et al., 1998). It is often possible to determine vertical variations in salinity from a single log over a depth of several kilometers.

## 6.5 Geochemical Data from the Same Formation Using Four Sampling Methods

A detailed field experiment of produced water and associated gas sampling was carried out by the USGS to investigate the differences in the chemical and isotopic compositions of fluids obtained from the fluvial sandstones of the Lower Cretaceous Paluxy Formation using four different sampling methods (Conaway et al., 2016). The fluids were obtained from a *characterization well* in the Citronelle Field, Alabama, as part of the SECARB Phase III Anthropogenic Test, which is an integrated carbon capture and storage project (Esposito et al., 2011).

In this experiment, produced water and gas samples were obtained from well D-9-8 #2 to a depth of 3,597 m and perforated between 2,866 to 2,875 m. This well was sampled in March and June of 2012 following its conditioning using coiled tubing and cleaning it of drilling fluids and KCl solutions by producing at least three wellbore volumes of formation water; this procedure was considered sufficient to obtain a representative uncontaminated sample. Conductivity was monitored periodically for the development of a consistent value to ensure representative formation water was being produced (Figure 22). In situ temperature and pressure as determined by a sensor associated with the U-tube were approximately 107 °C and 30 MPa.

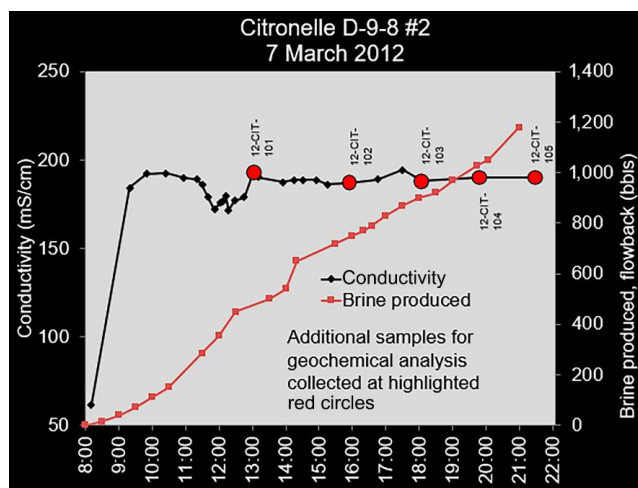


**Figure 22** – Electrical conductivity (mS/cm) versus time, with volume of brine produced (bbl) during and after initial well circulation using gas lift on March 7, 2012. Collection of the first five 12-CIT water samples are indicated by the red circles (from Conaway et al., 2016).

Fluid samples were obtained using four different sampling processes (Table 2): gas lift, electric submersible pump (ESP), downhole vacuum sampler (VS), and U-tube, and were subjected to similar field and laboratory analyses. Field chemical analyses included electrical conductivity, dissolved sulfide concentration, alkalinity, and pH. Laboratory analyses included major, minor, and trace elements; dissolved carbon; volatile fatty acids; and free and dissolved gas species. Sample handling and analysis conducted in this study follow protocols described in Lico and others (1982), Kharaka and others (2009), and Kharaka and Hanor (2014). These procedures and protocols are detailed in Conaway and others (2016) but are not discussed here.

**Table 2** - Summary of the four sampling methods used in the same well (Conaway et al., 2016).

Method	Summary of features
gas lift	Injects pressurized gas into the well, reducing the density of the wellbore fluid and stimulating flow driven by formation pressure. Can be used to clean a well and produces large brine volumes, but it may remove volatile components and raise pH, causing mineral-solution disequilibrium, mineral precipitation, and other chemical changes.
electric submersible pump (ESP)	In deep groundwater applications, this is typically a centrifugal pump above a sealed motor that is lowered into the well and pushes fluids to the surface. An ESP can be used to clean the well and produces large fluid volumes; however, this method can remove volatile components.
downhole vacuum sampler (VS)	Also called a closed chamber sampler, this tool is lowered into the well with a slickline and consists of a sample bottle with an inlet valve, two non-return valves, locking device, and timer. The sampler can be cleaned and evacuated, minimizing contamination, and placed at any depth in the well but has a small sampling volume (~1 L). Brine and gas can be sampled at in situ conditions. Requires a trained operator and can have a moderate rate of deployment failure.
U-tube	A fixed loop of narrow stainless steel sample tubing extending from the surface to the sampling depth of interest and back that is coupled with a positive pressure fluid displacement pump using high pressure gas or water drive. Tubing is fixed in the well, sampling only one depth, typically attached to the outside of production tubing string, and samples an area isolated by a packer. Samples tens of liters and can take pressurized samples.

Sampling using gas lift was performed in March and June 2012. Samples were taken after the well was conditioned, and water quality was monitored to establish that electrical

conductivity was stable. Samples were collected from the flowline at the wellhead. The ESP samples were taken in March 2012. The ESP was lowered to a depth of 213 m; the water level in the well before sampling was about 69 m. Samples were collected from a flow line at the wellhead. The VS was used in March and June 2012, and lowered to a depth of about 2,834 m, which is about 32 m above the perforations. The U-tube was installed between March and June 2012. U-tube samples were obtained in June 2012. Because of the depth of the sampling interval and the density of the brine, the sample column was too heavy to drive using N<sub>2</sub> pressure alone, so local groundwater was used as a drive fluid until the sample column was light enough to drive with N<sub>2</sub>. In addition to sampling in 2012, two U-tube samples were collected in May 2013.

The composition of gas that evolved from pressurized samples was determined on samples collected in 2012 using the VS in March and June and the U-tube in June. Gas samples were collected in low-carbon stainless steel sampling cylinders (Swagelok®), typically with a 75 or 300 mL volume. The cylinders were attached to the U-tube sampling manifold or a custom-built gas manifold to interface with the VS. Gas samples from the VS were collected into pre-evacuated cylinders, and U-tube samples were collected using both flow through and pre-evacuated techniques. Additional gas samples were collected from the annulus at the wellhead using a flow-through technique.

After sampling (and at ambient conditions), the cylinders typically contained both a water and gas phase. The volume and mass of brine obtained were determined analytically. The gas headspace was determined by the difference of the volume of the cylinder and volume of water recovered using the cylinder size. Pressure in gas cylinders for the VS and wellhead samples were lower (< 30 kPa) than atmospheric pressure after collection, whereas pressure in cylinders from U-tube sampling was 10 to 20 MPa, with an in-situ pressure of 30 MPa.

### 6.5.1 Results and Discussion

Results show the formation water obtained from this well is a Na-Ca-Cl-type brine with a salinity of approximately 200,000 mg/L (Table 3). Differences were evident between sampling methods, particularly for pH, Fe, and alkalinity (Table 3 through Table 6). Differences were evident between sampling methods, particularly for pH, Fe, and alkalinity (Tables 3-6). There was little gas in these samples, and gas composition results were strongly influenced by sampling methods (Table 7). The comparison demonstrates the difficulty and importance of preserving volatile analytes in samples, with the VS and U-tube system performing most favorably in this aspect. Conaway and others (2016) provide a detailed discussion of the origins of formation water and organic and inorganic solutes and gases from this well. Interested readers may want to read their paper for more information on that topic as we do not discuss it in further in this book.

**Table 3** - Sampling ID, field collected parameters electrical conductivity ( $\sigma$ ), temperature, and surface measured pH; and calculated total dissolved solids (TDS) for gas lift, electric submersible pump (ESP), downhole vacuum sampler (VS), and U-tube (from Conaway et al., 2016).

SAMPLE ID	Sampling method	Date and time <sup>a</sup> mm/dd/yy hh:mm	$\sigma$ (mS/cm) field <sup>b</sup>	$\sigma$ (mS/cm) laboratory <sup>b</sup>	T °C	Surface measured pH <sup>c,†</sup>	TDS <sup>d</sup> mg/L
12-CIT-100*	gas lift	03/07/12 08:10	61.6	62.3	20.5	-	37,000
12-CIT-101*	gas lift	03/07/12 13:05	193	-	39.0	-	196,000
12-CIT-102	gas lift	03/07/12 15:55	187	200	49.5	6.6	199,000
12-CIT-103*	gas lift	03/07/12 18:05	188	201	45.0	-	198,000
12-CIT-104	gas lift	03/07/12 19:50	190	201	41.3	6.4	203,000
12-CIT-105	gas lift	03/07/12 21:30	190	201	42.1	6.5	200,000
12-CIT-106	ESP	03/14/12 09:20	193	201	29.3	6.5	190,000
12-CIT-107	ESP	03/14/12 11:20	191	195	36.6	6.4	189,000
12-CIT-108	ESP	03/14/12 13:40	192	198	40.9	6.1	199,000
12-CIT-109	VS	03/15/12 11:25	196	199	33.7	5.3	200,000
12-CIT-110	VS	03/15/12 17:49	200	-	26.3	5.4	197,000
12-CIT-220	gas lift	06/04/12 13:15	187	203	42.4	6.4	201,000
12-CIT-221	gas lift	06/04/12 15:30	182	200	49.8	6.4	204,000
12-CIT-222	U-tube	06/04/12 19:30	195	202	27.2	6.0	202,000
12-CIT-223	VS	06/05/12 11:10	193	201	31.7	5.7	201,000
12-CIT-224	U-tube	06/05/12 15:10	186	193	31.7	6.2	185,000
12-CIT-225	VS	06/05/12 18:00	197	201	27.3	5.5	201,000
13-CIT-103	U-tube	05/20/13 13:00	182	-	30.5	6.1	202,000
13-CIT-105	U-tube	05/20/13 18:15	192	-	27.3	6.1	196,000

" = not determined

<sup>a</sup> all times are Central Time Zone

<sup>b</sup> measured conductivities are temperature-corrected to 25 °C by instrument software

<sup>c</sup> not corrected for in situ pressure-temperature conditions or loss of volatiles, in situ T and P were about 106.5 °C and 30 MPa

<sup>d</sup> calculated as the sum of all cation and anion mass, including estimated carbonate species and volatile fatty acids

\* analyses of these samples were limited to T, conductivity, anions, and cations

† considered estimates because of difficulty in measuring high conductivity (> 20 mS/cm) samples

**Table 4** - Cations determined by ICP-MS for samples obtained from the same formation by five sampling methods (from Conaway et al., 2016).

SAMPLE ID	Sampling method	Li mg/L	B mg/L	Na mg/L	Mg mg/L	K mg/L	Ca mg/L	Fe mg/L	Mn mg/L	Zn mg/L	Cu mg/L	Rb mg/L	Sr mg/L	Ba mg/L	Pb mg/L
12-CIT-100	gas lift	3.1	6	5,630	124	9400	2830	28	13	0.97	3.5	1.1	125	4	0.31
12-CIT-101	gas lift	11	47	45,090	2,220	645	24,600	155	56	49	< 0.3**	1.8	932	16	4.4
12-CIT-102	gas lift	11	48	45,600	2,280	647	24,900	136	57	50	< 0.3**	1.8	947	15	1.1
12-CIT-103	gas lift	11	47	45,800	2,150	650	25,000	118	57	50	< 0.2*	1.8	952	17	0.66
12-CIT-104	gas lift	11	46	47,000	2,200	672	26,300	107	57	50	< 0.3**	1.8	982	17	0.53
12-CIT-105	gas lift	11	48	45,900	2,180	648	25,500	102	57	51	< 0.2*	1.8	974	17	0.35
12-CIT-106	ESP	11	45	44,500	2,060	676	23,900	299	56	56	< 0.2*	1.8	921	16	0.29
12-CIT-107	ESP	11	45	44,300	1,970	667	23,500	309	51	51	< 0.2*	1.8	907	16	0.19
12-CIT-108	ESP	11	47	46,900	2,090	646	24,900	243	56	54	< 0.3**	1.9	957	17	0.61
12-CIT-109	VS	12	48	46,800	2,200	661	25,000	73	57	53	1.8	1.8	959	17	0.54
12-CIT-110	VS	11	47	46,300	2,100	649	25,300	101	57	53	0.79	1.8	962	17	0.52
12-CIT-220	gas lift	11	45	48,000	2,070	679	25,500	116	57	52	< 0.2*	1.8	986	17	1.8
12-CIT-221	gas lift	11	48	48,400	2,150	679	25,700	99	58	54	< 0.3**	1.9	992	17	0.51
12-CIT-222	U-tube	11	48	47,200	2,210	713	25,200	140	59	55	8.0	1.8	984	17	7.3
12-CIT-223	VS	11	47	48,800	2,140	690	23,500	129	56	53	4.4	1.8	905	17	9.6
12-CIT-224	U-tube	10	40	41,800	1,730	985	23,000	101	44	38	0.26	1.7	882	15	0.77
12-CIT-225	VS	11	47	48,000	2,110	685	25,300	115	56	53	1.7	1.8	990	17	9.0
13-CIT-103	U-tube	9.7	47	47,200	2,240	882	23,800	311	59	54	1.0	1.9	970	10	0.9
13-CIT-105	U-tube	9.5	48	45,700	2,200	814	23,800	271	59	53	0.8	1.9	959	15	1.3

\*Less than limit of detection (MDL); \*\*less than limit of quantitation (LOQ); Values in italics are not within the range of lowest to highest calibration standards. Results were below detection limit (< MDL) for Al (< 0.4), Si (< 20), V (< 0.2), Cr (< 0.6), Mo (< 0.4), Cs (< 0.4), and U (< 0.01).

**Table 5** - Anions determined by high-performance ion chromatography (from Conaway et al., 2016).

SAMPLE ID	Sampling method	Cl <sup>-</sup> mg/L	Br <sup>-</sup> mg/L	SO <sub>4</sub> <sup>-2</sup> mg/L
12-CIT-100	gas lift	18,700	90	148
12-CIT-101	gas lift	122,000	838	313
12-CIT-102	gas lift	123,000	861	321
12-CIT-103	gas lift	123,000	848	306
12-CIT-104	gas lift	125,000	861	319
12-CIT-105	gas lift	123,000	858	299
12-CIT-106	ESP	117,000	826	316
12-CIT-107	ESP	117,000	825	318
12-CIT-108	ESP	122,000	859	291
12-CIT-109	VS	123,000	832	277
12-CIT-110	VS	121,000	811	279
12-CIT-220	gas lift	123,000	858	294
12-CIT-221	gas lift	125,000	867	301
12-CIT-222	U-tube	124,000	856	287
12-CIT-223	VS	124,000	828	277
12-CIT-224	U-tube	115,000	764	318
12-CIT-225	VS	122,000	851	280
13-CIT-103	U-tube	125,000	937	311
13-CIT-105	U-tube	121,000	859	301

\*less than limit of detection (MDL)

concentrations of F<sup>-</sup>, NO<sub>3</sub><sup>-</sup>, NO<sub>2</sub><sup>-</sup>, and P<sub>4</sub><sup>3-</sup> were below the detection limit (< 1 mg/L) for all samples.

**Table 6** - Alkalinity and dissolved sulfide (from Conaway et al., 2016).

SAMPLE ID	Sampling method	Alkalinity <sup>†</sup> mg/L as HCO <sub>3</sub> <sup>-</sup>	δ <sup>13</sup> C – DIC (permil)	Sulfide mg/L	NH <sub>3</sub> mg/L	p <sup>226</sup> RaCi/L
12-CIT-100	gas lift	-	-	-	6	-
12-CIT-101	gas lift	-	-	-	-	-
12-CIT-102	gas lift	180	-10.6	< 1*	33	-
12-CIT-103	gas lift	-	-	-	34	-
12-CIT-104	gas lift	140	-13.3	< 1*	33	-
12-CIT-105	gas lift	130	-12.2	< 1*	33	-
12-CIT-106	ESP	90	-20.2	< 1*	32	-
12-CIT-107	ESP	78	-16.9	< 1*	33	-
12-CIT-108	ESP	240	-12.4	< 1*	33	-
12-CIT-109	VS	150	-17.3	-	33	-
12-CIT-110	VS	180	-17.7	-	-	-
12-CIT-220	gas lift	150	-	< 1*	34	-
12-CIT-221	gas lift	150	-11.9	< 1*	34	1,600 ± 400
12-CIT-222	U-tube	270	-11.6	-	33	-
12-CIT-223	VS	220	-17.5	-	33	-
12-CIT-224	U-tube	170	-16.2	-	32	1,700 ± 350
12-CIT-225	VS	190	-17.7	-	33	-
13-CIT-103	U-tube	182	-	-	-	-
13-CIT-105	U-tube	196	-8.4	-	-	-

" = not determined

\*less than limit of detection (MDL)

† alkalinity values are estimates due to difficulty measuring pH in high conductivity (> 20 mS/cm) samples

Alkalinity and dissolved sulfide by titration; ammonia by ion selective electrode; dissolved inorganic carbon isotopic composition and δ<sup>13</sup>C –dissolved inorganic carbon by combustion-interfaced cavity ring-down spectroscopy; naturally occurring radioactive materials (<sup>226</sup>Ra) by ultra-low background high-purity germanium (HPGe) well detector.

**Table 7** - Gas composition (in percent) for samples collected with downhole vacuum sampler (VS) sampler, U-tube, and at the wellhead in 2012 and 2013 (from Conaway et al., 2016). Dates are m/dd/yyyy.

ID	12-CIT-109	12-CIT-110	12-CIT-224	12-CIT-224-R <sup>‡</sup>	12-CIT-225	12-CIT-G1	12-CIT-G2
Well	D-9-8 #2	D-9-8 #2	D-9-8 #2	D-9-8 #2	D-9-8 #2	D-9-8 #2	D-9-8 #2
Sampler Date	VS 3/15/2012	VS 3/15/2012	U-tube 6/5/2012	U-tube 6/5/2012	VS 6/5/2012	Wellhead 3/13/2012	Wellhead 3/14/2012
H <sub>2</sub>	1.3	3.1	9.0	10	2.3	0.99	1.1
Ar	0.94	0.68	0.087	0.10	0.56	0.37	0.013
O <sub>2</sub>	1.5	< 0.0005	< 0.0005	< 0.0005	< 0.0005	2.8	< 0.0005
N <sub>2</sub>	79	71	58	53	64	90	96
CH <sub>4</sub>	15	21	24	29	32	5.1	3.0
CO <sub>2</sub>	2.6	3.9	9.2	7.8	0.74	0.029	0.0076
C <sub>2</sub> H <sub>6</sub>	0.029	0.046	0.050	0.052	0.082	0.0081	0.0053
CO	0.009	0.006	< 0.001	< 0.001	0.18	0.44	0.056
C <sub>3</sub> H <sub>8</sub>	0.0007	0.001	0.002	0.001	0.003	0.0009	< 0.0005
C <sub>2</sub> H <sub>4</sub>	0.0004	0.0006	0.002	0.003	0.001	0.01	0.01

"- " not determined

‡ field replicate

H<sub>2</sub>S, C<sub>4</sub>H<sub>10</sub>, and isobutane (also C<sub>4</sub>H<sub>10</sub>) were below the minimum detection limit (< 0.0005 percent) for all samples

The results demonstrate the difficulty of preserving volatile analytes in samples, particularly the loss of dissolved carbonate and associated increase of pH and the precipitation of calcite and possibly other minerals, that has also been documented in shallow groundwater studies for both gas lift and various types of ESP sampling (Conaway et al., 2016). The importance of sampling depth is shown in the results presented here, as evidenced by the shallow setting depth of the ESP and resulting loss of volatiles and increased contamination. Other work has suggested that with careful attention to setting depth and other parameters, ESP may be an effective sampling strategy in liquid-dominated geothermal and groundwater systems with low overall partial gas pressures (Wolff Boenisch & Evans, 2014). The VS and U-tube systems appear to perform most favorably in preserving volatile analytes. Further investigation should be performed to resolve sources of Cu and Pb contamination in some of the samples from VS and U-tube obtained in this study.

In addition to the preservation of volatile components, the importance of well conditioning before geochemical sampling is also demonstrated, as contamination by workover or drilling fluids was likely in the early gas lift samples as well as initial ESP samples. Although gas lift using coiled tubing substantially affected both brine and gas chemistry, it was essential in order to move a large volume of brine to clean the full length of the wellbore.

Because little gas was obtained from the pressurized samples in this study, the value of these analytical results is limited but some insight is provided for considering sampling methods. The gas composition results for samples collected by U-tube and VS are all influenced to some degree by contamination from air and residual N<sub>2</sub> gas from U-tube cycles or gas lift. Residual air in the vacuum chamber and sampling manifold appears to be an important consideration in VS-collected samples under these circumstances. Although correction for residual N<sub>2</sub> is a possibility for U-tube samples, as shown elsewhere (Freifeld et al., 2005), multiple sources of N<sub>2</sub> (residual N<sub>2</sub> from both U-tube and gas lift) make such an approach problematic for this study. Similar comparison studies in wells with a higher dissolved gas fraction, or even gas wells, would be valuable.

## 6.6 Inorganic Chemical Composition of Produced Water: A Basin and Country-Scale Perspective

In this section, we examine the chemical composition of produced water from two large data sets. The first is the USGS National Produced Waters Geochemical Database, where data for more than 120,000 oil and gas wells from the major sedimentary basins in the USA were obtained from published literature and received from oil companies and state oil and gas organizations. The data are listed in the updated USGS National Produced Waters Geochemical Database (Blondes et al., 2019).

The second major data set is from wells in the Alberta Basin, which is one of the largest petroleum basins in the world, has a more comprehensive and publicly available geochemical data set than other basins, and also has a new data set that includes information on potentially toxic elements seldom reported for other basins (Hitchon, 2023). Although the data set is relatively small ( $N = 631$ ), it is representative of the Alberta Basin both geographically and by major stratigraphic units (Figure 4 in Hitchon, 1995).

### 6.6.1 Culling Criteria for Standard Formation Water

Produced water is also called formation water and is by far the most common fluid recovered during exploration for and production of petroleum. In the Alberta Basin, there are at least ten times as many formation water analyses as there are crude oil and natural gas analyses. Further, most of the formation water analyses are so-called *standard* analyses reporting only Na (usually by difference between equivalent cation and anion concentrations), Mg, Ca, Cl,  $SO_4$  (sulfate),  $HCO_3$  (bicarbonate), and  $CO_3$  (carbonate), plus pH and specific gravity.

In the Alberta Basin, more than 118,000 standard analyses were conducted in mid-1993 when Hitchon and his colleague Michel Brulotte developed an electronic method for culling formation water samples from a database (Hitchon & Brulotte, 1994). They decided to cull erroneous analyses based on three criteria:

1. chemical analysis,
2. method of production and sampling, and
3. stratigraphic unit.

The stratigraphic unit was included to allow identification of KCl mud contamination using threshold values of  $K/Na \times 10^3$  that are specific for individual units in the Alberta Basin (Hitchon et al., 1995). The chemical criteria used for automatic (electronic) culling are summarized in Table 8. At the time that the software was developed, the Alberta Geological Survey Well Data Base included the method of production and sampling (Table 9). The final cull used a system of sequential removal of formation water analyses with fifteen criteria based on chemical analysis and by method of production and sampling. The final culling scheme is listed in Table 10, where the percent of total database removed shown in the last column is based on 141,337 analyses from the Western Canada Basin. After publication of Hitchon and Brulotte (1994), it became clear that some areas in Alberta with well documented uncontaminated freshwater recharge have formation water analyses reporting  $CO_3$ , thus rejection flag number 5 for analyses that report  $CO_3$  should be removed from the initial sequential culling system and used at the level of the individual stratigraphic unit.

**Table 8** - Automatic (electronic) culling criteria for formation water analyses based on chemical analysis (from Hitchon & Brulotte, 1994).

Flag	Criteria for rejection	Possible causes	Total analyses*	
			No.	Percent
1	Any of Ca, Mg, Cl, or SO <sub>4</sub> , with either HCO <sub>3</sub> or alkalinity, zero, missing, or reported as < or > value	Incomplete analysis; insufficient sample; very low content, hence difficulty in determination	39,018	27.8
2	Mg ≥ Ca	Commonly, loss of CO <sub>2</sub> and precipitation of CaCO <sub>3</sub> (calcium carbonate) before analysis due to a long time between sampling and analysis; very low (Ca + Mg), hence either difficulty in determination or incorrect entry as separate Ca and Mg values	6,901	4.9
3	pH < 5.0 or > 10.0 (0.0 is considered no pH reported)	Acid wash contamination or wash from cement job, respectively; typing error in decimal point	5,641	4.0
4	OH reported	Cement wash; poor analysis	3,509	2.5
5	CO <sub>3</sub> reported	Contamination by drilling mud (without significant effect on pH); poor sampling of separator or treater	36,307	25.8
6	Na (calculated) is negative	Poor analysis	88	0.06
7	Density < 1.0 (0.0 is considered no density reported)	Poor determination; organic matter contamination; contamination with alcohol additive to drilling mud	4,965	3.5
8	Ionic balance exceeds specific limits (usually 5 percent)	Poor analysis; incorrect transcription of original data sheet	–	–

“–” = not determined in the study.

\* based on 140,504 analyses from the Western Canada Basin

**Table 9** - Frequency of method of production for Alberta Basin data (from Hitchon & Brulotte, 1994).

Flag	Method of production	Percent	Flag	Method of production	Percent
0	Unclassified	19.2	11	Swabbing	2.3*
1	Drill stem test	73.6	12	Flowing	2.5
2	Formation wireline test	<.1*	13	Absolute open flow test	0.2*
3	Constant rate test	< 0.1	14	Production tank	< 0.1*
4	Pumped	0.8	15	Stock tank	< 0.1*
5	Bailed	0.5*	16	Formation interval test	< 0.1
6	Battery (multiple wells)	< 0.1*	17	Repeat formation test	0.1*
7	Separator	0.2	18	Blow down	< 0.1*
8	Treater	< 0.1	19	Formation test	< 0.1
9	Wireline test	0.1*	20	Frac-n-test	< 0.1*
10	Production test	0.5	21	Gas lift	< 0.1*

\* = rejected as an excluded method of production (flag 10)

**Table 10** - Scheme for the sequential removal of formation water analyses (from Hitchon & Brulotte, 1994).

Flag	Criteria	Number of analyses removed	Percent of total data base removed
1	Incomplete analysis	39,018	27.6
2	Mg ≥ Ca	6,475	4.6
3	pH < 5.0 or > 10.0	1,910	1.4
4	OH reported	1,766	1.2
5	CO <sub>3</sub> reported	25,292	17.9
6	Na (calculated) is negative	73	< 0.1
7	Density < 1.0	1,462	1.0
8	Poor ionic balance	595	0.4
9	No sampling interval	3,544	2.5
10	Excluded method of production	2,565	1.8
11	Excluded sampling point	4,968	3.5
12	Fe > 100 mg/L <sup>-1</sup> (probably “rust”)	2	< 0.1
13	Multiple DST	1,422	1.0
14	DST only non-aqueous	7,531	5.3
15	DST water < 10 percent of recovery	572	0.4
	Total analyses removed	97,195	68.8
	Total analyses remaining	4,142	31.2

Once the sequential culling has been completed the analyses can be assigned to their correct stratigraphic unit, at which stage an electronic cull for contamination by KCl mud may be carried out. Final culling is usually done manually using a variety of methods such as cumulative frequency plots of individual ions and maps of variations in regional salinity (or other components of interest).

The flag to remove analyses of samples obtained from separators and treaters where Fe is  $> 100$  mg/L was justified by a more recent study that identified *rust* contamination in formation water from producing wells. Analyses from drill stem tests showed no evidence of rust contamination (Hitchon, 2000). A word of caution is necessary here because high or low values used to exclude chemical data from the Alberta Basin may not be correct for basins in the USA or other parts of the world. In the case of Fe, for example, many produced water samples from the metal-rich Mississippi Salt Dome Basin have dissolved Fe values higher than 500 mg/L (Kharaka et al., 1987).

To demonstrate the speed and utility of sequential culling, this method was used for culling formation water samples in the Canadian portion of the Williston Basin along with map plotting software developed by the Alberta Geological Survey. The elapsed time to complete the study was only ten working days (Hitchon, 1996b).

For comparison with the Western Canada Basin, one other large publicly available database can be sorted using this method: the US Geological Survey National Produced Waters Geochemical Database. There are now nearly 166,000 analyses in the database, of which close to 60 percent ( $n = 98,192$ ) are classified as *conventional hydrocarbon* production.

In each data set, we selected only those analyses that passed the initial culling criteria set by Hitchon and Brulotte (1994), so with only minor variations, all the analyses include values for pH and the seven major elements: Na, K, Mg, Ca, Cl,  $\text{HCO}_3$ , and  $\text{SO}_4$ . These major elements make up more than 95 percent of the TDS in most produced water. The selection criteria also include a valid well location and perforation zone, an anion cation charge balance  $\leq 5$  percent, and the saturation state of calcite that is  $\leq 1$  kcal/mole. Hitchon and Brulotte (1994) and Hitchon (2023) provide more information on data selection.

### 6.6.2 Statistical Classification of Elements in Produced Water

The range of concentration for each element is given using the statistical distribution of the element in terms of percentiles (P-values). Thus, the value at P10 means that 10 percent of the analyses are less than the P-value and, conversely, 90 percent of the values are greater than P10. We may think of P50 as the median and it may differ from the average value.

For our purposes, we are not concerned with very low values, that is, those less than P10, which are closer to the composition of groundwater. But we are interested in the maximum amounts reported. Thus, we provide values for P10, P25, P50 (median), P75, and P90 to show the range found in produced water from most sedimentary basins (there are

exceptions, but they need not concern us at the level of this global overview). The P25 and P75 values can be directly compared with similar statistics from groundwater; P25, P50, and P75 are also known as the first, second, and third quartiles (Q1, Q2, and Q3), respectively.

The individual elements are presented in three groups: major elements, minor elements, and trace elements. For this book, we used a grouping based on the P75 values for elements in produced water in the Alberta Basin. Division boundaries are 500 mg/L and 10 mg/L. Elements considered in this section are listed below.

Although K is classed as a major element, it is not part of the original culling criteria; also, dissolved organic species, discussed in Section 7, are not included in these divisions. Only acetate ( $\text{CH}_3\text{COO}$ ) is of high enough concentration to be included with the major elements; a few short-chain, aliphatic-acid anions may plot with the minor elements, but the bulk of organics fall in the trace elements group.

- Major elements (P75 > 500 mg/L): Na, K, Mg, Ca, Cl,  $\text{HCO}_3$ ,  $\text{SO}_4$
- Minor elements (P75 10 to 499 mg/L): Li, Sr, Ba, Br, I, B,  $\text{SiO}_2$ ,  $\text{NH}_3$
- Trace elements (P75 < 10 mg/L): Rb, F, Pb, Zn, Fe, Mn, As, Se

For most major elements, the final culled data sets comprise 73,122 analyses from conventional hydrocarbon wells and 1,535 analyses from *un*conventional hydrocarbon wells (shale gas, tight oil, and coal bed methane) in the US National Geochemical Database, together with 631 analyses from conventional hydrocarbon wells in the Alberta Basin. For all other elements and ions, the number of analyses used to compile the statistics is given in the tables.

For comparison purposes, we cite average values for river water and ocean water from Taylor and McLennan (1985, Table 2.3). The data for groundwater have been summarized from cumulative frequency plots, citing the actual or estimated P25 and P75 statistical values for major and minor components from Appelo and Postma (1993, Figure 2.9), and for potentially toxic elements from Newcomb and Rimstidt (2002) and Lee and Helsel (2005). For major elements, the maximum amount in produced water worldwide is usually no more than 5 or 10 percent above the P90 value for that element. The information presented is, of necessity, rather generalized but offers a broad indication of the amounts of each element found in the specific situations considered.

To protect public health, the US EPA sets national enforceable MCLs and non-enforceable SMCLs for many inorganic, organic and radionuclide contaminants in drinking water. US EPA (2009) contains more information about the possible sources of contaminants, the nature of the risk to human health, and lists values for the maximum contaminant level goal (MCLG) which is the level of a contaminant in drinking water below which there is no known or expected risk to health. We listed the MCL or the SMCL (if it has been defined) in Table Box 2-1 for each element or compound discussed in this section.

There are also standards for irrigation water and water used for different animals. These are covered earlier in this book.

A final point before we consider the individual elements: Much of the preliminary general geochemistry and description of the aquatic behavior of the elements is summarized from *Introduction to Ground Water Geochemistry* (Hitchon et al., 1999b).

### 6.6.3 Salinity

Before we discuss the individual major elements, we need to describe the range of salinity (TDS) in natural and produced water (Table 11). In the USA, protected groundwater (also known as USDW) is defined as water with salinity < 10,000 ppm. This value is just less than P25 in the culled USGS data set; this means that three out of four samples of formation (produced) water in the USA have salinity high enough to potentially damage the local groundwater. The MCL value for salinity for drinking water is only 500 mg/L and almost all produced water has higher salinity and many organic and inorganic chemicals that may contaminate potable groundwater. With respect to salinity, we can consider formation water either as an extension of groundwater, or that groundwater may be thought of as *dilute* formation water. Effectively, there is a continuum between the two water classes in sedimentary basins.

**Table 11 - Salinity of natural and produced water.**

Source	Salinity (mg/L)
River water (average)	260
Ocean water (average)	35,335
Groundwater (P25–P75)	145–725
MCL value	500
<b>Produced water (P10–P25–P50–P75–P90)</b>	
Alberta Basin (N = 631)	11,000 - 25,000 - 53,000 - 120,000 - 200,000
USGS Conventional hydrocarbon (N = 72,843)	4,200 - 14,000 - 58,000 - 160,000 - 260,000
USGS Unconventional hydrocarbon (N = 1,535)	11,000 - 14,000 - 18,000 - 120,000 - 280,000

Alberta Basin (Hitchon, 2023) and USGS (Blondes et al., 2019)

Kharaka and Hanor (2014) have identified water-rock reactions as a major control on the composition of formation water at reservoir conditions. These reactions are temperature dependent and so information on formation temperature is essential for a proper understanding of how formation water composition is controlled. Table 12 lists available temperature information for the two data sets.

**Table 12 - Aquifer temperature of produced water.**

Source	Temperature (°C)
Produced water (P10–P25–P50–P75–P90)	
Alberta Basin (N = 631)	20 - 25 - 35 - 54 - 79
USGS Conventional hydrocarbon (N = 458)	32 - 64 - 82 - 95 - 116

Alberta Basin (Hitchon, 2023; Blondes et al., 2019)

There were no temperature values for the unconventional water

Maximum aquifer temperature for a gas field in the Alberta Basin is 152 °C at the Marsh Field: 49,390 kPa at 5,219.5 mKB (meters below Kelly Bushing). The maximum for

an oil field is 125 °C at the Karr Field: 61,097 kPa at 4,076.3 mKB. Both fields are in Devonian rocks.

### 6.6.4 Major Elements

Here, we classify seven elements as major elements in produced water (Figure 23). If formation water has all major elements determined (including organics), the ionic balance should be well within acceptable limits of 5 percent.

Group	1	2	3	4	5	6	7	8	9	10	11	12	13	14	15	16	17	18
Period 1	H																	He
2	Li	Be											B	C	N	O	F	Ne
3	Na	Mg											Al	Si	P	S	Cl	Ar
4	K	Ca	Sc	Ti	V	Cr	Mn	Fe	Co	Ni	Cu	Zn	Ga	Ge	As	Se	Br	Kr
5	Rb	Sr	Y	Zr	Nb	Mo	Tc	Ru	Rh	Pd	Ag	Cd	In	Sn	Sb	Te	I	Xe
6	Cs	Ba	La	Hf	Ta	W	Re	Os	Ir	Pt	Au	Hg	Tl	Pb	Bi	Po	At	Rn
7	Fr	Ra	Ac															

Figure 23 - Periodic Table showing the major elements in formation water.

### Sodium (Na)

Sodium is the most abundant alkali element on Earth in terms of atomic abundance and weight percent. In nature, sodium occurs only in coordination with oxygen and halogen atoms. Sodium is a lithophile element (literally, *rock-loving*; i.e., an element that forms silicates or oxides and is concentrated in the minerals of the Earth's crust). It is much less abundant than potassium in non-evaporite sedimentary rocks. The amounts of sodium held in evaporite sediments and in solution in the ocean are an important part of the total. In both cases, the amount of sodium far exceeds that of potassium. Table 13 shows the abundance of sodium in natural and produced water.

Table 13 - Sodium in natural and produced water.

Source	Sodium (mg/L)
River water (average)	6.3
Ocean water (average)	10,800
Groundwater (P25–P75)	10–100
MCL value	*
<b>Produced water (P10–P25–P50–P75–P90)</b>	
Alberta Basin (N = 631)	4,100 - 8,800 - 18,000 - 36,000 - 53,000
USGS Conventional hydrocarbon (N = 65,640)	1,100 - 4,000 - 18,000 - 49,000 - 78,000
USGS Unconventional hydrocarbon (N = 1535)	4,100 - 5,200 - 6,500 - 37,000 - 86,000
Alberta Basin (Hitchon, 2023); USGS (Blondes et al., 2019)	

\*no MCL value given, but a significant component of the 500 mg/l, the MCL for salinity

When sodium is brought into solution during weathering, it tends to remain in that state. This occurs because there is no important precipitation reaction that maintains low sodium concentrations in water in the way that the calcium content is controlled through

the precipitation of carbonate. Sodium is adsorbed onto mineral surfaces, especially clay minerals. In freshwater systems, cation exchange processes tend to extract divalent cations from solution and replace them with monovalent cations. Thus, sodium occurs mainly as the  $\text{Na}^+$  ion water with TDS < 1,000 mg/L. As the salinity increases, a variety of complex ions and ion pairs may form, including  $\text{NaHCO}_3^{\ominus}$ ,  $\text{NaSO}_4^+$ , and  $\text{NaF}^{\ominus}$  (sodium hydrogen carbonate/sodium bicarbonate, sodium sulfate, and sodium fluoride, respectively), although only in small amounts relative to the free ion.

High sodium concentrations can be reached before any precipitate is formed. In evaporated sea water, the sodium content can reach 150,000 mg/L when saturated with halite. In produced water, high sodium with high chloride (> 100,000 mg/L) and a high Cl/Br ratio (chlorine/bromine) suggests solution of halite. If considerable sulfate and calcium are also present, then mixed halite–anhydrite evaporite rocks may have been dissolved. When only sodium and sulfate are high, there may have been contact with fine-grained clastic rocks (i.e., rocks composed of fragments (clasts) of preexisting rocks). However, interpretation of the processes leading to the specific sodium content must be made in the context of both the other elements present and the local hydrogeology.

Shallow potable groundwater has a sodium content ranging from that of rainwater to 500 mg/L. Saturation with halite occurs at about 150,000 mg/L, so the range of concentration in formation water is considerable. Sedimentary basins with evaporites generally have some formation water with high contents of sodium.

### Potassium (K)

Potassium is a lithophile element with only one oxidation state (+1) and a strong affinity with oxygen and halogens. In the sedimentary environment, an essential feature of the behavior of potassium is its ease of adsorption onto colloids and clays, and its preferential fixation in cation-exchange reactions with clay minerals. Table 14 shows the abundance of potassium in natural and produced water.

**Table 14** - Potassium in natural and produced water.

Source	Potassium (mg/L)
River water (average)	2.3
Ocean water (average)	399
Groundwater (P25–P75)	1–5
MCL value	*
<b>Produced water (P10–P25–P50–P75–P90)</b>	
Alberta Basin (N = 631)	27 - 59 - 170 - 1,000 - 2,900
USGS Conventional hydrocarbon (N = 16,549)	13 - 38 - 160 - 1,200 - 1,400
USGS Unconventional hydrocarbon (N = 446)	90 - 1,600 - 3,300 - 4,900 - 6,200
Alberta Basin (Hitchon, 2023); USGS (Blondes et al., 2019)	

\* no MCL value given, but a significant component of the 500 mg/L, the MCL for salinity

During weathering, potassium enters the soil solution as  $\text{K}^+$ . Normally, because of its larger ionic size, it is expected to adsorb less strongly than sodium in ion-exchange reactions; but potassium is incorporated in a special way in some clay minerals. For

example, in the case of illite (mica-type clay minerals) it occupies spaces between the crystal layers, thus it cannot take part in ion-exchange reactions. In dilute natural water in which the sum of Na and K is less than about 10 mg/L, the amount of potassium may exceed that of sodium. At higher contents of these two alkali metals, the amount of potassium is considerably less than that of sodium, but the K/Na molar ratio increases with increasing reservoir temperature. Only in special situations in groundwater will the K/Na molar ratio approach or exceed that of formation water associated with halite-potash deposits (K/Na = 0.64).

The potassium content of potable groundwater ranges from that of rainwater to 12 mg/L, which is the drinking water limit in some jurisdictions. Potassium in formation water ranges from about 10 mg/L up to 21,800 mg/L (the maximum fully documented sample so far reported); but it is in sedimentary basins that include evaporites where formation water has the highest contents of both sodium and potassium. Potassium is held mainly as  $K^+$  but decreases with a corresponding increase in the importance of the KCl ion pair. Next in importance is the ion complex  $KSO_4^-$ .

### Magnesium (Mg)

Magnesium is an alkaline earth element and is strongly electropositive with a valence of 2. The  $Mg^{2+}$  ion is very stable and has characteristics similar to  $Fe^{2+}$ . In the sedimentary environment, most magnesium is associated with the carbonate anion, dominantly as dolomite:  $CaMg(CO_3)_2$ . Table 15 shows the abundance of magnesium in natural and produced water.

**Table 15 - Magnesium in natural and produced water.**

Source	Magnesium (mg/L)
River water (average)	4.1
Ocean water (average)	1,290
Groundwater (P25–P75)	5–20
MCL value	*
<b>Produced water (P10–P25–P50–P75–P90)</b>	
Alberta Basin (N = 631)	22 - 90 - 340 - 950 - 2,000
USGS Conventional hydrocarbon (N = 73,122)	13 - 68 - 450 - 1,500 - 2,600
USGS Unconventional hydrocarbon (N = 1535)	10 - 15 - 24 - 440 - 1,200

Alberta Basin (Hitchon, 2023); USGS (Blondes et al., 2019)

\* no MCL value given, but included in the 500 mg/L, the MCL for salinity

During weathering, magnesium enters the hydrosphere mainly through decomposition of dark ferromagnesian minerals, chlorites, Mg-calcite, and dolomite. In most dilute groundwater, the dominant form of magnesium in solution is  $Mg^{2+}$ . As the salinity increases, a variety of ion pairs and ion complexes is possible.

Most limestones contain significant amounts of magnesium. Dissolution brings  $Mg^{2+}$  into solution, but the precipitate that forms from the solution that has dissolved a Mg-limestone is nearly pure calcite. This means that the content of magnesium, relative to

calcium, increases down the flow path of formation water in contact with, and dissolving, a Mg-limestone aquifer.

In natural water, the magnesium content ranges from that of rainwater to just over 41,000 mg/L (Leman Field, North Sea). Concentrations above about 50,000 mg/L are often poorly documented. High salinity does not necessarily imply an elevated content of magnesium because the magnesium content depends on the chemical conditions that caused the high salinity. Most unpolluted groundwater with magnesium > 50 mg/L (the limit for potable water) owe their higher magnesium content to special situations. These include, but are not limited to, the presence of evaporite rocks, association with ultrabasic rocks, and unusual conditions such as that found in the San Joaquin Valley, California, where acidic seeps from weathered shales have resulted in elevated amounts of selenium and up to 7,550 mg/L of magnesium in nearby ephemeral streams (Barnes et al., 1973).

In the Alberta Basin, magnesium in formation water ranges up to 13,400 mg/L. As expected, formation water from other sedimentary basins containing carbonates and evaporites generally has higher magnesium content. Magnesium occurs dominantly as  $Mg^{2+}$ , with the ion pair  $MgSO_4$  and the bicarbonate complex  $MgHCO_3^+$  accounting for the rest.

## Calcium (Ca)

Calcium is a lithophile element and the most abundant of the alkaline-earth metals. It is a major constituent of many common rock types and minerals. In sedimentary rocks, calcium is most abundant in limestone and dolostone. Unlike magnesium, its ionic radius prevents it from fitting into the octahedral spaces of a close-packed oxygen arrangement. It is regarded as the smallest *large cation* and may be substituted by sodium and strontium. Table 16 shows the abundance of calcium in natural and produced water.

**Table 16 - Calcium in natural and produced water.**

Source	Calcium (mg/L)
River water (average)	15
Ocean water (average)	413
Groundwater (P25–P75)	10–50
MCL value	*
<b>Produced water (P10–P25–P50–P75–P90)</b>	
Alberta Basin (N = 631)	65 - 230 - 1,100 - 4,500 - 17,000
USGS Conventional hydrocarbon (N = 73,122)	42 - 330 - 1,800 - 7,700 - 15,000
USGS Unconventional hydrocarbon (N = 1,535)	32 - 40 - 80 - 3,900 - 14,000

Alberta Basin (Hitchon, 2023); USGS (Blondes et al., 2019)

\* no MCL value given, but included in the 500 mg/L, the MCL for salinity

Calcium is the dominant cation in most river water and is second only to sodium in most formation water. The major factor limiting the solubility of calcium in most natural water (including produced water) is equilibria involving carbonates, and so the system  $CaCO_3 - CO_2 - H_2O$  has been studied extensively. In dilute solutions, calcium is found as the divalent ion ( $Ca^{2+}$ ) but as the ionic strength (salinity) increases, a number of ion pairs and complexes are formed.

Shallow potable groundwater has a calcium content ranging from that of rainwater to 120 mg/L. In the Alberta Basin and the Palo Duro Basin (Texas, USA), calcium in formation water ranges up to nearly 100,000 mg/L—and possibly higher in other basins, although the samples are not always fully documented. Calcium-dominated brine is found deep in many sedimentary basins, including the Alberta Basin, and is of potential commercial interest.

In most formation water, calcium occurs as  $\text{Ca}^{2+}$ , but as the salinity increases, the amount of calcium held in this form decreases concomitantly with increase of the ion pair  $\text{CaCl}_2$ . There are much smaller amounts of other ion complexes and ion pairs.

In the Alberta Basin, calcium is found in all formation water. About 60 percent of formation water in the deeper strata are saturated or slightly undersaturated with respect to anhydrite ( $\text{CaSO}_4$ ). This is a direct reflection of the presence of anhydrite.

### Chlorine (Cl)

Chlorine is by far the most abundant halogen in the continental crust. It is a lithophile element and accumulates in terminal water reservoirs (oceans and, to a lesser extent, inland closed-basin lakes) because of the following:

- during migration, it is not affected by acid-alkaline or by oxidizing-reducing environments;
- it forms practically no insoluble salts; and
- chlorine occurs in nature only as chloride ( $\text{Cl}^-$ ) with a large ionic radius and high electronegativity.

As a result, three-fourths of crustal chlorine is found in the ocean.

In the sedimentary environment, where many rocks have been deposited under marine conditions, it is difficult to determine the true content of chlorine because

1. it is present in entrained formation water; and
2. it is readily leached by fresh water.

Thus, the abundances reported here are subject to much discussion. Not included in the above information are evaporites, which are a major source of chlorine in some formation water. Table 17 shows the abundance of chlorine in natural and produced water.

**Table 17 - Chlorine in natural and produced water.**

<b>Source</b>	<b>Chlorine (mg/L)</b>
River water (average)	7.8
Ocean water (average)	19,500
Groundwater (P25–P75)	10–50
SMCL value	250
<b>Produced water (P10–P25–P50–P75–P90)</b>	
Alberta Basin (N = 631)	5,800 - 14,000 - 32,000 - 73,000 - 120,000
USGS Conventional hydrocarbon (N = 73,122)	630 - 5,900 - 34,000 - 97,000 - 160,000
USGS Unconventional hydrocarbon (N = 1535)	6,000 - 7,500 - 9,500 - 71,000 - 170,000

Alberta Basin (Hitchon, 2023); USGS (Blondes et al., 2019)

Chlorine is present in, effectively, all natural water, predominantly as chloride ( $\text{Cl}^-$ ). The proportion of major anions in rainwater changes with the decrease in maritime influence from coastal to inland areas, that is, from chloride > sulfate > nitrate to sulfate > nitrate > chloride. In major unpolluted rivers, the order of major anions is bicarbonate > sulfate > chloride, a reflection of rock weathering by dissolved carbon dioxide in rainwater, which has a characteristic pH of about 5.0 or less. Within any drainage basin, however, there may be rivers that drain areas with evaporites or with significant groundwater baseflow from evaporite dissolution.

Potable groundwater varies in composition with respect to major anions. It is most desirable for bicarbonate to be the major anion with chloride < 250 mg/L and sulfate < 250 mg/L. As a general observation, increased depth (temperature) results in a gradual change from bicarbonate > sulfate > chloride to chloride > bicarbonate > sulfate, usually accompanied by a general increase in salinity, although potable formation water has been found at depths up to several kilometers, depending on the hydrodynamic situation.

In shallow groundwater and formation water, chloride may range from the global mean for precipitation, through the mean for river water, to > 200,000 mg/L in formation water in many sedimentary basins. Chloride content approaching the maximum reported so far (362,000 mg/L) is only found in formation water from deep sedimentary basins, with elevated temperatures, that are of the Ca–Na–Cl type.

In the Alberta Basin, chloride is found in all formation water, with concentrations up to 200,000 mg/L. The content of chloride increases with increasing temperature and salinity, a trend found in many sedimentary basins. As a general observation, the amount of chlorine held as  $\text{Cl}^-$  decreases with increasing salinity and temperature, concomitantly with slight increases of various chlorine-metal complexes.

## Carbon (C)

The inorganic geochemistry of carbon on Earth is concerned mainly with reactions involving carbon dioxide ( $\text{CO}_2$ ). Among minerals, carbonates are the most important carbon-containing compounds.

The content of carbon varies widely in major sedimentary rock types. Some sedimentary rocks are effectively free of both carbonate minerals and organic matter, for example, evaporites and some sandstones. The maximum content of carbon in a pure limestone without organic matter is 12 percent. Table 18 shows the abundance of bicarbonate in natural and produced water.

**Table 18** - Bicarbonate in natural and produced water.

Source	Bicarbonate (mg/L)
River water (average)	200
Ocean water (average)	142
Groundwater (P25–P75)	100–400
MCL value	*
<b>Produced water (P10–P25–P50–P75–P90)</b>	
Alberta Basin (N = 631)	130 - 220 - 410 - 800 - 1700
USGS Conventional hydrocarbon (N = 73,122)	61 - 140 - 340 - 830 - 1700
USGS Unconventional hydrocarbon (N = 1535)	140 - 300 - 850 - 1200 - 1400

Alberta Basin (Hitchon, 2023); USGS (Blondes et al., 2019)

\* no MCL value given, but included in the 500 mg/L, the MCL for salinity

In the aqueous environment, the geochemistry of carbon is the story of dissolved carbon dioxide species. Three main species are involved: carbonic acid ( $\text{H}_2\text{CO}_{3\text{aq}}$ ), bicarbonate ( $\text{HCO}_3^-$ ), and carbonate  $\text{CO}_3^{2-}$ . The boundaries between these species occur at pH 6.4 and pH 10.2. For most formation water, the  $\text{HCO}_3^-$  species is the dominant form, but in water with pH values  $< 4$ ,  $\text{H}_2\text{CO}_{3\text{aq}}$  is the dominant species. In water with pH values  $> 10.5$ , the carbonate ( $\text{CO}_3^{2-}$ ) species dominates.

The average bicarbonate in river water is 200 mg/L; in potable water, bicarbonate ranges from 10 to 500 mg/L. Although no jurisdiction has set an upper limit for bicarbonate in drinking water, some have set limits for pH and for salinity, which effectively results in the imposition of an upper limit for bicarbonate-plus-carbonate in the majority of water samples. In unpolluted groundwater, bicarbonate is generally  $< 1,500$  mg/L. White and others (1963) report the highest fully documented bicarbonate level so far found in formation water as 15,200 mg/L.

Analyses of formation water from the Alberta Basin were subject to adjustment for the loss of carbon dioxide upon bringing the samples to the surface; the pH calculated at aquifer temperature is shown in Table 19.

**Table 19** - pH calculated at aquifer temperature.

	Min.	P10	P25	P50	P75	P90	Max.
pH	4.3	5.4	5.9	6.4	6.9	7.1	8.9

In the Alberta Basin, bicarbonate is found in all formation water and ranges up to 13,900 mg/L. There is a broad trend of decreasing bicarbonate content with increasing salinity both in the Alberta Basin and the Beaufort-Mackenzie Basin (Hitchon et al., 1990). Using SOLMINEQ.88 (a computer program for geochemical modeling of water-rock interactions), we know that the amount of  $\text{HCO}_3^-$  decreases with increasing salinity, but there are no obvious trends for  $\text{H}_2\text{CO}_3$ . The balance of the analyzed bicarbonate is accounted for by various carbonate and bicarbonate metal complexes, and possibly acetate and other short-aliphatic acid anions.

## Sulfur (S)

Sulfur is the quintessential chalcophile element. Sulfur has several coordination numbers, of which the most common are 3, 4, and 6. For 3, examples are marcasite and pyrite ( $\text{FeS}_2$ ), examples of 4 include all sulfates and sphalerite ( $\text{ZnS}$ ), and an example for 6 is galena ( $\text{PbS}$ ). In nature, sulfur occurs in four oxidation states, two of which, -2 and +6, are common in geological materials. Sulfur is a primary constituent of three major mineral groups: sulfides, sulfates, and sulfo-salts. In sedimentary rocks, the highest abundances are in evaporites comprising gypsum,  $\text{CaSO}_4 \cdot 2\text{H}_2\text{O}$ , or anhydrite, ( $\text{CaSO}_4$ ). In shales, sulfur occurs mainly as pyrite, ( $\text{FeS}_2$ ), or similar iron sulfides. Coal is an important bearer of sulfur, both as pyrite and organic sulfur. Table 20 shows the abundance of sulfate in natural and produced water.

**Table 20 - Sulfate in natural and produced water.**

Source	Sulfate (mg/L)
River water (average)	11
Ocean water (average)	2,700
Groundwater (P25–P75)	10–100
SMCL value	250
<b>Produced water (P10–P25–P50–P75–P90)</b>	
Alberta Basin (N = 631)	13 – 31 – 110 – 590 – 1,200
USGS Conventional hydrocarbon (N = 73,122)	21 – 100 – 520 – 1,700 – 3,400
USGS Unconventional hydrocarbon (N = 1,535)	20 – 54 – 110 – 250 – 650

Alberta Basin (Hitchon, 2023); USGS (Blondes et al., 2019)

In most natural groundwater, sulfur is present as dissolved sulfate ( $\text{SO}_4^{2-}$ ). Depending on Eh and pH, however,  $\text{S}$ ,  $\text{H}_2\text{S}_{\text{aq}}$ ,  $\text{HS}^-$ , or  $\text{HSO}_4^-$  may be the dominant form. The concentration of sulfate varies over about six orders of magnitude from  $10^{-1}$  to  $10^5$  mg/L, depending on the processes controlling the aqueous system. For example, bacterial sulfate reduction can reduce the content of sulfate to extremely low amounts. If the water encounters large quantities of cations of very insoluble sulfates, such as barium, this also can significantly decrease the amount of sulfate remaining in solution. Conversely, solution of anhydrite or gypsum markedly increases the content of sulfate in formation water. A wide range of sulfate ion pairs with various cations occurs at high ionic strengths.

The global mean for sulfate in precipitation is 0.06 mg/L and the average in river water is 11 mg/L. In potable groundwater, sulfate ranges up to 250 mg/L. Very high contents of sulfate are found in special situations—for example, shallow groundwater in the Cheb Basin, Czech Republic, where Pačes (1987) reported 54,200 mg/L sulfate. By comparison, 19,230 mg/L is the maximum reported in formation water.

In the Alberta Basin, sulfate is found in all formation water with a maximum of 6,440 mg/L, reflecting the presence of anhydrite in the more saline, deeper water. Where anhydrite is absent, as in the Beaufort-Mackenzie Basin, sulfate amounts are much lower (Hitchon et al., 1990). In addition to  $\text{SO}_4^{2-}$ , sulfur is also present in small amounts as  $\text{HSO}_4^-$  and various metal-sulfate complexes.

The acid gases hydrogen sulfide (H<sub>2</sub>S) and carbon dioxide (CO<sub>2</sub>) play an important part in water–rock reactions. Generally, the increased content of both acid gases in deeper strata most likely results from thermochemical reactions associated with organic matter in the rocks.

### 6.6.5 Minor Elements

Here, we classify eight elements as minor elements (Figure 24). If formation water has all major and minor elements determined (including organics), the ionic balance should be well within acceptable limits (an imbalance of < 5 percent), and probably approaching an imbalance of < 1 percent.

Group	1	2	3	4	5	6	7	8	9	10	11	12	13	14	15	16	17	18
Period 1	H																	He
2	Li	Be											B	C	N	O	F	Ne
3	Na	Mg											Al	Si	P	S	Cl	Ar
4	K	Ca	Sc	Ti	V	Cr	Mn	Fe	Co	Ni	Cu	Zn	Ga	Ge	As	Se	Br	Kr
5	Rb	Sr	Y	Zr	Nb	Mo	Tc	Ru	Rh	Pd	Ag	Cd	In	Sn	Sb	Te	I	Xe
6	Cs	Ba	La	Hf	Ta	W	Re	Os	Ir	Pt	Au	Hg	Tl	Pb	Bi	Po	At	Rn
7	Fr	Ra	Ac															

Figure 24 - Periodic Table showing the minor elements in formation water.

### Lithium (Li)

Lithium exhibits many similarities with the other alkali metals, with differences being due mainly to the small size of the Li atom and of the Li<sup>+</sup> ion. In the sedimentary environment, lithium is concentrated in shales and is lowest in carbonates. Table 21 shows the abundance of lithium in natural and produced water.

Table 21 - Lithium in natural and produced water.

Source	Lithium (mg/L)
River water (average)	0.003
Ocean water (average)	0.17
Groundwater (P25–P75)	< 0.01–0.05
<b>Produced water (P10–P25–P50–P75–P90)</b>	
Alberta Basin (N = 629)	1.9 – 4.2 – 10 – 35 – 62
USGS Conventional hydrocarbon (N = 3572)	1.0 – 2.0 – 4.3 – 11 – 32
USGS Unconventional hydrocarbon (N = 23)	Range 0.0076–4

Alberta Basin (Hitchon, 2023); USGS (Blondes et al., 2019)

During weathering, lithium is released from the primary minerals to the soil solution as Li<sup>+</sup>. It is then removed with the soil solution into the hydrosphere. The relative bonding force holding monovalent cations is commonly Cs > Rb > K > Na > Li (where Cs is cesium and Rb is rubidium). This means that when lithium is brought into solution by weathering reactions it tends to remain in the dissolved state and is thus one of the most conservative elements. Lithium accumulates in the oceans, where it is sorbed from sea

water by clays, manganese hydroxides, and glauconite. Shales are therefore relatively enriched in lithium.

The concentration of lithium in rainwater is about 0.0005 mg/L. In river water, the mean concentration is 0.003 mg/L, although the variation is very high geographically and temporally. Lithium in potable groundwater is in the general range 0.05 to 0.5 mg/L. In most low-salinity formation water the minimum lithium content is about 1.0 mg/L, with contents up to tens of milligrams per liter, rarely > 100 mg/L. Effectively, all lithium in formation water occurs as  $\text{Li}^+$ .

In the Alberta Basin, lithium was found in all formation water and ranges up to 140 mg/L. Higher lithium contents are associated with higher aquifer temperatures. The maximum so far reported is 505 mg/L in the Jurassic (Oxfordian) Smackover Formation, Texas, USA (Collins, 1974).

### Strontium (Sr)

The ionic radius of strontium lies between those of calcium and barium, and is smaller than lead. Strontium therefore replaces, and may be replaced by, these ions in many minerals. Examples include the isotopes strontianite,  $\text{Sr}(\text{CO}_3)$ ; witherite,  $\text{Ba}(\text{CO}_3)$ ; cerussite,  $\text{Pb}(\text{CO}_3)$ ; and aragonite,  $\text{Ca}(\text{CO}_3)$ . Note that calcite forms an isomorphous series with carbonates of smaller cations. However, the bulk of the strontium in the continental crust occurs as a trace element dispersed in rock-forming and accessory minerals. In the sedimentary environment, strontium is most abundant in carbonate rocks and to a lesser extent in shales. Table 22 shows the abundance of strontium in natural and produced water.

**Table 22** - Strontium in natural and produced water.

Source	Strontium (mg/L)
River water (average)	0.07
Ocean water (average)	7.6
Groundwater (P25–P75)	0.01–0.5
<b>Produced water (P10–P25–P50–P75–P90)</b>	
Alberta Basin (N = 628)	3.2 – 20 – 80 – 200 – 500
USGS Conventional hydrocarbon (N = 4,077)	8 – 26 – 100 – 370 – 920
USGS Unconventional hydrocarbon (N = 22)	Range 59–2,250

Alberta Basin (Hitchon, 2023); USGS (Blondes et al., 2019)

During weathering, strontium enters the hydrosphere as  $\text{Sr}^{2+}$  ions, and its concentration is controlled with respect to the solubility of either strontianite,  $\text{Sr}(\text{CO}_2)$ , or celestite,  $\text{Sr}(\text{SO}_4)$ . In the Alberta Basin, the range of pH at reservoir conditions (P05 = 5.4 to P95 = 7.1) means that the concentration of strontium is controlled by celestite, not strontianite. This is the case in most sedimentary basins.

In potable groundwater, the content of strontium is generally < 5.0 mg/L. In formation water, contents of strontium range up to 4,700 mg/L (Smackover Formation, Arkansas, USA; Collins, 1974).

Strontium was found in all formation water in the Alberta Basin. Higher amounts are associated with higher temperatures and higher salinity in deeper aquifers, with a corresponding increase in formation water in which celestite is close to saturation. Strontium occurs dominantly as  $\text{Sr}^{2+}$  with the balance mainly made up of the ion pair  $\text{SrHCO}_3^+$ .

### Barium (Ba)

Of the divalent positive ions, barium has the largest ionic radius, closely followed by that of radium. This means that isostructural replacement with other large cations such as lead and strontium is fairly common. The replacement of potassium and calcium also occurs, but not as often. The crustal abundance of barium (250 ppm) and strontium (260 ppm) are similar, but their different geochemical characteristics result in different distributions in both igneous and sedimentary rocks. For example, barium is enriched in shales, whereas strontium is enriched in carbonate rocks. Table 23 shows the abundance of barium in natural and produced water.

**Table 23 - Barium in natural and produced water.**

Source	Barium (mg/L)
River water (average)	0.02
Ocean water (average)	0.014
Groundwater (P25–P75)	0.014–0.10
MCL value	2
<b>Produced water (P10–P25–P50–P75–P90)</b>	
Alberta Basin (N = 530)	0.3 – 0.8 – 2.9 – 13 – 70
USGS Conventional hydrocarbon (N = 5282)	0.6 – 3.0 – 14 – 50 – 140
USGS Unconventional hydrocarbon (N = 750)	1.0 – 3.0 – 7.0 – 19 – 38

Alberta Basin (Hitchon, 2023); USGS (Blondes et al., 2019)

The amount of barium in solution can be controlled by the solubility of either barite ( $\text{BaSO}_4$ ) or witherite ( $\text{BaCO}_3$ ), with the former having the lower solubility product, and hence occupying a major part of the Eh-pH field. Because natural water is rarely free of sulfate, the solubility product of barite is commonly the limiting factor for the barium content of formation water.

In formation water, the amount of barium ranges from < 1.0 mg/L to about 1,000 mg/L. Reports of much greater amounts are generally from old analyses using analytical methods less accurate than modern methods. Mixing of water containing barium with sulfate-rich water may result in the precipitation of barite.

In the Alberta Basin, barium was below detection (0.04 mg/L) in 3.4 percent of the samples analyzed, with a maximum of 315 mg/L. Barium is unlike most other cations and showed no general increase in content with either increasing temperature or salinity. We may interpret this to show that the amount of barium in formation water is strictly controlled by the solubility with respect to barite. The main control on the solubility of witherite (a barium carbonate mineral) is pH. The information from other sedimentary

basins is not sufficient to confirm these relations. Barium mainly occurs as  $Ba^{2+}$  in formation water, with the balance dominated by the ion pair  $BaHCO_3^+$ .

### Bromine (Br)

Bromine is similar to chlorine in geochemical characteristics and behavior but is considerably less abundant. It occurs only as  $Br^-$  (bromide) and its ionic radius is too large to be incorporated in most minerals. It occasionally substitutes for  $OH^-$  groups in hydroxyl-bearing minerals such as hornblendes, micas, and clay minerals. The high content of bromine in pelagic clay suggests that adsorption onto clay minerals is an important geochemical characteristic. Table 24 shows the abundance of bromine in natural and produced water.

**Table 24 - Bromine in natural and produced water.**

Source	Bromine (mg/L)
River water (average)	0.02
Ocean water (average)	67
Groundwater (P25–P75)	0.01–0.05
<b>Produced water (P10–P25–P50–P75–P90)</b>	
Alberta Basin (N = 601)	23 – 51 – 98 – 190 – 450
USGS Conventional hydrocarbon (N = 2,274)	15 – 60 – 190 – 720 – 1,700
USGS Unconventional hydrocarbon (N = 24)	Range 74–1,070
Alberta Basin (Hitchon, 2023); USGS (Blondes et al., 2019)	

In the marine environment, bromine accumulates through evaporation. In most shallow groundwater, the content of bromine is low ( $10^{-2}$  to  $10^{-1}$  mg/L). In the Alberta Basin, bromine was found in all formation water with a range of 0.5 to 2,785 mg/L.

Both chlorine and bromine are conservative elements, and therefore the Br/Cl ratio is particularly useful in distinguishing water from different sources, or water that has been subjected to different processes. Many authors used the Br/Cl weight ratio, but the Br/Cl molar ratio is more precise. Using data from Nova Scotia (Canada), Briggins and Cross (1995) provided a set of water analyses to demonstrate this point and we use their original data in Table 25. To simplify the table, small amounts of minor and trace elements were not entered.

**Table 25** - Chemical composition and physical properties of different types of water to illustrate the use of the Br/Cl ratio for distinguishing salt sources.

	Rock salt aqueous leach	Seawater	Diluted seawater	Groundwater affected by road salt	Groundwater affected by seawater	Groundwater affected by formation water
Na	1,260	10,500	2,000	390	206	525
K	0.4	390	70.8	3.9	5.7	3.2
Mg	0.2	1,350	229	23.5	49	4.6
Ca	49.8	410	84	72.6	234	111
Cl	1,800	19,000	3,360	696	797	882
Br	0.16	65	10.2	0.13	2.43	3.10
HCO <sub>3</sub>	< 1	71	13	10	37	46
SO <sub>4</sub>	61	2,700	511	65	60	28
pH (lab)	5.9	8.1	6.9	5.9	7.3	7.7
Br/Cl molar ( $\times 10^{-3}$ )	0.04	1.5	1.3	0.08	1.4	1.6
Br/Cl wt. ( $\times 10^{-3}$ )	0.09	3.4	3.0	0.19	3.0	3.5
$\Sigma$ cations (mEq/kg H <sub>2</sub> O)	57.3	598.2	111.8	22.62	25.01	29.06
$\Sigma$ anions (mEq/kg H <sub>2</sub> O)	52.0	593.3	105.6	21.15	24.34	26.21
Imbalance (percent)	4.84	0.41	2.85	3.36	1.36	5.16
Ionic strength	0.056	0.625	0.118	0.025	0.032	0.031
TDS	3,172	34,430	6,269	1,273	1,404	1,613

From: Briggins and Cross (1995)

Possible sources of groundwater contamination specific to Nova Scotia, Canada are road salt, seawater intrusion, and bedrock formation salt. Contamination of groundwater by road salt is commonly first recognized by elevated contents of sodium and chloride, with chloride the better indicator because it is chemically more conservative. But the Br/Cl ratio of an aqueous leach of rock salt ( $\text{Br/Cl} \times 10^{-3} = 0.09$ ) is a better indicator for distinguishing contamination by road salt ( $\text{Br/Cl} \times 10^{-3} = 0.19$ ) from contamination by seawater ( $\text{Br/Cl} \times 10^{-3} = 3.0$ ) or contamination by formation water ( $\text{Br/Cl} \times 10^{-3} = 3.5$ ). However, to separate the latter two, other chemical indicators are required.

## Iodine (I)

Iodine occurs as a minor constituent in various minerals and very rarely forms separate minerals. In 6-fold coordination, its ionic radius is large, allowing for only limited substitution. Like the other halides, it is univalent in nature, but—unlike them—iodine may occur in more than one oxidation state. The highest average abundances are found in shales, where it is associated with organic matter. Table 26 shows the abundance of iodine in natural and produced water.

**Table 26** - Iodine in natural and produced water.

Source	Iodine (mg/L)
River water (average)	0.007
Ocean water (average)	0.056
Groundwater (range)	0–0.07
<b>Produced water (P10–P25–P50–P75–P90)</b>	
Alberta Basin (N = 606)	4 – 8 – 12 – 19 – 26
USGS Conventional hydrocarbon (N = 1,815)	1.9 – 4.3 – 12 – 26 – 57
USGS Unconventional hydrocarbon (N = 13)	Range 0.3–57

Alberta Basin (Hitchon, 2023); USGS (Blondes et al., 2019)

Fuge and Johnson (2015) reviewed the geochemistry of iodine with specific reference to human health and provided a diagram of the iodine cycle showing the ocean as the major reservoir in the iodine cycle. In seawater, iodine occurs as iodide ( $I^-$ ), iodate ( $IO_3^-$ ), and various organic-bound forms. According to Hem (1985), iodate is the most likely form of iodine in groundwater. The Eh-pH diagram for the system I-O-H shows that iodate is present under strongly oxidizing conditions over a wide range of pH.

The typical range of iodine in potable groundwater is  $< 1 \mu\text{g/L}$  to  $70 \mu\text{g/L}$ , although extreme values may be up to  $400 \mu\text{g/L}$  ( $0.4 \text{ mg/L}$ ). Some of the higher values are found in coastal areas where seawater invasion has occurred. Collins and Egleson (1967) determined bromine and iodine in formation water, rocks, and oil from Carboniferous strata in the Anadarko Basin (USA). They found up to  $519 \text{ mg/L}$  iodine in formation water, the maximum so far recorded. They noted that I/Br ratios in formation water were similar to present-day seaweeds and corals, thus confirming an organic origin for iodine in formation water.

In the Alberta Basin, iodine was found in effectively all formation water in which iodine was measured with a maximum of  $66 \text{ mg/L}$ . The distribution of iodine in formation water in the Alberta Basin differs from other element profiles in that the general statistical distribution is similar in all major stratigraphic units. In other sedimentary basins in which iodine is reported, the profiles are similar to those in the Alberta Basin in some cases; in other cases, the amount of iodine is lower, although few data are available from other basins.

## Boron (B)

Boron is one of the less abundant elements and the only non-metal in Group 13 of the Periodic Table. It shows many similarities to its neighbor, carbon, and its diagonal relative, silicon. In the sedimentary environment, boron is adsorbed by clay minerals, hence the relatively high content in shales. With few exceptions, boron occurs in nature in chemical combination with oxygen, that is, as borates ( $BO_3$  in a plane triangular group) or borosilicates ( $BO_4$  in a regular tetrahedron). Table 27 shows the abundance of boron in natural and produced water.

**Table 27 - Boron in natural and produced water.**

Source	Boron (mg/L)
River water (average)	0.01
Ocean water (average)	4.5
Groundwater (P25–P75)	0.05 – 0.2
<b>Produced water (P10–P25–P50–P75–P90)</b>	
Alberta Basin (N = 579)	4 – 7 – 12 – 30 – 100
USGS Conventional hydrocarbon (N = 1,361)	3 – 8 – 22 – 48 – 90
USGS Unconventional hydrocarbon (N = 11)	Range 0.063–0.56

Alberta Basin (Hitchon, 2023); USGS (Blondes et al., 2019)

In general, the content of boron in groundwater and formation water is likely controlled by saturation with respect to alkaline earth borates, although even some of these are soluble in hot water. Orthoboric acid dissociates at pH 9.24, so it is the usual form of boron found in formation water.

The content of boron in most groundwater is quite low (in the range 0.05 to 1.0 mg/L). In the Alberta Basin, for example, boron was found in all formation water in which it was measured (range 0.7 to 285 mg/L). Up to 500 mg/L is reported in formation water from Silurian strata in the Michigan Basin.

The US EPA has not designated an MCL value for boron although boron is a major contaminant in groundwater impacted by produced water in California, USA (Kharaka, 2016). Although boron is an essential element in plants, it is extremely toxic to many fruit trees and vegetables, even at relatively low concentrations of 0.5 mg/L. The acceptable maximum concentration of boron in irrigation water for grape vines, citrus trees, and other fruit trees is only 0.75 mg/L, and most produced water in California has boron concentrations that are more than 100 times the maximum acceptable value for boron-sensitive trees and vegetables (Kharaka, 2016).

### Silicon (Si)

The two most abundant elements in the continental crust are oxygen and silicon, though silicon is only a minor constituent in crustal water. Oxygen and silicon occur together predominantly as  $[\text{SiO}_4]$  tetrahedra, which are the building blocks of most silicate minerals. The weathering of silicate minerals is perhaps the most important process that gives rise to ions in the hydrosphere. The relative order in which the silicates weather is related to their relative thermodynamic stability. As a broad generalization, the order of ease of weathering is as follows.

olivine = anorthite > pyroxene > amphibole > biotite = albite > K-feldspar > muscovite > quartz

With slight modifications, this is the same order as the classic Bowen reaction series that all geologists learn in their first college-level geology course. Table 28 shows the abundance of silica in natural and produced water.

**Table 28** - Silica ( $\text{SiO}_4$ ) in natural and produced water.

Source	Silica (mg/L)
River water (average)	14
Ocean water (average)	6
Groundwater (P25–P75)	10–30
<b>Produced water (P10–P25–P50–P75–P90)</b>	
Alberta Basin (N = 533)	4.5 – 6.5 – 9.8 – 17 – 28
USGS Conventional hydrocarbon (N = 1,938)	7.1 – 14 – 39 – 110 – 190
Alberta Basin (Hitchon, 2023); USGS (Blondes et al., 2019)	
Silica is not reported in the unconventional hydrocarbon class	

From knowledge of the composition of the major rock-forming silicates and their relative order of weathering, hydrogeologists have come to recognize that most of the silicic acid ( $H_4SiO_4$ ) in groundwater is from weathering of common rock-forming aluminosilicate minerals such as feldspars and micas. Therefore, quartz is effectively a residual mineral.

The average silica content of river water is 14 mg/L. In most unpolluted groundwater, the silica content ranges from 5 to 50 mg/L. Carbonate brine may have high contents of silica: for example, 1,712 mg/L in groundwater from the Okavango Delta, Botswana, and 1,055 mg/L in Lake Magadi, Kenya. In thermal water, the content of silica depends on temperature, and in hotter water may approach 1,000 mg/L. There are few reports of silica in polluted groundwater: one of the highest amounts is 259 mg/L from groundwater contaminated by coal pile leachates.

In the Alberta Basin, silica was found in all formation water and was close to equilibrium with quartz. Silica generally increases with increased temperature and salinity, as expected. All the Si occurred as  $H_4SiO_4$ , with  $H_3SiO_4^-$  accounting for about  $10^{-3}$  percent of the analyzed Si. This is expected because all these formation water samples are saturated with respect to quartz.

## Nitrogen (N)

Nitrogen is a typical atmophile element (i.e., found chiefly or exclusively in the form of gas) and comprises about 78 percent of the terrestrial atmosphere. Nitrogen is capable of exhibiting all the formal integral oxidation states from -3 to +5. By convention, the oxidation state of nitrogen in a particular molecule or ion containing fluorine, oxygen, or hydrogen is defined as the formal charge per atom of nitrogen if every fluorine, oxygen, and hydrogen present carries a charge of -1, -2, and +1, respectively. At Earth conditions, the most abundant valence states are 0 (74.9 percent as  $N_2$ ), -3 (25.1 percent  $NH_3$ , ammonium), and +5 (trace, as  $NO_3^-$  nitrates). In sedimentary rocks, the highest total nitrogen is found in shales. Table 29 shows the abundance of nitrogen in natural and produced water.

**Table 29** - Nitrogen in natural and produced water.

Source	Nitrogen (mg/L)
River water (average)	0.25 (as $NO_3^-$ )
Ocean water (average)	3.0 (as $NO_3^-$ )
Groundwater (P25–P75)	0.5 – 4.0 (as $NO_3^-$ )
MCL value	10 (as N)
<b>Produced water (P10–P25–P50–P75–P90) (as <math>NH_3</math>)</b>	
Alberta Basin (N = 255)	32 – 52 – 93 – 210 – 400
USGS Conventional hydrocarbon (N = 882)	12 – 27 – 51 – 120 – 230
USGS Unconventional hydrocarbon (N = 11)	Range 625 – 4,000
Alberta Basin (Hitchon, 2023); USGS (Blondes et al., 2019)	

Although the total amount of nitrogen present as nitrate is small compared to the total global nitrogen, effectively all of it is in the hydrosphere. Because other nitrogen compounds (including ammonium ion, nitrite, and organic nitrogen) may be present in

natural water, the specific reporting of the analysis as  $\text{NO}_3^-$  is often masked under *total nitrogen as  $\text{NO}_3$* . It is important to notice the manner in which nitrate, nitrite, and the ammonium ion are reported in water analyses because they are often given as *equivalent parts per million N*, and conversion to nitrate or ammonium is required for entry into programs such as SOLMINEQ.88.

The dominant aqueous species of nitrogen in surface water, groundwater, and formation water are nitrate under oxidizing conditions and ammonium under reducing conditions. Therefore, nitrogen typically occurs as ammonium in formation water.

The average river water has about 1.0 mg/L nitrate-nitrogen; the range of nitrate-nitrogen concentration in potable water is <0.1 to 10 mg/L. When agricultural pollution is suspected, the content of nitrate-nitrogen may be of the order of tens of milligrams and evaluation of the stable isotopes of  $^{15}\text{N}$  and  $^{18}\text{O}$  in nitrate can often deduce the source of the pollution. Ammonium commonly occurs in polluted water. A particularly high amount (7,900 mg/L) was found in a well near an abandoned tannery at Woburn, Massachusetts, USA. High amounts are also found in some thermal springs and water associated with ultrabasic rocks.

In the Alberta Basin, ammonium was determined in 255 formation water samples (range 5.6 to 1,150 mg/L). The content of ammonium is two to three times higher in hotter, more saline formation water. The highest ammonium content measured in formation water is 1,625 mg/L. Ammonium ( $\text{NH}_3$ ) is the dominant (>99 percent) form of nitrogen in formation water, with the balance being  $\text{NH}_4\text{OH}$ .

### 6.6.6 Trace Elements

Trace elements in formation water comprise the rest of the Periodic Table not classified as major or minor. Trace elements are not routinely determined—but perhaps some should be. We selected the elements to be considered here on the basis of their importance in the generation of commercial Mississippi Valley-type ore deposits (lead and zinc), their health effects (fluorine), their toxicity (arsenic and selenium), and their common occurrence in formation water. All the elements highlighted in the Periodic Table below (Figure 25) are discussed in *Formation Water Geochemistry* (Hitchon, 2023).

Group	1	2	3	4	5	6	7	8	9	10	11	12	13	14	15	16	17	18
Period 1	H																	He
2	Li	Be											B	C	N	O	F	Ne
3	Na	Mg											Al	Si	P	S	Cl	Ar
4	K	Ca	Sc	Ti	V	Cr	Mn	Fe	Co	Ni	Cu	Zn	Ga	Ge	As	Se	Br	Kr
5	Rb	Sr	Y	Zr	Nb	Mo	Tc	Ru	Rh	Pd	Ag	Cd	In	Sn	Sb	Te	I	Xe
6	Cs	Ba	La	Hf	Ta	W	Re	Os	Ir	Pt	Au	Hg	Tl	Pb	Bi	Po	At	Rn
7	Fr	Ra	Ac															

**Figure 25** - Periodic Table showing selected trace elements analyzed in formation water from the Alberta Basin.

### Rubidium (Rb)

Although rubidium is widely distributed, there are no minerals that are purely rubidium-containing. It is found most commonly in potassium minerals such as feldspar and in carnallite in some evaporite deposits. In sedimentary environments, rubidium is highest in shales. Table 30 shows the abundance of rubidium in natural and produced water.

**Table 30** - Rubidium in natural and produced water.

Source	Rubidium (mg/L)
River water (average)	0.001
Ocean water (average)	0.12
Groundwater (P25–P75)	-
<b>Produced water (P10–P25–P50–P75–P90)</b>	
Alberta Basin (N = 96)	0.09 - 0.18 - 2.4 - 4.9 - 11
USGS Conventional hydrocarbon (N = 320)	0.10 - 0.26 - 0.42 - 1.6 - 4.2
USGS Unconventional hydrocarbon (N = 11)	Range 2.1–27

Alberta Basin (Hitchon, 2023); USGS (Blondes et al., 2019)

Rubidium enters the hydrological cycle as  $\text{Rb}^+$ . Its route through the hydrological cycle is poorly understood. In the Alberta Basin, rubidium ranged from detection (0.09 mg/L) to 11 mg/L, the maximum found to date in formation water.

### Fluorine (F)

Elemental fluorine does not occur naturally in the free state. The most reactive form in which fluorine is found in nature as hydrogen fluoride (HF) in some volcanic gases. Fluorine is the lightest of the halogens; further, fluorine oxidizes water. Its ionic size is close to that of  $\text{OH}^-$  ( $\text{F}^-$  1.33Å versus  $\text{OH}^-$  1.4Å), so it is an isomorphous replacement of  $\text{OH}^-$  in many of the fluorine-bearing minerals. In sedimentary rocks, the general order of abundance of fluorine is shale > carbonates > sandstone. Table 31 shows the abundance of fluorine in natural and produced water.

**Table 31** - Fluorine in natural and produced water.

Source	Fluorine (mg/L)
River water (average)	0.001
Ocean water (average)	1.3
Groundwater (P25–P75)	0.05–0.5
SMCL value	2.0
<b>Produced water (P10–P25–P50–P75–P90)</b>	
Alberta Basin (N = 444)	0.47 - 0.74 - 1.2 - 2.0 - 3.3
USGS Conventional hydrocarbon (N = 228)	0.56 - 1.0 - 2.1 - 6.0 - 9.7
USGS Unconventional hydrocarbon (N = 11)	Range 2.9–17

Alberta Basin (Hitchon, 2023); USGS (Blondes et al., 2019)

Fluorine is the most electronegative of all the elements and in dilute solutions it occurs as  $F^-$  ions. Formation water with  $Ca < 100$  mg/L has 95 percent of the fluorine as  $F^-$ ; even formation water with  $Ca$  100 to 200 mg/L still has 80 percent as  $F^-$ . As salinity increases,  $MgF^+$  complexes become significant. Although aluminum, uranium, and vanadium form ion pairs and complexes with fluorine, the low amounts of these elements in most formation water means the content of fluorine is controlled almost solely by the concentration of calcium.

In average river water, fluorine is about 0.001 mg/L and the range in potable groundwater is  $< 0.05$  to 2 mg/L. However, in several parts of the world, drinking water may contain up to 10 mg/L F, resulting in endemic fluorosis. In unpolluted shallow groundwater, the content of fluorine is generally only a few milligrams per liter but can be up to 26 mg/L as found, for example, in the Piceance Creek Basin, Colorado, USA (Kimball, 1984). In the Alberta Basin, fluorine was found in all analyzed formation water with amounts ranging from 0.01 to 11.7 mg/L.

## Lead (Pb)

Among the so-called heavy elements with atomic number greater than 60, lead is the most abundant in the Earth's crust. This is due, in part, to the high amounts of lead resulting from radioactive decay of  $^{238}\text{U}$ ,  $^{235}\text{U}$ , and  $^{232}\text{Th}$  (thorium). Lead is a chalcophile element, and most commonly occurs as galena ( $\text{PbS}$ ), although the major portion of lead in the crust is camouflaged in silicate minerals. In the sedimentary environment, lead may be strongly adsorbed onto clay minerals, hence its higher abundance in shales. Table 32 shows the abundance of lead in natural and produced water.

**Table 32** - Lead in natural and produced water.

Source	Lead (mg/L)
River water (average)	0.001
Ocean water (average)	0.000,002
Groundwater (P25–P75)	0.0001 - 0.001
MCL value	0.015
<b>Produced water (P10–P25–P50–P75–P90)</b>	
Alberta Basin [N = 533]	[21 percent $< 0.02$ ] - 0.10 - 0.60 - 1.7 - 7.0 [Max. 360]
USGS Conventional hydrocarbon (N = 59)	0.0009 - 0.0021 - 0.0033 - 0.022 - 0.30 [Max. 100]
USGS Unconventional hydrocarbon (N = 7)	Range 0.0063 - 1.2

Alberta Basin (Hitchon, 2023); USGS (Blondes et al., 2019)

Lead enters the hydrological cycle as  $Pb^{2+}$  ions. Three situations tend to maintain low concentration in natural water, the:

1. very low solubility of lead hydroxy carbonates, phosphates, and sulfide;
2. adsorption of lead on organic surfaces; and
3. co-precipitation of lead with manganese dioxide.

This is extremely fortunate in view of the toxicity of lead in the biosphere.

In most river water and shallow groundwater, the content of lead is in the general range of  $10^{-3}$  to  $10^{-2}$  mg/L. The maximum for lead in potable groundwater is usually set at 0.015 mg/L. In natural water, the highest amount of lead is found in chloride-rich saline formation water in sedimentary basins. In the Alberta Basin, lead was below detection (0.02 mg/L) in 21 percent of the analyzed formation water samples and ranged up to 360 mg/L—the highest content of lead found to date in any formation water. In formation water, lead occurs predominantly as chloride complexes.

### Zinc (Zn)

Zinc occurs almost exclusively in compounds with other elements. Using a comparison of effective ionic radius, ionization potential, and electronegativity,  $Zn^{2+}$  shows a closer relation to  $Fe^{2+}$  than to  $Mg^{2+}$ . In igneous and sedimentary rocks, zinc occurs primarily in the structure of silicates and oxides and in sphalerite ( $ZnS$ ). Zinc is adsorbed onto clay minerals, iron oxides, and organic matter, hence the higher abundances in shales. Table 33 shows the abundance of zinc in natural and produced water.

**Table 33** - Zinc in natural and produced water.

Source	Zinc (mg/L)
River water (average)	0.02
Ocean water (average)	0.0004
Groundwater (P25–P75)	0.0016–0.02
SMCL value	5
<b>Produced water (P75–P90)</b>	
Alberta Basin [N = 635]	[52 percent < 0.02] - 0.84 - 4.7 [Maximum 360]
USGS Conventional hydrocarbon [N = 306]	0.01 - 0.11 - 1.0 - 2.0 - 6.5 [Maximum 250]
USGS Unconventional hydrocarbon (N = 7)	Range 0.13–23

Alberta Basin (Hitchon, 2023); USGS (Blondes et al., 2019)

Only sulfide, phosphate, oxide, and carbonate anions form low solubility zinc compounds. The ion  $Zn^{2+}$  is present at pH values less than about 7.5 under oxidizing conditions. At about pH 2.1, sphalerite dissolves to  $Zn^{2+}$ . Smithsonite ( $ZnCO_3$ ) is stable over only a narrow pH range and disappears altogether at higher  $pCO_2$  values.

In potable groundwater, the abundance of zinc ranges from that of rain water to about 1.0 mg/L. Higher amounts of zinc (up to 700 mg/L) are found in water from special situations such as acid mine drainage.

Zinc was below detection (0.02 mg/L) in slightly more than half the formation water samples analyzed from the Alberta Basin, with a maximum of 360 mg/L. For the data above detection, zinc content increases with increased temperature and salinity. The range and distribution of zinc in the deeper, hotter, and more saline formation water is similar to that found in the Smackover Formation, Texas, USA—the only other basin with enough data to allow comparison. The maximum reported thus far in formation water is 575 mg/L from the Smackover Formation.

Zinc is adsorbed onto some iron minerals, clay minerals, calcite, and amorphous aluminosilicates. Because shales have almost an order of magnitude more zinc than carbonate rocks and sandstones, one might expect zinc in formation water to be sourced from shales. Yet this does not appear to be the case, at least for the data examined so far. Interestingly, the independent nature of zinc was first observed using factor analysis with a small data set from Alberta (Hitchon et al., 1971) and it appears that the independent nature of zinc can also be observed in the larger data set used in this book.

### Iron (Fe)

Iron is the second most abundant metal in the continental crust after aluminum. Its geochemistry is governed by the ease with which it changes valence states from  $\text{Fe}^{2+}$  (ferrous) to  $\text{Fe}^{3+}$  (ferric) and the reverse. The ionic radius of  $\text{Fe}^{2+}$  (0.86Å) and  $\text{Mg}^{2+}$  (0.80Å) are similar and this allows considerable exchange in ferromagnesian minerals.

There are important redox reactions with iron in the sedimentary environment. Atmospheric oxygen reacts with primary ferrous minerals to form ferric oxides. In sediments, organic carbon is utilized by bacteria to reduce ferric oxides to ferrous compounds and dissolved sulfate to sulfide. Hence, iron sulfides may form. With low sulfide and high carbonate contents, siderite  $\text{FeCO}_3$  may form. If both sulfide and carbonate are low and silica is abundant, then glauconite may form. In addition to these possible reactions, iron is adsorbed onto clay minerals, hence the higher abundance in shales and pelagic clay. Table 34 shows the abundance of iron in natural and produced water.

**Table 34 - Iron in natural and produced water.**

Source	Iron (mg/L)
River water (average)	0.04
Ocean water (average)	0.000,06
Groundwater (P25–P75)	0.01 - 0.5
SMCL value	0.3
<b>Produced water (P10–P25–P50–P75–P90)</b>	
Alberta Basin (N = 329)	0.08 - 0.14 - 0.32 - 1.1 - 4.4
USGS Conventional hydrocarbon (N = 12,889)	1.0 - 3.0 - 15 - 59 - 160
USGS Unconventional hydrocarbon (N = 1,369)	5 - 11 - 24 - 44 - 110
Alberta Basin (Hitchon, 2023); USGS (Blondes et al., 2019)	

Weathering of ferromagnesian minerals releases iron into the hydrological cycle as  $\text{Fe}^{2+}$ . Most of the iron is probably rapidly re-deposited as pyrite, siderite, or iron

hydroxides, depending on the redox conditions and the presence of other cations and anions. In groundwater, iron most commonly occurs as  $\text{Fe}^{2+}$ .

The content of iron in potable groundwater ranges from less than that of the average river water (0.04 mg/L) to about 0.3 mg/L. Several iron-rich springs in western Canada, have iron concentration up to 450 mg/L, originating from sulfide mineralization in Devonian or Ordovician black shales (van Everdingen et al., 1985). Amounts up to several thousand milligrams per liter occur in some polluted groundwater; for example, close to 8,000 mg/L is found in groundwater contaminated with coal pile leachate at the Savannah River Site, North Carolina, USA. Contamination by tailings fluids from metal mining operations also commonly result in high iron content.

Hitchon (2000) showed that many formation water samples from wellheads, separators, and treaters in the Alberta Basin were contaminated by “rust,” compared to lower amounts in samples of formation water from drill stem tests. Here, we report iron in all formation water, regardless of source.

In the Alberta Basin, iron ranged from below detection (0.01 mg/L) to 87 mg/L. The iron content of formation water generally increases with increasing temperature and salinity.

The source of iron in formation water from drill stem tests is mainly from pyrite (as evidenced by iron–arsenic–selenium–chloride relations). Although we can rule out a contribution from rust, there could be a contribution from other sources that may be difficult to identify. Formation water from producing wells, separators, and treaters comes from a quite different environment where conditions are more oxidizing and bacterial action may have occurred, in addition to chemicals added by the operating company.

Siderite ( $\text{FeCO}_3$ ) has been reported as scale in wells in various parts of the world, and often with very small amounts of iron reported in an analysis of the produced water. For example, one analysis from a well with active siderite scale showed only 1 mg/L Fe. Calculations showed that saturation with respect to siderite at reservoir conditions occurs with as little as 0.68 mg/L Fe. This might have been reported as *trace* by some analysts, thereby giving a false impression of the scaling potential for siderite.

## Manganese (Mn)

Manganese is intermediate in its terrestrial abundance between a major and a minor element. Only one stable isotope of manganese ( $^{55}\text{Mn}$ ) occurs naturally. Manganese occurs in minerals as  $\text{Mn}^{2+}$ ,  $\text{Mn}^{3+}$ , or  $\text{Mn}^{4+}$ —sometimes with more than one valence state in the same mineral.  $\text{Mn}^{2+}$  (0.92Å) ion substitutes for ferrous iron  $\text{Fe}^{2+}$  (0.86Å) and  $\text{Mn}^{2+}$  (0.80Å) in igneous and metamorphic minerals (all in 6-fold coordination) and may also substitute for  $\text{Ca}^{2+}$  (1.08Å). At lower temperatures in sedimentary and weathering environments, minerals containing  $\text{Mn}^{3+}$  and  $\text{Mn}^{4+}$  occur almost exclusively because they are formed at a higher oxygen fugacity than found in igneous and metamorphic environments: for

example, fine-grained crypto-crystalline or poorly crystallized manganese dioxides and oxyhydroxides. In the sedimentary environment, the highest abundance, by far, is in pelagic clays, followed almost equally by carbonate rocks and shales. Table 35 shows the abundance of manganese in natural and produced water.

**Table 35 - Manganese in natural and produced water.**

Source	Manganese (mg/L)
River water (average)	0.007
Ocean water (average)	0.0003
Groundwater (P25–P75)	<< 0.01–0.01
SMCL value	0.05
<b>Produced water (P10–P25–P50–P75–P90)</b>	
Alberta Basin (N = 437)	0.09 - 0.19 - 0.62 - 1.9 - 5.0
USGS Conventional hydrocarbon (N = 658)	0.14 - 0.40 - 1.2 - 5.0 - 37
USGS Unconventional hydrocarbon (N = 11)	Range 0.0015–0.029
Alberta Basin (Hitchon, 2023); USGS (Blondes et al., 2019)	

Under most normal weathering conditions, manganese enters the hydrological cycle as  $Mn^{2+}$  and a large part of the Eh–pH space is occupied by this ion. The oxides and oxyhydroxides of manganese are commonly stable at higher pH values, except under very oxidizing conditions when  $Mn^{2+}$  is the preferred species (present as  $Mn(OH)_3^-$ ). In the system Mn–C–S–O–H, the dominant species is still  $Mn^{2+}$ , with the appearance of rhodochrosite,  $MnCO_3$ , and alabandite ( $MnS$ ). For slightly different activities of the carbonate species, the field of rhodochrosite may be much larger.

Groundwater and formation water are generally in the pH range 4 to 8, so manganese will occur as  $Mn^{2+}$ . Even under anoxic conditions, most natural water is undersaturated with respect to  $MnCO_3$ ,  $Mn(OH)_2$ , and  $MnS$ . This means that for most groundwater and formation water the concentration of  $Mn^{2+}$  is controlled by saturation with respect to rhodochrosite.

The concentration of manganese in groundwater ranges from that of average river water (0.007 mg/L) to about 10 mg/L. The maximum recommended (SMCL) manganese content in drinking water is generally set at 0.05 mg/L (Table Box 2-1). Manganese is one of the major geogenic contaminants in groundwater that results from reactions of water with geological materials in aquifers in the USA and many other countries (Erickson et al., 2021). Higher manganese contents may be found under a variety of circumstances including, but not limited to

- contamination by acid-mine drainage;
- very low pH for any of several reasons; and
- groundwater dissolving iron–manganese oxyhydroxides and then penetrating underlying strata where the conditions allow for precipitation of authigenic pyrite (marcasite), siderite, and rhodochrosite (Saunders and Swann, 1992).

At increased ionic strength, the formation of ion pairs and complexes may occur including  $\text{MnCl}^+$ ,  $\text{MnCl}_2$ ,  $\text{MnCl}_3^-$ ,  $\text{MnCl}_4^{2-}$ ,  $\text{MnHCO}_3^+$ ,  $\text{MnSO}_4$ ,  $\text{MnHPO}_4$ ,  $\text{MNOH}^+$ , and organic complexes with oxalate and succinate.

In the Alberta Basin, manganese ranges from the detection limit (0.005 mg/L) to 52 mg/L. There is a general increase in manganese content in formation water with increased temperature and salinity, accompanied by slightly lower SI values for rhodochrosite. Manganese is generally more abundant in formation water in the conventional hydrocarbon class of the culled USGS National Produced Waters Geochemical Database (Blondes et al., 2019), for reasons that are not clear.

### Arsenic (As)

Arsenic is a chalcophile element. In nature, it is found most commonly in compounds and in a formal oxidation state of 5 (arsenates) or 3 (arsenites). Arsenic-containing minerals are predominantly arsenates (60 percent) and sulfides (20 percent). Arsenic is adsorbed by hydrous iron oxide and co-precipitated with sulfide minerals in reducing muds on the bottom of water bodies. Therefore, the highest abundances in the sedimentary environment are in shales. These processes tend to keep the arsenic level low in the hydrosphere. Table 36 shows the abundance of arsenic in natural and produced water.

**Table 36** - Arsenic in natural and produced water.

Source	Arsenic (mg/L)
River water (average)	0.002
Ocean water (average)	0.0017
Groundwater (P25–P75)	0.0005 - 0.006
MCL value	0.010
<b>Produced water (P75–P90)</b>	
Alberta Basin (N = 535)	[72 percent < 0.13] - 0.76 - 2.9 [Max. 87]
USGS Conventional hydrocarbon (N = 51)	0.0008 - 0.0019 - 0.01 - 0.063 - 0.32
USGS Unconventional hydrocarbon (N = 11)	Range 0.063 - 0.57
Alberta Basin (Hitchon, 2023); USGS (Blondes et al., 2019)	

In acidic water, arsenic occurs as orthoarsenic acid ( $\text{H}_3\text{AsO}_4$ ) and the monovalent arsenate anion ( $\text{H}_2\text{AsO}_4^-$ ). In alkaline water (pH 7 to 11), the monovalent arsenate anion is replaced by the divalent arsenate anion ( $\text{HAsO}_4^{2-}$ ). These arsenic species are analogous to orthophosphoric acid and the phosphate species and to orthoboric acid and borates. Reducing conditions favor the uncharged arsenite anion, arsenious acid ( $\text{H}_3\text{AsO}_3$ ) and its anions (arsenites).

In the presence of sulfur, and under reducing conditions, there are Eh-pH fields for two arsenical sulfides, and a very small Eh-pH field for native arsenic under extreme reducing and basic conditions. These changes in the oxidation state of arsenic are important in studies of groundwater and formation water. Organo-arsenic compounds are found in

special situations in nature. Appelo and Postma (1993) included several examples of the oxidation of pyrite in an aquifer and the consequent release of arsenic to groundwater, and of the reduction of nitrate; Deutsch (1997) specifically stressed the importance of redox changes in the geochemistry of arsenic and discussed the methods that can be used in remediation of arsenic-contaminated soils or aquifers.

In river water, the maximum content of arsenic is about 0.005 mg/L. Due to its toxicity, the maximum content of arsenic in drinking water is set at 0.01 to 0.05 mg/L, depending on the jurisdiction. There is abundant literature, much written in the past decade, on the major problems with high-arsenic groundwater in Argentina, Bangladesh, Chile, Inner Mongolia, and Mexico, among other places. High contents of arsenic are also found in groundwater associated with sources of natural sulfide minerals, often exacerbated by mining activities.

In the Alberta Basin, arsenic was below detection (0.13 mg/L) in 72 percent of the formation water samples, with a maximum of 86.5 mg/L. Hotter, more saline formation water has higher amounts compared with other formation water in the basin. In the conventional hydrocarbon class of the culled USGS data set, there were fifty-one values for arsenic (range 0.0001 to 7 mg/L, median 0.01 mg/L).

The wealth of data on arsenic in formation water in the Alberta Basin, compared with other sedimentary basins, made it possible to study this toxic element and selenium with respect to CO<sub>2</sub> storage (Hitchon & Bachu, 2017).

### Selenium (Se)

In elements of the sulfur sub-group, the outer electronic configuration approaches those of the next noble gas. They are increasingly metallic in character with progression down the group and characteristically chalcophile in nature. Selenium commonly substitutes for sulfur in sulfide minerals, although it also forms independent metallic selenide minerals. In the sedimentary environment, selenium is concentrated in shales. Table 37 shows the abundance of selenium in natural and produced water.

**Table 37 - Selenium in natural and produced water.**

Source	Selenium (mg/L)
River water (average)	0.000,06
Ocean water (average)	0.000,13
Groundwater (P25–P75)	0.000,03 - 0.0008
MCL value	0.05
<b>Produced water (P75–P90)</b>	
Alberta Basin (N = 534)	[72 percent < 0.11] - 0.60 - 3.4 [Max. 44]
USGS Conventional hydrocarbon (N = 78)	0.010 - 0.036 - 0.056 - 0.48 - 1.3
Alberta Basin (Hitchon, 2023); USGS (Blondes et al., 2019)	
Selenium is not reported in the unconventional hydrocarbon class	

During weathering processes, selenium is oxidized over a wide pH range from selenide (Se<sup>2-</sup>) to selenate (SeO<sub>4</sub><sup>2-</sup>), which is an especially important species because of a link to adverse health effects. The selenate ion is analogous to the sulfate ion, highly soluble,

and not adsorbed onto iron oxyhydroxide surfaces. At intermediate redox levels, selenites ( $\text{SeO}_3^{2-}$ ) are the stable species. Under strongly reducing conditions, Se (native),  $\text{H}_2\text{Se}$  (selenium hydride), and  $\text{HSe}^-$  occur; the latter two are analogous to  $\text{H}_2\text{S}$  and  $\text{HS}^-$ .

Selenium most commonly occurs camouflaged in other minerals. Calcium and sodium selenites are soluble; iron selenites are nearly insoluble. Selenite ions are therefore very rapidly adsorbed by iron oxyhydroxides. At high concentrations, selenium is toxic to most organisms, so the very important process of *de-poisoning* the oceans is biologically vital.

In trace amounts, selenium is essential in the diet of both humans and animals. Edmunds and Smedley (1996) reviewed the geochemistry of selenium with respect to health and noted cases of both selenium toxicity and selenium deficiency in humans. They suggested that remoteness from the sea may lead to selenium deficiency. Because of its general toxicity, most jurisdictions have a maximum acceptable limit for selenium in drinking water (usually 0.01  $\mu\text{g/L}$ ).

Selenium enrichment in shales, coupled with weathering under acidic conditions, can lead to ecological problems such as at the Kesterson National Wildlife Refuge in California, USA, where selenium reached 3.5 mg/L in an ephemeral stream (Presser & Barnes, 1984).

Deutsch (1997) noted that the mobility of contaminant species such as selenium that are often present only in trace amounts ( $< 1.0$  mg/L) will be affected primarily by adsorption/desorption processes. Because the anionic form dominates in groundwater and formation water, the presence of a strong anion adsorber, such as ferrihydrite ( $\text{Fe}_{10}\text{O}_{15} \cdot 9\text{H}_2\text{O}$ ) has the greatest impact on movement of selenium in the environment. In the absence of ferrihydrite and other iron oxyhydroxides, clay minerals provide the most important exchange sites. Further, pH has a major effect on the amount of Se(IV) that can be adsorbed onto clay minerals, especially at near-neutral conditions. Under alkaline conditions, however, selenium will be mobile in the environment if clay minerals are the only solids available to retard movement.

In the Alberta Basin, selenium was below detection (0.11 mg/L) in 72 percent of the formation water samples, with a maximum of 44 mg/L. Hotter, more saline formation water has higher amounts of selenium compared to other formation water in the basin. In the conventional hydrocarbon class of the culled USGS data set there were seventy-eight values for selenium (range 0.0008 to 33 mg/L, median 0.056 mg/L).

### 6.6.7 Mineral Saturation Indices

So far, we have been concerned with the absolute values of elements and ions in produced water, albeit using statistics. This information can be used to determine more about the trends due to water-rock reactions as temperature and salinity increase with depth in sedimentary basins. However, there are specific limitations to the interpretation

of these trends. First, the trends are specific to each sedimentary basin, so to make use of the USGS data set requires separation of the data into the various basins. Second, the trends only show the direction—not the degree—of water-rock reactions.

Table 38 shows the input data for the Alberta Basin using the P-values previously described. Note the order of values for  $\text{HCO}_3$  has been reversed to reflect the field situation, that is, decreasing  $\text{HCO}_3$  with increasing salinity. Because the laboratory determination of pH reflects a variety of effects that may alter the pH but are unrelated to the composition trends, a neutral pH (7.00) was used for all calculations. Despite the statistically derived nature of the data, the analytical imbalances are generally quite good.

**Table 38** - Chemical composition (mg/L) and physical properties of formation water based on statistical distribution of the Alberta Basin data set.

Analytical values	P10	P25	P50	P75	P90
Li	1.9	4.2	10	35	62
Na	4,100	8,800	18,000	36,000	53,000
K	27	59	170	1,000	2,900
Mg	22	90	340	950	2,000
Ca	65	230	1,100	4,500	17,000
Sr	3.2	20	80	200	500
Ba	0.4	1.0	3.1	13	70
F	0.47	0.74	1.2	2.0	3.3
Cl	5,800	14,000	32,000	73,000	120,000
Br	23	51	98	190	450
I	4	8	12	19	26
$\text{HCO}_3$	1,700	800	410	222	125
$\text{SO}_4$	13	31	110	590	1,200
$\text{SiO}_2$	4.5	6.5	9.8	17	28
$\text{NH}_3$	32	52	93	210	400
B	4	7	12	28	100
TDS (at ignition)	10,060	22,970	50,960	113,800	190,270
pH (laboratory)	7.0	7.0	7.0	7.0	7.0
Specific gravity (15.56 °C)	1.0	1.0	1.0	1.1	1.1
Refractive index (25 °C)	1.3	1.3	1.3	1.4	1.4
Formation temperature (°C)	20	25	35	54	79
$\Sigma$ cations (meq/L)	186	414	920	2,148	4,215
$\Sigma$ anions (meq/L)	194	419	962	2,345	4,222
Analytical imbalance (percent)	-2.05	-0.64	-2.22	-4.37	-0.07

Table 39 shows calculations using SOLMINEQ GW (Hitchon et al., 1999b). To compensate for loss of  $\text{CO}_2$  as the produced water was brought to the surface,  $\text{CO}_2$  was added to the analysis to reach equilibrium with calcite. Aluminum was added to reach equilibrium with illite (the commonest clay mineral in the Alberta Basin rocks), thus allowing calculation of the saturation index (SI) of the other clay minerals and feldspars (these processes are described in Hitchon, 2023).

**Table 39** - Calculated values of chemical composition (mg/L) and physical properties of formation water based on statistical distribution of the Alberta Basin data set.

	P10	P25	P50	P75	P90
<b>Calculated values</b>					
Σ cations (meq/kg H <sub>2</sub> O)	182.51	396.62	841.72	1,775.50	3,078.10
Σ anions (meq/kg H <sub>2</sub> O)	188.27	398.74	875.87	1,937.11	3,059.62
Imbalance (percent)	-1.55	-0.27	-1.99	-4.35	0.30
Ionic strength	0.1877	0.4085	0.9091	2.0548	3.7066
TDS	11,794	24,138	52,402	116,920	197,890
<b>SOLMINEQ GW results</b>					
Saturation with respect to:	Calcite and illite at 20 °C	Calcite and illite at 25 °C	Calcite and illite at 35 °C	Calcite and illite at 54 °C	Calcite and illite at 79 °C
Al added (mg/L)	0.000744	0.000628	0.001006	0.000880	0.000958
pH	6.96 (at 20 °C)	6.75 (at 25 °C)	6.39 (at 35 °C)	6.00 (at 54 °C)	5.68 (at 79 °C)
<b>SI (Saturation Index)</b>					
Calcite	•	•	•	•	•
Dolomite	0.91	0.95	0.96	1.11	1.19
Strontianite	-0.85	-0.67	-0.80	-1.09	-1.31
Witherite	-2.61	-2.82	-3.05	-3.05	-2.89
Anhydrite	-3.70	-3.05	-2.07	-0.84	0.01
Barite	-0.74	-0.36	0.18	0.99	1.58
Celestite	-3.22	-2.38	-1.58	-0.74	-0.20
Halite	-3.40	-2.77	-2.18	-1.56	-1.14
Fluorite	-1.79	-1.10	-0.40	-0.10	-0.11
Quartz	-0.11	0.01	0.12	0.25	0.33
Albite	-0.02	0.25	0.38	0.47	0.67
Anorthite	-6.48	-6.31	-5.94	-5.34	-4.27
K-feldspar	0.71	0.88	0.99	1.33	1.49
Gibbsite	1.65	1.29	0.56	-1.01	-1.20
Illite	•	•	•	•	•
Kaolinite	2.95	2.61	2.25	1.56	0.99
Na-smectite	1.06	0.98	0.87	0.55	0.32
• = calculated at equilibrium					
SI values indicate oversaturated throughout the basin					
SI values at equilibrium (+0.5 to -0.5)					
SI values indicate undersaturated throughout the basin					

## 6.7 Inorganic Chemical Composition of Produced Water: A Field Scale Perspective

Comprehensive reports on the inorganic chemical composition of produced water first published by Hunt (1879) overwhelmingly come from wells in individual oil and gas fields in the USA and other countries including Canada and several countries in Europe. Over the last 50 years, the data were generally quite detailed and reported inorganic, organic, and isotopic composition of produced water. Thus, the data are more useful in geochemical modeling to investigate the origin of formation water and water-mineral interactions than basin-wide studies that provide averaged values (e.g., Kharaka & Hanor, 2014). Specifically, detailed data from individual petroleum fields are more useful in identifying the source of pollution in contaminated groundwater.

### 6.7.1 Water Salinity

Kharaka and Hanor (2014), Neff (2011), and Kharaka and others (2020) showed that the salinity of produced water in sedimentary basins varies by approximately three orders of magnitude from less than 3,000 mg/L in shallow meteoric flow regimes to more than 400,000 mg/L in evaporite-rich basins, such as the Michigan Basin, USA, and the Williston Basin in the USA and Canada. The highest salinity value reported in the literature is a 643,000 mg/L brine from the Salina Formation in the Michigan Basin (Case, 1945). However, not all sedimentary basins contain brine (salinity higher than that of ocean water). Well known examples include the evaporite-free Central Valley, California, USA (Kharaka & Berry, 1974), and the Pattani (Lundegard & Trevena, 1990) and Mahakam (Bazin et al., 1997) basins, Indonesia, where salinity is generally that of seawater or lower.

Salinity in individual petroleum fields generally increases with depth, but the rate of increase is highly variable (Figure 26 and Table 40). The variation can be large in water from the same petroleum field (Figure 27) and in water from different fields of the same basin (Table 41). Salinity in some basins with shale beds at depth—such as in the Central Valley, California, and the southern Louisiana and southeastern Texas Gulf Coast—show salinity decrease with increasing depth (Kharaka, 1971; Kharaka & Hanor, 2014). Nearly constant water salinity (~20,000 mg/L) has been documented over a depth interval of 700 to 2,800 m in widely varying lithologies in the North Slope, Alaska (Kharaka & Carothers, 1986).

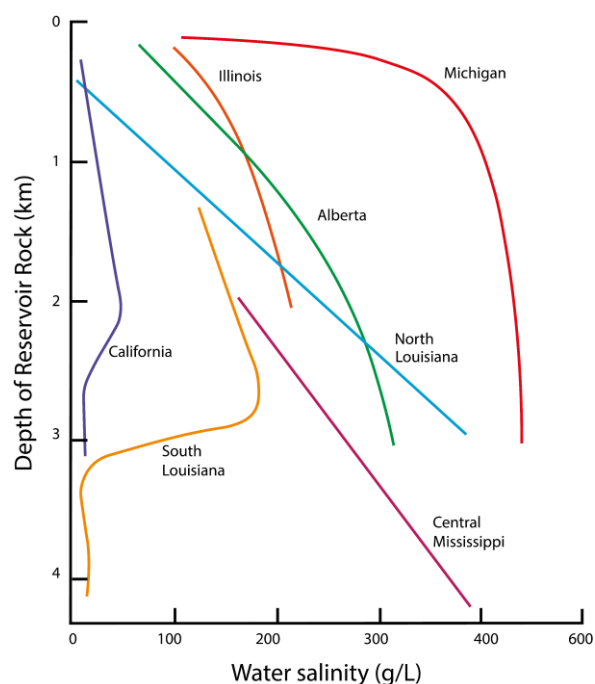


**Figure 26** - Variation in maximum reported salinity with depth for several major sedimentary basins in North America. Basins have different trends and the salinity in California and south Louisiana are reversed (modified from Kharaka & Thordsen, 1992; Hanor, 1979).

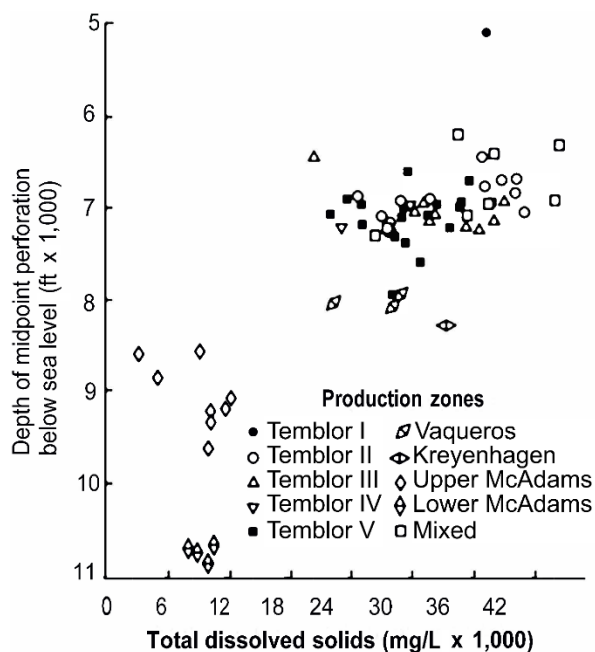


**Figure 27** - Distribution of salinity of formation water from Kettleman North Dome Field, California. Salinity of water in the deeper McAdams Formation is much lower than the Temblor Formation (from Kharaka & Berry, 1974).

**Table 40** - Chemical composition (mg/L) of produced water from Sacramento and San Joaquin Valleys, California; North Slope, Alaska; and the central Mississippi Salt Dome Basin, Mississippi (from Kharaka & Thordsen, 1992).

Location	Sacramento Valley, CA		San Joaquin Valley, CA			North Slope, AK		Central Mississippi	
Field	Grimes	Malton-Black Butte	San Emidio Nose	Wheeler Ridge	Kettleman North Dome	Barrow	Prudhoe Bay	Reedy Creek	West Nancy
Sample Number	81-NSV-15	81-NSV-1	74-SEN-3	75-WR-5	912-1	78-AX-52	78-AX-54	84-MS-11	84-MS-I
Well name	GOU4#2	19-1	21-15	21-28	323-21	S. Barrow 5	Arco 13	W.M. Geiger	W.L. West
Prod. zone <sup>a</sup>	Forbes	Forbes	Reef Ridge	Tejon	Lower McAdams	Barrow Sandstone	Sadlerochit Group	Rodessa	Smackover
Depth <sup>b</sup> (m)	2,074	1,524	3,337	2,691	3,520	728	2,820	3,486	4,428
Temperature (°C)	65	58	149	117	141	16	94	102	118
TDS <sup>c</sup>	18,600	21,400	10,900	44,300	10,000	22,100	21,900	320,000	275,000
Li	0.32	0.35	1.95	1.95	3.05	2.1	4.0	35	74
Na	6,830	7,510	4,000	7,450	3,760	7,980	7,600	61,700	54,800
K	35.5	28.4	620	135	92.4	3.0	86	990	6,500
Mg	72	148	7.0	27	3.4	67	20	3,050	3,350
Ca	182	331	67	5,550	30.7	119	182	46,600	33,900
Sr	14.3	18.8	8.0	187	4.4	16.1	20.2	1,920	1,670
Ba	6.4	4.6	4.2	12	3.98	175	3.8	60	48
Fe	0.58	54	0.36	2.8	0.31	5.5	63	465	0.47
NH <sub>3</sub>	34	30	73	32	8.9	19	17	34	119
F			3.0	2.0	0.3	1.6	1.5	1.5	11.5
Cl	11,000	12,700	3,460	21,450	4,680	11,800	10,600	198,000	170,000
Br	44	74	57	80	45	62	54	2020	2080
I	30	66	14	46	27	28	19	17	80
HCO <sub>3</sub> <sup>d</sup>	359	417	2,870	2,210	1,190	1,710	2,930	206	197
SO <sub>4</sub>	<0.5	0.9	38	50	0.5	n.d.	69	64	161
H <sub>2</sub> S	0.07	< 0.1	0.02	0.11	3.02	< 0.1	< 0.1	< 0.02	57.4
SiO <sub>2</sub>	31	18	109	46	128	11	62	28	34
B			92	600	43	42	158	59	342
pH	7.6	7.6	7.7	6.9	7.4	7.2	6.5	5.08	5.48

<sup>a</sup>Production zones are those used by oil companies. <sup>b</sup>Depth is depth below ground level of midpoint of perforation. <sup>c</sup>TDS is calculated total dissolved solids. <sup>d</sup>HCO<sub>3</sub> is field-titrated alkalinity and includes organic and inorganic species.

**Table 41** - Chemical composition (mg/L) of produced water and production data from wells in the geopressured zones from coastal Texas and Louisiana (from Kharaka & Thordsen, 1992).

Location	Lafayette, LA		Houston– Galveston, TX		Corpus Christi, TX		McAllen- TX	
Field	Weeks	Tigre Lagoon	Chocolate	Halls Bayou	Portland	East Midway	Pharr	La Blanca
Sample Number	77-GG-19	77-GG-55	76-GG-7	76-GG-24	76-GG-63	77-GG-73	77-GG-73	77-GG-117
Well name	St. Un. A	Edna Delcambre #1	Angle #3	Houston 'FF'	Portland A-3	Taylor E-2	Kelly A-1	La Blanca #12
Production zone <sup>a</sup>	S-Sand	Sand #3	Upper Weiting	Schenck	Morris	Lower Frio	Marks	7150 Sand
Depth <sup>b</sup> (m)	4,275	3,928	3,444	4,161	3,514	3,662	3,018	2,903
Temperature <sup>c</sup> (°C)	117	114	118	150	123	128	127	148
Pressure <sup>d</sup>	43.1	75.8	52.4	80.0	58.0	62.2	52.4	56.6
Fluid production <sup>e</sup>								
Oil/condensate	21.9	0	0.5	3.8	4.8	2.7	0	0.3
Water	56.0	633	6.7	57.9	7.5	0.2	7.1	51.0
Gas	6.1	7.9	5.1	70.8	25.1	4.9	3.2	17.1
TDS <sup>f</sup>	235,700	112,200	73,300	58,100	17,800	36,000	36,600	7,500
Na	78,000	40,000	26,500	20,500	6,500	13,250	9,420	2,680
Li	16	7.1	9.9	15	3.6	4.2	7.5	1.2
K	1,065	265	400	180	68	72	240	46
Rb	3.4	0.8	0.4	0.9	0.3	0.5	0.8	0.1
Cs	11.8	3.5	-	-	-	-	2.9	0.3
Mg	1,140	270	220	170	15	48	18	3.3
Ca	10,250	1,860	2,000	800	89	330	4,225	150
Sr	920	320	365	170	7.0	23	256	9.6
Ba	185	8.2	290	59	1.4	13	27	1.5
Fe	84	0.4	10.2	22	2.3	1.6	4.1	<0.1
Cl	143,000	67,900	42,700	34,500	9,270	21,000	22,000	3950
F	0.8	0.8	0.8	-	1.5	7.3	3.9	5.7
Br	419	63	52	32	19	45	78	15
I	18	26	16	11	25	45	22	16
B	44	57	35	91	62	35	105	117
NH <sub>3</sub>	100	69	29	13	5.8	13.5	21.5	4.2
H <sub>2</sub> S	0.4	0.5	1.2	1.4	< 0.1	0.04	< 0.1	<0.1
HCO <sub>3</sub> <sup>g</sup>	450	1,050	455	409	1,600	1,180	114	400
SO <sub>4</sub>	6.4	220	2.7	16	110	42	7.0	57
SiO <sub>2</sub>	48	57	87	110	93	132	90	88
pH	6.2	6.3	5.9	6.8	6.8	6.4	6.8	7.3

<sup>a</sup>Production zones are names used by oil companies. <sup>b</sup>Depth is depth below ground level of midpoint of perforation. <sup>c</sup>Temperature is measured subsurface temperature. <sup>d</sup>Pressure is original bottom-hole pressure in MPa (1 psi = 6.9 kPa). <sup>e</sup>Fluid production is in m<sup>3</sup>/d. <sup>f</sup>TDS is calculated total dissolved solids. <sup>g</sup>HCO<sub>3</sub> is field-titrated alkalinity and includes organic and inorganic species.

A wide range of explanations have been proposed over the years for the origin of the elevated formation water salinity observed in petroleum fields, but subaerial evaporation of seawater is one of the most important processes in determining the salinity and composition of fluids in sedimentary basins (Kharaka et al., 1987). The removal of H<sub>2</sub>O by progressive evaporation not only produces bittern brine (water remaining after evaporation of sea water) of high salinity and density that have the potential for infiltrating down into underlying sedimentary sequences but also results in the precipitation of a succession of Ca, Mg, Na, and K carbonate, sulfate, and chloride evaporite minerals, which may react with ambient pore fluids during burial, profoundly altering subsurface fluid compositions (Kharaka et al., 1987). Generally, the concentrations of cations and anions increase initially as evaporation increases, but the values for a number of cations (especially Ca and other divalent cations) as well as for Na start declining as evaporite salts begin precipitating when the saturation with CO<sub>3</sub>, SO<sub>4</sub>, and Cl are reached (Figure 28).

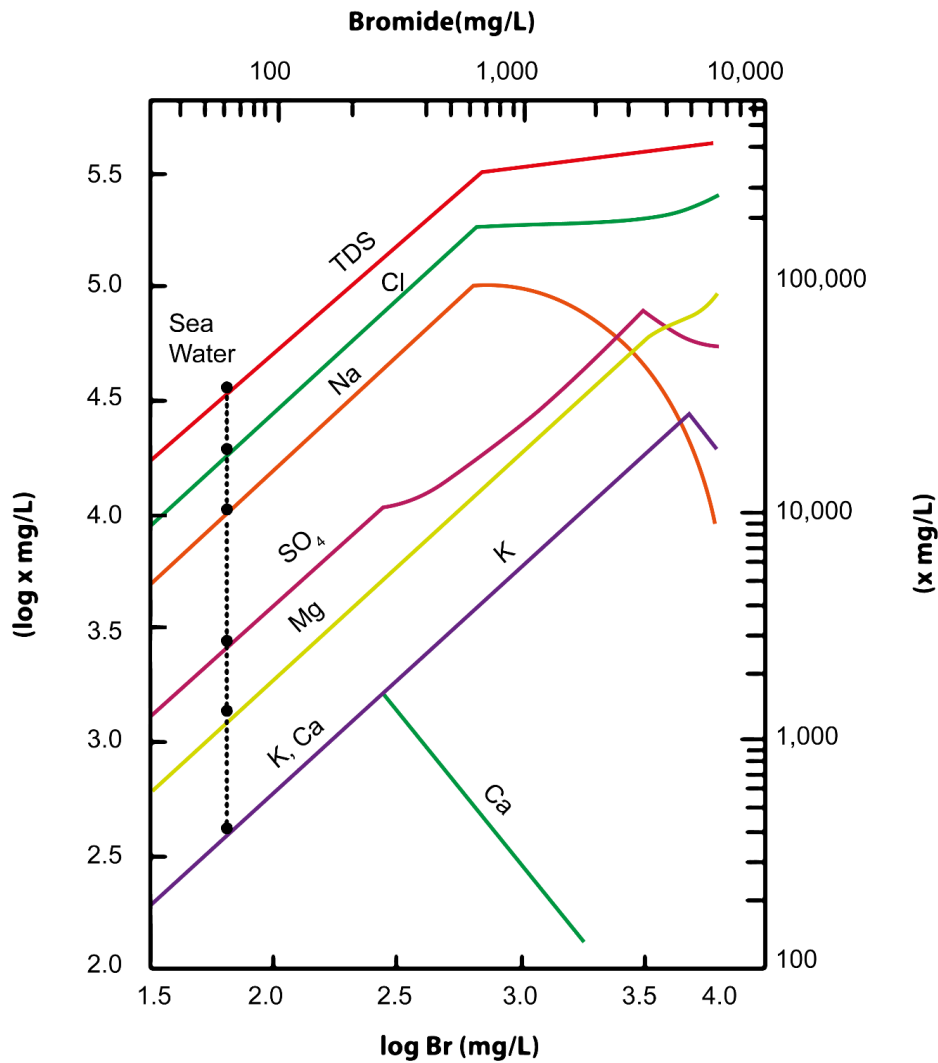


**Figure 28** - Concentration trends of salinity and several cations and anions as a function of Br concentration in evaporating seawater (modified from Carpenter, 1978; Kharaka & Thordsen, 1992).

Brine formed by subaerial evaporation of seawater can be distinguished as they have elevated Br/Cl ratios relative to ocean water. In contrast, brine formed by the dissolution of halite have low Br/TDS and Br/Cl ratios (Carpenter, 1978; Kharaka et al., 1987). Brine representing these end-members and mixtures of these and/or meteoric and/or connate marine water have been identified in sedimentary basins on the basis of their Br/Cl (Figure 29) and Br/TDS ratios (Hanor, 1987; Kharaka et al., 1987; Worden, 1996).

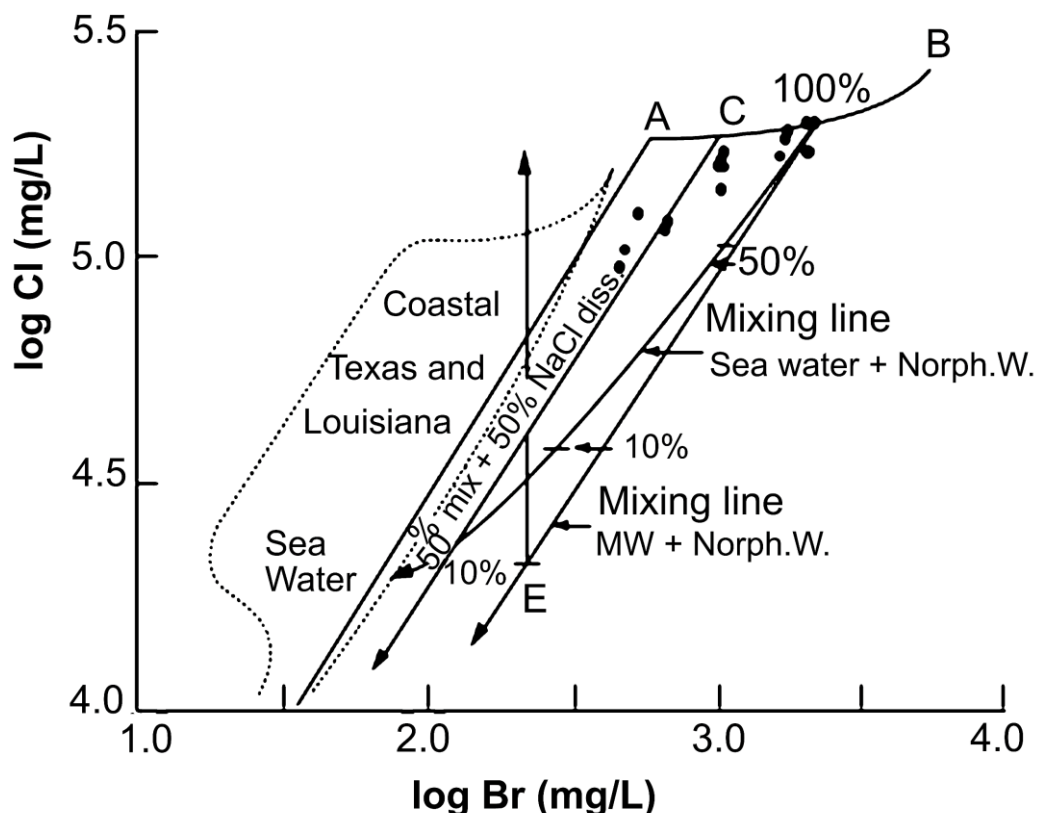


**Figure 29** - Distribution of Cl and Br in formation water from the central Mississippi Salt Dome Basin relative to the evaporation line for seawater (SW, A–B) and mixing lines between Norphlet water (Norph.W.) and meteoric (MW) and sea (SW) water. Line E–F gives the trend when the mixture of meteoric and Norphlet water dissolves halite with 70 ppm Br. Line C–D gives the trend where 50 percent of the Cl concentration in the mixture of meteoric and Norphlet water is from dissolution of halite. The samples from Coastal Texas and Louisiana (dashed field) plot in a different field (from Kharaka et al., 1987).

An alternative mechanism for producing subsurface brine of high salinity is the dissolution of chloride-bearing evaporites. Well documented field examples (Bennett & Hanor, 1987; Kharaka et al., 1978) exist in the US Gulf Coast, where the spatial variation in pore water salinity around some salt domes provides clear evidence for the dissolution of these halite-dominated diapirs as the source of brine. Field mapping of variations in salinity indicates that vertical transport of dissolved salts has occurred over distances of several kilometers vertically and tens of kilometers laterally throughout the surrounding sedimentary sequences (Bray & Hanor, 1990; Hanor & Sassen, 1990). The generally low

Br/Cl ratio of the pore fluids in this part of the Gulf Coast is consistent with dissolution of halite rather than subaerial evaporation as the source of Cl (Kharaka et al., 1987).

Spatial variation in salinity puts important constraints on the interpretation of the origin of basinal brine and on the quantification of diffusion, advection, and dispersion, which are responsible for subsurface solute transport. For example, lateral salinity plumes mapped around a number of shallow Gulf Coast salt domes (Bennett & Hanor, 1987) provide direct evidence for the dissolution of halite as the source of salinity in these areas. Salinity often increases with depth in basins where there is deep bedded salt and/or deep brine derived from the subaerial evaporation of seawater (Kharaka & Thordsen, 1992). Diffusive transport (Kharaka, 1986; Manheim & Bischoff, 1969), dispersive mixing of halite-saturated water and bittern brine with ambient formation water, and the near-surface recharge of low-TDS meteoric water into basins (McIntosh et al., 2002), produce formation water with a wide range in salinity. These field observations have led to studies involving numerical modeling to investigate the mechanisms and rates of solute transport driven by salt dissolution (Kharaka, 1986; Ranganathan & Hanor, 1987).

Field evidence shows that halite-derived brine can be transported over long distances in sedimentary basins. For example, the chemical compositions of water from the Houston–Galveston area, Texas, USA, and several other areas in the northern Gulf of Mexico Basin indicate dissolution of halite (Kharaka et al., 1985; Macpherson, 1992). However, in a number of these areas, there are no known salt domes within 50 km of the sampled sites. Large-scale fluid advection is probably the main mechanism for the transport of dissolved species there because large differences in hydraulic potential are present in the formations; and numerous faults can act as fluid conduits. Results from quantitative basin modeling have shown that fluid flow and solute transport can take place on the scale of hundreds of kilometers (Bjørlykke et al., 2010; Ortoleva et al., 1995; Wilson et al., 1999).

The influence of salt domes on the geochemistry of formation water is so important in many basins in the USA and throughout the world that we discuss it in more detail in Section 9, which is devoted to discussing the origin, flow, and composition of formation water of the south Louisiana salt dome province, a well-studied subregion within the Gulf of Mexico tectonic and sedimentary basin. A great deal of attention has been given to physical salt-sediment interactions in the Gulf of Mexico sedimentary basin because of their importance in the structural and tectonic evolution of the Gulf of Mexico and in the development of migration pathways and traps for crude oil and natural gas (e.g., Jackson et al., 1995). However, there are also important chemical salt-sediment interactions that include the subsurface dissolution of halite, the generation of dense subsurface brine, and the geochemical interaction of this brine with siliciclastic and carbonate sediments during burial diagenesis. Mixing of halite-derived brine with ambient marine and fresh water has

given rise to significant spatial variations in the salinity of formation water in the Gulf of Mexico Basin.

### 6.7.2 Cations in Produced Water

Sodium is the dominant cation in produced water, constituting 70 percent to >90 percent of the total cations by mass (Table 40, Table 41). Calcium is generally the second most abundant cation. Its concentration can rise, especially in Na-Ca-Cl-type water, to values of up to 50,000 mg/L (Table 40). The reason for the increase in calcium concentration with salinity can, however, be different for different fields in the same basin or different basins. The concentrations and proportions of magnesium are generally much lower than those in ocean water and decrease with increasing subsurface temperatures. The concentrations and proportions of strontium, barium, and iron are generally higher than those in ocean water and increase with increasing calcium concentration and chlorinity. The ratios of lithium, potassium, rubidium, and cesium to sodium generally increase with increasing subsurface temperatures, but again, there is a great deal of scatter in the data and their proportions vary from basin to basin (Hanor, 2001; Kharaka & Thordsen, 1992).

Plots of cation concentrations versus chloride differ in slope between the monovalent and divalent cations (Hanor, 1996, 2001). Both sodium and potassium show a 1:1 slope on log-log plots, but the divalent cations, magnesium, calcium, and strontium show a 2:1 slope. This difference in the rate of increase of sodium and calcium with salinity gives rise to the observed progression from Na-Cl to Na-Ca-Cl to Ca-Na-Cl water with increasing salinity in basinal water (Davisson & Criss, 1996; Hanor, 1987; Kharaka & Hanor 2014; Merino et al., 1997, 2006).

It is generally agreed that most of the chloride in basinal brine is derived from some combination of the subsurface dissolution of evaporites (Kharaka et al., 1985; Land, 1995) and the entrapment and/or infiltration of evaporated seawater (Carpenter, 1978; Kharaka et al., 1987; Moldovanyi & Walter, 1992). The dissolution of halite produces water dominated by sodium chloride. The evaporation of seawater produces water having the general trends shown for the bromide ion, but most formation water has neither the cation (nor anion) composition of a NaCl solution nor of evaporated modern seawater (Hanor, 2001; Stueber & Walter, 1991).

During the diagenetic evolution of formation water, there is up to an order of magnitude gain in calcium and strontium and up to an order of magnitude loss in magnesium and potassium relative to evaporated modern seawater. As brine derived from the dissolution of halite evolves diagenetically, dissolved sodium is lost and dissolved potassium, calcium, and strontium are gained. The observed 1:1 and 2:1 ratios discussed above with respect to the concentration of cations versus chloride can be accounted for largely by rock buffering (Hanor, 2001).

## Aluminum (Al)

Dissolved aluminum concentrations in subsurface water are generally < 0.5 mg/L; reported higher values are probably due to improper sample collection and/or treatment in the field (Kharaka et al., 1985, 1987). Determination of dissolved monomeric aluminum requires field filtration through a 0.1  $\mu\text{m}$  or smaller-size filter to prevent contamination with fine clay particles, followed by field solvent extraction as detailed in Lico and others (1982). There are presently insufficient high-quality data to establish the systematics of dissolved aluminum in produced water.

An alternative approach is to calculate values for dissolved aluminum using geochemical modeling—assuming brine equilibrium with respect to muscovite, microcline, albite, or other aluminosilicate minerals that are known to be present in the reservoir rocks. For example, Palandri and Reed (2001) calculated total dissolved aluminum values from 0.1 to 10  $\mu\text{g/L}$  for produced water from a number of sedimentary basins based on the assumption of local chemical equilibria among fluids, gases, and alteration minerals. Similar calculations by Bazin and others (1997a,b) for the Mahakam Basin, Indonesia, and the North Sea yield total aluminum concentrations on the order of 3  $\mu\text{g/L}$ .

The solubility of aluminum in natural water is commonly treated in terms of  $\text{Al}_{(\text{aq})}^{3+}$ , the aluminum fluoride  $\text{AlF}_{\text{n}(\text{aq})}^{3-\text{n}}$  and hydroxide complexes  $\text{Al}(\text{OH})_{\text{n}(\text{aq})}^{3-\text{n}}$  where  $n = 0, 1, 2,$  or  $3$ . However, thermodynamic calculations by Kharaka and others (2000) showed that organic acid anions—especially dicarboxylic acid anions—form strong complexes with aluminum. Thermodynamic calculations by Tagirov and Schott (2001) demonstrated that, in neutral to acidic fluids that contain dissolved fluoride in excess of 1 mg/L, the Al-F complexes  $\text{AlF}_{\text{n}(\text{aq})}^{3-\text{n}}$  should dominate aluminum speciation at temperatures below 100 °C. Moreover, hydroxy-fluoride complexes of aluminum, especially  $\text{Al}(\text{OH})_2\text{F}_{(\text{aq})}^{\square}$  and  $\text{AlOHF}_{2(\text{aq})}^{\square}$ , should be dominant at temperatures of 100 to 400 °C.

Calculations by these authors show that fluoride concentrations of 2 mg/L, which are common in produced water (Kharaka & Thordsen, 1992; Worden et al., 1999), could be enough to increase total aluminum concentrations as much as two orders of magnitude. Such an increase would adjust calculated aluminum concentrations in the above studies to values on the order of 0.01 to 1.0 mg/L. These values are similar to the range of aluminum values of 0.04 to 0.37 mg/L determined by careful sampling and direct chemical analysis by Kharaka and others (1987) in brine from the Mississippi Salt Dome Basin, USA.

## pH and Alkalinity

Because of changes in pressure-temperature ( $P$ - $T$ ) conditions and the possible loss of volatiles, especially  $\text{CO}_2$  as produced water is sampled at the wellhead, the measured and reported pH values are generally not equal to those at reservoir conditions. The true in situ pH values of produced water are largely unknown, but can be computed from field

measurements of pH and alkalinity that have been corrected for the lost CO<sub>2</sub> as the fluid flows from the reservoir to the sampling point (Kharaka et al., 1985). Another method for computing pH values is on the basis of assumed equilibrium relations with calcite under subsurface conditions (Merino, 1975; Merino et al., 1979; Palandri & Reed, 2001). Loss of acid volatiles such as CO<sub>2</sub> generally increases pH by 1 to 2 pH units (Kharaka et al., 1985).

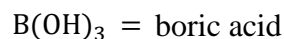
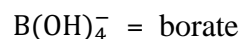
The pH values computed by these methods were in general agreement with those measured using a high P, T, and salinity probe (Kharaka et al., 2009). Many of the values for the in-situ pH of highly saline water of the Smackover Formation, Arkansas, that were calculated on the assumption of fluid equilibrium with respect to calcite, are substantially higher than field pH values reported by Moldovanyi and Walter (1992).

### Boron (B)

The boron cation B<sup>3+</sup> exists in aqueous solution as undissociated boric acid B(OH)<sub>3</sub> and as the borate ion B(OH)<sub>4</sub><sup>-</sup>. Formation water with pH values lower than 9 favor B(OH)<sub>3</sub> as the predominant species because the pK values for the reaction shown in Equation (2) are 4.77 at 25 °C and 3.42 at 100 °C (Kharaka et al., 1988).



where:



Bassett (1977) presented evidence for the existence of polynuclear boron species when boron concentrations are high. Organic–boron complexes may also exist; organically bound boron has the potential to be used to trace hydrocarbon migration paths in subsurface water (Mackin, 1987).

Boron is leached from rocks and organic matter, especially at high temperatures. Removal mechanisms for boron include adsorption on clay mineral surfaces at low temperatures (< 120 °C) and the incorporation of boron in exchange for tetrahedral silicon during higher-temperature silicate diagenesis (Spivack et al., 1987). Clay minerals play a key role in the boron budget. The clay mineral group illite/smectite contains an order of magnitude more boron than quartz, carbonate, and feldspar. Some types of organic matter contain several hundred ppm boron. Because metasedimentary graphite contains little boron, it is probable that boron is released together with hydrogen and oxygen during the thermal degradation of organic compounds (Kharaka & Hanor, 2014).

The reported boron concentrations in Gulf Coast (USA) brine ranges from a few milligrams per liter to ~700 mg/L (Kharaka et al., 1987; Land & Macpherson, 1992a). Dissolved boron shows no correlation with chloride concentration but shows some increase with depth and temperature (Kharaka et al., 1985). The B/Br ratios are highly elevated

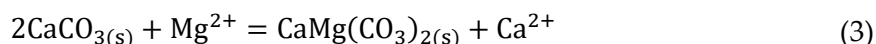
relative to the seawater evaporation trend for boron and bromide, which indicates the derivation of almost all of the boron from rock and/or organic sources.

### 6.7.3 Control of Cation Concentrations

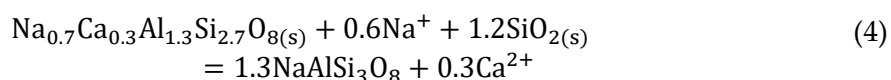
Dissolution of halite, as noted earlier, is probably the most important mechanism responsible for the increased sodium (and chloride) content in the very high salinity (> 100,000 mg/L) brine present in many sedimentary basins where evaporites are or were present. The concentrations of cations, especially multivalent species, are determined by the origin of the water and by the many temperature-controlled chemical, physical, and biological processes that modify the original composition of the water. These processes generally act together to increase or decrease the concentrations of the individual solutes.

The ultimate control on the concentration of a given solute is usually the solubility of the least soluble mineral of the solute at the subsurface temperature, pressure, and salinity conditions. For example, the concentration of calcium in water from a given reservoir may increase because of ion exchange, albitization (a chemically selective hydrous reaction) of plagioclase feldspar and/or dolomitization of limestone (Land, 1995). Eventually, the water will attain saturation with respect to calcite, the usual ultimate control on the calcium (and carbonate) concentrations.

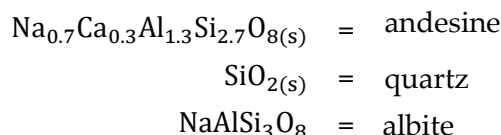
Congruent and incongruent dissolution and precipitation reactions (other than for halite) that probably control the major cation composition of formation water include dolomitization of limestone in the reaction shown in Equation (3), which results in a major increase of calcium and a major decrease of magnesium concentrations (Pokrovsky et al., 2009).



Albitization of plagioclase feldspar, as in the reaction shown in Equation (4), also increases calcium concentrations, but lowers the concentration of sodium.



where:

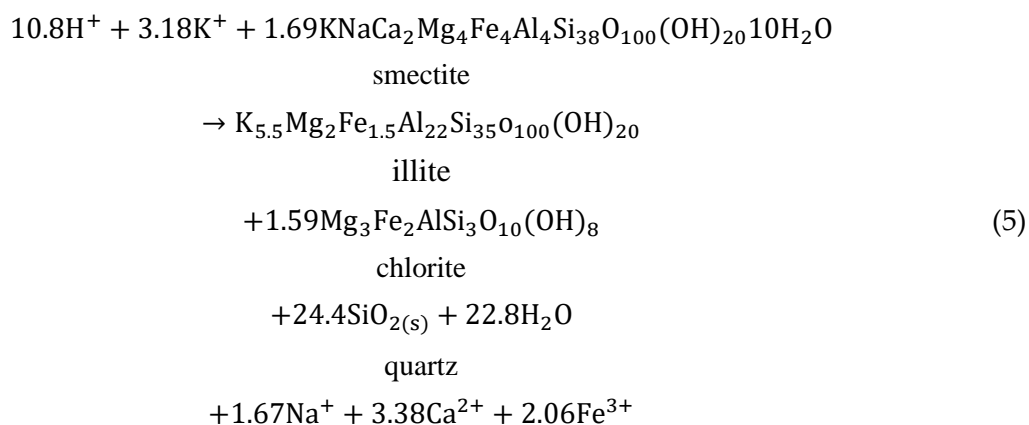


The concentrations of potassium in the samples obtained from the Norphlet Formation in the central Mississippi Salt Dome Basin of the USA are those expected from the Louann Salt bittern; potassium values in other samples obtained from reservoirs of Jurassic age are lower by a factor of ~2 (Kharaka et al., 1987). The decrease in the dissolved

potassium in these samples is attributed to the formation of authigenic (i.e., formed where found) illite and potassium feldspar (Carpenter et al., 1974; Kharaka et al., 1987).

The generally lower magnesium concentrations in formation water, in comparison to that of evaporated seawater, could result from diagenetic formation of chlorite, dolomite, and ankerite (Boles, 1978; Hower et al., 1976). Formation of ankerite (an iron-rich mineral related to dolomite) becomes important at subsurface temperatures higher than ~120 °C (Boles, 1978). In the absence of evaporites, the concentrations of alkali metals are strongly affected by temperature-dependent reactions with clays (transformation of smectite to mixed layer illite/smectite, then with increasing temperature to illite) and feldspar (e.g., Kharaka & Thordsen, 1992). The concentrations of potassium and sodium may be higher or lower than in seawater; the concentrations of lithium and rubidium are generally higher.

The transformation of smectite to mixed layer smectite-illite and (ultimately to illite) with increasing temperature is an extremely important reaction in many sedimentary basins, including the northern Gulf of Mexico Basin (Boles & Franks, 1979; Hower et al., 1976; Kharaka & Thordsen, 1992). The water and solutes released and consumed by this transformation are major factors in the hydrogeochemistry of these basins because of the enormous quantities of clays involved. Several reactions conserving aluminum or maintaining a constant volume have been proposed for this transformation (Boles & Franks, 1979; Hower et al., 1976; Merino & Canals, 2011, 2018). The proposed reaction shown in Equation (5) conserves aluminum and magnesium and is probably a closer approximation based on the composition of formation water in these systems. The  $\text{Fe}^{3+}$  in the reaction shown in Equation (5) will be reduced to  $\text{Fe}^{2+}$  by organics; some may precipitate as pyrite or ankerite. In summary, the overall reaction consumes large amounts of potassium and hydrogen and adds important amounts of calcium, sodium, and some  $\text{Fe}^{2+}$  to the formation water.



#### 6.7.4 Chemical Geothermometry and Barometry

Reservoir temperatures in particular—but also reservoir fluid pressures—are important parameters that affect water-mineral interactions and produced-water

compositions in the subsurface (e.g., Gunter & Perkins, 1991; Kharaka & Mariner, 1989). Gunter and Bird (1988) showed that significant amounts of CO<sub>2</sub> are produced in the heating of oil sands to generate oil production; Gunter and Perkins (1991) concluded that the relatively rapid calcite-CO<sub>2</sub> interaction was the best geobarometer for estimating CO<sub>2</sub> pressures and fluid pressures in the subsurface, including in thermally assisted oil recovery.

The concentration of certain chemicals and chemical ratios (especially Li/Na, K/Na, and Rb/Na) generally increase with increasing reservoir temperatures (depth of the reservoirs). The most useful *chemical markers* for increasing subsurface temperatures are the concentrations of silica, boron, and ammonia, and the Li/Mg, Li/Na, and K/Na ratios. The proportions of alkali metals alone or combined with those of alkaline-earth metals (magnesium and calcium in particular), and the concentrations of SiO<sub>2</sub> are so strongly dependent on subsurface temperatures that they have been combined into several chemical geothermometers (Table 42) that can be used to provide a good estimate of the reservoir temperatures (Fournier et al., 1974; Kharaka & Mariner, 1989, 2005; Land & Macpherson, 1992a; Pang & Reed, 1998).

**Table 42** - Equations for the general chemical geothermometers and their applicability for use in produced water from sedimentary basins (Kharaka et al., 1988).

Geothermometer	Equation <sup>1</sup>	Recommendation
Quartz	$t = \frac{1309}{0.41 - \log(k \cdot pf)} - 273.15$ $k = \frac{\alpha_{\text{H}_4\text{SiO}_4}}{\alpha_{\text{H}_2\text{O}}^2}; \quad pf = (1 - 7.862 \times 10^5 e^{(3.61 \times 10^{-3} \cdot t)}) p(b)$	70 °C to 250 °C
Chalcedony	$t = \frac{1032}{-0.09 - \log(k \cdot pf)} - 273.15$	30 °C to 70 °C
Mg-Li	$t = \frac{2200}{\log(\sqrt{\text{Mg/Li}}) + 5.47} - 273.15$	0 °C to 350 °C
Na-K	$t = \frac{1180}{\log\left(\frac{\text{Na}}{\text{K}}\right) + 1.31} - 273.15$	Do not use in produced water
Na-K-Ca	$t = \frac{699}{\log\left(\frac{\text{Na}}{\text{K}}\right) + \beta[\log(\sqrt{\text{Ca/Na}}) + 2.06] + 0.489} - 273.15$ $\beta = \frac{4}{3} \text{ for } t < 100; = \frac{1}{3} \text{ for } t > 100$	Do not use in produced water
Mg-Corrected, Na-K-Ca	<p>Same as Na-K-Ca (above) with Mg-corrections below</p> $t = t_5 - \Delta t_{\text{Mg}}$ <p>For R values of 0.5 to 5.</p> $\Delta t_{\text{Mg}} = 1.03 + 59.971 \log R + 145.05(\log R)^2 - \frac{36711(\log R)^2}{T(K)} - 1.67 \times 10^7 lo;$ <p>For 5 &lt; R &lt; 50</p> $\Delta t_{\text{Mg}} = 10.66 - 47415 R + 325.87(\log R)^2 - 1.032 \times 10^5 \left(\log \frac{R}{T}\right)^2 - 1.968 \times \frac{10^7(\log R)^2}{T^2} + 1.605 \times \frac{10^7(\log R)^3}{T^2};$ <p>No correction should be attempted if R &gt; 50.</p> $R = \frac{\text{Mg}}{\text{Mg} + 0.61 \text{Ca} + 0.31\text{K}} \cdot 100$	0 °C to 350 °C
Na/Li	$t = \frac{1590}{\log\left(\frac{\text{Na}}{\text{Li}}\right) + 0.779} - 273.15$	0 °C to 350 °C

<sup>1</sup>Concentrations in mg/L; *t* is temperature in °C; *T* in °K; *p* is pressure in bars; *α* is activity of the subscripted species (Na-K-Ca equation and Mg corrections from Fournier & Potter, 1979; for details see Kharaka & Mariner, 1989).

When temperatures calculated using chemical geothermometers are concordant and close to those obtained for that reservoir, the reliability of the chemical analyses is increased. When the calculated temperatures are not concordant and vary greatly from reported values, then the source of the discrepancy needs to be investigated, because may be a sampling problem, mixing with water from a leaked zone, or an analysis issue.

### 6.7.5 Major Anions in Produced Water

At salinity less than 10,000 mg/L and relatively shallow depths, the anionic composition of produced water is highly variable and can be dominated by sulfate, bicarbonate, chloride, or even acetate (Drever, 1997; Hem, 1985). Generally, shallow groundwater is dominated by sulfate, which is replaced by bicarbonate as the dominant species in deeper meteoric groundwater. Acetate may comprise a large portion of total anions, especially in Na – Cl – CH<sub>3</sub>COO-type water that are present mainly in some Cenozoic reservoir rocks at temperatures of 80 to 120 °C. In this water, acetate and other organic acid anions (Section 7) can reach concentrations of up to 10,000 mg/L and contribute up to 95 percent of the measured alkalinities (Kharaka et al., 2000; Willey et al., 1975).

Chloride is by far the dominant anion in nearly all formation water having salinity greater than ~30,000 mg/L (Table 40 and Table 41). Explaining the origin of saline water in sedimentary basins is, to some degree, the problem of explaining the origin of the dissolved chloride. Chloride and bromide are closely coupled in their subsurface geochemistry, but the other dissolved halogens—fluoride and iodide—have distinctly different systematics in basinal water. Sulfate, bicarbonate, and the organic acid anions provide valuable information on the effects of reactions involving petroleum and other organic matter on formation water chemistry. Other weak anionic species (e.g., borate and boric acid) may provide information on the degree of water–rock interaction (Kharaka & Hanor, 2014).

#### Chloride and Bromide

The principal sources of dissolved chloride in more saline produced water include the following:

1. dissolved chloride in water associated with sediments at their time of deposition;
2. chloride derived by refluxing of subaerially evaporated surface brine;
3. chloride derived from subsurface mineral dissolution, principally halite; and
4. marine aerosols.

The Cl–Br systematics of sedimentary brine provide useful constraints on interpreting the origin of chloride in this water (Carpenter, 1978; Kesler et al., 1996; Kharaka et al., 1987).

Although bromide and chloride are both monovalent anions of similar ionic radii (Br = 1.96 Å, Cl = 1.81 Å), Cl is strongly preferentially partitioned over Br into sodium, potassium, and magnesium halogen salts during precipitation (Hanor, 1987; Kharaka et al.,

1987). During the initial evaporation of seawater, both bromide and chloride increase in concentration in the residual hypersaline water; the Br/Cl ratio of the evaporated water does not vary (Figure 28 and Figure 29). When halite saturation is reached, chloride is preferentially precipitated as a constituent of halite. Because only a small fraction of the bromide is incorporated in the halite lattice as Na (Cl, Br), the Br/Cl ratio of the residual brine increases with progressive evaporation. As saturation with respect to K-Mg-Cl salts is reached, the slope of the Br-Cl curve begins to flatten out, because these minerals discriminate against bromide somewhat less than halite. The upper limit to bromide concentrations produced by evaporating seawater is ~6,000 mg/L; the upper limit for chloride is ~250,000 mg/L.

In theory, high salinity brine formed by subaerial evaporation of seawater should have elevated Br/Cl ratios. Brine formed by the dissolution of halite should have low Br/TDS and Br/Cl ratios (Carpenter, 1978; Kharaka et al., 1987). Brine representing these end-members and mixtures of these and/or meteoric and/or connate marine water (Figure 29) have been identified in sedimentary basins on the basis of their Br/Cl and Br/TDS ratios (Hanor, 1987; Kharaka et al., 1987; Worden, 1996).

The high Br/Cl ratios of water in the Smackover Formation, USA, for example, support the hypothesis that bromide-rich, subaerially produced brine is an important saline end-member in this system (Kharaka et al., 1987; Moldovanyi & Walter, 1992). The central Mississippi Salt Dome Basin provides an excellent example of a system where bittern (residual from evaporated seawater) water is an important component of the formation water (Figure 29). The very high salinity of brine (up to 350,000 mg/L) and its major ion concentrations are directly or indirectly related to its origin as bittern in the Louann Salt.

This conclusion is based on the relation between the chemical markers bromide and chloride, sodium, total cations, and the isotopic composition of the water (Carpenter et al., 1974; Kharaka et al., 1987; Stoessell & Carpenter, 1986). The bromide and chloride concentrations are much higher than those expected from dissolution of halite; the values (Figure 29) plot on or below the seawater evaporation line. Kharaka and others (1987) indicated the samples that plot on or below the seawater evaporation line result from mixing of bittern with meteoric water (Figure 29).

In contrast, the low Br/Cl values of water in south Louisiana, USA, indicate their high salinity is derived from the dissolution of halite-dominated salt domes (Hanor, 1987; Kharaka et al., 1978, 1985). Other examples include brine in the Paradox Basin (Hanshaw & Hill, 1969) and formation water in Devonian sediments of the Alberta Basin, Canada (Hitchon et al., 1971). Water of the Norwegian Shelf has an intermediate Br/Cl signature; this supports the conclusion of Egeberg and Aagaard (1989) that this water contains at least some contribution from subaerially produced brine in addition to brine generated by the dissolution of halite.

Several other processes modify the Cl-Br systematics in formation water. These include the incongruent dissolution of halite, the incongruent dissolution of chloride salts other than halite, the differential rates of molecular diffusion, and the introduction of bromide from organic compounds (Land & Prezbindowski, 1981). Br/Cl ratios in excess of those normally associated with subaerial evaporation may result from the incongruent dissolution of Na-K-Mg-Cl mineral assemblages during progressive burial (Hanor, 1987; Land et al., 1995).

### Iodide

The concentration of dissolved iodide typically ranges from < 0.01 to > 100 mg/L in basinal water (Collins, 1975; Worden et al., 1999). An exceptional value of 1,560 mg/L has been reported for a brine sample from Mississippian limestone of the Anadarko Basin, Oklahoma, USA, where iodide is extracted from the brine commercially (Johnson & Gerber, 1998). There is no correlation between the iodide and chloride concentrations, and the occurrence of iodide appears to be unrelated to either evaporative concentration or salt dissolution.

The probable source of iodide in produced water is organic matter. Iodide is an essential trace element in the biological cycle; it is estimated that 70 percent of crustal iodide resides in organic matter in marine sediments (Lu et al., 2014; Muramatsu et al., 2001). Iodide is released during the progressive thermal degradation of organic material and is preferentially partitioned into the aqueous phase as  $I^-$  (Collins, 1975; Kharaka & Thordsen, 1992).

### Fluoride

Fluorine exists in produced water primarily as fluoride,  $F^-$ , and cation-fluoride complexes such  $CaF$ ,  $CaF^+$ , and  $MgF^+$  (Richardson & Holland, 1979). The concentrations of fluoride in formation water varies from < 1 to > 30 mg/L (Worden et al., 1999). There appears to be a threshold value (100,000 mg/L) for chloride below which fluoride concentrations are typically below 5 mg/L and above which they are in the range of 10 to 20 mg/L. Occasionally, they are even higher. Sources of fluoride and controls on the concentrations of fluoride have not been extensively studied. Biogenic fluorapatite, bentonite, and smectite-bearing shales are potential sources.

The control of fluoride concentration by fluorite ( $CaF_2$ ) saturation is likely in some water. Fluorite solubility has been shown to be a complex function of temperature, salinity, and major ion chemistry (Richardson & Holland, 1979). Hitchon (1995) found that lower-salinity water of the Alberta Basin is generally undersaturated with respect to fluorite and that fluoride gradually increases to  $CaF_2$  saturation as temperature and salinity increase.

## Sulfate

Sulfur can exist in aqueous solution in at least five oxidation states, but data on sulfur species in basinal brine are limited primarily to sulfate, S(VI), and sulfide, S(-II); sulfate ( $\text{SO}_4^{2-}$ ) will be discussed in this section, while hydrogen sulfide ( $\text{H}_2\text{S}$ ) and bisulfide ( $\text{HS}^-$ ) will be discussed in the following section.

The concentration of  $\text{SO}_4^{2-}$  in produced water rarely exceeds 1,000 mg/L, even though it is present in high concentration in seawater (2,700 mg/L) and in even higher concentrations in residual brine formed by seawater evaporation (Table 40 and Table 41). Unlike major cations and alkalinity, there is no significant correlation between the concentration of  $\text{SO}_4^{2-}$  and chloride or salinity, but the solubility of anhydrite decreases rapidly with increasing temperature and provides the ultimate control on  $\text{SO}_4^{2-}$  concentrations (Kharaka & Thordsen, 1992; Kharaka & Hanor, 2014). The wide variations in sulfate concentrations that exist on the basinal—and even the oil-field scale—may also reflect rate-controlled processes involving the following:

1. release of sulfate by the dissolution of sulfate minerals such as gypsum and anhydrite (Land et al., 1995; Hitchon, 1996b) and the oxidation of pyrite (Dworkin & Land, 1996);
2. dispersive fluid mixing;
3. precipitation as barite ( $\text{BaSO}_4$ );
4. removal by bacterial sulfate reduction (BSR) at shallow and deeper zones, particularly in the presence of hydrocarbons (Gavrieli et al., 1995); and
5. removal by thermochemical sulfate reduction that becomes important at temperatures  $> 100^\circ\text{C}$  (Machel, 2001).

## Inorganic Carbon Species

The alkalinity of most formation water—operationally defined by titration of a given volume of water with  $\text{H}_2\text{SO}_4$  to an inflection pH—is contributed predominantly by bicarbonate and organic acid anions. The inflection pH for inorganic alkalinity is close to 4.5. For organic acid anions, it is at a pH value of 2 to 3 (Carothers & Kharaka, 1978; Willey et al., 1975). Total inorganic (organic anions are discussed in more detail later in this section) alkalinity, comprised mainly of  $\text{HCO}_3^-$  and  $\text{CO}_3^{2-}$  species, is generally less than a few hundred milligrams per liter in water having salinity greater than  $\sim 30,000$  mg/L.

Alkalinity generally decreases with increasing salinity. There are two main reasons for this decrease. Both are related to the solubility of carbonate minerals, primarily calcite. First, in a calcium carbonate-buffered system, carbonate alkalinity should decrease with the marked increase in dissolved calcium that generally occurs with increasing salinity. Second, the increase in  $\text{H}^+$  (lower pH) with increasing salinity shifts dissolved carbonate and bicarbonate toward carbonic acid as shown in Equation (6).



### 6.7.6 Metal-Rich Brine

The concentrations of heavy metals in oil-field water, with the exception of iron and manganese, are generally low (Hitchon et al., 2001; Kharaka & Thordsen, 1992). In the case of lead, zinc, and copper, and with the exception of fewer than half a dozen localities worldwide, the concentrations are < 100 mg/L. The concentrations of trace metals (e.g., mercury, gold, and silver) are generally one to several orders of magnitude lower (e.g., Giordano, 2000; Kharaka & Hanor, 2014).

The central Mississippi Salt Dome Basin is a metal-rich brine locality that has been studied extensively (Carpenter et al., 1974; Kharaka et al., 1987). The brine (Table 43) is Na-Ca-Cl-type water of extremely high salinity (up to  $3.5 \times 10^5$  mg/L) but with low concentrations of aliphatic acid anions. The metal concentrations in many samples are very high, reaching values of 100 mg/L for lead, 250 mg/L for zinc, 500 mg/L for iron, and 200 mg/L for manganese (Table 43). Brine with such high toxic metal content causes higher toxicity when it enters a USDW.

**Table 43** - Selected metal concentrations (mg/L; \* $\mu\text{g/L}$ ; - not measured) in produced water from central Mississippi Salt Dome Basin (Kharaka et al., 1987).

Sample ID	Fe	Mn	Pb	Zn	Al*	Cd	Cu*
84-MS-1	137	57.5	8.39	49.6	-	0.49	< 20
84-MS-2	97.4	38.2	0.07	1.22	59	0.05	< 20
84-MS-3	61.9	10.6	0.04	0.53	133	0.02	< 20
84-MS-4	346	63.9	53.2	222	267	0.83	< 20
84-MS-5	407	70.2	60.5	243	42	0.81	61
84-MS-6	284	21.0	26.8	95.1	67	0.63	21
84-MS-7	261	83.5	34.6	172	79	0.86	< 20
84-KS-8	194	69.3	22.8	107	132	0.67	34
84-MS-9	0.54	15.5*	< 0.5*	12.0*	-	< 0.2*	< 0.2
84-MS-10	84.9	44.8	0.08	0.31	-	0.02	< 20
84-MS-11	465	212	70.2	243	367	0.99	21
84-MS-12	65.3	16.4	0.17	0.28	-	0.03	< 20
84-MS-14	0.75	2.78	0.16	0.20	-	< 0.02	< 20
84-MS-15	223	53.2	2.28	4.10	-	0.02	< 20
84-MS-16	0.53	9.98	0.02	0.07	142	< 0.02	< 20
84-MS-18	0.15	3.2*	< 0.5*	13*	-	0.08*	0.61
84-MS-19	0.47	1.64	0.04	0.06	-	0.03	< 20
84-MS-20	0.07	1.46	0.03	0.16	-	0.05	< 20
Field blank*	10.6	1.05	1.04	12.6	-	0.08	< 0.20

The samples with high metal content have extremely low concentrations (< 0.02 mg/L) of  $\text{H}_2\text{S}$ . Samples with high concentrations of  $\text{H}_2\text{S}$  have low metal content typical of oil-field water (Kharaka et al., 1987). Exceptionally rich sources of metals such as red beds can provide sufficient amounts of metals for the formation of ore deposits. Red beds are a likely source of the ore deposits for this reason; because they contain so little

reduced sulfur, leached metals will tend to remain in solution, precipitating as ore deposits when mixed with a brine of higher H<sub>2</sub>S content.

### Solubilization of Heavy Metals

A major problem in explaining metal transport in basinal brine is the very low solubility of base metal sulfides, particularly at temperatures less than 150 °C. For example, the calculated activity product for solutions in equilibrium with sphalerite, using SUPCRT92 (Johnson et al., 1992), is only 10 to 15.1 at 100 °C, 500 bar, and a neutral pH of 6.04. The activity product for lead and H<sub>2</sub>S for a solution in equilibrium with galena under these conditions is only 10 to 17.7. Thus, the aqueous complexes of base metals are required to account for the minimum concentrations of the ore-forming metals, for example as shown for sphalerite in Equation (7).



Experimental work and thermodynamic calculations have focused primarily on metal-chloride, metal-bisulfide, and metal-organic complexes as possible solubilizing agents (Giordano, 2000; Kharaka & Hanor, 2014). There is some disagreement on the relative importance of these complexing agents, although most authors today favor chloride complexing as discussed in the remainder of this section.

### Bisulfide Complexing

Considerable attention has been paid to complexing of metals by reduced sulfur species. Some complexes of zinc and lead that have been considered include Zn(HS)<sub>3</sub><sup>-</sup>, Zn(HS)<sub>2</sub><sup>2-</sup>, Pb(HS)<sub>3</sub><sup>-</sup>, Pb(HS)<sub>2</sub><sup>2-</sup>, and Pb(H<sub>2</sub>S)<sub>2</sub><sup>2-</sup> (Barnes, 1979; Kharaka et al., 1987). On the basis of experimental studies, Giordano and Barnes (1981) concluded that ore-forming solutions at temperatures less than 200 °C, with total dissolved sulfur contents of less than 1 mole/L, cannot transport significant quantities of lead as bisulfide complexes. Extensive metal complexing by the bisulfide complexes requires much higher pH values than those found in saline formation water (Kharaka et al., 2000).

### Organic Complexing

In recent years there has also been considerable interest in the possible role of organic ligands as complexing agents of metals in basinal water (e.g., Kharaka et al., 1987, 2000). Aliphatic acid anions such as acetate, which are generally the most abundant of the reactive organic species, have received the most attention (Giordano & Kharaka, 1994). There is, however, an inverse correlation between metal content and organic acid concentrations in basinal water (Hanor, 1994). Concentrations of lead and/or zinc well above 1 mg/L have been reported only in low-acetate water. At acetate concentrations greater than 50 mg/L, reported metal concentrations are low. Dicarboxylic acid anions form

stronger metal–organic complexes, but field data and geochemical modeling indicate the occurrence of high metal concentrations is not directly related to high concentrations of dissolved organic species (Hanor, 1996; Kharaka et al., 2000).

The solubility of PbS and ZnS in produced water containing dissolved chloride is enhanced by the formation of metal–chloro-complexes. Defining Me to stand for a divalent metal like Pb, then the following complexes are formed:  $\text{MeCl}^+$ ,  $\text{MeCl}_2^0$ ,  $\text{MeCl}_3^-$ , and  $\text{MeCl}_4^{2-}$ . Most formation water that has concentrations of dissolved lead and dissolved zinc exceeding 1 mg/L, also have chloride concentrations in excess of  $1 \times 10^5$  mg/L (TDS =  $1.7 \times 10^5$  mg/L). A few water samples from the Gulf Coast with a slightly lower chloride concentration between  $6 \times 10^4$  mg/L and TDS of  $1 \times 10^5$  mg/L have metal concentrations in excess of 1 mg/L.

Thermodynamic calculations using Pitzer equations of state show that several properties of typical basinal fluids combine to increase the solubility of PbS and ZnS, at a fixed temperature and activity of dissolved  $\text{H}_2\text{S}$ , 15 orders of magnitude through an order of magnitude increase in salinity and chlorinity (Hanor, 1996). These properties include the following:

- significant decrease in pH with increasing salinity;
- onset of the predominance of the tetrachloro complexes ( $\text{MeCl}_4^{2-}$ ), whose activities increase by a factor of  $10^4$  with increasing chloride concentration; and
- strongly non-ideal behavior of Cl, which results in activity coefficient terms that are significantly greater than unity in very saline water.

### 6.7.7 Geochemical Modeling of Ore Fluids

Geochemical modeling is a valuable tool for assessing the importance of ligands including chlorides, bisulfides, and organic acid anions in the transport of significant quantities of metals in ore solutions (Giordano & Kharaka, 1994; Kharaka et al., 2000; Zhu et al., 2016). The geochemical code used in such modeling must include the following:

1. thermochemical data for the dominant inorganic and organic species present in formation water and the minerals of interest;
2. temperature and pressure corrections for the thermochemical data; and
3. ability to treat high-salinity solutions using Pitzer or comparable ion-interaction formulations.

In geochemical modeling, two approaches have been used to study the importance of organic ligands, bisulfides, and chlorides in the transport and deposition of metals. In the first approach, simulations are carried out using variable concentrations of known organic and other ligands that are added to model compositions for the ore fluids, especially fluids for Mississippi Valley-type and red bed-related base metal deposits (Giordano & Kharaka, 1994; Hanor, 2000).

In the second approach, Kharaka and others (1987) used the measured chemical composition of metal-rich and metal-poor brine from the central Mississippi Salt Dome Basin to compute the concentrations of sodium, calcium, magnesium, aluminum, iron, lead, and zinc complexed with acetate and other measured organic ligands, and with chlorides and bisulfides under subsurface conditions.

Results from both approaches indicate the following.

1. High concentrations (100 mg/L) of lead and zinc can be present in oil-field brine only if the concentration of total H<sub>2</sub>S is at the µg/L level; in this case significant quantities of dissolved lead and zinc can be transported as carboxylate complexes.
2. Lead and zinc in Mississippi Valley-type ore fluids are transported dominantly as chloride complexes.
3. The brine is close to equilibrium with galena and sphalerite under the likely subsurface temperatures, pressures, and pH (Giordano, 2000; Kharaka et al., 1987).

## 6.8 The Influence of Shale and Other Geologic Membranes

The ability of clays, mudstones, and shale to serve as semipermeable geologic membranes has been conclusively demonstrated by laboratory experimental data (Fritz & Marine, 1983; Kharaka et al., 1973; Mazurek et al., 2015; Whitworth & Fritz, 1994) and field evidence (Berry, 1973; Hanshaw & Hill, 1969; Kharaka & Berry, 1974). The chemical composition of water in sedimentary basins, including pore water in shale and the flow of water and chemicals into and out of shale following hydraulic fracturing, can be significantly affected by interaction with geologic membranes in four ways.

1. Compacted clays and shale serve as semipermeable membranes that retard, to varying degrees, the flow of dissolved chemical species with respect to water. Subsurface water that has flowed through a geologic membrane (effluent water) is lower in TDS and has a chemical composition different from that of the original solution (input water) or from the solution remaining in the formation on the input side of the membrane (hyperfiltrated water).
2. Subsurface water has been squeezed out of massive shale and siltstone is present in large areas in many sedimentary basins such as the Gulf Coast (Kharaka & Berry, 1980) and the Central Valley, California, USA (Berry, 1973; Kharaka et al., 1985). This water also exhibits increasing *membrane effluent* characteristics with increasing depth of the reservoir. The lowest salinity of water in these two basins is 5,000 to 10,000 mg/L. These values are about a quarter of the salinity of formation water at comparable depths in these basins, where the water is not affected by the membrane filtration process. Water

squeezed from clays and shales in laboratory experiments was equilibrated with a solution of similar composition as the field setting that exhibits membrane effects show comparable compositions. As compaction pressure increases, the salinity of squeezed water decreases and shows selectivity values and other membrane filtration characteristics described above (Kharaka & Berry, 1974; Kryukov et al., 1962).

3. Clay minerals have cation exchange capacities that are approximately 5 meq/100 g (milliequivalents per 100 grams) for kaolinite, 70 meq/100 g for illite, and 150 meq/100 g for smectite. The chemical composition of pore water within the double layer and membrane properties of clays are directly related to their selectivities and exchange capacities. Exchange reactions are relatively fast and can rapidly modify the composition of pore water in shale. Thus, chemicals in the fracturing fluids will mix with those present in shale pore water and selectively exchange with chemicals on the mineral exchange sites and within the *stern* layer (the layer with concentrated cations).
4. Clay-mineral transformations, especially the conversion of smectite to illite, are important reactions in many sedimentary basins at temperatures higher than 80 °C. The exchange capacity of illite is about half that of smectite. This transformation can therefore result in the uptake of potassium on clays and the release of quantitatively important amounts of adsorbed species to subsurface water.

Kharaka (1986) reported detailed studies of membrane effluent effects in the Central Valley, California; in the northern Gulf of Mexico Basin; and in the North Slope, Alaska. In each basin, the compositions of effluent and hyper-filtered water were compared. The membrane effluent characteristics observed include the following chemical markers: lower TDS, lower Ca/Na and Br/Cl ratios, and higher Li/Na, NH<sub>3</sub>, B/Cl, HCO<sub>3</sub>/Cl, and F/Cl ratios. These chemical markers are similar to those predicted from laboratory studies when extrapolated to the temperature, pressure, and hydraulic pressure gradients in sedimentary basins (Demir, 1988; Haydon & Graf, 1986; Kharaka & Smalley, 1976).

Nevertheless, the importance of membrane filtration in modifying the chemical composition of subsurface water is controversial (Hanor, 1987). Manheim and Horn (1968) discussed the difficulties of producing brine by shale membrane filtration and concluded that the pressure requirements for significant membrane filtration were not encountered in geologic environments. Fluid pressure or hydraulic potentials are needed to force water through shale. However, membrane filtration will lead to an increase in the concentration of solution on the input side of shale relative to the output side. Flow and membrane filtration will cease when the osmotic head thus generated equals the original hydraulic potential. For a more detailed coverage of this complex topic, the interested reader is directed to the discussion reported in Kharaka and Hanor (2014).

## 6.9 Secular Variations in Seawater Chemistry: Impact on Composition of Basinal Brine

Studies of the composition of fluid inclusions in ancient evaporites suggest there have been significant secular (over geologic time) variations in seawater chemistry (Horita et al., 2002; Lowenstein et al., 2003). Modern seawater is rich in  $\text{SO}_4$  and relatively poor in Ca. As a consequence, when modern seawater is evaporated to gypsum saturation,  $\text{Ca}^{2+}$  is effectively precipitated nearly entirely from solution, leaving behind a Ca-depleted and  $\text{SO}_4$ -enriched brine. However, fluid inclusion evidence developed to date suggests that during much of the early to middle Paleozoic and the Cretaceous, the oceans were  $\text{SO}_4$ -poor and Ca-rich. The evaporation of this water would have produced brine depleted in sulfate, enriched in  $\text{Ca}^{2+}$ , and with elevated Ca/Na ratios.

Calculations by Berner (1980) suggest that Ca-rich seas were the norm over the Phanerozoic. Berner found that variations in seawater composition could be accounted for by variations in the rates of precipitation of calcium sulfate, burial of pyrite, weathering, and the exchange of Mg for Ca as a result of basalt–seawater reactions and dolomitization. Holland (2005) proposed that changes in seawater composition resulted from sedimentary processes rather than circulation through mid ocean ridges. Lowenstein and others (2003) proposed that basinal brines inherited their chemistry from evaporated paleo seawater that was Ca-rich and  $\text{SO}_4$ -poor.

Hanor and McIntosh (2006) reviewed the hypothesis by Lowenstein and others and noted that there is little evidence to support the proposal that brines in Phanerozoic sedimentary basins necessarily inherited their chemistries from evaporated marine waters at times when the oceans were Ca-rich and  $\text{SO}_4$ -poor. For example, basinal brines in Silurian–Devonian formations of the Illinois and Michigan basins do not show the same compositional trends as that of evaporated  $\text{CaCl}_2$ -rich Silurian seawater. Significant diagenetic alteration is required to explain their composition. The Mississippian, Permian, and Middle Jurassic were not periods of pronounced Ca enrichment in seawater, yet the evaporated marine waters formed during these times yielded brines that subsequently became enriched in calcium. Further discussion is provided in Section 9.

## 6.10 Exercises Pertinent to Section 6

[Link to Exercise 7](#) ↓

[Link to Exercise 8](#) ↓

[Link to Exercise 9](#) ↓

## 7 Organic Compounds in Produced Water

### 7.1 Introduction to Organic Composition

Beginning in the 1970s, interest has grown in the origin and interactions of dissolved organic species in subsurface water, especially in produced water (Connor et al., 1997; Khan et al., 2016; Kharaka et al., 1986; MacGowan & Surdam, 1990; Orem et al., 2017; Willey et al., 1975). Geochemical interest in organic species was initially related to their important role in mineral diagenesis (Kharaka & Hanor, 2014; Neff et al., 2011; Seewald, 2001; Surdam et al., 1989). They are present in relatively high concentrations (up to 10,000 mg/L) in produced water, and act as proton donors for a variety of pH-dependent water-mineral reactions as pH and Eh buffering agents. They also form complexes with metals such as aluminium, iron, lead, and zinc. Additionally, they can be used as proximity indicators in petroleum exploration (Carothers & Kharaka, 1978; Collins, 1975) and they may serve as precursors for natural gas (Drummond & Palmer, 1986; Kharaka et al., 1983).

More recently, interest in organic compounds has increased substantially because significant concentrations of nonpolar (but highly toxic) dissolved organic compounds may be present in oil-field water including benzene, toluene, ethylbenzene, and xylenes (up to 60 mg/L for total BTEX), phenols (20 mg/L), and PAHs (up to 10 mg/L for total PAHs). These highly toxic organic compounds, together with dispersed tiny globules of oil, are of concern for their environmental impacts including contaminating soil, surface water, and groundwater (Bekins et al., 2016, 2021; Hidalgo et al., 2020; Kharaka et al., 2009; Kharaka & Hanor, 2014; McDevitt et al., 2022; Orem et al., 2017, 2014; Varonka et al., 2020; US EPA, 2019).

### 7.2 Monocarboxylic Acid Anions

The concentration of dissolved organic species (DOC)—especially monocarboxylic acid anions—in produced water is generally very high, reaching 10,000 mg/L (DOC = 170 mg/L). This is much higher than concentration in uncontaminated groundwater, where the DOC is generally < 1 mg/L (Kharaka & Hanor, 2014; Thurman, 1985). Acetate concentration alone may reach as high as 10,000 mg/L (Kharaka & Carothers, 1986; MacGowan & Surdam, 1990). Acetate, propionate, butyrate, and valerate were identified as the dominant organic species in produced water (Carothers & Kharaka, 1978; Willey et al., 1975). The presence of these organic acid anions in groundwater at concentrations higher than about 1 mg/L is reason to suspect contamination from a petroleum source.

Prior to the identification of these aliphatic acid anions in produced water by Willey and others (1975), these organics were generally grouped with and recorded as *bicarbonate alkalinity* because they are titrated with H<sub>2</sub>SO<sub>4</sub> that is used to measure field alkalinities.

Willey and others (1975) and Carothers and Kharaka (1978) showed these organic acid anions contribute up to 99 percent of the measured alkalinities in some produced water (Figure 30). Their concentration in produced water is controlled primarily by subsurface temperature and the age of the reservoir rocks, which indicates the time of their generation.

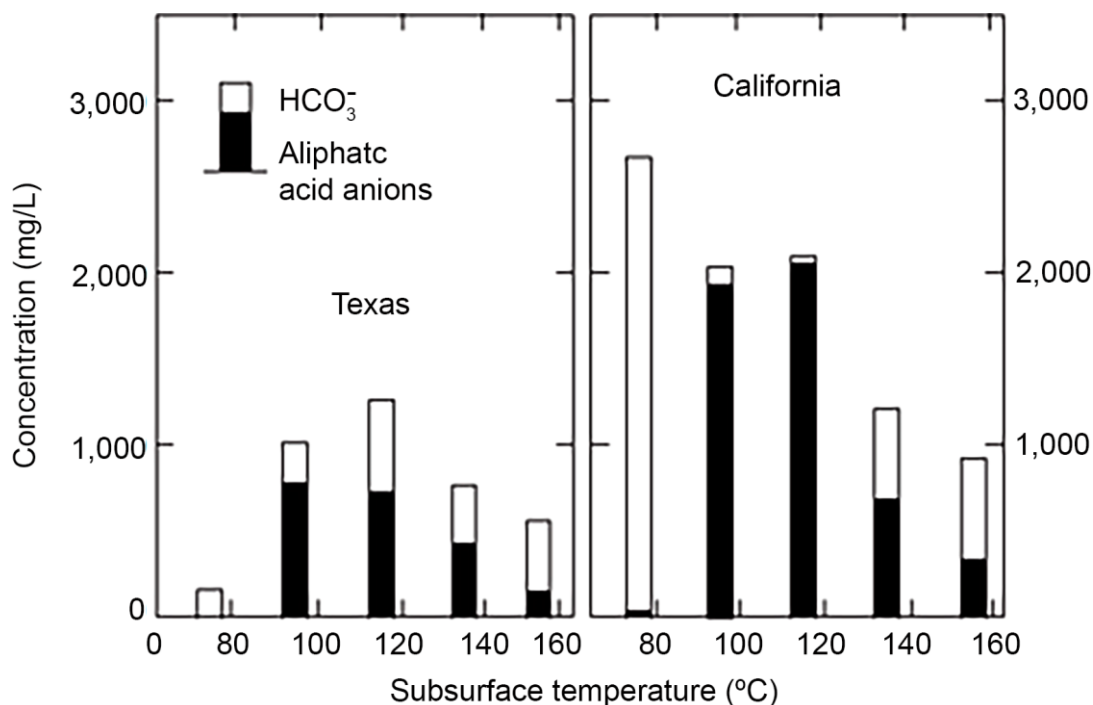


**Figure 30** - Average concentrations of aliphatic acid anions and bicarbonate alkalinity as  $\text{HCO}_3^-$  in oil-field water from Texas and California, USA. Note that organic acid anions contribute most of the total alkalinity at temperatures between 80 and 140 °C (after Carothers & Kharaka, 1978).

The distribution of aliphatic acid anions in oil-field water from several basins shown in Figure 31 reveals three distinct temperature zones (Kharaka et al., 2000). Zone 1 is characterized by concentrations of acid ions < 500 mg/L and reservoir temperatures < 80 °C. The concentrations of acetate in this zone are generally low and propionate generally dominates. Bacterial degradation is believed to be responsible for the low concentration of organic species in Zone 1 (Carothers & Kharaka, 1978). The highest concentrations of aliphatic acid anions are observed in the youngest (Tertiary age) and shallowest reservoir rocks of Zone 2 (temperatures 80 to 120 °C). Their concentration generally decreases with increasing subsurface temperatures (Figure 31) and with the age of the reservoir rocks (Kharaka et al., 1993a). Acetate constitutes more than 90 percent of acid anions; propionate comprises ~5 percent of these anions (Carothers & Kharaka, 1978; Lundegard & Kharaka, 1994). The high temperature limit of Zone 3, where no measurable acid anions are present, is placed at ~220 °C, a value obtained by extrapolating the points of Zone 2 (Kharaka et al., 1986).

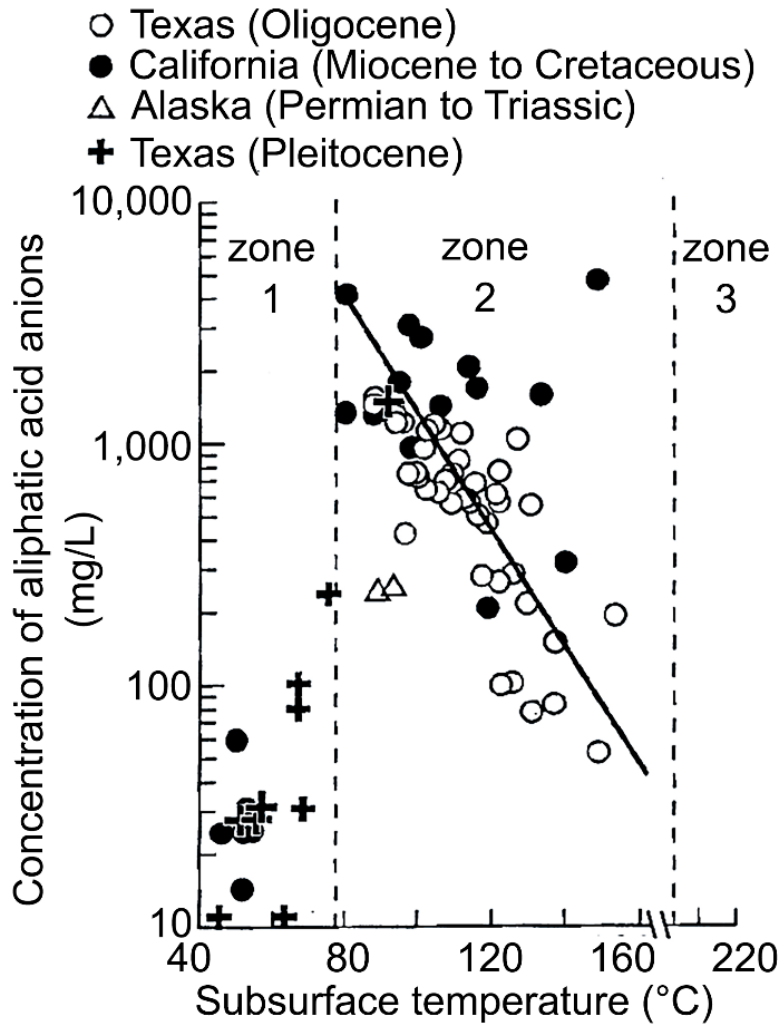


**Figure 31** - Concentrations of aliphatic acid anions with 2-5 carbon atoms in produced water from three sedimentary basins. Note that the highest concentrations are at a temperature of 80 °C and concentrations decrease with increasing temperatures (from Kharaka et al., 1988).

The decrease in the concentration of acid anions with increasing temperature (Figure 31) and with the age of the reservoir rocks (Carothers & Kharaka, 1978; Kharaka et al., 1993b, 2000) indicates that thermal decarboxylation is responsible for the conversion of acid anions to CO<sub>2</sub> and hydrocarbon gases. In the case of acetic acid, the reaction produces methane in addition to CO<sub>2</sub> as shown in Equation (8).



Further evidence for the importance of thermal decarboxylation in the destruction of acid anions is obtained from the  $\delta^{13}\text{C}$  values of dissolved bicarbonate, CO<sub>2</sub> and CH<sub>4</sub> in natural gas, and diagenetic calcite and ankerite from basins in the Gulf Coast and California (Boles, 1978; Carothers & Kharaka, 1980; Lundegard & Kharaka, 1994; Lundegard & Land, 1986). These  $\delta^{13}\text{C}$  values indicate that the carbon in CO<sub>2</sub> gas, dissolved carbonate, and carbonate cement was derived largely from an organic source.

Laboratory experiments show that decarboxylation rates for acetic acid are extremely sensitive to both temperature and the types of available catalytic surfaces on the containers. Rate constants for acetic acid decarboxylation at 100 °C differ by more than fourteen orders of magnitude between experiments conducted in stainless steel and in catalytically much less active titanium (Drummond & Palmer, 1986; Kharaka et al., 1983). Naturally occurring mineral surfaces provide rather weak catalysts (Bell, 1991). Decarboxylation rates calculated from field data indicate half-life values of 10 to 60 million years at 100 °C (Kharaka, 1986; Lundegard & Kharaka, 1994).

### 7.3 Dicarboxylic Acid Anions

Data for the concentrations of dicarboxylic acid anions in produced water are much more limited than for monocarboxylic anions. Some of the reported values are also controversial (Hanor et al., 1993; Kharaka et al., 1993a). The total reported range is 0 to 2,640 mg/L (further discussion and references are found in Kharaka et al., 2000). The highest concentrations of dicarboxylic acid anions are those reported by MacGowan and Surdam (1988, 1990) for water samples from ~40 petroleum wells located mainly in the San Joaquin Valley and Santa Maria Basin, California, USA, and in the northern Gulf of Mexico Basin. They reported values of up to 494 mg/L oxalate, 2,540 mg/L malonate, and 66 mg/L maleate from wells in the North Coles Levee Field, San Joaquin Valley Basin, California.

Several wells in the North Coles Levee Field and the nearby Paloma Field were re-sampled by other investigators (Fisher & Boles, 1990; Kharaka & Hanor, 2014; MacGowan & Surdam, 1990). These authors found much lower and more typical concentrations of dicarboxylic acid anions (maximum of ~200 mg/L). The concentration is probably limited by a rapid rate of thermal decomposition (Crossey, 1991; MacGowan & Surdam, 1988) and by the low solubility of calcium oxalate and calcium malonate (Harrison & Thyne, 1992; Kharaka et al., 1986).

From the above discussion, we conclude there are large variations and some uncertainty in the reported maximum concentrations of mono- and dicarboxylic acid anions in produced water. The use of these maximum values in computer simulations of water-mineral interactions leads to erroneous results and conclusions. Maximum reported values together with more reasonable and likely maximum values are listed in Table 44. Only when measured concentrations of organic and inorganic species from petroleum wells are available should rigorous geochemical simulations be carried out (Kharaka et al., 1987).

**Table 44** - Maximum and most likely maximum concentrations of mono- and dicarboxylic acid anions reported in produced water (Kharaka et al., 2000).

Acid anion IUPAC	Maximum Concentration (mg/L)			References for maximum reported values**
	Common	Reported*	Likely	
<b>Monocarboxylic anions</b>				
Methanoate	Formate	174	10	1
Ethanoate	Acetate	10,000	5,000	2
Propanoate	Propionate	4,400	2,000	1
Butanoate	Butyrate	682	500	3
Pentanoate	Valerate	371	200	3
Hexanoate	Caprolate	107	100	4
Heptanoate	Enanthate	99	100	1
Octanoate	Caprylate	42	100	1
<b>Dicarboxylic anions</b>				
Ethanedioate	Oxalate	494	10	1
Propanedioate	Malonate	2,540	100	1
Butanedioate	Succinate	63	100	4
Pentanedioate	Glutarate	95	100	5
Hexanedioate	Adipate	0.5	10	4
Heptanedioate	Pimelate	0.6	10	4
Octanedioate	Suberate	5.0	10	4
Cis-Butenedioat	Maleic	26	50	1

\*for geochemical simulations, use of the listed "Likely" maximum value is more appropriate

\*\*references: 1 = MacGowan and Surdam (1988); 2 = Surdam and others (1984); 3 = MacGowan and Surdam (1990); 4 = Kharaka and others (1985); 5 = Kharaka and others (2000)

## 7.4 Other Reactive Organic Species

Data for the concentration of organic species other than the mono- and dicarboxylic acid anions are few. Degens and others (1964) and Rapp (1976) identified several amino acids including serine, glycine, alanine, and aspartic acid, but their concentrations were < 0.3 mg/L. Produced water of the High Island Field, offshore Texas, contained a number of other organic compounds including phenol, 2-, 3-, and 4-methylphenol, 2-ethylphenol, 3-, 4-, and 3-, 5-dimethylphenol, cyclohexanone, and 1- and 4-dimethylbenzene (Kharaka et al., 1986). Fisher and Boles (1990) identified various polar aliphatics (fatty acids to C9 with various methyl and ethyl substituents), cyclics (phenols and benzoic acids), and heterocyclics (quinolines). They were able to determine, at the ppm or sub-ppm level, the concentrations of phenol, methyl-substituted phenols, and benzoic acid.

Lundegard and Kharaka (1994) reported data showing that waters from oil and gas wells in the Sacramento Valley, California, contained the following organic species: phenols (up to 20 mg/L), 4-methylphenol (up to 2 mg/L), benzoic acid (up to 5 mg/L), 4-methylbenzoic acid (up to 4 mg/L), 2-hydroxybenzoic acid (up to 0.2 mg/L), 3-hydroxybenzoic acid (up to 1.2 mg/L), 4-hydroxybenzoic acid (up to 0.2 mg/L), and citric acid (up to 4 mg/L). Additional dissolved organic species including organosulfur compounds will likely be discovered as analytical procedures improve (Kharaka et al., 2000).

Significant concentrations of nonpolar—but highly toxic—dissolved organic compounds may be present in oil-field waters including benzene, toluene, ethylbenzene,

and xylenes (60 mg/L total BTEX), phenols (20 mg/L), and polycyclic aromatic hydrocarbons (up to 10 mg/L total PAHs). These highly toxic organic compounds are of concern in the leakage of produced waters and in geologic sequestration of CO<sub>2</sub> because they are partitioned preferentially into the supercritical CO<sub>2</sub> and, potentially, could leak with it and contaminate the overlying shallow groundwater (Kharaka et al., 2009; Kharaka et al., 2010a).

## 7.5 Origin of Major Reactive Organic Species

Hydrous pyrolysis experiments of crude oil generated relatively large concentrations of mono- and di-carboxylic acid anions with relative abundances generally similar to those observed in sedimentary basin water. But analysis of all of the pertinent data indicates that the major part of the organic acid anions in formation water is probably generated by the thermal alteration of kerogen in source rocks (Kharaka & Hanor, 2014; Lewan & Fisher, 1994). This conclusion is based on several observations.

1. The oxygen content of oil (0 to 1 wt. percent) is ~20 times lower than that of kerogen (Tissot & Welte, 1984).
2. The yields of organic acid anions per unit weight are approximately two orders of magnitude lower in experiments with oil than in kerogen experiments (Barth et al., 1989; Kharaka & Hanor, 2014; Lundegard & Senftle, 1987).
3. Oil is much less abundant than kerogen in sedimentary basins.
4. High concentrations of organic acid anions have been reported from gas fields (e.g., the Sacramento Valley Basin, California) where liquid petroleum has probably never existed (Lundegard & Kharaka, 1994).

## 7.6 Toxicity of Produced Water and Crude Oil Releases

The benefits of petroleum and coal consumption are clear but carry major environmental impacts that may be regional or global in scale including air pollution, global climate change, and major oil spills. Exploration and production of petroleum have also caused local detrimental impacts to soil, air, surface water, groundwater, and ecosystems in the thirty-six producing states in the USA and throughout the world (Kharaka & Dorsey, 2005). These impacts generally arise primarily from the improper disposal of large volumes of saline water produced with oil and gas, accidental hydrocarbon and produced water releases, and flow pathways associated with abandoned petroleum wells that were orphaned or incorrectly plugged (Kharaka & Otton, 2007).

Both crude oil and produced water contain chemical components that are toxic to humans, plants, and other biota as well as to ecosystems (McDevitt et al., 2022). These toxic chemicals will contaminate any groundwater that they contact, thereby impacting water quality—which means the chemical, physical, and biological characteristics of water based

on the standards of its usage. Contamination is most frequently determined by reference to a set of standards against which compliance, generally achieved through treatment of the water, can be assessed (US EPA, 2019, and Table Box 2-1 of this book). The most common standards used to monitor and assess water quality concern the health of ecosystems, the safety of human contact, and the condition of drinking water. Water quality has a significant impact on water supply and often determines supply options.

### 7.6.1 Toxicity Resulting from Crude Oil and Organic Chemicals

Crude oil is toxic and causes two main kinds of injury: physical and biochemical (Overton et al., 1994). The physical effects of freshly spilled crude oil are seen when birds, insects, and other animals coated in crude oil struggle to survive. Crude can completely cover and smother plants and animals living along its flow path.

Crude oil not only destroys the insulating properties of animal fur and bird feathers, which can lead to hypothermia, but it also impairs animals' abilities to fly and swim, sometimes causing oiled animals to drown. For example, during the months after the major 1989 *Exxon Valdez* oil spill mentioned earlier, researchers collected approximately 30,000 dead birds including more than ninety different species from oiled areas and estimated that perhaps ten times as many birds died.

The presence of oil may also render fertile land unfit for plant life by reducing the ability of the soil to hold oxygen. Because oxygen is a key element for plant growth and photosynthesis, existing vegetation may suffocate. Crude oil, especially heavy crude oil, also saturates the ground and acts as a barrier that prevents water from being absorbed, further inhibiting plants from being nourished.

Spilled crude oil can harm life because it has chemical constituents that are toxic including some that are cancerous, mutagenic, and cause damage to the immune system, the brain and nervous system, liver, and other organs (Bekins et al., 2016; Kharaka et al., 2020). Although crude oil is a complex mixture of thousands of chemical compounds, the elemental components (by weight) are carbon (82 to 85 percent), hydrogen (10 to 14 percent), nitrogen (0.1 to 2 percent), oxygen (1.0 to 1.5 percent), and sulfur (0.5 to 6 percent), with a few trace metals making up a very small percentage of the remainder. The properties of petroleum are defined by the range of the four main hydrocarbon groups: paraffins (15 to 60 percent), naphthenes (30 to 60 percent), and aromatics (3 to 30 percent), with asphaltenes making up the remainder.

Two important components of crude oil are extremely toxic—in some cases at very low levels: the volatile organic compounds (VOCs) that include benzene and other BTEX compounds, and PAHs that are present in all crude oil and produced water. Benzene comprises approximately 0.16 percent of USA crude oils and 0.33 percent of Canadian crude oil and is acutely toxic when inhaled (MCL benzene is 5 µg/L; MCLG is 0; Table Box 2-1), in addition to being potentially cancer-causing (US EPA, 2019). At the site

of a fresh oil spill, benzene and other VOCs can threaten nearby residents, responders working on the spill, and air-breathing animals. However, VOCs are generally a response concern only right after oil is spilled because they quickly evaporate and oxidize to harmless compounds.

The concentration of PAHs in produced water is low; however, they have high concentrations in all crude oil with  $K_{OW}$  values in the many thousands, where  $K_{OW}$  is the equilibrium ratio of concentration of a chemical in n-octanol and water at a specified temperature as discussed by Hoffman and others (2002) and Kharaka and Hanor (2014). At a crude oil spill, PAHs remain in the crude for a much longer time than VOCs, so their health and environmental impacts last much longer—likely until all the crude is physically removed and the site remediated (Bekins et al., 2021; Kharaka & Hanor, 2014; US-EPA, 2019).

PAHs are aromatic hydrocarbons with two to seven fused hydrocarbon rings, which may have substituted groups attached to the rings. As with VOCs many of the PAHs are extremely toxic, some at a lower level than benzene (MCL for benzo(a)pyrene is 0.2  $\mu\text{g/L}$ ). Sixteen PAHs are designated by the EPA as priority pollutants (US EPA, 2019). But, in contrast to VOCs, PAHs partition more heavily into oil (with partition coefficient  $K_{OW}$  values in many thousands) comprising 0.2 to 7 percent of the crude oil. The concentrations of PAHs are highest in heavy crude oil, and they can persist in the environment for many years, in some cases continuing to harm organisms and the environment until all crude is removed and the site remediated (Bekins et al., 2021; Hoffman et al., 2002; Kharaka & Hanor, 2014).

At Bemidji, Minnesota, transformations and interactions of organic compounds in the crude oil also result in the formation of metabolites (some toxic) in contaminated groundwater (Bekins et al., 2016; 2021). Cozzarelli and others (2015) and Ziegler and others (2021) reported the release of toxic arsenic (up to 230  $\mu\text{g/L}$ ; MCL 10  $\mu\text{g/L}$ ) to groundwater, not from the crude oil but by dissolution of iron oxyhydroxides in the aquifer rocks at the Bemidji oil study site (contamination at Bemidji is discussed in detail in Section 10).

Benzene and other toxic BTEX compounds are also present in produced water (up to 60 mg/L) but at lower concentration than in crude oil because the partition coefficients favor the oil;  $K_{OW} = 130$  for benzene (McMahon et al., 2017). However, produced water is generally more mobile than crude oil, impacting larger areas when the produced water flows into creeks or penetrates into the unsaturated zone and, at times, reaches local groundwater. The highest reported total concentration of PAHs in produced water is 10 mg/L, with much higher values in the associated crude oil (Kharaka & Hanor, 2014).

### 7.6.2 Toxicity Resulting from Inorganic Chemicals

Produced water generally has salinity and several inorganic and organic chemicals and radionuclides that are above the MCL values for drinking water and standards in irrigation water, which makes it toxic to humans, plants, and other biota as well as the local ecosystem (Gillespie et al., 2019; McMahon et al., 2021). This can be seen when the concentrations of chemicals in produced water (e.g., Table 40 and Table 41) are compared with the MCL and SMCL values (Table Box 2-1). For example, produced water salinity may be 10 to 1,000 times more concentrated than the SMCL value of 500 mg/L TDS, the National Secondary Drinking Water Regulation (US EPA, 2019). Concentrations of chloride, sodium, and other inorganic chemicals in the produced water are also 10 to 1,000 times more concentrated than the SMCL values (250 mg/L for Cl) reported in Table Box 2-1 (US EPA, 2019). Concentrations of many highly toxic chemicals (including Pb, Zn, Cd, Fe, As, and H<sub>2</sub>S) in produced water are also often 10 to 1,000 times higher than the MCL and SMCL values.

Produced water has salinity and several inorganic chemicals that make it unsuitable, even toxic, for crops, fruit trees, vines, and soils. Many fruit trees and other cultivars, for example, are susceptible to injury from salt toxicity. Most plants are tolerant of irrigation water with salinity of 1,000 mg/L TDS, and some may tolerate salinity as high as 5,000 mg/L (Kharaka, 2016; Maas & Grattan, 1999). However, produced water salinity is generally 10 to 100 times higher than the threshold value for most plants.

Build-up of salinity in the root zone increases osmotic pressure of the soil solution and causes a reduction in both the rate of water absorption by the plants and soil water availability. Plant growth is then delayed, with considerable reduction in yield. In addition to salinity, the high concentrations of sodium, chloride, and boron in produced water are among the most toxic chemicals for plants. Chloride, sodium, and boron are absorbed by the roots and transported to the leaves where they accumulate to harmful amounts, causing leaf burn, leaf necrosis, and plant death.

Although boron is an essential element for plants, it is extremely toxic to many fruit trees and vegetables when present in excessive amounts, even at relatively very low concentrations of 0.5 mg/L. The threshold concentration of boron in irrigation water for grape vines, citrus trees, and other fruit trees is only 0.75 mg/L. Toxicity occurs with uptake of boron from the soil solution. The boron tends to accumulate in leaves until it becomes toxic to the leaf tissue and results in death of the plant. In arid regions like southern California, boron is considered the most harmful element in irrigation water (Maas & Grattan, 1999). Produced water from California oil fields (Table 42) has high boron concentrations (up to 600 mg/L) that are approximately thirty to one hundred times the threshold value for boron-sensitive trees and vegetables (Kharaka, 2016; Kharaka et al., 1998).

Ammonia is another toxic compound that can adversely affect the health of fish and other aquatic life even at low concentration. The nature and degree of toxicity depends on many factors including the chemical form of ammonia, the pH and temperature of the water, the length of exposure, and the life stage of the exposed fish. Issues associated with toxicity testing and the consequences of ammonia exposure are discussed by the US EPA (1989). The toxicity of ammonia solutions does not usually cause problems for humans and other mammals, as a specific mechanism exists to prevent its build-up in the bloodstream (i.e., the body treats ammonia as a waste product and gets rid of it through the liver).

A literature review of the threat posed by ammonia to fisheries from mining and other industrial operations was conducted by McKenzie and others (2008). When dissolved in water, ammonia exists in two forms:  $\text{NH}_3$  (unionized) and  $\text{NH}_4^+$  (ionized). Ionized ammonia does not easily cross fish gills and is less bioavailable than the unionized form (US EPA, 1989). The unionized form can cross from water into fish and, once inside, some converts to the ionized form, which then causes cellular damage (US EPA, 1989). The primary form of total body ammonia in fish at physiological pH (7.0 to 8.0) is ammonium, and it is this chemical species that is responsible for toxic effects.

Although unionized ammonia is the more toxic form, toxicity is most commonly expressed as total ammonia, that is, as the sum of ionized and unionized ammonia in water. Ammonia toxicity is also a function of ionic strength, i.e., the salinity of the water. Ammonia is more toxic to aquatic life at higher temperature and pH values. As pH increases, so does the fraction of unionized ammonia and the toxicity to fish (US EPA, 1999). The ratio of  $\text{NH}_3$  to  $\text{NH}_4^+$  increases the rise of each pH unit by a factor of ten and by approximately two times for each 100 °C rise in temperature from 0 to 300 °C (US EPA, 2009).

## 7.7 Exercises Pertinent to Section 7

[Link to Exercise 10](#) ↴

[Link to Exercise 11](#) ↴

[Link to Exercise 12](#) ↴

[Link to Exercise 13](#) ↴

## 8 Isotopic Composition of Produced Water

### 8.1 Introduction to Isotopic Composition

In the last few decades, isotopes—atoms of the same element but with different mass—have become an essential part of geochemistry and have contributed significantly to the solution of a wide variety of geoscientific problems that span the entire field of earth sciences. Continued improvements in methods such as the use of double spike-thermal ionization mass spectrometry (Russel et al., 1978), and the invention of new mass-spectrometer systems—such as multi-collector, inductively-coupled, plasma mass spectrometers (MC-ICP-MS)—have enabled investigations of isotope variations of a wide range of transition and heavy elements that could not previously be measured with adequate precision. This has allowed many of the stable and radioactive isotopic systems to be investigated and applied to a huge variety of inorganic and organic samples including water-mineral-petroleum interactions (Bullen, 2011; Bullen et al., 2001; Kharaka & Hanor, 2014).

As detailed in Clark and Fritz (1997), Faure and Mensing (2005), Kendall and McDonnell (2012), and other textbooks on isotopes, a chemical element is defined by the number of protons in the nucleus of its atom. Atoms consist of a nucleus of protons and neutrons surrounded by a cloud of electrons. The number of protons, which defines the atomic number, is fixed for a chemical element, but the number of neutrons can vary. The various combinations of protons and neutrons are called isotopes of the element, which have a slightly different atomic mass. For example, the element carbon has six protons, whereas sodium has eleven, and lead has eighty-two. Carbon can have six, seven, or eight neutrons, resulting in three carbon isotopes:  $^{12}\text{C}$ ,  $^{13}\text{C}$ , and  $^{14}\text{C}$ , respectively.

When the number of neutrons increases beyond a specific limit for each element, the nucleus can become unstable (radioactive) and decays to a more stable isotope of the same or another element. The isotope  $^{14}\text{C}$  is radioactive because it undergoes spontaneous decay to the isotope  $^{14}\text{N}$ . The radioactive decay of  $^{14}\text{C}$  (half-life of 5,730 years) is extremely important in geochemistry as it is the basis for radiocarbon (carbon-14) dating. In contrast,  $^{12}\text{C}$  and  $^{13}\text{C}$  are called stable isotopes because they do not decay.

Isotopes of the same chemical element have almost identical physical and chemical properties. However, because of their small mass differences, they have different reaction rates and different abundances in two chemical compounds or phases that are in isotopic exchange. Physical processes such as diffusion, evaporation, condensation, and melting produce isotopic differentiation. The variations in the isotopic composition produced by chemical, physical, or biological processes in compounds or phases and present in the same system are called *isotopic fractionations* (e.g., Clark & Fritz, 1997).

Stable isotope geochemistry investigates variations in the ratios of stable isotopes such as  $^2\text{H}/^1\text{H}$ ,  $^{13}\text{C}/^{12}\text{C}$ ,  $^{18}\text{O}/^{16}\text{O}$ , and  $^{34}\text{S}/^{32}\text{S}$ . Isotopic ratios are measured in the laboratory on an instrument known as a mass spectrometer. Before a sample can be analyzed for its isotopic ratio, the element of interest in the sample must be converted to a gaseous form. For example, isotopes of hydrogen, oxygen, and sulfur are measured by converting the samples to hydrogen gas, carbon dioxide, and sulfur dioxide, respectively.

The primary use of radioactive isotopes is for dating the age of water and rocks. For groundwater, the clock begins ticking as soon as the radionuclide enters the groundwater at the time of recharge. The time unit is given by the half-life  $t_{1/2}$  during which the radioactivity of a specific isotope decays by 50 percent. After seven half-lives, the activity has decreased to only 1 percent of the original activity. The range of half-lives for environmental isotopes is large: from 15.7 million years ( $^{29}\text{I}$ ) to 300,000 years for ( $^{36}\text{Cl}$ ), 5,730 years for ( $^{14}\text{C}$ ), and 12.43 years for ( $^3\text{H}$ ) (e.g., Faure & Mensing, 2005).

Both stable and radioactive isotopes have a number of scientific applications. Typically, stable isotopes have been successfully used to determine the presence of different water sources/types and to investigate the hydraulic connections between different aquifers or formations. To identify a source of water, the stable isotopes of oxygen ( $^{18}\text{O}$ ) and hydrogen ( $^2\text{H}$ ) are most relevant. To investigate the origin of formation water or to explore the geochemical evolution processes that influence formation water chemistry in sedimentary basins, chlorine ( $^{37}\text{Cl}$ ), bromine ( $^{81}\text{Br}$ ), and strontium ( $^{87}\text{Sr}/^{86}\text{Sr}$ ) isotopes can be valuable tools (Duane et al., 2004; Saeed, 2021; Shouakar-Stash, 2008; Shouakar-Stash et al., 2006; Wood et al., 2005).

The stable sulfur isotope ( $^{34}\text{S}$ ) is mainly used to determine the source of sulfur. Moreover, additional information about the sources of sulfate and about the geochemical environment in which the sulfate was formed can be obtained from analysis of the stable oxygen isotope ( $^{18}\text{O}$ ) of dissolved sulfate. Berner and others (2002) used  $^{34}\text{S}$  and  $^{18}\text{O}$  of  $\text{SO}_4$  to identify zones of variable groundwater mixing and significant amounts of bacterial sulfate reduction.

To assess water-mineral interactions—especially where marked hydrogeological variations occur—the strontium isotopes ( $^{87}\text{Sr}/^{86}\text{Sr}$ ) are commonly applied. For example, Müller and others (1990) used Sr isotopes to separate groundwater and marine water in sabkhas (i.e., flat areas between desert and ocean) in Abu Dhabi.

Insights on water-mixing zonation can be obtained from analyses of the stable isotopes of boron ( $^{11}\text{B}$ ).

Radioactive isotopes are generally used for age dating of water. Information about the age of groundwater can be used to differentiate between different water sources. Generally, several radiogenic isotopes are used for age dating of water. In groundwater studies, tritium ( $^3\text{H}$ ) and carbon ( $^{14}\text{C}$ ) isotopes have been the most used. Analyses of  $^3\text{H}$

allow groundwater to be dated up to about fifty years in age and it has been used to identify hydraulic connections between an aquifer and water input from different sources. However, it has lost its value because the source of  $^3\text{H}$  occurred in the 1950s and 60s so the 50-year clock has expired. Analysis of  $^{14}\text{C}$  allows estimation of age (i.e., groundwater residence time) up to 30,000 years and provides patterns in ages, which can be useful for comparison of water from different aquifers. To use isotopes when investigating the origin or fate of formation water, it is crucial to understand the isotopic behaviors associated with various natural processes (Faure & Mensing, 2005; McMahon et al., 2019, 2021; Saeed, 2021).

## 8.2 Water Isotopes

The oxygen and hydrogen isotopes of  $\text{H}_2\text{O}$  have become the most useful tools in the study of the origin and evolution of subsurface water. Reviews of this topic are provided by Kharaka and Thordsen (1992), Sheppard (1986), and Faure and Mensing (2005). Prior to the use of isotopes, it was generally assumed that most of formation water in marine sedimentary rocks were trapped in the pores of sedimentary rocks as they were deposited (i.e., connate marine water) (White et al., 1963). Clayton and others (1966) were the first to use the isotopic composition of  $\text{H}_2\text{O}$  to show that water in several sedimentary basins are not connate but predominantly of local meteoric origin.

The connate water in sedimentary basins is generally lost by compaction, mixing, and flushing. The extensive use of isotopes of water, solutes, and associated minerals—coupled with studies of the regional geology and paleohydrology—has shown that subsurface water has a complicated history for the most part, and they are commonly mixtures of water of different origin (Birkle et al., 2002, 2009; Graf et al., 1965; Kharaka & Hanor, 2014; Kharaka & Thordsen, 1992).

The distribution of and controls on the isotopic composition of present-day precipitation and surface water are complex, especially in mountainous terrains. Their isotopic composition, together with data for paleoclimates and regional paleogeography, can be used to deduce the isotopic composition of old surface water including ocean water. An understanding of these parameters is needed to interpret the origin of deep basin brine (Kharaka & Thordsen, 1992). Reactions between water and minerals, dissolved species, associated gases, and other liquids with which they come into contact can modify the isotopic composition of water, especially the value of  $\delta^{18}\text{O}$  (O'Neil & Kharaka, 1976; Kharaka & Hanor, 2014). The del ( $\delta$ ) notation indicates the relative difference, in parts per thousand, of the isotopic ratios of a sample and of a reference standard. In addition to mixing of water of different isotopic composition, the following are the main processes that modify the isotopic composition of formation water in sedimentary basins:

1. isotopic exchange between water and minerals;
2. evaporation and condensation;

3. fractionation caused by the membrane properties of rocks; and
4. isotopic exchange between water and other fluids, especially petroleum compounds.

### 8.2.1 Formation Water Derived from Holocene Meteoric Water

The isotopic composition of water in some basins indicates that formation water is related principally to recent local meteoric water (Clayton et al., 1966; Hitchon & Friedman, 1969; Kharaka & Thordsen, 1992). The  $\delta D$  values of formation water related principally to recent local meteoric water (Figure 32) show a *hydrogen isotope shift* in addition to the generally observed *oxygen isotope shift*. The origin of these shifts varies, but the lines fitted to the  $\delta D$  and  $\delta^{18}O$  plots (Figure 32) in each case intersect the global meteoric water line (GMWL; Craig, 1961) at values that approximate those of present-day meteoric water in the area of recharge (Clayton et al., 1966; Kharaka & Thordsen, 1992).

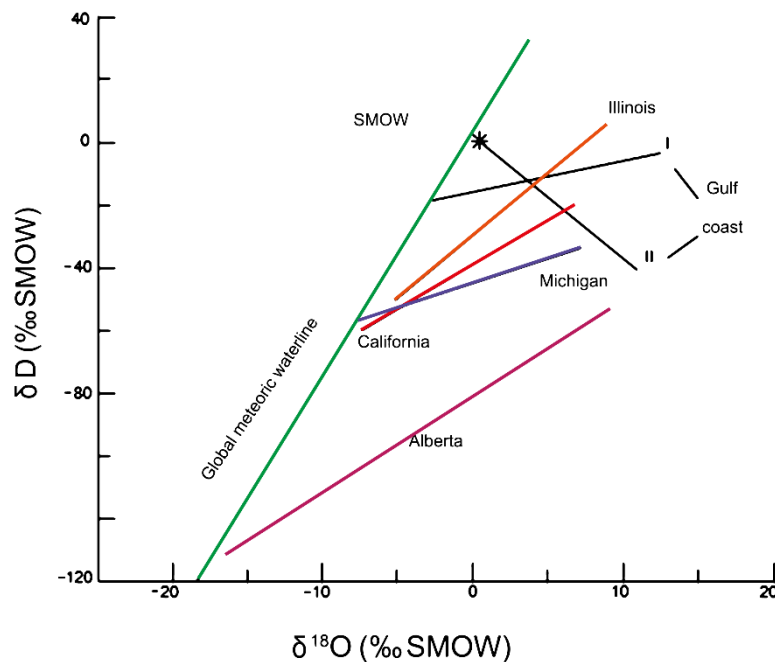


**Figure 32** - Isotopic compositions of produced water from several basins in North America (original lines from Clayton et al., 1966; Hitchon & Friedman, 1969; Kharaka et al., 1973, 1979). Except for Gulf Coast II, the isotope lines intersect the Global Meteoric Water Line (GMWL; Craig, 1961) at points with isotopic values of present-day meteoric water of the area (Kharaka & Thordsen, 1992). The \* indicates the isotopic value for SMOW, the standard mean ocean water.

Oxygen and hydrogen isotopes of formation water are sometimes not sufficient by themselves to indicate the origin of the water. Kharaka and others (1973) showed that plots of  $\delta D$  values and TDS as well as the geology and paleogeography indicate a connate marine origin for the water from the McAdams Formation (Eocene) of Kettleman North Dome, California, USA, and a meteoric origin for those from the overlying formations. The isotope data alone (Figure 32) could indicate a meteoric origin for both the water types as they plot

on the same trend. In the Alberta Basin, Canada, water isotope data (Hitchon & Friedman, 1969) combined with formation water flow regime, salinity, and geologic data (Bachu, 1995; Karsten & Bachu, 2002) indicate a complex origin for formation water. Some formation water is dominated by meteoric water, but formation water in parts of deeper zone is dominated by modified connate water. A mixture of the two water types is present in many parts of the basin.

### 8.2.2 Formation Water Originating from “Old” Meteoric Water

A combination of stable isotopes of water, in addition to age determinations based on  $^{14}\text{C}$  and other radioactive isotopes, have shown that the waters in many petroleum fields are ‘old’ meteoric water, that is, older than Holocene and probably older than Pleistocene (Bath et al., 1978; Clark and Fritz, 1997; Kharaka and Thordsen, 1992). Clayton and others (1966) were the first to show that a number of formation water samples from the Michigan and Illinois basins were probably recharged during the Pleistocene epoch because the  $\delta^{18}\text{O}$  values in those samples were much lower than those for present-day meteoric water.

Kharaka and others (1979) and Kharaka and Carothers (1986, 1988) presented evidence for meteoric water older than the Pleistocene in sedimentary basins. These authors presented isotopic and chemical data for formation water from exploration and production oil and gas wells on the North Slope of Alaska. The water samples were obtained from reservoir rocks between 700 and 2,800 m depth that range in age from Mississippian to Triassic. The water from all these rocks, however, is remarkably similar in TDS ( $1.9$  to  $2.4 \times 10^4$  mg/L) and in the concentration of the major cations and anions. The least-squares regression line through the  $\delta D$  and  $\delta^{18}\text{O}$  values for these water samples (Figure 33) intersects the meteoric water line at  $\delta D$  and  $\delta^{18}\text{O}$  values of 65 permil (parts per thousand) and 7 permil, respectively. This line does not pass through the values for standard mean ocean water (SMOW) or for the present-day meteoric water. The conclusion drawn from these studies was that the formation water was meteoric in origin, but recharge occurred when the North Slope had an entirely different climate. The relationship between mean annual temperature and the isotopic composition of meteoric water (Dansgaard, 1964) suggests the mean annual temperature at the Brooks Range, Alaska—the most likely recharge area—was 15 to 20 °C higher at the time of recharge than in 2023. Paleoclimatic indicators show that annual temperatures in northern Alaska were as high as this during the Miocene, as well as throughout most of the early Cenozoic and the Mesozoic (Bryant, 1997).

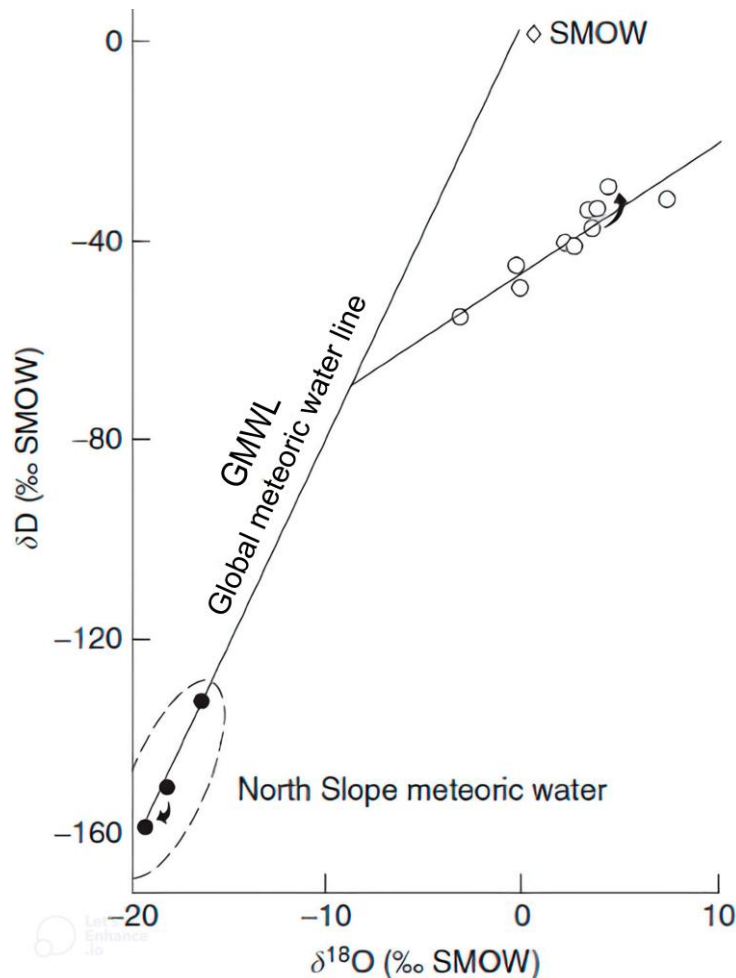


**Figure 33** - Isotopic composition of produced water from the North Slope, Alaska, USA with the least-squares regression line drawn through the data (open circles). Also shown are values for SMOW, meteoric water in the area, and the GMWL. The line through the data does not pass through SMOW nor the local meteoric water, but it intersects the GMWL in a location that would have had a much warmer climate than that of the present day. Arrows indicate corrected values as described in Kharaka and Carothers (1988).  $\diamond$  indicates isotopic values for SMOW, the standard mean ocean water.

### 8.2.3 Formation Water of Connate Marine Origin

Connate marine water is an important end-member component of fluid in sedimentary basins. Fluid flow and solute transport in many marine sediments, particularly deep-sea pelagic and semi-pelagic sediments, are dominated by compaction-driven advection and molecular diffusion (Berner, 1980). More dynamic fluid environments are found on continental shelves, where topographically driven meteoric water can mix with marine pore water (Hesse, 1990). As noted earlier, seawater is a Na-Cl-dominated fluid with  $\text{SO}_4$ , Mg, Ca, and K as the other major species. The relative proportion of these solutes is nearly constant throughout the world's oceans, with the exception of depleted, anoxic bottom water in closed submarine basins. Much of the water trapped in marine sediments at the time of deposition was seawater. This water, however,

underwent continuous early chemical diagenesis and a change in composition with time and depth of burial (Hesse, 1990; Schulz, 2000). Typically, Ca systematically increases while Mg and K systematically decrease with depth, with little change in salinity.

The variations in Ca and Mg are generally thought to be the result of hydrolysis of silicate minerals in underlying oceanic basement basalts (Hesse, 1990). The downward decrease in dissolved K may be related to the formation of the potassium-bearing zeolite, phillipsite, and adsorption by ion exchange on clays. There is often a distinct downward decrease in  $\delta^{18}\text{O}$  in marine interstitial water reflecting preferential removal of heavy oxygen during formation of phyllosilicates in altered igneous rocks and volcanoclastic sediments. Increases in  $\delta^{18}\text{O}$  levels, however, have been noted in gas hydrate-bearing sections of Deep-Sea Drilling Project cores. Silica concentrations are typically highly variable with depth and are dependent on lithology. Elevated silica concentrations, for example, are found in siliceous oozes. The recrystallization of biogenic pelagic carbonates releases substantial amounts of Sr but does not seem to have a significant effect on Ca concentration gradients.

With the exception of dissolution of evaporite minerals, chloride does not participate in mineral-fluid reactions in the subsurface in marine sections. The changes in chloride that have been observed in evaporite-free sections are due to mixing with freshwater released from gas hydrates, loss of water in hydration reactions, and possibly slight changes in seawater chlorinity during glacial–interglacial cycles. In more organic-rich hemipelagic sediments, redox conditions become progressively reducing with depth. As a result of a progression of redox reactions similar to those that characterize continental groundwater, dissolved ammonia, phosphate, and alkalinity typically increase in the upper part of the sediment column and dissolved sulfate decreases, primarily by reduction to sulfide (Berner, 1980).

The Gulf of Mexico Basin is a prime example of where formation water was originally connate marine in origin. The extensive drilling for petroleum, especially in the northern half of this basin, has documented a very thick sequence (up to 15,000 m) of Cenozoic terrigenous shales, siltstones, and sandstones; there are no major unconformities. Fine-grained sediments contain the largest percentage of connate water at the time of deposition (initial porosity was up to 80 percent). Most of this water was squeezed out into the interbedded sandstones during compaction (Kharaka & Thordsen, 1992).

Abnormally high fluid pressures (geopressured zones) are another important characteristic of these basins. In the northern Gulf of Mexico Basin, geopressured zones with hydraulic pressure gradients higher than hydrostatic (10.5 kPa/m; 0.465 psi/ft) are encountered at depths that range from 2,000 m in south Texas to more than 4,000 m in parts of coastal Louisiana (Kharaka et al., 1985). Calculated fluid potentials show hydraulic heads higher than heads in any recharge area of the basin, indicating that upward gradients drove

groundwater flow up the dip of geologic strata. The geologic and paleogeographic history of the northern Gulf of Mexico Basin suggest the flow has always been updip and toward the recharge areas to the north and northwest, indicating that much of the water is connate water squeezed from the marine shales and siltstones of the basin (Kharaka & Carothers, 1986; Land & Fisher, 1987).

The isotopic composition of formation water from many fields in the northern Gulf of Mexico Basin (Figure 34) falls on a general trend that passes through SMOW and away from the meteoric water of the area. Isotopic data show the formation water in the geopressured and normally pressured zones is neither meteoric in origin nor the result of mixing of meteoric with ocean water. Kharaka and Carothers (1986) used mass balance equations to show that the isotopic interaction between connate marine water and clay minerals—having a very light original  $\delta D$  value (70 permil)—is responsible for this unusual isotopic trend.

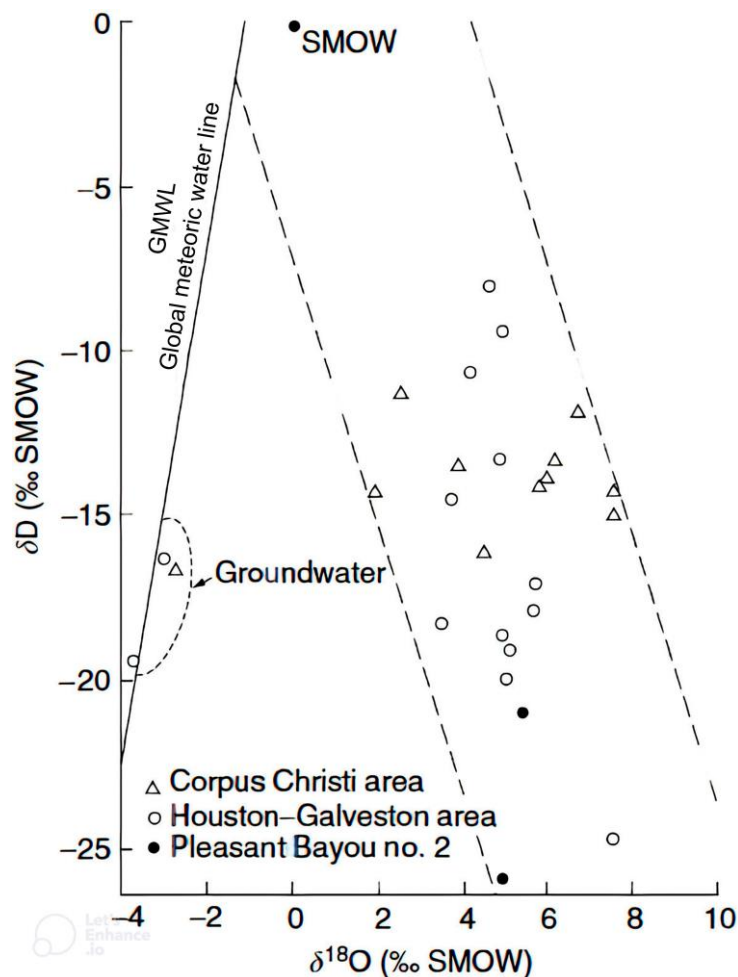


**Figure 34** - Isotopic composition of produced water from the northern Gulf of Mexico Basin. The trend shows decreased  $\delta D$  values with increasing  $\delta^{18}O$  values and that the trend goes through SMOW and away from the local groundwater, indicating a connate marine origin (from Kharaka et al., 1979). • indicates isotopic values for SMOW, the standard mean ocean water.

The concentration and isotopic composition of noble gases in natural gas produced from wells in the Gulf of Mexico Basin also support the conclusion that the formation water is marine connate in origin (Mazor & Kharaka, 1981; Kharaka & Specht, 2088). Finally, age determinations using  $^{129}\text{I}/^{127}\text{I}$  ratios for 60 formation water samples from several oil fields in Texas and Louisiana gave ages of 53 to 55 Ma. This points to the Wilcox Group shale as the main source of iodide. Moran and others (1995) pointed out that even older (Mesozoic age) shale could not be ruled out, because of uncertainties in estimating the composition of the fission component.

#### 8.2.4 Bittern Connate Water Associated with Evaporites

Evaporated seawater trapped in precipitated salt and associated sediments and adjacent rocks (bittern water) is probably an important component of formation water in several sedimentary basins (Carpenter et al., 1974; Kharaka et al., 1987; Moldovanyi & Walter, 1992). The central Mississippi Salt Dome Basin is such a basin. The isotopic composition of its formation water (Figure 35) belongs to three main groups. Samples from rocks of Jurassic age (Smackover and Norphlet formations) have  $\delta\text{D}$  values ranging from -1 to -3 permil, comparable to that of SMOW; they also have  $\delta^{18}\text{O}$  values ranging from 5.1 to 7.3 permil, which are highly enriched in  $^{18}\text{O}$ . Samples obtained from rocks of Cretaceous age have  $\delta\text{D}$  values (-9 to -13 permil) that are depleted in deuterium relative to both SMOW and the samples from rocks of Jurassic age. Finally, samples obtained from shallow groundwater in the area have  $\delta\text{D}$  and  $\delta^{18}\text{O}$  values that plot close to the GMWL. The  $\delta^{\text{a}}\text{D}$  values (Figure 35) give the D/H measurements in terms of the activities of deuterium in high salinity solutions calculated using a correction factor from Sofer and Gat (1972).

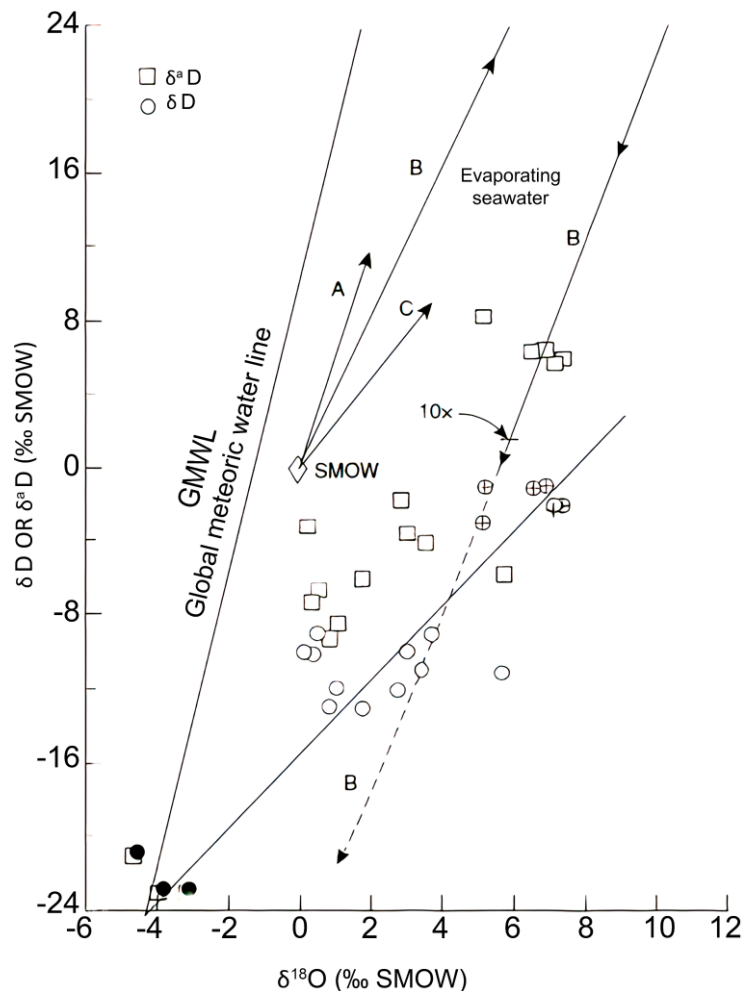


**Figure 35** - Isotopic composition of local shallow groundwater (solid circles), formation water from Jurassic (open circles with +), and Cretaceous (open circles) rocks from the central Mississippi Salt Dome Basin.  $\delta^2D$  values (squares) were computed from  $\delta D$  values and a correction factor from Sofer and Gat (1972). Lines originating from SMOW are the range of trajectories for seawater undergoing evaporation, with line B being from Holser's (1979) estimate of evaporating seawater in the Gulf Coast. The least-squares regression line for the  $\delta D$  and  $\delta^{18}O$  values is also indicated (after Kharaka et al., 1987).  $\diamond$  indicates isotopic values for SMOW, the standard mean ocean water.

The isotopic composition of these waters supports the conclusion, based on plots of bromide versus chloride and combinations of other chemical constituents (Carpenter et al., 1974; Kharaka et al., 1987; Stoessell and Carpenter, 1986), that the formation water in rocks of Jurassic age are evaporated seawater. The  $\delta D$  and  $\delta^{18}O$  values of evaporating seawater (line B in Figure 35) initially increase with increasing evaporation, but at higher degrees of evaporation, the line loops (loop not shown), then reverses direction (Holser, 1979). There are several trajectories for changes in water isotopes as seawater evaporates; Knauth and Beeunas (1986) have shown that line B in Figure 36 is the most likely trajectory for evaporating seawater in the Gulf Coast. This line passes very close to the point giving the

d-values (point of interception with the x axis) for the water in the Norphlet Formation, which is what is expected from evaporating seawater at the point of halite precipitation. The d-values of the samples from the Smackover Formation were initially close to those from the Norphlet Formation; the 1-2 permil shifts in the d-values are probably related to isotopic exchange with the enclosing carbonate minerals (Heydari and Moore, 1989).

### 8.2.5 Brine of Mixed Origin

Formation water in sedimentary basins is highly mobile; this leads to mixing of water of different ages or of different origin and ages (Kharaka & Carothers, 1986; Worden et al., 1999; Ziegler & Coleman, 2001). Hitchon and Friedman (1969) made a very detailed isotopic and chemical study of the surface and formation water in the Western Canada Basin. Using mass balance calculations for deuterium and TDS, they concluded that the observed distribution of deuterium in the formation water could best be explained by mixing of diagenetically modified seawater with 2.9 times its volume of fresh meteoric water. They attributed the  $^{18}\text{O}$  enrichment of formation water to extensive exchange with carbonate rocks.

Other examples of deep-basin water related to simple mixing of meteoric water with marine connate water have been documented in the Dnepr–Donets Basin, Ukraine (Vetshteyn et al., 1981), and in the Sacramento Valley, California, USA (Berry, 1973; Kharaka et al., 1985). Knauth (1988) used water isotopes and chemical data for water in the Palo Duro Basin, Texas, USA, to indicate extensive mixing between bittern brine and two pulses of meteoric water with different isotopic compositions.

Mixing of water of the same origin but affected by different processes is likely common in sedimentary basins. Kharaka and others (1985) used  $\delta\text{D}$  and  $\delta^{18}\text{O}$  values and the chemical composition of formation water from High Island Field, offshore Texas, USA, to show (Figure 36) that the formation water in Pleistocene reservoir rocks involved mixing of two types of connate marine water. One end member is an essentially unmodified marine connate water of Pleistocene age (samples 6 and 7 in Figure 36); the other (sample 5) is a chemically and isotopically modified marine connate water, possibly of Miocene age. Approximately the same mixing proportions were obtained using stable isotope values (Figure 36) and concentrations of sodium, chloride, calcium, and lithium.

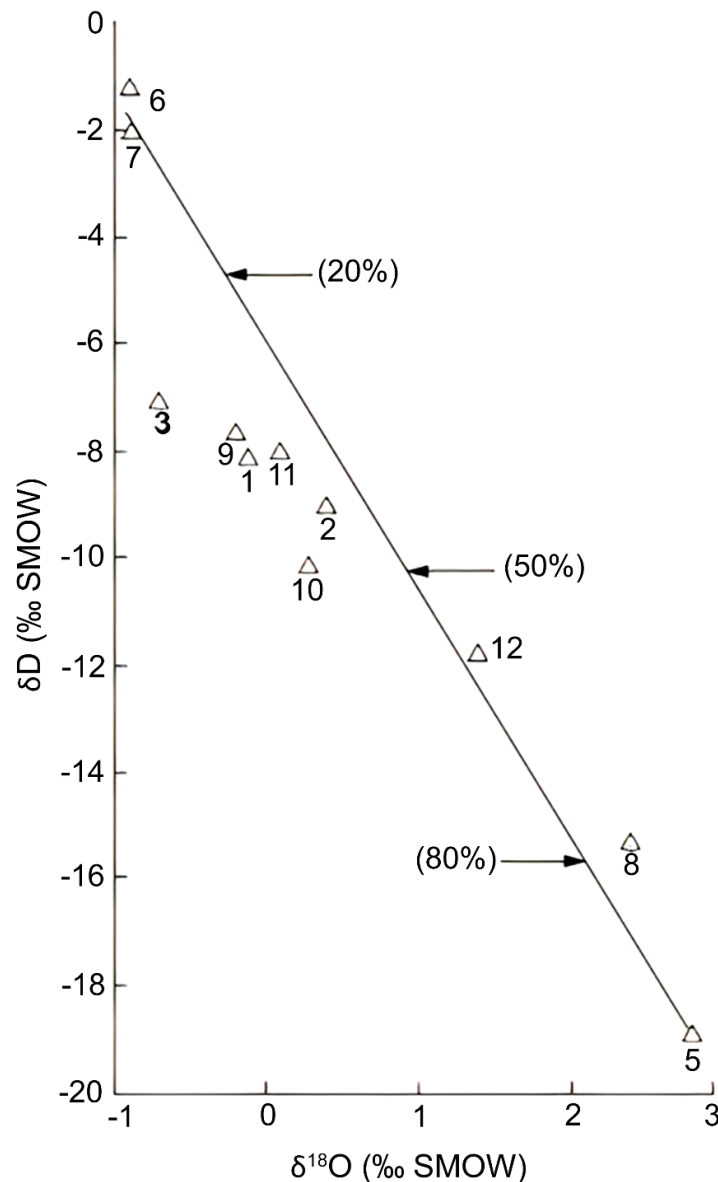


**Figure 36** - Isotopic composition of produced water from High Island Field, offshore Texas, USA. Percentages represent mixing proportions of the deep brine with Pleistocene connate seawater. Samples 6 and 7 are essentially unmodified marine connate water of Pleistocene age; sample 5 is a chemically and isotopically modified marine connate water, possibly of Miocene age (from Kharaka et al., 1985). SMOW is standard mean ocean water.

### 8.3 Isotopic Composition of Solutes

Significant advances in isotope analytical techniques over the last several decades have greatly expanded our knowledge of the isotopic composition of natural water (Ajemigbitse et al., 2020; Bagheri et al., 2014; Birkle et al., 2010; Bullen et al., 2001; Capo et al., 2014; Fantle & Bullen, 2009; Kharaka et al., 2017; McMahon et al., 2019, 2021; Tasker et al., 2020). Precise data are now available for isotopic compositions of hydrogen, oxygen, carbon, and sulfur, and a large body of data is available for strontium, boron, and noble gas

isotopes. More recently, data for isotope systematics of lithium, chloride, bromide, and iodide in basinal water have been accumulating. The applications of isotope geochemistry in studies of sedimentary basins have included identifying the sources of solutes and  $H_2O$ , quantifying the degree of rock–water exchange, tracing fluid flow paths, determining paleotemperatures, and calculating the age and residence time of basinal fluids. The systematics of many isotopic systems, such as those of strontium, have been well determined for formation water. Some systems, such as that of bromide, are in their infancy; others, such as the stable isotope geochemistry of chloride, are beset by unresolved questions regarding their interpretation.

This section discusses the stable isotopes of boron, lithium, carbon, sulfur, chloride, bromide, strontium, and calcium; we divide the stable isotopes into traditional and nontraditional isotopes and provide a summary discussion of radioactive isotopes and age dating. Recent reviews of other isotopic systems, including noble gases, have been used in subsurface hydrogeology and are reported in Cook and Herczeg (2000), Bullen (2011), and Kharaka and Hanor (2014).

### 8.3.1 Boron Isotopes

Boron has stable isotopes with atomic masses of 10 and 11. These have natural abundances of 19.82 percent and 80.18 percent, respectively (Aggarwal et al., 2000; Marschall & Foster, 2018; Palmer & Swihart, 1996). The analyses of  $^{11}B/^{10}B$  isotopic ratios are reported in the standard  $\delta^{11}B$  notation permil. Natural water ranges in  $\delta^{11}B$  from -16 to +60 permil relative to the SRM NBS 951 standard. This exceptionally wide range reflects the large variability in the isotopic composition of boron sources and the large fractionation factors attendant to the partitioning of boron between aqueous and solid phases (Barth, 1998). The major factors in the isotopic fractionation of boron are the preference of  $^{10}B$  for tetrahedral coordination with oxygen (either in the borate ion  $B(OH)_4^-$  or in silicate mineral surface and lattice sites) and the preference of  $^{11}B$  for trigonal coordination with oxygen as in dissolved boric acid  $B(OH)_3$ .

Under diagenetic conditions, boron is present largely in trigonal coordination in fluids but in tetrahedral coordination in silicates. Fractionation is less mineral-specific than coordination-specific (Williams et al., 2001a). Lighter isotopes are generally concentrated in the more volatile phase because of their higher vibration frequency, but boron is an important exception because of the significance of the coordination state in the fractionation of its isotopes.

The value of  $\delta^{11}B$  in seawater is 40 permil; in marine carbonates, 10 to 30 per permil; and in continental rocks and siliclastic sediments, 15 to 5 per permil (Aggarwal et al., 2000; Palmer & Swihart, 1996). Boron isotopic values for Gulf Coast formation water range from 1 to 50 permil (Land & Macpherson, 1992a). There is a general decrease in  $\delta^{11}B$  and

an increase in boron with increasing depth and temperature, reflecting the release of light boron during silicate mineral diagenesis.

During deep burial diagenesis, some boron is reincorporated into crystal lattices. The  $\delta_{\text{B}}^{11}$  of diagenetic mineral phases should therefore reflect the  $\delta_{\text{B}}^{11}$  of the ambient fluid. Since boron substitution for silicon involves the breaking of Si–O bonds, there should be a coincident change in the  $\delta_{\text{O}}^{18}$  of mineral phases. However, boron fractionation is so large that the value of  $\delta_{\text{B}}^{11}$  may be more sensitive than  $\delta_{\text{O}}^{18}$  to fluid–rock exchange under diagenetic conditions. Williams and others (2001b) have developed a boron fractionation equation based on this concept that can possibly be used to determine paleotemperatures.

### 8.3.2 Lithium Isotopes

Lithium has two stable isotopes ( ${}^6\text{Li}$  and  ${}^7\text{Li}$ ) that have abundances of 7.5 percent and 92.5 percent, respectively. Lithium is a soluble alkali element. Because its ionic radius is small (0.78 Å), it behaves more like magnesium (0.72 Å) than the other alkalis.  $\text{Li}^+$  tends to substitute for  $\text{Al}^{3+}$ ,  $\text{Fe}^{2+}$ , and especially for  $\text{Mg}^{2+}$ . Because of their large relative mass difference, lithium isotopes have the potential to exhibit sizable fractionation, as has been demonstrated by high-precision isotopic analysis.

Lithium isotopic compositions generally are reported in terms of  $\delta_{\text{Li}}^6$ , an unusual formulation because the abundance of the heavier isotope is in the denominator (Chan et al., 2002).  $\delta_{\text{Li}}^6$  is defined in Equation (9).

$$\delta_{\text{Li}}^6(\text{permil}) = \left[ \frac{\left( \frac{{}^6\text{Li}}{{}^7\text{Li}} \right)_{\text{sample}}}{\left( \frac{{}^6\text{Li}}{{}^7\text{Li}} \right)_{\text{std}}} - 1 \right] \times 1,000 \quad (9)$$

Lithium in seawater, with an average  $\delta_{\text{Li}}^6$  value of -32 permil, is therefore isotopically heavy. Marine sediments, with  $\delta_{\text{Li}}^6$  values of +1 to -15 permil, are much lighter. Other reported ranges in  $\delta_{\text{Li}}^6$  values for geological materials include those of mid-ocean-ridge basalts, -8 to -21 permil; hemipelagic clays, -9 to -15 permil; and continental crustal rocks, -8 to -21 permil (Huh et al., 1998). All lithium isotopes are referenced to the NBSL-SVEC  $\text{Li}_2\text{CO}_3$  standard (Clark & Fritz, 2013).

Chan and others (2002) studied the isotopic composition of lithium in oil-field brine in the Heletz-Kokhav Field in the southern coastal plain of Israel. The formation water has chloride concentrations of 18,000 to 47,000 mg/L and are thought to represent seawater evaporated into the gypsum stability field and subsequently altered by the dissolution of halite. Lithium concentrations range from 0.97 mg/L to 2.3 mg/L and increase with increasing chloride. The  $\delta_{\text{Li}}^6$  values range from -198 to -30 permil and are thus lighter than

seawater (-32 permil), reflecting a rock-dominated source for lithium rather than an evaporated seawater source.

### 8.3.3 Carbon Isotopes

The origin of inorganic and organic carbon in sedimentary basins and the systematics of its isotopes have received a great deal of attention (e.g., Clark & Fritz, 1997; Kharaka & Hanor, 2014). The stable carbon isotopic composition of dissolved carbon species—such as  $\text{HCO}_3^-$ ,  $\text{CO}_2(\text{aq})$ ,  $\text{CH}_4(\text{aq})$ , and the organic acids—is normally reported as  $\delta^{13}\text{C}$  permil PDB (Pee Dee Belemnite, a sample of shells of an extinct organism collected on banks of the Pee Dee River in California, USA). There are two major reservoirs of carbon in sedimentary basins: marine carbonate having  $\delta^{13}\text{C}$  values of  $0 \pm 4$  permil and organic carbon with values between -10 permil and -35 permil. Bacterial and thermogenic reduction of organic matter to methane produces two isotopically distinct  $\text{CH}_4$  reservoirs: biogenic  $\text{CH}_4$  with  $\delta^{13}\text{C}$  of -50 to 90 permil, and thermogenic  $\text{CH}_4$  with  $\delta^{13}\text{C}$  between -20 permil and -50 permil.

Carothers and Kharaka (1980) reported  $\delta^{13}\text{C}$  values of inorganic carbon dissolved in oil-field water from California and Texas and discussed the sources and reactions that yield  $\delta^{13}\text{C}$  of -20 to 28 permil. Dissolution of carbonate minerals and the oxidation of reduced carbon both produce bicarbonate as a byproduct. Emery and Robinson (1993) reported a range from -60 to 10 permil, depending on the source of the carbon and the fractionation factors accompanying the production of  $\text{HCO}_3^-$ .

An increasing body of evidence indicates that the large volumes of  $\text{CO}_2$ —observed in basins such as the Pannonian Basin, Hungary; the Cooper-Eromanga Basin, Australia; and the South Viking Graben, North Sea—may have deep-seated sources (Wycherley et al., 1999). The isotopic composition of  $\text{CO}_2$  released by mantle, deep crustal, and shallow high-temperature processes is estimated to be intermediate between values for inorganic marine carbonate and organic carbon. Wycherley and others (1999) cited the following values: magmatic origin/mantle degassing, -4 to -7 permil; regional metamorphism, 0 permil to 10 permil; contact metamorphism of carbonates, -2 permil to -12 permil; and contact metamorphism of coals, -10 to -20 permil. It should be noted that as the result of the number of sources for carbon of varying  $\delta^{13}\text{C}$  values, and especially due to the ease of isotopic exchange and re-equilibration as well as mixing, carbon isotopes are not highly diagnostic and cannot be used alone to identify carbon sources (Kharaka et al., 1999b). Carbon isotopes in shallow groundwater are discussed by Kendall and Doctor (2014).

### 8.3.4 Sulfur Isotopes

The isotopic composition of sulfur in geologic materials is reported in the usual  $\delta^{34}\text{S}$  notation as  $\delta^{34}\text{S}$  permil relative to Vienna Canyon Diablo Troilite (VCDT). The isotopic geochemistry of sulfur is complex because it exists in several redox states, each with a wide variety of fractionation mechanisms (Seal et al., 2000). The three principal redox states of

concern here are sulfur as sulfate (VI), sulfide (-II), and elemental sulfur (0). Below ~200 °C, the nonbiologic rate of isotopic exchange between dissolved sulfate and sulfide is slow and isotopic equilibrium between the species is rare (Ohmoto & Lasaga, 1982). Kinetic effects therefore dominate the isotopic systematics of sulfur in sedimentary basins. The principal kinetic effects are associated with the reduction of sulfate to elemental sulfur or sulfide S(-II). This can be achieved both microbially with large fractionation effects and thermochemically with minimal fractionation. Fractionation is usually minor during the oxidation of sulfide to sulfate (Seal et al., 2000).

The principal sources of sulfate in formation water are dissolved marine sulfate, sulfate derived from the dissolution of evaporites, and sulfate formed by the oxidation of sulfides. Sulfate is destroyed by reduction to hydrogen sulfide. The value of  $\delta^{34}\text{S}$  in gypsum is only ~1.6 permil heavier than sulfate in solutions from which it precipitates. The isotopic composition of sulfur in gypsum in Phanerozoic deposits precipitated from seawater during evaporation tracks the secular changes in the isotopic composition of sulfur in seawater (~10 to 30 permil).

The lighter isotopes of sulfur are preferentially partitioned into sulfide during microbial SO reduction. Hydrogen sulfide is much lighter than the precursor sulfate, whereas residual sulfate is heavier. Therefore, sulfate reduction during early diagenesis drives the  $\delta^{34}\text{S}$  of residual pore-water sulfate toward higher values. Thermochemical reduction of sulfate at higher basinal temperatures, however, typically produces sulfide similar in isotopic composition to the parent sulfate (Machel, 2001).

Dworkin and Land (1996) found that the  $\delta^{34}\text{S}$  values of sulfate in Frio (Oligocene) formation water were modified by the addition of light sulfur derived from the probable inorganic oxidation of pyrite at elevated temperatures. The  $\delta^{18}\text{O}$  values of dissolved sulfate in this water fall within the range found in Mesozoic and Cenozoic seawater and are interpreted by Dworkin and Land to reflect sulfate derived from deeper Jurassic evaporites.

However, this conclusion must be qualified because at temperatures > 100 °C, oxygen isotopes equilibrate between oxygen in water and in sulfate (e.g., Kharaka & Mariner, 1989). Gavrieli and others (1995) documented two stages in the evolution of the isotopic composition of sulfate-sulfur in oil fields of southwestern Israel. Early shallow bacterial reduction increased the  $\delta^{34}\text{S}$  of residual dissolved Miocene sulfate from 20 to 26 permil. In the presence of crude oil, additional sulfate was reduced and increased the  $\delta^{34}\text{S}$  values to a maximum of 54 permil.

### 8.3.5 Chlorine Isotopes

Chlorine has two stable isotopes,  $^{37}\text{Cl}$  and  $^{35}\text{Cl}$ , and one radioactive isotope:  $^{36}\text{Cl}$  (half-life 301,000 years). The stable isotopic composition of chloride in geologic materials is reported in the conventional del notation as  $\delta^{37}\text{Cl}$ . Seawater, which is used as the isotopic standard, has a  $\delta^{37}\text{Cl}$  of 0 permil. Natural water typically has  $\delta^{37}\text{Cl}$  values between -

1 permil and +1 permil. However, values of -8 permil have been measured in marine pore water. Minerals in which chloride substitutes for OH at high temperatures have  $\delta^{37}\text{Cl}$  values as high as 7 permil (Banks et al., 2000).

During halite precipitation from evaporated seawater,  $^{37}\text{Cl}$  is preferentially partitioned into the solid phase, so the  $\delta^{37}\text{Cl}$  of the residual brine and of subsequently precipitated halite become progressively lighter. However, during the last stages of evaporation, preferential incorporation of  $^{35}\text{Cl}$  into potassium and magnesium salts reverses the fractionation trend; the residual brine and the precipitated salts become isotopically heavier (Banks et al., 2000; Eastoe et al., 1999). The  $\delta^{37}\text{Cl}$  of halite precipitated from evaporated seawater with a  $\delta^{37}\text{Cl}$  value of 0 is -0.29 permil. Eastoe and others (1999) found a minimum  $\delta^{37}\text{Cl}$  value of -0.9 permil in brine produced during the laboratory evaporation of seawater at the beginning of the potash facies.

The mechanisms that fractionate chloride isotopes during diagenesis are still not well established (Eastoe et al., 1999). Eggenkamp (1998) found a range from -0.27 permil to 4.96 permil in the  $\delta^{37}\text{Cl}$  of formation water from North Sea oil fields. In some fields,  $\delta^{37}\text{Cl}$  decreased with decreasing chloride concentration. Water from oil reservoirs had a much smaller range in  $\delta^{37}\text{Cl}$ , from 0 percent to -1.5 permil over a wide range of chloride concentrations. Bedded salt in the Gulf of Mexico Basin has  $\delta^{37}\text{Cl}$  values of -0.5 permil to 0.3 permil (Eastoe et al., 2001), values consistent with a  $\delta^{37}\text{Cl}$  value of 0.0 permil for Jurassic seawater.

Eastoe and others (2001) suggested that the slightly heavier values for diapiric salt (0.0 to 0.5 permil) are the result of the incongruent dissolution of halite, which presumably releases lighter chloride preferentially. The  $\delta^{37}\text{Cl}$  values of formation water from the Gulf of Mexico Basin range from -1.9 permil to 0.7 permil. Water having  $\delta^{37}\text{Cl}$  values < 0.6 permil are found in siliciclastic strata of Eocene to Miocene age but not in Plio-Pleistocene sediments or in Mesozoic carbonates, which contain water of higher  $\delta^{37}\text{Cl}$  composition. Eastoe and others (2001) invoked differences in the rate of diffusion of  $^{35}\text{Cl}$  and  $^{37}\text{Cl}$  as a possible fractionation mechanism.

### 8.3.6 Bromine Isotopes

Bromine isotope geochemistry is in its developing stages but is proving useful to understand the evolution of brine in sedimentary basins (Shouakar-Stash, 2008; Shouakar-Stash et al., 2006). Bromine has two stable isotopes,  $^{79}\text{Br}$  and  $^{81}\text{Br}$ , having relative mass abundances of 50.7 percent and 49.3 percent, respectively (Eggenkamp & Coleman, 2000). Variations in isotopic composition are reported as  $\delta^{81}\text{Br}$  (SMOB), where SMOB is standard mean oceanic bromide.

Several processes have the potential for causing significant fractionation of the bromide isotopes. These include concentration of bromide during the evaporation of seawater, oxidation of bromide to  $\text{Br}_2$ , and the natural production of organobromide

compounds. Eggenkamp and Coleman (2000) found a range of 0.08 to 1.27 permil in  $\delta^{81}\text{Br}$  in formation water of the Norwegian North Sea. The negative correlation between  $\delta^{81}\text{Br}$  and  $\delta^{37}\text{Cl}$  reflects differences in fractionation mechanisms of the two isotopic systems.

### 8.3.7 Strontium Isotopes

The strontium isotopic composition of formation water has shown great utility as a means to identify sources of strontium in formation water, the degree of water-rock exchange, and the degree of mixing along regional fluid flow paths and in groundwater contamination plumes (e.g., Armstrong et al., 1998; Capo et al., 2014; Peterman et al., 2010). The strontium isotopic composition of geologic materials is expressed as the ratio of  $^{87}\text{Sr}/^{86}\text{Sr}$ , which can be measured with great analytical precision.

Strontium has four stable isotopes:  $^{84}\text{Sr}$  (0.56 percent),  $^{86}\text{Sr}$  (9.86 percent),  $^{87}\text{Sr}$  (7.0 percent), and  $^{88}\text{Sr}$  (82.58 percent), and a radiogenic  $^{87}\text{Sr}$  isotope that is produced by the decay of Rb (half-life =  $4.88 \times 10^{10}$  years). Rocks having high initial concentrations of rubidium, such as granites, are characterized by high  $^{87}\text{Sr}/^{86}\text{Sr}$  ratios. Rocks derived from materials having low rubidium concentrations, such as mantle-derived rocks, have correspondingly low  $^{87}\text{Sr}/^{86}\text{Sr}$ . Since the Precambrian, the  $^{87}\text{Sr}/^{86}\text{Sr}$  of seawater has fluctuated between  $\sim 0.7070$  and  $\sim 0.7092$  as the result of variations in the relative rates of input of  $^{87}\text{Sr}$ -enriched strontium from continental weathering and  $^{87}\text{Sr}$ -depleted strontium from mantle sources.

Fluids in sedimentary basins containing Paleozoic strata typically have  $^{87}\text{Sr}/^{86}\text{Sr}$  ratios in excess of current seawater values that are contemporaneous or coeval with the depositional age of the current host sediment. The enrichment is due to the release of strontium attending the alteration of silicates. Due to the significant increase of  $^{87}\text{Sr}/^{86}\text{Sr}$  in seawater since the Jurassic, some formation water in Cenozoic sedimentary basins actually has  $^{87}\text{Sr}/^{86}\text{Sr}$  ratios lower than those of contemporaneous seawater due to the addition of strontium dissolved from older and deeper sedimentary sources (McManus & Hanor, 1993). Precipitates derived from such sources, such as barite in Holocene seafloor vents in the Gulf of Mexico, have lower  $^{87}\text{Sr}/^{86}\text{Sr}$  values than present-day seawater (Fu, 1998).

### 8.3.8 Calcium Isotopes

Reliable results for Ca isotopes were not obtained until Russel and others (1978) published an accurate method for determining Ca stable isotope compositions using double spike-thermal ionization mass spectrometry. Only a few studies have focused on Ca stable isotopes until the late 1990s. Since then, the number of studies dealing with Ca stable isotope fractionation has steadily increased, reflecting both analytical advances and promising results obtained in a large variety of applications in earth and life sciences. In their book *Nontraditional Stable Isotopes*, Teng and others (2017) provide detailed analytical methods including protocols for sample preparation and isotope analysis, various fields of

application (such as low-temperature mineral precipitation and biomineralization), and indicate future research directions.

Calcium isotopes are fractionated during inorganic precipitation from aqueous solutions according to their relative mass differences. The magnitude and sign of isotope fractionation depend on the composition and structure of the solid and the physicochemical conditions of the aqueous environment. Ca isotope fractionation during precipitation experiments at well-defined conditions—where results for Mg, Sr, and Ba, are included for the discussion of fractionation mechanisms—are reported (Blättler et al., 2015; Böttcher et al., 2012). Teng and others (2017) cover the different conceptual models for Ca isotope fractionation between carbonate minerals and aqueous solutions; they include Ca isotope variability found in inorganic minerals from natural environments, and Ca isotope fractionation related to ion diffusion, ion exchange, and ion adsorption in aqueous systems.

## 8.4 Traditional and Nontraditional Isotopes

Stable isotopes have shown highly versatile applications in the field of geochemistry. Two types of stable isotopes have been used: traditional stable isotopes including C, N, O, S, and H and nontraditional stable isotopes such as Ca, Zn, Cu, Fe, Pd, Cd, and other metals (Cramer & Jarvis, 2020; Kay et al., 2002; Farkas et al., 2012; Gussone & Dietzel, 2016; Teng et al., 2017). On the one hand, traditional isotopes have been utilized for more than 100 years as geothermometers, and tracers in hydrological systems including formation water, ore deposits, and hydrothermal systems. On the other hand, nontraditional isotopes have had limited study due to a lack of advanced techniques and methods. Fortunately, recent advancements in techniques and development of advanced methods have increased their application in various fields (Bullen 2009, 2011). The nontraditional isotopes have been used in various geochemical applications such as for tracing of toxic environmental pollutants like Cr and Hg, in mining and petroleum operations. There is great value in using multiple isotope systems together with solute concentrations in a multi-tracer approach, rather than relying on the results of a single system analysis (Bullen, 2011).

Traditional stable isotope geochemistry involves isotopes measured predominantly by gas-source mass spectrometry (Teng et al., 2017). Even though Li isotope geochemistry was developed in the 1980s based on thermal ionization mass spectrometry, the real flourishing of so-called nontraditional stable isotope geochemistry was made possible by the development of MC-ICP-MS (multi-collector, inductively-coupled, plasma mass spectrometers). Since then, isotopes of both light (e.g., Li, Mg) and heavy (e.g., Tl, U) elements have been routinely measured with a precision high enough to resolve natural variations. Large variations have been documented in both natural samples and laboratory experiments for nontraditional stable isotopes. These studies suggest that the following

factors control the degree of isotope fractionation in non-traditional stable isotopes during various processes: the relative mass difference between isotopes, change of the oxidation state, biological sensitivity, and volatility. Among these elements, Li displays the largest isotopic variation in terrestrial samples. Since Li is neither volatile during geological processes nor sensitive to redox reactions and biological processes, the large isotope fractionation is controlled mainly by the large relative mass difference.

For many of the other elements, other factors may be equally, if not more, important. For example, chlorine exhibits the second largest isotopic variation due to kinetic isotope fractionation during volcanic degassing. Selenium isotopes also show large isotopic variations, but this reflects redox-controlled Se isotope fractionation, while the large mercury isotopic variations are mainly associated with biological processes (Teng et al., 2017).

## 8.5 Radioactive Isotopes and Age Dating

A number of radioactive isotopes that are produced primarily by cosmic ray interactions in the upper atmosphere, especially  $^{14}\text{C}$  (Clark & Fritz, 1997; Mazor, 1997),  $^{36}\text{Cl}$  (Andrews et al., 1994; Phillips, 2000),  $^{129}\text{I}$  (Fabryka-Martin, 2000; Moran et al., 1995),  $^{39}\text{Ar}$ , and  $^{81}\text{Kr}$  (Aggarwal, 2013; Loosli & Purtschert, 2005; Porcelli et al., 2002; Purtschert et al., 2021), as well as total dissolved  $^4\text{He}$  (Solomon, 2000)—have been used, in conjunction with data for stable isotopes and calculated flow rates, to determine the residence time (age) of natural water including fluids in sedimentary basins (Bethke & Johnson, 2002; Bethke et al., 1999, 2000; Plummer, 2005). The 5.73 ka half-life of  $^{14}\text{C}$  is so short that it is useful only for dating basinal meteoric water younger than 40 ka.  $^{36}\text{Cl}$  ( $t_{1/2}=0.301$  Ma) is useful for dating water of up to 2 Ma in age. These isotopic systems are reviewed by Phillips and Castro (2014).

The ratio of  $^{129}\text{I}$  ( $t_{1/2}=15.7$  Ma) to total iodide can be used to estimate ages up to 80 Ma. The determination of even greater ages is theoretically possible by using  $^4\text{He}$  generated from the decay of uranium and thorium in rocks (Froehlich et al., 1991). However, the ages obtained carry large uncertainties because the radioactive isotopes can have several sources (e.g., Fabryka-Martin, 2000) and are often subject to fractionation due to isotopic exchange and partitioning. In addition, the origin and age of  $\text{H}_2\text{O}$  in formation water is generally different from that of the radioactive and other isotopes used for age determinations (Clark & Fritz, 1997; Kharaka & Thordsen, 1992; Froehlich et al., 1991).

The ratio of  $^{129}\text{I}$  to total I, at times in combination with  $^{36}\text{Cl}/\text{Cl}$  ratios, has been successfully used to estimate the residence time of subsurface water, to trace the migration of brines and to identify hydrocarbon sources (e.g., Fabryka-Martin, 2000). However, this method can also be used to illustrate the difficulties of dating “very old” formation water. These difficulties include the following.

1. The ratios of  $^{129}\text{I}/\text{I}$  generally are between  $20 \times 10^{-15}$  and  $1,500 \times 10^{-15}$ , requiring the use of an accelerator MS for their measurement.
2. There are major uncertainties in the correct value of the initial  $^{129}\text{I}/\text{I}$  ratios.
3. Errors may occur in the estimation of the rate of subsurface release of  $^{129}\text{I}$  by spontaneous fission of  $^{238}\text{U}$ .
4. Additional (diagenetic) release of  $^{129}\text{I}$  from organic-rich sediments may occur (Fabryka-Martin, 2000; Moran et al., 1995).

For several of these reasons, the  $^{129}\text{I}/\text{I}$  and  $^{36}\text{Cl}/\text{Cl}$  ratios could not be used to estimate the residence nor the travel time of water in the Milk River aquifer, Alberta, Canada (Fabryka-Martin, 2000).

The age of brine inclusions in Louisiana salt domes was estimated to be 8 Ma by  $^{129}\text{I}/\text{I}$  ratios that assumed no significant in-situ production of  $^{129}\text{I}$  because of the low uranium concentration in salt (Fabryka-Martin et al., 1985). Moran and others (1995) found the comparison between measured ratios and the decay curve for hydrospheric  $^{129}\text{I}$  results in minimum source ages much older than present host formation ages, indicating migration of brine from older and deeper sources. Corrections for the fissiogenic (i.e., formed by nuclear fission) component of  $^{129}\text{I}$  gave Eocene ages (53 to 55 Ma) for brine residing in Miocene reservoirs. However, Mesozoic sources could not be ruled out because of uncertainties in estimating the magnitude of the fissiogenic component. Some of the measured  $^{129}\text{I}/\text{I}$  ratios showed that the brine had resided in formations with locally high uranium values (Moran et al., 1995).

## 8.6 Exercises Pertinent to Section 8

[Link to Exercise 14](#) ↴

[Link to Exercise 15](#) ↴

## 9 Geochemistry of Produced Water in Basins with Salt Domes

### 9.1 Introduction to Water Geochemistry near Salt Domes

The salinity of water co-produced with crude oil and natural gas often exceeds freshwater and normal marine salinity. This elevated salinity is usually spatially associated with the presence of evaporites, in particular halite-dominated evaporites. This highly saline water may reflect in part the presence of evaporated marine water but is more often the result of the subsurface dissolution of evaporites. Sedimentary basins with major salt domes are of particular interest in the study of the origin of saline formation water and water co-produced with oil and gas. This is because salt domes and salt sheets can extend vertically upward across many kilometers of sedimentary section and influence the salinity and chemical composition of formation water within large volumes of sediment.

This section addresses the origin and properties of formation water of the south Louisiana salt dome province, a well-studied subregion within the Gulf of Mexico tectonic and sedimentary basin. We use the term *Gulf of Mexico* to refer to the Gulf of Mexico geological basin, not to the Gulf of Mexico oceanic body of water.

A great deal of attention has been given to physical salt-sediment interactions in the Gulf of Mexico sedimentary basin because of their importance in the structural and tectonic evolution of that basin and in the development of migration pathways and traps for crude oil and natural gas (e.g., Jackson et al., 1995). However, there are also important chemical salt-sediment interactions, which include the subsurface dissolution of halite, the generation of dense subsurface brine, and the geochemical interaction of brine with siliciclastic and carbonate sediments during burial diagenesis.

Mixing of halite-derived brine with ambient marine and fresh water has given rise to significant spatial variation in the salinity of formation water in the Gulf of Mexico Basin. The variation in salinity contributes to spatial variation in fluid density, which has the potential for driving both local and long-distance fluid flow. Variation in salinity on smaller field and reservoir scales has been used to document fluid expulsion up faults (Esch & Hanor, 1995; Lin & Nunn, 1997; Roberts & Nunn, 1995) and to provide evidence for reservoir compartmentalization and continuity (Bruno & Hanor, 2003). Salinity is also a major control on the properties of water such as density, viscosity, and interfacial tension within hydrocarbon reservoirs, which are required for accurate reservoir modeling (Willhite, 1986) and for predicting the behavior and fate of produced water during disposal.

The south Louisiana salt dome province (Figure 37) has been a prolific producer of hydrocarbon waste, oil field brine, and other wastes. Some portions of the discussion of south Louisiana salt domes and associated formation water in this section are based on previous reviews by Hanor (2004) and Hanor and McIntosh (2007). The terms *autochthonous*

and *allochthonous* (literally, *same earth* and *other earth*) are often used in the study of salt tectonics. In this book, we used the term *autochthonous* to refer to salt masses such as salt beds that lie in their original stratigraphic position; those, such as salt domes and salt sheets, which have been physically displaced from their original depositional location, are referred to as *allochthonous*.

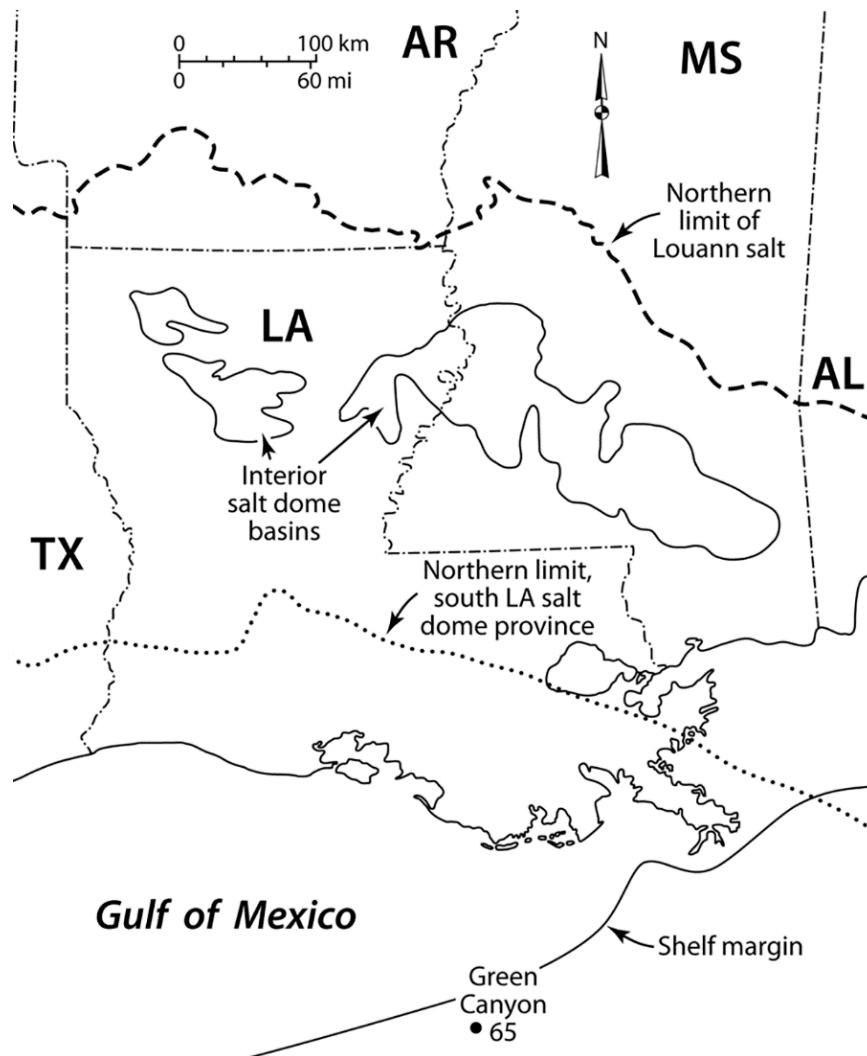


**Figure 37** - Map of the south-central USA and northern Gulf of Mexico showing the northern limit of the Louann Salt, the principal evaporite unit in the Gulf of Mexico Basin, and several salt dome basins. The focus of this section is on the south Louisiana (LA) salt dome province. Abbreviations: TX = Texas, LA = Louisiana, AR = Arkansas, MS = Mississippi, AL = Alabama (from Hanor & McIntosh, 2007).

## 9.2 Geologic Setting of the Gulf of Mexico Basin

The Gulf of Mexico Basin began to form in the Triassic as a result of lithospheric stretching and seafloor spreading associated with the breakup of Pangea (Salvador, 1991; Worrall & Snelson, 1989). Widespread marine incursions in the Middle Jurassic, associated with broad regional subsidence, resulted in the deposition of thick intervals of halite-dominated evaporites known as the Louann Salt over much of the Gulf region.

Non-marine quartzose sandstones, red beds, and conglomerates were deposited directly over the Louann Salt throughout most of the basin (Figure 37). The first major marine transgression occurred in the Late Jurassic, resulting in the deposition of the shallow water carbonates of the Smackover Formation. This was followed by a major influx of siliciclastic sediments in the Late Jurassic and Cretaceous.

The depositional style within the Gulf of Mexico basin changed dramatically at the beginning of the Cenozoic as a result of an influx of large quantities of siliciclastic sediments from the north and northwest. These sediments were deposited primarily in a series of major depocenters situated basinward of a Late Cretaceous continental shelf. South Louisiana became the principal region of deposition in the Gulf Coast in the early Miocene as major depocenters shifted in position and generally prograded basinward to the south.

This progradation in south Louisiana and the Louisiana shelf created a largely sand-dominated section approximately 3 km thick that overlies a thick sequence of Cenozoic mudstone-dominated marine sediments. Fluids in the mudstone-dominated section are typically overpressured (Hanor & Sassen, 1990). The total thickness of Middle Jurassic and younger sediments in south Louisiana is approximately 15 km.

The original depositional thickness of the Louann Salt is estimated to have varied from a few meters along the northern rim of the Gulf of Mexico to more than a kilometer in the interior salt basins (Figure 37) and as much as several kilometers within the area of the present Texas-Louisiana continental slope (Salvador, 1991). The thickness and spatial distribution of salt have been highly modified by salt tectonics. Local differential subsidence of salt, relative to the surrounding denser clastic sediments, occurred in areas of thick salt including the interior salt dome basins in northeastern Texas, northern Louisiana, central Mississippi, and the south Louisiana coastal (Figure 38) and offshore salt basins (Figure 37). This differential movement produced subvertical diapirs and subhorizontal allochthonous sheets of Jurassic salt that today are surrounded by shallower and much younger sediments (Worrall & Snelson, 1989). However, in other areas of the Gulf Coast—such as the northernmost Gulf of Mexico rim of Texas, Arkansas, Mississippi, and Alabama—the salt is still primarily in its original, near-basal, autochthonous position within the section (Figure 37).

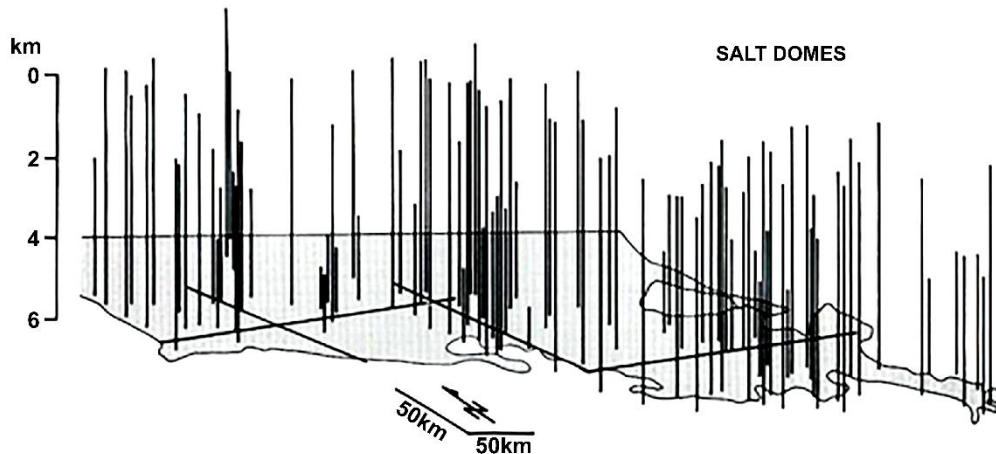


**Figure 38** - Schematic three-dimensional diagram showing the spatial distribution of salt domes in the south Louisiana salt dome province. The distribution of salt is complex. The map outline is drawn at a depth of 6 km below mean sea level. Horizontal lines on the map represent the location of a fence diagram shown later in this book (from Hanor et al., 1986).

### 9.3 Chemical Composition of Water Associated with Salt Domes

Most of the information on the salinity of deep formation water in the Gulf of Mexico Basin has come either indirectly from borehole logs or directly from analyses of water co-produced with crude oil and natural gas. The basic spontaneous potential (SP) log technique (Bateman & Konen, 1977) has been widely used to estimate formation water salinity and was used in many of the studies referenced in this book.

The thermodynamic basis of the SP response is described by Hearst and Nelson (1985). An additional technique developed by Revil and others (1998) uses the combined responses from density, gamma ray, and resistivity logs to calculate both formation water electrical conductivity and salinity. The technique can be used where oil-based drilling muds make the SP technique impossible. Borehole logs are particularly useful in establishing spatial variations of salinity because these can often be determined over large depth intervals from a single log. Techniques for the direct sampling and analysis of produced water for their chemical and isotopic composition are described in Kharaka and Hanor (2014).

#### 9.3.1 Salt, Salinity, and Hydrogeology

Although the hydrogeology of the Gulf of Mexico Basin has been described as an interplay between topographically driven flow and the development of over-pressure or compaction-driven flow (Bjørlykke, 1988, 1994), the presence of salt significantly complicates that interpretation. The high thermal conductivity of salt has the ability to heat ambient formation water, thus lowering its density. However, the dissolution of salt introduces solutes, principally NaCl, that significantly increase salinity and fluid density. The term *free convection* refers to flow driven by density differences arising from spatial variations in salinity and temperature. Depending on the dominant controls on fluid

density, such flow may be termed thermal convection, haline convection, or thermohaline convection.

Considerable work has been done on the numerical modeling of free convection, solute, and heat transport around salt domes—research stimulated in part by the field documentation of large salinity plumes extending laterally away from the top of some diapirs (described in early work by Evans et al., 1991; Ranganathan & Hanor, 1987; Williams & Ranganathan, 1994). Fluid flow velocities are still poorly known for many deep sedimentary systems but presumably range over many orders of magnitude, probably up to and exceeding meters per year. However, even where the magnitude of the driving force is reasonably well known, there is often insufficient information available on the scale-dependence of the permeability field to make accurate calculations of flux and velocity.

Several published studies have provided evidence for the dissolution of individual salt structures and fluid flow in the Louisiana and Texas Gulf Coast on the basis of spatial variation in formation water salinity in proximity to salt. These include the early studies of the Welsh salt dome (Bennett & Hanor, 1987), the Black Bayou dome (Leger, 1988), the Iberia dome (Esch & Hanor, 1995; Workman & Hanor, 1985), the Port Barré dome (Hanor & Workman, 1986), the St. Gabriel and Darrow domes (Bray & Hanor, 1990), the Bay St. Elaine dome (Cassidy & Ranganathan, 1992), and Weeks Island dome (Ausburn, 2013)—all in Louisiana—and the South Liberty dome in Texas (Banga et al., 2002). Information is also available on salt dissolution and fluid flow around coastal and offshore salt structures including Eugene Island 128 (Esch & Hanor, 1995), Eugene Island 330 (Lin & Nunn, 1997; Losh et al., 2002), South Timbalier 54 (Little, 2003), Bay Marchand (Bruno & Hanor, 2003), and Green Canyon 65 (Hanor, 2004). No two of these field areas exhibit the same pattern of spatial variations in salinity. Several contrasting field examples are included in various places in this section including: Bay Marchand, Welsh, Iberia dome, St. Gabriel, and Darrow.

### 9.3.2 Salt Dissolution: Bay Marchand Salt Dome

Bruno and Hanor (2003) documented the existence of a large plume of saline formation water originating from a solution cavity on the northeast flank of the Bay Marchand salt dome, coastal Louisiana (Figure 39). The saline plume extends laterally and downward to the southeast and south within sandy Pliocene and Miocene sediments. The plume appears to be the basal leg of a large fluid convection system driven by fluid density differences resulting from the dissolution of salt near the top of the dome. The downward leg of the system is pulling shallow formation water of normal marine salinity down across the salt-sediment interface, resulting in continuing dissolution of salt. The upward and upper legs of the convection system may involve highly diffuse rather than focused fluid flow. Lateral fluid flow downward and away from salt is rapid enough that isotherms in

the vicinity of the saline plume are depressed as much as 400 m vertically. Heat balance calculations (Hanor & Bruno, 2013) suggest that lateral fluid flow rates on the order of one meter per year within the plume could account for the observed temperature perturbations.

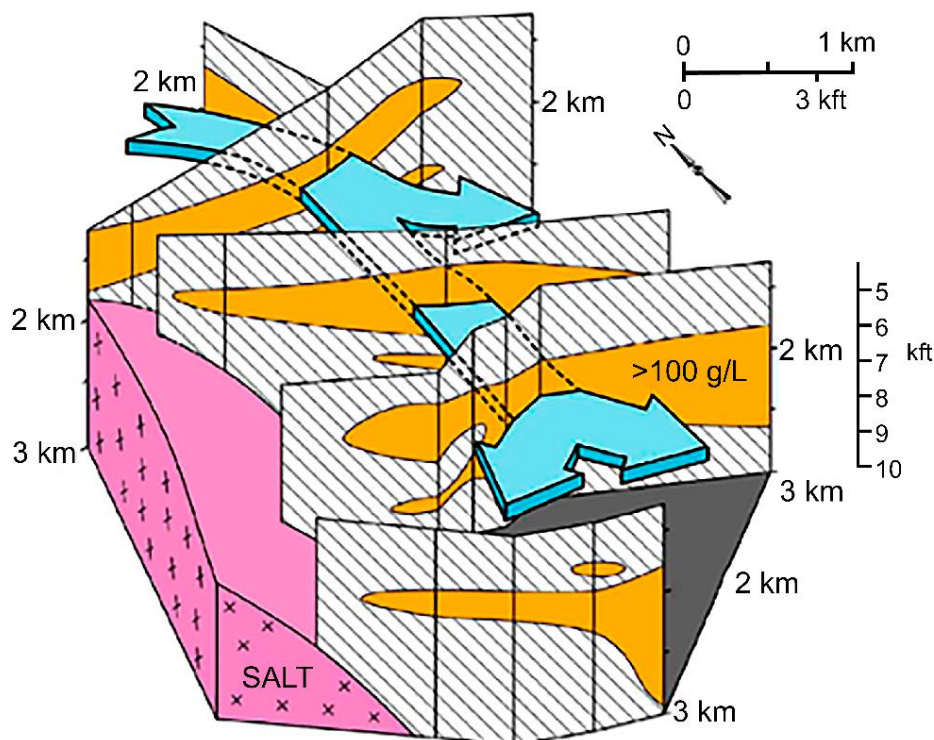


**Figure 39** - Diagram showing the location of a plume of saline formation water with salinity in excess of 100 g/L on the eastern flank of the Bay Marchand dome, coastal Louisiana (Hanor & Bruno, 2013). Blue arrows indicate inferred directions of subsurface fluid flow. Depths are below sea bottom. kft is kilofeet; 1,000 feet = 304.8 meters (from Bruno & Hanor, 2003).

Evans and others (1991) presented the results of numerical modeling of free convection in sediments having an intrinsic permeability of 10 to 14 m<sup>2</sup> near a hypothetical cylindrical salt stock. When ambient formation water salinity was less than 150 g/L, salinity effects on density dominated and flow was down the salt-sediment interface. At higher salinities, temperature effects resulting from the high thermal conductivity of halite dominated, and it is possible (in theory) to generate fluid flow up the side of the salt. In the example of downwelling shown in Evans and others (1991), a maximum Darcy flux of 0.145 meters per year was generated with a significant depression of the isotherms near the salt. At a porosity of 30 percent, which was assumed by Evans and others (1991), this flux corresponds to a fluid velocity of 0.48 meters per year or roughly the same order of magnitude as the possible estimate at Bay Marchand reported by Bruno and Hanor (2003). Although some skepticism has been raised regarding how effective convective fluid flow may be in perturbing subsurface temperatures (e.g., Bjørlykke, 2010, p. 256), the fluid flow regime at Bay Marchand appears to be sufficiently dynamic to have a significant influence on formation water temperatures.

### 9.3.3 Salt Dissolution: Welsh Salt Dome

In marked contrast to the Bay Marchand dome, the highest salinity water at the Welsh salt dome, southwest Louisiana, is perched in sediments well above the top of the dome (Figure 40). There appears to be a preferential migration of salty water to the northwest away from the dome (Bennett & Hanor, 1987). The salinity pattern at Welsh obviously cannot be explained by the downwelling of dense brine, as is the case at Bay Marchand. Bennett and Hanor (1987) proposed that the upward transport above the salt might be related to the episodic vertical expulsion of over pressured fluids that then dissolved the salt. The feasibility of this mechanism was established through the numerical modeling experiments of Ranganathan and Hanor (1989) and Williams and Ranganathan (1994). An additional possibility is that the elevated temperature at the top of the dome heated the fluids, thus contributing to their upward migration (Evans et al., 1991).

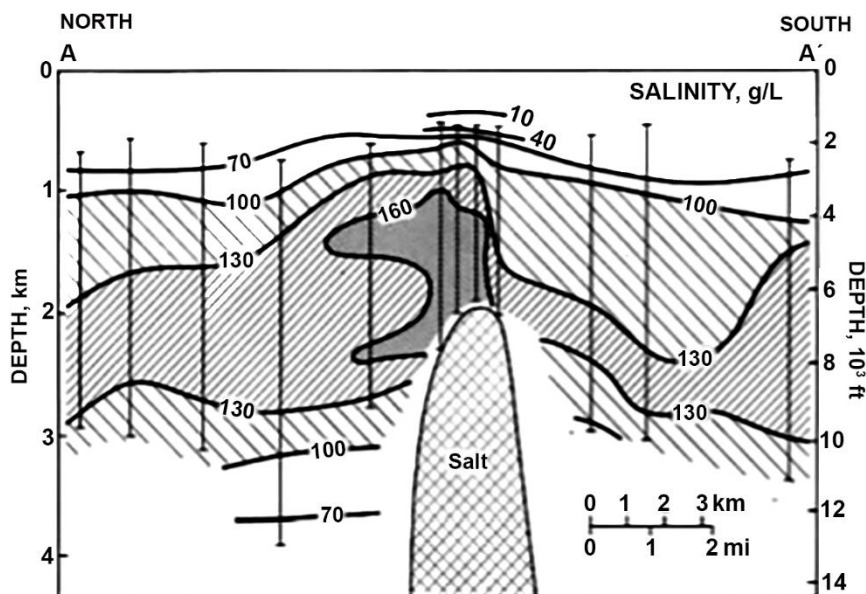


**Figure 40** - Cross section through the area of the Welsh salt dome, southwest Louisiana, showing spatial variations in formation water salinity. Vertical lines show geophysical log control locations. The most saline water occurs in a sand-dominated section between 1.0 and 3.5 km below land surface. Salinity decreases downward into over-pressured sediments. Vertical exaggeration = 5X (after Bennett & Hanor, 1987).

From mapping salinity in a large volume of sediment surrounding the dome, Bennett and Hanor (1987) determined that the dissolution of at least two vertical kilometers of salt from the top of the Welsh dome was required to account for the elevated salinity in the field area. There is no documented extensional feature above the Welsh dome. In fact, the Welsh Field was originally discovered because it was below a gentle topographic high. Apparently, as salt has been dissolved near the top, additional salt moved vertically to keep the top of the dome at approximately the same elevation.

### 9.3.4 Regional Variations in Salinity

The dissolution of salt and the coalescence of brine plumes from the large number of individual salt structures (Figure 38) in the south Louisiana salt dome province have produced spatially complex regional variations in salinity reflecting fluid flow and solute transport over large vertical and lateral distances (Figure 41). In contrast to some other sedimentary basins and sediments of the Gulf rim where salinity typically progressively increases with depth above autochthonous salt, the most saline water in south Louisiana occurs in the sand-dominated section between intermediate depths of 0.5 to 4 km. This salinity reflects the dissolution of salt domes at relatively shallow depths, rather than having been derived from deeply buried autochthonous salt (Bray & Hanor, 1990; Hanor & Sassen, 1990).

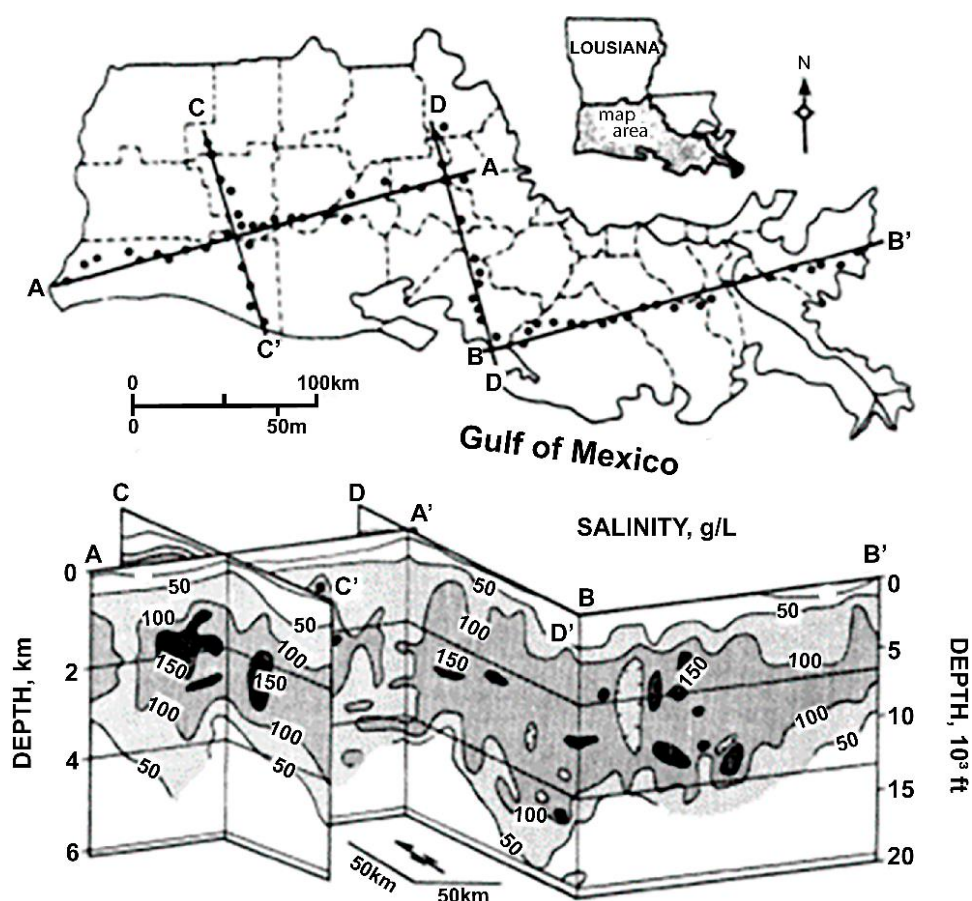


**Figure 41** - Fence diagram showing regional variation in formation water salinity in the south Louisiana salt dome basin. The highest salinity water is found in sand-dominated sedimentary sequences between depths of 0.5 and 4 km. Salinity decreases to marine values of 35 g/L or less in underlying, over-pressured mudstone sequences. The upper diagram shows the location of borehole logs used to calculate salinity. The distribution of salt domes is shown in Figure 38 (from Hanor et al., 1986).

Porewater salinity in the Cenozoic section of the south Louisiana salt dome province typically ranges from 100 to 150 g/L, although values as high as 300 g/L have been found in the immediate vicinity of some salt structures (Szalkowski & Hanor, 2003). In the

underlying mudstone-dominated over-pressured section, pore water salinity often decreases with depth to original marine salinity of 35 g/L or less, although higher salinity has been documented (Kharaka et al., 1978; Szalkowski & Hanor, 2003). Salinity below a depth of 6 or 7 km is largely unknown due to lack of data.

#### 9.4 Geochemical Composition of Gulf of Mexico Formation Water

Hanor and McIntosh (2007) compared the compositional systematics of Gulf of Mexico formation water hosted by Mesozoic carbonates above autochthonous salt (analyses from Hawkins et al., 1963; Land & Prezbindowski, 1981; Moldovanyi & Walter, 1992) with formation water from Cenozoic siliciclastics (i.e., clastic noncarbonate sedimentary rocks composed primarily of silicate minerals) penetrated by salt domes and allochthonous salt sheets (analyses from Hawkins et al., 1963; Land et al., 1988; Land & Macpherson, 1992b; Macpherson, 1992). They also compared compositional trends with the calculated evaporation trends for Cretaceous seawater (Timofeeff et al., 2006) and the measured evaporation trend for modern seawater (McCaffrey et al., 1987) to determine whether the compositional trends for Gulf of Mexico basinal water reflects evaporated marine water. The following is a brief summary of some of Hanor and McIntosh's (2007) findings.

All Gulf formation water shows an increase in Na with increasing Cl, but there are significant differences between the Na versus Cl for the Cenozoic siliciclastic-hosted water and the Mesozoic, largely carbonate-hosted, water (Figure 42). The Cenozoic siliciclastic-hosted water have higher Na/Cl ratios than do the Mesozoic-hosted water and plot slightly below the trend predicted by the dissolution of halite and above the two seawater evaporation trends.

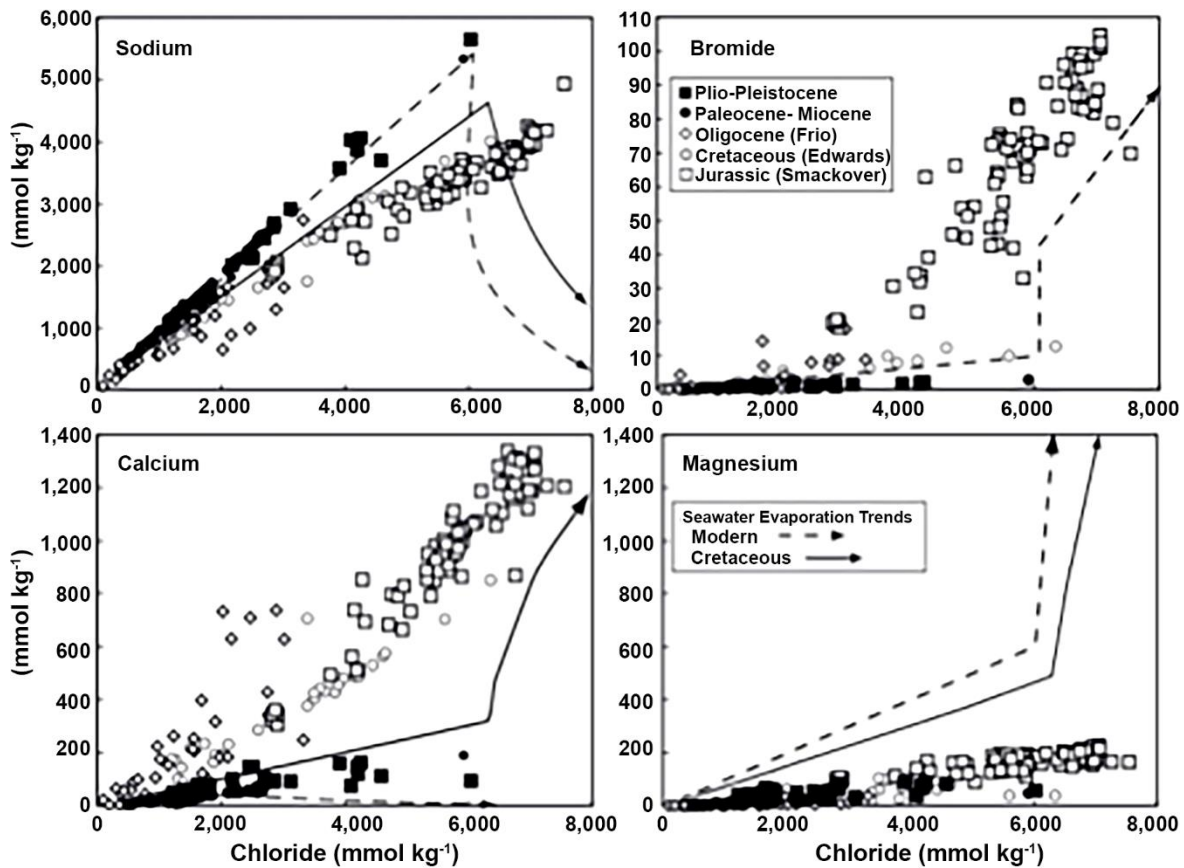


**Figure 42** - Compositional trends for some Gulf of Mexico formation water. Open symbols are for water spatially associated with bedded, autochthonous salt; closed symbols represent water spatially associated with allochthonous salt domes and salt sheets. Neither group follows compositional trends predicted by evaporating seawater as discussed in the references cited in the accompanying text (from Hanor & McIntosh, 2007).

The carbonate-hosted water plots broadly along a trend having lower Na/Cl ratios than the evaporated seawater trend. Calcium increases with increasing Cl, but the Ca/Cl ratios are significantly higher in the Mesozoic-hosted water (Figure 42). Calcium in the Cenozoic-hosted water is enriched relative to the modern seawater evaporation trend and is generally depleted relative to Jurassic and Cretaceous water. Magnesium, in contrast, is depleted in all of the water relative to the seawater evaporation trend (Figure 42). The Ca/Mg ratios of the Cenozoic-hosted water is broadly similar and much lower than the Ca/Mg ratios of water in Jurassic to Oligocene-age reservoirs. The Ca/Mg ratios of all of water in Jurassic to Oligocene-age reservoirs are significantly higher than either Ca-poor evaporated modern seawater or Ca-rich Cretaceous seawater. In contrast to brine associated with autochthonous salt, which generally have high Br/Cl ratios, brine associated with salt domes typically have low Br/Cl ratios, reflecting derivation primarily from halite dissolution rather than evaporation of marine water or dissolution of marine bittern (Figure 42).

Hanor and McIntosh (2007) agreed with previous workers—such as Land (1995), who in his study of fluids in the Frio Formation found that the Na-Mg-Ca-Cl compositions

of brine in the Gulf Coast sedimentary basin are products of diagenesis and do not reflect the composition of the connate marine or evaporated marine water present at the time of sediment deposition. One of the more important diagenetic reactions to have occurred in the Gulf Coast basins since the deposition of the Louann Salt has been the dissolution of halite, which has provided a continuing source of dissolved chloride and is a driving force for subsequent water-mineral reactions (Hanor, 2001).

Other questions remain, including what specific diagenetic reactions control the relative proportions of the major cations. Of interest are the significant differences in Na and Ca versus Cl trends for water hosted by Mesozoic and Cenozoic sediments (Figure 42) and the wide range in Ca/Mg ratios in the water we have examined here. It is not known whether these variations reflect differences in

- the source of salinity (evaporated seawater for some of the Mesozoic sediments, dissolution of salt for some of the Cenozoic sediments), or
- sediment lithology (dominantly carbonates for much of the Mesozoic sediments, predominantly siliciclastics for the Cenozoic sediments), or
- when brine was first introduced into these sediments (tens of millions of years ago versus today), or
- mixing of water of different composition.

Hanor (2001) proposed that the observed progression from Na-Cl to Na-Ca-Cl to Ca-Na-Cl brine with increasing salinity can be explained by rock buffering involving metastable equilibria between the fluid and ambient carbonate and silicate minerals. If that is the case, it would appear that different buffering assemblages are operating in the Mesozoic and Cenozoic sediments considered here. These problems require additional research.

#### 9.4.1 Chemical Composition of Formation Water at Individual Salt Structures

Although a number of studies examined spatial variation in salinity in proximity to individual salt structures as described previously in this section, fewer studies document variation in the chemical and isotopic composition of formation water on the individual field scale.

Ausburn (2013) re-examined controls on the composition of formation water in some south-central and offshore Louisiana fields to provide insight into water-rock reactions that might be expected as a result of lowering reservoir temperatures and/or mixing of native formation water associated with in situ heat extraction. Data from the Weeks Island salt dome, Green Canyon 65, and a proprietary salt dome field called Bellatrix were used to document the existence of significant spatial variation in formation water composition within individual reservoir sands and fault blocks. Ausburn found that most significant, in terms of the potential for precipitation of mineral cements or scale, are the inverse relations between the concentration of dissolved barium and sulfate (Figure 43) and of dissolved calcium and alkalinity. In theory, mixing of water within these sands could

cause the precipitation of barite and/or calcite within a downhole heat exchanger or within conventional production tubing.

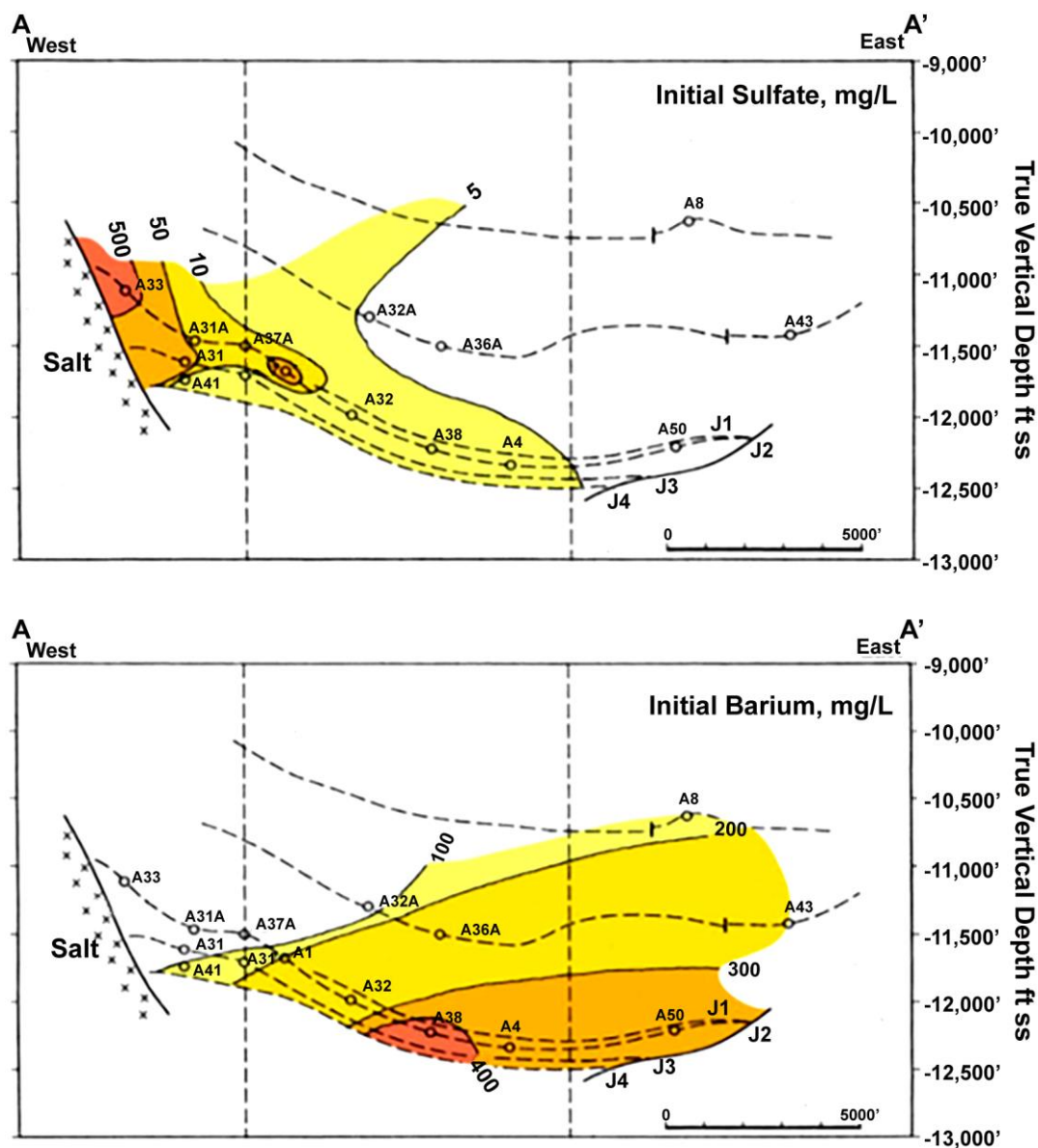


**Figure 43** - Vertical cross-section showing spatial variation in dissolved sulfate and dissolved barium in produced water in relation to the salt-sediment (ss) interface at the Green Canyon 65 field, offshore Louisiana. Letters H through J4 refer to hydrocarbon-bearing sands (dashed lines). Small circles show the location of the screens of producing wells. For y axes ss=subseafloor. The generally inverse relation between sulfate and barium may reflect buffering of fluid compositions by barite. The term 'initial' refers to the composition of the first water produced at each well (from Ausburn, 2013).

Workman and Hanor (1985) established evidence for the existence of a complex flow regime around the Iberia salt dome, south-central Louisiana, using spatial variation in volatile fatty acid concentration, chloride, temperature, and the isotopic composition of formation water as indicators of flow direction (Figure 44). There is evidence, deep in the section, for upward flow of salty water to the north along the margin of the dome. However,

the saltiest water exists at the very crest of the dome and is driving a second plume that is moving out to the south and above the deeper plume (Figure 44a). Esch and Hanor (1995) subsequently showed that some of the circulation around the Iberia dome is preferentially controlled by faults and fractures, which act as conduits for fluid flow.

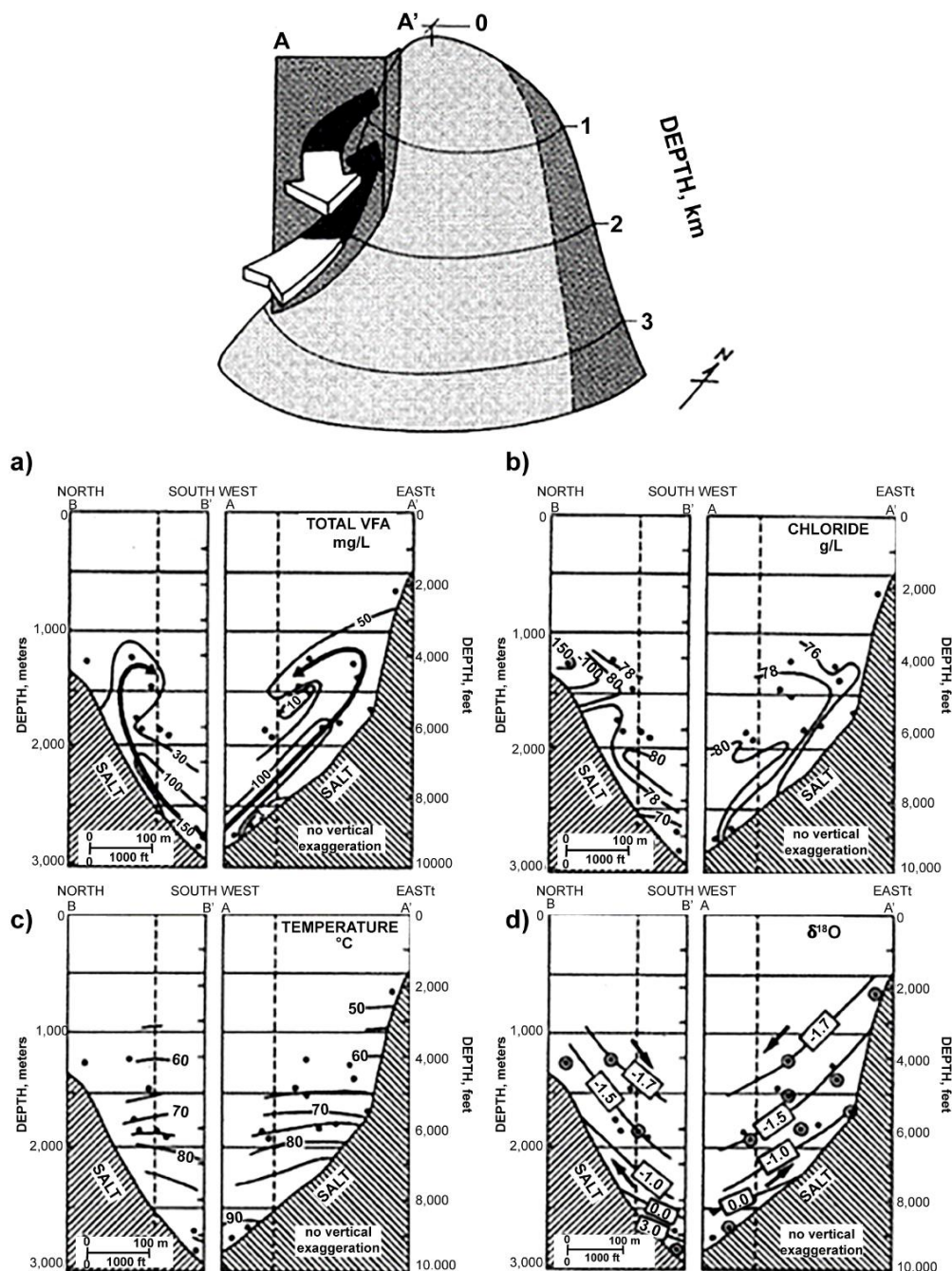


**Figure 44** – (Top) Three-dimensional representation of fluid flow on the southwestern flank of the Iberia salt dome as deduced from spatial variation in formation water chemistry and temperature in cross sections. West-east (A-A') and north-south (B-B') cross sections display the distribution of: a) total volatile fatty acids (VFA); b) chloride; c) temperature; and d)  $\delta^{18}O$  (Workman & Hanor, 1989).

### 9.4.2 Effect of Salt Dissolution on Groundwater Resources

The subsurface dissolution of salt domes has played a major role in the distribution of fresh groundwater resources in south Louisiana. The discharge areas of the regional groundwater systems in sediments in the US Atlantic Coastal Plain are situated at or near the Atlantic coastline (Meisler et al., 1988). In some areas, fresh groundwater lenses extend far out into the Atlantic continental shelf (Meisler, 1989).

In contrast, the principal pre-development discharge areas of the coastal plain aquifer systems in Louisiana (Martin & Whiteman, 1988) are located as much as 100 km inland from the Gulf of Mexico (Figure 45). The distal end of the deep part of the aquifer systems corresponds, spatially, to the northern limit of the South Louisiana salt dome province (Figure 46). The subsurface dissolution of salt has produced a regional mass of dense brine at shallow depth (Figure 46; Bray & Hanor, 1990). Anderson and others (2013) proposed that topographically driven fresh water is forced to ride up and over the much denser water, resulting in a pronounced thinning of the zone of freshwater and the development of groundwater discharge areas located far from the coast.

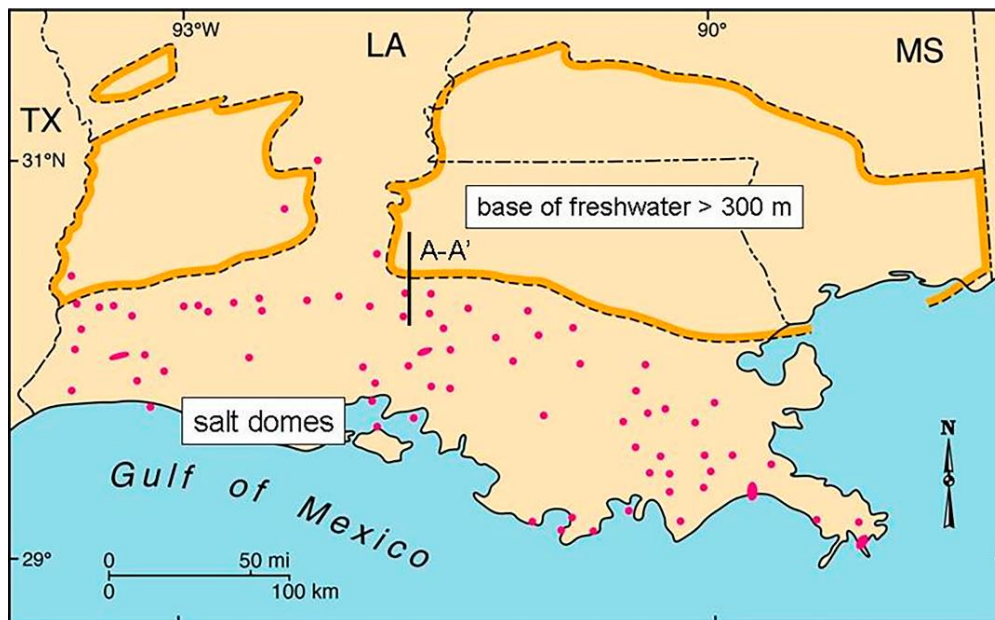


**Figure 45** - Map showing the location of coastal plain aquifers where fresh groundwater extends to a depth of at least 300 m. The general groundwater flow direction is from north to south. The southernmost extent of deep groundwater corresponds spatially to the northern boundary for the south Louisiana salt dome province. Line A-A' shows location of cross section in Figure 46. Red dots show the location of onshore salt domes (Hanor, unpublished data).

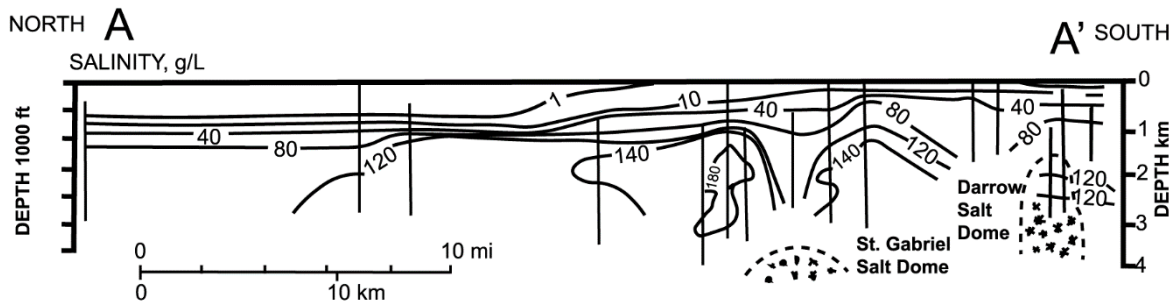


**Figure 46** - Cross section (A-A' located as shown in Figure 45) in part of southeast Louisiana near Baton Rouge showing spatial variation in formation water salinity as calculated from spontaneous potential response of geophysical logs. A large mass of brine has been generated by the subsurface dissolution of salt at the St. Gabriel and Darrow salt domes. Fresh groundwater from the north is forced to ride up and over the dense brine (Modified from Bray and Hanor, 1990).

## 9.5 Exercises Pertinent to Section 9

[Link to Exercise 16](#) ↴

[Link to Exercise 17](#) ↴

[Link to Exercise 18](#) ↴

## 10 Field Studies of Groundwater Contamination by Produced Water and Petroleum

In this section, we provide detailed field case studies of groundwater contaminated by produced water and associated petroleum in existing oil fields and legacy sites where petroleum production ended many years ago (Hanor, 2007; Kharaka & Otton, 2007). We also discuss the Bemidji crude oil spill, where approximately 10,000 bbl (1,590 m<sup>3</sup>) of crude petroleum spilled from a 34-inch (86.36-cm) broken pipeline near Bemidji, Minnesota, USA, in 1979; petroleum seeped through the soil and is floating on the water table in the outwash aquifer (Delin et al., 1998, 2020).

Although we noted in Section 1 that major pollution from large oil spills due to international conflicts, ocean transport, and major well blowouts are infrequent, we cover the Bemidji oil spill in this section. We do this because, from the point of view of groundwater contamination, breaks in the 400,000 km of crude oil pipelines in the USA are quite frequent, occurring at a rate of ~300 significant pipeline incidents yearly since 1986. Equally significant, even though the number of pipeline accidents has been decreasing over the past two decades, they pose a substantial risk to groundwater and the environment (US Pipeline and Hazardous Materials Safety Administration, 2021).

Groundwater contamination from pipeline accidents in other countries are comparable and sometimes the frequency and extent of contamination is higher.

### 10.1 Case Study 1: Groundwater Contamination by a Crude Oil Spill

This case study was established by the USGS in 1982 in response to the research and regulatory community's need for in situ field-scale studies to improve understanding of the mobilization, transport, and fate of crude oil compounds in the shallow subsurface (Baedecker et al., 2018; Delin et al., 2020; Essaid et al., 2011). Contamination at this site began when an oil pipeline near the city of Bemidji, Minnesota, ruptured—spraying approximately 1.6 million liters (10,000 bbl) of light (33°API) crude oil across an area of 6500 m<sup>2</sup> as shown in Figure 47 (Essaid et al., 2011). The spilled oil contained 0.56 percent sulfur and 0.28 percent nitrogen with a composition of 58 to 61 percent saturated hydrocarbons, 33 to 35 percent aromatics, 4 to 6 percent resins, and 1 to 2 percent asphaltenes.

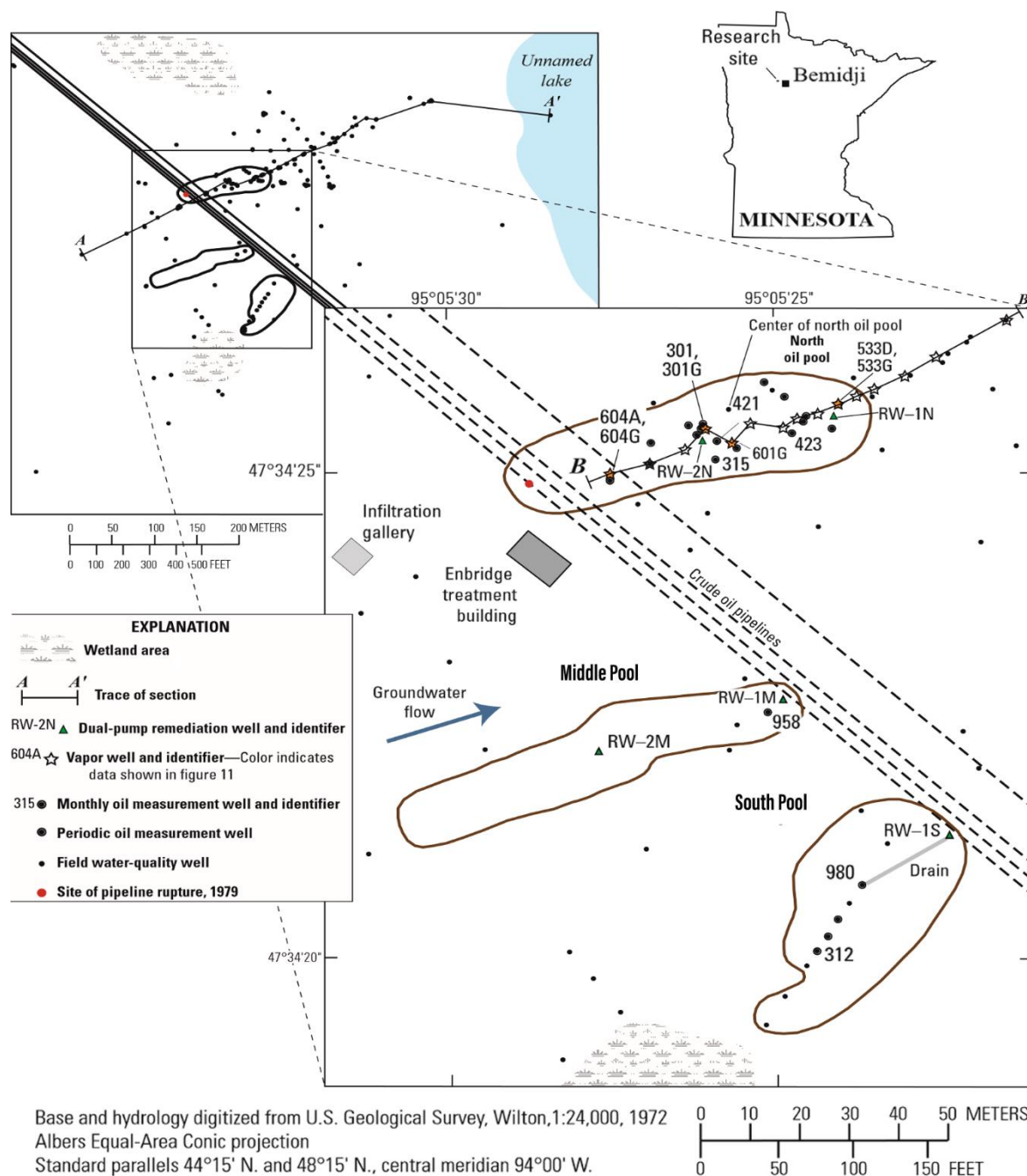


**Figure 47** - Location map showing observation wells and other features at the National Crude Oil Spill Fate and Natural Attenuation Research site near Bemidji, Minnesota, USA (from Delin et al., 2020).

### 10.1.1 Remediation at the Bemidji Site

Initial cleaning following the pipeline break in 1979 removed about 75 percent of the crude oil, but approximately 2,500 bbl (400 m<sup>3</sup>) remained, contaminating the soil and groundwater at the site. In 1997, the Minnesota Pollution Control Agency demanded that the pipeline company remove any remaining crude to a “sheen” level in all wells at the Bemidji site. To do that, the company installed a dual-pump recovery system in selected remediation wells (Figure 48). This additional remediation resulted in removal of about

723 bbl (115 m<sup>3</sup>) of crude oil, representing ~40 percent of the estimated crude oil present in the aquifer in 1998. The effects of the remediation on groundwater plumes and unsaturated-zone vapor concentrations were evaluated by the USGS using several methods including measurement of:

- oil thickness in individual wells;
- water temperature and water-quality parameters including dissolved oxygen, specific conductance, and pH in groundwater; and
- vapor concentration of methane, carbon dioxide, nitrogen, and oxygen in wells completed in the unsaturated zone.

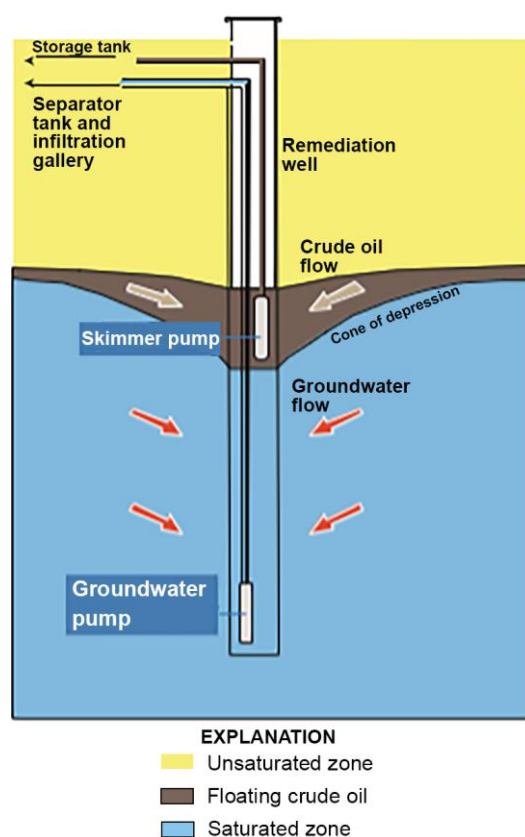


**Figure 48** - Conceptual diagram of the crude-oil-recovery system for the removal of oil and contaminated groundwater at the Bemidji site, Minnesota, USA (from Delin et al., 2020).

Although the recovery system decreased oil thickness near the remediation wells, average oil thickness measured in all wells at the site were not reduced substantially (Figure 49). Dissolved oxygen and specific conductance measurements indicated that a secondary plume was created during the remediation, caused by the disposal of pumped water from the remediation wells in an upgradient infiltration gallery. This plume expanded rapidly, resulting in expansion of the anoxic zone of groundwater upgradient and beneath the existing plume that was undergoing natural attenuation. The measured conductance increased in many wells at the North Pool from about 400 to more than 700  $\mu\text{S}/\text{cm}$  (micro

siemens per cm) as shown in Figure 50. The trends in vapor data collected before, during, and after the remediation generally support the hypothesis that crude oil removal would have an insignificant effect on vapor concentrations in the unsaturated zone. Oil-phase recovery at this site was determined to be challenging and resulted in considerable volumes of mobile and entrapped oil remaining in the subsurface despite ~40 years of natural attenuation and five years of pump-and-skim remediation (Delin & Herkelrath, 2014; Delin et al., 2020).

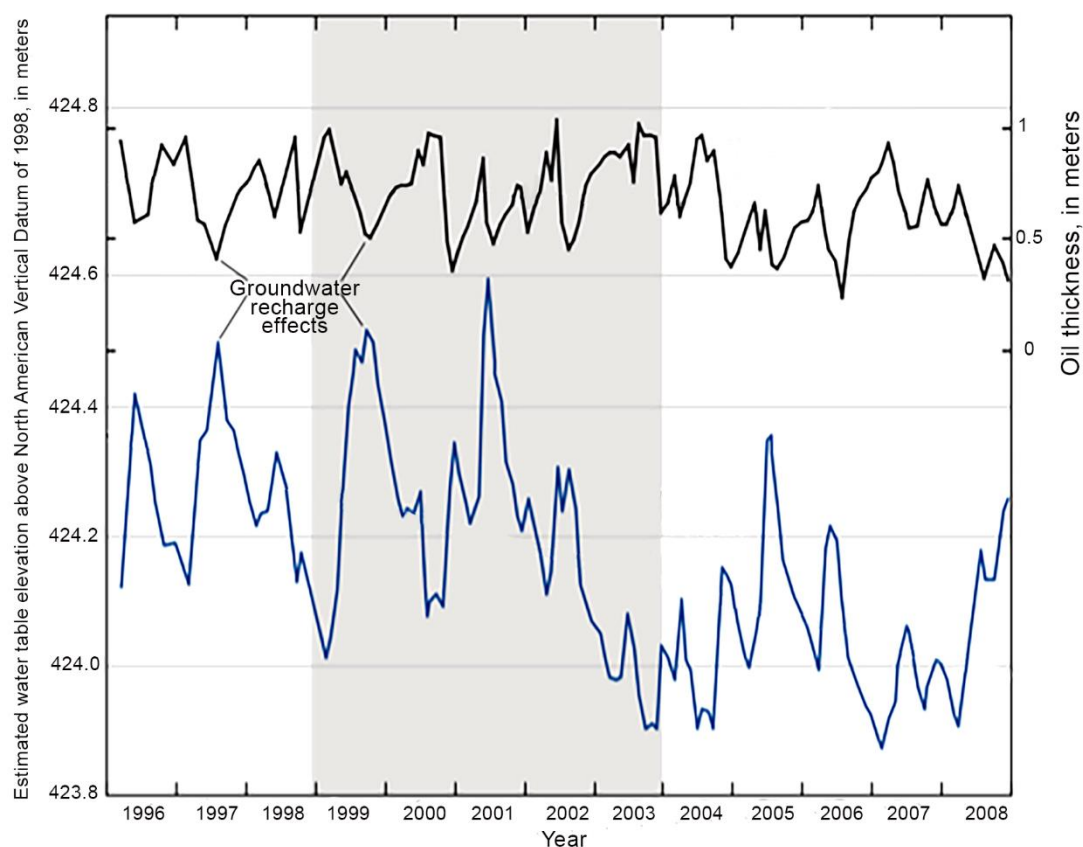


**Figure 49** - Oil thickness (black line) and estimated water table elevation (blue line) for well 315 at the North Pool of the Bemidji site, Minnesota, 1996–2008. The shaded zone is the remediation period. Effects of groundwater recharge are apparent as rises in the water table are coupled with declines in oil thickness, and vice versa (from Delin et al., 2020).

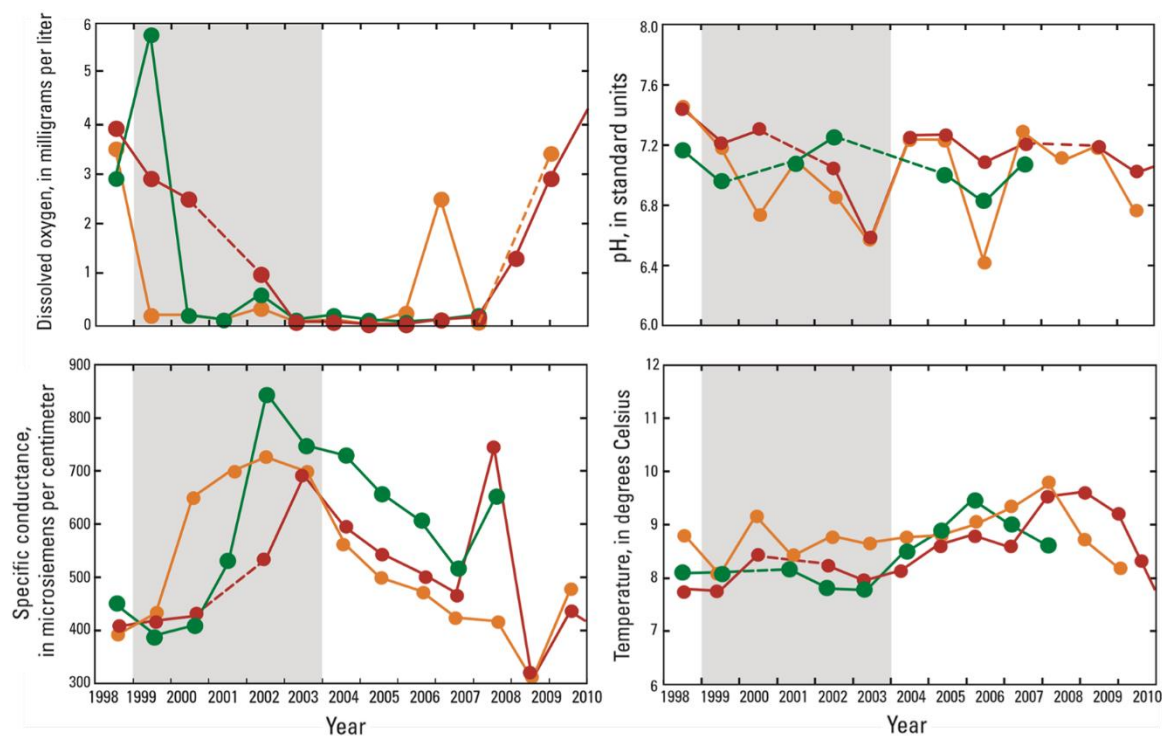


**Figure 50** - Concentrations of dissolved oxygen, pH, specific conductance, and temperature for selected wells from 1998 through 2010; well 801C (green circles), well 8315E (red circles), well 532D (orange circles). Shaded area is the remediation period (from Delin et al., 2020).

The Bemidji site has been well characterized through collection and analysis of more than 1,000 core samples over four decades. Cores have been collected by many research groups for project-specific objectives. Core samples have been analyzed in many ways including grain size distribution, moisture content, microbial community biomass and composition, geochemistry, oil saturation, and other characteristics. Moreover, the site has an extensive array of groundwater monitoring wells along the core of the plume that enables sampling at high spatial resolution (Figure 51); results have documented east-northeast flow of the groundwater at an average velocity of 22 m/year at this site (Delin et al., 2020).

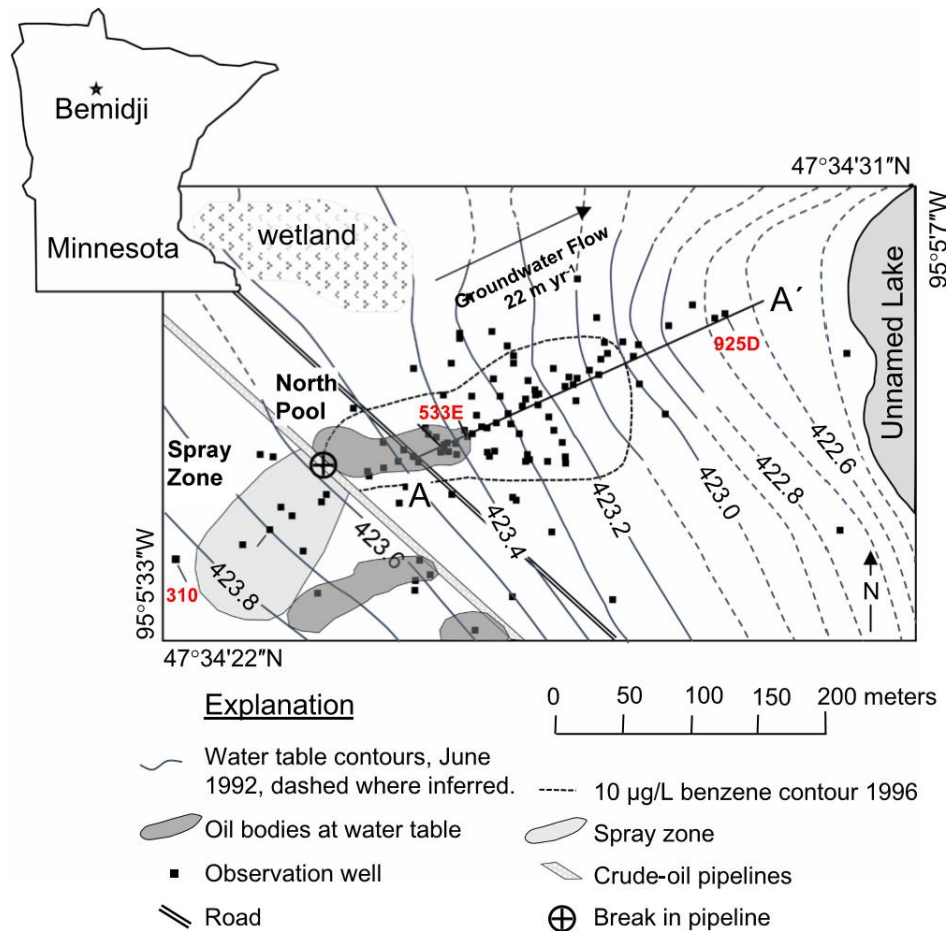


**Figure 51** - Map showing the North Pool and resulting DOM<sub>HC</sub> (petroleum-derived dissolved organic matter) plume at the National Crude Oil Spill Fate and Natural Attenuation Research Site near Bemidji, Minnesota, USA. The samples characterized here were collected down the centerline A-A' of the plume in the direction of groundwater flow. The 310 well nest (non-plume affected), 533E (adjacent to the oil body), and 925D (toe of the plume) are labeled in red for reference (modified from Bekins et al., 2016).

Currently, the site consists of four distinct research areas: North Pool, Middle Pool, South Pool, and Spray Zone (Figure 47 and Figure 51). Most research at the site has focused on the North Pool and groundwater plume. This is the location of the *Underground Observatory* initially established to investigate biodegradation and natural attenuation.

This area has more than 200 water wells, which are screened at different depths in the aquifer and provide a three-dimensional view of the interaction between subsurface crude oil, aquifer sediments, and groundwater (Figure 52). Additionally, a network of multi-port vapor wells installed in the unsaturated zone above the aquifer provide a way to sample and measure soil gas composition. A variety of instruments are also installed including electrode arrays and probes for measuring self-potential (SP), soil moisture, temperature, CO<sub>2</sub>, and O<sub>2</sub>. The Middle and South Pools have oil present in the subsurface but—like the Spray Zone—have been less studied.

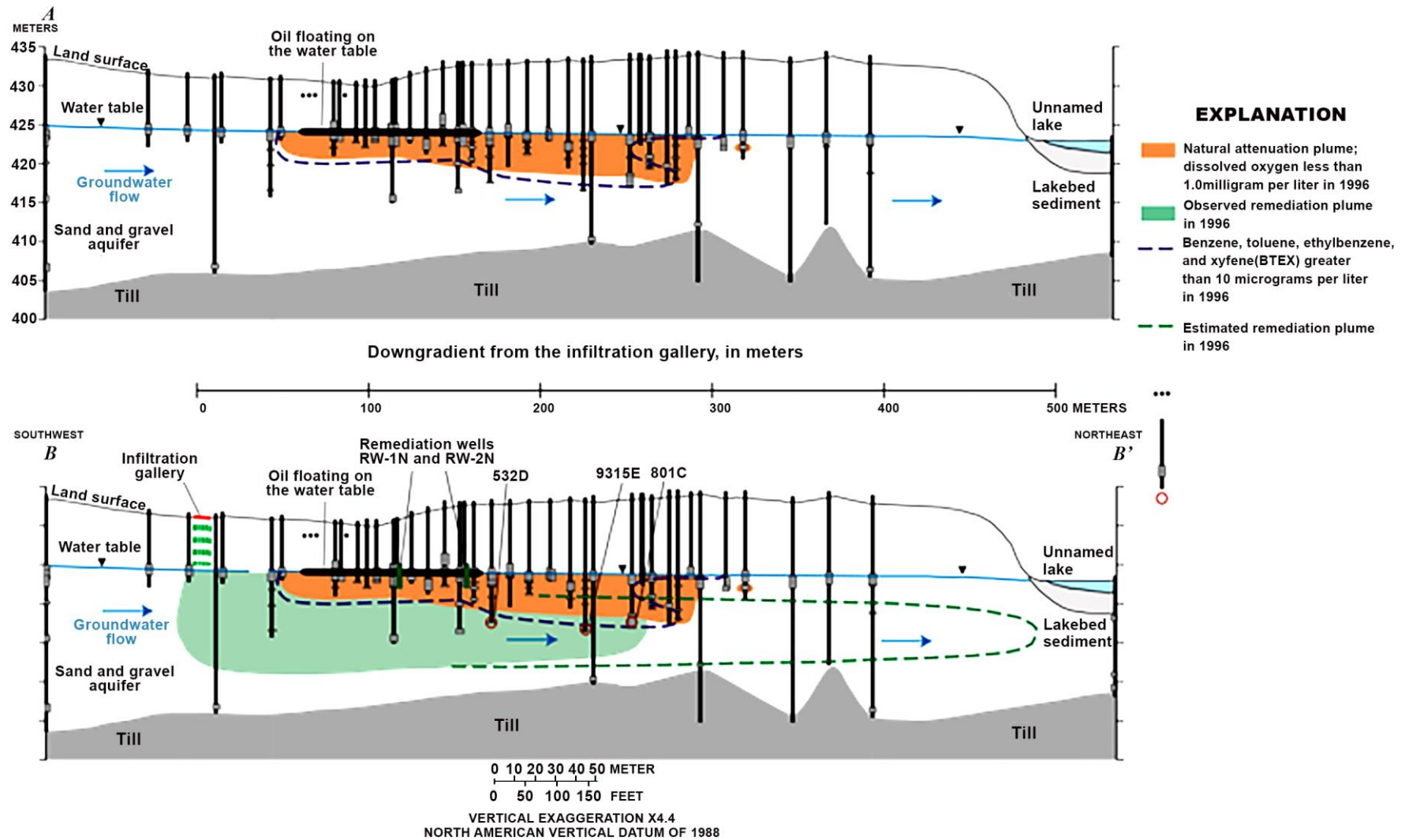
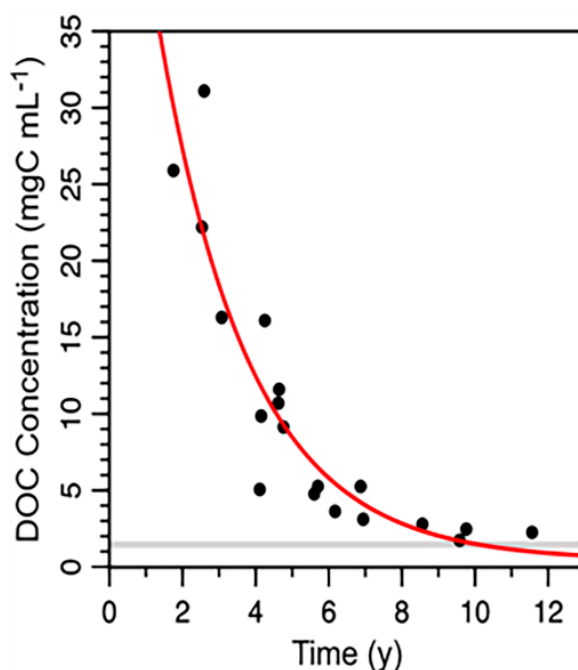


Figure 52 - Diagrams showing the natural attenuation and the remediation plumes in the saturated zone at the Bemidji site, Minnesota (from Delin et al., 2020).

### 10.1.2 Results and Discussion

The crude oil at the spill site has undergone weathering since the time of the spill about forty years ago. The relative contributions to weathering by volatilization, dissolution, and biodegradation vary depending on compound properties and location in the oil body (Baedecker et al., 1993, 2018). Biodegradation and dissolution have continuously produced a plume that extends approximately 340 m downgradient from the source to a lake. The plume comprises dissolved hydrocarbons, partially oxidized hydrocarbon metabolites, and hydrocarbon oxidation products (Bekins et al., 2021; Eganhouse et al., 1993).

Results of dissolved organic carbon (DOC) measurements (Figure 53) show DOC concentrations measured for the nineteen sampled wells as a function of time from the center of the oil body. The concentration of DOC in the wells directly adjacent to the oil body is 31 mg/L, decreasing to 2.3 mg/L in a well located 254 m downgradient from the center of the source (Cozzarelli et al., 2010; Essaid et al., 2011). Most of the decrease in DOC occurred in the iron-reducing portion of the plume during the first seven years after the spill. The estimated DOC degradation rate of 0.40/year is similar to previously modeled DOC decay estimates at the site of 0.46/year (Ng et al., 2014).



**Figure 53** - DOC concentration in the groundwater plume versus time from the center of the oil body fit to a three-parameter exponential decay model (red line). The gray line represents the range of DOC concentrations measured in background wells 310B and 310E (from Podgorski et al., 2021).

Degradation rates of individual gas chromatography-amenable compounds are reported in detail by Cozzarelli and others (2010) and Eganhouse and others (1996).

Collectively, these results indicate that the complex mixture of oil hydrocarbons is comprised of labile, semi-labile, and persistent fractions.

Cozzarelli and others (2010) used an in-situ microcosm (ISM) technique to investigate volatile aromatic hydrocarbon biodegradation processes and rates in the aquifer at the Bemidji site in an area downgradient from a subsurface oil body where biodegradation was predominantly by iron reduction. Installation occurred in August 1998 and the experiment continued through August 2001. The objective in this study was to provide a comparison of the rates determined by this approach to those estimated from monitoring well data and rates presented in the literature for other contaminated sites. The experiment was conducted in a well-characterized region of the aquifer that has been identified as iron-reducing based on geochemical and microbiological measurements. Sediments analyzed from this location (Rooney-Varga et al., 1999) were found to be enriched in microorganisms of the *Geobacter* cluster and were capable of anaerobic benzene degradation.

Benzene; toluene; ethylbenzene; o-, m- and p-xylenes; and four pairs of C<sub>3</sub>- and C<sub>4</sub>-benzenes were added to an in-situ microcosm and studied over a three-year period. The microcosm allowed for a mass-balance approach and quantification of hydrocarbon biodegradation rates within a well-defined iron-reducing zone of the anoxic plume. Among the BTEX compounds, the apparent order of persistence is ethylbenzene > benzene > m,p-xylene > o-xylene ≥ toluene. Threshold concentrations much higher than the MCL values were observed for several compounds (including benzene) in the ISM, below which degradation was not observed, even after hundreds of days. In addition, long lag times were observed before the onset of degradation of benzene or ethylbenzene.

The isomer-specific degradation patterns were compared to observations from a multi-year study conducted using data collected from monitoring wells along a flow path in the contaminant plume. The data were fit with both first-order and Michaelis-Menten models. First-order kinetics provided a good fit for hydrocarbons with starting concentrations below 1 mg/L and Michaelis-Menten kinetics were a better fit when starting concentrations were above 1 mg/L, as was the case for benzene.

The biodegradation rate data from this study were also compared with rates from other investigations reported in the literature. Results showed that the spatial variability of hydraulic properties influenced subsurface oil and water flow, vapor diffusion, and the progression of biodegradation. Pore-scale, capillary pressure versus saturation hysteresis and the presence of fine-grained sediments impeded oil flow, causing entrapment and relatively large residual oil saturations. Hydrocarbon attenuation and plume extent was a function of groundwater flow, compound-specific volatilization, dissolution and biodegradation rates, and availability of electron acceptors, especially Fe<sup>3+</sup> (Essaid et al., 2011).

Podgoriski and others (2021) examined water samples from wells located on transect A to A' (Figure 51) to determine the source and chemical composition of the compounds that persist downgradient in the North Pool of the Bemidji site. Results reported here, in Trost and others (2020), and in Bekins and others (2021) show an exponential decrease in dissolved organic carbon concentration from 28.4 mg/L in the plume zone to 2.6 mg/L at 254 m downgradient, as the result of biodegradation along the plume transect (Figure 52).

Compositional results indicated that changes in the dissolved organic compounds in the groundwater plume were gradual. Relatively low molecular weight (MW) and reduced aliphatic compounds from the oil source were selectively degraded, while high MW and alicyclic/aromatic (including PAHs and unsaturated oxidized compounds) persisted (Figure 54). The team concluded that biodegradation follows a continuum model where the most labile compounds degrade first, and that benzene carboxylic acids are quantitative conservative tracers of the groundwater plumes contaminated by petroleum.

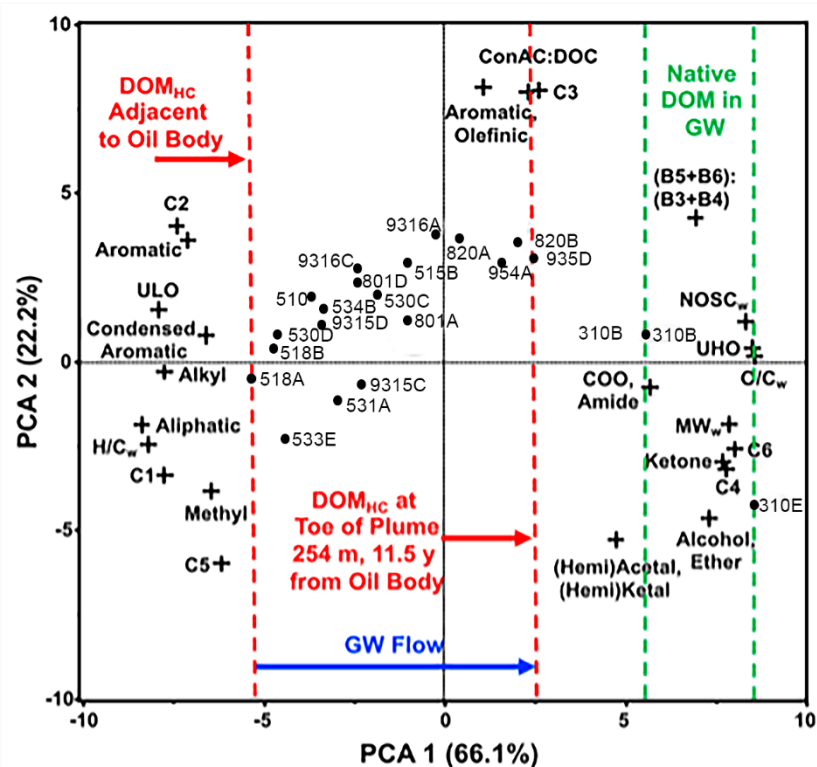


**Figure 54** - Principal Component Analysis (PCA) plot of plume degradation and distribution and source of relatively high-molecular weight compounds and dissolved organic matter (DOM). The blue arrow indicates the direction of groundwater flow. The background wells (green line) are upgradient from the oil body and not in the flow path of the contaminated water. Dots indicate groundwater monitoring wells and crosses are PCA loading variables. Podgoriski et al. (2021) provide a detailed interpretation of data in this figure.

Not all the toxic contaminants in the groundwater at the Bemidji oil site come directly from the spilled petroleum hydrocarbons. Cozzarelli and others (2015), Schreiber and

Cozzarelli (2021), and Ziegler and others (2021) report the release of arsenic (As)—a known human toxin and carcinogen (MCL for As is 10 µg/L)—at the Bemidji oil site to groundwater at concentrations that reach 230 µg/L by dissolution of iron oxyhydroxides. These elevated concentrations of As are geogenic and originate within the aquifer.

At this site, the rocks of the aquifer contain significant amounts of iron oxyhydroxides that have absorbed As, which can be mobilized into groundwater in the anoxic zone through biogeochemical reactions triggered by hydrocarbon biodegradation. At Bemidji, the concentration of As (as well as Mn, Pb, and other toxic metals) is directly related to the concentration of Fe in the contaminated plume (Figure 55).

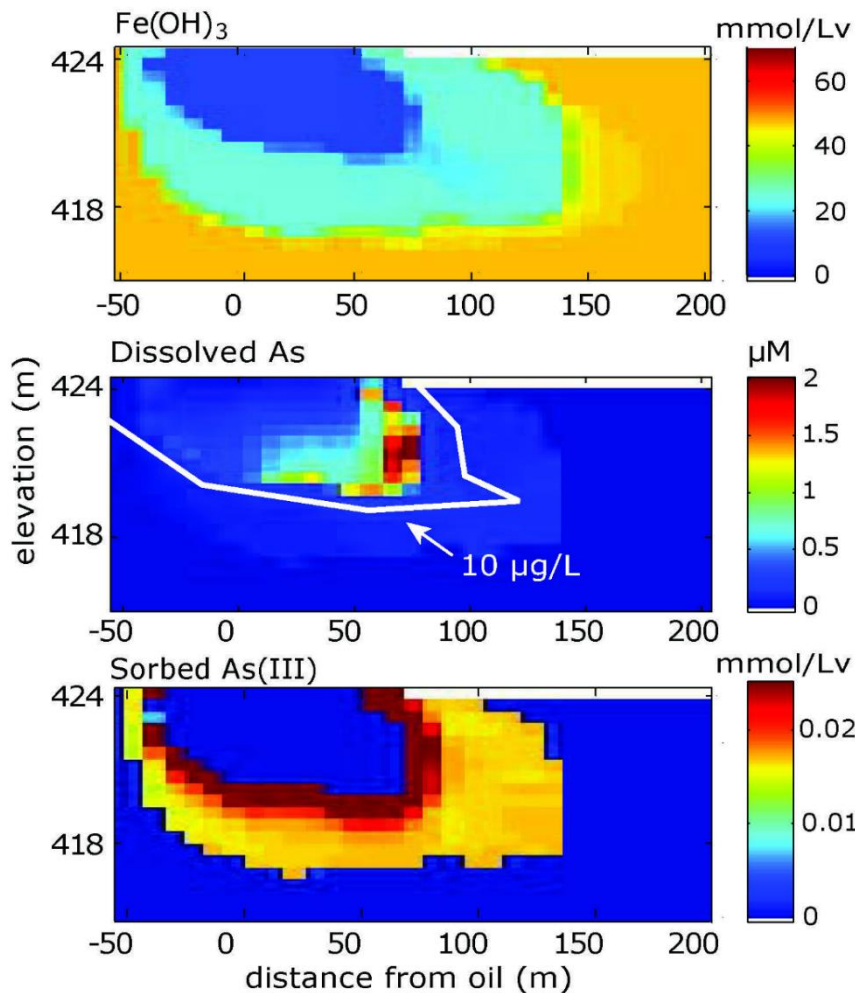


**Figure 55** - Cross sections showing the spatial distribution of dissolved and sorbed As, as well as Fe(OH)<sub>3</sub> relative to the location of the oil spill. As values are very high in the region of Fe(OH)<sub>3</sub> dissolution (from Ziegler et al., 2021).

In the uncontaminated (oxic) groundwater, the dissolved Fe concentration is low (< 0.5 mg/L) because dissolved oxygen (DO) values are high; the concentration of As in this oxic zone is < 0.5 µg/L and that of benzene is also very low at < 0.1 µg/L. As we approach the oil plume, the groundwater redox state changes from oxic to anoxic (reducing) to highly

anoxic, dissolving more of the iron oxyhydroxides (dissolved Fe > 30 mg/L) and mobilizing more As, until a high value of 230 µg/L (i.e., about 2µM per liter volume) is reached (Figure 55). As expected, when As values are high adjacent to the oil pool, DO values are very low < 0.1 mg/L. Benzene values reach a high value of 4.0 mg/L—800 times the MCL value for benzene.

## 10.2 Case Study 2: Groundwater Contamination by Produced Water and Petroleum at Osage Sites, Oklahoma

### 10.2.1 Introduction

The USGS tenth annual V.E. McKelvey forum held in Washington, DC, February 13 to 17, 1995, focused on the USA energy resources and the environment. Kharaka and Wanty (1995) presented a talk on water quality degradation associated with natural energy sources and also convened a small group of attendees to discuss plans for expanded USGS research in the field of water energy nexus. That discussion led to two significant research projects:

1. compilation of a comprehensive national produced water geochemical data base; and
2. location of a national petroleum field site for detailed investigation of transport, fate, and natural attenuation; impacts of inorganic salts, trace metals, hydrocarbons, and other organic compounds on soils, sedimentary rocks, surface water, and groundwater; and radionuclides present in produced water releases (Kharaka & Wanty, 1997).

The latest USGS National Produced Waters Geochemical Database provides detailed geochemical data from the published literature, oil companies, and state divisions of oil and gas for more than 120,000 oil and gas wells from the major sedimentary basins in the USA (Blondes et al., 2019).

After developing site selection criteria, Kharaka and Otton (2007) visited oil fields in several petroleum-producing states including the East Poplar Field in Montana (Ball et al., 2019a; Thamke & Smith, 2014), where significant surface contamination was observed. Because of potential liability issues, however, some oil companies were reluctant to encourage selection of their fields for research. The Osage-Skiatook Petroleum Environmental Research (OSPER) A and B Sites, located in the southeastern part of the Osage Reservation in Osage County, northeast Oklahoma (Figure 56), were selected for detailed multidisciplinary investigations in June 2000 following a two-year national search effort.

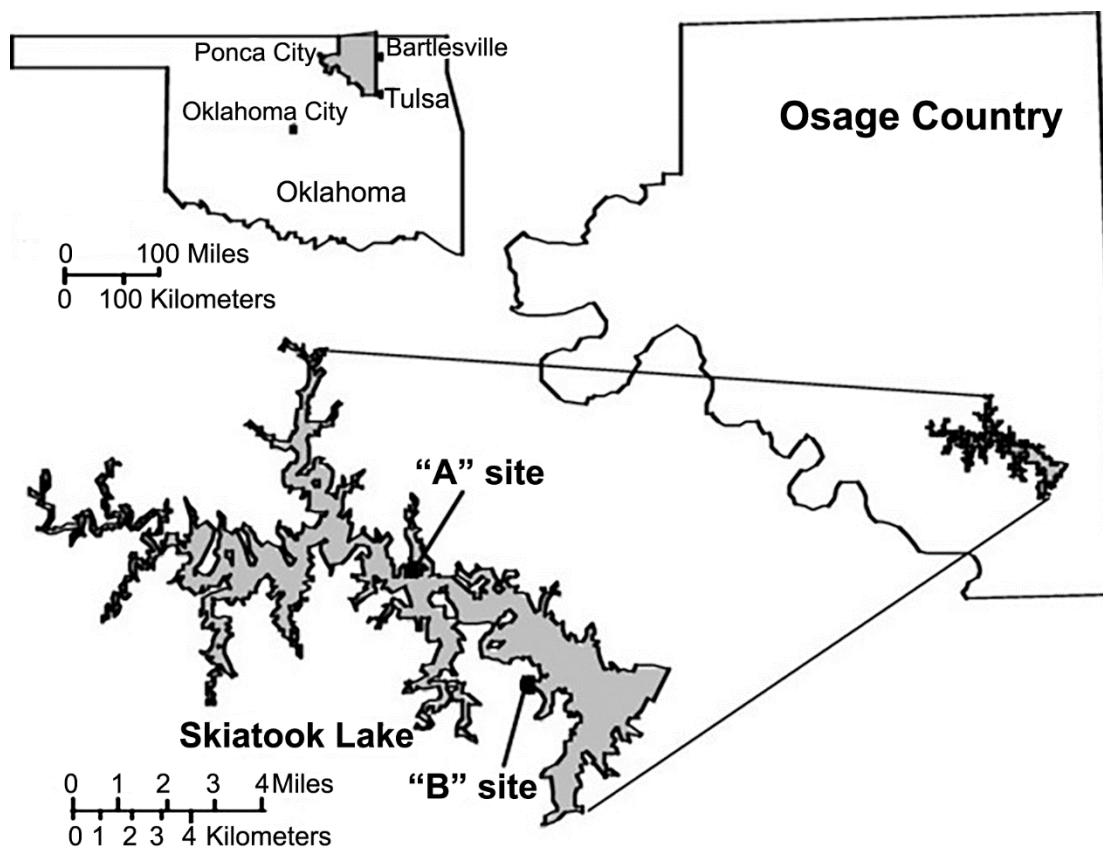


**Figure 56** - Map showing the Osage-Skiatook Petroleum Environmental Research (OSPER) A and B Sites, located in the southeastern part of the Osage Reservation in Osage County, northeast Oklahoma (from Kharaka et al., 2007).

The sites are located in oil leases typical of many depleted and aging petroleum fields in Osage County, which ranks among the top oil and gas producing counties in Oklahoma with about 39,000 wells (Abbott, 2000). Although oil and gas production has occurred in Osage County for over one hundred years, current production is mainly from stripper wells (averaging ~2.8 bbl/d (0.44 m<sup>3</sup>/d) oil and > 30 bbl/d brine, i.e., 4.79 m<sup>3</sup>/d) that are shallow—mostly 300 to 700 m deep—and produce from several sandstones of Pennsylvanian age.

The geologic and climatic settings of these sites resemble those of much of the major southern mid-continent oil- and gas-producing areas of the USA. The long history of oil and gas production in these leases has resulted in impacts that include soil salinization that led to destruction of soil texture and deep erosion, death of proximal vegetation, stress on peripheral vegetation, contamination of surface water and groundwater, saturation of soil with crude oil of varying age, and weathering and dispersal of crude oil components and trace elements.

An important selection criterion that was met is that the sites are located on federal land; the Osage Nation holds the mineral rights, while the Bureau of Indian Affairs (BIA) and the Environmental Protection Agency (EPA) have trust responsibility. The Army Corps

of Engineers owns the surface rights at these sites and manages adjacent Skiatook Lake. The 4,250-hectare Skiatook Lake provides drinking water to local Tulsa suburban communities and a rural water district and offers recreational fishing and boating opportunities to tens of thousands of visitors each year (Kharaka & Otton, 2003).

Starting in 2001, these two sites—the active OSPER B and the legacy OSPER A—have been the subject of intensive multidisciplinary studies by a team of approximately twenty scientists from the USGS and other governmental agencies as well as academia. The objective is to investigate the transport, fate, natural attenuation, and impacts of inorganic salts, trace metals, hydrocarbons, and other organic compounds, and radionuclides present in produced water releases. Impacts at these sites include salt scarring, tree and grass kills, soil salinization, and groundwater and surface-water contamination caused by the leakage of produced water and hydrocarbons from brine channels and pits, as well as accidental releases from flow lines and tank batteries. The goal was to improve understanding of the long- and short-term impacts of surface disturbances, produced water, and hydrocarbon releases from petroleum fields to minimize future impacts and develop science-based remediation plans (Dadrasnia, 2015; Kharaka & Otton, 2003, 2007).

After several years of research on repairing salt- and hydrocarbon-damaged soils in the tallgrass prairie of northeastern Oklahoma, Sublette and others (2007) have learned many lessons about what works and what does not in this geologic and climatic setting. These techniques simplify the remediation process and lower costs, thus benefiting the smaller producers who now are responsible for much of the petroleum production in the USA. For example, fertilizers added incrementally over a period of time seem more effective than large single application of fertilizer. Incremental applications increase and maintain rates of bioremediation by improving N recycling and microbial diversity.

Other lessons learned are that nematode community structure, which can be measured inexpensively, provides a simple estimate of the health of the recovering soil during remediation. In many cases, tilled hay is more effective in the reestablishment of vegetation than the more expensive gypsum applications on brine sites. However, subsurface drainage systems may be needed in some cases of low slope and excessive salinity, and reinjection of the recovered fluids may be necessary. Such science-based remediation plans are particularly needed in many of the aging and depleted fields—not only in Oklahoma, but throughout the world where land use is changing from petroleum production to residential, agricultural, or recreational uses (Kharaka & Dorsey, 2005; Miller et al., 2020).

The complexity of the multiple physical, chemical, and microbiological processes operating at these two sites requires a multidisciplinary team to examine the geology, geophysics, hydrology, geochemistry, microbiology, and ecosystem dynamics to generate a credible interpretive analysis useful to stakeholders and the scientific community. The

research team for this investigation comprised scientists from the Geologic, Water Resources, and Biologic Resources Disciplines of the USGS and from the US EPA, US BIA, and regional universities. This team was uniquely able to address the relevant issues including the characterization and fate of contaminants from produced water in soils, bedrock, surface water, and groundwater, and then generate data on site remediation and land use.

### 10.2.2 Site Investigations

Intensive investigations aimed at mapping the geology, impacted areas, and other cultural features at the OSPER sites started in February 2001 (Otton et al., 2005, 2007; Otton & Zielinski, 2003). Water, oil, and gas samples were taken from eight oil wells located in the Branstetter lease (OSPER B) and in areas adjoining the Lester Lease (OSPER A) to characterize the crude oil and produced water contaminant sources. Water samples were also obtained from Skiatook Lake, shallow groundwater wells in the region, and brine pits, seeps, and creeks in both sites (Kharaka et al., 2003, 2005, 2007a). Initial surface soil sampling (0 to 15 cm) was conducted at the B site in March 2001 to determine the chemical signature of added salts and the spatial distribution of soil salinity in relation to areas of visible salt scarring (Zielinski et al., 2003). Ground electromagnetic (EM) and DC (direct current) resistivity geophysical surveys were carried out in September 2001; the data were used to interpret the subsurface distribution of saline soil, water, and bedrock at both sites (Smith et al., 2003).

A total of sixty Geoprobe, auger, and rotary wells (1 to 71 m deep) were drilled, cored, completed, and sampled at both sites in February and March 2002. Three deep rotary wells were drilled as stratigraphic holes in nearby unimpacted areas. The location of the other wells was based on the following three criteria:

1. presence of salt scars, excessive soil and rock erosion, brine and asphalt pits, degraded oil, dead trees and shrubs, and other visible surface features;
2. results of electrical conductance, Cl, Br, and  $\text{SO}_4^{2-}$  measurements on aqueous leachates from samples of shallow soil (0 to 15 cm) and selected soil profiles (0.5 to 1.7 m); and
3. results of shallow penetrating (< 10 m) electromagnetic (EM) and deeper (30 to 60 m) DC resistivity surveys. Additional Geoprobe and auger wells were drilled at both sites in November 2002 and in March and April 2003; results from these and other wells are discussed in Kharaka and Otton (2007) and the references listed in that publication.

The shallow wells (0.5 to 4 m) were drilled without using water, employing an EPA Geoprobe (direct push) rig that was unable to penetrate the unweathered sandstones. The deeper (71 m) well, BR-01, and (38 m) well, BR-02, were drilled using a rotary rig that required water (a possible contaminant) for cooling; the other deeper wells were drilled

with an auger rig without water. The Geoprobe wells were completed using 2.5 cm PVC tubing that generally had a 0.61 m screened interval with a bottom cap starting at total depth. The deeper rotary and auger wells had two completions using 5.1 cm PVC tubing, usually with 1.5 m screened intervals selected based on indications of water-bearing zones while drilling the wells. Clean and graded sand was placed around the screened intervals, and bentonite pellets and chips were used to isolate the screened intervals in wells with multiple completions.

Core samples from impacted and pristine areas were studied (Rice et al., 2003) using visual and microscopic description, X-ray powder diffraction of the bulk soil and clay-sized fraction, particle size analysis, cation exchange capacity, and selective extraction of iron species to establish the differences in the mineralogy, sorption of Na and other chemicals, and geochemical behavior of soils impacted by saline water compared to those from unimpacted areas. Grab and core samples from impacted and pristine areas were also used by Campbell and others (2003) to determine key parameters, including nitrates, organic matter, total petroleum hydrocarbons (TPH), conductivity, chlorides, and dehydrogenase activity (DHA: a measure of viable biomass) that are essential for the development of guidelines for stabilizing or restoring impacted areas. A series of oil, water, brine, and soil samples were characterized and analyzed for geochemical parameters that are indicative of microbial activity (McIntosh et al., 2017).

Characterization of the resident microbial populations and the varying stages of weathering and biodegradation of oils were completed for some of these samples and are reported by Godsy and others (2003). Characterization of the discrete (i.e., organic acid anions, BTEX, phenols, and so on) and non-discrete organic matrix (NOM) of produced water in three petroleum wells and one groundwater monitoring well at the OSPER sites were investigated and are discussed by Sirivedhin and Dallbauman (2004).

Based on repeated water table measurements in wells, chemical analyses of water samples, and field observations, Herkelrath and Kharaka (2003) and Herkelrath and others (2007) developed conceptual models of the hydrology and solute transport mechanisms near the major brine pit at OSPER A and B sites. They proposed two main mechanisms for solute transport from the waste pit to the lake. One mechanism is the relatively slow and steady flow of saline groundwater from the waste pit to the lake in a near-surface aquifer. The other mechanism is relatively fast overland flow of salt-laden runoff during rainfall. Using the USGS model SUTRA, they simulated steady-state groundwater flow and solute transport from the pit to the lake. Preliminary modeling results indicated that the solute travel time from the pit (OSPER B) to the lake for saline groundwater is two to four years.

All the wells, other sampling sites, and features were surveyed with high accuracy real-time kinematic (RTK) GPS equipment in June and July 2002. This differential correction method of surveying requires a GPS base station, a GPS rover unit, and radio link between

the units. The accuracy achieved is better than  $\pm 10$  cm horizontally and vertically (Abbott, 2003).

Details of all these investigations, including field and laboratory methods used and results obtained, appear as separate reports primarily in three major publications (Kharaka & Otton, 2003, 2007; Kharaka & Dorsey (2005)).

### 10.2.3 Case Study 2A: Groundwater Contamination at an Active Oil Field

The OSPER B site is located in the Branstetter oil lease in sections 29 and 32, T22N, R10E. The Township-Section-Range system of location used in the USA is described on [Wikipedia](#)<sup>7</sup>. The site is actively producing oil and has ongoing hydrocarbon releases and salt scars that have impacted an area of approximately one hectare. The site includes an active production tank battery and adjacent large brine pit (Figure 57), as well as two injection-well sites—one with an adjacent small pit—and an old tank battery. The large pit is about 15 m from the shoreline of Skiatook Lake (Figure 58); all the other sites are within 45 m of the lake. Three salt scars (partially remediated in 2000 by saline soil removal, tilling, and soil amendments) extend downslope from the active tank battery, the injection well/pit, and the old tank battery site to the lake's edge. Two small creeks cross the northern and southern parts of the site. The upper part of the site is characterized by a thin surface layer of eolian sand mixed with sandstone-clast colluvium underlain by weathered and unweathered shale, whereas the lower part of the site is underlain by

- a surface layer of eolian sand (20 to 70 cm thick);
- colluvial apron and alluvial deposits of varying thickness comprised of sandstone pebbles, cobbles, and boulders with a fine sandy to clayey matrix;
- weathered shale; and
- unweathered bedrock (Otton et al., 2007; Otton & Zielinski, 2003).

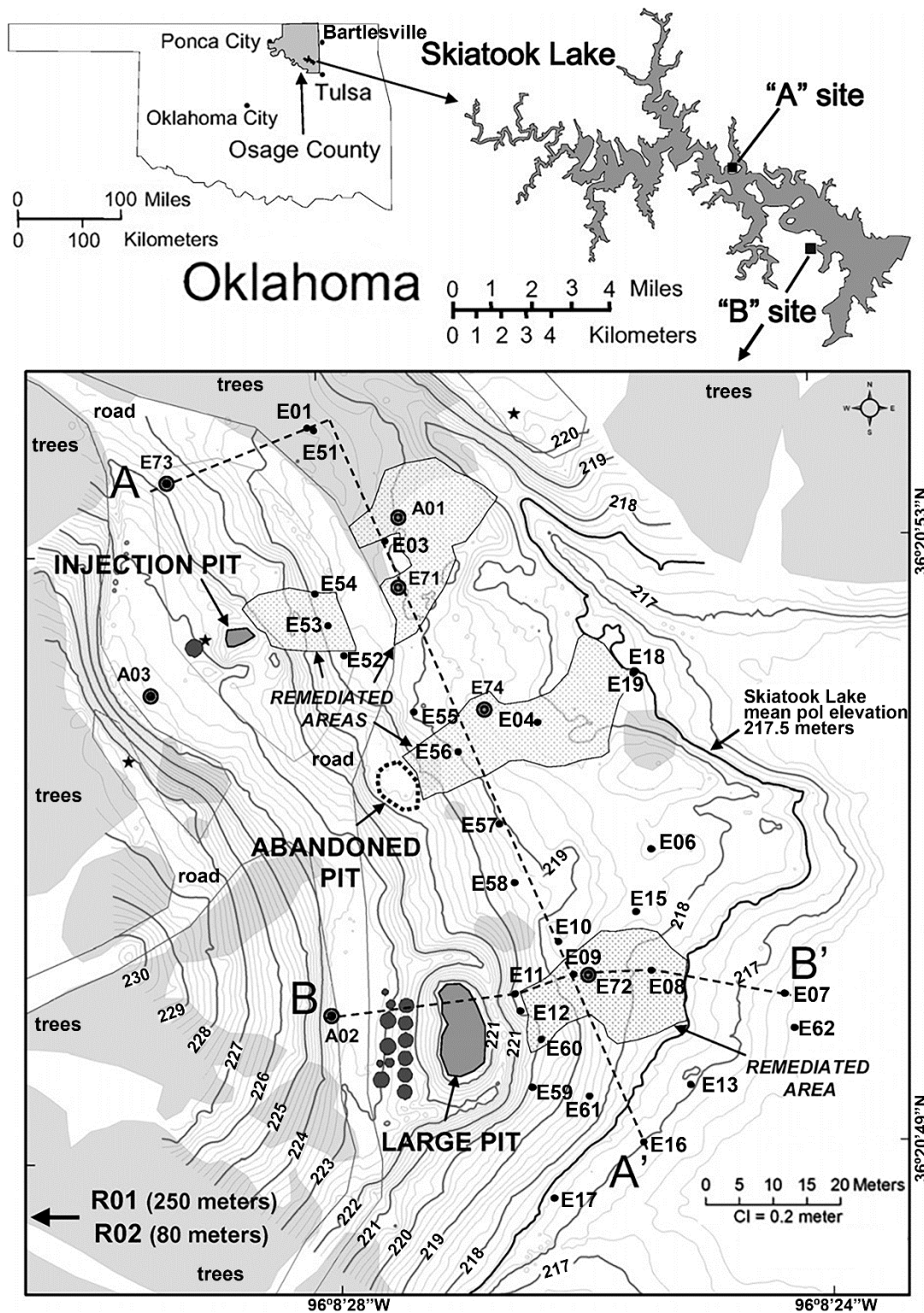


**Figure 57** - The OSOPER A and B sites on Skiatook Lake in Osage County, Oklahoma, USA are shown on the overview map. The expanded surface elevation map (contours in m) of the OSOPER B site shows locations of brine pits, other production features, drilled water wells, outlines of treed areas, impacted and remediated areas, and transect lines (from Kharaka et al., 2007).



**Figure 58** - Aerial photograph of part of the OSPER B site showing the fluid tanks and the active brine pit near Skiatook Lake. Oil operations have caused the scarred and partially remediated area between the brine pit and the reservoir (photo courtesy of Ken Jewell, USEPA, Ada, Oklahoma; from Kharaka & Dorsey, 2005).

The Branstetter lease was initially drilled in 1938 and increased activity occurred from 1947 to 1951. Approximately 110,000 barrels (~17,488.60 m<sup>3</sup>) of oil were produced from the lease before water flooding for enhanced recovery began in 1953. In 2006, ten wells produced 1 to 3 bbl/d (0.16 to 0.48 m<sup>3</sup>/d) oil and 50 to 100 bbl/d brine; all the produced fluid is collected and separated in the tank battery adjacent to the large brine pit. The two brine pits at this site are not lined and receive brine and hydrocarbon releases from broken pipes and tank leaks. They also receive large volumes of surface-water flow from precipitation. The brine in these pits is generally pumped into collection tanks by submersible pumps, but these occasionally fail causing filling and overflow of brine pits as occurred in November and December 2001 for the large brine pit.

## Results and Discussion

Concentrations of inorganic and organic chemicals in selected surface and groundwater samples from the OSPER B site and adjoining areas are listed in Table 45. The data listed are generally for water samples collected during February 2005, the last field sampling. For each of the forty-one wells at this site—especially the deeper rotary (BR) and auger (BA) wells—chemical and water isotope data for water samples are reported that were collected from repeated (up to eight times) sampling in February 2005 (Thordsen et al., 2007). Repeated sampling is necessary for all wells because drilling operations generally introduce contaminants to the pore water, especially in rotary wells drilled with fresh water and rotary and auger wells with multiple completions that may have been subject to downward and cross formational flow prior to well completions. The last sample is most representative of undisturbed conditions.

**Table 45** - Chemical composition (mg/L) of water from the separator, Skiatook Lake, and selected boreholes from the OSPER B site (from Kharaka et al., 2007). Dates are m/dd/yy (TDS = total dissolved solids).

Site	Separator	Skiatook Lake	BR-01 deep	BA-01 deep	BA-03 shallow	BA-03deep	BE-55	BE-62	BE-71	BE-72	BE-73	BE-74
Sample	02OS-314	02OS-310	04OS-241	05OS-107	05OS-105	05OS-104	04OS-245	03OS-152	05OS-109	05OS-108	05OS-111	05OS-110
Date	2/24/02	2/22/02	5/24/04	2/4/05	2/3/05	2/3/05	5/25/04	4/2/03	2/4/05	2/4/05	2/4/05	2/4/05
TDS	133,600	165	1,260	6,560	12,900	6,590	26,600	15,700	11,600	11,400	14,300	18,600
pH	6.50	8.14	6.67	7.03	6.45	6.58	6.40	6.66	6.60	6.64	6.89	6.49
Na	40,400	16	109	901	2,120	792	5,270	3,720	1,210	1,290	1,740	2,120
K	232	2.5	2.2	14	19	12	12	12.0	19	22	20	32
Mg	1,580	5.7	60.7	396	1,180	475	2,320	756	1,210	1,190	1,480	2,140
Ca	7,640	22	142	464	775	447	997	751	656	569	665	949
Cl	82,100	29.1	94.7	963	7110	1230	13,600	7640	2850	2550	4270	7630
SO <sub>4</sub>	2.5	11.3	271	3190	792	2780	3620	2150	4680	4710	4740	4700
HCO <sub>3</sub>	139	76	558	571	861	791	653	480	949	1,010	1,280	978
Li	8.5	0.0017	0.04	0.08	0.14	0.11	0.06	0.18	0.19	0.23	0.19	0.31
Sr	472	0.21	0.92	16	13	12	30	31	15	11	10.0	23
Ba	460	0.06	0.04	0.016	0.130	0.012	0.068	0.093	0.013	0.013	0.016	0.013
Mn	0.84	0.032	0.33	2.3	10.4	0.24	5.6	71	0.96	0.27	0.39	0.42
Fe	36	< 0.006	1.96	2.2	2.8	1.4	0.4	59	3.0	< 0.5	2.8	1.6
Br	338	0.14	0.36	3.1	31	4.2	53	33	10.3	9.7	18	30
NO <sub>3</sub>	< 0.5	0.7	0.18	< 0.2	< 0.4	< 0.2	< 2	< 1	< 0.25	< 0.25	< 0.25	< 0.4
SiO <sub>2</sub>	< 32	1.4	22	15	16	15	10	9	14	12	14	13
B	2.9	0.03	0.34	4.4	0.8	4.9	< 0.8	0.41	2.4	2.3	0.9	2.2
DOC	5	4	0.6	0.5	5	0.4	7	32	1	1	4	1
Formate	0.26	-	0.02	< 0.06	< 0.06	< 0.1	< 0.16	0.4	< 0.2	< 0.16	0.17	< 0.3
Acetate	0.7	-	0.06	< 0.1	< 0.06	< 0.1	0.6	0.13	< 0.1	< 0.1	0.27	0.3
C <sub>6</sub> H <sub>6</sub>	4.0	-	< 0.005	< 0.005	< 0.005	< 0.005	< 0.005	0.058	< 0.005	< 0.005	< 0.005	< 0.005

Results of repeated samples obtained from the BR-01d (deep perforation) well (Figure 59a) show the initial dilution with fresh drilling water, followed by high salinity water (which was also high in Na and Cl) from the overlying zone. A reasonably constant salinity and chemical composition is achieved in the fourth and subsequent samples, giving the presumed pre-drilling composition of groundwater in the perforated section of this well. Results also indicate a uniform composition of groundwater in the vicinity of this perforated section, since three or more well-pore volumes were pumped from this and other wells before each sampling and they all had similar chemistry.

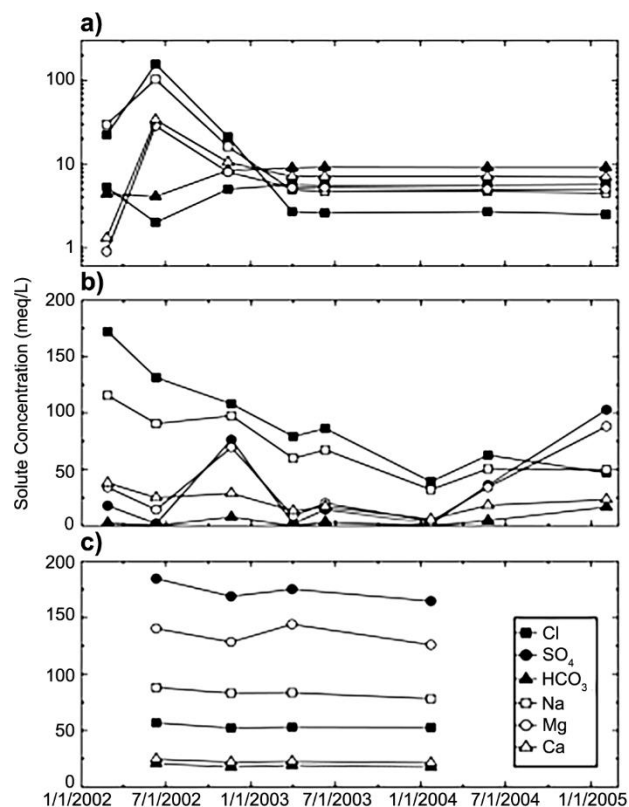


**Figure 59** - Temporal variation in the concentrations of major cations and anions in water obtained from selected boreholes from the OSPER B site showing a) significant initial changes as a result of drilling operations in well BR-01d, b) continued changes likely resulting from variations in composition of water in the aquifer in the vicinity of well BA-01s, and c) relatively constant composition of water from BE-71 (from Kharaka et al., 2007).

Results of repeated samples from the BA-01s (shallow perforation) well, on the other hand, show variable increases and decreases in salinity and concentrations of chemical components (Figure 59b). The likely reactions leading to these changes are listed in Table 46, but such changes are not caused by drilling operations. They likely represent spatial variability in the chemical composition of groundwater in the vicinity of the perforated section from this well.

**Table 46** - Important water-mineral interactions at OSPER sites (from Kharaka et al., 2007a).

Reactions	
$2\text{FeS}_2 + 7\text{O}_2 + 2\text{H}_2\text{O} \leftrightarrow 2\text{Fe}^{++} + 4\text{SO}_4^{--} + 4\text{H}^+$	(1)
$\text{FeS}_2 + 2\text{NO}_3^- + 2\text{H}_2\text{O} \leftrightarrow \text{Fe}^{++} + 2\text{SO}_4^{--} + 4\text{H}^+\text{N}_2$	(2)
$4\text{Fe}^{++} + \text{O}_2 + 10\text{H}_2\text{O} \leftrightarrow 4\text{Fe}(\text{OH})_3 + 8\text{H}^+$	(3)
$8\text{Fe}^{+++} + \text{CH}_3\text{COOH} + 2\text{H}_2\text{O} \leftrightarrow 8\text{Fe}^{++} + 2\text{CO}_2 + \text{H}^+$	(4)
$\text{Fe}^{++} + \text{HS}^- \leftrightarrow \text{FeS} + \text{H}^+$	(5)
$2\text{H}^+ + \text{CaMg}(\text{CO}_3)_2 \leftrightarrow \text{Ca}^{++} + \text{Mg}^{++} + 2\text{HCO}_3^-$	(6)
$\text{Ca}^{++} + \text{HCO}_3^- \leftrightarrow \text{H}^+ + \text{CaCO}_3$	(7)
$4.8\text{H}^+ + 0.2\text{Ca} + 0.8\text{Na}^+ + 2\text{Al} + 2.8\text{Si} + 8\text{O} + 3.2\text{H}_2\text{O}$	(8)
$\quad \quad \quad \leftrightarrow 0.2\text{Ca}^{++} + 0.8\text{Na}^+ + 1.2\text{Al}^{+++} + 2.8\text{H}_4\text{SiO}_4$	
$\text{Ca}^{++} + \text{SO}_4^{--} + 2\text{H}_2\text{O} \leftrightarrow \text{CaSO}_4 \cdot 2\text{H}_2\text{O}$	(9)

Results from the shallow and single completion well (BE-71) are much more uniform (Figure 59c) in water salinity (15,000 to 16,700 mg/L) and concentration of chemical components including DOC values (6 to 9 mg/L) than the other wells. The salinity (134,000 mg/L) and chemical composition of water from the separator of the active tank battery (Table 45) are similar to those for the produced water from the seven oil wells (115,000 to 185,000 mg/L) reported in Kharaka and others (2003). The hypersaline brine is a Na-Ca-Cl type and has notably high concentrations of Mg, Sr, Ba and  $\text{NH}_4$ , but very low amounts of  $\text{H}_2\text{S}$  (<0.4 mg/L, not shown),  $\text{SO}_4$ , and  $\text{HCO}_3$  (Table 45). With the exception of Fe, the concentrations of metals in produced water are low, and the values of organic acid anions and other dissolved organic species are relatively low (Table 45, separator sample). Relative concentrations of major ions in water from Skiatook Lake, BR01d, produced water from the tank battery and OSPER B site boreholes are shown in Figure 60.

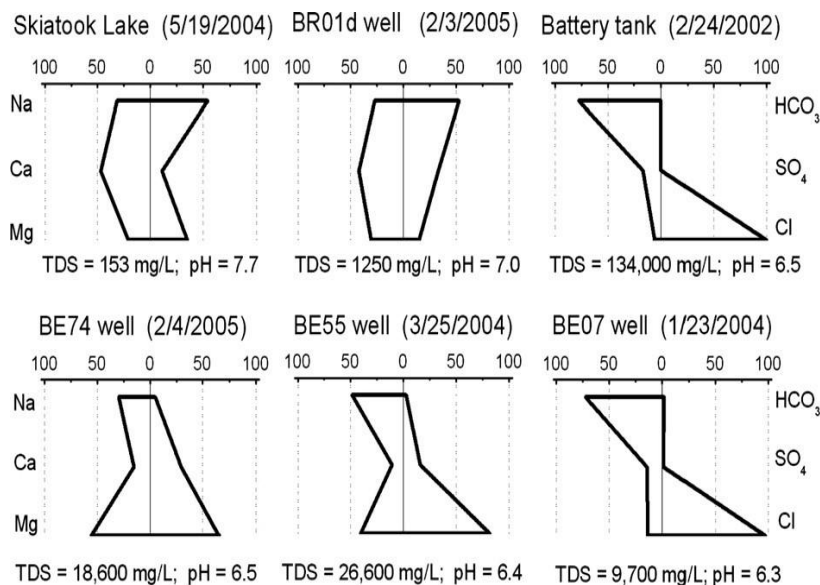


**Figure 60** - Modified Stiff diagrams showing the salinity of water and the relative concentrations (in eq/L normalized to 100 percent) of major cations and anions in water from Skiatook Lake, in local well BR01d, in produced water from the tank battery and in water from selected boreholes at the OSPER B site (from Kharaka et al., 2007).

The salinity and chemical composition of water in the two brine pits (Figure 57) vary greatly with time, reflecting primarily the mixing of produced brine with dilute water from precipitation and runoff into the pits; evaporation also plays an important role, especially during the hot summer season. The measured salinity of water in the two brine pits have ranged from 1000 to > 40,000 mg/L total dissolved solids (TDS), with changes occurring over relatively short times. The salinity of water in the brine pit adjacent to the injection well, for example, was 13,000 mg/L on December 11, 2001, and 42,000 mg/L on February 25, 2002. The proportions of major anions and cations in the samples from the brine pits are generally similar and comparable to those of produced water, but the concentrations are reduced by factors of 3 to 100.

The chemical composition of Skiatook Lake water (Table 45 and Figure 60) and two potable groundwater wells used by local farmers show major contrast from that of produced water (Kharaka et al., 2003). The water has low salinity (150 to 1,000 mg/L) and comparable values for the equivalent concentrations of Na, Mg, and Ca as well as those of Cl, SO<sub>4</sub>, and HCO<sub>3</sub> as is generally the case with uncontaminated groundwater (Hem, 1985; Kharaka & Hanor, 2014; Richter & Kreitler, 1993). The local groundwater reported in Kharaka and others (2003) has a composition comparable, but with lower salinity to that shown in sample BR01d (Figure 60, Table 45). Local groundwater, then, has much higher Mg and Ca concentrations relative to Na and much higher HCO<sub>3</sub> and SO<sub>4</sub> relative to Cl when compared to produced water (Figure 60, Table 45).

The average concentration of DOC in pristine groundwater is 0.7 mg/L, so values higher than 1 mg/L—together with the presence of organic acid anions and BTEX—are considered good indicators of contamination with produced water and/or oil (Kharaka et al., 2000; Thurman, 1985).

Uncontaminated groundwater is also generally oxic with DO values > 2 mg/L, resulting in low concentrations of Fe (<0.3 mg/L), Mn, and other metals (Hem, 1985). In anoxic environments, present in produced water and petroleum contaminated groundwater at OSPER B, Fe and Mn are mobilized from sediments and reach high values, generally > 2 and up to 59 mg/L for Fe (Table 45).

Based on these criteria, together with  $\delta D$  and  $\delta^{18}O$  values of water, which are isotopically lighter for pristine groundwater relative to produced water (Kharaka et al., 2003), groundwater from the perforated section of only one well, BR-01d, (Table 45) located 330 m upslope and west of the large brine pit appears to be uncontaminated by the petroleum operations.

No significant amount of oil was observed in contaminated groundwater at this site, but oil globules in water, strong oil odor, and relatively high values for VOC gases measured by a field PID instrument (that excludes CH<sub>4</sub> and C<sub>2</sub>H<sub>6</sub>) were observed mainly in wells E-07 (3 ppm total VOC) and E-09 (24 ppm) located down gradient from the large brine

pit (Figure 57). Strong oil odor and oil globules were also observed in water from well R-02d (indicated as R02 in Figure 57), located adjacent to an active oil well, 150 m upslope, and west of the large brine pit. Evidence of CH<sub>4</sub> and other flammable VOC gases was found in well E-71 as the evolving gas was ignited at the wellhead, indicating relatively little contamination. A cross-sectional view of the site is provided in Figure 61.

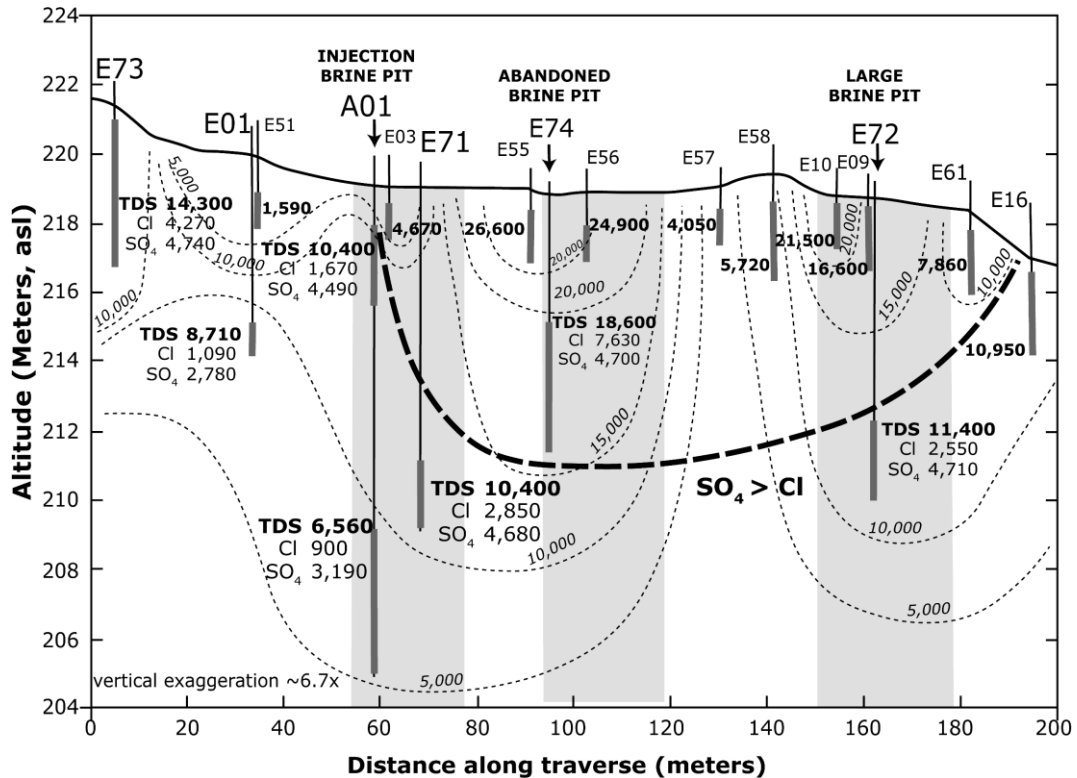


**Figure 61** - Water salinity and concentrations of Cl and SO<sub>4</sub> in samples from perforated sections of wells along a north–south transect A–A (Figure 57) at the OSPER B site’ with a factor of 6.7 vertical exaggeration. Three interconnected plumes of high salinity water are present below the small injection pit, the abandoned brine pit (highest salinity of up to 30,000 mg/L) and the large brine pit (from Kharaka et al., 2007). Shaded zone represent the section below the pits.

The average concentration of DOC in pristine groundwater is 0.7 mg/L. In general, DOC values higher than 1 mg/L occurring with organic acid anions and BTEX, are considered good indicators of contamination with produced water and/or oil (Thurman, 1985; Kharaka et al., 2000; Sirivedhin & Dallbauman, 2004). All wells at the OSPER B site had DOC values and other dissolved organic compounds that indicate contamination, but DOC values in water from deeper sections of a few wells (e.g., A-01d) were lower than 1 mg/L for samples collected more recently. The higher DOC values (up to 83 mg/L) were obtained from shallow wells (e.g., E-7, 8, 9) located down slope from the large brine pit. Water from the deeper BE wells drilled in May 2004 (E-71, 72, 73, and 74) had relatively low DOC concentrations (1 to 4 mg/L). The observed higher DOC values indicate recent contamination with brine from the brine pit. In time the DOC values decrease by biodegradation and dilution.

Carboxylic acid anion concentrations for the OSPER B site are much lower than for the OSPER A site, ranging from 0 to 4 mg/L, and generally correlate positively with DOC values. The anions are mainly acetate and occasionally succinate. Concentrations of BTEX compounds generally ranged from 0 to 1 mg/L, with benzene being the dominant component. One exceptionally high BTEX value of 10 mg/L was found in the first sample from BA03s, but values declined in subsequent samples, and BTEX concentrations were below the detection limit of 5 µg/L in the last sample collected in 2005; a similar pattern is observed in the other BA wells.

All the water samples obtained from pools, seeps, and boreholes at the OSPER B site show variable impacts from produced water operations. The most saline (82,000 mg/L TDS) sample outside the brine pits was obtained in December 2001 from a well (EPA-1; Table 3 in Kharaka et al., 2003) located about 15 m down gradient and to the east from the large brine pit, which generally contains 0.2 to 2 m of produced water covered with a thin layer of oil. The brine in this pit is generally pumped into collection tanks by a submersible pump, but the pump occasionally fails causing filling and overflow of the brine pit as happened in November and December 2001, resulting in high salinity water reaching wells located down gradient. Water obtained from the same well in February 2002 had a salinity of only 17,400 mg/L, but the proportions of major cations and anions were similar to those of produced water.

Brine leaks and overflows from the large pit likely are the source of the high salinity groundwater plume centered below this pit (Figure 61). The most recent data (mainly from February 2005) depicted in the figure show a maximum salinity close to 30,000 mg/L, but as discussed above, a salinity of 82,000 mg/L was measured in December 2001. Water samples obtained from the other wells, especially the shallow ones (Figure 62), also show major changes in salinity and chemical composition. In the case of well BE-07, located in the littoral zone of Skiatook Lake about 65 m down gradient and to the east from the large brine pit, water salinity in 2002 was 20,000 to 24,000 mg/L TDS, decreasing to 9,000 and 10,000 in 2003 and 2004, respectively. The chemical composition of water from this well has characteristics similar to that of produced water, that together with the presence of oil globules in the water, strong oil odor, and high values measured for hydrocarbon gases and other VOCs (Godsy et al., 2003; Kharaka et al., 2003) show that brine and minor amounts of hydrocarbons from the large brine pit reach Skiatook Lake.

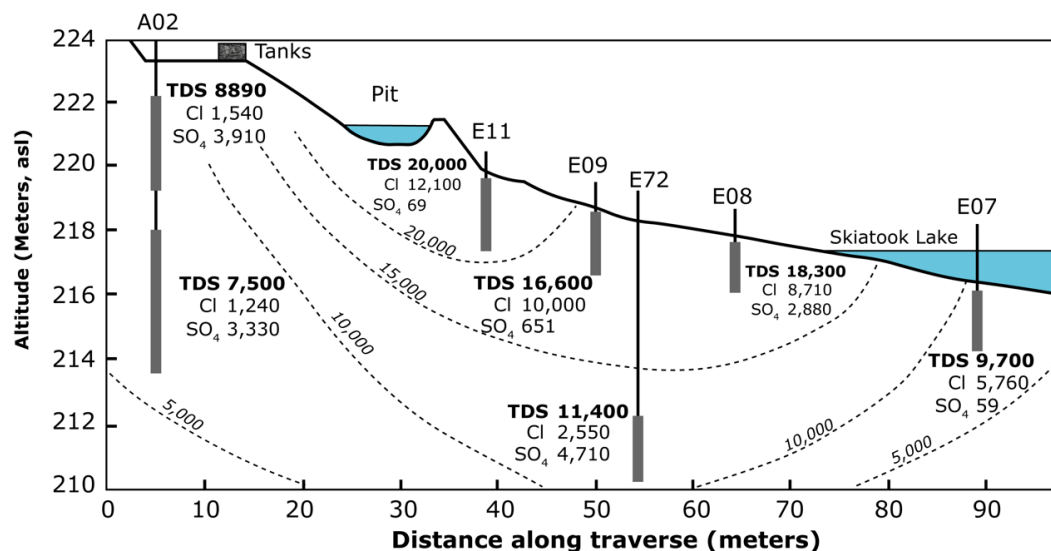


**Figure 62** - Water salinity and concentrations of Cl and SO<sub>4</sub> in samples from perforated sections of wells along a west-east transect B-B' (Figure 57) at the OSPER B site. A plume of high salinity (up to 20,000 mg/L) contaminated groundwater is present below the large, active, brine pit (from Kharaka et al., 2007).

Brine leaks and overflows from the abandoned brine pit and tank battery are likely the main source of the higher salinity (26,600 mg/L) groundwater plume depicted in Figure 62. Leaks from the injection brine pit have flowed northward toward well BE-73 and westward toward well BA03, with the bulk flowing down gradient toward BA-01 and the northern creek (Figure 61). The two adjacent plumes have coalesced into a larger plume centered below the abandoned brine pit, with salinity decreasing with increasing depth.

Significant amounts of produced water, but no oil, continue to reach the wells, water pool, and even the creek adjacent to the scarred, but "remediated" area down gradient from the reinjection pit (Figure 61). The salinity of water from BE-03 and other wells, small pools, and a large pool close to the creek has varied widely (2,500 to 13,000 mg/L), modified by evaporation and mixing with water from precipitation and Skiatook Lake water, but the chemical composition is that of diluted produced water.

Profiles of specific conductance in creek water show two areas of brine discharge. The first is located near well E-19 and had conductance values up to 8,000  $\mu\text{S}/\text{cm}$ ; the second, located to the east of well A-01, had higher conductance (up to 20,000  $\mu\text{S}/\text{cm}$ ). A composite sample collected from that location had a salinity of 2,500 mg/L and chemical properties of diluted produced water.

Data obtained from the four relatively deep auger wells (BE71 to 74) completed in May 2004 allow for the construction of the cross sections (Figure 61 and Figure 62) showing a general decrease of salinity with depth. The organic and inorganic compositions of water from these wells, together with  $\delta^3\text{H}$  values indicate contamination with produced water high in Na and Cl. The water from these and other wells, however, have very high (up to 10,000 mg/L) concentrations of SO<sub>4</sub> that are higher than those for Cl in samples from relatively shallow (1.5 to 2 m) wells located to the south of the large brine pit (BE-16, 17, 18)

and for many samples from deeper sections of wells (Table 45). The concentrations of Mg are also very high and generally higher (on equivalent basis) than Na for samples with  $\text{SO}_4$  values greater than 4,000 mg/L. The concentrations of  $\text{HCO}_3$  in this water are elevated relative to those of Cl in produced water (Figure 60); the concentrations of Ca are about the same or only slightly elevated relative to those of Na in produced water (Figure 60).

The chemical composition of groundwater in general, and the very high concentrations of  $\text{SO}_4$  and Mg in particular, cannot be explained by simple proportional mixing of produced water with low salinity local groundwater and/or precipitation water. In addition to mixing that can be ascertained from the concentrations of conservative solutes (e.g., Cl, Na) in the mixed water, several important water–mineral–bacterial interactions leading to mineral dissolution and precipitation are necessary to explain the observed compositions. The very light  $\delta^{34}\text{S}$  values (generally -10 permil to -30 permil) for  $\text{SO}_4$  obtained for samples from the OSPER A site show oxidation of pyrite (Table 46; reactions 5 and 9) that is ubiquitous in the unweathered shale (Otton & Zielinski, 2003), is likely the main source of high  $\text{SO}_4$ . The highest  $\text{SO}_4$  values present in water from relatively shallow wells (e.g., BE-16, 17) require significant amounts of the main oxidant,  $\text{O}_2$ , possibly indicating reaction in the unsaturated zone together with relatively long reaction time. High  $\text{SO}_4$  in water from deeper wells could result from downward flow of water from overlying sections, which is indicated by the presence of contaminant inorganic and organic compounds in that water; it could also indicate a significant rise in groundwater levels in the area as a result of completion of the Skiatook Lake as a reservoir in 1987 (Herkelrath & Kharaka, 2003).

The increases in Mg concentrations are positively correlated with increases in  $\text{SO}_4$  and  $\text{HCO}_3$ , and likely result mainly from dissolution of dolomite present in sandstones (Table 46; reaction 6), with the  $\text{H}^+$  provided from pyrite oxidation. The absence of significant Ca increases with higher Mg values is explained by precipitation of calcite (Table 46; reaction 7), that also lowers the concentration of  $\text{HCO}_3$  to half of that resulting from dissolution of dolomite.

Results of geochemical modeling using the latest version of SOLMINEQ (Kharaka et al., 1988) show that samples of groundwater (and produced water) are generally at saturation with calcite (Figure 63), and addition of any Ca and/or  $\text{HCO}_3$  would result in calcite supersaturation and precipitation. Modeling also shows that groundwater high in  $\text{SO}_4$  are at saturation with gypsum but produced water and most other groundwater is undersaturated with gypsum (Figure 63). This modeling indicates that gypsum, because of faster rates of mineral dissolution and precipitation compared to dolomite and calcite, could be the ultimate control on the concentrations of  $\text{SO}_4$  and Ca, but any gypsum precipitated (e.g., by evaporation in the shallow sections) would quickly redissolve in lower salinity surface water and/or groundwater.

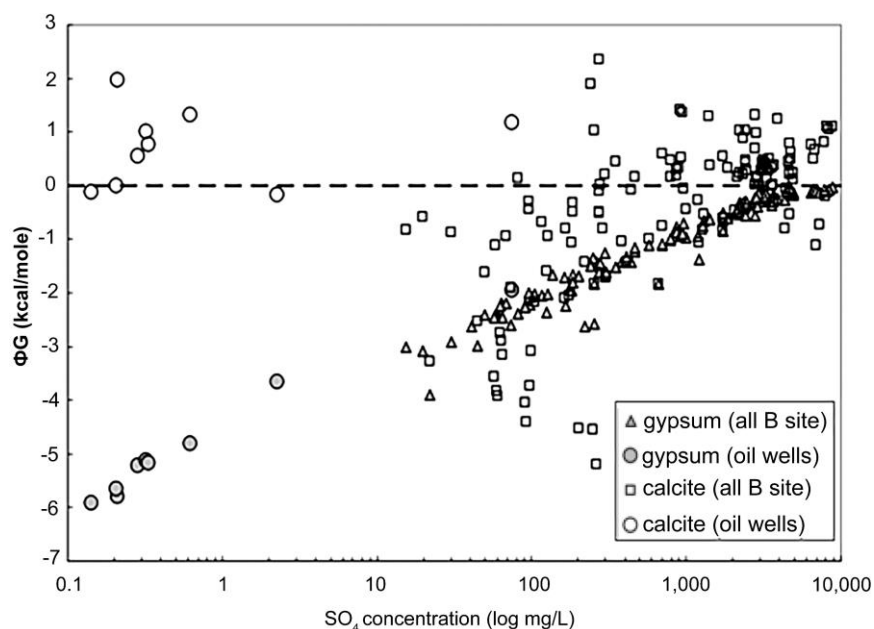


**Figure 63** - Saturation states of calcite and gypsum in produced water from oil wells in and near the Branstetter lease and from boreholes drilled at the OSPER B site. Most of the water samples, including those from oil wells, cluster near the saturation line for calcite (dashed line) but are undersaturated with respect to gypsum except when  $\text{SO}_4$  concentrations are higher than  $\sim 4,000$  mg/L (from Kharaka et al., 2007).

The three plumes (Figure 61) are interconnected, but the middle plume that is centered below the older and now abandoned brine pit has higher salinity and high salinity contours extend to greater depth, indicating deeper brine penetration and possibly increased residence time. The lateral boundaries of the larger plume are not defined because all wells at this site are impacted by produced water. The bottom of the plume is also not defined because the authors interpret the data from the deeper section of well BA-01d as indicating impact. The eight samples collected from the deeper section of this well could be interpreted to indicate initial mixing by higher salinity water (also high in Na and Cl) from the overlying zone during drilling. Later samples show relatively high (up to 3 mg/L) DOC values, organic acid anions (up to 0.5 mg/L), and BTEX (0.5 mg/L)—all indicators of contamination. The concentration of some of these organics are relatively high in the three samples collected in 2004–2005 that yielded relatively high and constant salinity (6,600 to 6,700 mg/L) as well as chemical composition (Table 45).

#### 10.2.4 Case Study 2B: Groundwater Contamination at a Legacy Site

The OSPER A site (located in section 13, T22N, R10E) has an area of about 1.5 hectare. The Township-Section-Range system of location used in the USA is described on [Wikipedia](#)<sup>7</sup>. The site is impacted by produced water and hydrocarbon releases that occurred primarily 75 to 100 years ago. The site is underlain with the following as shown in Figure 64:

- a surface layer of eolian sand of varying thickness (up to about 80 cm);

- colluvium that ranges from large boulders of sandstone to thin, granule-pebble conglomerate;
- weathered shale, siltstone, and sandstone; and
- underlying unweathered bedrock.

Much of the site appears to have been impacted by early salt-water releases that killed the pre-existing oak forest. The salt-impacted soil subsequently prevented younger oak trees from colonizing much of the site except where a single tree or clump of trees found favorable conditions. The gently sloping upper part of the site is slightly eroded in places and has been mostly revegetated with grasses, forbs, sumac, and a few trees. This area drains into the main arm of Skiatook Lake just off the map (Figure 57) to the southwest.

The lower, steeper, more heavily salt-impacted portion has been eroded to depths of as much as 2 m. Seepage of salt water from a shallow sandstone aquifer continues and active salt scarring persists. This area drains into the Cedar Creek arm of Skiatook Lake to the north (Figure 65).

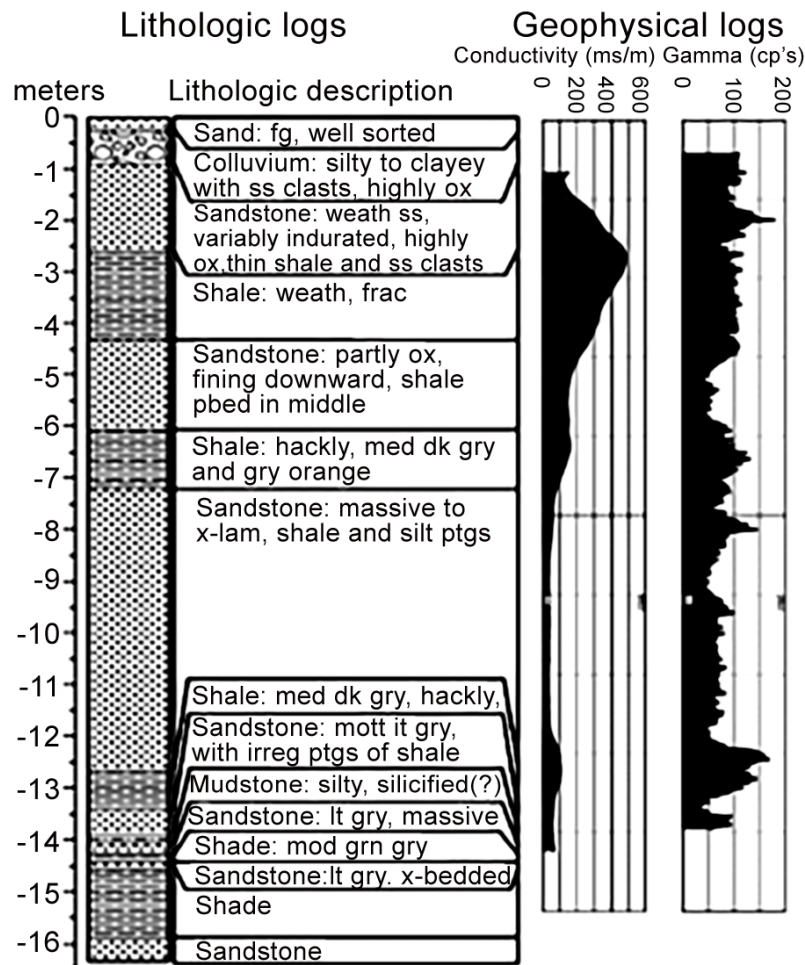


**Figure 64** - Lithologic and geophysical logs of the AA02 well at OSPER A site. Notations: Fg = fragments; ss = sandstone; ox = oxygenated; weath = weathered; frac = fractured; med = medium; dk = dark; gry = gray; mott = mottled; lt = light; irreg = irregular; ptgs = partings; lam = laminated; grn = green (from Kharaka et al., 2005).

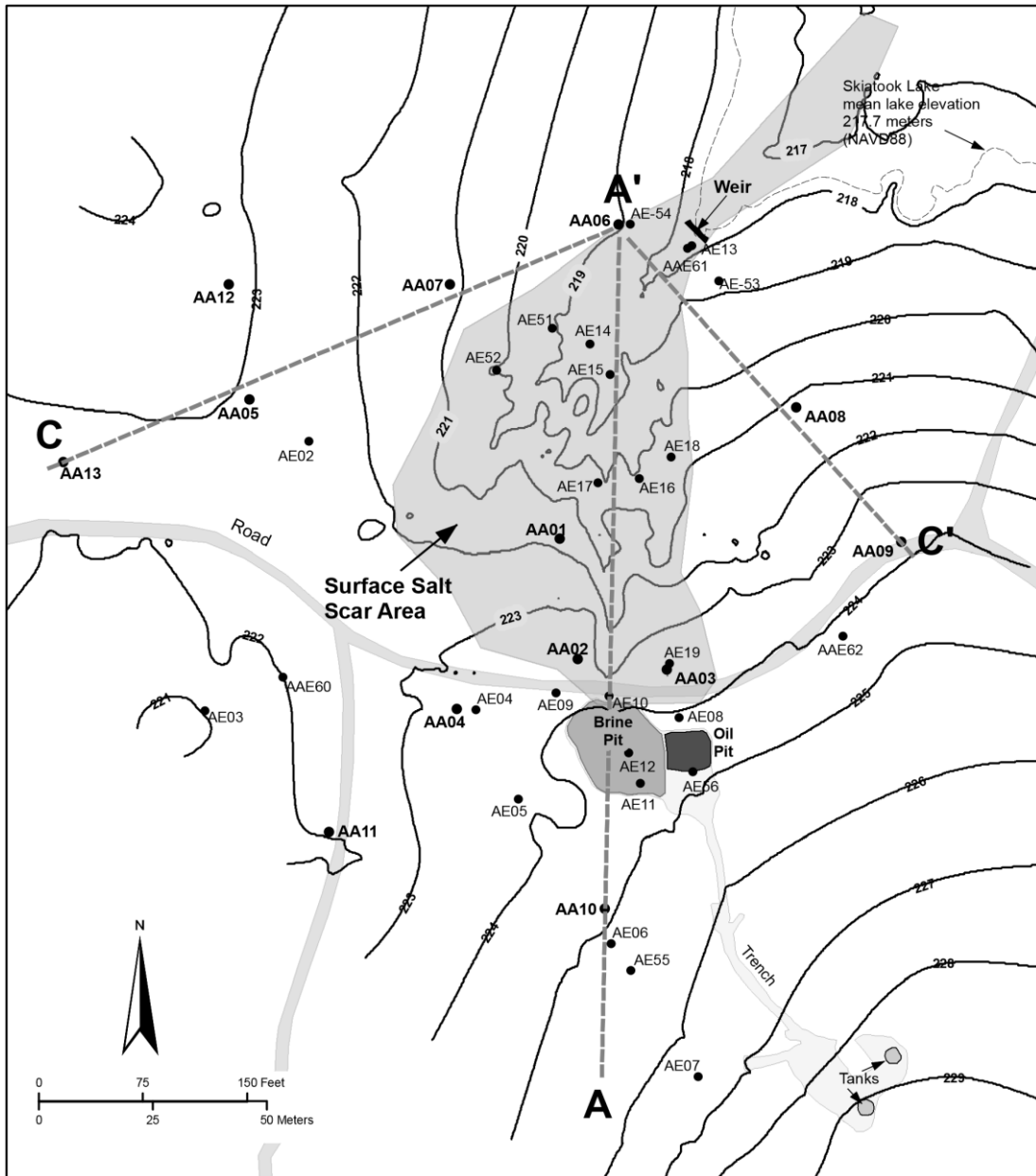


**Figure 65** - Topographic map of OSPER A site showing the location of the drilled auger wells (AA), Geoprobe (direct push) wells, oil and brine pits, redwood tanks (southeast corner), a weir close to Skiatook Lake, and other main features at this site. The transect C-A'-C' is also indicated (from Herkelrath et al., 2005).

Drilling at the Lester Lease started in 1912, and most of the over 100,000 bbl of oil produced was obtained prior to about 1937. Oil production, which was entirely from the Bartlesville sand at depths of 450 to 524 m, ended in 1973. Oil and produced water were collected in two redwood tanks at the top of the site and transported via a ditch to two roadside pits at mid-site (Figure 65). Remnants of decades-old, produced water and hydrocarbon spills (now highly degraded and weathered oil) are scattered around the site. One pit at this site contains relatively fresh asphaltic oil and high salinity brine (Godsy et al., 2003).

**Results and Discussion**

The concentrations of selected inorganic and organic chemicals from an oil well and surface and groundwater samples from OSPER A site and adjoining areas in Osage County, Oklahoma, are illustrated in Figure 66 and Figure 67 and listed in Table 47. As with OSPER B, the results show that produced water obtained from the oil well Lebow 8 (Figure 67) and seven other oil wells reported in Kharaka and others (2003) have similar chemical composition: The water is a hypersaline (115,000 to 185,000 mg/L) Na-Ca-Cl brine dominated by Na and Cl with relatively high concentrations of Ca, Mg, Sr, Ba, and NH<sub>4</sub> but very low values for SO<sub>4</sub>, HCO<sub>3</sub>, and H<sub>2</sub>S (Figure 67). With the exceptions of Fe and Mn, the concentrations of trace metals are low, and the values of organic acid anions and other dissolved organic species are relatively low.

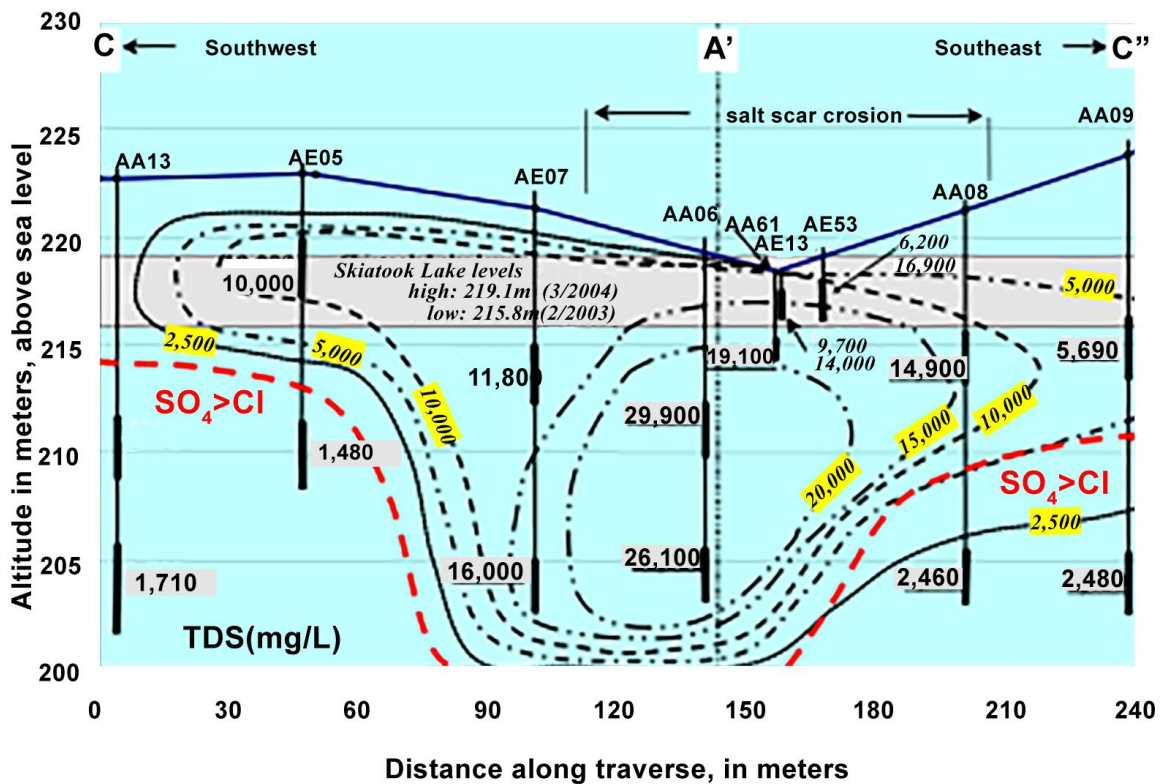


**Figure 66** - Showing salinity of groundwater at the OSPER A site along transect C-A-C' (Figure 65). The depth below which the concentrations of SO<sub>4</sub> are greater than Cl (red dotted line) and the high and low levels of the Skiatook Lake are indicated. The high salinity (30,000 mg/L) plume of contaminated groundwater is centered at the middle depth of well AA06 (from Kharaka et al., 2005).

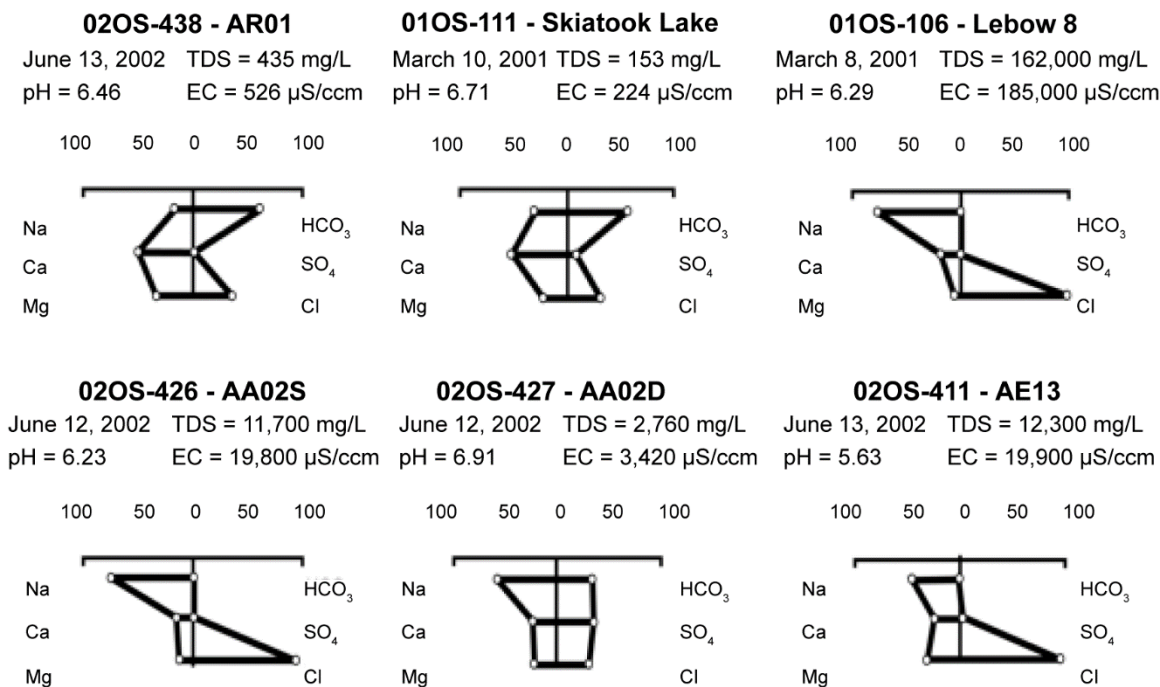


**Figure 67** - Modified Stiff diagrams showing the salinity of water and the relative concentrations (in equivalent units normalized to 100 percent) of major cations and anions in Skiatook Lake and produced water from selected oil and water wells at or near the OSPER A site (from Kharaka et al., 2005).

**Table 47** - Chemical composition (mg/L) of water samples from wells drilled at the OSPER A site. Dates are mm/dd/yy (from Kharaka et al., 2003).

Well Name	AA-01d	AA-02d	AA-02s	AA-03d	AA-03s	AA-04d	AA-04s	AE-04	AE-05	AE-06
Sample No.	02OS-430	02OS-427	02OS-42	02OS-429	02OS-428	02OS-425	02OS-424	02OS-434	02OS-332	2OS-435
Date	06/13/02	06/12/02	06/12/02	06/12/02	06/12/02	06/12/02	06/12/02	06/13/02	03/03/02	06/13/02
pH	6.5	6.9	6.2	6.7	6.6	7.0	5.7	-	-	-
T (°C)	16	18	19	16	19	-	-	22	-	23
Li	0.16	0.05	0.07	0.13	0.04	0.08	0.04	0.001	0.001	0.002
Na	2,180	525	3,400	3,250	1,110	1,150	1,670	60	11.8	4
K	27	6.8	16	25	3.2	28	5.3	1.0	0.03	0.8
Mg	2,520	102	272	166	41	234	63	0.4	0.03	1.1
Ca	3,460	176	564	419	98	567	202	2.1	0.18	5.9
Sr	8.6	2.9	8.4	5.2	3.4	4.9	7.7	0.07	0.004	0.26
Ba	0.3	0.1	0.6	1.2	1.9	1.3	6.3	0.026	0.003	0.25
Mn	5.1	0.49	1.7	14.5	2.2	4.3	12.5	0.013	0.001	0.23
Fe	< 10	3	< 5	6	6.5	< 2.5	< 2.5	0.1	0.07	0.2
Cl	16,100	436	7,020	5,630	1,860	3,410	3,240	76.7	3.3	2.2
Br	56	1.5	23	19.3	6.4	11.6	11.7	0.27	0.08	0.12
SO <sub>4</sub>	696	668	137	23.4	5.7	56.8	5.9	10.2	14.2	6.0
HCO <sub>3</sub>	445	824	255	894	301	279	54	ND	ND	ND
NO <sub>3</sub>	< 1	< 0.2	< 1	< 0.2	< 0.2	< 0.5	1.8	1.2	1.1	0.32
SiO <sub>2</sub>	< 43	24	< 21	< 21	19	18	29	11	10	16
B	-	0.4	-	-	0.1	-	-	0.04	0.023	0.033
TDS	25,500	2,760	11,700	10,500	3,450	5,760	5,310	180	50	62
DOC	99	113	2	203	53	2	4	-	-	-
Acetate	171	200	0.08	517	101	< 0.04	< 0.04	-	-	-
Formate	< 0.08	< 0.08	0.09	< 0.08	< 0.08	< 0.08	< 0.04	-	-	-
Propionate	< 0.2	< 0.2	< 0.2	0.7	3.3	< 0.1	< 0.05	-	-	-
Butyrate	< 0.2	< 0.2	< 0.2	0.5	< 0.2	< 0.1	< 0.05	-	-	-

The water sample obtained from the oil pit (AP01; (Table 47) has a salinity (110,000 mg/L) and chemical composition comparable to that of the produced water from nearby oil wells (e.g., Lebow 8; (Table 47). The salinity of water obtained from the boreholes in the adjacent pit, which has more weathered and degraded oil (Godsy et al., 2003), and from those boreholes located close to the two pits, all have fresh water ( $\leq 1,000$  mg/L) indicating that the brine in the oil pit is of limited volume and extent. In addition, all the shallow ( $< 2$  m;  $< 6.6$  ft) direct-push wells located to the south and west of the two oil pits have fresh water with compositions that indicate no mixing with produced water (Kharaka et al., 2003, 2007). It is possible that produced water was present in these shallow wells because they are located downgradient from the brine source in the redwood tanks (Figure 65). If so, then the brine was subsequently flushed and replaced with meteoric water from precipitation events. Results from soil analysis (Zielinski et al., 2003) and geophysical surveys (Smith et al., 2003) are in general agreement with this interpretation.

Except for well AA-13, the salinity and chemical composition of water obtained from the auger wells—designated AA—and from those direct-push wells—designated AE—located to the north and west of the two oil pits in the salt-scarred area at the A site (Figure 65, Figure 66, and Figure 68) show major impact from produced-water operations. A three-dimensional (3-D) plume of high-salinity water (2,000 to 30,000 mg/L) dominated by Na and Cl intersects Skiatook Lake near well AE-13 that has water salinity of about 10,000 mg/L. This plume is not limited to the salt-scarred area ( $\sim 0.5$  ha;  $\sim 1.2$  ac) and the visibly impacted area of this site ( $\sim 1.2$  ha;  $\sim 2.9$  ac); it extends beneath a total area of about 3 ha (7.4 ac). The trees, shrubs, and grass in the outlying areas show no visible impacts from oil operations (Figure 68).

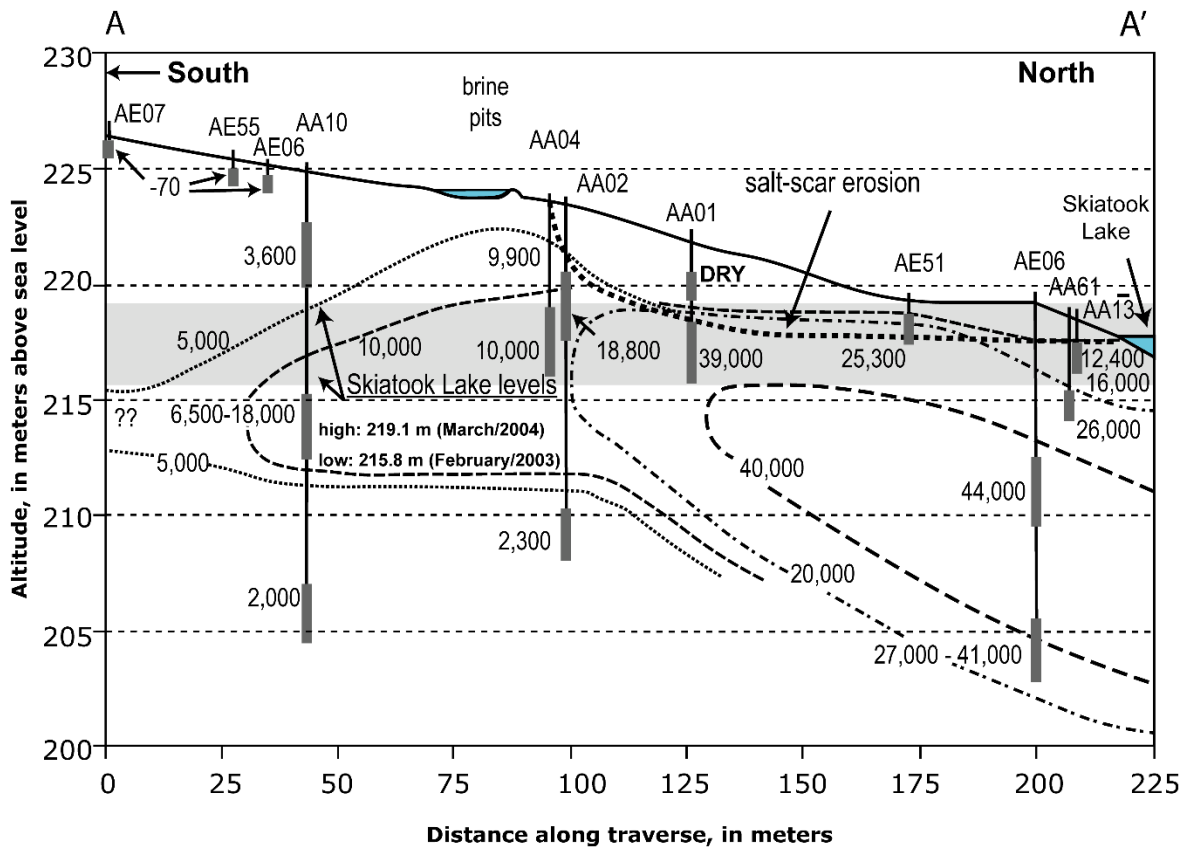


**Figure 68** - Water levels and salinity of water (from January 2004) in wells along a south-north transect A-A' (Figure 65), from well AE-07 north to AE-13, located in the littoral zone of Skiatook Lake at the OSPER A site. A plume of high-salinity water is present at intermediate depths, especially in wells located below the brine pits. The highest and lowest water levels of Skiatook Lake are shown and indicated by shading (from Kharaka et al., 2003).

Water levels in Skiatook Lake and water salinity (from January 2004) in wells along a south-north transect A-A' (Figure 65), from well AE-07 north to AE-13 (located in the littoral zone of Skiatook Lake at this site) show a plume of high-salinity water is present at intermediate depths, especially in wells located below the brine pits. The highest water salinity in the plume, ~30,000 mg/L, is found at the intermediate depth of well AA-06 (Figure 66, Figure 68), also located close to Skiatook Lake. The plume extension underneath Skiatook Lake to the north of well AA-06 (Figure 68) is presently unknown because we have no wells drilled there, but data from existing wells show water salinity decreasing in all directions from this well. No liquid petroleum was found in the contaminated groundwater. However, soluble petroleum by-products—including organic acid anions, BTEX, and other VOCs—are present (Table 47).

The salinity decrease is more rapid to the east of well AA-06 (Figure 67), which is consistent with our conceptual model of water moving at higher rates westward along the dip ( $1^{\circ}$  to  $2^{\circ}$  west) of the sandstone aquifers. The shape of the plume indicates recharge from the brine pit located at mid site (Figure 67 and Figure 68), which is also consistent with local topography and production practices at this site, where large volumes of saline

water and oil, collected in redwood tanks at the south end of the site (near AE-07, Figure 66), were allowed to flow in a ditch to two oil and brine pits located at mid site.

During peak oil production (from 1913 to 1937), most of the produced water likely flowed downgradient in a creek channel into the northern eroded part of the site and then flowed beyond the site because the Skiatook reservoir was not completed until 1987. Because of its higher density, a large portion of this produced water infiltrated through the bottom of pits and channels into the underlying sandstone beds. Dissolution, precipitation reactions, and especially mixing with precipitation water, groundwater, and/or recently with Skiatook Lake water, resulted in modifying brine composition (Figure 68), including lowering brine salinity from about 150,000 mg/L TDS to that of water residing in the sandstone beds (up to 30,000 mg/L).

The boundaries of the plume were delineated during deep drilling completed in January 2004. The chemical compositions of water samples obtained from the two perforated zones of well AA-13 (Figure 66), as well as a sample collected from a depth of 6.4 m while drilling the well, indicated the groundwater is not impacted by produced water, thus delineating the western limit of the plume. The bottom of the plume, although problematic, is tentatively defined by the 1,200 mg/L salinity contour obtained from several wells. The difficulty of defining the lower boundary of the plume can be appreciated by examining the chemical data for water from the deeper perforated section (13.8 to 15.2 m below ground level) of well AA-02. The salinity and concentrations of major cations and anions of water for this section (AA-02D, Table 47; Figure 68) indicate groundwater that is not contaminated by a NaCl-rich produced water source. However, the concentrations of DOC, acetate, and other VOCs, as well as Fe and Mn (Table 47), indicate reducing conditions and contamination by degradation products from an oil source.

Defining the impacts of produced water and associated hydrocarbons on the shallowest beds—which may be unsaturated or may be unconfined, confined, or contain perched water—is also difficult. In wells located to the north of the brine and oil pits, contamination by produced water is shown by high salinity and high concentrations of Na and Cl relative to other cations and anions (Figure 68). In shallow (< 2 m; < 6.6 ft) wells located to the south of the brine pit, the shallowest sandstone is generally dry but has a perched water zone following precipitation; water salinity is very low (~70 mg/L) and dominated by Na and Cl, with Na likely residual from produced water.

Contamination by oil and its degradation products is more obvious in a background well drilled 0.6 km (0.4 mi) downdip to the northwest of the OSPER A site. Initially (March, 2002), groundwater in this well was fresh (salinity 450 mg/L) with low DOC values and other characteristics of the pristine local groundwater (AR-01, Table 47). Repeated sampling did not change the inorganic composition of water from this well appreciably, but DOC concentrations continued to increase. A sample collected in June 2003 from this

well showed no significant change in the inorganic composition of water, but small oil globules and relatively high concentrations of DOC and BTEX were observed. The source of this petroleum contamination was initially not clear because no plugged oil well was mapped close to this site. However, additional searching led to discovery of some concrete and other trace remains of an old abandoned oil well located about 10 m southeast of the groundwater well.

The hydrology and subsurface transport of brine at OSPER A site (which was abandoned in 1973) was investigated by Herkelrath and others (2007). Based on detailed geological (Otton et al., 2007) and hydrochemical (Kharaka et al., 2005) data from 41 boreholes that were cored and completed with monitoring wells, a large (~200 m × 200 m × 20 m) plume of saline groundwater was mapped that extends in the subsurface far beyond the area of a surface salt scar at this site. As discussed, the main dissolved species in the plume are Na and Cl, with salinity ranging as high as 30,000 mg/L.

Continuous monitoring revealed that water levels in the wells respond rapidly to changes in barometric pressure. A multiple-regression deconvolution analysis was used to filter out barometric effects. The barometric response function indicates the wells are completed in confined aquifers; slug tests run on the wells are consistent with a confined aquifer model. Hydraulic conductivity was low, ranging from 0.3 to 7.0 cm/d. Water level-versus-time data indicate no significant change in water level in response to rainfall events, suggesting recharge is limited. On the other hand, water levels moved up and down in an annual cycle, suggesting some long-term recharge. Only one well, which is quite close to Skiatook Lake, responded to lake level changes.

To explore, compare, and illustrate conceptual models of the site, the finite-difference model STOMP (White & Oostrom, 2000) was used to simulate the evolution of a subsurface salt plume. A simple two-dimensional model did a reasonable job of simulating the salinity distribution measured in 2005 (Kharaka et al., 2005). Modeling results support the hypothesis that although recharge and hydraulic conductivity are low, production at this site occurred for a long enough time (approximately sixty years) for a sufficient volume of brine to leak from pits to fill the pore space beneath the pits and create the plume. According to the model, after the site was abandoned, spreading and natural attenuation of the brine plume caused by mixing with fresh groundwater recharge was limited. The model suggests that—partly because of the filling of Skiatook Lake in 1987—the plume has largely stagnated.

Results indicate that under present conditions the brine plume will exist for 100 or more years, with continued deleterious environmental impact at groundwater discharge points. Because hydraulic conductivity is low, remediation by flushing or fluid injection is probably impractical at this site. Conditions at this site are likely to be typical of oil production sites in Oklahoma where underlying rocks are relatively impermeable.

The rate of salt removal from this site by surface runoff was determined by measuring the volume and chemical composition of water flowing over a weir installed close to the Skiatook reservoir in a location that captures most of the surface and base flow from this site following precipitation (Figure 65). The weir and an automated precipitation gauge were installed close to Skiatook Lake to investigate the natural overland transport of salts from this site by measuring the volume and chemical composition of surface runoff from precipitation events draining a 1.7 ha (4.2 ac) area. Results show that the initial runoff that leaches the previously precipitated surficial salts can have a relatively high salinity (up to 3,000 mg/L), but that only small amounts of total salts (500 to 1,000 kg/year) are removed by this process (Kharaka et al., 2005). This too indicates that natural attenuation at this site will be very slow.

### 10.3 Case Study 3: Potential Effects of Cation Exchange on the Composition and Mobility of Produced Water

The first geological materials impacted by oil field wastes released into near-surface environments are often clay and silt beds. Clay minerals within these siliciclastic sediments have the potential to both alter the composition of produced water and influence the relative mobility of environmentally sensitive components such as dissolved barium and radium through cation exchange. Interpretation of soil data generated during the investigation of a site contaminated by produced water in southern Louisiana, USA, provides an example of these processes.

#### 10.3.1 Site History

The study site is located within the Napoleonville oil and gas field located on the eastern flank of the Napoleonville salt dome in southeastern Louisiana, USA. The site surface facilities are situated within fine-grained natural levee deposits of a former distributary of the Mississippi River. The Napoleonville Field first produced crude oil and natural gas in 1958.

Produced water from a well in that field was encountered that same year and originally stored in an unlined evaporation pond excavated to a depth of approximately 4 m. A wastewater injection well was installed in 1962 but produced water continued to be stored in the pond prior to injection. A closed produced-water handling system was eventually installed near the pond in 1970 and used to store produced water in tanks prior to injection. Pre-1970 leakage of saline waste from the storage pond and soil contamination at other sites within the field resulted in litigation that began in 1998. A variety of field studies and sampling programs were performed by environmental and engineering consulting firms in support of both plaintiffs and site operators in this litigation.

Despite the obvious spatial association of contaminated sediments with the principal produced water storage site indicated as "Pit" on Figure 69, a consultant for the

site operators proposed that the saline contamination was actually due to the natural presence of “an old, buried swamp” (Hanor, 2007, p.195). Although an extensive study was made of soil properties at the site by this consultant, no chemical analyses were made of the groundwater. In addition, no analyses of produced water were available from the well in question. The question thus arose: Was it possible to determine the probable source of contamination from soil analyses alone?

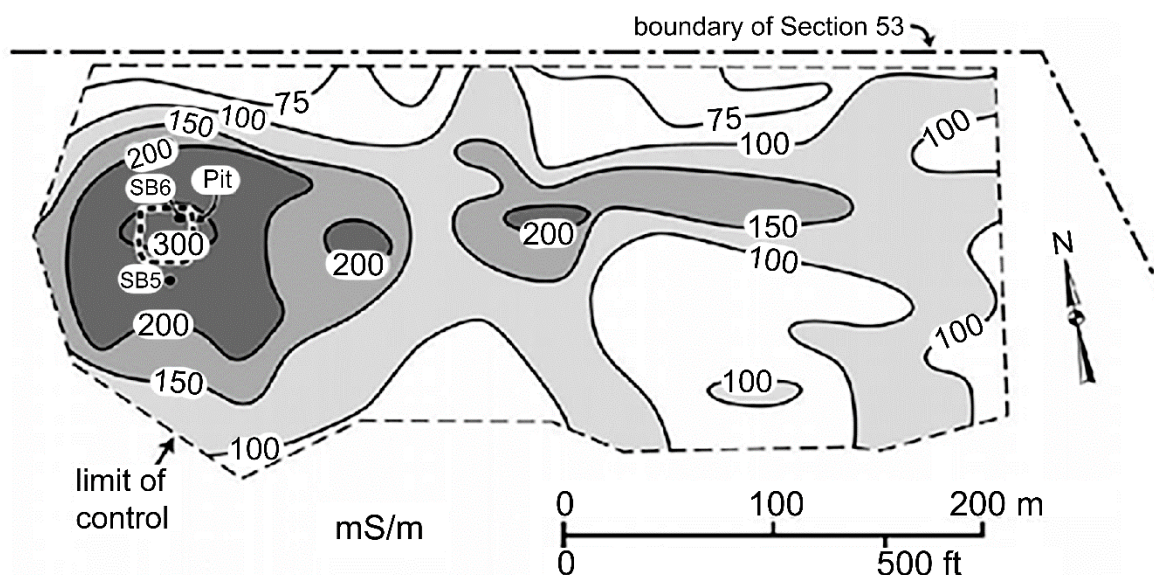


**Figure 69** - Map showing locations of a former produced water storage pit and two soil borings (SB-5 and 6). Contours are of sediment electrical conductivity in mS/m, measured by a Geonics EM31 conductivity meter in the vertical mode, which had a reported depth of penetration of approximately 6 m (from Hanor, 2007).

### 10.3.2 Field Techniques

An electromagnetic (EM) survey (Figure 69) was made at the site in 1998 by litigant consultants forty years after produced water was first encountered. The reported depth of penetration of the survey was approximately 6 m. The electromagnetic survey revealed the presence of electrically conductive, brine-contaminated sediments centered around the former site of the brine storage pit. A plume of brine-contaminated groundwater extended several hundred meters to the east of the pit area.

### 10.3.3 Soil Data

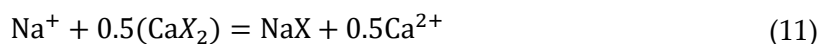
Two soil borings having total depths of approximately 8 and 6 m were made at the site of the produced water storage pond (Figure 69) by site operator consultants. No groundwater samples were taken or analyzed. However, soil analyses of samples from these borings by the operator consultants included the exchangeable cations Na, K, Mg, and Ca per unit weight of dry sediment; sediment exchange capacity; water soluble anions chloride, sulfate, and bicarbonate per unit weight of bulk sediment; and total soil moisture. From these data, Hanor (2007) calculated the aqueous concentrations of each of the reported anions and the concentration of total dissolved anionic charge on the assumption that

adsorption of anions was negligible. Chloride contributed over 90 percent of the total anionic charge for the great majority of samples. Pore-water salinity, calculated as NaCl, ranged from less than 1,200 mg/L in near surface sediments (presumably by dilution with fresh groundwater) to over 53,000 mg/L at depth.

#### 10.3.4 Multicomponent Cation Exchange

Produced water generally contains Na, Ca, Mg, K, and Sr in decreasing order of relative abundance as the principal dissolved cationic components (Kharaka & Hanor, 2014). Cation exchange between produced water and sediment involves a complex multicomponent system. Several conventions have been developed to quantify multicomponent exchange involving cations of mixed charge (Appelo, 1996; Appelo & Postma, 1993). Calculating thermodynamic activities of dissolved solutes is now a fairly straightforward matter, even in very saline water (Kharaka & Hanor, 2014). However, different conventions have been used in calculating the thermodynamic standard state and activities of adsorbed species (Appelo & Postma, 1993; Drever, 1997). The approach followed here uses the Gaines-Thomas convention where it is assumed that the activity of an adsorbed cation is proportional to the *equivalent fraction* of the adsorbed cation (Appelo & Postma, 1993, pages 156–159) The Gaines-Thomas convention is the default approach used in the equilibrium modeling programs PHREEQM (Appelo & Postma, 1993) and PHREEQC (Parkhurst & Appelo, 1999).

Following the development by Appelo and Postma (1993), but using a slightly different notation, let the equivalent fraction—i.e., the fraction in units of equivalents,  $\beta(CX_i)$ —of exchangeable cation  $C^{i+}$  of charge  $i+$  adsorbed on exchange site(s)  $X_i$  on a sediment, be defined as  $\beta(CX_i) = [(meq\ CX_i\ per\ 100\ g\ sediment)/CEC]$ , where  $CEC$  is the total cation exchange capacity of the sediment (in units of meq/100 g of sediment) and  $CX_i$  represents the adsorbed cation  $C$  on exchange site(s)  $X_i$ . As noted earlier in this book, in the Gaines-Thomas convention, it is assumed that the thermodynamic activity of an adsorbed cation,  $\alpha(CX_i)$ , is proportional to the equivalent fraction of the adsorbed cation,  $\beta(CX_i)$ . This leads to the following stoichiometries for the exchange reactions between Na and K and between Na and Ca as shown in Equation (10) and Equation (11), respectively.



The exchange coefficients are defined by the reactions shown in Equation (12) and Equation (13), respectively.

$$K_{Na-K} = \frac{(\beta(NaX))(\alpha(K^+))}{(\beta(KX))(\alpha(Na^+))} \quad (12)$$

$$K_{\text{Na-Ca}} = \frac{\left(\beta(\text{NaX})(\alpha(\text{Ca}^{2+}))^{0.5}\right)}{\left(\beta(\text{CaX}_2)(\alpha(\text{Na}^+))\right)} \quad (13)$$

where:

$$\alpha = \text{activity}$$

In a multicomponent exchange system, the equivalent fractions and cation exchange reactions involving Na, K, Mg and Ca are coupled together in the reaction shown in Equation (14).

$$\beta(\text{NaX}) + \beta(\text{KX}) + \beta(\text{MgX}_2) + \beta(\text{CaX}_2) = 1 \quad (14)$$

Molalities ( $m$ ) of the dissolved cations are related to activity ( $\alpha$ ) through the stoichiometric activity coefficients,  $x_{tot}$ , which for aqueous Na is defined by the reaction shown in Equation (15).

$$\alpha(\text{Na}^+) = (x_{tot}(\text{Na}^+)) (m(\text{Na}_{tot})) \quad (15)$$

where:

$$\begin{aligned} \alpha(\text{Na}^+) &= \text{stoichiometric activity coefficient for Na} \\ x_{tot}(\text{Na}^+) &= \text{stoichiometric activity coefficient} \\ m(\text{Na}_{tot}) &= \text{sum of the molality of each Na species in solution} \end{aligned}$$

As shown by Appelo and Postma (1993, p. 61), if the activities of the exchangeable cations in free solution are known, the composition of the exchangeable cations can be calculated by rewriting the exchange coefficient equations, for example Equation (12) and Equation (13) in terms of  $\beta(\text{NaX})$  as the unknown variable, substituting these into Equation (14), and solving the resulting quadratic equation for  $\beta(\text{NaX})$ . Once  $\beta(\text{NaX})$  is known, the equivalent fractions of the other cations are calculated by back substitution in the exchange coefficient equations. Although not discussed by Appelo and Postma, the calculation scheme presented above can be inverted and the composition of an aqueous phase in exchange equilibrium with a sediment can be calculated if the equivalent fractions of the exchangeable cations are known. In this case, the charge balance equation is used instead of Equation (14) to tie all of the exchange reactions together as shown in Equation (16).

$$m\text{Na}^+ + m\text{K}^+ + 2m\text{Ca}^{2+} + 2m\text{Mg}^{2+} = A \quad (16)$$

where:

$$A = \text{the total concentration of anionic charge in solution in units of meq/kg H}_2\text{O}$$

This time, the exchange coefficient equations are rewritten with  $\alpha(\text{Na}^+)$  as the unknown variable and substituted in Equation (16). An approximate conversion between aqueous activities and modalities was made using stoichiometric activity coefficients at

25 °C calculated for typical produced water compositions as a function of  $\text{Cl}^-$  concentration by Morse and others (1997) using the Pitzer approach. The resulting quadratic equation is solved for  $\alpha(\text{Na}^+)$  and the activities of the other cations are calculated by back substitution. The following values of the Gaines-Thomas exchange coefficients were used in the calculations of interstitial water chemistry done as part of the Napoleonville study (Hanor, 2007): Na–K (0.20), Na–Mg (0.50), Na–Ca (0.40), and Na–Ba (0.35) (Appelo & Postman, 1993, Table 5.5).

Because calculated values for sediment porosity were available, it was also possible to calculate the total mass of each cation in the adsorbed phase and in the interstitial aqueous phase per unit mass of water-saturated bulk sediment. This information was then used to calculate the fraction of the total adsorbed and dissolved cation that was present as an adsorbed cation for each sediment sample. In the case of estimating the partitioning of Ba, where chemical analyses were not available, an arbitrary concentration of 100 mg/L was assigned to  $\text{Ba}^{2+}$  and a value for the equivalent fraction of adsorbed Ba,  $\beta(\text{BaX}_2)$ , was calculated by the techniques described in this section.

### 10.3.5 Calculated Pore Water Compositions

Sodium is the dominant cation by an order of magnitude in all but one of the calculated pore water compositions; K was more abundant in that sample (Figure 70). Calcium and K are generally the next two most abundant cations; Ca was consistently the second most abundant cation in the higher salinity water.

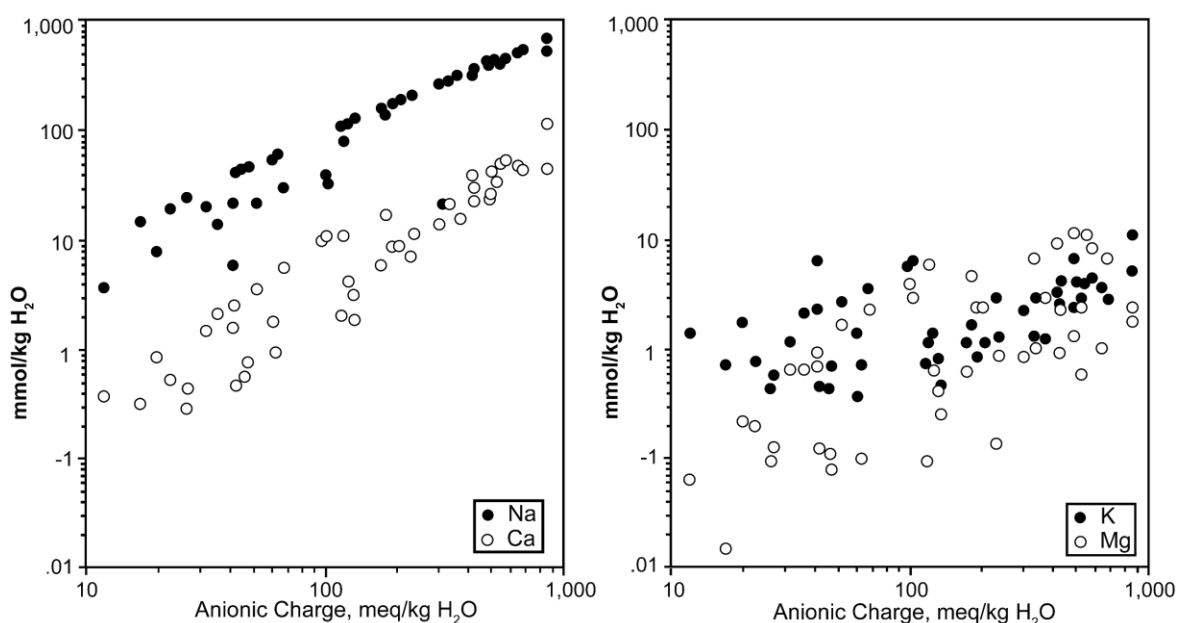


**Figure 70** - Fluid compositions calculated from the composition of adsorbed cations assuming exchange equilibrium. Sodium is the most abundant cation in the fluids, followed by calcium for most of the samples (from Hanor, 2007).

### 10.3.6 Composition of Adsorbed Cations as a Function of Anionic Charge and Salinity

In the lowest salinity water at the site, where total dissolved anionic charge  $A^-$  is less than 20 meq/kg  $H_2O$  (salinity  $< \approx 1,200$  mg/L), Ca is the dominant adsorbed cation followed by Mg and then K (Figure 71). There is a transition in the composition of adsorbed cations over the interval of total anionic charge of 20 meq to 100 meq/kg  $H_2O$  (salinity = 5,800 mg/L) in which Na replaces Ca as the dominant adsorbed cation. Between 100 and 900 meq of anionic charge per/kg  $H_2O$  (salinity approximately 53,000 mg/L), there is no further systematic increase in adsorbed Na nor a decrease in adsorbed Ca. The fraction of adsorbed Na in equivalents (i.e., equivalent fraction) varies between approximately 0.60 and 0.75, and the equivalent fraction of adsorbed Ca varies between 0.2 and 0.35.

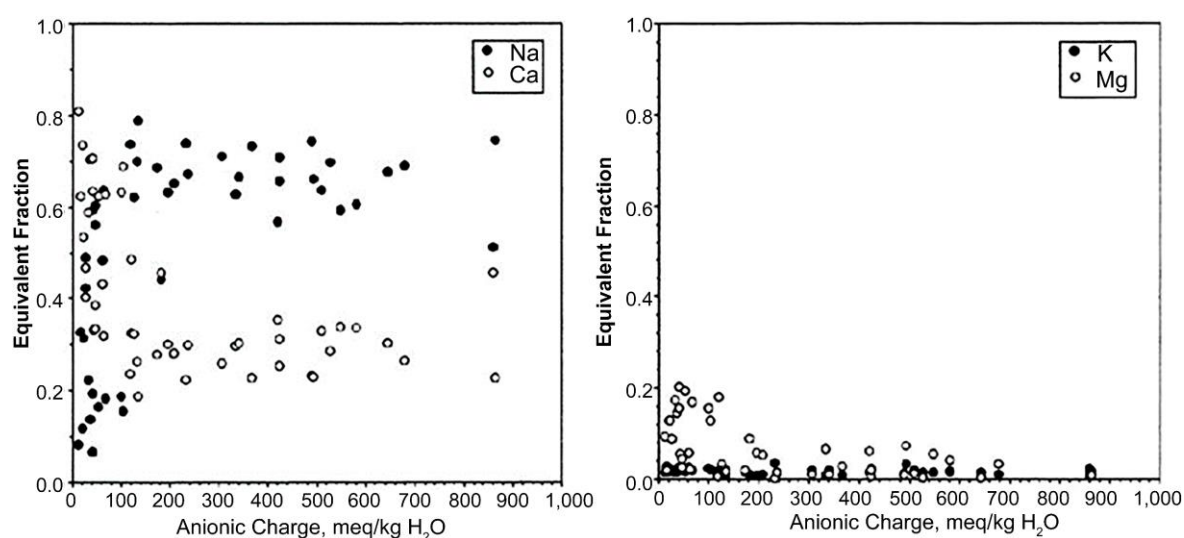


**Figure 71** - Fraction of adsorbed cations in equivalents versus anionic charge in aqueous solution. Note that adsorbed Mg and K are present in much lower abundances than Na and Ca (from Hanor, 2007).

There is also scatter in the equivalent fraction of Mg. The equivalent fraction of adsorbed Mg decreases from approximately 0.20 for  $A^- < 100$  meq/kg  $H_2O$  to less than 0.01 as anionic charge increases. The equivalent fraction of K fluctuates between 0.01 and 0.04, with no clear trend with increases in anionic charge.

The calculated fraction of Na, Ca, and Ba present as adsorbed cations decreases with increasing anionic charge and salinity (Figure 72). At values of  $A^- < 100$  meq/kg  $H_2O$  (salinity  $< 5800$  mg/L), the fraction of Ba adsorbed exceeds 0.95. The fraction of Ba adsorbed then systematically decreases (Figure 72) with increasing anionic charge to values that range between approximately 0.55 and 0.86 at values of anionic charge approaching 900 meq/  $H_2O$ , corresponding to a salinity of approximately 53,000 mg/L. Hence, barium is preferentially partitioned into the more mobile aqueous phase under more saline conditions.

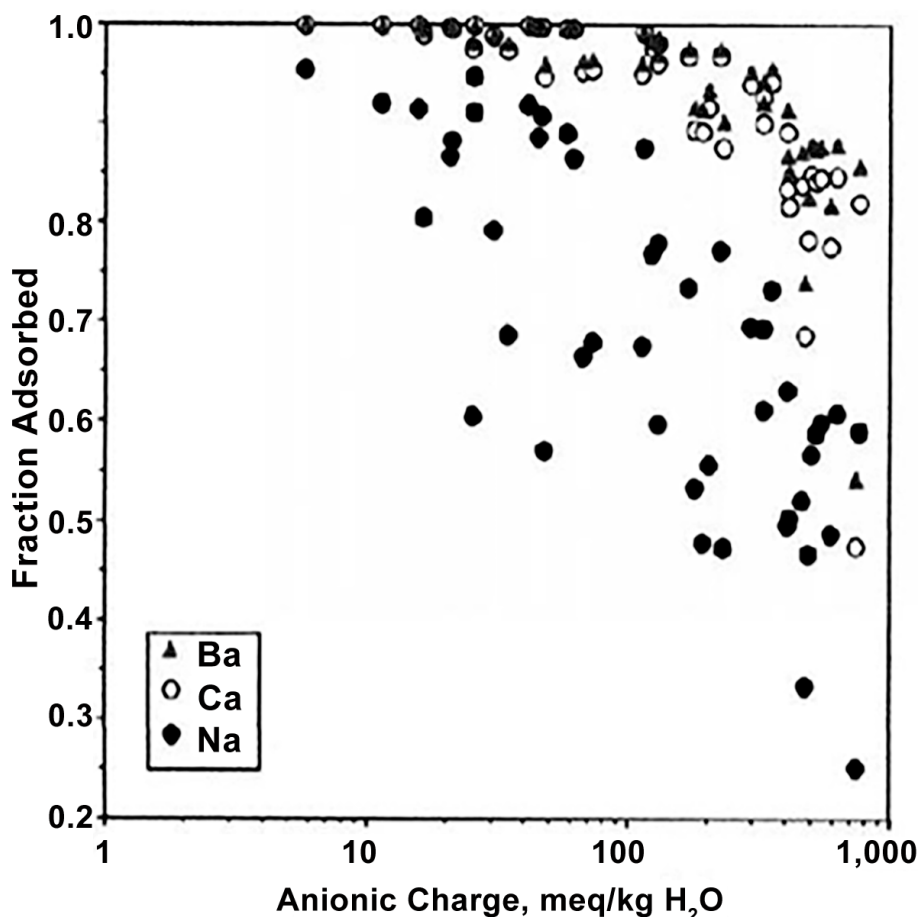


**Figure 72** - Calculated partitioning of Ba, Ca, and Na as a function of aqueous anionic charge. Partitioning is represented by the fraction adsorbed of the total adsorbed plus the dissolved cation per unit volume of sediment. The fraction of Ba adsorbed (triangles) systematically decreases with increasing anionic charge to values that range between approximately 0.55 and 0.86 at values of anionic charge approaching 900 meq/kg H<sub>2</sub>O (salinity = 53,000 mg/L). The dissolved anionic charge is presented on a logarithmic scale (from Hanor, 2007).

### 10.3.7 Discussion

The general relation between the composition of adsorbed cations and salinity in the contaminated samples from the Napoleonville oil and gas production facility are consistent with previous studies of multicomponent exchange in natural groundwater systems of varying salinity (e.g., Appelo, 1994, 1996; Appelo & Postma, 1993). These studies have shown that divalent cations Ca and Mg dominate as adsorbed cations at low salinity and thus low total dissolved cation concentrations, but Na is the dominant adsorbed cation at moderate to high salinity. The exchange is a non-linear function of salinity, and the transition from Ca-dominated adsorption to Na-dominated adsorption occurs over a fairly narrow range of salinity.

There are no reported analyses of produced water from the particular well in question. There are, however, analyses of produced water from wells elsewhere in the Napoleonville Field (Blondes et al., 2019) that report concentrations of Na > Ca > Mg.

Concentrations of K are not listed for these wells. The calculated interstitial water compositions at the Napoleonville contaminated site are thus consistent with the original source of produced water typical of the Louisiana Gulf Coast (Hanor & McIntosh, 2007; Kharaka & Hanor, 2014) where Na is the dominant dissolved cation followed by  $Ca > Mg$ , rather than being some other type of saline contamination such as a pure NaCl brine, marine water where  $Mg > Ca$ , or  $CaCl_2$  drilling fluids.

The spatial variations in sediment electrical conductivity at the site (Figure 70) are consistent with the former produced water storage pit having been a source of saline water contamination. The maximum pore water salinity in the samples from the two boreholes is approximately 53,000 mg/L. This value is less than the 100,000 to 150,000 mg/L range typical of most produced water in south Louisiana (Hanor, 1997) and the salinity values for Napoleonville produced water reported by Blondes and others (2019). This may reflect dilution of produced water by meteoric water.

The calculated fractionation for Ba indicates that in low to moderate salinity samples, Ba—and, by extension, Ra—are near completely adsorbed on the clays and would thus be of low mobility in an advective groundwater system of low salinity. However, Ba and Ra are likely to remain mobile when the anionic charge is greater than approximately 100 meq/kg  $H_2O$ . Most produced water is sufficiently saline (Fisher, 1998) that this threshold of anionic charge is exceeded; hence Ba and Ra would not be preferentially adsorbed.

The fate of Ba and Ra is also influenced by the presence of sulfate, which can cause the precipitation of radioactive barite,  $(Ba, Ra) SO_4$  (Hanor, 2000). The next logical step in the study of cation adsorption at this site is to utilize the information and concepts generated in this section to investigate the chromatographic separation of cations both during the infiltration and migration of produced water into the sediments at the site and the possible subsequent dilution of produced water contaminants by mixing with meteoric water. In such a study, it will be necessary to consider vertical and lateral variations in sediment lithology. It would be of interest to determine how far wastes would have to travel through such sediments for significant removal of dissolved Na to occur, and if remediation by natural attenuation by meteoric water is feasible at this site.

At the beginning of this study the following question was asked: Was it possible to determine the probable source of contamination from soil analyses alone? Yes, there was sufficient information in the bulk soil analyses to establish that the source of contamination was produced water, not natural marine waters.

## 10.4 Case Study 4: Limitations on the Use of Water Levels to Infer Directions of Fluid Flow in Variable-Density Groundwater Systems—a Field Example

Produced saline water and other possible oil field fluids permeated over  $2.2 \times 10^6 \text{ m}^3$  of shallow sediments near a former oil and gas well near the town of Fordoche in Pointe Coupee Parish, south Louisiana, USA, (Hanor, 1997). Saline water radiated out laterally in all directions from an area of former brine storage pits at distances of 150 to 900 m over a forty-five-year period. Contamination in the late 1990s extended at least 14 m below land surface into shallow sediments with fresh groundwater. This site provides an instructive example of the limitations of conventional groundwater monitoring and sampling techniques and the non-applicability of the concept of hydraulic head in characterizing sediments permeated by variable-density, single-phase mixes of produced saline water and native fresh groundwater. The following discussion is modified from Hanor (1997).

### 10.4.1 Site Location and History

The study site is located in and around a group of three former produced water storage pits located within the Fordoche Field in Pointe Coupee Parish, southern Louisiana, USA. At some time after wells in this field began producing salt water in the late 1940s, an oil well in the field was recompleted for disposal of produced water. Three pits were excavated to depths of approximately 1.2 m below ground surface in the vicinity of this well and used to store produced water prior to subsurface injection. The development of dead vegetation in the vicinity of the pits lead to pit closure in 1984–85. Closure procedures included capping the pits with fly ash.

Geotechnical characterization of the site began in 1986 by an engineering consulting firm hired by the field operators. Data on site geology, hydrology, and water quality were collected by these and other consultants intermittently between 1986 and 1989 and again between 1990 to 1995. A French drain was emplaced in the late 1990s along the southern margin of the former pits with the intent of intercepting and removing contaminated groundwater.

### 10.4.2 Site Geology

The site is located within the alluvial flood plain of the present Mississippi River. Sediments to a depth of 30 m consist of three clayey-silt and silty-sand beds, designated by the operator consultants as *permeable zones* separated by beds of clay-dominated sediments (Figure 73).

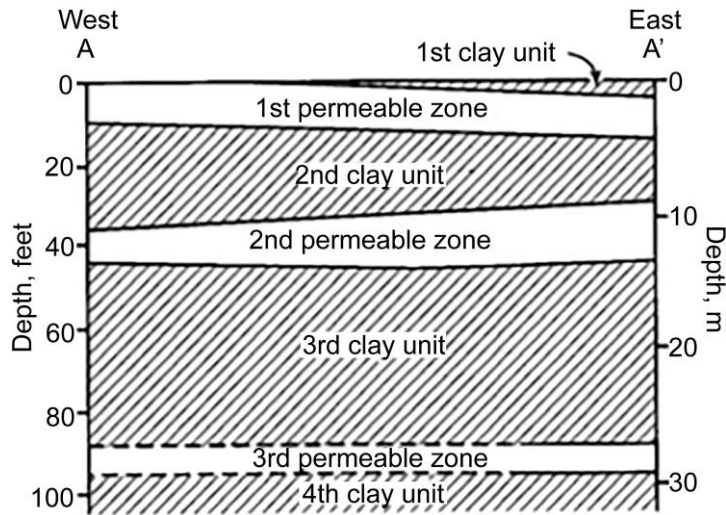


**Figure 73** - Generalized cross-section of the Fordoche site from soil boring logs (from Hanor, 2007).

### 10.4.3 Extent of Saline Contamination near Pits

Salinity of contaminated groundwater collected from wells screened in the first permeable zone in the immediate vicinity of the pits varied from less than 20,000 to over 50,000 mg/L in August 1986 when the first samples were collected (Figure 74). Groundwater salinity increased systematically from west to east. Salinity of water samples collected from the second permeable zone varied from 1,000 mg/L to over 10,000 mg/L and increased from south to northwest. By June 1992, during the last synoptic or comprehensive sampling prior to 1995, salinity of groundwater collected from the first permeable zone had decreased very slightly, while salinity of groundwater in the second permeable zone had increased.

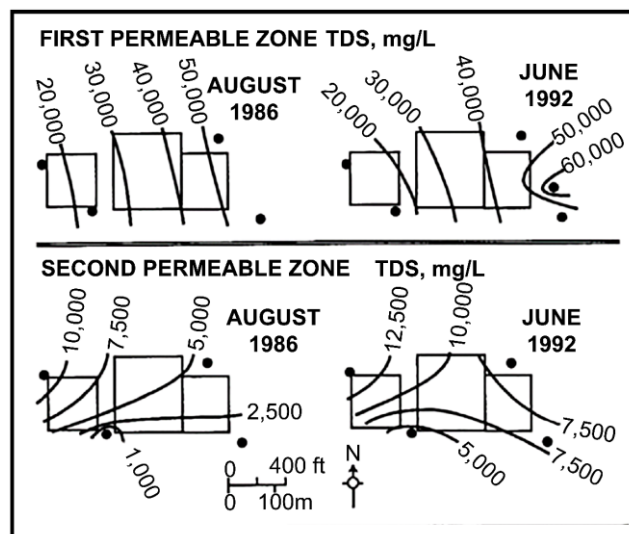


**Figure 74** - Areal variation in groundwater salinity in permeable units 1 and 2 in vicinity of three former evaporation pits (rectangles). Black dots represent the location of boreholes used in groundwater sampling (from Hanor, 1997).

#### 10.4.4 Total Lateral Extent of Saline Contamination

In the first permeable zone, the approximate lateral extent of contamination away from the immediate area of the brine pits was delineated by site consultants from geophysical terrain conductivity surveys and chemical analyses of ground water collected at or near the water table in shallow boreholes. Two geophysical terrain conductivity surveys were made using a Geonics EM-31 TC meter in a vertical dipole mode that, according to the site consultants, recorded the average weighted conductivity from the land surface to a depth of approximately 6 m. This depth interval thus includes the base of the first permeable zone, which has an average depth of 3.9 m in the pit area. Ground-truth verification of the geophysical results was done between 1992 and 1993 by collecting and analyzing groundwater samples using a hand auger drilled to the top of the water table, which was approximately 1.2 m below land surface.

Figure 75 shows the results of the terrain conductivity surveys as derived from maps in the consultant reports. High conductivity values reflect the presence of saline contaminants within a vertical interval from the ground surface to a depth of 6.1 m. The lateral limit of contamination was taken by the consultants to be the 100 mmho/m contour (where mmho/m is milli mho/meter; mho is the inverse of an ohm and was the usual unit of conductance at the time, now replaced by siemens). This contour is a boundary that defines areas where conductivity readings were above that of the background. There are many areas of the site, particularly in the west in the 1986 survey and in the south in the 1992 survey, where saline contamination extended up to and presumably beyond the boundaries of the terrain conductivity surveys.

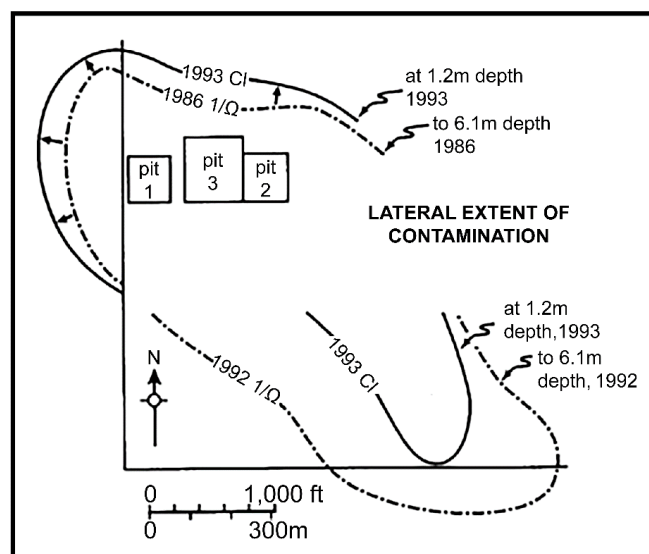


**Figure 75** - Map showing the lateral extent of saline water contamination at various times and depths below ground surface at the Fordoche site as determined by chloride analyses (solid lines) and terrain conductivity measurements (dot-dash lines). The areas marked pits 1 to 3 show the location of evaporation ponds used to store produced water wastes (from Hanor, 1997).

A consultant map showing the spatial variation in dissolved chloride in shallow groundwater samples collected at the water table in 1992 and 1993 was used by the consultant to determine the lateral extent of contamination near the top of the first permeable zone (Figure 75). Shallow groundwater outside of the area of impact typically have dissolved chloride values of less than 20 mg/L. The areal limit of the extent of near-surface contamination is taken to be their plot of the 100 mg/L dissolved chloride contour.

The area of groundwater contamination at a depth of 1.2 m near the top of the first permeable zone in 1992 and 1993 was smaller in lateral extent than the area of contamination from terrain conductivity over a total depth interval of 6.1 m (Figure 75). This is consistent with observations from deeper boreholes that fluids within the first permeable zone are salinity stratified, with the most saline water occurring at the base of the unit. The lateral extent of contamination in the first permeable zone in 1992–93 was from 150 to 250 m to the west, north, and east of the boundary of the pits, and from 300 to over 900 m to the south and southeast. The axis of the furthestmost extension of contamination to the south is approximately coincident with the location of what is identified on consultant site maps as a “possible [buried] pipeline” (Hanor, 1997, p. 198).

No conclusions can be made about the total lateral extent of contamination below the first permeable zone other than the fact that groundwater contamination must have extended beyond the perimeter of well and borehole control in the immediate vicinity of the pits. A borehole was drilled 430 m WNW of the pit area with the express purpose of sampling the second permeable zone upgradient of the inferred direction of groundwater flow. This borehole was drilled to a total depth of only 11 m, however, and thus missed the lower section and base of the second permeable zone, which extends to a depth of 14 m in the vicinity of the pits.

#### 10.4.5 Site Hydrology: Constant Fluid Density Model

What can be deduced from the directions and rates of contaminated groundwater flow at this site? One conventional groundwater approach would be to calculate directions and rates of flow from water level measurements and measured, or assumed, hydraulic conductivities. Water levels were measured by consultants at semi-regular intervals in wells screened in the first and second permeable zones. Water levels for January 1995 are shown in Figure 76 (Hanor, 1997). Hydraulic conductivities were calculated by site consultants from slug tests conducted in each of four wells in both the first and second permeable zones. The reported geometric mean of hydraulic conductivities for the first permeable zone was  $1.2 \times 10^{-3}$  cm/s and  $2.6 \times 10^{-4}$  cm/s was reported for the second permeable zone. These values are within the ranges reported for unconsolidated sands and silty sands (e.g., Figure 32 of Woessner & Poeter, 2020). In their report, the consultants tacitly assumed that water levels at the site are equivalent to hydraulic head,  $h$ . Sediment porosity was

apparently not measured but was assumed to be 30 percent in the consultant reports, again a reasonable value (e.g., Table 2 of Woessner & Poeter, 2020). If the assumption that groundwater at the site can be modeled as a constant density fluid system is correct, then the rates and directions of fluid flow horizontally within and vertically between these zones can be calculated from Darcy's Law as shown by Equation (17).

$$v = - \left( \frac{K}{n} \right) (\nabla h) \quad (17)$$

where:

$v$  = fluid velocity ( $LT^{-1}$ )

$K$  = hydraulic conductivity ( $LT^{-1}$ )

$n$  = porosity (dimensionless)

$\nabla h$  = hydraulic head gradient (dimensionless)

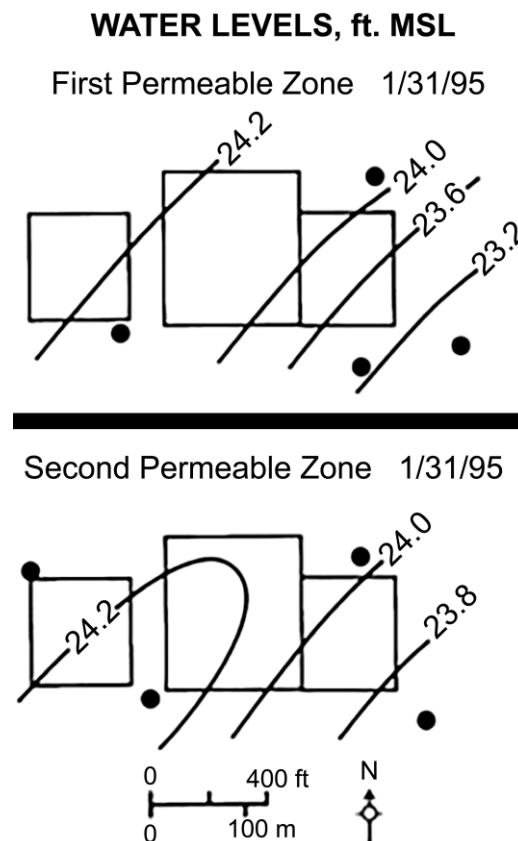


**Figure 76** - Water levels in wells emplaced in the first and second permeable zones in early 1995 (from Hanor, 1997).

According to the consultant reports the average water level gradients measured at different times between 1986 and 1995 in both the first and second permeable zone are  $9 \times 10^{-3}$ . These gradients are similar in magnitude to the gradients which can be determined from the mapped water levels shown Figure 76 for January 1995 (Hanor, 1997). Given the consultant values for hydraulic conductivity and an assumed porosity of 0.30, the velocities

of groundwater flow should be on the order of 1.1 m/y in the first permeable zone and 0.3 m/y in the second permeable zone. Water level measurements were made by the consultants for only four wells in each of the two permeable zones. On the basis of these sparse data for January 1995, one could infer that the direction of fluid flow at that time was generally to the southeast in both zones (Figure 76). Measured water levels in the second permeable zone are typically higher than in the shallower first zone (Figure 76). Fluids should thus be moving upward here through the second clay from the second permeable zone to the first permeable zone.

It is an easy matter to test the validity of using Equation (17) to evaluate rates and directions of solute transport at the site by observing the actual spatial distribution of contaminated groundwater. According to Equation (17), contaminated groundwater in the first permeable zone would have migrated a distance of approximately 50 m to the southeast during the 42-year period from 1950, when the site was first established, to 1992, the year of mapping shown in Figure 75. Total distances of lateral solute transport within this zone, however, were significantly greater (Figure 75). Wastes migrated from 60 to 240 m from the pit area by 1992, not 50 m. In addition, contaminated groundwater migrated not only to the southeast, but in all directions radially from the pit area. Also, on the basis of water levels, one would conclude that fluids migrated vertically up from the second to the first permeable zone in the southeastern area of the pits. It is clear from the increase in salinity with time in the second permeable zone (Figure 74), however, that the net direction of vertical transport of salt was actually downward.

#### 10.4.6 Site Hydrology: Variable Density Considerations

Measured groundwater salinity in the study area ranges from 100 mg/L to over 60,000 mg/L, which corresponds to water having fluid densities of approximately 997 to 1,040 kg/m<sup>3</sup>. In fluid systems of spatially varying salinity—and hence, fluid density—static water levels do not provide a usable indication of hydraulic force; Darcy's Law expressed in terms of hydraulic head in Equation (17) is no longer valid (McWhorter et al., 2020). It is necessary instead to formulate hydraulic force in terms of fluid pressure and fluid specific weight as shown in Equation (18).

$$v = -\frac{k}{n\eta}(\nabla P - \rho g) \quad (18)$$

where:

- $v$  = fluid velocity (LT<sup>-1</sup>)
- $k$  = intrinsic permeability (L<sup>2</sup>)
- $n$  = sediment porosity (dimensionless)
- $\eta$  = dynamic fluid viscosity (MLT<sup>-1</sup>)
- $\nabla P$  = fluid pressure gradient (dimensionless)

$$\begin{aligned}\rho g &= \text{fluid specific weight (ML}^{-2}\text{T}^{-2}\text{)} \\ \rho &= \text{density (ML}^{-3}\text{)} \\ g &= \text{gravitational force (LT}^{-2}\text{)}\end{aligned}$$

Measurements of water level and calculations of water level gradients cannot be used as reliable indicators of hydraulic force, and independent determinations or calculations of fluid pressure gradients. Density must be used instead. It is possible that assumptions could be made regarding the fluid pressure and fluid density fields at this site that would permit an analysis of the complex problem of variable density flow.

#### 10.4.7 Site Hydrology: Conceptual Model for Site

Contaminated groundwater at the site traveled much faster and in directions far different from those predicted on the basis of conventional water level measurements, reported values for porosity and hydraulic conductivity, and Darcy's Law described in Equation (17). Fluids within the first permeable zone are salinity-stratified, with the highest salinity—hence, density—occurring at the base of the unit (Figure 77). Wastes have also migrated down through the underlying clay into the second permeable zone in the vicinity of the brine pits and probably elsewhere on the site.

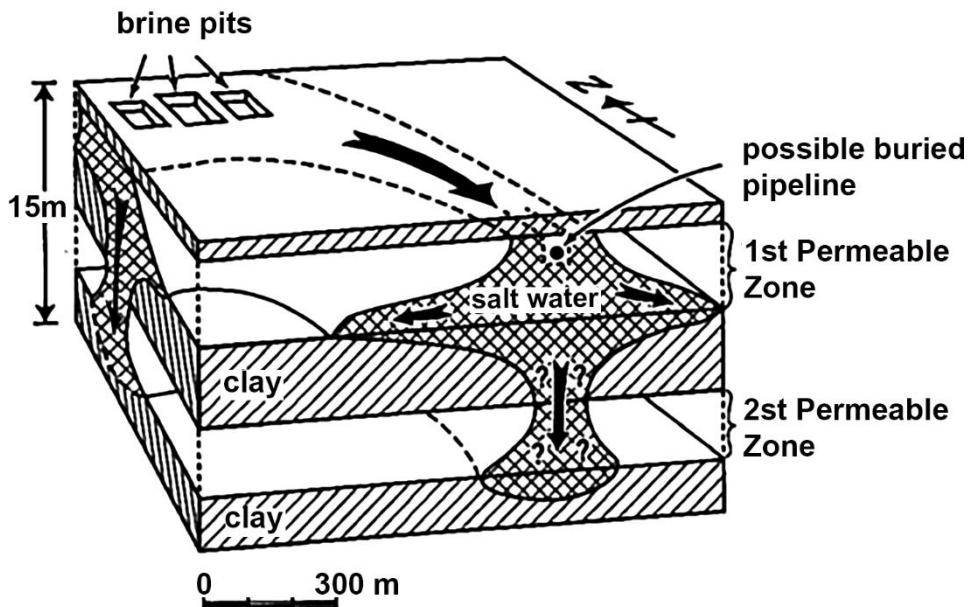


**Figure 77** - Conceptual model for the transport and dispersal of produced water wastes at the Fordoche site, as of 1992-93. Arrows show inferred directions of saline water flow (from Hanor, 1997).

It is unlikely that a French drain or horizontal well emplaced at shallow depths in the first permeable zone along the southern margin of the former pits would be effective in remediating the site. The clays underlying the first permeable zone have not acted as a confining layer, and brines collected in the drains would in part migrate vertically

downward, thus bypassing the shallow remediation efforts. The apparent relatively high hydraulic conductivity of these clays is consistent with measurements of hydraulic conductivity that have been made of clay beds at other shallow Gulf Coast sites where the presence of secondary porosity in the form of fractures and worm burrows has enhanced vertical permeability (Hanor, 1993; Capuano & Jan, 1996).

## 10.5 Exercises Pertinent to Section 10

[Link to Exercise 19](#) ↴

[Link to Exercise 20](#) ↴

[Link to Exercise 21](#) ↴

[Link to Exercise 22](#) ↴

[Link to Exercise 23](#) ↴

[Link to Exercise 24](#) ↴

# 11 Geologic Storage of CO<sub>2</sub>: Environmental Impacts on Potable Groundwater

## 11.1 Introduction

The clear benefits of hydrocarbon fossil fuels (coal, oil, and natural gas) also carry major detrimental health and environmental impacts that may be local, regional, or global in scale (Kharaka & Dorsey, 2005; US EPA, 2020). Global impacts include air pollution and the interrelated global warming that results from continued addition of large and increasing amounts of CO<sub>2</sub> to the atmosphere (40.1 B tonnes CO<sub>2</sub> added in 2019, compared with 31 B tonnes in 2011 and 20 B tonnes in 1991) obtained largely from the burning of fossil fuels (Friedlingstein et al., 2020; Kharaka et al., 2013). The increased anthropogenic emissions of CO<sub>2</sub> have raised Earth's atmospheric concentrations from about 280 ppmv during preindustrial times to 423 ppmv as of January 23, 2024 (National Oceanic and Atmospheric Administration, NOAA, 2024). Based on several defined scenarios, CO<sub>2</sub> concentrations are projected to increase up to 1,100 ppmv by 2100 (Intergovernmental Panel on Climate Change (IPCC), 2007; NRC, 2020).

Preliminary results of CO<sub>2</sub> emissions from USA sources in 2023 could indicate that global CO<sub>2</sub> levels may stabilize at a lower level than that listed above (King et al., 2024). In 2023, the US greenhouse gas emissions were 1.9 percent lower than in 2022, even while the economy expanded by 2.4 percent. The US emissions remained below pre-pandemic levels and dropped to 17.2 percent below 2005 levels. A decline in emissions in 2023 is a step in the right direction. But the deadline for the US 2030 climate target under the Paris Agreement of a 50 to 52 percent reduction in GHG emissions below 2005 levels is rapidly approaching, and achievement of that goal requires the US to average a 6.9 percent emissions reduction every year from 2024 through 2030—more than triple the 1.9 percent drop in 2023 (King et al., 2024).

There is now a broad scientific consensus that current global warming (average temperature is 1.2 °C higher than during preindustrial times) and related climate changes are related to atmospheric CO<sub>2</sub> increases caused mainly by human activities (Figure 78). According to new data from the Copernicus Climate Change Service, the Earth's average temperature in 2023 was the hottest in recorded human history, reaching 1.48 °C (2.66 °F) hotter than the preindustrial average and dangerously close to a long feared warming threshold of 1.5 °C listed in the Paris Agreement of 2016 (Dance et al., 2024). Average global temperatures are projected to increase by 2 to 5 °C by 2100 (Figure 79) (IPCC 2017, 2021a, 2021b, 2023; NRC, 2020).

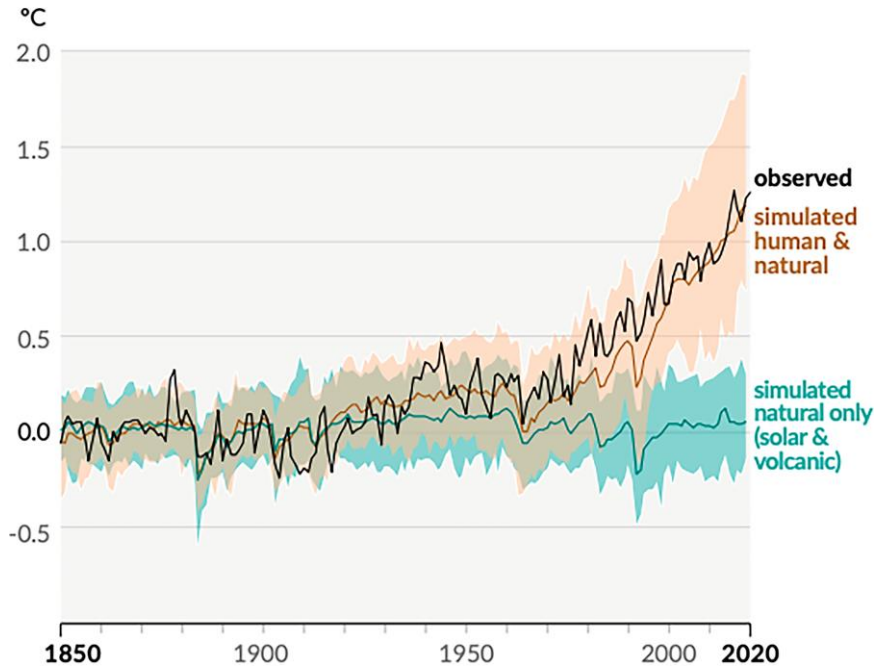


**Figure 78** - Change in global average surface temperature from 1850 to 2020 as observed and simulated using only natural (blue) and combined (beige) human and natural factors (IPCC, 2021).

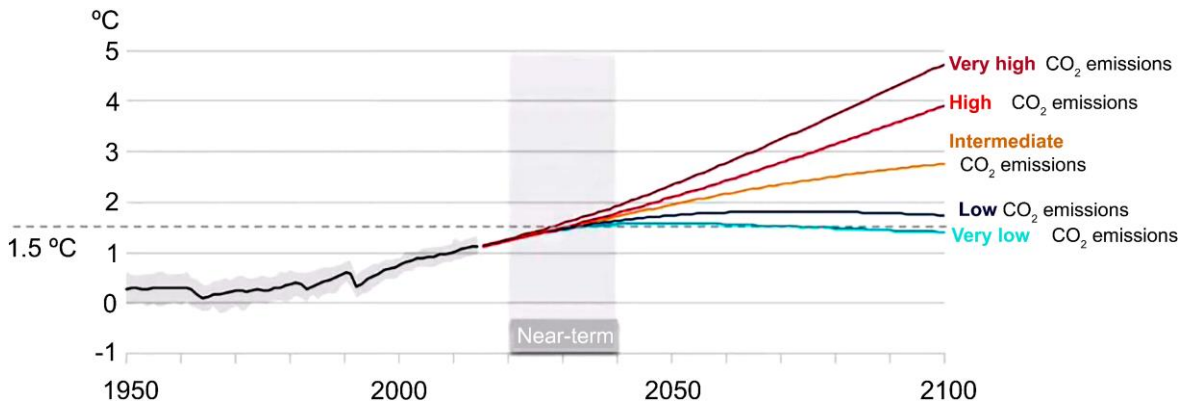


**Figure 79** - Expected global temperature increases as a function of CO<sub>2</sub> emissions. Note that only two emission scenarios will keep warming this century below 2 °C, and in only one does warming stay below 1.5 °C (from IPCC, 2021).

Related climate changes with potential adverse impacts include sea-level rise from the melting of mountain glaciers and polar ice sheets and ocean warming; increased frequency and intensity of wildfires, floods, droughts, and tropical storms; and changes in the amount, timing, and distribution of rain, snow, and runoff. Rising atmospheric CO<sub>2</sub> is also increasing the amount of CO<sub>2</sub> dissolved in ocean water, increasing its acidity (i.e., lowering its pH from 8.1 to 8.0), with potentially disruptive effects on coral reefs, marine plankton, and some marine ecosystems (Kharaka & Hanor 2014; NRC, 2020; Sundquist et al., 2009).

## 11.2 Sea Level Rise from Global Warming

The issue of sea level rise and coastal flood hazard in the USA is discussed in detail in a new report by scientists at several US government agencies including NOAA, NASA, USGS, and others (Sweet et al., 2022). The report makes the following major points.

1. The average rise in the US coastal sea level in the next thirty years (2020 to 2050) is predicted to be 25 to 30 cm, which is equal to the rise measured over the last 100 years. Approximately 40 percent of the rise is due to the thermal expansion of seawater and the remainder is due to melting of mountain glaciers and polar ice sheets in Greenland and Antarctica that are diminishing at rates faster than natural systems can replace them (Figure 80).

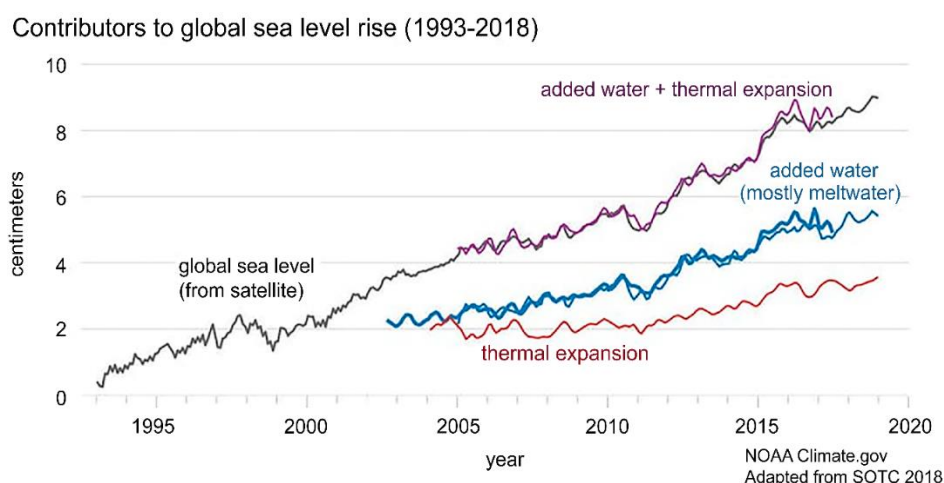


**Figure 80** – Graphs showing how thermal expansion and melting land ice combine to create enhanced sea level rise over time. The black line is observed sea level since the start of the satellite altimeter record in 1993 (from Sweet et al., 2022).

2. Sea level rise in the coastal USA varies regionally, being 25 to 35 cm for the east coast, 35 to 45 cm for the Gulf of Mexico, and only 10 to 20 cm for the west coast. Areas along the Gulf of Mexico and the east coast will rise higher as those shorelines are sinking because of geological factors and because melting ice in Greenland is already changing currents in the Atlantic Ocean.
3. Sea level rise will create a profound shift in coastal flooding over the next thirty years by causing tide and storm surge heights to increase and reach farther inland. By 2050, so called “moderate” flooding is expected to occur, on average, more than ten times as often as it does today and can be intensified by local factors such as precipitation events. “Major” (often destructive) flooding is expected to occur five times as often in 2050 as it does today (Figure 81). Coastal infrastructure, communities, and ecosystems will face increased impacts without additional measures to reduce risks.

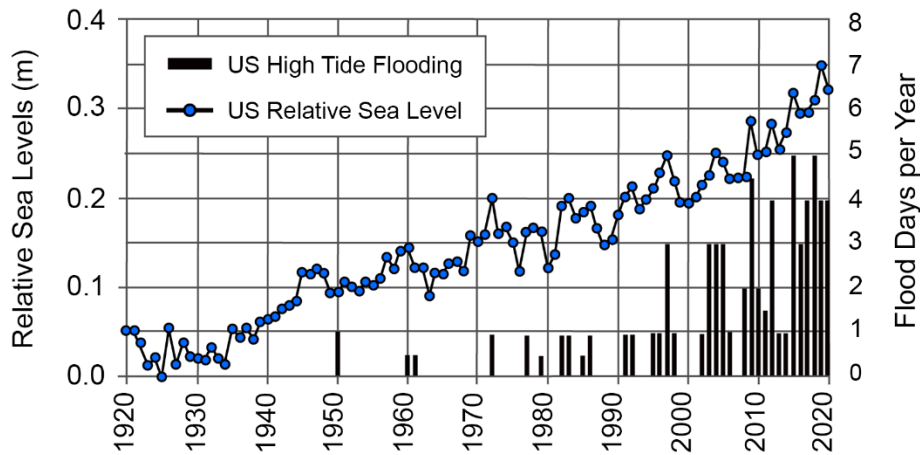


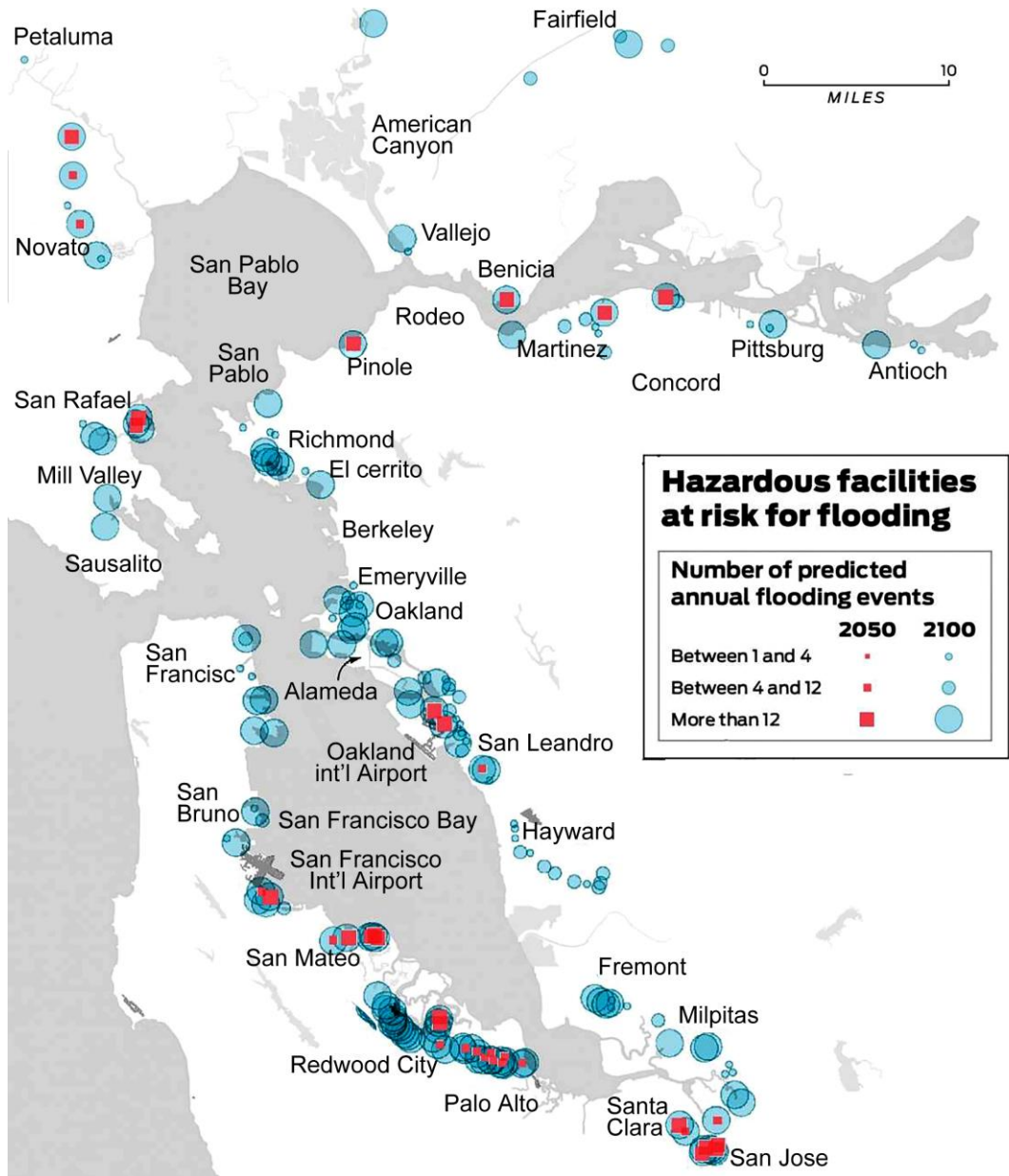
**Figure 81** - The rate of minor high-tide flooding and sea level rise, in meters, from 98 NOAA tide gauges along US coastlines outside Alaska (from Sweet et al., 2022).

4. Current and future greenhouse gas emissions will determine the amount of additional sea level rise in coastal USA and globally. Approximately 60 cm of additional sea level rise is expected between 2020 and 2100 if present day emission rates continue. An additional rise of up to 1.5 m, for a total of 2.1 m, could occur by 2100 if future emissions are not controlled. If global temperatures rise above 3 °C, much greater sea level rise becomes possible in the USA and globally because of the potential for rapid melting of ice sheets in Greenland and Antarctica.
5. Plans for adaptation to sea level rise require tracking how and why sea level is changing. US federal agencies are performing continuous monitoring and assessments of key sea level rise source contributions affecting the coastlines. These contributions include ocean temperature, ice mass loss from Greenland and Antarctica, vertical land motion from geological factors, and changes in the Gulf Stream. These contributing factors can be tracked separately and compared with measurements of global ocean levels and ice sheet thicknesses using satellites (Figure 80). Results from these measurements can provide early indications of change in the trajectory of sea level rise, which can be used to change the adaptation planning.

The rising sea levels will bring profound flood risks to large parts of the coastal USA—especially in the Gulf of Mexico and Atlantic coasts—over the next three decades. Without significant adaptations, high tides will more frequently pour into streets and disrupt coastal infrastructure including ports that are essential for supply chains and the economy. The higher ocean will also bring seawater farther inland, contaminating surface and groundwater.

The flooding threatens to spread toxic materials from landfills, refineries, oil wells, hazardous waste sites, and other toxic facilities. In coastal California, 400 hazardous facilities in low-lying areas are likely to experience regular flooding by the end of the

century, according to the report dubbed *Toxic Tides*. The sites likely to be impacted by these toxic tides in 2050 and 2100 have been mapped in the San Francisco Bay area, (Figure 82), and remedial action is planned for some of them. These toxic tides are likely to impact the infrastructure as well as surface and groundwater.



Source: *Toxic Tides*  
 John Blanchard/ The Chronicle  
**Figure 82** - Hazardous facilities at risk of flooding in the San Francisco Bay area, California, in 2050 and 2100 (John Blanchard / San Francisco Chronicle, 2022).

To tackle climate change and its many negative global impacts, world leaders from 196 countries at the UN Climate Change Conference (COP21) in Paris reached the historic Paris Agreement on December 12th, 2015. The parties pledged to substantially reduce their countries' greenhouse gas emissions to limit the global temperature increase by 2100 to well

below 2 °C and to pursue efforts to limit the temperature increase to 1.5 °C relative to pre-industrial times. The countries also pledged to review and strengthen their emission commitments every five years, thus providing a durable framework guiding the global effort for many decades (UN, 2015).

In 2021, the UN IPCC released its first major assessment of human-caused global warming since 2013. The report shows a world that has starkly changed in eight years, warming by more than 0.3 °C to nearly 1.2 °C above preindustrial levels (1885–1900). Weather has grown more severe, seas are measurably higher, and mountain glaciers and polar ice have shrunk sharply. And after years of limited action, many countries—pushed by a concerned public and corporations—seem willing to curb their carbon emissions (IPCC, 2021a).

In the past, the IPCC team relied on temperature data provided by a few national centers with supercomputers to project the average temperature increases to 2100. However, results from these computers recently provided unrealistically warmer temperatures; so, the IPCC team (IPCC, 2021a) is using field measurements of warming over the past few decades to constrain the computer projections to 2100 (Figure 83).

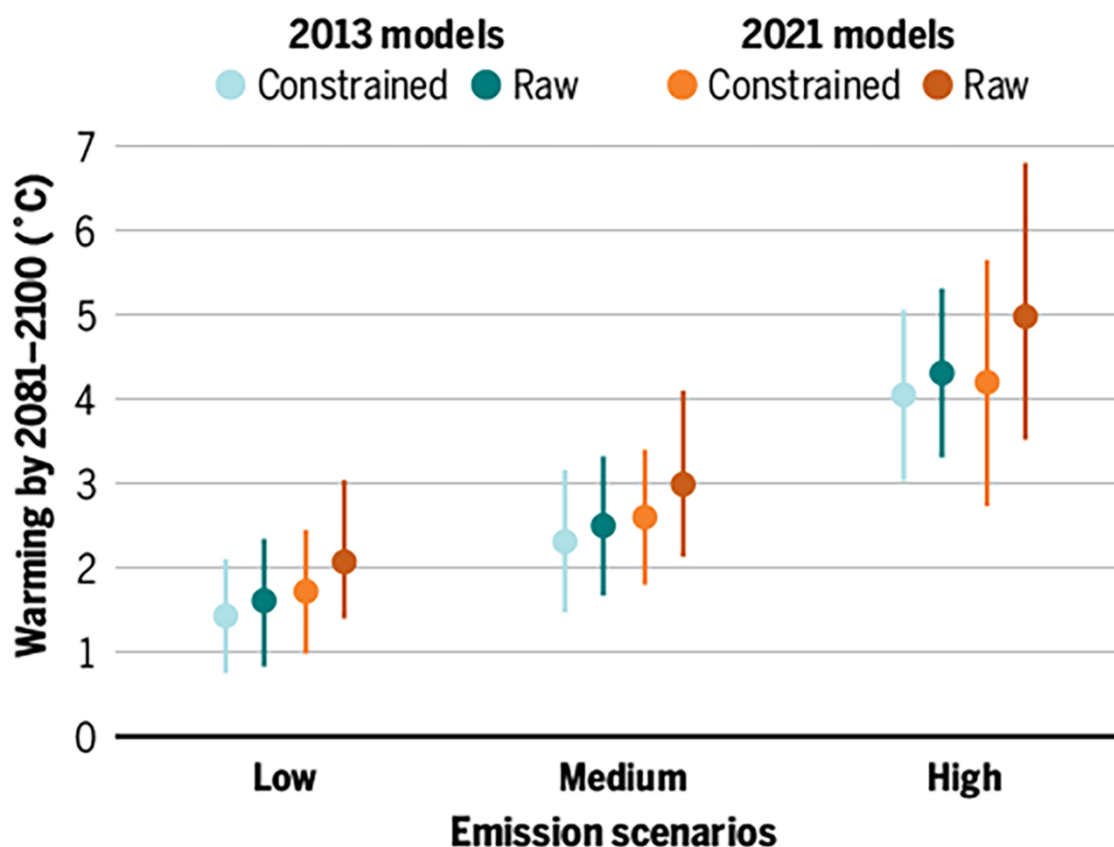
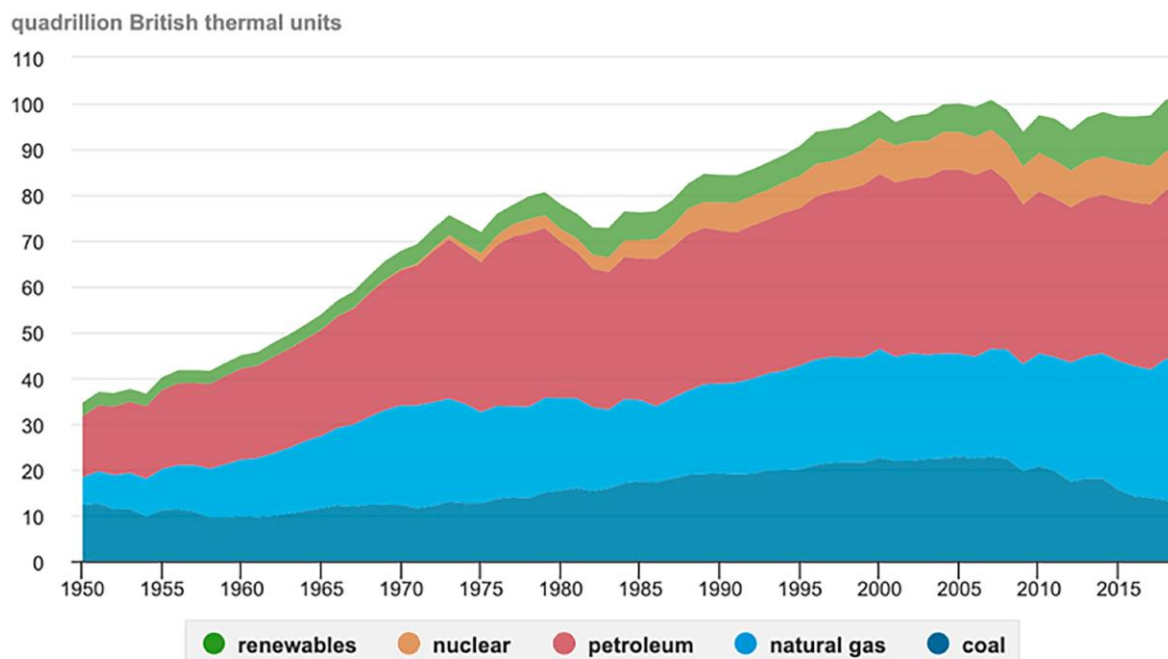


**Figure 83** - Climate models used by IPCC projected more warming over the adjusted 1850–1900 baseline temperature than those in a 2013 report as shown by the points labeled raw in this graph. Scientists then used field measurements of warming to constrain the calculations of future temperature increases resulting in the points labeled constrained. The lines extending from the points are 95 percent confidence intervals indicating the uncertainty associated with the predicted values (from IPCC, 2021a).

Fossil fuels continue to dominate the energy system in the USA (Figure 84), providing approximately 80 percent of the current source of energy. A sharp decline in their extraction and use, in addition to the deployment of clean energy, must be realized to keep the global temperature increase below 1.5 °C, the lower limit stipulated by the Paris Agreement (Luderer et al., 2018; MacDowell et al., 2017; Rogelj et al., 2018, 2020).



Note: Petroleum is petroleum products excluding biofuels, which are included in renewables.

Source: U.S. Energy Information Administration, *Monthly Energy Review*, Table 1.3, April 2020, preliminary data for 2019

**Figure 84** - USA primary energy consumption by major sources from 1950–2019 shows a major decline in energy from coal with increases from natural gas and renewables over the last fifteen years (from US Energy Information Administration (EIA), 2020).

A recent modeling investigation by Welsby and others (2021) assessed the amount of fossil fuels that would need to be left in the ground, regionally and globally, to allow for a 50 percent probability of limiting warming to 1.5 °C. Their results showed that by 2050, unextractable oil, natural gas, and coal reserves are estimated to be 58 percent, 59 percent, and 89 percent, respectively, as a percentage of their 2018 reserve base. This means that high proportions of reserves considered economic today would not be extracted under a global 1.5 °C target. They also estimate that to achieve this goal, oil and gas production must decline globally by 3 percent annually until 2050.

As we noted in Section 1, at the November 2021 COP26 summit held in Glasgow, Scotland, diplomats from nearly 200 countries reached a major agreement aimed at intensifying efforts to fight climate change by limiting the rise in global temperatures to just 1.5 °C above preindustrial levels. Scientists have warned this is the threshold beyond which the risks of calamities like deadly heat waves, water shortages, and ecosystem collapse grow immensely.

### 11.3 Carbon Capture and Storage (CCS)

The IPCC and other experts agree that carbon capture and storage (CCS) will need to play a critical role if the USA and other countries are to meet the emission-reduction goals stipulated in the Paris Agreement of 2015 (US EPA, 2020). Carbon dioxide storage in deep geological formations is now considered an important component of the portfolio of options for reducing greenhouse gas (GHG) emissions to stabilize atmospheric levels of these gases and global temperatures at acceptable values that would not severely impact global economic growth (Benson & Cook, 2005; Hitchon, 1996a; Holloway, 1996, 2001; IPCC, 2017; Knauss et al., 2005; Pang et al., 2010; US EPA, 2020).

Sedimentary basins in general, and deep saline aquifers in particular, are being investigated as possible repositories for large volumes of anthropogenic CO<sub>2</sub> that must be sequestered to mitigate global warming and related climate changes (Benson & Cole, 2008; Hitchon, 1996a, 2009; Kharaka et al., 2006c, 2013). These basins are attractive for CO<sub>2</sub> storage because they have huge potential capacity, estimated at 350 to 11,000 Gt (giga ton) of CO<sub>2</sub> worldwide as well as advantageous locations close to major CO<sub>2</sub> sources (Bradshaw et al., 2007; Hitchon et al., 1999a; NRC, 2020). In addition, a great deal of relevant geologic, geochemical, and hydrologic information can be obtained from the large number of wells (five million in the USA) drilled for oil and gas operations (Kharaka & Dorsey, 2005; Kharaka et al., 2020).

In 2011, only five commercial projects were operating worldwide that captured and injected approximately seven million tonnes of CO<sub>2</sub> annually and provided valuable experience for assessing the efficacy of CCS (Kharaka et al., 2013). Three are the Sleipner Project, offshore Norway; the Weyburn-Midale enhanced oil recovery (EOR) project in the Williston Basin, Saskatchewan, Canada; and the In Salah gas field project in Algeria. Two other projects started in 2008: the Snøhvit Field in the Barents Sea, offshore Norway, and the Cranfield Field sequestration-EOR project in Mississippi (Kharaka & Hanor, 2014; Lu et al., 2012).

The Sleipner Project, operated by StatoilHydro since 1996, is the world's first industrial-scale operation. Approximately one million tonnes of CO<sub>2</sub> are extracted annually from the produced gas that has ~10 percent CO<sub>2</sub> to meet quality specifications and is stored ~1,000 m below sea level in the Utsira Formation (Chadwick et al., 2004, 2009; Hermanrud et al., 2009). The Utsira Formation consists of thick, poorly consolidated sandstones with high porosity (35 to 40 percent) and permeability (1 to 3 Darcy) and is overlain by the thick Nordland shale caprock (Bickle, 2009).

The number of capture and storage projects has increased dramatically, as reported in the US Department of Energy (US DOE) NETL (2018) database, which lists 305 CCS projects worldwide, with 299 sites identified. The 299 site-located projects include 76 capture, 76 storage, and 147 for capture and storage in more than thirty countries across six

continents. While several of the projects are still in the planning and development stage, 37 have been completed and are actively capturing and/or injecting CO<sub>2</sub>. The Shute Creek Gas Processing Plant, located in LaBarge, Wyoming, USA, is the largest operational CCS facility in the world. The CO<sub>2</sub> is obtained from CO<sub>2</sub>-rich natural gas fields in Wyoming. It has a storage capacity of seven million tonnes per year and also provides CO<sub>2</sub> for use in EOR projects in Wyoming and Colorado (Madhumitha, 2021). Other large global CCS operations (Global CCS Institute, 2020) include the following:

- The Century Plant, Pecos County, West Texas, USA: 5 million tonnes per year;
- Petrobras Santos Basin Pre-Salt Field CCS, Brazil: 4.6 million tonnes per year;
- Gorgon Carbon Dioxide Injection, Australia 4 million tonnes per year;
- Qatar LNG CCS, Qatar: 2.1 million tonnes per year;
- Great Plains Synfuels Plant and Weyburn-Midale, Canada-USA: 2 million tonnes per year;
- Petra Nova Carbon Capture, USA: 1.4 million tonnes per year;
- Alberta Carbon Trunk Line (ACTL) with North West Redwater Partnership's Sturgeon Refinery CO<sub>2</sub> Stream, Canada: 1.4 million tonnes per year;
- Quest, Canada: 1.2 million tonnes per year;
- Illinois Industrial Carbon Capture and Storage, USA: 1 million tonnes per year; and
- Sleipner CO<sub>2</sub> Storage, Norway: 1 million tonnes per year.

The story of CCS has largely been one of unmet expectations: Its potential to mitigate climate change has been recognized for decades, but deployment has been slow and so it has had only a limited impact on global CO<sub>2</sub> emissions. This slow progress is a major concern in view of the urgent need to reduce emissions across all regions and sectors in order to reach global net-zero emissions as quickly as possible. Yet there are clear signs that CCS and carbon capture, utilization, and storage (CCUS) may be gaining traction in spite of the economic uncertainty created by the COVID-19 pandemic, with more projects coming online, more plans to build new ones, and increased policy ambition and action. The coming decade will be critical to scaling up investment in developing and deploying CCUS and realizing its significant potential to contribute to the achievement of net-zero emissions by 2050.

A radical transformation of the way we produce and consume energy will be needed to bring about a rapid reduction in emissions of GHGs consistent with the Paris Agreement goal of holding the increase in the global average temperature to well below 2 °C above pre-industrial levels and pursuing efforts to limit the temperature increase to 1.5 °C above pre-industrial levels. The Paris Agreement also seeks to achieve a balance between anthropogenic emissions by sources and removals by sinks in the second half of this century (IPCC, 2018).

In practice, this translates to net zero emissions. Net zero requires that any CO<sub>2</sub> released into the atmosphere from human activity be balanced by an equivalent amount being removed, either through nature-based solutions (including afforestation, reforestation, and other changes in land use) or technological solutions that permanently store CO<sub>2</sub> captured (directly or indirectly) from the atmosphere. The sooner net zero emissions are achieved, the greater the chances of meeting the most ambitious climate goals.

The IEA report *Energy Technology Perspectives 2020* highlights the central role that CCUS must play as one of four key pillars of global energy transitions alongside renewables-based electrification, bioenergy, and hydrogen (US EPA, 2020). CCUS can reduce emissions from large stationary sources—essentially, power stations and industrial plants—in a variety of ways and generate negative emissions by combining it with bioenergy or through direct air capture. Carbon removal technologies will almost certainly be required due to the practical and technical difficulties in eliminating emissions in certain sectors, including some types of industry, notably steel, chemicals and cement, aviation, road freight, and maritime shipping. Another key attraction of CO<sub>2</sub> capture technology is that it can be retrofitted to existing power and industrial plants, which could operate for many years to come. CCUS can also provide a least-cost pathway for producing low-carbon hydrogen (based on natural gas or coal) in countries with low-cost resources. Captured CO<sub>2</sub> can be used in a number of ways including to produce clean aviation fuels (US EPA, 2020).

At the global level, both the IPCC and IEA indicate that huge CCS deployment will be required to reduce CO<sub>2</sub> emissions to net zero by 2050 and economically meet long-term climate targets (IES, 2022; IPCC, 2023). The IPCC climate pathways include up to 1,200 Gt of CO<sub>2</sub> cumulatively stored by 2100. In the IEA Sustainable Development Scenario, which is consistent with meeting the goals of the Paris Agreement, global CO<sub>2</sub> storage increases to 2.8 Gt/year by 2050 (Global CCS Institute, 2020).

In addition to the active injection sites, many geologic sequestration field demonstration projects in the USA are at various stages of planning and deployment, and a large number of tests are also being implemented in other countries to investigate the storage of CO<sub>2</sub> in various rock formations (clastic, carbonate, or basalt) using different injection schemes, monitoring methods, hazards assessment protocols, and mitigation strategies (Gislason et al., 2010; IEA, 2022; Kharaka & Hanor, 2014; NRC, 2020).

### 11.3.1 Concept of Hubs

So far, CCUS has not lived up to its promise. Although its relevance for reducing CO<sub>2</sub> emissions to reach global climate goals has long been recognized, actual deployment has been slow. Annual CCUS investment has generally accounted for less than 0.5 percent of global investment in clean energy and efficiency technologies (US EPA, 2020). However, stronger climate targets (e.g., 1.5 °C temperature increase by 2100) and governmental

investment incentives are injecting new momentum into CCUS. Plans for more than thirty new integrated CCUS facilities have been announced since 2017, mostly in the USA and Europe, although projects are also planned in Australia, China, Korea, the Middle East, and New Zealand. Projects at advanced stages of planning represent a total estimated investment of more than \$ 27 B USD, almost double the investment in projects commissioned since 2010 (US EPA, 2020).

To speed up CCUS, the concept of hubs is being investigated and results prove promising (Meckel et al., 2021; Oil and Gas Climate Initiative (OGCI), 2021; US EPA, 2020). A CCUS Hub is a location where multiple industrial point sources of CO<sub>2</sub> are aggregated and connected to a shared transport and storage network. The location will have access to a large geological storage area with high capacity to store the CO<sub>2</sub> from different sources permanently and safely for hundreds of years. The project will be commercially viable as the unit cost of CO<sub>2</sub> storage will be kept low because of economies of scale. The hub's shared existing and added infrastructure likely would attract new clean industries as well as innovation and negative emissions technologies.

In 2019, the OGCI launched CCUS KickStarter Hubs to help drive down costs of CO<sub>2</sub> capture and storage, demonstrate the impact of CCUS-enabling policies, and attract widespread commercial investment. Table 48 lists the first nine KickStarter Hubs in the world identified by the OGCI. Many more potential hubs have been identified in North America, Europe, Saudi Arabia, Australia, and South America.

**Table 48** - The Oil and Gas Climate Initiative (OGCI) global list of the first nine launched CCUS KickStarter Hubs to help drive down costs of CO<sub>2</sub> capture and storage.

OGCI Climate Initiative KickStarter Hubs	Potential impacts by 2030
Hub 1: Net Zero Teesside, UK	Over 10 million tonnes CO <sub>2</sub> per year
Hub 2: Northern Lights, Norway	5 million tonnes CO <sub>2</sub> per year
Hub 3: Rotterdam, Netherlands	10 million tonnes CO <sub>2</sub> per year
Hub 4: Xinjiang, China	Over 3 million tonnes CO <sub>2</sub> per year
Hub 5-7: Gulf of Mexico, Texas, Louisiana, USA	Over 200 million tonnes CO <sub>2</sub> per year
Hub 8: Edmonton, Alberta, Canada	Close to 2 million tonnes CO <sub>2</sub> per year
Hub 9: Adriatic Blue, Italy	In the planning stage

North-central Gulf of Mexico is one of the most heavily industrialized regions in the USA, spanning approximately 1,600 km from the Louisiana industrial corridor along the lower Mississippi River in the east to Corpus Christi in the west. The region hosts some of the largest current and planned energy and refined product generation facilities in North America; its role as a leader in the future of energy development and management of CO<sub>2</sub> is an appropriate fit for several CCUS hubs. The Houston area of Texas, for example, has several features that make it an ideal site for a CCUS Hub.

- Many large industrial emission sources are located there including petrochemical, manufacturing, and power generation facilities.

- It is near geologic formations in the Gulf of Mexico that could store large amounts of CO<sub>2</sub> safely, securely, and permanently.
- A significant portion of the captured CO<sub>2</sub> can be used for several beneficial purposes, especially for CO<sub>2</sub>-EOR in depleted oil fields nearby.

The US DOE estimates that storage capacity along the US Gulf Coast in Texas and Louisiana is enough to hold 500 B tonnes of CO<sub>2</sub> — more than 130 years of the country's total industrial and power generation emissions, based on 2018 data. The CO<sub>2</sub> would be captured from all the industrial sources and piped into geologic formations thousands of feet under the sea floor. Offshore storage in the Houston area and Gulf of Mexico is particularly attractive, as it presents minimal risks to underground sources of drinking water (USDW) and populated areas, and it has proven reservoir volume and quality (Bump & Hovorka, 2023; Meckel et al., 2021; Smyth & Hovorka, 2018).

The development of CCUS hubs could play a critical role in accelerating the deployment of CCUS. Efforts to develop CCUS hubs have commenced in at least twelve locations around the world (nine listed in Table 48). These hubs have an initial CO<sub>2</sub> capture capacity of about 25 million tonnes/year but could be expanded to more than 50 million tonnes/year.

A major legal barrier to the development of CCUS was resolved in 2019 when an amendment to the London Protocol was ratified to permit cross-border transportation of CO<sub>2</sub>. The principal benefit of a hub approach to CCUS deployment is the possibility of sharing CO<sub>2</sub> transport and storage infrastructure. This can support economies of scale and reduce unit costs, including through greater efficiencies and reduced duplication in the infrastructure planning and development phases. The initial oversizing of infrastructure increases the capital cost of the project and so can make it harder to raise financing, but it can also reduce unit transport and storage costs substantially in the longer term. Developing CCUS hubs with shared infrastructure can also make it feasible to capture CO<sub>2</sub> at smaller industrial facilities, for which dedicated CO<sub>2</sub> transport and storage infrastructure may be both impractical and uneconomic.

Government leadership and co-ordination are vitally important to the early development of CCUS hubs, notably in supporting or underwriting investment in new CO<sub>2</sub> transport and storage infrastructure. In Canada, the ACTL, which came online in June 2020, is an example of strong government support for the CO<sub>2</sub> transport infrastructure required to enable the future expansion of CCUS. The 240-km pipeline has been oversized with almost 90 percent of its capacity available to accommodate future CO<sub>2</sub> sources (ACTL, 2022).

In the USA, Section 45Q of the Internal Revenue Service (IRS) tax code describes currently available tax credits that provide a powerful commercial incentive for deploying CCUS (<https://www.irs.gov/pub/irs-pdf/f8933.pdf><sup>7</sup>). These federal tax credits for

permanent subsurface storage of CO<sub>2</sub> have existed since 2009 but were significantly and notably expanded in 2019. They provide \$ 22 USD per tonne of CO<sub>2</sub> for projects that produce oil or other products through utilization or \$ 31 USD per tonne for projects that permanently store CO<sub>2</sub> in a deep geologic saline formation. Both values increase incrementally through time, creating a predictable financial future. A minimum volume is needed to qualify and a twelve-year tax credit eligibility; these projects have a minimum net tax credit value of about \$ 10 million USD for utilization projects, \$ 40 million USD for EOR projects, and \$ 57 million USD for geologic storage projects.

The European Union (EU) uses a carbon price in the form of the Emissions Trading System, which works on a cap-and-trade principle. It covers 45 percent of the EU's GHG emissions (the power, manufacturing, and aviation sectors). A carbon-pricing system that accurately conveys the true costs of GHG emissions can raise the relative cost of coal, oil, and natural gas to reflect the environmental harm they cause. This can also lower the overall cost of green technologies and fuels relative to fossil-based alternatives. Currently, many industrial facilities receive free emissions allowances that will continue until at least 2030. To ensure continued decarbonization of European industries, free allowances for all sectors should phase out in favor of other policies addressing carbon leakage risks and so that future carbon prices are at a high enough level to drive clean energy investments.

### 11.3.2 Field Scale Demonstration Projects of Geologic Storage of CO<sub>2</sub>

Carbon capture and underground storage of CO<sub>2</sub> was investigated by several groups (IEA, 2022). One of the earliest studies was the JOULE Program funded by the Commission of the European Communities (Holloway, 1996, 2001). That same year saw the publication of a book based on research in the Alberta Basin (Hitchon, 1996a) in which the disposal of CO<sub>2</sub> into a Lower Cretaceous glauconitic sandstone and an Upper Devonian carbonate were evaluated as possible disposal aquifers. The source of the CO<sub>2</sub> was a coal-fired power plant near Edmonton, Alberta, Canada. As late as 2012, power companies in Canada still considered the concept of CO<sub>2</sub> disposal to be uneconomic. By late 2021 effectively all thermal coal plants in Alberta were not only converted to natural gas but many will be able to use hydrogen when it becomes economically available.

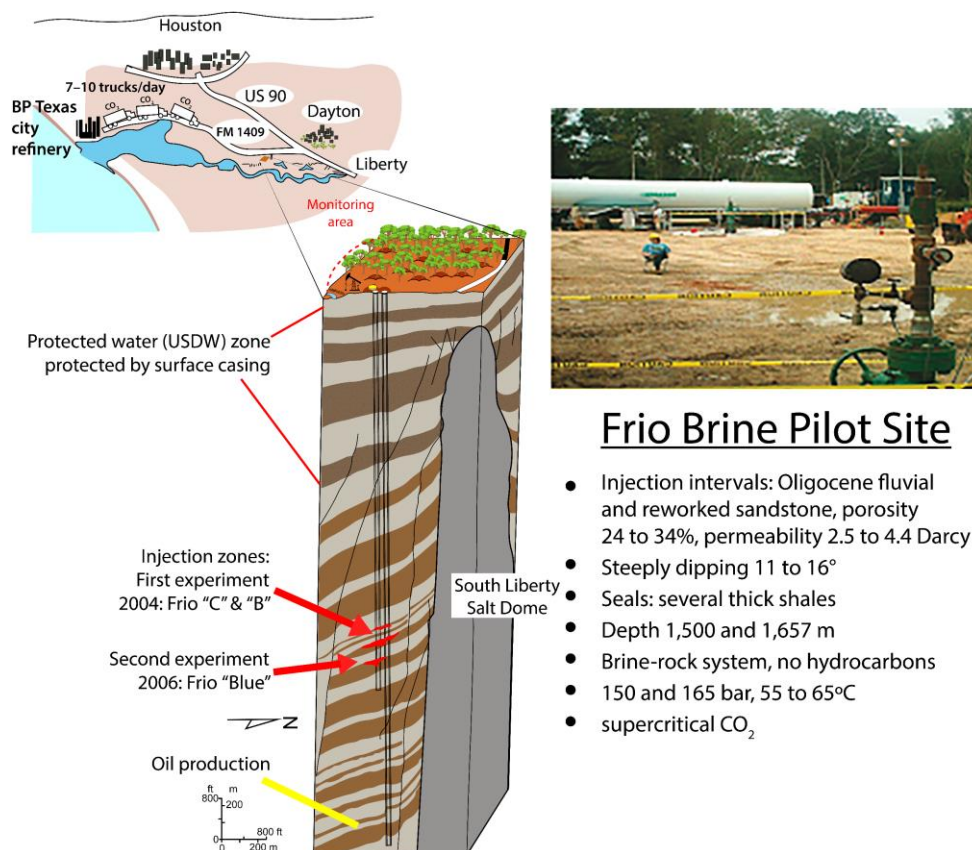
In the intervening decade, the first disposal site for CO<sub>2</sub> started operation in 2015 in Alberta, also near Edmonton, Canada. This is the Quest Carbon Capture and Storage Project where more than one million tonnes of CO<sub>2</sub> per year are captured from the Scotford oil sands bitumen upgrader northeast of Edmonton, piped 65 km, and sequestered in the highly permeable Basal Cambrian Sandstone. Multiple technologies used to measure, monitor, and verify, indicate that the CO<sub>2</sub> is where it is expected to be. Also, microseismic monitoring has revealed very low magnitude events that do not represent a risk to containment (IEA, 2022; Quest CCS, 2022).

In Australia, extensive field, laboratory, and simulation tests are being carried out in the CO<sub>2</sub> CRC Otway Project, where several major CO<sub>2</sub> storage trials between 2008 and 2020 injected over 95,000 tonnes of CO<sub>2</sub> into a depleted gas field and saline formations (Cook, 2014; Enis-King et al., 2017; Otway International Test Centre, 2022; Underschultz et al., 2011). The storage of this CO<sub>2</sub> is being monitored using an internationally renowned program to test advanced geochemical and geophysical technologies and techniques. The monitoring program is the most comprehensive of its type in the world and aims to demonstrate how the cost of storage and plume monitoring can be significantly reduced (Jenkins, 2013; Otway International Test Centre, 2022).

Another important CCS project is the Gorgon Gas Development Project located off the northwest coast of Western Australia. Natural gas in the huge Gorgon natural gas fields contain approximately 14 percent CO<sub>2</sub> that, starting in 2019, is being captured and injected at an ultimate rate of approximately four million tonnes per year. With a predicted project lifespan of more than forty years, the injection project is expected to be the largest long-term CO<sub>2</sub> storage project in the world. The Department of Mines Industry Regulation and Safety (DMIRS, 2022) will monitor the performance of the project over the long term ([online@dmirs.wa.gov.au](mailto:online@dmirs.wa.gov.au) ↗).

### Storage of CO<sub>2</sub> in the Frio Formation

As noted, several projects in the USA capture and inject large volumes of CO<sub>2</sub> annually. To investigate the potential for geologic storage of CO<sub>2</sub> in saline aquifers, a multi-laboratory experiment, called the Frio Brine I and II field tests, was conducted between 2004 and 2008 to investigate the potential for geologic storage of CO<sub>2</sub> in saline aquifers (Figure 85). For Frio I, approximately 1,600 tons of refinery CO<sub>2</sub> was injected into a 24-m sandstone in the Oligocene Frio Formation—an extensive regional petroleum and brine reservoir in the US Gulf Coast (Hovorka et al., 2006; Meckel et al., 2021). Downhole and surface samples of formation water and gas were obtained from the injection well and an observation well that was completed about 30 m up dip using a variety of sampling tools and methods (Kharaka et al., 2006b, 2009). Samples were obtained from both wells before CO<sub>2</sub> injection for baseline data.



### Frio Brine Pilot Site

- Injection intervals: Oligocene fluvial and reworked sandstone, porosity 24 to 34%, permeability 2.5 to 4.4 Darcy
- Steeply dipping 11 to 16°
- Seals: several thick shales
- Depth 1,500 and 1,657 m
- Brine-rock system, no hydrocarbons
- 150 and 165 bar, 55 to 65°C
- supercritical CO<sub>2</sub>

**Figure 85** - Surface area and a sketch of the geological section at the Frio Brine I and II field tests near Houston, Texas, conducted from 2004 to 2008 to investigate the potential for geologic storage of CO<sub>2</sub> in saline aquifers. For Frio I, approximately 1,600 metric tons of refinery CO<sub>2</sub> were injected into a 24 m sandstone zone of the Oligocene Frio Formation. Downhole and surface samples of formation water and gas were obtained from the injection well and an observation well about 30 m up dip using a variety of sampling tools and analytical methods (Kharaka et al., 2006b, 2009).

A large number of samples were taken from the observation well during the injection to track CO<sub>2</sub> breakthrough and investigate temporal changes in fluid composition; some were collected post-injection to investigate the “residual” CO<sub>2</sub> (Hovorka et al., 2006) and its possible leakage into the overlying “B” sandstone (Kharaka et al., 2006a, 2009). Also, surface and wellbore geophysical logging using electrical, seismic, and the Schlumberger reservoir saturation tool was carried out to provide baseline characterization and to investigate changes in the composition and distribution of the CO<sub>2</sub> plume (Daley et al., 2007, 2008; Hovorka et al., 2006a, 2013).

The results of chemical analyses of Frio I samples prior to CO<sub>2</sub> injection show that the brine is a Na–Ca–Cl-type water with a salinity of 93,000 mg/L (Figure 86), with relatively high concentrations of Mg and Ba, but with low values for SO<sub>4</sub>, HCO<sub>3</sub>, DOC, and organic acid anions. The high salinity and the low Br/Cl ratio (0.0013) relative to seawater indicate dissolution of halite from the nearby salt dome (Kharaka et al., 2006a). The brine has 40 to 45 mM dissolved CH<sub>4</sub>, which is close to saturation at reservoir conditions (60 °C and 150 bar.; CH<sub>4</sub> comprises 95 percent of total gas, but the CO<sub>2</sub> content is low at 0.3 percent (Table 49).

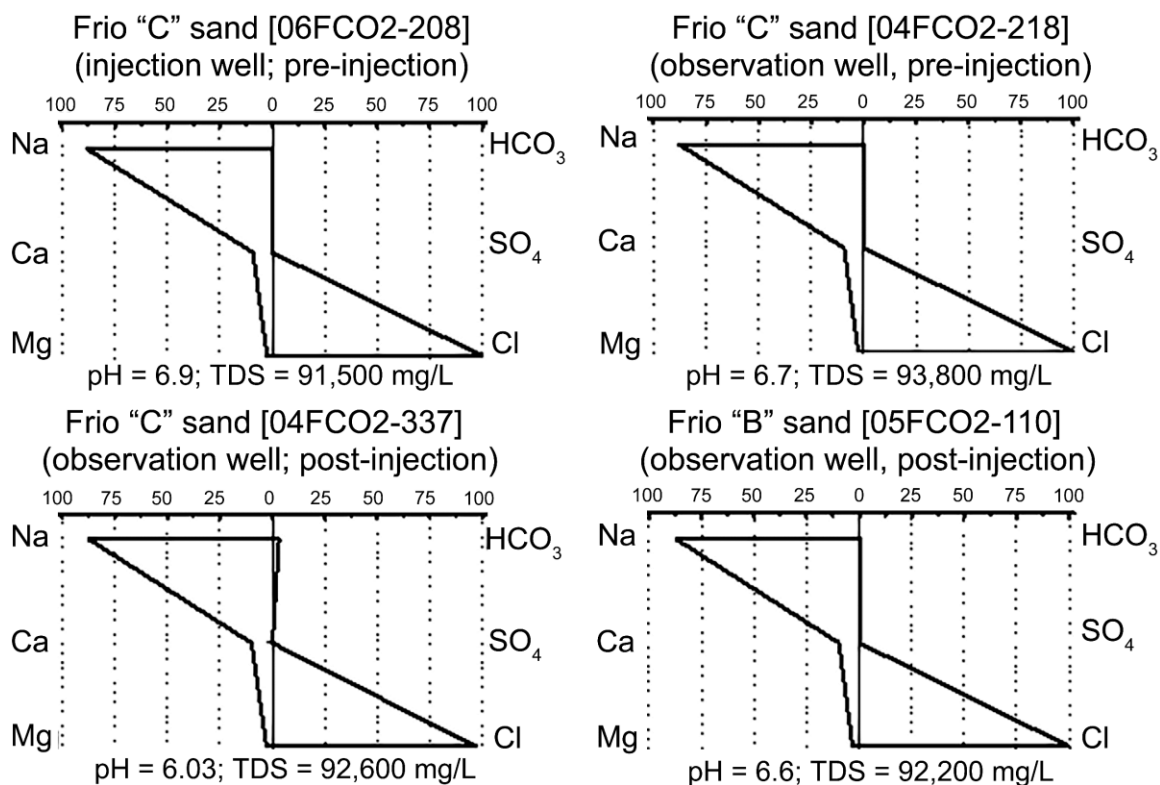


**Figure 86** - Modified Stiff diagrams showing concentrations of major cations and anions (equivalent units normalized to 100 percent), together with salinity and pH of Frio I and II brine from the "Blue," "C," and "B" sandstones before and after CO<sub>2</sub> injection (reproduced from Kharaka et al., 2009).

**Table 49** - Chemical composition of gases (mole percent) from Frio I "C" and "B" sandstones. The relatively high CO<sub>2</sub> concentration in "B" indicates leakage from the underlying injection zone.

Gas	"C" <sup>a</sup>	"C" <sup>b</sup>	"B" <sup>c</sup>	"B" <sup>d</sup>
He	0.008	0	0.001	0.011
H <sub>2</sub>	0.040	0.19	0.92	0.012
Ar	0.041	0	0.13	0.010
CO <sub>2</sub>	0.31	96.8	2.86	0.28
N <sub>2</sub>	3.87	0.037	1.51	1.12
CH <sub>4</sub>	93.7	2.94	94.3	98.3
C <sub>2</sub> H <sub>6</sub> <sup>+</sup>	1.95	0.005	0.12	0.11

<sup>a</sup>background sample from the injection well, before CO<sub>2</sub> injection

<sup>b</sup>from the observation well, after CO<sub>2</sub> breakthrough

<sup>c</sup>from the observation well, ~6 months after completion of injection

<sup>d</sup>from the observation well, ~15 months after injection

During CO<sub>2</sub> injection between October 4th and 14th, 2004, on-site measurements of electrical conductance (EC) exhibited only a small increase from a pre-injection value of 120 mS/cm at 22 °C. However, there were major changes in some chemical parameters (Figure 87) when CO<sub>2</sub> reached the observation well, including a sharp drop in pH from 6.5 to 5.7 (measured in a 150 ml bottle at surface conditions) and large increases in alkalinity from 100 to 3,000 mg/L as HCO<sub>3</sub> (Kharaka et al., 2006a). Additionally, laboratory determinations showed major increases in dissolved Fe (from 30 to 1,100 mg/L) and Mn,



modeling, convinced Kharaka and others (2010a) that the high Fe values following CO<sub>2</sub> injection had a mixed origin: dissolution of Fe-oxyhydroxide minerals and the carbon steel tubing (Figure 89).

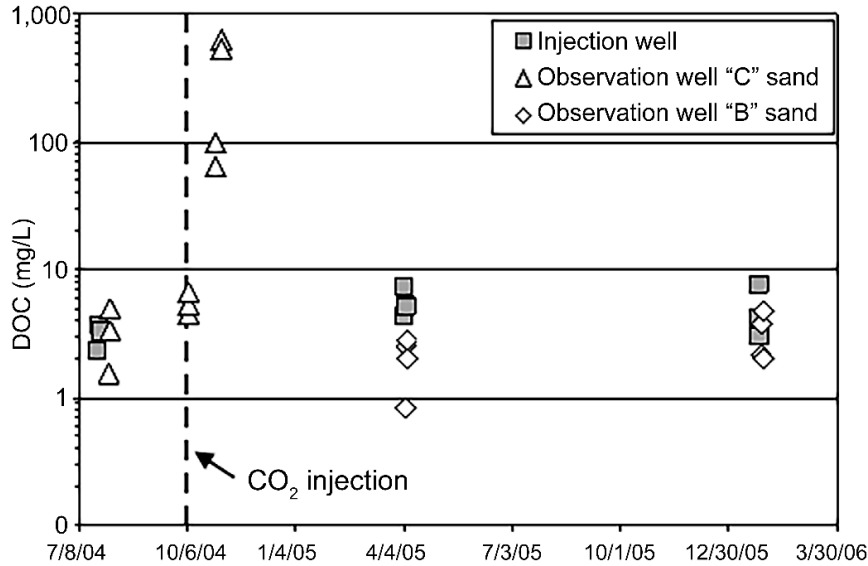


**Figure 88** - Concentration of dissolved organic carbon (DOC) in Frio I brine. The extremely high values of DOC obtained in November 2004, measured twenty days after the end of CO<sub>2</sub> injection also indicate the presence of CO<sub>2</sub> (Kharaka et al., 2009).

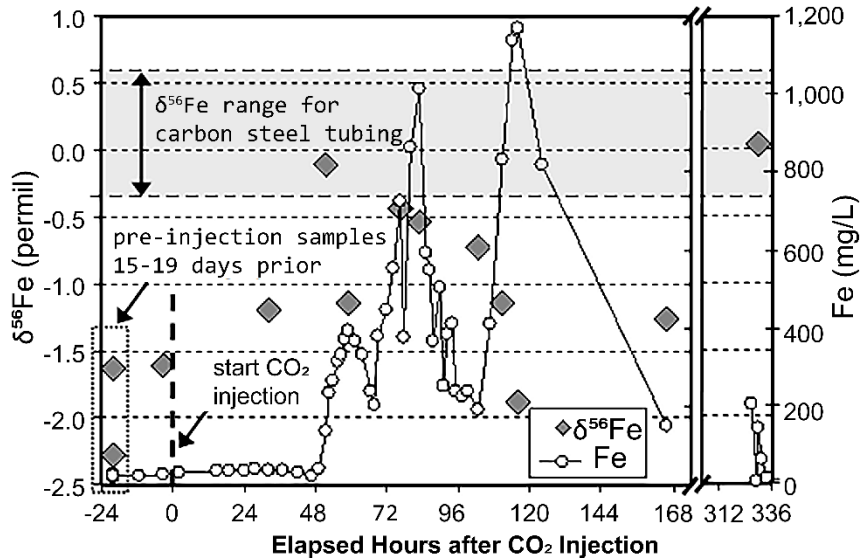


**Figure 89** - Concentrations of Fe and  $\delta^{56}\text{Fe}$  values for selected brine samples from Frio II. Samples with high Fe values following CO<sub>2</sub> injection have  $\delta^{56}\text{Fe}$  values that fall between those of the carbon steel tubing and pre-injection brine, indicating a mixed origin for dissolved Fe (Kharaka et al., 2010a).

### 11.4 Carbon Dioxide for EOR and Other Uses

The injection of CO<sub>2</sub> into oil fields to enhance recovery of oil has been practiced for many years. Western Canada has been at the forefront of large projects using CO<sub>2</sub> in EOR. The longest running fully documented project is in the Weyburn-Midale fields in

Saskatchewan. The CO<sub>2</sub> is purchased from the Great Plains Synfuels Plant of Dakota Gasification Company in Beulah, North Dakota. The gas is about 95 percent CO<sub>2</sub> and is transported through a 320-km pipeline to the Weyburn and Midale fields. Injection is into Mississippian carbonates with a total of about 30 Mega-tonnes (Mt) of CO<sub>2</sub> to be injected over the course of the project. Research into many aspects of the project is an international collaboration led by the Petroleum Technology Research Centre in Regina, Saskatchewan. The project started in 2000; the first five years are described by Wilson and Monea (2004). This was followed by an update covering research to 2012 (Hitchon, 2012).

One other large EOR research project concerned CO<sub>2</sub> injection into the Upper Cretaceous Cardium Formation at the Pembina Field, Alberta. This project was supported by the Alberta Government and involved staff from the Alberta Research Council, the Alberta Geological Survey, the University of Alberta, and the University of Calgary. The project ran from 2004 to 2008 and cost about \$ 4.25 M CAD. The summary report covers all aspects from regional and local geology, hydrogeology, seismic analysis, reservoir modeling, fluid and rock geochemistry, environmental monitoring, and the tools and techniques developed for the project (Hitchon, 2009).

EOR projects in the USA began in 1972; currently, 6 percent of oil production is from EOR operations with CO<sub>2</sub> sales for EOR reaching three billion cf/d in 2008 (US DOE, NETL, 2009); Moritis, 2009; Warwick et al., 2022). Commercial CO<sub>2</sub>-EOR projects worldwide have been increasing. By 2017, there were 166 EOR projects worldwide with ~80 percent in the USA, primarily in the Permian Basin of Texas and New Mexico (Kharaka et al., 2013; US EPA, 2019). Research indicates that CO<sub>2</sub>-EOR is a proven and cost-attractive technology for increasing oil production in maturing fields. Initially, a CO<sub>2</sub> slug is followed by injections of water and CO<sub>2</sub> into a depleted reservoir to obtain an additional 10 to 15 percent of original oil-in-place (Figure 90).

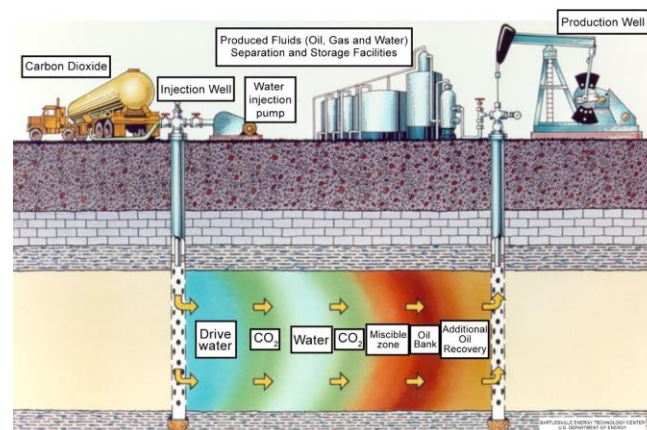


**Figure 90** - Carbon dioxide flooding reduces viscosity of the oil to provide a more efficient miscible displacement process for enhanced oil recovery (EOR) that is applicable to many reservoirs. The most feasible approach is an initial CO<sub>2</sub> slug in an injection well followed by alternating water and CO<sub>2</sub> injections. Then oil, produced water, and natural gas are obtained from a production well (sketch from US DOE, 2020).

Nichols and others (2014) report on the sources of CO<sub>2</sub> for EOR operations in the USA, which amounted to 58 million tonnes CO<sub>2</sub> in 2010. Production from natural accumulations of CO<sub>2</sub> accounted for 85 percent of the 2010 supply and natural gas accounted for 13 percent of the supply. The rate of CO<sub>2</sub> supply in 2015 was 93 million tonnes CO<sub>2</sub>, a 60 percent increase over the 2010 level. Hydrocarbon conversion facilities with CO<sub>2</sub> capture accounted for 36 percent of the growth between 2010 and 2015. Twenty-one CO<sub>2</sub> fields in the contiguous USA contain an estimated 311 Tcf of CO<sub>2</sub> gas in-place. Of that, 168 Tcf (54 percent) is estimated to be accessible and technically recoverable. The estimated economically recoverable resource (ERR) is 96.4 Tcf, based on a CO<sub>2</sub> price of \$ 1.06 USD/mcf (\$20 USD/ton) at the field gate. Cumulative production to date is 18.9 Tcf, leaving 77.5 Tcf remaining or net ERR. The Big Piney-LaBarge Field in Wyoming contains an estimated net ERR of 52 Tcf, 67 percent of the total for the USA. The remaining ERR lies in reservoirs that feed into the Permian Basin and Gulf Coast and comprises on the order of ten to twenty years of supply (Nichols et al., 2014).

Although CO<sub>2</sub> accumulations occur globally, those found in the western USA, particularly in the Colorado Plateau and adjoining Rocky Mountain regions, have received a great deal of interest in terms of application of various geochemical tools to assess the origin of CO<sub>2</sub> and its interaction with surrounding host rocks (e.g., Gilfillan et al., 2008; Moore et al., 2005; Nichols et al., 2014). At least nine producing or abandoned gas fields within or near the plateau region contain close to 100 Tcf of natural gas; a number of these are used for EOR (Allis et al., 2005). The dominant producing lithologies of the region are either limestone or sandstone. Mineralogically, it is noteworthy that Moore and others (2005) documented the formation of late-stage dawsonite and kaolinite from dissolution of carbonate cements and detrital feldspars in the Springerville-St. Johns CO<sub>2</sub> field along the Arizona-New Mexico border. Dawsonite (NaAlCO<sub>3</sub>(OH)<sub>2</sub>) is a phase predicted by various thermodynamic water-rock interaction codes (e.g., Johnson et al., 2004) and is thought to be one of the key carbonate phases to form during CO<sub>2</sub> injection into feldspar-bearing sandstones (Bénézech et al., 2007; Palandri et al., 2005).

In addition to using the captured CO<sub>2</sub> for EOR, it may be converted into products such as chemicals, plastics, fuels, building materials, and other commodities as noted by the Office of Fossil Energy's [Carbon Capture and Storage program](#) managed by the National Energy Technology Laboratory. This approach could be especially valuable in reducing carbon emissions in areas of the country where geologic storage of CO<sub>2</sub> is not practical. The use of the CO<sub>2</sub> for an industrial purpose can provide a potential revenue stream for CCUS facilities (National Energy Technology Laboratory, 2013). Until now, the vast majority of CCUS projects have relied on revenue from the sale of CO<sub>2</sub> to oil companies for EOR, but there are many other potential uses of the CO<sub>2</sub> including as a feedstock for the production of synthetic fuels, chemicals, and building materials.

CCUS technologies can provide a means of removing CO<sub>2</sub> from the atmosphere (i.e., *negative emissions*) to offset emissions from sectors in which reaching zero emissions may not be economically or technically feasible (Fujikawa et al., 2020). Bioenergy with carbon capture and storage (BECCS), involves capturing and permanently storing CO<sub>2</sub> from processes where biomass (which extracts CO<sub>2</sub> from the atmosphere as the biomass grows) is burned to generate energy. A power station fueled with biomass and equipped with CCUS is a type of BECCS technology. Direct air capture involves the capture of CO<sub>2</sub> directly from ambient air (as opposed to a point source). For example, the CO<sub>2</sub> can be used as a CO<sub>2</sub> feedstock in synthetic fuel, or it can be permanently stored to achieve negative emissions. These technology-based approaches for carbon removal can complement and supplement nature-based solutions, such as afforestation and reforestation.

Underground injection and storage of CO<sub>2</sub> has been proposed as a solution for mitigating CO<sub>2</sub> emissions into the atmosphere from stationary sources of burning fossil fuels. In this process, CO<sub>2</sub> is compressed into a supercritical fluid and injected underground for EOR or for geologic sequestration. Both operations use wells to place CO<sub>2</sub> into deep subsurface geologic formations, but they are regulated differently both by the US EPA and individual states (Jones, 2020). Recent discussions in the US Congress regarding underground carbon storage—including debate about tax credits for geologic sequestration and EOR CO<sub>2</sub> injection—have raised interest in the similarities and differences between these operations and associated regulations.

EOR is a process used in the oil industry since the 1970s whereby fluids are injected underground to increase production from partially depleted oil reservoirs, with CO<sub>2</sub> the most common injection fluid used in EOR projects. The CO<sub>2</sub> can be pumped out for reuse after injection, although some of the CO<sub>2</sub> remains trapped underground. In the USA there are more than 134,000 Class II EOR wells that inject 68 million tonnes/year (as of 2014) CO<sub>2</sub>. They are predominantly located in California, Texas, Kansas, Illinois, and Oklahoma. Unfortunately, most CO<sub>2</sub> injected for EOR comes from naturally occurring underground CO<sub>2</sub> reservoirs, but roughly 20 percent comes from industrial sources.

The CO<sub>2</sub> is typically injected into a partially depleted oil reservoir using the existing well infrastructure from the original oil production process. According to a 2019 National Energy Technology Laboratory report, between 30 percent and 40 percent of the CO<sub>2</sub> is generally considered to be stored after each injection cycle, depending on the reservoir characteristics. Geologic sequestration of CO<sub>2</sub> is considered to be long-term containment.

However, there are uncertainties and scientific gaps in our understanding of CO<sub>2</sub>-brine-mineral interactions under reservoir conditions because supercritical CO<sub>2</sub> is buoyant, displaces huge volumes of formation water, and becomes reactive when dissolved in the formation water (Benson & Cole, 2008; Kharaka et al., 2009). Dissolved CO<sub>2</sub> is likely to react with the reservoir and cap rocks, causing dissolution, precipitation, and

transformation of minerals, which changes the porosity, permeability, and injectivity of the reservoir and impacts the extent of CO<sub>2</sub> and brine leakage that, as noted by Kharaka and others (2009) and Benson and Cole (2008), could contaminate USDW. Reservoir capacity, performance, and integrity are strongly affected by four possible CO<sub>2</sub> trapping mechanisms (Benson & Cole, 2008; Benson & Cook, 2005; Friedmann, 2007):

1. *structural and stratigraphic trapping*, where the injected CO<sub>2</sub> is stored as a supercritical and buoyant fluid below a cap rock or adjacent to an impermeable barrier;
2. *residual trapping* of CO<sub>2</sub> by capillary forces in the pores of reservoir rocks away from the supercritical plume;
3. *solution trapping*, where CO<sub>2</sub> is dissolved in formation water forming aqueous species such as H<sub>2</sub>CO<sub>3</sub><sup>\*</sup>, HCO<sub>3</sub><sup>-</sup>, and CO<sub>3</sub><sup>-2</sup>; and
4. *mineral trapping*, with the CO<sub>2</sub> precipitated as calcite, magnesite, siderite, and dawsonite (Gunter et al., 1993; Palandri & Kharaka, 2005; Xu et al., 2010).

Initially, the bulk of injected CO<sub>2</sub> will be stored as a supercritical fluid because the target reservoirs are likely to have temperatures and pressures higher than 31 °C and 74 bar—the critical values for CO<sub>2</sub>. The injected CO<sub>2</sub> will rapidly dissolve in formation water that contacts the fluid, but mineral trapping—which would depend on the availability of reactive Ca, Mg, Fe, and other divalent cations in formation water or the reservoir rocks—could be slower, yet more permanent, because many carbonate phases can remain stable for geologically significant time periods (Gunter et al., 1993; Hitchon, 1996a; Palandri & Kharaka, 2005).

Understanding gas–water–mineral interactions in sedimentary basins could facilitate the isolation of anthropogenic CO<sub>2</sub> in the subsurface for thousands of years, thus moderating rapid increases in the concentrations of atmospheric CO<sub>2</sub> and mitigating global warming (Kharaka & Hanor, 2014; White et al., 2005). Given the economic benefits and more than 30 years of commercial application, it is expected that injection into depleted petroleum fields for EOR will be the earliest method of CO<sub>2</sub> disposal. However, as the amounts of CO<sub>2</sub> to be sequestered increase, deep saline aquifers will likely become preferred storage sites, because of their huge potential capacity and advantageous locations close to CO<sub>2</sub> sources (Hitchon et al., 1999a; Holloway, 2001). In addition to storage capacity, key environmental questions include CO<sub>2</sub> leakage related to the storage integrity and the physical and chemical processes that are initiated by injecting CO<sub>2</sub> underground (Hepple & Benson, 2005; Kharaka & Cole, 2011).

## 11.5 Monitoring CO<sub>2</sub> and Brine Leakage from Storage Sites

Carbon dioxide capture and storage in high-capacity geologic formations has become a promising approach for the stabilization of atmospheric CO<sub>2</sub> levels and global

temperatures (Bachu, 2003; Benson & Cook, 2005; White et al., 2003). As attractive as the capacity potential of geologic formations may be, environmental concerns and possible risks must be addressed. Leakage of CO<sub>2</sub> from the reservoir rocks via faults, fracture systems, or improperly abandoned boreholes is the main concern. Leakage of CO<sub>2</sub> into shallow groundwater could also occur via pathways created by mineral dissolution that results from the lowered pH of formation water in contact with the injected CO<sub>2</sub> (Hepple & Benson, 2005; Kharaka et al., 2009; Wells et al., 2007; White et al., 2005).

Laboratory and field studies suggest that in such scenarios, the increase in acidity will lead to dissolution of sulfide, carbonate, and iron oxyhydroxide minerals present in the rocks. Leakage of CO<sub>2</sub> into groundwater could initiate adsorption and desorption reactions that may mobilize hazardous trace elements such as Fe, Pb, U, As, and Cd into groundwater, with some possibly exceeding the MCLs mandated by the US EPA (Apps et al., 2011; Kharaka et al., 2009; Smyth et al., 2008; Wang & Jaffe, 2004).

### 11.5.1 Subsurface Monitoring at the Frio Site, Texas

Monitoring at and close to the ground level for CO<sub>2</sub> and brine leakage into soil gas and shallow (~30 m depth) groundwater was not effective at the Frio site, primarily because of perturbation caused by injection operations (Kharaka et al., 2009; Everett et al., 2020). Because of such difficulties, and the long time that would be required for a potential CO<sub>2</sub> and/or brine leakage to reach the surface, a rigorous program for deep subsurface monitoring was carried out. Results of brine and gas analyses of fluid samples obtained from the "B" sandstone, that was perforated and sampled six months after CO<sub>2</sub> injection, showed the following:

- slightly elevated concentrations of bicarbonate, Fe, and Mn;
- significantly depleted  $\delta^{13}\text{C}$  values (-17.5 to -5.9 permil versus ~-4 permil) of dissolved inorganic carbon (Figure 91); and
- somewhat depleted  $\delta^{18}\text{O}$  values of brine (Figure 92), relative to pre-injection values obtained for the "C" samples.

A more definitive proof of the migration of injected CO<sub>2</sub> into the "B" sandstone was obtained from the presence of the two Perfluorocarbon tracers PFT (PMCH and PTCH) that were added to the injected CO<sub>2</sub> and migrated with the initial CO<sub>2</sub> breakthrough (Phelps et al., 2006). Additional proof of the migration of injected CO<sub>2</sub> into the "B" sandstone is obtained from the high concentration (2.9 versus to 0.3 percent) of CO<sub>2</sub> in dissolved gas obtained from one of the two downhole Kuster samples (Table 49).

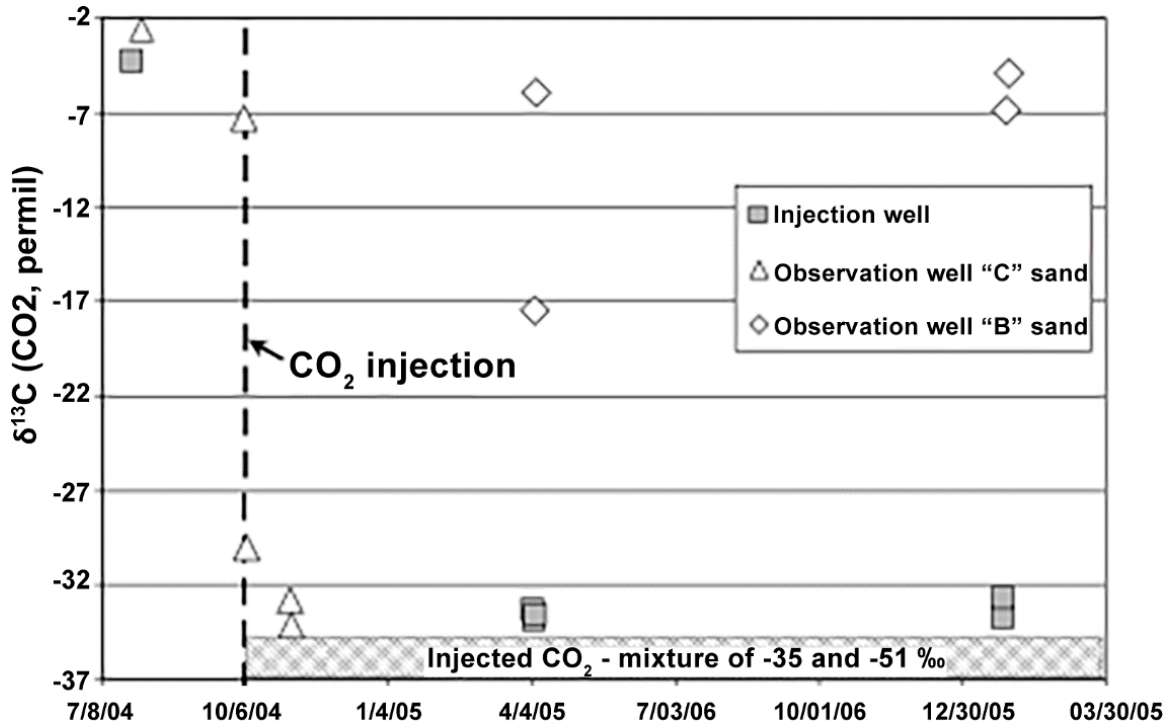


**Figure 91** - The  $\delta^{13}\text{C}$  values of dissolved inorganic carbon in Frio I samples obtained before, during and after  $\text{CO}_2$  injection. Values obtained from the "C" sandstone following  $\text{CO}_2$  injection are highly depleted relative to those before injection. The  $\delta^{13}\text{C}$  values obtained from the "B" sandstone show some depletion, especially in samples collected six months after completion of injection (Kharaka et al., 2009).

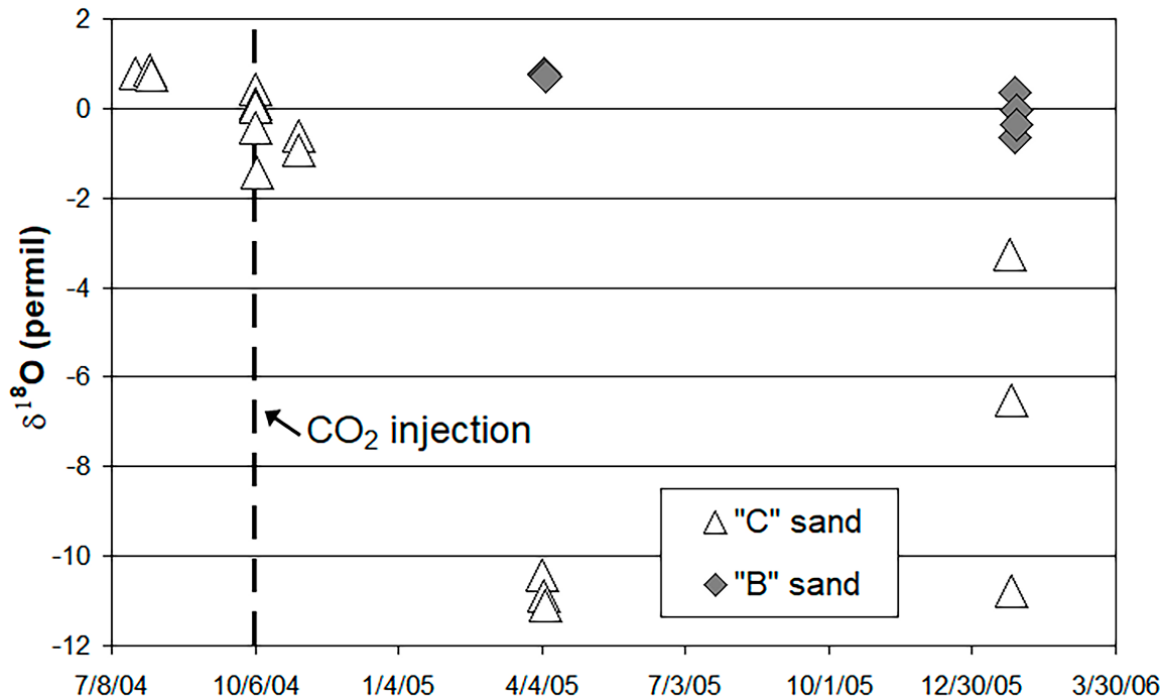


**Figure 92** - The  $\delta^{18}\text{O}$  values of Frio I brine samples collected before, during and after  $\text{CO}_2$  injection. Values obtained from the "C" sandstone following  $\text{CO}_2$  injection are depleted relative to those before injection. The  $\delta^{18}\text{O}$  values obtained from the "B" sandstone show some depletion, especially in samples collected fifteen months after completion of injection (Kharaka et al., 2009).

Results of samples collected from Frio "B" approximately fifteen months after CO<sub>2</sub> injection, gave brine and gas compositions that are similar to those obtained from the "C" sandstone before CO<sub>2</sub> injection (Figure 86). The  $\delta^{13}\text{C}$  values of dissolved inorganic carbon (Figure 91) and the  $\delta^{18}\text{O}$  values of brine (Figure 92) are slightly depleted in the heavy isotopes relative to pre-injection values obtained for the "C" samples. These overall results indicate the absence of significant amounts of injected CO<sub>2</sub> in the "B" fluids sampled.

However, a contrary conclusion is indicated from the fact that PMCH and PTCH were measured in the six samples also analyzed for PFT tracers (Phelps et al., 2006). It is possible that the PMCH and PTCH measured in January 2006 represent desorbed PFT tracers introduced into "B" earlier so their presence does not require migration of additional injected CO<sub>2</sub> into the "B" sandstone.

Results from the "B" sandstone show some CO<sub>2</sub> migration from the "C" sandstone after about six months following injection. These results can neither be used to estimate the volume of CO<sub>2</sub> that migrated to "B" nor the path of migration, but they highlight the importance of subsurface monitoring for detecting early leaks (Kharaka et al., 2009). These results are comparable to those observed at Sleipner, where CO<sub>2</sub> is injected into the bottom of the Utsira sandstone but has migrated through intervening shale beds (one of the shale beds is extensive and ~5 m thick) into nine different sandstone layers. Results from seismic investigations show that no CO<sub>2</sub> is leaking out of the cap rocks at Sleipner (Bickle, 2009; Chadwick et al., 2004). Leakage of CO<sub>2</sub> injected into the Shatuck sandstone (Permian) in a pilot study similar to Frio was detected at the surface at the West Pearl Queen Field, New Mexico, where 2,090 tons of CO<sub>2</sub>, tagged with perfluorocarbon tracers (PFTs), were injected at a depth of 1,400 m. Using an array of PFTs capillary absorption tubes placed 2 m below ground, a leakage rate of 0.009 percent of injected CO<sub>2</sub> per year was measured by Wells and others (2007).

### 11.5.2 Near Surface Monitoring at the ZERT Site, Bozeman, Montana

The ZERT facility was developed at a field site close to Bozeman, Montana, USA, to allow controlled studies of near-surface CO<sub>2</sub> transport and detection technologies. The ZERT site is located on a relatively flat 12-hectare agricultural plot close to the Montana State University campus in Bozeman. At this site, the topsoil of organic-rich silt and clay with some sand ranges in thickness from 0.2 to 1.2 m, with a caliche layer, high in calcite (~15 percent) at depths of ~0.5 to 0.8 m.

Beneath the topsoil layer is a cohesionless deposit of coarse sandy gravel extending to 5 m, the maximum depth investigated (Spangler et al., 2009). Gravels comprise ~70 percent of rock volume; andesite is the chief rock fragment among the gravels and coarse sands, but there are also minor amounts of detrital limestone and dolostone. The sand- and silt-sized fraction of this sediment consists of approximately 40 percent quartz,

40 percent magnetite and magnetic rock fragments, and 20 percent grains of amphibole, biotite/chlorite, and feldspar.

A slotted horizontal pipe (well) divided into six zones was installed horizontally 2 to 2.3 m deep. Controlled releases of CO<sub>2</sub> tagged with PFTs and other tracers were administered via the horizontal pipe in the summers of 2007, 2008, and 2009. A wide variety of detection techniques, including soil gas flux, composition and isotopes, eddy covariance measurements, hyperspectral and multispectral imaging of plants, and differential absorption measurements using laser-based instruments were deployed by many collaborators from many institutions. Even at relatively low CO<sub>2</sub> fluxes, most techniques were able to detect elevated levels of CO<sub>2</sub> in the soil or atmosphere. Additionally, modeling of CO<sub>2</sub> transport and concentrations in the saturated soil and vadose zone was successfully conducted. Details of the study program are provided by Spangler and others (2009).

As part of this multidisciplinary research, the USGS team carried out a study with the main objective to investigate changes in the concentrations of major, minor, and trace inorganic and organic compounds during and following CO<sub>2</sub> injection (Kharaka et al., 2010b). Kharaka and colleagues obtained 80 samples of water during the 2008 summer season from ten shallow monitoring wells (1.5 or 3.0 m deep) installed 1 to 6 m from the injection pipe and from two distant monitoring wells (Figure 93). Approximately 300 kg/day of food-grade CO<sub>2</sub> was injected through the perforated pipe between July 9th and August 7th, 2008, at the field test site. Samples were collected before, during, and after CO<sub>2</sub> injection. The injected CO<sub>2</sub> flows mainly upward and to the right, in the direction of groundwater flow (Figure 94).

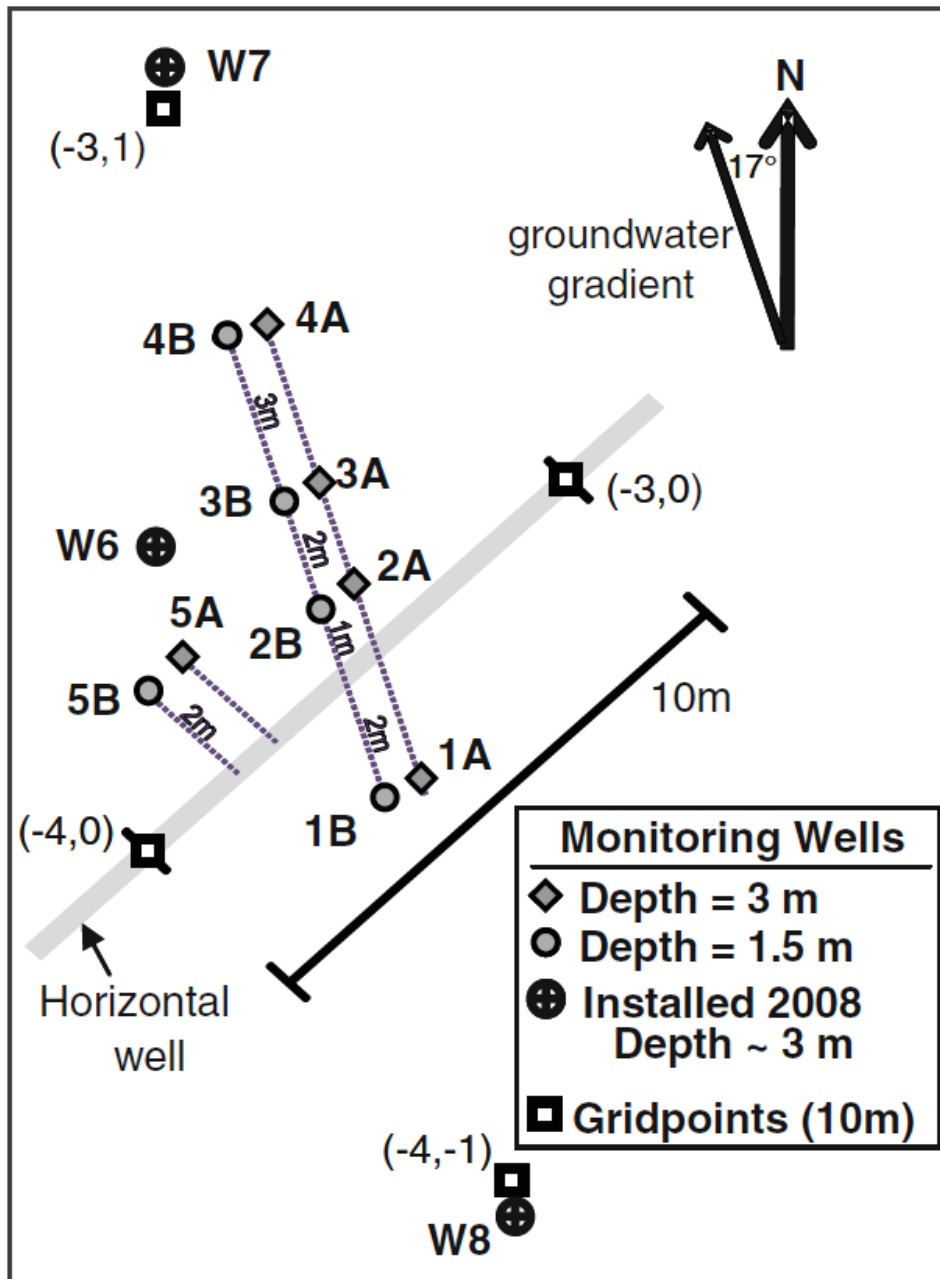


**Figure 93** - Map of the locations of the water-monitoring wells in relation to the surface trace of the slotted horizontal CO<sub>2</sub> injection pipe in zone VI of the ZERT site (Kharaka et al., 2010).

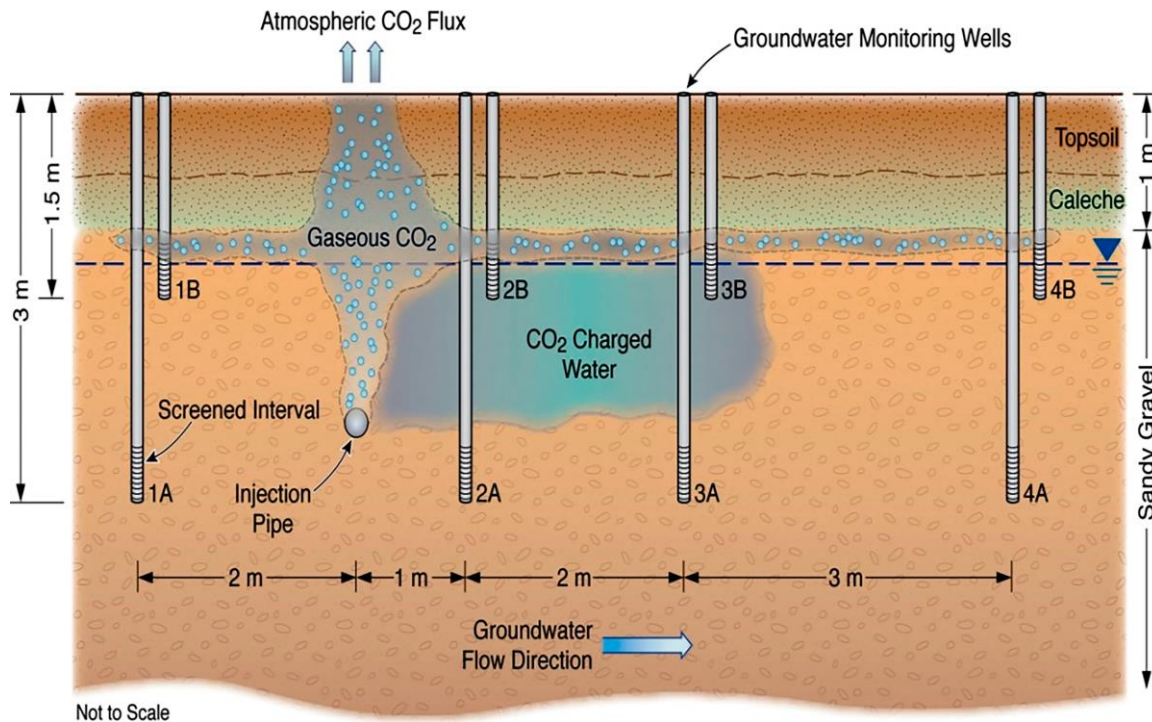


**Figure 94** - Schematic of the CO<sub>2</sub> plume in selected water-monitoring wells at the ZERT site (Kharaka et al., 2010).

### 11.5.3 Dissolved Inorganic Chemicals

The chemical data for samples collected prior to CO<sub>2</sub> injection show that the groundwater at the ZERT site is a Ca – Mg – Na – HCO<sub>3</sub> type water, with a fresh-water salinity of about 600 mg/L (sample collected 7/8/2008, Table 50). The groundwater has a pH of approximately 7 and HCO<sub>3</sub><sup>-</sup> is the dominant anion, but the concentrations of Cl<sup>-</sup> and SO<sub>4</sub><sup>2-</sup> are relatively low. The concentrations of Fe, Mn, Zn, Pb, and other trace metals are expectedly low at ppb levels.

**Table 50** - Chemical composition of water samples obtained from the ZERT monitoring well 2B in 2008 before and following CO<sub>2</sub> release (from Kharaka et al., 2010b).

Sample No.	ZRT-2B	ZRT-2B	ZRT-2B	ZRT-2B	ZRT-2B
Date (m/dd/yyyy)	7/8/2008	7/12/2008	7/17/2008	7/19/2008	7/23/2008
<b>~1.5 m depth</b>					
EC (µS/cm)	651	952	1,193	1,342	1,424
pH	7.04	6.4	5.91	5.97	5.96
<b>Major solutes (mg/L)</b>					
HCO <sub>3</sub>	434	664	924	1120	1150
Na	9.1	9.7	9.5	9.9	10.2
K	5.4	7.1	8.0	7.4	7.4
Mg	28.0	40.8	48.8	54.6	54.9
Ca	91.9	141.9	191.0	223.0	239.0
Sr	0.30	0.45	0.63	0.57	0.69
Ba	0.10	0.19	0.27	0.26	0.23
Mn	0.0	0.2	0.13	0.14	0.01
Fe	0.0	0.08	0.39	0.5	0.0
F	0.01	0.08	0.39	0.53	0.03
Cl	5.35	5.31	5.47	5.55	5.54
Br	0.04	0.05	0.05	0.05	0.06
NO <sub>3</sub>	0.26	0.12	0.20	0.20	0.25
PO <sub>4</sub>	0.10	0.05	0.02	0.02	0.24
SO <sub>4</sub>	7.17	7.39	7.69	7.77	8.35
SiO <sub>2</sub>	32.3	40.3	43.7	37.3	38.1
TDS	614	917	1,234	1,468	1,516
<b>Trace solutes (µg/L)</b>					
Al	3.3	5.2	6.8	5.8	6.0
As	1.32	1.05	1.32	0.42	0.88
B	0.0	0.0	0.0	0.0	0.0
Cd	0.29	0.45	0.61	0.4	0.2
Co	0.38	1.18	1.24	1.17	0.45
Cr	11.58	53.88	71.55	21.15	7.16
Cu	2.48	2.27	2.65	2.17	2.37
Li	7.0	9.1	8.2	7.7	7.5
Mo	0.66	0.51	0.54	0.51	0.50
Pb	0.06	0.08	0.1	0.1	0.1
U	4.28	3.83	4.52	4.28	4.12
Zn	3.80	8.96	3.24	2.34	2.84

Following CO<sub>2</sub> injection, field measured pH values decreased systematically to values around 6.0; early response (within one day) occurred in well 2B, only 1 m from the injection pipe and in the direction of groundwater flow, with pH decreasing to 5.7 (Figure 95). The pH of water for samples from well 4B (6 m from pipe) started decreasing after three days following CO<sub>2</sub> injection, but pH values remained above pH 6.0 (Figure 95). The measured pH values of groundwater were controlled primarily by pCO<sub>2</sub>, which was measured by Strazisar and others (2008) in capped wells and computed with SOLMINEQ (Kharaka et al., 1988) using the measured temperature, pH, alkalinity, and other chemical parameters. The pCO<sub>2</sub> values measured and computed for the ZERT samples were 0.035 bar before CO<sub>2</sub> injection; they increased to values close to 1.0 bar following CO<sub>2</sub> injection. These results show that pH is an excellent early indicator for detection of CO<sub>2</sub> intrusion into groundwater at this and similar sites.

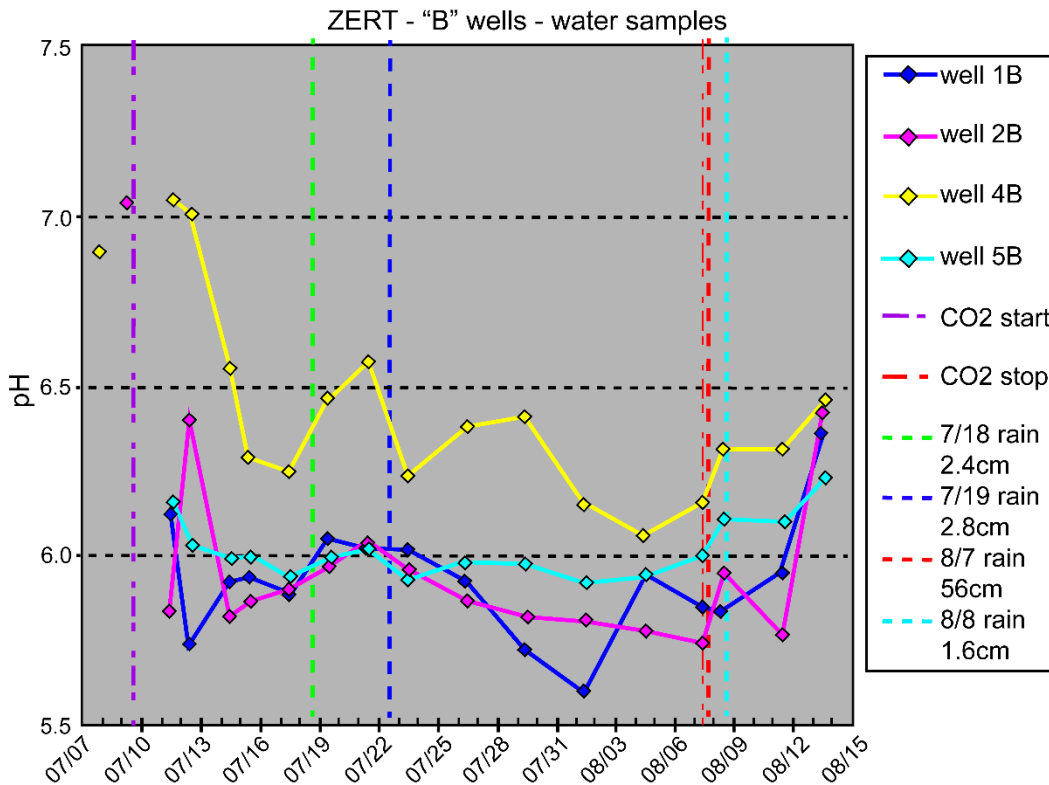


**Figure 95** - Results of pH measurements in water samples obtained from the shallow monitoring wells (B) at the ZERT site before and following CO<sub>2</sub> release (Kharaka et al., 2010).

The alkalinity of groundwater increased from about 400 mg/L as HCO<sub>3</sub> to 1330 mg/L, following CO<sub>2</sub> injection (Figure 96). Alkalinity values for different wells, as with the pH values, show variable trends reflecting distance from the CO<sub>2</sub> injection pipe, impacts from precipitation events, and possibly local variations in the mineral composition of soils and sediments. Values for the EC show similar trends as alkalinity, increasing from ~600 μS/cm before CO<sub>2</sub> injection to ~1,800 μS/cm following CO<sub>2</sub> injection (Figure 97). EC and

alkalinity, as with pH, are easily measured field parameters that could provide early detection of CO<sub>2</sub> leakage into shallow groundwater from deep storage operations.

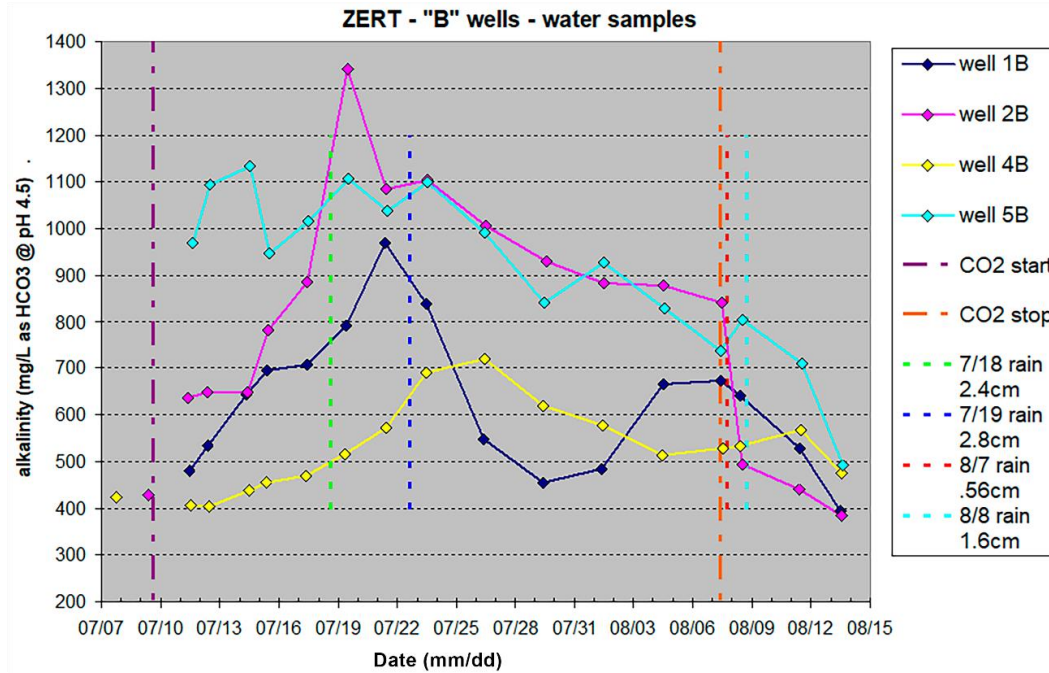


**Figure 96** - Results of alkalinity measurements in water samples obtained from shallow monitoring wells (B) at the ZERT site before and following CO<sub>2</sub> release (Kharaka et al., 2010).

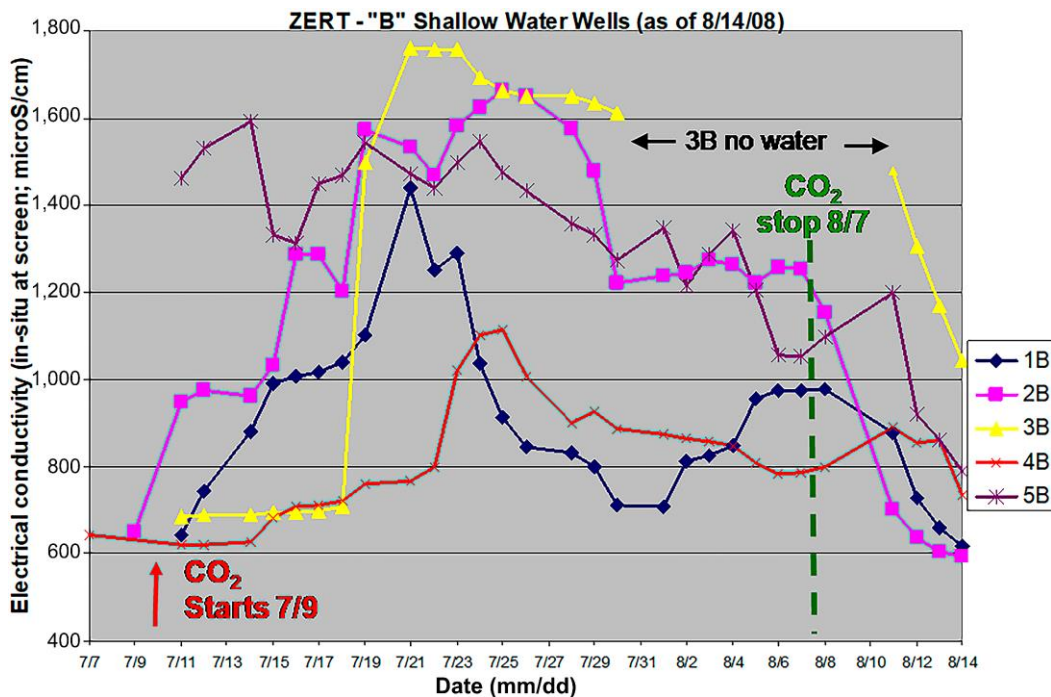
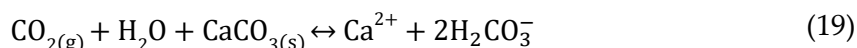


**Figure 97** - Results of EC measurements of water samples obtained from shallow monitoring wells (B) at the ZERT site before and following CO<sub>2</sub> release (Kharaka et al., 2010).

The alkalinity increases following CO<sub>2</sub> injection are balanced primarily by increases in the concentrations of Ca and Mg, whereas the concentrations of Na (10 ±2 mg/L) are

relatively constant. The concentrations of Ca increase from ~80 to 240 mg/L and those for Mg from ~25 to 70 mg/L. Dissolution of both calcite as shown in Equation (19), and dolomite as shown in Equation (20), are required to explain the changes in alkalinity and concentrations of Ca and Mg (Table 50).



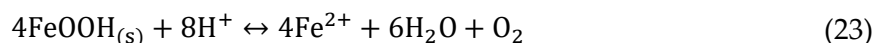
These conclusions are supported by the initial characterization of minerals in core samples that show that calcite is abundant in a caliche layer observed at depths of ~0.5 to 0.8 m. Traces of carbonates were also observed in fines at depths shallower than 2.5 m; minor amounts of detrital limestone and dolostone were observed in the gravel section. Results of geochemical modeling with SOLMINEQ (Kharaka et al., 1988) also support dissolution of calcite and disordered dolomite as possible reactions at all pH values. Desorption-ion exchange reactions on clay minerals with  $\text{H}^+$  have been suggested as an alternative explanation (Zheng et al., 2009) for the increases in the concentrations of Ca and Mg.

The concentrations of Fe and Mn, the two most abundant trace metals in groundwater, also increase following  $\text{CO}_2$  injection. Increased concentrations of Fe could reflect dissolution of several Fe(II) and Fe(III) minerals including siderite and ferrihydrite, depicted in Equations (21) and (22), respectively. The concentration of Fe in groundwater is a strong function of Eh, which was measured in water from the deeper wells not impacted by  $\text{CO}_2$  injection (150 to 200 mV) and indicate oxidizing conditions that account for the low concentration of dissolved Fe; much higher Fe values are possible under reducing conditions because of the higher solubility of Fe(II) minerals (Hem, 1985). The Fe concentrations increase from ~5 to 1200 ppb but show very low values between July 20th and July 26th, 2008, following significant precipitation events even when pH values were low.



Dilution alone cannot explain the low Fe concentrations, but they can be attributed to oxidizing conditions that may have been caused by increased dissolved  $\text{O}_2$  content in groundwater transported with percolating water from precipitation events. Ion exchange reactions on clays with  $\text{H}^+$  and major dissolved cations such as Ca, Mg, and Na, are other possible controls on Fe concentrations (Jenne, 1968; Zheng et al., 2009).

Geochemical modeling indicates the large increases observed in concentrations of Fe could result from dissolution of siderite as in Equation (21) but are most likely caused by dissolution of iron oxyhydroxides, as depicted in redox-sensitive reactions Equations (23) and (24).



The concentration of Mn shows similar trends to those of Fe, increasing from ~5 to 1,400 ppb following CO<sub>2</sub> injection, but also having low values between July 20th and July 26th.

The concentrations of Pb, As, Zn, and other trace metals (Table 50) generally show an increase with increasing alkalinity (lower pH value) following CO<sub>2</sub> injection. The values reported, however, carry high uncertainties as they are, in some cases, close to the analytical detection limit. The concentration increases are likely caused by desorption-ion exchange reactions with H<sup>+</sup>, Ca, and Mg resulting from lowered pH values (Zheng et al., 2011). The concentrations, it should be noted, are all significantly below the MCLs for the respective trace metals (e.g., 15 ppb for Pb, 6 ppb for As; US EPA, 2009). The initial values and the increases in concentrations of these trace metals, although small, are readily measured by the sampling and analytical methods used in this study.

The chemical changes observed in the ZERT groundwater are similar in trends, though much lower in concentration, to the changes observed in the Frio Brine Pilot tests discussed earlier in this section. The differences between pH results from Frio (pH as low as 3) and ZERT results are related to several geochemical parameters, but one important reason for the difference relates to the subsurface pCO<sub>2</sub> value for Frio of approximately 150 bar (Kharaka et al., 2009) compared to the pCO<sub>2</sub> value measured (Stratizar et al., 2008) and computed with SOLMINEQ (Kharaka et al., 1988) for the ZERT samples, which ranged from 0.035 to ~1 bar.

The maximum amount of CO<sub>2</sub> dissolved in water is a strong function of fluid pressure. Field determinations showed rapid and systematic changes in pH (7.0 to 5.6), alkalinity (400 to 1300 mg/L as HCO<sub>3</sub>) and EC (600 to 1800 μS/cm). These easily monitored and sensitive chemical changes could provide early detection of CO<sub>2</sub> leakage into shallow groundwater from deep storage operations. Laboratory results could be used to confirm such leaks.

#### 11.5.4 Carbon Isotopes

The isotopic composition of carbon was measured by Fessenden and others (2009, 2010) on dominant plants, soil cores (from 0 to 70 cm depth), dissolved inorganic carbon in groundwater, and in the local and regional CO<sub>2</sub>. The δ<sup>13</sup><sub>‰</sub>C values were measured during

several seasons before and during CO<sub>2</sub> releases. Results show that the dominant vegetation has a C-isotope signature typical of C<sub>3</sub> plants, with values for grasses and alfalfa as low as –25 permil and –29 permil, respectively. Once the CO<sub>2</sub> was released in the 2007 experiment, vegetation growing over the pipe and as far as 7 m to the north of the pipe experienced a change in δ<sup>13</sup>C signatures. The δ<sup>13</sup>C of the CO<sub>2</sub> released from the tank was –52 permil and the δ<sup>13</sup>C of the leaf tissues became increasingly depleted over the course of the experiment.

The soils remained constant through each of the experiments, but the δ<sup>13</sup>C signature of the soil column became enriched in <sup>13</sup>C with depth. Groundwater showed a CO<sub>2</sub> signature from the tank with a depletion of <sup>13</sup>C in the dissolved inorganic carbon that was observed within a day of the release and as far as 6 m north and down gradient from the pipe. The local air showed a CO<sub>2</sub> tank signature within one day of the release. This experiment showed that C-isotope analysis in the carbon reservoirs was a useful tool to detect CO<sub>2</sub> seepage either within days or weeks of release (Fessenden et al., 2010; Spangler et al., 2009).

## 11.6 Potential Environmental Impacts and Health Risks

The potential major environmental risks associated with a CO<sub>2</sub> storage site include induced seismicity in vulnerable locations and leakage of CO<sub>2</sub> and brine that may impact groundwater and other natural resources or cause harm to humans, animals, and ecosystems (Meckel et al., 2023; US EPA, 2020). Fluid leakage could occur along unmapped fracture systems and faults, improperly sealed abandoned and orphaned wells (Nordbotten et al., 2009; Celia et al., 2006), corroded well casings and cements (Carey et al., 2007), or even via pathways created in the rock seals as a result of CO<sub>2</sub>-brine-rock interactions (Figure 98) (Kharaka et al., 2006a; 2009). Maintaining reservoir integrity that limits CO<sub>2</sub> leakage to very low levels (less than 0.01 percent) is essential to the long-term success of injection operations (Hepple & Benson, 2005). Preventing brine migration into overlying drinking water supplies is equally important because dissolution of minerals following CO<sub>2</sub> injection would mobilize Fe, Mn, and other metals, as well as toxic organics, including BTEX, phenols, and other toxic compounds observed in the Frio Brine tests (Kharaka et al., 2009).



Furthermore, CO<sub>2</sub> could migrate into other strata, with the potential for contaminating potable groundwater or causing other problems. If the formation into which CO<sub>2</sub> is injected is below the seabed, leakage of CO<sub>2</sub> into the marine environment could affect ocean pH and chemistry and have potentially serious consequences for marine life.

Results from the Frio Brine tests indicate that the injected supercritical CO<sub>2</sub>, which is a very effective solvent for organic compounds (Kolak & Burruss, 2006), could mobilize and transport organics including BTEX, phenols, PAHs, and other toxic organic compounds that have been reported in relatively high concentrations (10 to 60 mg/L) in oil field brine (Kharaka & Hanor, 2014; Kharaka et al., 2009). Preventing brine migration into overlying potable groundwater is equally important because dissolution of minerals following CO<sub>2</sub> injection would mobilize Fe, Mn, and other metals in addition to the high concentration of other chemicals present in the original brine having salinity from 5,000 to more than 200,000 mg/L (Kharaka & Hanor, 2014).

Additional risks could arise from potential damage to nearby hydrocarbon resources caused by the displacement of fluids by the injected CO<sub>2</sub> such as saline water production at wells that had been producing oil or gas. Finally, if a project does not operate within prescribed injection rates and pressures, there is the potential for initiating seismic activity (Friedmann, 2007). This implies that injection sites should not be located near major active faults (such as the San Andreas fault in California) because results from recent simulations indicate that large earthquakes along such faults would cause intense ground motions leading to rock fracturing and possible CO<sub>2</sub> leakage over large areas (up to 300 by 50 km) (US Geological Survey, 2008).

### 11.6.2 Health and Safety Concerns

Information on the responses of humans, animals, and plants to elevated and potentially hazardous levels of CO<sub>2</sub> and associated low levels of oxygen is provided by Deel and others (2006), National Institute of Occupational Safety (NIOSH/OSHA; 1981), and US EPA (2020). They have determined that human time-weighted average (8 hours TWA) exposure limits to CO<sub>2</sub> of 1 percent (10,000 ppm), and short-term exposure limit (15-minute STEL) of 3 percent are appropriate maximum exposure values (NIOSH/OSHA, 1981, 1989). Human exposure to levels to CO<sub>2</sub> higher than these limits can be hazardous in two ways: by a reduction in the oxygen content of the ambient air causing hypoxia or through direct CO<sub>2</sub> toxicity.

In most cases of hazardous CO<sub>2</sub> exposure, the gas is presumed to act as a simple asphyxiant. However, extensive research indicates that exposure to elevated CO<sub>2</sub> concentrations higher than 3 percent has significant effects— including kidney damage— before oxygen dilution becomes physiologically significant. Concentrations higher than 10 percent have caused difficulty in breathing, impaired hearing, nausea, vomiting, a strangling sensation, sweating, and loss of consciousness within fifteen minutes. As O<sub>2</sub>

concentration drops below 17 percent, increasingly severe physiological effects occur until, at below 6 percent  $O_2$ , loss of consciousness is rapid and death takes place within minutes.

Another potential safety problem could result from accidents at facilities required to capture, condense, transport, and inject the  $CO_2$ . If  $H_2S$  is sequestered along with  $CO_2$ , health risks are significantly increased as  $H_2S$  is highly toxic. Also, the health impacts would increase substantially if significant amounts of BTEX, PAHs, and other mobilized organics are carried with the leaking  $CO_2$  (Kharaka et al., 2009).

To minimize the environmental hazards and risks associated with  $CO_2$  storage, a rigorous program should be implemented for the measurement, monitoring, and verification (MMV) of the injected  $CO_2$  and associated brine (Benson & Cook, 2005; Doughty et al., 2008; Friedmann, 2007). MMV is concerned with the capability to measure the amount of  $CO_2$  stored at a specific sequestration site, map its spatial disposition through time, develop techniques for surface and subsurface monitoring for the early detection of leakage, and verify that the  $CO_2$  is stored or isolated as intended and will not adversely impact the host ecosystem including potable groundwater. MMV for geologic sequestration consists of three parts:

1. modeling and analysis of the geology and hydrology of the total injection system before injection occurs;
2. tracking and monitoring the movement of the  $CO_2$  plume; and
3. above-surface measurements that verify the  $CO_2$  remains sequestered (US EPA, 2020).

Optimization of the MMV technologies is needed to ensure the full range of spatial and temporal scales are covered. Results from pilot studies highlight the importance of using the more sensitive geochemical markers (Kharaka et al., 2006a, 2009; Wells et al., 2007) and the importance of subsurface monitoring for detecting any early leakage of injected  $CO_2$  and brine to minimize damage to groundwater and the local environment.

## 11.7 Exercises Pertinent to Section 11

[Link to Exercise 25](#) ↴

[Link to Exercise 26](#) ↴

## 12 Summary and Wrap Up

Water is an essential resource throughout the world and maintaining its quality is of utmost importance to safeguard the health of the public and the environment. Currently, more than two billion people live without adequate safe drinking water and the number is likely to grow in the future due to increased population, poor water management, and climate change (UN, 2021). Groundwater, is the source for domestic use by approximately half the world's population. Of all the fresh water on the planet (excluding polar ice caps), 95 percent is groundwater. Therefore, groundwater must play a major role in alleviating the current and future global water stress, which requires science-based groundwater assessment, management, and protection from all sources of contamination.

Energy is also an essential commodity that powers the expanding global economy. Starting in the 1950s, oil and natural gas became the main sources of energy for the rapidly increasing world population; their dominance continues today and likely will continue in the near future. Oil and gas reservoirs, in contrast to aquifers, are generally located thousands of meters below ground level and deep wells drilled through one or more aquifers are required to produce the resource. Groundwater protection techniques have long played a crucial role in protecting environmental and human health during oil and gas production (Allison & Mandler, 2018).

The clear benefits of hydrocarbons, coal, oil, and natural gas consumption, however, carry major detrimental health and environmental impacts that range from local to global in scale (Kharaka & Otton, 2007; US EPA, 2019). Global impacts include air pollution and the interrelated global warming that results from continued addition to the atmosphere of large and increasing amounts of CO<sub>2</sub> obtained largely from the burning of fossil fuels. This is discussed but not addressed in detail in this book, and neither are the details of major pollution from large oil spills or major well blowouts such as the 2010 Deepwater Horizon disaster in the Gulf of Mexico (NOAA, 2020).

This book is devoted primarily to environmental impacts on groundwater that occur during exploration for and production of oil and natural gas including coal-bed natural gas. These operations have caused detrimental impacts to air, soil, surface water, groundwater, and ecosystems in the USA and throughout the world (e.g., Kharaka & Hanor, 2014). These impacts have arisen primarily from the improper disposal of some of the large volumes of saline water produced with oil and gas, from petroleum blowouts and accidental hydrocarbon and produced water releases, and from abandoned oil wells that were orphaned or not correctly plugged (Kharaka & Otton, 2007; Veil, 2020). Over the past twenty years, impacts have increased dramatically in the USA from production of oil and natural gas from shale and tight reservoirs that require the injection of large volumes of water with added proppant and chemicals at fluid pressures high enough to fracture the rocks (US EPA, 2021).

Impacts and ground surface disturbances, on the order of a few hectares per well, have arisen from related activities such as site clearance, construction of roads, tank batteries, brine pits and pipelines and other land modifications necessary for the drilling of exploration and production wells and construction of production facilities, especially in “sensitive” areas. The cumulative impacts from these operations are high because, for example, about five million oil and gas wells have been drilled in the USA, although only about 900,000 are currently in production (IHS, 2021).

## 12.1 Summary of the Three Major Parts of this Book

The first three sections of this book include introductory remarks provided in Section 1, which is followed by an introduction to the oil and natural gas industry that describes its history as well as how petroleum and produced water are brought to the surface with wells drilled into conventional and unconventional sources of energy. We summarize the history of petroleum production and the management of produced water in the USA. Although oil and natural gas may themselves contaminate potable groundwater, we emphasize contamination of groundwater by produced water.

In Sections 4 through 9, we describe the chemical and isotopic compositions of produced water obtained mainly from conventional sources of energy through discussion of two comprehensive geochemical data sets. One data set is from the Alberta Basin (Hitchon, 2023); the other is from petroleum fields and basins in the USA (Blondes et al., 2019; Kharaka and Hanor, 2014). This information is compared and contrasted with chemical and isotopic data from average groundwater that shows how much average groundwater chemistry differs from produced water chemistry. We discuss the organic and inorganic chemicals and isotopes that are toxic to human health and the environment as well as those that could provide unique criteria for distinguishing contamination from petroleum sources. We devote Section 9 to describing the geochemistry of formation water in basins with major salt domes. These basins are found worldwide and are major controls on the composition and movement of formation water that is an important potential contaminant of local groundwater.

The third part of this book, Sections 10 and 11, is the most important because it describes the pathways through which groundwater may be contaminated by produced water and petroleum. Section 10 provides case studies of groundwater contaminated by produced water and petroleum in several existing oil fields as well as in legacy sites where petroleum production ended many years ago (Hanor, 2007; Kharaka & Otton, 2007). We also discuss groundwater contaminated by crude oil from a pipeline at Bemidji, Minnesota, where extensive remediation efforts have failed to completely remove oil and toxic chemicals from the groundwater (Delin et al., 2020). Section 11 covers the important topic of CCUS. We provide results from the Frio (Texas) injection field study and the ZERT (Montana) monitoring case study (Kharaka & Hanor, 2014). We also discuss the major

environmental risks associated with CO<sub>2</sub> storage sites that, potentially, may include induced seismicity in vulnerable locations and leakage of CO<sub>2</sub> and brine that may damage groundwater and other natural resources or cause harm to humans, animals, and ecosystems (Kharaka & Hanor, 2014; US EPA, 2020).

## 12.2 The Importance of Produced Water

Produced water containing petroleum hydrocarbons from oil field operations has been a major source of groundwater contamination at thousands of sites across the USA and the world (e.g., Kharaka & Otton, 2007). From 1859 to about 1950s, oil producers in the USA disposed of their saline produced water simply by letting their wastewater run freely over natural channels into streams, rivers, and lakes. Some of the wastewater percolated into and contaminated groundwater (Gorman, 1999).

In general, disposal of this saline water was not a major concern until the 1960s when the total volume of produced water increased as oil production increased. By 1965, 23 million bbl/d (3.65 million m<sup>3</sup>/d) of water was generated with 7.67 million bbl/d (1.22 million m<sup>3</sup>/d) of oil, for a W/O ratio of 3.0 (Gorman, 1999). As expected, the W/O ratio today is approximately 10 because the ratio from a given field generally increases as the years of production increase.

The W/O ratios in petroleum fields in Saudi Arabia and other countries are generally much lower than the values in the USA because petroleum fields in those countries generally have not had as many years of production to deplete the reservoirs. For example, in 2015, the global volume of produced water was 310 million bbl/d (~50 million m<sup>3</sup>/d) and the W/O ratio was only 3.8 (Fakhru'l-Razi et al., 2014).

The W/O ratio in the USA is highly variable from state to state and even in fields from the same state. The highest W/O ratios are obtained in states that have fields that have been producing petroleum for a long time and have limited unconventional petroleum production. For example, Kansas had a high ratio of 33.6 in 2017; California—with increasing production starting in 1865—had a W/O ratio of 18 in 2017 (Kharaka et al., 2019; Veil, 2020). The W/O ratio in Colorado is low, measuring only 2.34 for 2017.

The W/O ratio is much lower for oil and gas obtained from unconventional wells that generally produce much more crude oil and lower volumes of produced water. Thus, the W/O ratio is only 0.47 for Weld County, Colorado, with dominantly unconventional production, but the W/O is much higher (18.2) for Garfield County (Piceance Basin) that has no unconventional petroleum production (Kharaka et al., 2019).

Currently, about 60 percent of produced water in the USA is injected into the same petroleum reservoir for pressure maintenance and EOR and about 30 percent is injected into shallower reservoirs. The balance is discharged to surface water, ocean water, and other uses such as road application and for livestock. Significant surface water and

groundwater contamination has resulted because there were no local, state, or federal regulations until around the 1950s to control the disposal of brine wastewater. It was not until the 1980s that there was general acceptance that compliance with well-defined federal regulations was a logical way to maintain the level of environmental quality desired by the broad society.

The resulting wave of pollution control legislation enacted in the 1970s gave the EPA the authority to enforce pollution-control legislation. The EPA required operators to monitor the integrity of all injection wells through regular pressure tests and inspect their wells for mechanical integrity every five years. In addition, operators drilling new injection wells were required to search for and fix any leaky well located within one-quarter mile of the new injection well.

We examined the chemical composition of produced water from two large data sets. The first is the USGS National Produced Waters Geochemical Database where data from conventional and unconventional sources of energy for more than 100,000 oil and gas wells from the major sedimentary basins in the USA were obtained from the published literature and received from oil companies and state oil and gas organizations (Blondes et al., 2019). The second major data set was obtained from wells in the Alberta Basin, which is one of the largest petroleum basins in the world. The Alberta Basin has a more comprehensive, publicly available, and culled geochemical data set than other basins, and also has a new data set that includes information on potentially toxic elements seldom reported for other basins (Hitchon, 2023).

### 12.2.1 The Composition of Produced Water

These data sets show that produced water has salinity in the general range of from 3,000 to over 300,000 mg/L, dominated by Na and Cl, and with high concentrations of Ca, K, and Sr, especially in high salinity brine. Some produced water has relatively high concentrations of  $\text{HCO}_3$ ,  $\text{SO}_4$ , DOC, and  $\text{CH}_3\text{COO}$ . The concentrations of Fe and Mn are generally moderate (50 to 100 mg/L) but concentrations of Pb, Zn, Cu, Hg, Ra, and several other toxic metals are almost always very low (< 1 mg/L) because they are controlled by the very low solubility of their respective sulfide minerals.

Exceptionally high concentrations of metals (e.g., Pb values of hundreds of mg/L) are reported from a few localities worldwide including the central Mississippi Salt Dome Basin (Kharaka et al., 1987). Produced water may also contain high concentrations of mono- and dicarboxylic acid anions, phenols, BTEX, PAHs, and other reactive and toxic organic species (up to 10,000 mg/L).

Detailed inorganic and organic chemical analyses—together with measurements of the oxygen and hydrogen isotopes in water and of a diverse suite of other stable and radioactive isotopes—have been reported for produced water from many sedimentary basins worldwide. The application of these data, together with information on local and

regional geology as well as paleo-hydrology, has shown that these fluids are more mobile and their origins and interactions with rocks and sediments are more complex than previously realized (Hitchon, 2023; Kharaka & Hanor, 2014).

The data show that the formation water in sedimentary basins are predominantly of local meteoric or marine connate origin. However, bittern (residual) water, geologically old meteoric water, and especially water of mixed origin are important components in many sedimentary basins. The original water has evolved to Na – Cl, Na – Cl – CH<sub>3</sub>COO, or Na – Ca – Cl type water by a combination of several major processes, including the following:

1. dissolution of halite;
2. incorporation of bittern;
3. dissolution and precipitation of minerals other than halite;
4. interaction of the water with organic matter present in sedimentary rocks;
5. interaction with rocks, principally clays, siltstones, and shale that behave as geologic membranes; and
6. diffusion, which appears to be more important than previously thought.

The important processes responsible for the chemical evolution of water and mineral diagenesis in each basin can be identified using chemical markers and isotopes.

The salinity and chemical composition of potable groundwater discussed in Section 4 is sharply different from that of produced water. In the USA, the MCL value for the salinity of drinking water is only 500 mg/L and almost all produced water has 1 to 3 orders of magnitude higher salinity. Protected groundwater in the USA, also known as USDW, that may be used now or in the future for drinking or irrigation, is defined as water with salinity < 10,000 mg/L. Groundwater generally has approximately equal concentrations of Na, Mg, and Ca, but generally HCO<sub>3</sub> > SO<sub>4</sub> > Cl. Metal concentrations, organic acid anions, and DOC values are very low.

The contrast in salinity (easily measured by a conductance electrode) between groundwater and produced water may provide the first tool for detection of contamination by produced water. A more definitive answer may be obtained from the contrast in the concentrations or the ratios of individual conservative ions such as Cl, Br, B, and Li. The presence of high DOC values, organic acid anions, BTEX, and especially long-lived PAHs could also be definitive diagnostic compounds that indicate contamination from oil or produced water. Further confirmation using the isotopes of water, especially the more conservative  $\delta D$  values, and those of many solutes (e.g., B, Li, Sr) should confirm the source of contamination.

We conclude that potential contamination of groundwater by activities of the petroleum industry may be evaluated using detailed hydrological, chemical, and isotopic

data. This research can assist in accurately determining or tracing a particular water contaminant to its source, and help in designing proper remediation protocols.

### 12.3 Future Research

Water-rock interactions in sedimentary basins are and will continue to be the subject of intensive research. The following areas are receiving particular attention because of their scientific, environmental, or economic importance and/or the arrival of new analytical equipment and techniques.

1. A plethora of stable and radioactive isotope data are being used to study mineral diagenesis, the origin and age of water, and the sources and sinks of solutes in sedimentary basins with particular emphasis on injection sites for CO<sub>2</sub> sequestration and waste disposal. The determination of accurate fractionation factors and rates of isotopic exchange between water and minerals for in-situ conditions of sedimentary basins are needed for a better interpretation of the isotope data (Bullen, 2011).
2. Major advances have been made since the early 1990s in documenting the nature, distribution, and organic and inorganic interactions of reactive organic species. Additional investigation is needed, especially in determining the toxicity and stability of organic-inorganic complexes, the rates of decarboxylation and other transformations under field conditions, and the importance of dissolved organic sulfur and nitrogen compounds.
3. Geochemical, hydrologic, and solute transport computer codes are being applied to sedimentary basins. To obtain reliable information from this endeavor, accurate and detailed data on aqueous and solid phases must be available, with more accurate thermodynamic data for clay minerals, minerals of highly variable composition, and brine. Data on the kinetics of dissolution/precipitation under field conditions are also needed.
4. Improved reaction kinetics could be obtained by employing quantitative fluid flow models to integrate data describing field measurement of the spatial variation of fluid composition with detailed knowledge of the spatial variation of sediment mineralogy.
5. Chemical and isotopic evolution of the components of aqueous wastes, including produced water injected into the subsurface are required to answer the question: What can be deduced about the mixing and fate of this waste from what is known about the composition and interactions of formation water?
6. Understanding water-mineral-CO<sub>2</sub> interactions in the subsurface is vital to the success of EOR operations as well as the safe geologic storage of large amounts of anthropogenic CO<sub>2</sub> in depleted petroleum fields and saline aquifers to mitigate

global warming, which is arguably the most important environmental issue facing the world today (IPCC, 2021).

7. Develop large-scale survey methods to locate existing oil and gas wells that, if inadequately plugged, can provide a conduit for the rapid vertical migration of injected produced water and CO<sub>2</sub> causing groundwater contamination and environmental damage.

Several important questions need to be further investigated to improve understanding of the geochemistry of natural formation water in shale and tight reservoirs, and to minimize potential environmental impacts, especially groundwater contamination, related to petroleum exploration and production operations. These investigations include:

1. determine the spatial and temporal contamination of pore water in shale and tight reservoirs with drilling and fracturing fluids, using natural and human-made chemical and isotopic tracers;
2. identify the detailed differences in the chemical and isotopic compositions of produced water obtained from shale and from adjoining conventional reservoirs within the same basin/sub-basin at comparable temperature and pressure conditions;
3. investigate ionic selectivities and membrane efficiencies because of the importance of geological membranes in controlling the flow of solutes through shale and out of shale;
4. explore the role of dissolved organics and organic matter (quantity, type, maturity, and transformations) in modifying the chemical composition of pore water and the general behavior of shale and tight reservoirs; and
5. determine the list of chemicals added to fracturing fluids and their toxicity, transformations and interactions with natural fluids and rocks.

It would be beneficial to direct more research to remediation of many thousands of depleted petroleum fields—legacy sites worldwide that have been contaminated by produced water and petroleum. After several years of research on repairing salt and hydrocarbon-damaged soils in the tallgrass prairie of northeastern Oklahoma, Kerry Sublette and others (2007) discovered many techniques that simplify the remediation process and lower costs.

1. Fertilizers added incrementally over a period of time are more effective than large amounts of simultaneous fertilization. The former applications increase and maintain rates of bioremediation by improving N recycling and microbial diversity.
2. Nematode community structure, which can be measured inexpensively, provides a simple estimate of the health of the recovering soil during remediation.

3. Tilled hay is more effective in the reestablishment of vegetation than the more expensive gypsum applications on brine sites.
4. Subsurface drainage systems may be needed in some cases of low slope and excessive salinity and reinjection of the recovered fluid may be necessary.

Such science-based remediation plans are particularly needed in many of the aging and depleted petroleum fields that exist—not only in the USA but worldwide—where land use is changing from petroleum production to residential, agricultural, or recreational uses (Kharaka & Dorsey, 2005).

## 13 Exercises

### Exercise 1

Fossil fuels, oil, natural gas, and coal are essential commodities that have provided the main sources of primary energy for more than 100 years to fuel the rapidly increasing world population. Consumption of fossil fuels, however, carries major detrimental health and environmental impacts that may be local, regional, or global in scale. List five health and/or environmental impacts of fossil fuels.

[Click to return to where text linked to Exercise 1 ↑](#)

[Click for solution to Exercise 1 ↓](#)

### Exercise 2

Oil and gas operations today are multi-billion-dollar industries that started modestly around 1850, when commercial wells were dug or drilled in several countries to obtain crude oil primarily for kerosene and oil lamps. The question of where or when the first commercial oil well was drilled is difficult to answer. However, Edwin L. Drake's 1859 well, in the Oil Creek Valley near Titusville, Pennsylvania, is popularly considered the first modern well. Give four reasons why the Drake's well is singled out for this honor.

[Click to return to where text linked to Exercise 2 ↑](#)

[Click for solution to Exercise 2 ↓](#)

### Exercise 3

The main concern about the use of fossil fuels today is related to global warming and associated climate issues that result from continual addition of large and increasing amounts of CO<sub>2</sub> to the atmosphere, mainly from the burning of fossil fuels. The global temperature has already warmed 1.2 °C relative to pre-industrial times and is predicted to increase to 2.7 °C by 2100. Name four global potential adverse impacts of climate warming and rising atmospheric CO<sub>2</sub> concentrations.

[Click to return to where text linked to Exercise 3 ↑](#)

[Click for solution to Exercise 3 ↓](#)

## Exercise 4

What produced water to oil (W/O) ratio at the well head for every barrel of crude oil produced today in the USA? What was the W/O ratio for the US in 1965? Speculate on this ratio in 2050.

[Click to return to where text linked to Exercise 4 ↑](#)

[Click for solution to Exercise 4 ↓](#)

## Exercise 5

Hydraulic fracturing of shale is carried out by injecting large volumes of generally fresh water with added proppant and both disclosed and undisclosed organic and inorganic chemicals at pressures high enough to fracture the shale, and fractures are kept open by the proppant particles.

- a. How much water is needed per well in the USA to fracture an average horizontal shale for oil production?
- b. What is the composition of the fluid used for fracturing shale or tight reservoirs?

[Click to return to where text linked to Exercise 5 ↑](#)

[Click for solution to Exercise 5 ↓](#)

## Exercise 6

There may be several objectives for obtaining produced water from wells in a petroleum field for chemical and isotope analyses. The three primary objectives are:

1. investigating the chemistry of pristine formation water in the production zone to improve understanding of water–rock interactions,
2. locating leakage of formation water from a different production zone or aquifer, and
3. safe environmental disposal of produced water.

It is much more challenging to sample wells to obtain accurate geochemical data to meet the first objective. Name four criteria that should be used when selecting wells to obtain produced water to meet this objective.

[Click to return to where text linked to Exercise 6 ↑](#)

[Click for solution to Exercise 6 ↓](#)

## Exercise 7

Geochemical data sets obtained from oil companies are available and useful but are often incomplete, especially with regard to chemical and isotopic compositions of produced water. The chemical lists reported in Blondes and others (2019) underwent some basic culling that involved removing many wells that did not include a specific location, a valid perforation zone, all the major cations and anions, and anion cation charge balance > 10 percent. More detailed culling criteria are discussed in Hitchon and Brulotte (1994).

List five additional culling criteria that are needed to make data sets from oil companies more useful and acceptable.

[Click to return to where text linked to Exercise 7 ↑](#)

[Click for solution to Exercise 7 ↓](#)

## Exercise 8

Because the solutes Cl and Br are relatively conservative in formation water, the Cl/Br ratio can be used as an indicator of the origin of salinity. The Cl/Br weight ratio in modern seawater is approximately 300; Its value is much higher in formation water impacted by dissolution of halite as in salt domes. The Cl/Br ratios are much lower in produced water originating as bittern water from subaerial evaporation of seawater past the point of precipitation of halite, which has high Cl/Br ratios. Examine the composition of following produced water in samples shown in Table 40 and Table 41: 75-WR-5, 84-MS-11, and 77-GG-55 and decide on the origin of the salinity for each sample.

[Click to return to where text linked to Exercise 8 ↑](#)

[Click for solution to Exercise 8 ↓](#)

## Exercise 9

What are chemical geothermometers and why are they important in produced water?

[Click to return to where text linked to Exercise 9 ↑](#)

[Click for solution to Exercise 9 ↓](#)

## Exercise 10

Aliphatic acid anions such as acetate may be present in produced water at concentrations as high as 10,000 mg/L. Chemical data obtained from oil companies generally do not identify these organic solutes, but they list them as bicarbonate and add them to the measured alkalinity because they are titrated with  $\text{H}_2\text{SO}_4$  that is used to measure field alkalinities. In some produced water, more than 95 percent of measured alkalinity is attributed to these organics. As a result, the calculated saturated states of calcite in produced water show erroneous supersaturation by three kcal/mole or more.

Discuss the main controls on the concentrations of these organic acid anions.

[Click to return to where text linked to Exercise 10](#) ↑

[Click for solution to Exercise 10](#) ↓

## Exercise 11

What are polycyclic aromatic hydrocarbons (PAHs)? Describe their distribution and toxicity in produced water.

[Click to return to where text linked to Exercise 11](#) ↑

[Click for solution to Exercise 11](#) ↓

## Exercise 12

Boron is an essential element for the health of humans and biota. However, it is extremely toxic to many fruit trees and vegetables where present in excessive amounts in soils or irrigation water. Describe the toxicity of boron to fruit trees and vegetables, and why irrigation water contaminated with produced water is highly toxic to these fruit trees and vegetables.

[Click to return to where text linked to Exercise 12](#) ↑

[Click for solution to Exercise 12](#) ↓

## Exercise 13

The salinity and chemical composition of potable groundwater is distinctly different from that of the produced water. List five chemical parameters that, if encountered in groundwater, would indicate contamination with produced water. A detailed hydrogeological investigation would still be required to confirm the source of contamination.

[Click to return to where text linked to Exercise 13](#) ↑

[Click for solution to Exercise 13](#) ↓

## Exercise 14

The strontium isotopic composition of formation water has shown great utility as a means of identifying sources of strontium, the degree of water–rock exchange, the degree of mixing along regional fluid flow paths, and contaminated groundwater. The strontium isotopic composition of geologic materials is expressed as the ratio of  $^{87}\text{Sr}/^{86}\text{Sr}$ , which can be measured with precision. Describe the sources of high and low  $^{87}\text{Sr}/^{86}\text{Sr}$  ratios in produced water.

[Click to return to where text linked to Exercise 14](#) ↴

[Click for solution to Exercise 14](#) ↴

## Exercise 15

What are the most useful isotopes for dating the residence time of produced water?

[Click to return to where text linked to Exercise 15](#) ↴

[Click for solution to Exercise 15](#) ↴

## Exercise 16

What do the terms *allochthonous* and *autochthonous* mean both literally and in the context of the position of masses of salt within sedimentary basins? Which Gulf of Mexico salt masses are examples of each?

[Click to return to where text linked to Exercise 16](#) ↴

[Click for solution to Exercise 16](#) ↴

## Exercise 17

The following questions refer to Figure 42. A sample of produced water waste is found to contain 4,000 mmol/kg dissolved chloride. Based on the information in Figure 42, what geochemical parameters could be used to determine whether the water is more likely from Jurassic or from Paleocene-Miocene-Pleistocene host reservoirs, even if the water were partially diluted by mixing with fresh groundwater? Does the composition of basinal brine reflect the composition of either ancient seawater or evaporated ancient seawater?

[Click to return to where text linked to Exercise 17](#) ↴

[Click for solution to Exercise 17](#) ↴

## Exercise 18

Given the field examples of salt structures and surrounding sediments discussed in Section 9, would you characterize flow of formation water and transport of solutes in these Gulf Coast sediments as having been largely stagnant over time (no fluid flow) and/or dynamic (active fluid flow)? What is the evidence for either case? If dynamic, what forces are driving fluid flow? Give examples.

[Click to return to where text linked to Exercise 18](#) ↑

[Click for solution to Exercise 18](#) ↓

## Exercise 19

Contamination at the Bemidji, Minnesota, USA, site began when an oil pipeline ruptured in 1979 and sprayed approximately 11,000 bbl (1.7 million liters) of crude oil across an area of 6,500 m<sup>2</sup>. Petroleum seeped through the soil and is floating on the water table in the outwash aquifer. Extensive research by scientists from the USGS, universities, and oil companies over more than 40 years has resulted in major discoveries. Discuss the four most important findings from this research.

[Click to return to where text linked to Exercise 19](#) ↑

[Click for solution to Exercise 19](#) ↓

## Exercise 20

Examine the concentration of solutes in water of the Skiatook Lake and from well BE-62 reported in Table 45. Is the water from Skiatook Lake suitable for human consumption? The groundwater from well BE-62 is highly contaminated from oil field operations. What different dilution factors with distilled water would you have to employ to make groundwater from BE-62 suitable for human consumption with regard to each contaminant?

[Click to return to where text linked to Exercise 20](#) ↑

[Click for solution to Exercise 20](#) ↓

## Exercise 21

The OSPER A legacy site, located in Osage County, Oklahoma, has an area of about 1.5 hectare that is impacted by produced water and hydrocarbon releases that occurred primarily 75 to 100 years ago. A three-dimensional plume of high-salinity water (2,000 to 30,000 mg/L TDS) dominated by Na and Cl extends beneath a total area of about 3 ha and intersects Skiatook Lake. Discuss the main conclusion from the rate of surface salt removal and natural attenuation at this site.

[Click to return to where text linked to Exercise 21](#) ↑

[Click for solution to Exercise 21](#) ↓

## Exercise 22

The OSPER B site, located in Osage County, Oklahoma, is actively producing oil and has ongoing hydrocarbon releases and salt scars that have impacted an area of approximately one hectare. The site includes an active production tank battery and adjacent large brine pit, two injection-well sites (one with an adjacent small pit), and an old tank battery. The large brine pit generally contains a 0.2 to 2 m depth of produced water with a thin layer of oil. The brine in this pit is generally pumped into collection tanks by a submersible pump but this occasionally fails causing filling and overflow of the brine pit that contaminates soil, groundwater, and Skiatook Lake. How would you investigate the source of brine in a sample obtained from a borehole below the brine pit and close to Skiatook Lake? How would you confirm this source?

[Click to return to where text linked to Exercise 22 ↑](#)

[Click for solution to Exercise 22 ↓](#)

## Exercise 23

Figure 70 shows the calculated composition of waste water at an oil field waste site as determined from the composition of exchangeable cations on sediments from the site. Assuming that the concentration of anionic charge shown Figure 70 is largely dissolved chloride, compare the calculated composition of the oil field waste water with the composition of formation water shown in Figure 42.

[Click to return to where text linked to Exercise 23 ↑](#)

[Click for solution to Exercise 23 ↓](#)

## Exercise 24

Migration of oil field waste under variable density conditions can be complex. Print out or visually inspect Figure 74 and Figure 76. Draw or visualize an arrow on the map in Figure 74 of the First Permeable Zone for August 1986 perpendicular to the TDS (or salinity) contours in the direction of decreasing TDS. One might conclude that the source of saline contamination is to the east of the rectangular pits on the map. Now draw or visualize an arrow on the map in Figure 76 for the first permeable zone perpendicular to the water level contours and in the direction of decreasing water level. In a fresh groundwater system, one would assume that this second arrow represents the direction of groundwater flow. Briefly discuss your findings. Is groundwater contamination increasing, decreasing, or constant over the six-year period 1986 to 1992?

[Click to return to where text linked to Exercise 24 ↑](#)

[Click for solution to Exercise 24 ↓](#)

## Exercise 25

The increased anthropogenic emissions of heat trapping CO<sub>2</sub> have raised its atmospheric concentrations from about 275 ppmv (parts per million; 10<sup>6</sup> by volume) during preindustrial times to approximately 420 ppmv today. So far, CCUS has not lived up to its promise for reducing CO<sub>2</sub> emissions to reach global climate goals. To speed up the use of CCUS, the concept of hubs is being investigated and results prove promising. What is a CCUS Hub and why are hubs considered an important tool to achieve global climate goals?

[Click to return to where text linked to Exercise 25 ↑](#)

[Click for solution to Exercise 25 ↓](#)

## Exercise 26

The ZERT facility was developed at a field site close to Bozeman, Montana, USA, to allow controlled studies of near-surface CO<sub>2</sub> transport and detection technologies. A slotted horizontal pipe (well) divided into six zones was installed horizontally 2 to 2.3 m deep. Controlled releases of CO<sub>2</sub> tagged with perfluorocarbon and other tracers were performed in the summers of 2007, 2008, and 2009. As part of this multidisciplinary research, the USGS team carried out a study with the main objective to investigate changes in the concentrations of major, minor, and trace inorganic and organic compounds during, and following, CO<sub>2</sub> injection. Eighty samples of water were obtained during the 2008 season from ten shallow monitoring wells (1.5 or 3.0 m deep, installed 1 to 6 m from the injection pipe) and from two distant monitoring wells. Approximately 300 kg/day of food-grade CO<sub>2</sub> was injected through the perforated pipe between July 9th and August 7th, 2008, at the field test. Samples were collected before, during, and after CO<sub>2</sub> injection.

Describe the three main changes in the composition of groundwater CO<sub>2</sub> injection. How was the change in pH at the ZERT site different from the Frio Brine test, and why?

[Click to return to where text linked to Exercise 26 ↑](#)

[Click for solution to Exercise 26 ↓](#)

## 14 References

- Abbott, M. M. (2000). *Water quality of the Quaternary and Ada Vamoosa aquifers on the Osage reservation, Osage County, Oklahoma, 1997* (Water Resources Investigation Report number 99-4231). US Geological Survey. <https://doi.org/10.3133/wri994231>.
- Abbott, M. M. (2003). *Real-time kinematic (RTK) surveying at the Osage Skiatook Petroleum Environmental Research sites, Osage County, Oklahoma* (Water Resources Investigations number 03-4260) (pp. 147–155). US Geological Survey. [pubs.er.usgs.gov/publication/70216521](https://pubs.er.usgs.gov/publication/70216521).
- ACTL (Alberta Carbon Trunk Line). (2022). Alberta carbon capture, utilization and storage-funded projects and reports. [Alberta CCUS projects & reports](#).
- Aggarwal, J. K., Palmer, M. R., Bullen, T. D., Ragnarsdottir, K. V., & Arnorsson, S. (2000). The boron isotope systematics of Icelandic geothermal water. 1: Meteoric water charged systems. *Geochimica et Cosmochimica Acta*, 64(4), 579–585. [https://doi.org/10.1016/S0016-7037\(99\)00300-2](https://doi.org/10.1016/S0016-7037(99)00300-2).
- Aggarwal, P. K. (2013). Introduction. In A. Suckow, P. K. Aggarwal, & L. Araguas-Araguas (Eds.), *Isotope methods for dating old groundwater* (pp. 1–4). International Atomic Energy Agency.
- Ajemigbitse, M. A., Cannon, F. S., & Warner, N. R. (2020). A rapid method to determine  $^{226}\text{Ra}$  concentrations in Marcellus Shale produced water using liquid scintillation counting. *Journal of Environmental Radioactivity*, 220–221, 106300. <https://doi.org/10.1016/j.jenvrad.2020.106300>.
- AKOB, D. M., Cozzarelli, I. M., Dunlap, D. S., Rowan, E. L., & Lorah, M. M. (2015). Organic and inorganic composition and microbiology of produced water from Pennsylvania shale gas wells. *Applied Geochemistry*, 60, 116–125. <https://doi.org/j.apgeochem.2015.04.011>.
- Alberta Energy and Utilities Board. (2004). Alberta's reserves 2003 and supply/demand outlook 2004–2013: Bitumen, crude oil and natural gas basic reserve data tables: Statistical Series 2004–98 (CD-ROM). [eub.gov.ab.ca](http://eub.gov.ab.ca).
- Alley, B., Beebe, A., Rodgers J., & Castle J. W. (2011). Chemical and physical characterization of produced water from conventional and unconventional fossil fuel resources. *Chemosphere*, 85(1), 74–82. [j.chemosphere.2011.05.043](http://j.chemosphere.2011.05.043).
- Allis, R., Bergfeld, D., Moore, J., McClure, K., Morgan, C., Chidsey, T., Heath, J., & Macpherson, B. (2005). Implications of results from CO<sub>2</sub> flux surveys over known CO<sub>2</sub> systems for long-term monitoring. *Proceedings. Fourth Annual Conference on Carbon Capture and Sequestration DOE/NETL, May 2–5, 2005* (pp. 1367–1388). (CD-ROM).
- Allison, E., & Mandler, B. (2018). Groundwater protection in oil and gas production: Identifying and mitigating contamination of groundwater from oil and gas activity. In *Petroleum and the Environment, Part 6/24 of American Geosciences Institute Critical Issues Program as supported by the American Association of Petroleum Geologists (AAPG)*

- Foundation. [www.americangeosciences.org/geoscience-currents/groundwater-protection-oil-and-gas-production](http://www.americangeosciences.org/geoscience-currents/groundwater-protection-oil-and-gas-production).
- Anderson, C. E., Hanor, J. S., & Tsai, F. T. C. (2013). Sources of salinization of the Baton Rouge aquifer system, southeastern Louisiana. *Gulf Coast Association of Geological Societies Transactions*, 63, 3–12. [semanticscholar.org/paper/Sources-of-Salinization-of-the-Baton-Rouge-Aquifer-Anderson-Hanor](http://semanticscholar.org/paper/Sources-of-Salinization-of-the-Baton-Rouge-Aquifer-Anderson-Hanor).
- Andrews, J. N., Edmunds, W. M., Smedley, P. L., Fontes, J. C., Fifield, L. K., & Allan, G. L. (1994). Chlorine-36 in groundwater as a palaeoclimatic indicator: The East Midlands Triassic sandstone aquifer (United Kingdom). *Earth and Planetary Science Letters*, 122, 159–177. [https://doi.org/10.1016/0012-821X\(94\)90057-4](https://doi.org/10.1016/0012-821X(94)90057-4).
- Appelo, C. A. J. (1994). Some calculations on multicomponent transport with cation exchange in aquifers. *Ground Water*, 32, 968–975. [go.gale.com/ps/i.do?id=](http://go.gale.com/ps/i.do?id=).
- Appelo, C. A. J. (1996). Multicomponent ion exchange and chromatography in natural systems. *Reviews in Mineralogy*, 34, 193–227. <https://doi.org/10.1515/9781501509797-007>.
- Appelo, C. A. J., & Postma, D. (1993). Geochemistry, groundwater and pollution. *Applied Geochemistry*, 131(5), 479–480. <https://doi.org/10.1002/esp.3290200510>.
- Apps, J. A., Zheng, L., Spycher, N., Birkholzer, J., Kharaka, Y. K., Thordsen, J., Kakouros, E., & Trautz, R. C. (2011). Transient changes in shallow groundwater chemistry during the MSU ZERT CO<sub>2</sub> injection experiment. *Energy Procedia*, 4, 3231–3238. <https://doi.org/10.1016/j.egypro.2011.02.241>.
- Armstrong, S. C., Sturchio, N. C., & Hendry, M. J. (1998). Strontium isotopic evidence on the chemical evolution of pore water in the Milk River aquifer, Alberta, Canada. *Applied Geochemistry*, 13, 463–475.
- Arthur, M. A., & Cole, D. R. (2014). Unconventional hydrocarbon resources: Prospects and problems. *Elements*, 10, 257–264. <https://doi.org/10.2113/gselements.10.4.257>.
- Ausburn, M. E. (2013). *Controls on the composition of saline formation water from coastal and offshore Louisiana* (Identifier No. etd-05302013-141118) [Masters' thesis, Department of Geology and Geophysics, Louisiana State University]. LSU Digital Commons. [digitalcommons.lsu.edu/gradschool\\_theses/2149/h](http://digitalcommons.lsu.edu/gradschool_theses/2149/h).
- Ayers, A. S., & Westcot, D. W. (1976). *Paper Number 9: Water quality for agriculture, irrigation and drainage*. Food and Agriculture Organization of the United Nations.
- Bachu, S. (1995). Synthesis and model of formation-water flow, Alberta Basin, Canada. *American Association of Petroleum Geologists Bulletin*, 79, 1159–1178. <https://doi.org/10.1306/8D2B2209-171E-11D7-8645000102C1865D>.
- Bachu, S. (2003). Screening and ranking of sedimentary basins for sequestration of CO<sub>2</sub> in geological media in response to climate change. *Environmental Geology*, 44, pages 277–289. <https://doi.org/10.1007/s00254-003-0762-9>.

- Baedecker, M. J., Cozzarelli, I. M., Eganhouse, R. P., Siegel, D. I., & Bennett, P. C. (1993). Crude oil in a shallow sand and gravel aquifer – III. Biogeochemical reactions and mass balance modeling in anoxic groundwater. *Applied Geochemistry*, 8, 569–586. [https://doi.org/10.1016/0883-2927\(93\)90014-8](https://doi.org/10.1016/0883-2927(93)90014-8).
- Baedecker, M. J., Eganhouse, R. P., Haiping, Q. I., Cozzarelli, I. M., Trost, J. J., & Bekins, B. A. (2018). Weathering of oil in a surficial aquifer. *Groundwater*, 56, 797–809. <https://doi.org/10.1111/gwat.12619>.
- Bagheri, R., Nadri, A., Raeisi, E., Eggenkamp, H. G. M., Kazemi, G. A., & Montaseri, A. (2014). Hydrochemical and isotopic ( $\delta^{18}\text{O}$ ,  $\delta^2\text{H}$ ,  $\delta^{87}\text{Sr}/^{86}\text{Sr}$ ,  $\delta^{37}\text{Cl}$ , and  $\delta^{81}\text{Br}$ ) evidence for the origin of saline formation water in a gas reservoir. *Chemical Geology*, 384, 62–75. [j.chemgeo.2014.06.017](https://doi.org/10.1016/j.chemgeo.2014.06.017).
- Baldwin, H. (1959). Oil strategy in World War II. *American Petroleum Institute Quarterly-Centennial Issue, Archive 2009-08-15*, 10–11.
- Ball, L., Deszcz-Pan, M., Thamke, J. & Smith, B. (2019). Monitoring brine contamination using time-lapse airborne electromagnetic surveys, East Poplar Oil Field, Montana. In *Proceedings of the 7th annual conference on airborne electromagnetics, June 17–20, 2018, Kolding, Denmark*. <https://pubs.er.usgs.gov/publication/70203035h>.
- Ball, L. B., Gillespie, J. M., Minsley, B., Davis, T., & Landon, M. K. (2019). Mapping protected groundwater adjacent to oil and gas fields, San Joaquin Valley, California. In *Proceedings of the 7th annual conference on airborne electromagnetics, June 17–20, 2018, Kolding, Denmark*. <https://pubs.er.usgs.gov/publication/70203036>.
- Banga, T., Capuano, R. M., & van Nieuwenhuise, D. S. (2002). Fluid flow, stratigraphy and structure in the vicinity of the South Liberty salt dome, Texas. *Gulf Coast Association of Geological Societies Transactions*, 52, 25–36. <https://researchgate.net/publication/285700215> Fluid flow stratigraphy and structure in the vicinity of the South Liberty salt dome Texas.
- Banks, D. A., Gleeson, S. A., & Green, R. (2000). Determination of the origin of salinity in granite-related fluids; evidence from chloride isotopes in fluid inclusions. *Journal of Geochemical Exploration*, 69–70, 309–312. [https://doi.org/10.1016/S0375-6742\(00\)00076-5](https://doi.org/10.1016/S0375-6742(00)00076-5).
- Barnes, H. L. (1979). Solubilities of ore minerals. In H. L. Barnes (Ed.), *Geochemistry of hydrothermal ore deposits* (pp. 404–460). John Wiley & Sons.
- Barnes, I., O’Neil, J. R., Rapp, J. B., & White, D. E. (1973). Silica-carbonate alteration of serpentine: Wall rock alteration in mercury deposits of the California Coast Ranges. *Economic Geology*, 68, 388–398. <https://doi.org/10.2113/gsecongeo.68.3.388>.
- Barth, T. (1987). Quantitative determination of volatile carboxylic acids in formation water by isotachopheresis. *Analytical Chemistry*, 59, 2232–2237. <https://doi.org/10.1021/ac00145a004>.

- Barth, S. (1998). Application of boron isotopes for tracing sources of anthropogenic contamination in groundwater. *Water Research*, 32, 685–690. [https://doi.org/10.1016/S0043-1354\(97\)00251-0](https://doi.org/10.1016/S0043-1354(97)00251-0).
- Barth, T., Borgund, A. E., & Hopland, A.L. (1989). Generation of organic compounds by hydrous pyrolysis of Kimmeridge oil shale-bulk results and activation energy calculations. *Organic Geochemistry*, 14, 69–76. [https://doi.org/10.1016/0146-6380\(89\)90020-X](https://doi.org/10.1016/0146-6380(89)90020-X).
- Bassett, R. L. (1977). *The geochemistry of boron in thermal water* [Unpublished doctoral dissertation]. Stanford University.
- Bateman, R. M., & Konen, C. E. (1977). Wellsite log analysis and the programmable pocket calculator. *Transactions of the Society of Professional Well Log Analysts (Annual Logging Symposium)*, 18, B.1–B.35. <https://onepetro.org/SPWLAALS/proceedings-abstract>.
- Bath, A., Edmunds, W. M., & Andrews, J. N. (1978). Paleoclimatic trends deduced from the hydrochemistry of Triassic sandstone aquifer, United Kingdom. *Isotope Hydrology*, 2, 545–568. [https://inis.iaea.org/search/search.aspx?orig\\_q=RN:10462983](https://inis.iaea.org/search/search.aspx?orig_q=RN:10462983).
- Bauder, T. A., Waskom, R. M., Sutherland, P. L., & Davis, J. G. (2014). *Fact Sheet Number 0.506: Irrigation water quality criteria*. Colorado State University.
- Bazin, B., Brosse, E., & Sommer, F. (1997a). Chemistry of oil-field brines in relation to diagenesis of reservoirs. 1: Use of mineral stability fields to reconstruct in situ water composition, example of the Mahakam basin. *Marine and Petroleum Geology*, 14, 481–495. [https://doi.org/10.1016/S0264-8172\(97\)00004-4](https://doi.org/10.1016/S0264-8172(97)00004-4).
- Bazin, B., Brosse, E., & Sommer, F. (1997b). Chemistry of oil-field brines in relation to diagenesis of reservoirs: 2. Reconstruction of paleo-water composition for modeling illite diagenesis in the Greater Alwyn area (North Sea). *Marine and Petroleum Geology*, 14, 497–511. [https://doi.org/10.1016/S0264-8172\(97\)00005-6](https://doi.org/10.1016/S0264-8172(97)00005-6).
- Bekins, B. A., Hostetter, F. D., Herkelrath, W. N., Delin, G. N., Warren, E., & Essaid, H. I. (2005). Progression of methanogenic degradation of crude oil in the subsurface. *Environmental Geosciences*, 12(2), 139–152. <https://doi.org/10.1306/eg.11160404036>.
- Bekins, B. A., Cozzarelli, I. M., Erickson, M. L., Steenson, R. A., & Thorn, K. A. (2016). Crude oil metabolites in groundwater at two spill sites. *Groundwater*, 54, 681–691. <https://doi.org/10.1111/gwat.12419>.
- Bekins, B. E., Brennan, J., Tillitt, D. E., Illig, J. M., Cozzarelli, I. M., & Martinovic-Weigelt, D. (2020). Biological Effects of hydrocarbon degradation intermediates: Is the total petroleum hydrocarbon analytical method adequate for risk assessment? *Environmental Science and Technology*, 54, 11396–11404. <https://doi.org/10.1021/acs.est.0c02220>.
- Bekins, B. E., Podgorski, D. C., Wagner, S., Thorn, K. A., Cozzarelli, I. M., Tillitt, D. E., & Leet, J. K. (2021). New approaches for characterization of petroleum hydrocarbon partial transformation products [abstract id. H44C-01]. In *Proceedings of the American*

- Geophysical Union Fall Meeting 2021, December 13–17, 2021, New Orleans, LA.*  
<https://ui.adsabs.harvard.edu/abs/2021AGUFM.H44C..01B/abstract>↗.
- Beloe, W. (1830). *Herodotus*. H. Colburn and R. Bentley.
- Bénézech, P., Palmer, A. D., Anovitz, L. M., & Horita, J. (2007). Dawsonite synthesis and re-evaluation of its thermodynamic properties from solubility measurements: Implications for mineral trapping of CO<sub>2</sub>. *Geochimica et Cosmochimica Acta*, 71, 4438–4455. <https://doi.org/10.1016/j.gca.2007.07.003>↗.
- Bennett, S. C., & Hanor, J. S. (1987). Dynamics of subsurface salt dissolution at the Welsh Dome, Louisiana Gulf Coast. In I. Lerche & J. J. O'Brien (Eds.), *Dynamical geology of salt and related structures* (pp. 653–677). Academic Press.  
<https://doi.org/10.1016/B978-0-12-444170-5.50021-X>↗.
- Benson, S. M., & Cole, D. R. (2008). CO<sub>2</sub> sequestration in deep sedimentary formations. *Elements*, 4(5), 325–331. <https://doi.org/10.2113/gselements.4.5.325>↗.
- Benson, S. M., & Cook P. (Coordinating Lead Authors). (2005). Underground geological storage. In O. Davidson, H.C. de Coninck, M. Loos, & L. A. Meyer (Eds.), *Intergovernmental Panel on Climate Change (IPCC) special report on carbon dioxide capture and storage* (pp. 195–276). Cambridge University Press.  
[researchgate.net/publication/264453028](https://www.researchgate.net/publication/264453028)↗.
- Berner, R. A. (1980). *Early diagenesis: A theoretical approach*. Princeton University Press.
- Berner, Z. A., Stüben, D., Leosson, M. A., & Klinge H. (2002). S- and O-isotopic character of dissolved sulphate in the cover rock aquifers of a Zechstein salt dome. *Applied Geochemistry*, 17(12), 1515–1528. [https://doi.org/10.1016/S0883-2927\(02\)00046-X](https://doi.org/10.1016/S0883-2927(02)00046-X)↗.
- Berry, F. A. F. (1973). High fluid-potentials in the California coast ranges and their tectonic significance. *American Association of Petroleum Geologists Bulletin*, 57, 1229–1249. <https://doi.org/10.1306/83D90E8A-16C7-11D7-8645000102C1865D>↗.
- Bethke, C. M., Torgersen, T., & Park, J. (2000). The “age” of very old groundwater: Insights from reactive transport models. *Journal of Geochemical Exploration*, 69–70, 1–4.  
[https://doi.org/10.1016/S0375-6742\(00\)00115-1](https://doi.org/10.1016/S0375-6742(00)00115-1)↗.
- Bethke, C. M., Zhao, X., & Torgersen, T. J. (1999). Groundwater flow and the <sup>4</sup>He distribution in the Great Artesian Basin of Australia. *Journal of Geophysical Research: Biogeosciences*, 104, 12999–13011. <https://doi.org/10.1029/1999JB900085>↗.
- Bethke, C. M., & Johnson, T. C. (2002). Paradox of groundwater age: correction. *Geology*, 30, 385–388. [https://doi.org/10.1130/0091-7613\(2002\)030<0386:POGAC>2.0.CO;2](https://doi.org/10.1130/0091-7613(2002)030<0386:POGAC>2.0.CO;2)↗.
- Bethke, C. (2015). *The geochemist's workbench* (Version 10.0.3) [Computer software]. Aqueous Solutions LLC.
- Bickle, M. J. (2009). Geological carbon storage. *Nature Geoscience*, 2(12), 815–818.
- Birdwell, J. E., Bowker, K., Burke, B., Chidsey, T., Hammes, U., Henk, B., Hollon, Z., Jiang, S., Li, P., Marra, K. R., McCracken, J., Nyahay, R., Seyedolali, A., Schmid, K., Tinnin, B., & Whidden, K. J. (2020). *Energy and minerals division tight oil and gas committee: Activities and commodity report for 2019–2020*. American Association of Petroleum

- Geologists (AAPG) Energy Minerals Division Tight Oil and Gas Committee.  
<https://pubs.er.usgs.gov/publication/70217638> ↗.
- Birkle, P., García, B. M., & Padrón, C. M. M. (2009). Origin and evolution of formation water at the Jujo-Tecominoacán oil reservoir, Gulf of Mexico. Part 1: chemical evolution and water-rock interaction. *Applied Geochemistry*, 24, 543–554.  
<https://doi.org/10.1016/j.apgeochem.2008.12.009> ↗.
- Birkle, P., García, B. M., Padrón, C. M. M., & Eglington, B. M. (2010). Origin and evolution of formation water at the Jujo-Tecominoacán oil reservoir, Gulf of Mexico. Part 2: Isotopic and field-production evidence for fluid connectivity. *Applied Geochemistry*, 24, 555–573. <https://doi.org/10.1016/j.apgeochem.2008.12.010> ↗.
- Birkle, P., Aragón, J. J. R., Portugal, E., & Fong Aguilar, J. L. (2002). Evolution and origin of deep reservoir water at the Activo Luna oil field, Gulf of Mexico, Mexico. *American Association of Petroleum Geologists Bulletin*, 86, 457–484.  
<https://doi.org/10.1306/61EEDB0C-173E-11D7-8645000102C1865D> ↗.
- Bjørlykke, K. (1988). Sandstone diagenesis in relation to preservation, destruction and creation of porosity in diagenesis. *Developments in Sedimentology*, 41(1988), 555–588.  
[https://doi.org/10.1016/S0070-4571\(08\)70180-8](https://doi.org/10.1016/S0070-4571(08)70180-8) ↗.
- Bjørlykke, K. (1994). Fluid-flow processes and diagenesis in sedimentary basins in Geofluids: Origin, Migration and Evolution of fluids in sedimentary basins. *Geological Society London Special Publication*, 78, 127–140,  
<https://doi.org/10.1144/GSL.SP.1994.078.01.11> ↗.
- Bjørlykke, K. (2010). *Petroleum geoscience: From sedimentary environments to rock physics*. Springer. [imash.ru/netcat\\_files/file/BIBLIO/GEOLOG/Bjorlykke%20K\\_%20-%20Petroleum%20Geoscience%20-%202011.pdf](http://imash.ru/netcat_files/file/BIBLIO/GEOLOG/Bjorlykke%20K_%20-%20Petroleum%20Geoscience%20-%202011.pdf) ↗.
- Bjørlykke, K., Jahren, J., Aagaard, P., & Fisher, Q. (2010). Role of effective permeability distribution in estimating overpressure using basin modeling. *Marine and Petroleum Geology*, 27, 1684–1691. <https://doi.org/10.1016/j.marpetgeo.2010.05.003> ↗.
- Black, B. C. (2012). *Crude reality: Petroleum in world history*. Rowman & Littlefield.  
<https://rowman.com/ISBN/9781538142479> ↗.
- Blättler, C. L., Miller, N. R., & Higgins, J. (2015). Mg and Ca isotope signatures of authigenic dolomite in siliceous deep-sea sediments. *Earth and Planetary Science Letters*, 419, 32–42. <https://doi.org/10.1016/j.epsl.2015.03.006> ↗.
- Blondes, M. S., Gans, K. D., Thordsen, J. J., Reidy, M. E., Engle, M. A., Kharaka, Y. K., & Rowan, E. L. (2019). *National produced waters geochemical database (Version 2.3) (Provisional)*. US Geological Survey. <https://www.usgs.gov/programs/energy-resources-program> ↗.
- Blondes, M. S., Shelton, J. L., Engle, M. A., Trembly, J., Doolan, C. A., Jubb, A. M., Chenault, J., Rowan, E. L., Haefner, R. J., & Mailot, B. E. (2020). Utica shale play oil and gas brines: Geochemistry and factors influencing wastewater management.

- Environmental Science & Technology*, 54(21), 13917–13925.  
<https://doi.org/10.1021/acs.est.0c02461>.
- Blondes, M. S., Gans, K. D., Engle, M. A., Kharaka, Y. K., Reidy, M. E., Saraswathula, V., Thordsen, J. J., Rowan, E. L., & Morrissey, E. A. (2016). *National produced waters geochemical database* (Version 2.3) (Provisional). US Geological Survey.  
[archive.org/stream/USGSProducedWaterV2.2c/USGSProducedWaterDatabasev2.2.Documentation\\_djvu.txt](https://archive.org/stream/USGSProducedWaterV2.2c/USGSProducedWaterDatabasev2.2.Documentation_djvu.txt).
- Boles, J. R. (1978). Active ankerite cementation in the subsurface Eocene of southwest Texas. *Contributions to Mineralogy and Petrology*, 68, 13–22.  
<https://link.springer.com/article/10.1007/BF00375443>.
- Boles, J. R., & Franks, S. G. (1979). Clay diagenesis in Wilcox sandstones of southwest Texas: implications of smectite diagenesis on sandstone cementation. *Journal of Sedimentary Petrology*, 49, 55–70. <https://doi.org/10.1306/212F76BC-2B24-11D7-8648000102C1865D>.
- Bonetti, P., Leuz, C., & Michelon, G. (2021). Large-sample evidence on the impact of unconventional oil and gas development on surface water. *Science*, 373, 896–899.  
<https://doi.org/10.1126/science.aaz2185>.
- Böttcher, M. E., Geprägs, P., Neubert, N., von Allmen, K., Pretet, C., Samankassou, E., & Nägler, T. F. (2012). Barium isotope fractionation during experimental formation of the double carbonate BaMn(CO<sub>3</sub>)<sub>2</sub> at ambient temperature. *Isotopes in Environmental and Health Studies*, 48(3), 457–463. <https://doi.org/10.1080/10256016.2012.673489>.
- Boverton, R. (1911). Petroleum. In H. Chisholm (Ed.), *Encyclopædia britannica, volume 21* (11th ed.). (pp. 316–323). Cambridge University Press.
- BP. (2020). *Statistical review of world energy 2020* (69th ed.). BP. [BP Statistical Review of World Energy 2020](https://www.bp.com/content/dam/bp/pdf/statistical-review/bp-statistical-review-of-world-energy-2020.pdf).
- Bradshaw, J., Bachu, S., Bonijoly, D., Burruss, R., Holloway, S., Christensen, N. P., & Magne Mathiassen, O. (2007). CO<sub>2</sub> storage capacity estimation: issues and development of standards. *International Journal of Greenhouse Gas Control*, 1, 62–68.  
[https://doi.org/10.1016/S1750-5836\(07\)00027-8](https://doi.org/10.1016/S1750-5836(07)00027-8).
- Bray, R. B., & Hanor, J. S. (1990). Spatial variations in subsurface pore fluid properties in a portion of southeast Louisiana: Implications for regional fluid flow and solute transport. *Gulf Coast Association of Geological Societies Transactions*, 40, 53–64.  
[doi.org/10.1306/20B22F8F-170D-11D7-8645000102C1865D?sid=semanticscholar](https://doi.org/10.1306/20B22F8F-170D-11D7-8645000102C1865D?sid=semanticscholar).
- Breit, G. N., Kharaka, Y. K., & Rice, C. A. (2001). National database on the chemical composition of formation water from petroleum wells. In K. L. Sublette (Ed.), *Proceedings of the 7th IPEC Meeting: Environmental issues and solutions in petroleum exploration, production, and refining, November 2000, Albuquerque, NM*.
- Brice, W. R. (2009). *Myth, legend, reality: Edwin Laurentine Drake and the early oil industry*. Oil Region Alliance of Business, Industry and Tourism.

[worldcat.org/title/myth-legend-reality-edwin-laurentine-drake-and-the-early-oil-industry/oclc/501813103](http://worldcat.org/title/myth-legend-reality-edwin-laurentine-drake-and-the-early-oil-industry/oclc/501813103).

- Briggins, D. R., & Cross, H. J. (1995). *Well contamination by road salt: Problems and possible solutions in Nova Scotia* (Preprint). Proceedings XXVI International Association of Hydrogeologists Congress, Edmonton, Alberta, Canada.
- Bruno, R. S., & Hanor, J. S. (2003). Large-scale fluid migration driven by salt dissolution, Bay Marchand dome, offshore Louisiana. *Gulf Coast Association of Geological Societies Transactions*, 53, 97–107.
- Bryant, E. A. (1997). *Climate processes and change*. Cambridge University Press.
- Bullen, T. D. (2011). Stable isotopes of transition and post-transition metals as tracers in environmental studies. In M. Baskaran (Ed.), *Advances in isotope geochemistry: Handbook of environmental isotope geochemistry* (pp. 177–203). Springer-Verlag. [https://doi.org/10.1007/978-3-642-10637-8\\_10](https://doi.org/10.1007/978-3-642-10637-8_10).
- Bullen, T. D., & Eisenhauer, A. (2009). Metal stable isotopes in low-temperature systems: A primer. *Elements*, 5(6), 349–352. <https://doi.org/10.2113/gselements.5.6.349>.
- Bullen, T. D., White, A. F., Childs, C.W., & Horita, J. (2001). Reducing ambiguity in isotope studies using a multi-tracer approach. In R. Cidu (Ed.), *Proceedings of the 10<sup>th</sup> International Symposium on the Water Rock Interaction* (pp. 19–28).
- Bullen, T. D., & Walczyk T. R. (2009). Environmental and biomedical applications of metal stable isotopes. *Elements*, 5, 381–385. <https://doi.org/10.2113/gselements.5.6.381>.
- Bump, A. P., and Hovorka, S. D., (2023), Fetch-trap pairs: exploring definition of carbon storage prospects to increase capacity and flexibility in areas with competing uses: *International Journal of Greenhouse Gas Control*, 122, no. 103817, 10 pages. <http://doi.org/10.1016/j.ijggc.2022.103817>.
- Capo, R. C., Stewart, B. W., Rowan, E. L., Kolesar, C. A., Wall, A. J., Chapman, E. C., & Hammack, R. W. (2014). The strontium isotopic evolution of Marcellus Formation produced water, southwestern Pennsylvania. *International Journal of Coal Geology*, 26, 57–63 <https://doi.org/10.1016/j.coal.2013.12.010>.
- Capuano, R. M., & Jan, R. Z. (1996). In situ hydraulic conductivity of clay and silt-clay fluvial-deltaic sediments, Texas Gulf Coast. *Groundwater*, 34, 545–555. <https://doi.org/10.1111/j.1745-6584.1996.tb02036.x>.
- Carey, J. W., Wigand, M., Chipera, S. J., Wolde, G., Pawar, R., Lichtner, P. C., Wehner, S. C., Raines, M. A., & Guthrie, G. D. (2007). Analysis and performance of oil well cement with 30 years of CO<sub>2</sub> exposure from the SACROC Unit, West Texas, USA. *International Journal of Greenhouse Gas Control*, 1, 75–85. [https://doi.org/10.1016/S1750-5836\(06\)00004-1](https://doi.org/10.1016/S1750-5836(06)00004-1).
- Carothers, W. W., & Kharaka, Y. K. (1978). Aliphatic acid anions in oil-field water. Implications for origin of natural gas. *American Association of Petroleum Geologists Bulletin*, 62, 2441–2453. <https://doi.org/10.1306/C1EA5521-16C9-11D7-8645000102C1865D>.

- Carothers, W. W., & Kharaka, Y. K. (1980). Stable carbon isotopes of  $\text{HCO}_3$  in oil-field water. Implications for the origin of  $\text{CO}_2$ . *Geochimica et Cosmochimica Acta*, 44, 323–333. [https://doi.org/10.1016/0016-7037\(80\)90140-4](https://doi.org/10.1016/0016-7037(80)90140-4).
- Carpenter, A. B. (1978). Origin and chemical evolution of brines in sedimentary basins. *Oklahoma Geological Survey Circular*, 79, 60–77. <https://doi.org/10.2118/7504-MS>.
- Carpenter, A. B., Trout, M. L., & Pickett, E. E. (1974). Preliminary report on the origin and chemical evolution of lead- and zinc-rich brines in central Mississippi. *Economic Geology*, 52, 1191–1206. <https://doi.org/10.2113/gsecongeo.69.8.1191>.
- Case, L. C. (1955). Origin and current usage of the term, “connate water.” *American Association of Petroleum Geologists Bulletin*, 39, 1879–1882.
- Cassidy, D. P., & Ranganathan, V. (1992). Groundwater upwelling near Bay St. Elaine salt dome in southeastern Louisiana, as inferred from fluid property variations. *American Association of Petroleum Geologists Bulletin*, 76, 1560–1568. <https://doi.org/10.1306/BDF8A4C-1718-11D7-8645000102C1865D>.
- Celia, M. A., Kavetski, D., Nordbotten, J. M., Bachu, S., & Gasda, S. E. (2006). Implications of abandoned wells for site selection. In *Proceedings of the CO2SC 2006 International Symposium on Site Characterization for CO2 Geological Storage, Berkeley, CA* (pp. 157–159). Lawrence Berkeley National Laboratory.
- Chadwick, R. A., Noy, D., Arts, R., & Eiken, O. (2009). Latest time-lapse seismic data from Sleipner yield new insights into  $\text{CO}_2$  plume development. *Energy Procedia*, 1, 2103–2110. <https://doi.org/10.1016/j.egypro.2009.01.274>.
- Chadwick, R. A., Zweigel, P., Gregersen, U., Kirby, G. A., Holloway, S., & Johannessen, P. N. (2004). Geological reservoir characterization of a  $\text{CO}_2$  storage site: The Utsira Sand, Sleipner, northern North Sea. *Energy*, 9, 1371–1381. <https://doi.org/10.1016/j.energy.2004.03.071>.
- Chan, L. H., Starinsky, A., & Katz, A. (2002). The behavior of lithium and its isotopes in oilfield brines: Evidence from the Heletz-Kokhav Field, Israel. *Geochimica et Cosmochimica Acta*, 66, 615–623. [https://doi.org/10.1016/S0016-7037\(01\)00800-6](https://doi.org/10.1016/S0016-7037(01)00800-6).
- Chaudhary, B. K., Sabie, R., Engle, M. A., Xu, P., Willman, S., & Carroll, K. C. (2019). Spatial variability of produced-water quality and alternative-source water analysis applied to the Permian Basin, USA. *Hydrogeology Journal*, 27(8), 2889–2905. <https://doi.org/10.1007/s10040-019-02054-4>.
- Clark, C. E., & Veil, J. A. (2009). *Produced water volumes and management practices in the United States*. Argonne National Laboratory Report ANL/EVS/R-09/1. US Department of Energy. <https://doi.org/10.2172/1007397>.
- Clark, I. D. (2015). *Groundwater geochemistry and isotopes*. CRC. <https://doi.org/10.1201/b18347>.
- Clark, I. D., & Fritz, P. (2013). *Environmental isotopes in hydrogeology*. CRC. <https://doi.org/10.1201/9781482242911>.

- Collins, A. G. (1974). *Geochemistry of liquids, gases, and rocks from the Smackover Formation: Report of investigations number 7897*. US Department of Energy, Office of Scientific and Technical Information. <https://www.osti.gov/biblio/7258153>.
- Collins, A. G. (1975). *Geochemistry of oil field water*. Elsevier.
- Collins, A. G., & Egleson, G. C. (1967). Iodide abundance in oilfield brines in Oklahoma. *Science*, 156(3777), 934–935. <https://doi.org/10.1126/science.156.3777.934>.
- Conaway, C. H., Thordsen, J. J., Manning, M. A., Cook, P. J., Trautz, R. C., Thomas, R. B., & Kharaka, Y. K. (2016). Comparison of geochemical data obtained using four brine sampling methods at the SECARB phase III anthropogenic test CO<sub>2</sub> injection site, Citronelle oil field, Alabama. *International Journal of Coal Geology*, 162, 85–95. <https://doi.org/10.1016/j.coal.2016.06.001>.
- Connor, B. F., Rose, D. L., Noriega, M. C., Murtaugh, L. K., & Abney, S. R. (1997). *Methods of analysis by the US Geological Survey National Water Quality Laboratory – Determination of 86 volatile organic compounds in water by gas chromatography/mass spectrometry, including detections less than reporting limits (Open-File Report)* (pp. 97–829). US Geological Survey. <https://pubs.er.usgs.gov/publication/ofr97829>.
- Cook, P. G., & Herczeg, A. L. (2000). *Environmental tracers in hydrology*. Kluwer Academic.
- Cozzarelli, I. M., Bekins, B. A., Eganhouse, R. P., Warren, E., & Essaid, H. I. (2010). In situ measurements of volatile aromatic hydrocarbon biodegradation rates in groundwater. *Journal of Contaminant Hydrology*, 111(1–4), 48–64. <https://doi.org/10.1016/j.jconhyd.2009.12.001>.
- Cozzarelli, I. M., Schreiber, M. E., Erickson, M. L., & Ziegler, B. A. (2015). Arsenic cycling in hydrocarbon plumes: Secondary effects of natural attenuation. *Groundwater*, 54(1), 35–45. <https://doi.org/10.1111/gwat.12316>.
- Craig, H. (1961). Isotopic variations in meteoric water. *Science*, 133, 1702–1703.
- Cramer, B. D., & Jarvis, I. (2020). Carbon isotope stratigraphy. In F. M. Gradstein, J. G. Ogg, M. D. Schmitz, & G. M. Ogg (Eds.), *Geologic time scale 2020, Vol 1*, 309–343. <https://doi.org/10.1016/B978-0-12-824360-2.00011-5>.
- Crossey, L. J. (1991). Thermal degradation of aqueous oxalate species. *Geochimica et Cosmochimica Acta*, 55, 1515–1527.
- Crossey, L. J., Surdam, R. C., & Lahann, R. (1985). Application of organic/inorganic diagenesis to porosity prediction. D. L. Gautier (Ed.), *Relationship of organic matter and mineral diagenesis, Special Publication*, 38, 147–156. <https://doi.org/10.2110/pec.86.38.0147>.
- Dadrasnia, A., Salmah, I., Emenike, C. U., & Shahsavari, N. (2015). Remediation of oil contaminated media using organic material supplementation. *Petroleum Science and Technology*, 33, 1030–1037. <https://doi.org/10.1080/10916466.2014.925920>.
- Daley, T. M., Myer, L. R., Peterson, J. E., Majer, E. L., & Hoversten, G. M. (2008). Time-lapse cross-well seismic and VSP monitoring of injected CO<sub>2</sub> in a brine aquifer. *Environmental Geology*, 54, 1657–1665. <https://doi.org/10.1007/s00254-007-0943-z>.

- Daley, T. M., Solbau, R. D., Ajo-Franklin, J. B., & Benson, S. M. (2007). Continuous active-source monitoring of CO<sub>2</sub> injection in a brine aquifer. *Geophysics*, 72(5), A57–A61. <https://10.1190/1.2754716>.
- Dance, S., Kaplan, S., & Penney, V. (2024). Scientists knew 2023's heat would be historic — but not by this much. *Washington Post*, January 9, 2024.
- Dansgaard, W. (1964). Stable isotopes in precipitation. *Tellus*, 16, 436–468.
- Darrah, T. H., Vengosh, A., Jackson, R. B., Warner, N. R., & Poreda, R. J. (2014). Noble gases identify the mechanisms of fugitive gas contamination in drinking-water wells overlying the Marcellus and Barnett Shales. In *Proceedings of the National Academy of Sciences*, 111(39), 14076–14081. <https://doi.org/10.1073/pnas.1322107111>.
- Das, N., Horita, J., & Holland, H. D. (1990). Chemistry of fluid inclusions in halite from the Salina Group of the Michigan Basin: Implication for Late Silurian seawater and the origin of sedimentary brines. *Geochimica et Cosmochimica Acta*, 54, 319–327. [https://doi.org/10.1016/0016-7037\(90\)90321-B](https://doi.org/10.1016/0016-7037(90)90321-B).
- Davis, S. N. (1964). The chemistry of saline water by R.A. Krieger. Discussion. *Groundwater*, 2, 51.
- Davisson, M. K., & Criss, R. E. (1996). Na–Ca–Cl relations in basinal fluids. *Geochimica et Cosmochimica Acta*, 60, 2743–2752. [https://doi.org/10.1016/0016-7037\(96\)00143-3](https://doi.org/10.1016/0016-7037(96)00143-3).
- Deel, D., Mahajan, K., Mahoney, C. R., McIlvried, H. G., & Srivastava, R. D. (2006). Risk assessment and management for long-term storage of CO<sub>2</sub> in geologic formations. *Journal of Systemics, Cybernetics and Informatics*, 5, 79–85. <https://www.iiisci.org/journal/pdv/sci/pdfs/P807791.pdf>.
- Degens, E. T., Hunt, I. M., Reuter, J. H., & Reed, W. E. (1964). Data on the distribution of amino acids and oxygen isotopes in petroleum brine water of various geologic ages. *Sedimentology*, 3, 199–225. <https://doi.org/10.1111/j.1365-3091.1964.tb00460.x>.
- Delin, G. N., & Herkelrath, W. N. (2014). Effects of a dual-pump crude-oil recovery system, Bemidji, Minnesota, USA. *Groundwater Monitoring & Remediation*, 34(1), 57–67. <https://ngwa.onlinelibrary.wiley.com/toc/17456592/2014/34/1>.
- Delin, G. N., Essaid, H. I., Cozzarelli, I. M., Lahvis, M. H., & Bekins, B. A. (1998). *Ground-water contamination by crude oil near Bemidji, Minnesota (Fact sheet number 084-98)*. US Geological Survey. <https://doi.org/10.3133/fs08498>.
- Delin, G. N., Herkelrath, W. N., & Trost, J. J. (2020). *Effects of a crude-oil recovery remediation system operated 1999–2003 on groundwater plumes and unsaturated-zone vapor concentrations at a crude-oil spill site near Bemidji, Minnesota (Scientific investigations report 2020-5111)*. US Geological Survey. <https://doi.org/10.3133/sir20205111>.
- Demir, I. (1988). Studies of smectite membrane behavior: electrokinetic, osmotic, and isotopic fractionation processes at elevated pressures. *Geochimica et Cosmochimica Acta*, 52, 727–737. [https://doi.org/10.1016/0016-7037\(88\)90333-X](https://doi.org/10.1016/0016-7037(88)90333-X).

- DeSimone, L. A., McMahon, P. B., & Rosen, M. R. (2014). *The quality of our nation's water: Water quality in principle aquifers of the United States, 1991–2010* (Circular number 1360). US Geological Survey. <https://doi.org/10.3133/cir1360>.
- Deutsch, W. J. (1997). *Groundwater geochemistry: Fundamentals and applications to contamination*. Lewis. <https://doi.org/10.1201/9781003069942>.
- Dieter, C. A., Maupin, M. A., Caldwell, R. R., Harris, M. A., Ivahnenko, T. I., Lovelace, J. K., Barber, N. L., & Linsey, K. S. (2018). *Estimated use of water in the United States in 2015* (Circular number 1441). US Geological Survey. <https://doi.org/10.3133/cir1441>.
- Doughty, C., Freifeld, B. M., & Trautz, R. C. (2008). Site characterization for CO<sub>2</sub> geologic storage and vice versa: the Frio brine pilot, Texas, USA, as a case study. *Environmental Earth Sciences*, 54(8), 1635–1656. <https://doi.org/10.1007/s00254-007-0942-0>.
- Drever, J. I. (1997). *The geochemistry of natural water* (3rd ed.). Prentice Hall. <https://agris.fao.org/agris-search/search.do?recordID=XF2016034002>.
- Drummond, S. E., & Palmer, D. A. (1986). Thermal decarboxylation of acetate. II: Boundary conditions for the role of acetate in the primary migration of natural gas. *Geochimica et Cosmochimica Acta*, 50, 813–824. [https://doi.org/10.1016/0016-7037\(86\)90358-3](https://doi.org/10.1016/0016-7037(86)90358-3).
- Dusseault, M. B. (2001). *Comparing Venezuelan and Canadian heavy oil and tar sands* [Paper presentation]. In Proceedings of Petroleum Society's Canadian International Conference, Calgary, AB, June 2001. <https://doi.org/10.2118/2001-061>.
- Dworkin, S. I., & Land, L. S. (1996). The origin of aqueous sulfate in Frio pore fluids and its implication for the origin of oil-field brines. *Applied Geochemistry*, 11, 403–408.
- East Texas Salt Water Disposal Corporation. (1953). *Salt water disposal in the East Texas Field, Report*. Austin, Texas, USA.
- Eastoe, C. J., Long, A., Land, L. S., & Kyle, J. R. (2001). Stable chloride isotopes in halite and brine from the Gulf Coast Basin: Brine genesis and evolution. *Chemical Geology*, 176, 343–360.
- Editor. (1993). Editorial: EPA drafts tougher injection well rules. *Oil and Gas Journal*, 91.
- Edmunds, W. M., & Smedley, P. L. (1996). Groundwater geochemistry and health: An overview. *Geological Society Special Publication 113*, 91–105. <https://doi.org/10.1144/GSL.SP.1996.113.01.08>.
- Eganhouse, R. P., Baedeker, M. J., Cozzarelli, I. M., Aiken, G. R., Thorn, K. A., & Dorsey, T. F. (1993). Crude oil in a shallow sand and gravel aquifer-II. Organic geochemistry. *Applied Geochemistry*, 8(6), 551–567. [https://doi.org/10.1016/0883-2927\(93\)90013-7](https://doi.org/10.1016/0883-2927(93)90013-7).
- Eganhouse, R. P., Dorsey, T. F., Phinney, C. S., & Westcott, A. M. (1996). Processes affecting the fate of monoaromatic hydrocarbons in an aquifer contaminated by crude oil. *Environmental Science and Technology*, 30, 3304–3312. <https://doi.org/10.1021/es960073b>.

- Egeberg, P. K., & Aagaard, P. (1989). Origin and evolution of formation water from oil fields on the Norwegian shelf. *Applied Geochemistry*, 4, 131–142. [https://doi.org/10.1016/0883-2927\(89\)90044-9](https://doi.org/10.1016/0883-2927(89)90044-9).
- Eggenkamp, H. G. M. (1998). The stable isotope geochemistry of the halogens Cl and Br: A review of 15 years development. *Mineralogical Magazine*, 62-A(1), 411–412.
- Eggenkamp, H. G. M., & Coleman, M. L. (2000). Rediscovery of classical methods and their application to the measurement of stable bromide isotopes in natural samples. *Chemical Geology*, 167, 393–402. [https://doi.org/10.1016/S0009-2541\(99\)00234-X](https://doi.org/10.1016/S0009-2541(99)00234-X).
- Ellsworth, W. L. (2013). Injection-induced earthquakes. *Science*, 341(6142). <https://www.science.org/doi/10.1126/science.1225942>.
- Ellsworth, W., Hickman, S., Llenos, E., McGarr, A., Michael, A., & Rubinstein, J. (2012). Are seismicity rate changes in the midcontinent natural or manmade? *Seismological Research Letters*, 83(2), 403. <https://disaster-sts-network.org/content/are-seismicity-rate-changes-midcontinent-natural-or-manmade-1>.
- Emery, D., & Robinson, A. (1993). *Inorganic geochemistry: Applications to petroleum geology*. Blackwell Scientific.
- Engelder, T. (2012). Capillary tension and imbibition sequester frack fluid in Marcellus gas shale. *Proceedings of the National Academy of Sciences*, 109(52), E3625. <https://doi.org/10.1073/pnas.1216133110>.
- Engle, M. A., & Rowan, E. L. (2014). Geochemical evolution of produced water from hydraulic fracturing of the Marcellus Shale, northern Appalachian Basin: A multivariate compositional data analysis approach. *International Journal of Coal Geology*, 126, 45–56. <https://doi.org/10.1016/j.coal.2013.11.010>.
- Engle, M. A., Reyes, F. R., Varonka, M. S., Orem, W. H., Ma, L., Ianno, A. J., Schell, T. M., Xu, P., & Carroll, K. C. (2016). Geochemistry of formation water from the Wolfcamp and “Cline” shales: Insights into brine origin, reservoir connectivity, fluid flow in the Permian Basin, USA. *Chemical Geology*, 425, 76–92. <https://doi.org/10.1016/j.chemgeo.2016.01.025>.
- Engle, M. A., Doolan, C. A., Pitman, J. A., Varonka, M. S., Chenault, J., Orem, W. H., McMahon, P. B., & Jubb, A. M. (2020). Origin and geochemistry of formation water from the Lower Eagle Ford group, Gulf Coast Basin, south central Texas. *Chemical Geology*, 550(119754), 1–12. <https://doi.org/10.1016/j.chemgeo.2020.119754>.
- Erickson, M. L., Elliott, S. M., Brown, C. J., Stackelberg, P., Ransom, K. M., Reddy, J. E., & Cravotta, C. A. (2021). Machine-learning predictions of high arsenic and high manganese at drinking water depths of the glacial aquifer system, northern continental United States. *Environmental Science & Technology*, 55(9), 5791–5805. <https://pubs.acs.org/doi/10.1021/acs.est.0c06740>.
- Ennis-King, J., LaForce, T., Paterson, L., Black, J., Vu, H., Haese, R., Sernod, S., Gilfilland, S., Johnson, G., Freifeld, B., & Singh, R. (2017). Stepping into the same river twice:

- Field evidence for the repeatability of a CO<sub>2</sub> injection test. *Energy Procedia*, 114, 2760–2771. <https://doi.org/10.1016/j.egypro.2017.03.1392>.
- Esch, W. L., & Hanor, J. S. (1995). Fault and fracture control of fluid flow and diagenesis around the Iberia salt dome, Iberia Parish, Louisiana. *Gulf Coast Association of Geological Societies Transactions*, 45, 181–187. <https://www.osti.gov/biblio/150551>.
- Esposito, R. A., Rhudy, R., Trautz, R. C., Koperna, G. J., & Hill, G. (2011). Integrating carbon capture with transportation and storage. *Energy Procedia*, 4, 5512–5519. <https://10.1016/j.egypro.2011.02.537>.
- Essaid, H. I., Bekins, B. A., Herkelrath, W. N., & Delin, G. N. (2011). Crude oil at the Bemidji site-25 years of monitoring, modeling and understanding. *Groundwater*, 49, 706–726. <https://doi.org/10.1111/j.1745-6584.2009.00654.x>.
- Evans, D. G., Nunn J. A., & Hanor, J. S. (1991). Mechanisms driving groundwater flow near salt domes. *Geophysical Research Letters*, 18, 927–930. <https://doi.org/10.1029/91GL00908>.
- Everett, R. R., Brown, A. A., Gillespie, J. M., Kjos, A., & Fenton, N. C. (2020). *Multiple-well monitoring site adjacent to the North and South Belridge Oil Fields, Kern County, California (Open-File Report 2020-1116)*. US Geological Survey. <https://doi.org/10.3133/ofr20201116>.
- Fabryka-Martin, J. (2000). Iodine-129 as a groundwater tracer. In P. Cook & A. L. Herczeg (Eds.), *Environmental tracers in subsurface hydrogeology* (pp. 504–510). Kluwer Academic.
- Fakhru'l-Razi, A., Pendashteh, A., Abdullah, L. C., Biak, D. R. A., & Madae, S. S. (2009). Review of technologies for oil and gas produced water treatment. *Journal of Hazardous Materials*, 170(2–3), 530–551. <https://doi.org/10.1016/j.jhazmat.2009.05.044>.
- Fantle, M. S., & Bullen, T. D. (2009). Essentials of iron, chromium and calcium isotope analysis of natural materials by thermal ionization mass spectrometry. *Chemical Geology*, 258, 50–64. <https://doi.org/10.1016/j.chemgeo.2008.06.018>.
- Farkäs, J., Chakrabarti, R., Jacobsen, S., Kump, L. R., & Melezhik, V. A. (2012). Ca and Mg isotopes in sedimentary carbonates. *Frontiers in Earth Sciences, Springer*, 8, [https://doi.org/10.1007/978-3-642-29670-3\\_10](https://doi.org/10.1007/978-3-642-29670-3_10).
- Kump, L. R., Kuznetsov, A. B., Gorokhov, I. M., Melezhik, V. A., Farkäs, J., Chakrabarti, R., Jacobsen, S. B., Reinhard, C. T., Lyons, T. W., Rouxel, O., Asael, D., Dauphas, N., van Zuilen, M., Schoenberg, R., Tissot, F. L. H., Hannah, J. L., & Stein, H. J. (2013). 7.10 Chemical Characteristics of Sediments and Seawater. In V. A. Melezhik, L. R. Kump, H. Strauss, E. J. Hanski, A. R. Prave, & A. Lepland (Eds.), *Reading the archive of earth's oxygenation (Volume 3: Global events and the Fennoscandian Arctic Russia–Drilling early earth project)* (pp. 1457–1514). Springer. [https://doi.org/10.1007/978-3-642-29670-3\\_10](https://doi.org/10.1007/978-3-642-29670-3_10).
- Faure, G. (1986). *Principles of isotope geology* (2nd ed.). Wiley. <https://www.osti.gov/biblio/7100564>.

- Faure, G., & Mensing, T. M. (2005). *Isotopes: Principles and applications* (3rd ed.). Wiley. [Faure & Mensing 2005 \(pdf\)](#).
- Fessenden, J. E., Clegg, S. M. Rahn, T. A., Humphries, S. D., & Baldrige, W. S. (2010). Novel MVA tools to track CO<sub>2</sub> seepage, tested at the ZERT controlled release site in Bozeman, MT. *Environmental Earth Sciences*, 60, 325–334. <https://link.springer.com/article/10.1007/s12665-010-0489-3>.
- Fessenden, J. E., Stauffer, P. H., & Viswanathan, H. S. (2009). Natural analogs of geologic CO<sub>2</sub> sequestration: Some general implications for engineered sequestration. In B. J. McPherson & E. T. Sundquist (Eds.), *Carbon sequestration and its role in the global carbon cycle* (Geophysical Monograph Series, 183, 135–146). American Geophysical Union. [https://ui.adsabs.harvard.edu/link\\_gateway/2009GMS...183..135F/doi:10.1029/2006GM000384](https://ui.adsabs.harvard.edu/link_gateway/2009GMS...183..135F/doi:10.1029/2006GM000384).
- Fipps, G. (2021). Irrigation water quality standards and salinity management. *Texas Cooperative Extension, EB-1667*. The Texas A&M University System. <https://gfipps.tamu.edu/files/2021/11/EB-1667-Salinity.pdf>.
- Fisher, R. S. (1998). Geologic and geochemical controls on naturally occurring radioactive materials (NORM) in produced water from oil, gas and geothermal operations. *Environmental Geosciences*, 5, 139–150. [doi.org/10.1046/j.1526-0984.1998.08018.x](https://doi.org/10.1046/j.1526-0984.1998.08018.x).
- Fisher, J. B., & Boles, J. R. (1990). Water rock interaction in Tertiary sandstones, San Joaquin Basin, California, USA: Diagenetic controls on water composition. *Chemical Geology*, 82, 83–101. [https://doi.org/10.1016/0009-2541\(90\)90076-J](https://doi.org/10.1016/0009-2541(90)90076-J).
- Forbes, R. J. (1958). *Studies in early petroleum history*. Brill. <https://books.google.com.br/books?hl=pt-BR&lr=&id>.
- Fournier, R. O., White, D. E., & Truesdell, A. H. (1974). Geochemical indicators of subsurface temperature. I: Basic assumptions. *Journal of Research of the US Geological Survey*, 2, 259–262, <https://doi.org/10.3133/ofr741033>.
- FracFocus. (2021). *Chemical disclosure registry*. <https://fracfocus.org>.
- Franks, K. A., & Lambert, P. F. (1985). *Early California oil: A photographic history, 1865–1940*. Texas A& M University Press. <https://www.tamupress.com/book/9780890969892/early-california-oil/>.
- Freeze, R. A., & Cherry, J. A. (1979). *Groundwater*. Prentice Hall. <https://gw-project.org/books/groundwater/>.
- Freifeld, B. M., Trautz, R. C., Kharaka, Y. K., Phelps, T. J., Myer, L. R., Hovorka, S. D., & Collins, D. J. (2005). The U-tube: A novel system for acquiring borehole fluid samples from a deep geologic CO<sub>2</sub> sequestration experiment. *Journal of Geophysical Research*, 110, B10203. <https://doi.org/10.1029/2005JB003735>.
- Friedlingstein, P., O'Sullivan, M., Jones, M. W. (2020). Global carbon budget 2020. *Earth System Science Data*, 12, 3269–3340. <https://doi.org/10.5194/essd-12-3269-2020>.
- Friedmann, S. J. (2007). Geological carbon dioxide sequestration. *Elements*, 3, 179–184. <https://education.aapg.org/carbonsequestration/friedmann.pdf>.

- Fritz, S. J., & Marine, I. W. (1983). Experimental support for a predictive osmotic model of clay membranes. *Geochimica et Cosmochimica Acta*, 47, 1515–1522.  
[https://doi.org/10.1016/0016-7037\(83\)90310-1](https://doi.org/10.1016/0016-7037(83)90310-1).
- Fritz, P., & Fontes, J. C. (1986). *Handbook of environmental isotope geochemistry. The Terrestrial Environment*, 2. Elsevier.  
[https://inis.iaea.org/search/search.aspx?orig\\_q=RN:20059224https://inis.iaea.org/search/search.aspx?orig\\_q=RN:20059224](https://inis.iaea.org/search/search.aspx?orig_q=RN:20059224https://inis.iaea.org/search/search.aspx?orig_q=RN:20059224).
- Froehlich, K., Ivanovich, M., Hendry, M. J., Andrews, J. N., Davis, S. N., Drimmie, R. J., Fabryka-Martin, J., Florkowski, T., Fritz, P., Lehmann, B. E., Loosli, H. H., & Nolte, E. (1991). Application of isotopic methods to dating of very old groundwater: Milk River aquifer, Alberta, Canada. *Applied Geochemistry*, 6, 465–472.  
[https://doi.org/10.1016/0883-2927\(91\)90045-Q](https://doi.org/10.1016/0883-2927(91)90045-Q).
- Fromkin, D. (1989). *A peace to end all peace: The fall of the Ottoman empire and the creation of the modern Middle East*. Macmillan.  
<https://us.macmillan.com/books/9780805088090/apecetoendallpeace>.
- Fu, B. (1998). *A study of pore fluids and barite deposits from hydrocarbon seeps: Deepwater Gulf of Mexico* [Unpublished doctoral dissertation]. Louisiana State University.
- Fuge, R., & Johnson, C. C. (2015). Iodine and human health, the role of environmental geochemistry and diet, a review. *Applied Geochemistry*, 63, 282–302.  
<https://doi.org/10.1016/j.apgeochem.2015.09.013>.
- Fujikawa, S., Selyanchyn, R., & Kunitake, T. (2020). A new strategy for membrane-based direct air capture. *Polymer Journal*, 53, 111–119.  
<https://doi.org/10.1038/s41428-020-00429-z>.
- Gallegos, T. J., Varela, B. A., Haines, S. S., & Engle, M. A. (2015). Hydraulic fracturing water use variability in the United States and potential environmental implications. *Water Resources Research*, 51(7). <https://doi.org/10.1002/2015WR017278>.
- Gans, K. D., Kharaka, Y. K., Conaway, C. H., Blondes, M. S., Reidy, M. E., Thordsen, J. J., Rowan, E. L., & Engle, M. (2015). *Management of reclaimed produced water in California, enhanced with the expanded United States Geological Survey Produced Water Geochemical Database* [Poster presentation]. Groundwater Resources Association of California, October 2015.
- Gavrieli, I., Starinsky, A., Spiro, B., Aizenshat, Z., & Nielsen, H. (1995). Mechanisms of sulfate removal from subsurface chloride brines: Heletz-Kokhav oilfields, Israel. *Geochimica et Cosmochimica Acta*, 59, 3525–3533. [https://doi.org/10.1016/0016-7037\(95\)00229-S](https://doi.org/10.1016/0016-7037(95)00229-S).
- Gilfillan, S. M. V., Ballentine, C. J., Holland, G., Blagburn, D., Sherwood-Lollar, B., Stevens, S., Schoell, M., & Cassidy, M. (2008). The noble gas geochemistry of natural CO<sub>2</sub> gas reservoirs from the Colorado Plateau and Rocky Mountain provinces, USA. *Geochimica et Cosmochimica Acta*, 72, 1174–1198.  
<https://doi.org/10.1016/j.gca.2007.10.009>.

- Gillespie, J. M., Davis, T., Stephens, M. J., Ball, L. B., & Landon, M. K. (2019). Groundwater salinity and the effects of produced water disposal in the Lost Hills-Belridge oilfields, Kern County, California. *Environmental Geosciences*, 36, pages 73–96. <https://doi.org/10.1306/eg.02271918009>.
- Giordano, T. H. (2000). Organic matter as transport agent in ore-forming systems. *Reviews in Economic Geology*, 9, 133–156. <https://doi.org/10.5382/Rev.09.07>.
- Giordano, T. H., & Barnes, H. L. (1981). Lead transport in Mississippi Valley-type ore solutions. *Economic Geology*, 76, 2200–2211. <https://doi.org/10.2113/gsecongeo.76.8.2200>.
- Giordano, T. H., & Kharaka, Y. K. (1994). Organic ligand distribution and speciation in sedimentary basin brines, diagenetic fluids, and related ore solutions. In J. Palmer (Ed.), *Geofluids: Origin, migration, and evolution of fluids in sedimentary basins. Special Publication Number 78* (pp. 175–202). Geological Society of London. <https://www.lyellcollection.org/doi/abs/10.1144/GSL.SP.1994.078.01.14?download=true>.
- Gislason, S. R., Boenisch, D. W., Stefansson, A., Oelkers, E. H., Gunnlaugsson, E., Sigurdardottir, H., Sigfusson, B., Broecker, W. S., Matter, J. M., Stute, M., Axelsson, G., & Fridriksson, T. (2010). Mineral sequestration of carbon dioxide in basalt: A pre-injection overview of the CarbFix project. *International Journal of Greenhouse Gas Control*, 4, 537–545. <https://doi.org/10.1016/j.ijggc.2009.11.013>.
- Global CCS Institute. (2020). *Capacity of operational large-scale carbon capture and storage facilities worldwide as of 2020 (in million metric tons per year)*. Statista. <https://www.statista.com/statistics/1108355/largest-carbon-capture-and-storage-projects-worldwide-capacity/><https://www.statista.com/statistics/1108355/largest-carbon-capture-and-storage-projects-worldwide-capacity/>.
- Godsy, E. M., Hostettler, F. D., Warren, E., Paganelli, V. V., & Kharaka, Y. K. (2003). The fate of petroleum and other organics associated with produced water from the Osage-Skiatook petroleum environmental research site, Osage County, Oklahoma. In Kharaka, Y. K., & Otton, J. K. (Eds.), *Environmental impacts of petroleum production: Initial results from the Osage-Skiatook petroleum environmental research (OPER) sites, Osage County, Oklahoma* (pp. 84–102). US Geological Survey Water-Resources Investigations Report 03-4260
- Gorman, H. S. (1999). Efficiency, environmental quality and oil field brines: The success and failure of pollution control by self-regulation. *Business History Review*, 73(4), 601–640. <https://doi.org/10.2307/3116128>.
- Government Accountability Office (GAO). (1989). GAO finds brine still contaminate aquifers. *Oil and Gas Journal*, 87(16 October 1989), 38.
- Government Accountability Office (GAO). (2014). *Freshwater: Supply concerns continue and uncertainties complicate planning*. US Government Report to Congressional Requesters 14–430. <https://www.gao.gov/assets/gao-14-430.pdf>.

- Government of Canada. (2020). *Oil sands: A strategic resource for Canada, North America and the global market*. Water Management. [https://natural-resources.canada.ca/sites/www.nrcan.gc.ca/files/energy/pdf/oilsands-sablesbitumineux/14-0704%20Oil%20Sands%20-%20Water%20Management\\_e.pdf](https://natural-resources.canada.ca/sites/www.nrcan.gc.ca/files/energy/pdf/oilsands-sablesbitumineux/14-0704%20Oil%20Sands%20-%20Water%20Management_e.pdf).
- Government of Canada. (2021). *Environment and natural resources/ energy*. <https://www.canada.ca/en/services/environment.html>.
- Graf, D. L. (1982). Chemical osmosis and the origin of subsurface brines. *Geochimica et Cosmochimica Acta*, 46, 1431–1448. [https://doi.org/10.1016/0016-7037\(82\)90277-0](https://doi.org/10.1016/0016-7037(82)90277-0).
- Graf, D. L., Meents, W.F., Friedman, I., & Shimp, N.F. (1966). *The origin of saline formation waters, III. Calcium chloride waters*. Illinois State Geological Survey Circular 397.
- Gregory, K. B., Vidic, R. D., & Dzombak, D. A. (2011). Water management challenges associated with the production of shale gas by hydraulic fracturing. *Elements*, 7, 181–186. <https://doi.org/10.2113/gselements.7.3.181>.
- Ground Water Protection Council and ALL Consulting. (2009). *Modern shale gas development in the United States: A primer*. US Department of Energy, National Energy Technology Laboratory, DE-FG26-04NT15455. <https://www.energy.gov/fecm/articles/modern-shale-gas-development-united-states-primer>.
- Ground Water Protection Council. (2019). *Produced water report: Regulations, current practices and research needs*. Groundwater Protection Council. [https://www.gwpc.org/wp-content/uploads/2019/06/Produced Water Full Report Digital Use.pdf](https://www.gwpc.org/wp-content/uploads/2019/06/Produced-Water-Full-Report-Digital-Use.pdf).
- Ground Water Protection Council, (2023), *Produced Water Report: update*. Groundwater Protection Council, 95 pages. <https://gwpc.org>.
- Gunter, W. D., & Bird, G. W. (1988). CO<sub>2</sub>-production in tar sand reservoirs under in situ steam temperatures: reactive calcite dissolution. *Chemical Geology*, 70, 301–331.
- Gunter, W. D., & Perkins, E. H.. (1991). Use of calcite as a CO<sub>2</sub> geobarometer for estimation of reservoir pressures in thermally assisted oil recovery. *The Canadian Mineralogist*, 29, 755–765.
- Gunter, W. D., Perkins, E. H., & McCann T. J. (1993). Aquifer disposal of CO<sub>2</sub>-rich gases: Reaction design for added capacity. *Energy Conversion and Management*, 34, 941–948. [https://doi.org/10.1016/0196-8904\(93\)90040-H](https://doi.org/10.1016/0196-8904(93)90040-H).
- Gunter, W. D., Perkins, E. H., & Hutcheon, I. (2000). Aquifer disposal of acid gases: Modeling of water rock reactions for trapping of acid wastes. *Applied Geochemistry*, 15, 1085–1095.
- Gussone, N., & Dietzel, M. (2016). Calcium isotope fractionation during mineral precipitation from aqueous solution. In N. Gussone, A.-D. Schmitt, A. Heuser, F. Wombacher, M. Dietzel, E. Tipper, & M. Schiller (Eds.), *Calcium stable isotope geochemistry* (pp. 75–110). [https://doi.org/10.1007/978-3-540-68953-9\\_3](https://doi.org/10.1007/978-3-540-68953-9_3).

- Haines, S. S., Varela, B. A., Hawkins, S. J., Gianoutsos, N. J., Thamke, J. N., Engle, M. A., Tennyson, M. E., Schenk, C. J., Gaswirth, S. B., Marra, K. R., Kinney, S. A., Mercier, T. J., & Martinez, C. D. (2017). *Assessment of water and proppant quantities associated with petroleum production from the Bakken and Three Forks Formations, Williston Basin Province, Montana and North Dakota, 2016 (Fact Sheet 2017-3044)*. US Geological Survey. <https://doi.org/10.3133/fs20173044>.
- Haluszczak, L. O., Rose, A. W., & Kump, L. R. (2013). Geochemical evaluation of flowback brine from Marcellus gas wells in Pennsylvania, USA. *Applied Geochemistry*, 28, 55–61. <https://doi.org/10.1016/j.apgeochem.2012.10.002>.
- Hamlin, H. S. (2006). Salt domes in the Gulf Coast aquifer. In R. E. Mace, S. C. Davidson, E. S. Angle, & W. F. Mullican (Eds.), *Aquifers of the Gulf Coast of Texas: Report*, 365 (pp. 217–230). Texas Water Development Board. [http://www.twdb.texas.gov/publications/reports/numbered\\_reports/doc/r365/r365\\_composite.pdf](http://www.twdb.texas.gov/publications/reports/numbered_reports/doc/r365/r365_composite.pdf).
- Hanor, J. S. (1987). *Origin and migration of subsurface sedimentary brines. Short Course 21*. Society for Sedimentary Geology. <https://doi.org/10.2110/scn.87.21>.
- Hanor, J. S. (1993). Effective hydraulic conductivity of fractured clay beds at a hazardous waste landfill, Louisiana Gulf Coast. *Water Resources Research*, 29, 3691–3698. <https://doi.org/10.1029/93WR01913>.
- Hanor, J. S. (1994). Origin of saline fluids in sedimentary basins. *Geological Society Special Publications*, 78(1), 151–174. <https://doi.org/10.1144/GSL.SP.1994.078.01.13>.
- Hanor, J. S. (1996). Variations in chloride as a driving force in siliciclastic diagenesis. In L. J. Crossey, R. Loucks, & M. W. Totten (Eds.), *Diagenesis and fluid flow: Concepts and applications*. Society for Sedimentary Geology (SEPM) Special Publication 55 (pp. 3–12). <https://doi.org/10.2110/pec.96.55.0003>.
- Hanor, J. S. (1997). Limitations on the use of conventional ground water techniques in characterizing the fate of produced water in on-shore Gulf Coast sediments. *Gulf Coast Association of Geological Societies Transactions*, 47, 193–199.
- Hanor, J. S. (2000). Barite-celestine geochemistry and environments of formation. *Reviews in Mineralogy and Geochemistry*, 40, 193–275. <https://doi.org/10.2138/rmg.2000.40.4>.
- Hanor, J. S. (2001). Reactive transport involving rock-buffered fluids of varying salinity. *Geochimica et Cosmochimica Acta*, 65, 3721–3732. [https://doi.org/10.1016/S0016-7037\(01\)00703-7](https://doi.org/10.1016/S0016-7037(01)00703-7).
- Hanor, J. S. (2004). The role of salt dissolution in the geologic, hydrologic and diagenetic evolution of the northern Gulf Coast sedimentary basin. In P. J. Post, D. L. Olson, K. T. Lyons, D. L. Palmer, P. F. Harrison, & N. C. Rosen (Eds.), *Salt sediment interactions and hydrocarbon prosperity: Concepts, applications, and case studies for the 21st century* (pp. 464–501). Society for Sedimentary Geology. <https://doi.org/10.5724/gcs.04.24.0464>.
- Hanor, J. S. (2007). Variation in the composition and partitioning of adsorbed cations at a brine-contaminated crude oil production facility in southeastern Louisiana, USA.

- Applied Geochemistry*, 22, 2115–2124.  
<https://doi.org/10.1016/j.apgeochem.2007.04.003>↗.
- Hanor, J. S., & McIntosh, J.C. (2006). Are secular variations in seawater chemistry reflected in the compositions of basinal brines? <http://refhub.elsevier.com/B978-0-08-095975-7.00516-7/rf0650> <https://doi.org/10.1016/j.gexplo.2005.11.054>↗.
- Hanor, J. S., & McIntosh, J.C. (2007). Diverse origins and timing of formation of basinal brines in the Gulf of Mexico sedimentary basin. *Geofluids*, 7, 227–237.  
<https://doi.org/10.1111/j.1468-8123.2007.00177.x>↗.
- Hanor, J. S., & Sassen, R. (1990). Evidence for large-scale vertical and lateral migration of formation water, dissolved salt and crude oil in the Louisiana Gulf Coast. In D. Schumacher & B. F. Perkins (Eds.), *Gulf Coast oils and gases: Their characteristics, origin, distribution, and exploration and production significance* (293–296). Gulf Coast Section Society of Petrologists and Mineralogists Foundation.  
<https://doi.org/10.5724/gcs.90.09.0283>↗.
- Hanor, J. S., & Workman, A. L. (1986). Dissolved fatty acids in Louisiana oil-field brines. *Applied Geochemistry*, 1(9), 37–46.  
<https://archives.datapages.com/data/bulletns/1984-85/data/pg/0069/0009/1400/1431c.htm>↗.
- Hanor J. S., Kharaka, Y. K., & Land, L. S. (1988). Geochemistry of water in deep sedimentary basins. *Geology*, 16(6), 560–561  
[https://doi.org/10.1130/0091-7613\(1988\)016<0560:PCRGOW>2.3.CO;2](https://doi.org/10.1130/0091-7613(1988)016<0560:PCRGOW>2.3.CO;2)↗.
- Hanor, J. S., Bailey, J. E., Rogers, M. C., & Milner, L. R. (1986). Regional variations in physical and chemical properties of South Louisiana oil field brines. *Gulf Coast Association of Petroleum Geologists Transactions*, 36, 143–149.
- Hanor J. S., Land, L. S., & Macpherson, L. G. (1993). Carboxylic acid anions in formation water, San Joaquin Basin and Louisiana Gulf Coast, USA – Implications for clastic diagenesis: Critical comment. *Applied Geochemistry*, 8, 305–307.  
[https://doi.org/10.1016/0883-2927\(93\)90046-J](https://doi.org/10.1016/0883-2927(93)90046-J)↗.
- Hanshaw, B. B., & Hill, G. A. (1969). Geochemistry and hydrodynamics of the Paradox Basin Region, Utah, Colorado and New Mexico. *Chemical Geology*, 4, 264–294.  
[https://doi.org/10.1016/0009-2541\(69\)90050-3](https://doi.org/10.1016/0009-2541(69)90050-3)↗.
- Harkness, J. S., Darrah, T. H., Warner, N. R., Whyte, C. J., Moore, M. T., Millot, R., Kloppmann, W., Jackson, R. B., & Vengosh, A. (2017). The geochemistry of naturally occurring methane and saline groundwater in an area of unconventional shale gas development. *Geochimica et Cosmochimica Acta*, 208, 302–334.  
<https://doi.org/10.1016/j.gca.2017.03.039>↗.
- Harkness, J. S., Warner, N. R., Ulrich, A., Millot, R., Kloppmann, W., Ahad, J. M. E., Savard, M. M., Gammon, P., & Vengosh, P. (2018). A characterization of the boron, lithium, and strontium isotopic variations of oil sands process-affected water in

- Alberta, Canada. *Applied Geochemistry*, 90, 50–62.  
<https://doi.org/10.1016/j.apgeochem.2017.12.026>↗.
- Harmon, R. S., & Vannucci, R. (2006). Frontiers in analytical geochemistry – an IGC 2004 perspective. *Applied Geochemistry*, 21, 727–729.
- Harrison, W., & Thyne, G. D. (1992). Predictions of diagenetic reactions in the presence of organic acids. *Geochimica et Cosmochimica Acta*, 56, 565–586.
- Hawkins, M. E., Dietman, W. D., & Seward, J. M. (1963). *Analysis of brines from oil-productive formations in south Arkansas and north Louisiana. Report of Investigations*. US Department of Energy, Office of Scientific and Technical Information.  
<https://www.osti.gov/biblio/7356250>↗.
- Haydon, P. R., & Graf, D. L. (1986). Studies of smectite membrane behavior: temperature dependence, 20–1801C. *Geochimica et Cosmochimica Acta*, 50, 115–122.  
[https://doi.org/10.1016/0016-7037\(86\)90055-4](https://doi.org/10.1016/0016-7037(86)90055-4)↗.
- Head, I. M., Jones, D. M., & Larter, S. R. (2003). Biological activity in the deep subsurface and the origin of heavy oil. *Nature*, 426(20), 344–352.  
<https://doi.org/10.1038/nature02134>↗.
- Healy, R. W., Alley, W. M., Engle, M. A., McMahon, P. B., & Bales, J. D. (2015). *The water-energy nexus—An earth science perspective (Circular 1407)*. US Geological Survey.  
<https://doi.org/10.3133/cir1407>↗.
- Hearst, J. R. & Nelson, P. H. (1985). *Well logging for physical properties*. McGraw-Hill.  
[inis.iaea.org/search/search.aspx?orig\\_q=RN:18057914h](inis.iaea.org/search/search.aspx?orig_q=RN:18057914h)↗.
- Helgeson, H. C., Owens, C. E., Knox, A. M., & Richard, L. (1998). Calculation of the standard molal thermodynamic properties of crystalline, liquid, and gas organic molecules at high temperatures and pressures. *Geochimica et Cosmochimica Acta*, 62, 985–1081. [https://doi.org/10.1016/S0016-7037\(97\)00219-6](https://doi.org/10.1016/S0016-7037(97)00219-6)↗.
- Hem, J. D. (1985). *Study and interpretation of the chemical characteristics of natural water. (Water-supply paper 2254) (3rd ed.)*. US Geological Survey.  
<https://books.google.com.br/books?hl=pt-BR&lr=&id=>↗.
- Hepple, R. P., & Benson, S. M. (2005). Geologic storage of carbon dioxide as a climate change mitigation strategy: Performance requirements and the implications of surface seepage. *Environmental Geology*, 47, 576–585.  
<https://link.springer.com/article/10.1007/s00254-004-1181-2>↗.
- Herkelrath, W. N., & Kharaka, Y. K. (2003). *Hydrologic controls on the subsurface transport of oil-field brine at the Osage-Skiatook petroleum environmental research “B” site, Oklahoma (Water Resources Investigations 03-4260) (pp. 111–123)*. US Geological Survey.  
<https://pubs.er.usgs.gov/publication/70216512>↗.
- Herkelrath, W. N., Kharaka, Y. K., Thordsen, J. J., & Abbott, M. M. (2007). Hydrology and subsurface transport of oil-field brine at the US Geological Survey OSPER site “A”, Osage County, Oklahoma. *Applied Geochemistry*, 22, 2155–2163.  
<https://doi.org/10.1016/j.apgeochem.2007.04.004>↗.

- Hermanrud, C., Andresen, T., Eiken, O., Hansen, H., Janbu, A., Lippard, J., Bolas, H. N., Simmenes, T. H., Teige, G. M. G., & Ostmo, S. (2009). Storage of CO<sub>2</sub> in saline aquifers: Lessons learned from 10 years of injection into the Utsira Formation in the Sleipner area. *Energy Procedia*, 1, 1997–2004.  
<https://doi.org/10.1016/j.egypro.2009.01.260>.
- Hesse, R. (1990). Early diagenetic pore water/sediment interaction: Modern offshore basins. In I. A. McIlreath & D. W. Morrow (Eds.), *Diagenesis. Geoscience Canada Reprint Series 4*, 277–316.
- Heydari, E., & Moore, C. H. (1989). Burial diagenesis and thermochemical sulfate reduction, Smackover Formation, southeastern Mississippi Salt Basin. *Geology*, 17, 1080–1084. [https://doi.org/10.1130/0091-7613\(1989\)017<1080:BDATSR>2.3.CO;2](https://doi.org/10.1130/0091-7613(1989)017<1080:BDATSR>2.3.CO;2).
- Hidalgo, K. J., Sierra-Garcia, I. N., Dellagnezze, B. M., & de Oliveira, V. M. (2020). Metagenomic insights into the mechanisms for biodegradation of polycyclic aromatic hydrocarbons in the oil supply chain. *Frontiers in Microbiology*, 11, 2250.  
<https://doi.org/10.3389/fmicb.2020.561506>.
- Hitchon, B. (1995). Fluorine in formation water, Alberta Basin, Canada. *Applied Geochemistry*, 10, 357–367. [https://doi.org/10.1016/0883-2927\(95\)00004-4](https://doi.org/10.1016/0883-2927(95)00004-4).
- Hitchon, B. (Ed.). (1996a). *Aquifer disposal of carbon dioxide: Hydrodynamic and mineral trapping – Proof of concept*. Geoscience Publishing.  
[https://inis.iaea.org/search/search.aspx?orig\\_q=RN:28064116](https://inis.iaea.org/search/search.aspx?orig_q=RN:28064116).
- Hitchon, B. (1996b). Rapid evaluation of the hydrochemistry of a sedimentary basin using only “standard” formation water analysis: Example from the Canadian portion of the Williston Basin. *Applied Geochemistry*, 11, 789–795.  
[https://doi.org/10.1016/S0883-2927\(96\)00043-1](https://doi.org/10.1016/S0883-2927(96)00043-1).
- Hitchon, B. (2000). “Rust” contamination of formation water from producing wells. *Applied Geochemistry*, 15, 1527–1533. [https://doi.org/10.1016/S0883-2927\(00\)00006-8](https://doi.org/10.1016/S0883-2927(00)00006-8).
- Hitchon, B. (Ed.). (2009). *Pembina Cardium CO<sub>2</sub> monitoring pilot: A CO<sub>2</sub>-EOR project, Alberta, Canada*. Geoscience Publishing. <https://geosciencepublishing@gmail.com>.
- Hitchon, B. (Ed.). (2012). *Best practices for validating CO<sub>2</sub> geological storage: Observations and guidance from the IEAGHG Weyburn-Midale CO<sub>2</sub> monitoring and storage project*. Geoscience Publishing. <https://geosciencepublishing@gmail.com>.
- Hitchon, B. (2023). *Formation water geochemistry: New perspectives*. Geoscience Publishing. For more details, please contact [geosciencepublishing@gmail.com](https://geosciencepublishing@gmail.com).
- Hitchon, B. & Friedman, I. (1969). Geochemistry and origin of formation water in the western Canada sedimentary basin I: Stable isotopes of hydrogen and oxygen. *Geochimica et Cosmochimica Acta*, 33, 1321–1349.  
[https://doi.org/10.1016/0016-7037\(69\)90178-1](https://doi.org/10.1016/0016-7037(69)90178-1).
- Hitchon, B., & Brulotte, M. (1994). Culling criteria for “standard” formation water analyses. *Applied Geochemistry*, 9, 637–645.  
[https://doi.org/10.1016/0883-2927\(94\)90024-8](https://doi.org/10.1016/0883-2927(94)90024-8).

- Hitchon, B., Billings, G. K., & Klovan, J. E. (1971). Geochemistry and origin of formation water in the western Canada sedimentary basin III: Factors controlling chemical composition. *Geochimica et Cosmochimica Acta*, 35, 567–598.  
<https://ui.adsabs.harvard.edu/abs/1971GeCoA..35..567H/abstract>↗.
- Hitchon, B., Underschlutz, J. R., Bachu, S., & Sauveplane, C. M. (1990). Hydrogeology, geopressures and hydrocarbon occurrences, Beaufort-Mackenzie Basin. *Bulletin of Petroleum Geology*, 38(2), 215–235. <https://doi.org/10.35767/gscpgbull.38.2.215>↗.
- Hitchon, B., Bachu, S., Underschlutz, J. R., & Yuan, L. P. (1995). Industrial mineral potential of Alberta formation water. *Alberta Research Council Bulletin No. 62*.
- Hitchon, B., Gunter, W. D., Gentzis, T., & Bailey, R. T. (1999a). Sedimentary basins and greenhouse gases: A serendipitous association. *Energy Conversion and Management*, 40, 825843. [https://doi.org/10.1016/S0196-8904\(98\)00146-0](https://doi.org/10.1016/S0196-8904(98)00146-0)↗.
- Hitchon, B., Perkins, E. H., & Gunter, W. D. (1999b). *Introduction to ground water geochemistry*. Geoscience Publishing.
- Hitchon, B., Perkins, E. H., & Gunter, W. D. (2001). Recovery of trace metals in formation water using acid gases from natural gas. *Applied Geochemistry*, 16, 1481–1497.  
[https://doi.org/10.1016/S0883-2927\(01\)00004-X](https://doi.org/10.1016/S0883-2927(01)00004-X)↗.
- Hitchon, B., & Bachu, S. (2017). Arsenic and selenium in formation water: Environmental implications for carbon dioxide storage in geological media. *Transactions of Ecology and the Environment*, 224, 477–488. <https://doi.org/10.2495/ESUS170441>↗.
- Holland, H. D. (2005). Sea level, sediments, and the composition of seawater. *American Journal of Science*, 305, 220–239. <https://doi.org/10.2475/ajs.305.3.220>↗.
- Holloway, S. (Ed.). (1996). *The underground disposal of carbon dioxide. Final report*. British Geological Survey.
- Holloway, S. (2001). Storage of fossil fuel derived carbon dioxide beneath the surface of the Earth. *Annual Review of Energy and the Environment*, 26, 145–166.  
<https://doi.org/10.1146/annurev.energy.26.1.145>↗.
- Holser, W. T. (1979). Review: Trace elements and isotopes in evaporites. In R. G. Burns (Ed.), *Mineralogy, Marine Minerals* (pp. 295–346). Mineral Society of America.
- Horita, J., Zimmerman, H., & Holland, H. D. (2002). Chemical evolution of seawater during the Phanerozoic: Implications from the records of marine evaporites. *Geochimica et Cosmochimica Acta*, 66, 3733–3756. [https://doi.org/10.1016/S0016-7037\(01\)00884-5](https://doi.org/10.1016/S0016-7037(01)00884-5)↗.
- Horner, R. M., Harto, C. B., Jackson, R. B., Lowry, E. R., Brandt, A. R., Yeskoo, T. W., Murphy, D. J., & Clark, C. E. (2016). Water use and management in the Bakken Shale Oil Play in North Dakota. *Environmental Science and Technology*, volume 50(6), 3275–3282. <https://doi.org/10.1021/acs.est.5b04079>↗.
- Hovorka, S. D., Benson, S. M., Doughty, C. K., Freifeld, B. M., Sakurai, S., Daley, T. M., Kharaka, Y. K., Holtz, M. H., Trautz, R. C., Nance, H. S., Myer, L. R., & Knauss, K. G. (2006). Measuring permanence of CO<sub>2</sub> storage in saline formations—The Frio

- Experiment. *Environmental Geoscience*, 13, 105–121.  
<https://doi.org/10.1306/eg.11210505011> ↗.
- Hovorka, S. D., Meckel, T., & Treviño, R. H. (2013). Monitoring a large-volume injection at Cranfield, Mississippi—Project design and recommendations. *International Journal of Greenhouse Gas Control*, 18, 345–360. <https://doi.org/10.1016/j.ijggc.2013.03.021> ↗.
- Hower, J., Eslinger, E. V., Hower, M. E., & Perry, E. A. (1976). Mechanism of burial metamorphism of argillaceous sediments. 1: Mineralogical and chemical evidence. *Geological Society of America Bulletin*, 87, 725–737. [https://doi.org/10.1130/0016-7606\(1976\)87<725:MOBMOA>2.0.CO;2](https://doi.org/10.1130/0016-7606(1976)87<725:MOBMOA>2.0.CO;2) ↗.
- Huh, Y., Chan, L. H., Zhang, L., & Edmond, J. M. (1998). Lithium and its isotopes in major world rivers: Implications for weathering and the oceanic budget. *Geochimica et Cosmochimica Acta*, 62, 2039–2051. [https://doi.org/10.1016/S0016-7037\(98\)00126-4](https://doi.org/10.1016/S0016-7037(98)00126-4) ↗.
- Hunt, J. M. (1996). *Petroleum geochemistry and geology* (2nd ed.). W.H. Freeman.
- Hunt, T. S. (1879). *Chemical and geological essays*. Osgood and Company.
- Igunnu, E. T., & Chen, G. Z. (2014). Produced water treatment technologies, *International Journal of Low-Carbon Technologies*, 9(3), 157–177. <https://doi.org/10.1093/ijlct/cts049> ↗.
- Ilggen, A. G., Heath, J. E., Akkutlu, I. Y., Bryndzia, L. T., Cole, D. R., Kharaka Y. K., Kneafsey, T. J., Milliken, K. L., Pyrak-Nolte, L. J., & Suarez-Rivera, R. (2017). Shales at all scales: Exploring coupled processes in mudrocks. *Earth-Science Reviews*, 166, 132–152. <https://doi.org/10.1016/j.earscirev.2016.12.013> ↗.
- Information Handling Service (IHS) Energy Group. (2018). *US production and well data*. [Database]. <https://www.oilandgasonline.com/doc/pidwights-plus-information-database-0001> ↗.
- Information Handling Service (IHS) Energy Group. (2020). *Enerdeq-energy information access and integration platform* [Database]. <https://www.spglobal.com/commodityinsights/en/ci/products/oil-gas-tools-enerdeq-browser.html> ↗.
- Information Handling Service (IHS) & Cambridge Energy Research Associates (CERA). (2010). *Oil Sands, Greenhouse Gases, and US Oil Supply: Getting the Numbers Right, Special Report*. <https://cdn.ihs.com/ihs/cera/Oil-Sands-Greenhouse-Gases-and-European-Oil-Supply.pdf> ↗.
- Intergovernmental Panel on Climate Change (IPCC). (2007). Climate change 2007: The physical science basis. In S. Solomon, D. Qin, M. Manning, Z. Chen, M. Marquis, K. B. Averyt, M. Tignor, & H. L. Miller (Eds.), *The fourth assessment report of the Intergovernmental Panel on Climate Change*. Cambridge University Press.
- Intergovernmental Panel on Climate Change (IPCC). (2017). *AR6 scoping meeting, Addis Ababa, Ethiopia, 1-5 May 2017, AR6-SCOP/Document 2*.
- Intergovernmental Panel on Climate Change (IPCC). (2018). Summary for policymakers. In V. Masson-Delmotte, P. Zhai, H. O. Pörtner, D. Roberts, J. Skea, P. R. Shukla, A. Pirani, W. Moufouma-Okia, C. Péan, R. Pidcock, S. Connors, J. B. R. Matthews, Y.

- Chen, X. Zhou, M. I. Gomis, E. Lonnoy, T. Maycock, M. Tignor, & T. Waterfield (Eds.), *Global warming of 1.5 °C*. World Meteorological Organization.
- Intergovernmental Panel on Climate Change (IPCC). (2021a). Climate change 2021: The physical science basis. In V. Masson-Delmotte, P. Zhai, A. Pirani, S. L. Connors, C. Péan, S. Berger, N. Caud, Y. Chen, L. Goldfarb, M. I. Gomis, M. Huang, K. Leitzell, E. Lonnoy, J. B. R. Matthews, T. K. Maycock, T. Waterfield, O. Yelekçi, R. Yu, & B. Zhou (Eds.), *Sixth assessment report of the Intergovernmental Panel on Climate Change*. Cambridge University Press. <https://ipcc.ch/report/ar6/wg1/>.
- Intergovernmental Panel on Climate Change (IPCC). (2021b). Summary for policymakers. In V. Masson-Delmotte, P. Zhai, A. Pirani, S. L. Connors, C. Péan, S. Berger, N. Caud, Y. Chen, L. Goldfarb, M. I. Gomis, M. Huang, K. Leitzell, E. Lonnoy, J. B. R. Matthews, T. K. Maycock, T. Waterfield, O. Yelekçi, R. Yu, & B. Zhou (Eds.), *Climate change 2021: The physical science basis: Sixth assessment report of the Intergovernmental Panel on Climate Change*. Cambridge University Press. [ipcc.ch/report/ar6/wg1/](https://ipcc.ch/report/ar6/wg1/).
- International Energy Agency (IEA). (2013). *World energy outlook 2013*. [IEA world energy outlook 2013.pdf](#).
- International Energy Agency (IEA). (2019). *Number of EOR projects in operation globally, 1971-2017*. [IEA # projects globally 1971-2017](#).
- International Energy Agency (IEA). (2020). *Energy technology perspectives 2020: Special report on carbon capture utilization and storage (CCUS in clean energy transitions)*. <https://iea.org/reports/ccus-in-clean-energy-transitions>.
- International Energy Agency (IEA). (2022). *Greenhouse gases*. <https://www.iea.org/fuels-and-technologies/carbon-capture-utilisation-and-storage>.
- IPCC, (2023). Sixth Assessment report. (AR6)- Final section, Synthesis report. 20 March 2023. <https://www.ipcc.ch/assessment-report/ar6/>.
- Ivahnenco, T., Szabo, Z., & Gibs, J. (2001). Changes in sample collection and analytical techniques and effects on retrospective comparability of low-level concentrations of trace elements in ground water. *Water Research*, 35, 3611–3624. [https://doi.org/10.1016/S0043-1354\(01\)00094-X](https://doi.org/10.1016/S0043-1354(01)00094-X).
- Jackson, M. P. A., Roberts, D. G., & Snelson, S. (1995). *Salt tectonics: A global perspective. Memoir 65*. American Association of Petroleum. <https://doi.org/10.1306/M65604>.
- Jackson, R. B., Vengosh, A., Darrah, T. H., Warner, N. R., Down, A., Poreda, R. J., Osborn, S. G., Zhao, K., & Karr, J. D. (2013). Increased stray gas abundance in a subset of drinking water wells near Marcellus shale gas extraction. *Proceedings of the National Academy of Sciences of the United States of America* 110, 11250–11255.
- Jasechko, S., Seybold, H., Perrone, D. et al. (2024). Rapid groundwater decline and some cases of recovery in aquifers globally. *Nature*, 625, 715–721. <https://doi.org/10.1038/s41586-023-06879-8>.
- Jenkins, C. (2013). Statistical aspects of monitoring and verification. *International journal of Greenhouse Gas Control*, 13, 215–229.

- Jenne, E. A. (1968). Controls on Mn, Fe, Co, Ni, Cu and Zn concentrations in solid and water: The significant role of hydrous Mn and Fe oxides. In R.A. Baker (Ed.), *Trace inorganics in water* (pp. 337–387). American Chemical Society.  
<https://doi.org/10.1021/ac60280a848>.
- Johnson, C., Beard, B., & Weaver, S. (2020). *Iron geochemistry: An isotopic perspective*. Springer International.
- Johnson, J. W., Oelkers, E. H., & Helgeson, H. C. (1992). SUPCTR92: A software package for calculating the standard molal thermodynamic properties of minerals, gases, aqueous species, and reactions from 1 bar to 5,000 bar and 0 °C to 1,000 °C. *Computer Geosciences*, 7, 899–947.
- Johnson, J. W., Nitao, J. J., & Knauss, K. G. (2004). Reactive transport modeling of CO<sub>2</sub> storage in saline aquifers to elucidate fundamental processes, trapping mechanisms and sequestration partitioning. In S. J. Baines & R. H. Worden (Eds.), *Geological storage of carbon dioxide: Special publication 233* (pp. 107–128). British Geological Society.
- Johnson, K. S., & Gerber, W. R. (1998). Iodide geology and extraction in northwestern Oklahoma. *Oklahoma Geological Survey Circular*, 10, 73–79.
- Jones, A. C. (2020). CO<sub>2</sub> underground injection regulations: Selected differences for enhanced oil recovery and geologic sequestration. *InFocus*, 16 June 2020. Congressional Research Service.  
<https://crsreports.congress.gov/product/pdf/IF/IF11578>.
- Kampbell, D. H., An, Y. J., Smith, M. W., & Abbott, M. A. (2003). *Impact of oil production releases on some soil chemical properties at the OSPER sites (Water-Resources Investigations number 03-4260)* (pp. 103-110). US Geological Survey.  
[pubs.er.usgs.gov/publication/70216510](https://pubs.er.usgs.gov/publication/70216510).
- Kargbo, D. M., Wilhelm, R. G., & Campbell, D. J. (2010). Natural gas plays in the Marcellus Shale: Challenges and potential opportunities. *Environmental Science & Technology*, 44, 5679–5684. <https://doi.org/10.1021/es903811p>.
- Karsten, M., & Bachu, S. (2002). Origin, chemistry and flow of formation water in the Mississippian–Jurassic sedimentary succession in the west-central part of the Alberta Basin, Canada. *Marine and Petroleum Geology*, 19, 289–306.  
[https://doi.org/10.1016/S0264-8172\(02\)00018-1](https://doi.org/10.1016/S0264-8172(02)00018-1).
- Kay, R. T., Bayless, E. R., & Solak, R. A. (2002). Use of isotopes to identify sources of ground water, estimate ground-water-flow rates, and assess aquifer vulnerability in the Calumet Region of northwestern Indiana and northeastern Illinois: US Geological Survey Water-Resources Investigations Report 2002–4213.  
<https://doi.org/10.3133/wri024213>.
- Kendall, C., & McDonnell, J. J. (Eds.). (2012). *Isotope tracers in catchment hydrology*. Elsevier Science. <https://doi.org/10.1016/C2009-0-10239-8>.

- Kendall, C., & Doctor, D. H. (2014). 5.11 Stable isotope applications in hydrologic studies. In H. D. Holland, & K. K. (Eds.), *Treatise on geochemistry, volume 5* (2nd ed.) (pp. 319–365). US Geological Survey. <https://doi.org/10.1016/B0-08-043751-6/05081-7>.
- Kennedy, V. C., Zellweger, G. W., & Jones, B. F. (1974). Filter pore size effects on the analysis of Al, Fe, Mn, and Ti in water. *Water Resources Research*, 10, 785–789. <https://doi.org/10.1029/WR010i004p00785>.
- Kesler, S. E., Martini, A. M., Appold, M. S., Walter, L. M., Huston, T. J., & Furman, F. C. (1996). Na–Cl–Br systematics of fluid inclusions from Mississippi Valley-type deposits, Appalachian Basin: Constraints on solute origin and migration paths. *Geochimica et Cosmochimica Acta*, 60, 225–233. [https://doi.org/10.1016/0016-7037\(95\)00390-8](https://doi.org/10.1016/0016-7037(95)00390-8).
- Khan, N. A., Engle, M., Dungan, B., Holquin, F. O., Xu, P., Carroll, K. C. (2016). Volatile-organic molecular characterization of shale-oil produced water from the Permian Basin. *Chemosphere*, 148, 126–136. [j.chemosphere.2015.12.116](https://doi.org/10.1016/j.chemosphere.2015.12.116).
- Kharaka, Y. K. (1971). *Simultaneous flow of water and solutes through geological membranes: Experimental and field investigations* (Unpublished doctoral dissertation). University of California, Berkeley.
- Kharaka, Y. K., & Berry, F. A. F. (1973). Simultaneous flow of water and solutes through geological membranes: I. Experimental investigation. *Geochimica et Cosmochimica Acta*, 37, 2577–2603. [https://doi.org/10.1016/0016-7037\(73\)90267-6](https://doi.org/10.1016/0016-7037(73)90267-6).
- Kharaka, Y. K., Berry, A. F. A., & Friedman, I. (1973). Isotopic composition of oil-field brines from Kettleman North Dome oil field, California and their geologic implications. *Geochimica et Cosmochimica Acta*, 37, 1899–1908. [https://doi.org/10.1016/0016-7037\(73\)90148-8](https://doi.org/10.1016/0016-7037(73)90148-8).
- Kharaka, Y. K., & Berry, F. A. F. (1974). The influence of geological membranes on the geochemistry of subsurface water from Miocene sediments at Kettleman North Dome, California. *Water Resources Research*, 10, 313–327. <https://doi.org/10.1029/WR010i002p00313>.
- Kharaka, Y. K., & Smalley, W. C. (1976). Flow of water and solutes through compacted clays. *American Association of Petroleum Geologists Bulletin*, 60, 973–980. <https://doi.org/10.1306/C1EA35F0-16C9-11D7-8645000102C1865D>.
- Kharaka, Y. K., Brown, P. M., & Carothers, W. W. (1978). Chemistry of water in the geopressured zone from coastal Louisiana—Implications for geothermal development. *Geothermal Resources Council Transactions*, 2, 371–374.
- Kharaka, Y. K., Lico, M. S., Wright, V. A., & Carothers, W. W. (1979). Geochemistry of formation water from Pleasant Bayou number 2 well and adjacent areas in coastal Texas. In W. L. Dorfman & M. H. Fisher (Eds.), *Proceedings of the Fourth United States Gulf Coast Geopressured/Geothermal Energy Conference: Research and Development*. Austin, TX, USA, October 29–31, 1, 168–193.

- Kharaka, Y. K., Berry, F. A. F., & Campbell, A. (1980). Geochemistry of geopressed geothermal water from the northern Gulf of Mexico and California basins. *Proceedings of the Third International Symposium on Water-Rock Interaction, July 14, 1980, Edmonton, AB, Canada*. <https://www.osti.gov/etdeweb/biblio/8473242>.
- Kharaka, Y. K., Lico, M. S., & Carothers, W. W. (1980). Predicted corrosion and scale formation properties of geopressed-geothermal water from the northern Gulf of Mexico Basin. *Journal of Petroleum Technology*, 32, 319–324. <https://doi.org/10.2118/7866-PA>.
- Kharaka, Y. K., Carothers, W. W., & Rosenbauer, R. J. (1983). Thermal decarboxylation of acetic acid: Implications for origin of natural gas. *Geochimica et Cosmochimica Acta*, 47, 397–402. [https://doi.org/10.1016/0016-7037\(83\)90262-4](https://doi.org/10.1016/0016-7037(83)90262-4).
- Kharaka, Y. K., Hull, R. W., & Carothers, W. W. (1985). Water-rock interactions in sedimentary basins. In D. L. Gautier, Y. K. Kharaka, & Surdam, R. C. (Eds.), *Relationship of organic matter and mineral diagenesis. Short course 17 (79–176)*. Society of Economic Paleontologists and Mineralogists. [sedimentary-geology-store.com/catalog/book/relationship-organic-matter-and-mineral-diagenesis](https://sedimentary-geology-store.com/catalog/book/relationship-organic-matter-and-mineral-diagenesis).
- Kharaka, Y. K., Law, L. M., Carothers, W. W., & Goerlitz, D. F. (1986). Role of organic species dissolved in formation water in mineral diagenesis. In D. L. Gautier (Ed.), *Relationship of organic matter and mineral diagenesis. Special issue 38 (pp. 111–122)*. Society of Economic Paleontologists and Mineralogists.
- Kharaka, Y. K., & Carothers, W. W. (1986). Oxygen and hydrogen isotope geochemistry of deep basin brine. In P. Fritz, & J. C. Fontes (Eds.), *Handbook of environmental isotope geochemistry* (pp. 305–360). International Atomic Energy Agency. [https://inis.iaea.org/search/search.aspx?orig\\_q=RN:20059224h](https://inis.iaea.org/search/search.aspx?orig_q=RN:20059224h).
- Kharaka, Y. K. (1986). Origin and evolution of water and solutes in sedimentary basins. In B. Hitchon, S. Bachu, & C. M. Sauveplane (Eds.), *Hydrology of sedimentary basins: Application to exploration and exploitation*. Proceedings of 3rd Canadian/American Conference on Hydrogeology, Banff, AB, Canada, June 22–26, 1986. National Water Well Association. <https://searchworks.stanford.edu/view/223135>.
- Kharaka, Y. K., Maest, A. S., Carothers, W. W., Law, L. M., & Fries, T. L. (1987). Geochemistry of metal-rich brines from central Mississippi Salt Dome Basin, USA. *Applied Geochemistry*, 2, 543–561. [https://doi.org/10.1016/0883-2927\(87\)90008-4](https://doi.org/10.1016/0883-2927(87)90008-4).
- Kharaka, Y. K., & Specht, D. J. (1988). The solubility of noble gases in crude oil at 25–100 °C. *Applied Geochemistry*, 3, 137–144. [https://doi.org/10.1016/0883-2927\(88\)90001-7](https://doi.org/10.1016/0883-2927(88)90001-7).
- Kharaka, Y. K., Gunter, W. D., Aggarwal, P. K., Perkins, E. H., & DeBraal, J. D. (1988). SOLMINEQ 88: A computer program for geochemical modeling of water-rock interactions. *Water-Resources Investigations Report 88-4227*. <https://doi.org/10.3133/wri884227>.

- Kharaka, Y. K., & Carothers, W. W. (1988). Geochemistry of oil-field water from the North Slope, Alaska. *United States Geological Survey Professional Paper, 1399*, 551–561, [dggs.alaska.gov/pubs/id/4168](https://pubs.usgs.gov/pubs/id/4168).
- Kharaka, Y. K., & Specht, D. J. (1988). The solubility of noble gases in crude oil at 25–100 °C. *Applied Geochemistry, 3*, 137–144.
- Kharaka, Y. K., & Mariner, R. H. (1989). Chemical geothermometers and their application to formation water from sedimentary basins. In N. D. Naeser, & T. H. McCulloh (Eds.), *Thermal history of sedimentary basins* (pp. 99–117). Springer-Verlag. [https://link.springer.com/chapter/10.1007/978-1-4612-3492-0\\_6](https://link.springer.com/chapter/10.1007/978-1-4612-3492-0_6).
- Kharaka, Y. K., & Thordsen, J. J. (1992). Stable isotope geochemistry and origin of water in sedimentary basins. In N. Clauer, & S. Chaudhuri (Eds.), *Isotope signatures and sedimentary records* (pp. 411–466). Springer-Verlag. <http://link.springer.com/book/10.1007/BFb0009858>.
- Kharaka, Y. K., Ambats, G., & Thordsen, J. J. (1993a). Distribution and significance of dicarboxylic acid anions in oil-field water. *Chemical Geology, 107*, 499–501. [https://doi.org/10.1016/0009-2541\(93\)90239-F](https://doi.org/10.1016/0009-2541(93)90239-F).
- Kharaka, Y. K., Lundegard, P. D., Ambats, G., Evans, W. C., & Bischoff, J. L. (1993b). Generation of aliphatic acid anions and carbon dioxide by hydrous pyrolysis of crude oils. *Applied Geochemistry, 8*, 317–324. [https://doi.org/10.1016/0883-2927\(93\)90001-W](https://doi.org/10.1016/0883-2927(93)90001-W).
- Kharaka, Y. K., Thordsen, J. J., & Ambats, G. (1995). Environmental degradation associated with exploration for and production of energy sources in USA. In Y. K. Kharaka, & O. V. Chudaeu (Eds.), *WRI-8: Proceedings of the Eighth International Symposium on the Water Rock Interaction, Vladivostok, Russia, August 15–19, 1995*. (pp. 25–30). Balkema. <https://www.worldcat.org/title/water-rock-interaction-proceedings-of-the-8th-international-symposium-on-water-rock-interaction-wri-8-vladivostok-russia-15-19-august-1995/oclc/33452759>.
- Kharaka, Y. K., & Wanty, R. B. (1995). *Water quality degradation associated with natural energy sources* (Circular number 1108, 25–27). US Geological Survey.
- Kharaka, Y. K., & Wanty, R. B. (1997). *United States Geological Survey research on saline water co-produced with energy sources* (Fact Sheet FS-003-97). US Geological Survey. [pubs.usgs.gov/fs/1997/fs003-97/FS-003-97.html](https://pubs.usgs.gov/fs/1997/fs003-97/FS-003-97.html).
- Kharaka, Y. K., Thordsen, J. J., Evans, W. C., & Kennedy, B. M. (1999). Geochemistry and hydromechanical interactions of fluids associated with the San Andreas fault system, California. In W. C. Haneberg, L. B. Goodwin, P. S. Mozley, & J. C. Moore (Eds.), *Faults and subsurface fluid flow in the shallow crust. AGU Geophysical Monograph Series, 113*, 129–148. American Geophysical Union.
- Kharaka, Y. K., Leong, L. Y. C., Doran, G., & Breit, G. N. (1998, October). Can produced water be reclaimed? Experience with the Placerita oil field, California. In K. L. Sublette (Ed.), *Environmental issues in petroleum exploration, production and refining*.

*Proceedings of the 5th Integrated Petroleum Environmental Consortium Meeting, Albuquerque, New Mexico.* [CD-ROM].

- Kharaka, Y. K., Lundegard, P. D., & Giordano, T. H. (2000). Distribution and origin of organic ligands in subsurface water from sedimentary basins. *Reviews in Economic Geology*, 9, 119–132. <https://doi.org/10.5382/Rev.09.06>.
- Kharaka, Y. K., & Otton, J. K. (2003). *Environmental impacts of petroleum production: Initial results from the Osage-Skiatook Petroleum Environmental Research Sites, Osage County, Oklahoma (Water-Resources Investigations Report 03-4260)*. US Geological Survey. <https://doi.org/10.3133/wri034260>.
- Kharaka, Y. K., Thordsen, J. J., Kakouros, E., & Herkelrath, W. N. (2005). Impact of petroleum production on ground and surface water: Results from the Osage-Skiatook petroleum environmental research site A, Osage County, Oklahoma. *Environmental Geosciences*, 12, 127–138. <https://doi.org/10.1306/eg.11160404038>.
- Kharaka, Y. K., & Dorsey, N. (2005). Environmental issues of petroleum exploration and production. *Environmental Geosciences*, 12(2), 61–63. <https://archives.datapages.com/data/deg/2005/INTRO/INTRO.HTM>.
- Kharaka, Y. K., & Mariner, R. H. (2005). Geothermal systems. In J. K. Aggarwal, & K. Froehlich (Eds.), *Isotopes in the water cycle: Past, present and future of a developing science* (pp. 243–270). Springer-Verlag. <https://ink.springer.com/book/10.1007/1-4020-3023-1>.
- Kharaka, Y. K., Cole, D. R., Hovorka, S. D., Gunter, W. D., Knauss, K. G., & Freifeld, B. M. (2006a). Gas-water-rock interactions in Frio formation following CO<sub>2</sub> injection: Implications to the storage of greenhouse gases in sedimentary basins. *Geology*, 34, 577–580. <https://doi.org/10.1130/G22357.1>.
- Kharaka, Y. K., Cole, D. R., Thordsen, J. J., Kakouros, E., & Nance, H. S. (2006b). Gas-water-rock interactions in sedimentary basins: CO<sub>2</sub> sequestration in the Frio Formation, Texas, USA. *Geology*, 34(7), 577–580. <https://doi.org/10.1130/G22357.1>.
- Kharaka, Y. K., Cole, D. R., Thordsen, J. J., Kakouros, E., & Nance, H. S. (2006c). Gas-water-rock interactions in sedimentary basins: CO<sub>2</sub> sequestration in the Frio Formation, Texas, USA. *Journal of Geochemical Exploration*, 89(1–3), 183–186. [https://doi.org/10.1016/j.jge\(1-3\), plo.2005.11.077](https://doi.org/10.1016/j.jge(1-3), plo.2005.11.077).
- Kharaka, Y. K., & Otton, J. K. (2007). Environmental issues related to oil and gas exploration and production. *Applied Geochemistry*, 22, 2095–2098.
- Kharaka, Y. K., Kakouros, E., Thordsen, J. J., Ambats, G., & Abbott, M. M. (2007a). Fate and groundwater impacts of produced water releases OSPER "B" site, Osage County, Oklahoma. *Applied Geochemistry*, 22(2), 164–176. <https://doi.org/10.1016/j.apgeochem.2007.04.005>.
- Kharaka, Y. K., Thordsen, J. J., Hovorka, S. D., Cole, D. R., Phelps, T. J., & Bullen, T. D. (2007b). Potential environmental issues of CO<sub>2</sub> storage in saline aquifers: Geochemical

- results from the Frio Brine pilot tests, Texas, USA. *Geochimica et Cosmochimica Acta*, 71, A481–A481. <https://doi.org/10.1016/j.apgeochem.2009.02.010>.
- Kharaka, Y. K., Thordsen, J. J., Hovorka, S. D., Nance, H. S., Cole, D. R., Phelps, T. J., & Knauss, K. G. (2009). Potential environmental issues of CO<sub>2</sub> storage in deep saline aquifers: Geochemical results from the Frio-I Brine Pilot test, Texas, USA. *Geochimica et Cosmochimica Acta*, 74, 1106–1112. <https://doi.org/10.1016/j.apgeochem.2009.02.010>.
- Kharaka, Y. K., Thordsen, J., Kakouros, E., Ambats, G., Herkelrath, W. N., Beers, S. R., Birkholzer, J. T., Apps, J. A., Spycher, N. F., Zheng, L., Trautz, R. C., Rauch, H. W., & Gullickson, K. S. (2010a). Changes in the chemistry of shallow groundwater related to the 2008 injection of CO<sub>2</sub> at the ZERT field site, Bozeman, Montana. *Environmental Earth Sciences*, 7, 417–422. <https://doi.org/10.1007/s12665-009-0401-1>.
- Kharaka, Y. K., Thordsen, J. J., Bullen, T. D., Cole, D. R., Phelps, T. J., Birkholzer, & Hovorka, J., S. (2010b). Near surface and deep subsurface monitoring for successful geologic sequestration of CO<sub>2</sub>. In P. Birkle, & I. S. Torres-Alvarado (Eds.), *Proceedings of WRI-13* (pp. 867–870). Balkema. <https://www.researchgate.net/publication/328696085>.
- Kharaka, Y. K., & Cole, D. R. (2011). Geochemistry of geologic sequestration of carbon dioxide. In R. S. Harmon, A. Parker (Eds.), *Frontiers in geochemistry: Contribution of geochemistry to the study of the Earth* (pp. 136–174). Blackwell. <https://doi.org/10.2138/am.2012.594>.
- Kharaka, Y. K., Thordsen, J. J., Conaway, C. H., & Thomas, R. B. (2013). The energy-water nexus: Potential groundwater-quality degradation associated with production of shale gas. *Procedia Earth and Planetary Science*, 7, 417–422. <https://doi.org/10.1016/j.proeps.2013.03.132>.
- Kharaka, Y. K., & Hanor, J. S. (2014). 7.14 Deep fluids in sedimentary basins. In H.D. Holland, & K. K. Turekian (Eds.), *Treatise on geochemistry, volume 7* (2nd ed.) (pp. 471–515). Elsevier. <https://doi.org/10.1016/B978-0-08-095975-7.00516-7>.
- Kharaka, Y. K. (2016). *Chemical composition and fate of produced water and crude releases from the Greka Energy Petroleum Production facilities, Cat Canyon and Zaka oil fields, Santa Barbara County, California. Expert witness report*. US Environmental Protection Agency.
- Kharaka, Y. K., Thordsen, J. J., Bullen, T., Ambats, G., & Fitzpatrick, J. (2017). Iron isotopes used to investigate water-rock interactions and well-pipe corrosion as sources of dissolved Fe in brine from CO<sub>2</sub> storage sites. *Proceedings of the 12th International Symposium on Applied Isotope Geochemistry (AIG-12), September 17-22, Copper Mountain, Colorado*.
- Kharaka, Y. K., Abedini, A. A., Gans, K. D., Thordsen, J. J., Beers, S. R., & Thomas, R. B. (2018). Changes in the chemistry of groundwater reacted with CO<sub>2</sub>: Comparison of results from laboratory experiments and the ZERT field site, Bozeman, Montana,

- USA. *Applied Geochemistry*, 98, 75–81.  
<https://doi.org/10.1016/j.apgeochem.2018.08.017>.
- Kharaka, Y. K., Gans, K., Thordsen, J., Blondes, M., & Engle, M. (2019). Geochemical data for produced water from conventional and unconventional oil and gas wells: Results from Colorado, USA. *E3S Web of Conferences*, 98(03002).  
<https://doi.org/10.1051/e3sconf/20199803002>.
- Kharaka, Y. K., Gans, K., Thordsen, J., Rowan, E., Blondes, M., Engle, M., & Conaway, C. (2020). Chemical composition of formation water in shale and tight reservoirs: A basin-scale perspective. In T. Dewers, J. Heath, & M. Sanchez (Eds.), *Shale: Subsurface science and engineering* (pp. 27–44). John Wiley & Sons.  
<https://books.google.com.br/books?hl=pt-BR&lr=&id=>.
- Kimball, B. A. (1984). Ground water age determinations, Piceance Creek Basin, Colorado. In B. Hitchon, & E. I. Wallick (Eds.), *Proceedings, First Canadian/American Conference on Hydrogeology: Practical Applications of Ground Water Geochemistry* (pp. 267–283). National Water Well Association.
- King, B., Gaffney, M., & Rivera, A. (2024). Preliminary US Greenhouse Gas Emissions Estimates for 2023. Note: Rhodium Group (rhg.com) January 10, 2024.
- Knauss, K. G., Johnson, J. W., & Steefel, C. I. (2005). Evaluation of the impact of CO<sub>2</sub>, co-contaminant gas, aqueous fluid and reservoir-rock interactions on the geologic sequestration of CO<sub>2</sub>. *Chemical Geology*, 217(3–4), 339–350.  
<https://doi.org/10.1016/j.chemgeo.2004.12.017>.
- Knauth L. P. (1988). Origin and mixing history of brines, Palo Duro Basin Texas, U.S.A. *Applied Geochemistry*, 3(5), 455–479. [https://doi.org/10.1016/0883-2927\(88\)90019-4](https://doi.org/10.1016/0883-2927(88)90019-4).
- Knauth, L. P., & Beeunas, M. A. (1986). Isotope geochemistry of fluid inclusions in Permian halite with implications for the isotopic history of ocean water and the origin of saline formation water. *Geochimica et Cosmochimica Acta*, 50(3), 419–433.  
[https://doi.org/10.1016/0016-7037\(86\)90195-X](https://doi.org/10.1016/0016-7037(86)90195-X).
- Kolak, J. J., & Burruss, R. C. (2006). Geochemical investigation of the potential for mobilizing non-methane hydrocarbons during carbon dioxide storage in deep coal beds. *Energy Fuels*, 20(2), 566–574. <https://doi.org/10.1021/ef050040u>.
- Kondash, A. J., Redmon, J. H., Lambertini, E., Feinstein, L., Weinthal, E., Cabrales, L., & Vengosh, A. (2020). The impact of using low-saline oilfield produced water for irrigation on water and soil quality in California. *Science of the Total Environment*, 733, 139392. <https://doi.org/10.1016/j.scitotenv.2020.1393920048-9697>.
- Kraemer, T. F., & Reid, D. F. (1984). The occurrence and behavior of radium in saline formation water of the United States Gulf Coast region. *Isotope Geosciences*, 2(2), 153–174. [https://doi.org/10.1016/0009-2541\(84\)90186-4](https://doi.org/10.1016/0009-2541(84)90186-4).
- Kraemer, T. F., & Kharaka, Y. K. (1986). Uranium geochemistry in geopressured geothermal aquifers of the United States Gulf Coast. *Geochimica et Cosmochimica Acta*, 50(6), 1233–1238. [https://doi.org/10.1016/0016-7037\(86\)90406-0](https://doi.org/10.1016/0016-7037(86)90406-0).

- Kryukov, P. A., Zhuchkova, A. A., & Rengarten, E. F. (1962). Change in the composition of solutions pressed from clays and ion exchange resins. *Akademiia Nauk SSSR Earth Sciences Section*, 144, 167–169.
- Land, L. S. (1995). The role of saline formation water in crustal cycling. *Aquatic Geochemistry*, 1, 137–145.
- Land, L. S. & Macpherson, G. L. (1992a). Geothermometry from brine analyses: Lessons from the Gulf Coast, U.S.A. *Applied Geochemistry*, 7(4), 333–340.  
[https://doi.org/10.1016/0883-2927\(92\)90023-V](https://doi.org/10.1016/0883-2927(92)90023-V).
- Land, L. S., & Macpherson, G. L. (1992b). Geochemistry of formation water, Plio-Pleistocene reservoirs, offshore Louisiana. *American Association of Petroleum Geologists Bulletin*, 100(6), 943–967. [10.1306/02101615027](https://doi.org/10.1306/02101615027).
- Land, L. S., & Prezbindowski, D. R. (1981). The origin and evolution of saline formation water, Lower Cretaceous carbonates, south central Texas, U.S.A. *Journal of Hydrology*, 54(1–3), 51–74. [https://doi.org/10.1016/0022-1694\(81\)90152-9](https://doi.org/10.1016/0022-1694(81)90152-9).
- Land, L. S., & Fisher, R. S. (1987). Wilcox sandstone diagenesis, Texas Gulf Coast: A regional isotopic comparison with the Frio Formation. In J. D. Marshall (Ed.), *Diagenesis of sedimentary sequences. Special publication number 36* (pp. 219–235). Geological Society of America.
- Land, L. S., Macpherson, G. L., & Mack, L. E. (1988). The geochemistry of saline formation water, Miocene offshore Louisiana. *Gulf Coast Association of Geological Societies Transactions*, 38, 503–511.  
<https://archives.datapages.com/data/gcags/data/038/038001/0503.htm>.
- Land, L. S., Eustice, R. A., Mack, I. E., & Horita, J. (1995). Reactivity of evaporites during burial: an example from the Jurassic of Alabama. *Geochimica et Cosmochimica Acta*, 59(18), 3765–3778. [https://doi.org/10.1016/0016-7037\(95\)00262-X](https://doi.org/10.1016/0016-7037(95)00262-X).
- Lane, A. C. (1908). *Annual Report for 1908 / Notes on the Geological Section of Michigan*. Board of Geological Survey.
- Larter, S., Huang, H., Adam, J., Bennett, B., Jokanola, O., Oldenburg, T., Jones, M., Head, I., Riediger, C., & Fowler, M. (2006). The controls in the composition of biodegraded oils in the deep subsurface: Part II. Geological controls on subsurface biodegradation fluxes and constraints on reservoir-fluid property prediction. *American Association of Petroleum Geologists Bulletin*, 90(6), 921–938. <https://doi.org/10.1306/01270605130>.
- Lattanzio, R. K. (2014). Canadian oil sands: Life-cycle assessments of greenhouse gas emissions. *Congressional Research Service Report for Congress 7-5700*.  
[https://www.everycrsreport.com/files/20130315\\_R42537](https://www.everycrsreport.com/files/20130315_R42537).
- Lee, L., & Helsel, D. (2005). Baseline models of trace elements in major aquifers of the United States. *Applied Geochemistry*, 20(8), 1560–1570,  
<https://doi.org/10.1016/j.apgeochem.2005.03.008>.

- Leger, W. L. (1988). Salt dome related diagenesis of Miocene sediments, Black Bayou Field, Cameron Parish, Louisiana. *Gulf Coast Association of Geological Societies Transactions*, 38, 525–534. <https://www.osti.gov/biblio/6180778h>.
- Lewan, M. D., & Fisher, J. B. (1994). Organic acids from petroleum source rocks. In E. D. Pittman, & M. D. Lewan (Eds.), *Organic acids in geological processes* (pp. 70–114). Springer.
- Lewis, J. (2022). Carbon capture and storage project in Western Australia only operated at just over half of its stated capacity in the 2021 financial year. *Upstream*, February 16, 2022.
- Lico, M. S., Kharaka, Y. K., Carothers, W. W., & Wright, V. A. (1982). *Methods for collection and analysis of geopressured, geothermal and oil-field water* (Water Supply Paper Report W 2194). US Geological Survey. <https://doi.org/10.2172/5407477>.
- Lin, G., & Nunn, J. A. (1997). Evidence for recent migration of geopressured fluids along faults in Eugene Island, Block 330, offshore Louisiana, from estimates of pore water salinity. *Gulf Coast Association of Geological Societies Transactions*, 47, 419–424. <https://archives.datapages.com/data/gcags/data/047/047001/0419.htmh>.
- Little, R. E., Jr. (2003). *An investigation of a salt dome environment at South Timbalier 54, Gulf of Mexico* [Unpublished master's thesis]. Louisiana State University.
- Liu, D., Li, J., Zou, C., Cui, H., Ni, Y., Liu, J., Wu, W., Zhang, L., Coyte, R., Kondash, A. J., & Vengosh, A. (2020). Recycling flowback water for hydraulic fracturing in Sichuan Basin, China: Implications for gas production, water footprint, and water quality of regenerated flowback water. *Fuel*, 272, 117621. <https://doi.org/10.1016/j.fuel.2020.117621>.
- Loosli, H. H., & Purtschert, R. (2005). Rare gases. In P. K. Aggarwal, J. R. Gat, & K. F. O. Froehlich(Eds.), *Isotopes in the water cycle: Past, present and future of a developing science* (pp. 91–96). Springer.
- Losh, S., Walter, L., Muelbroek, P., Martini, A., Cathles, L., & Whelan, J. (2002). Reservoir fluids and their migration into the South Eugene Island Block 330 reservoirs, offshore Louisiana. *American Association of Petroleum Geologists Bulletin*, 86, 1463–1488. <https://doi.org/10.1306/61EEDCCE-173E-11D7-8645000102C1865D>.
- Lowenstein, T. K., & Timofeeff, M. N. (2008). Secular variations in seawater chemistry as a control on the chemistry of basinal brines: A test of the hypothesis. *Geofluids*, 8, 77–92. <https://doi.org/10.1111/j.1468-8123.2007.00206.x>.
- Lowenstein, T. K., Hardie, L. A., Timofeeff, M. N., & Demicco, R. V. (2003). Secular variation in seawater chemistry and the origin of calcium chloride basinal brines. *Geology*, 31, 857–860. <https://doi.org/10.1130/G19728R.1>.
- Lu, J. M., Kharaka, Y. K., Thordsen, J. J., Horita, J., Karamalidis, A., Griffith, C., Hakala, J. A., Ambats, G., Cole, D. R., Phelps, T. J., Manning, M. A., Cook, P. J., & Hovorka, S. D. (2012). CO<sub>2</sub>-rock-brine interactions in Lower Tuscaloosa Formation at Cranfield

- CO<sub>2</sub> sequestration site, Mississippi, U.S.A. *Chemical Geology*, 291, 269–277.  
<https://doi.org/10.1016/j.chemgeo.2011.10.020> ↗.
- Lu, Z., Hummel, S. T., Lautz, L. K., Hoke, G. D., Zhou, X., Leone, J., & Siegel, D. I. (2014). Iodine as a sensitive tracer for detecting influence of organic-rich shale in shallow groundwater. *Applied Geochemistry*, 60, 29–36.  
<https://doi.org/10.1016/j.apgeochem.2014.10.019> ↗.
- Luderer, G., Vrontisi, Z., Bertram, C., Edelenbosch, O. Y., Pietzcker, R. C., Rogelj, J., De Boer, H. S., Drouet, L., Emmerling, J., Fricko, O., Fujimori, S., Havlík, P., Iyer, G., Keramidas, K., Kitous, A., Pehl, M., Krey, V., Riahi, K., Saveyn, B., ... Kriegler, E. (2018). Residual fossil CO<sub>2</sub> emissions in 1.5-2 °C pathways. *Nature Climate Change*, 8, 626–633. <https://doi.org/10.1038/s41558-018-0198-6> ↗.
- Lund, S., & Dvory, N. Z. (2020). Magnitude 5.0 earthquake shakes West Texas,  
<https://doi.org/10.6084/m9.figshare.12045213> ↗.
- Lundegard, P. D., & Kharaka, Y. K. (1994). Distribution of organic acids in subsurface water. In E. D. Pittman, & M. D. Lewan (Eds.), *Organic acids in geological processes* (pp. 40–69). Springer.
- Lundegard, P. D., & Trevena, A. S. (1990). Sandstone diagenesis in the Pattani Basin (Gulf of Thailand): History of water–rock interaction and comparison with the Gulf of Mexico. *Applied Geochemistry*, 5, 669–685.
- Maas, E. V., & Grattan, S. R. (1999). Crop yields as affected by salinity in agricultural drainage. In R. W. Skaggs, & J. van Schilfhaarde (Eds.), *Agronomy monograph* (volume 38). ASA, CSSA, SSSA.
- MacDowell, N., Fennell, P. S., Shah, N., & Maitland, G. C. (2017). The role of CO<sub>2</sub> capture and utilization in mitigating climate change. *Nature Climate Change*, 7, 243–249.  
<https://doi.org/10.1038/nclimate3231> ↗.
- Macêdo-Júnior, B. S., Silva, L., Silva, D., & Ruzene, D. (2020). Produced water: an overview of treatment technologies. *International Journal for Innovation Education and Research*, 8(4), 207–224. <https://doi.org/10.31686/ijer.vol8.iss4.2283> ↗.
- MacGowan, D. B., & Surdam, R. C. (1990). Importance of organic–inorganic interactions during progressive clastic diagenesis. In D. C. Melchior, & R. L. Bassett (Eds.), *Chemical modeling of aqueous systems II. Symposium series 416* (pp. 494–507). American Chemical Society.
- Machel, H. G. (2001). Bacterial and thermochemical sulfate reduction in diagenetic settings: Old and new insights. *Sedimentary Geology*, 140, 143–175.  
[https://doi.org/10.1016/S0037-0738\(00\)00176-7](https://doi.org/10.1016/S0037-0738(00)00176-7) ↗.
- Mackin, J. E. (1987). Boron and silica behavior in salt-marsh sediments: Implications for paleo-boron distributions and the early diagenesis of silica. *American Journal of Science*, 287, 197–241. <https://doi.org/10.2475/ajs.287.3.197> ↗.
- Macpherson, G. L. (1992). Regional variations in formation water chemistry: Major and minor elements, Frio Formation fluids, Texas. Association of Petroleum Geologists



- McDevitt, B., A.M. Jubb, M.S. Varonka, M.S. Blondes, M.A. Engle, T.J. Gallegos, & J.L. Shelton (2022). Dissolved organic matter within oil and gas associated wastewaters from U.S. unconventional petroleum plays: Comparisons and consequences for disposal and reuse. *Science of the Total Environment*, 838, 26 Pages. <https://doi.org/10.1016/j.scitotenv.2022.156331>.
- McFeeley, M. (2012). *State hydraulic fracturing disclosure rules and enforcement: A comparison (Issue Brief 1b:12-06-A)*. Natural Resources Defense Council. <https://nrdc.org/resources/state-hydraulic-fracturing-disclosure-rules-and-enforcement-comparison>.
- McIntosh, J. C., Walter, L. M., & Martini, A. M. (2002). Pleistocene recharge to midcontinent basins: effects on salinity structure and microbial gas generation. *Geochimica et Cosmochimica Acta*, 66, 1681–1700. [https://doi.org/10.1016/S0016-7037\(01\)00885-7](https://doi.org/10.1016/S0016-7037(01)00885-7).
- McIntosh, P., Schulthess, C. P., Kuzovkina, Y. A., Guillard, K. (2017). Bioremediation and phytoremediation of total petroleum hydrocarbons (TPH) under various conditions. *International Journal of Phytoremediation*, volume 19, 755–764. <https://doi.org/10.1080/15226514.2017.1284753>.
- McMahon, P. B., Barlow, J. R. B., Engle, M. A., Belitz, K., Ging, P. B., Hunt, A. G., Jurgens, B. C., Kharaka, Y. K., Tollett, R. W., & Kresse, T. M. (2017). Methane and benzene in drinking-water wells overlying the Eagle Ford, Fayetteville and Haynesville shale hydrocarbon production areas. *Environmental Science & Technology*, 51(12), 6727–6734. <https://doi.org/10.1021/acs.est.7b00746>.
- McMahon, P. B., Kulongoski, J. T., Vengosh, A., Cozzarelli, I. M., Landon, M. K., Kharaka, Y. K., Gillespie, J. M., & Davis, T. A. (2018). Regional patterns in the geochemistry of oil-field water, southern San Joaquin Valley, California, USA. *Applied Geochemistry*, 98, 127–140. <https://doi.org/10.1016/j.apgeochem.2018.09.015>.
- McMahon, P. B., Vengosh, A., Davis, T. A., Landon, M. K., Tyne, R. L., Wright, M. T., Kulongoski, J. T., Hunt, A. G., Barry, P. H., Kondash, A. J., Wang, Z., & Ballentine, C. J. (2019). Occurrence and sources of radium in groundwater associated with oil fields in the southern San Joaquin Valley, California. *Environmental Science & Technology*, 53, 9398–9406. <https://doi.org/10.1021/acs.est.9b02395>.
- McMahon, P. B., Landon, M. K., Davis, T., Wright, M., Rosecrans, C. Z., Anders, R., Land, M., Kulongoski, J. T., & Hunt, A. (2021). Relative risk of groundwater-quality degradation near California (USA) oil fields estimated from  $^3\text{H}$ ,  $^{14}\text{C}$  and  $^4\text{He}$ . *Applied Geochemistry*, 131, 105024. <https://doi.org/10.1016/j.apgeochem.2021.105024>.
- McManus, K. M., & Hanor, J. S. (1993). Diagenetic evidence for massive evaporite dissolution, fluid flow, and mass transfer in the Louisiana Gulf Coast. *Geology*, 21, 727–730. [https://doi.org/10.1130/0091-7613\(1993\)021<0727:DEFMED>2.3.CO;2](https://doi.org/10.1130/0091-7613(1993)021<0727:DEFMED>2.3.CO;2).
- McMillion, L. G. (1965). Hydrological aspects of disposal of oil-field brines in Texas. *Groundwater*, 3(4), 36–42. <https://doi.org/10.1111/j.1745-6584.1965.tb01228.x>.

- McNutt, M. K., Camilli, R., Crone, T. J., Guthrie, G. D., Hsieh, P. A., Ryerson, T. B., Savas, O., & Shaffer, F. (2012). Review of flow rate estimates of the Deepwater Horizon oil spill. *Proceedings of the National Academy of Sciences*, 109(5), 20260–20267. <https://doi.org/10.1073/pnas.1112139108>.
- McWhorter, D. B., Poeter, E. P., & Woessner, W. W. (2020). Box 3 Foundation for understanding hydraulic head and hydraulic potential. In W. W. Woessner, & E. P. Poeter, *Hydrogeologic properties of earth materials and principles of groundwater flow* (pp. 142–148). The Groundwater Project. <https://gw-project.org/books/hydrogeologic-properties-of-earth-materials-and-principles-of-groundwater-flow/>.
- Meckel, T. A., Bump, A. P., Hovorka, S. D., & Treviño, R. H. (2021). Carbon capture, utilization, and storage hub development on the Gulf Coast: Greenhouse Gases. *Science and Technology*, 11(4), 619–632. <https://doi.org/10.1002/ghg.2082>.
- Meckel, J., R. H. Treviño, S. Hovorka, & Bump, A. (2023). Mapping existing wellbore locations to compare technical risks between onshore and offshore CCS activities in Texas: Greenhouse Gases. *Science and Technology*, 13, 493-504. <https://doi.org/10.1002/ghg.2220>.
- Meisler, H. (1989). *The occurrence and geochemistry of salty ground water in the northern Atlantic coastal plain (Professional Paper 1404-D)*. US Geological Survey. <https://doi.org/10.3133/pp1404D>.
- Meisler, H., Miller, J. A., Knobel, L. L., & Wait, W. (1988). Region 22, Atlantic and eastern gulf coastal plain in the geology of North America. In W. Back, J. S. Rosenshein, & P. R. Seaber (Eds.), *Hydrogeology* (pp. 209–218). Geological Society of America. <https://doi.org/10.1130/DNAG-GNA-O2.209>.
- Merino, E. (1975). Diagenesis in tertiary sandstones from Kettleman North Dome. California—II. Interstitial solutions: Distribution of aqueous species at 100 °C and chemical relation to the diagenetic mineralogy. *Geochimica et Cosmochimica Acta*, 39, 1629–1645. [https://doi.org/10.1016/0016-7037\(75\)90085-X](https://doi.org/10.1016/0016-7037(75)90085-X).
- Merino, E., Girard, J. P., & May, M. T. (1997). Diagenetic mineralogy, geochemistry, and dynamics of Mesozoic arkoses, Hartford rift basin, Connecticut, U.S.A. *Journal of Sedimentary Research*, 67, 212–224. <https://doi.org/10.1306/D4268536-2B26-11D7-8648000102C1865D>.
- Merino, E., Canals, À., & Fletcher, R. (2006). Genesis of self-organized zebra textures in burial dolomites: Displacive veins, induced stress, and dolomitization. *Geologica Acta*, 4, 383–393. [https://www.researchgate.net/publication/28118502\\_Genesis\\_of\\_self-organized\\_zebra\\_textures\\_in\\_burial\\_dolomites\\_displacive\\_veins\\_induced\\_stress\\_and\\_dolomitization](https://www.researchgate.net/publication/28118502_Genesis_of_self-organized_zebra_textures_in_burial_dolomites_displacive_veins_induced_stress_and_dolomitization).
- Merino, E., & Canals, À. (2011). Self-accelerating dolomite-for-calcite replacement: Self-organized dynamics of burial dolomitization and associated mineralization. *American Journal of Science*, 311, 573–607. <https://doi.org/10.2475/07.2011.01>.

- Merino, E., & Canals, À. (2018). Reply to Comment by D. W. Morrow on Self-accelerating dolomite-for-calcite replacement: Self-organized dynamics of burial dolomitization and associated mineralization. *American Journal of Science*, 318, 887–892. <https://doi.org/10.2475/07.2011.01>.
- Meyer, R. F., Attanasi, E. D., & Freeman, P.A. (2007). *Heavy oil and natural bitumen resources in geological basins of the world (Open-File Report 2007-1084)*. US Geological Survey. <https://doi.org/10.3133/ofr20071084>.
- Michel, J. (2011). 1991 Gulf war oil spill. In M. Fingas (Ed.), *Oil spill science and technology* (2nd ed.) (pp. 1127–1132). Elsevier. <https://sciencedirect.com/book/9780128094136/oil-spill-science-and-technologyht>.
- Michel, J., Owens, E. H., Zengel, S., Graham, A., Nixon, Z., Allard, T., Holton, W., Reimer, P.D., Lamarche, A., White, M., Rutherford, N., Childs, C., Mauseth, G., Challenger, G., & Taylor, E. (2013). Extent and degree of shoreline oiling: Deepwater horizon oil spill, Gulf of Mexico, USA. *PLoS ONE*, 8(6), e65097. <https://doi.org/10.1371/journal.pone.0065087>.
- Miller, H., Dias, K., Hare, H., Borton, M. A., Blotvogel, J., Danforth, C., Wrighton, K., Ippolito, J.A., & Borch, T. (2020). Reusing oil and gas produced water for agricultural irrigation: effects on soil health and the soil microbiome. *Science of the Total Environment*, 722, 137888. <https://doi.org/10.1016/j.scitotenv.2020.137888>.
- Mir-Babayev, Y. (2021). The Bibi-Heybat oil field: The 175th anniversary of the first oil well in the world. *American Association of Petroleum Geologists Explorer*, 42(8), 16–21. <https://explorer.aapg.org/story/articleid/61005/the-bibi-heybat-oil-field>.
- Moldovanyi, E. P., & Walter, L. M. (1992). Regional trends in water chemistry, Smackover Formation, southwest Arkansas: Geochemical and physical controls. *American Association of Petroleum Geologists Bulletin*, 76, 864–894. <https://doi.org/10.1306/BDF890C-1718-11D7-8645000102C1865D>.
- Molofsky, L. J., Connor, J. A., Farhat, S. K., Wylie, A. S., & Wagner, T. (2011). Methane in Pennsylvania groundwater unrelated to Marcellus shale hydraulic fracturing. *Oil and Gas Journal*, 109. <https://www.ogj.com/home/article/17298166/methane-in-pennsylvania-water-wells-unrelated-to-marcellus-shale-fracturing>.
- Molofsky, L. J., Connor, J. A., McHugh, T. E., Richardson, S. D., Woroszlyo, C., & Alvarez, P. A. (2016). Environmental factors associated with natural methane occurrence in the Appalachian Basin. *Groundwater*, 54(7), 656–668. <https://doi.org/10.1111/gwat.12401>.
- Moore, J., Adams, M., Allis, R., Lutz, S., & Rauzi S. (2005). Mineralogical and geochemical consequences of the long-term presence of CO<sub>2</sub> in natural reservoirs: An example from the Springerville–St. Johns Field, Arizona, and New Mexico, U.S.A. *Chemical Geology*, 217, 365–385. <https://doi.org/10.1016/j.chemgeo.2004.12.019>.

- Moran, J. E., Fehn, U., & Hanor, J. S. (1995). Determination of source ages and migration patterns of brines from the US Gulf Coast using  $^{129}\text{I}$ . *Geochimica et Cosmochimica Acta*, 59, 5055–5069. [https://doi.org/10.1016/0016-7037\(95\)00360-6](https://doi.org/10.1016/0016-7037(95)00360-6).
- Moritis, G. (2009). Special Report: More CO<sub>2</sub>-EOR projects likely as new CO<sub>2</sub> supply sources become available. *Oil & Gas Journal*, December 2009.
- Morse, J. W., Hanor, J. S., & He, S. (1997). The role of brines in carbonate mineral mass transport in sedimentary basins. *Society of Economic Petrologists and Mineralogists Special Publication*, 57, 41–52.
- Müller, D. W., McKenzie, J. A., & Mueller, P. A. (1990). Abu Dhabi sabkha, Persian Gulf, revisited: Application of strontium isotopes to test an early dolomitization model. *Geology*, 18(7), 618–621. [https://doi.org/10.1130/0091-7613\(1990\)018<0618:ADSPGR>2.3.CO;2](https://doi.org/10.1130/0091-7613(1990)018<0618:ADSPGR>2.3.CO;2).
- Muramatsu, Y., Fehn, U., & Yoshida, U. (2001). Recycling of iodide in fore-arc areas: evidence from the iodide brines in Chiba, Japan. *Earth and Planetary Science Letters*, 192, 583–593. [https://doi.org/10.1016/S0012-821X\(01\)00483-6](https://doi.org/10.1016/S0012-821X(01)00483-6).
- National Academies of Sciences, Engineering, and Medicine. (2018). *Onshore unconventional hydrocarbon development: Induced seismicity and innovations in managing risk—Day 2: Proceedings of a workshop*. The National Academies Press. <https://doi.org/10.17226/25083>.
- National Energy Technology Laboratory (NETL). (2013). *Quality guidelines for energy system studies: Estimating plant costs using retrofit difficulty factors*. US DOE/NETL.
- National Institute for Occupational Safety and Health (NIOSH). (1989). *Toxicologic review of selected chemicals: Carbon dioxide*. Centers for Disease Control. <https://www.cdc.gov/niosh/pel88/124-38.html>.
- National Institute for Occupational Safety and Health (NIOSH). (1981). *Occupational health guidelines for chemical hazards (Number 81-123)*. United States Government Printing Office.
- National Oceanic and Atmospheric Administration (NOAA). (2020). Deepwater horizon. National Oceanic and Atmospheric Administration. [Oil spills | National Oceanic and Atmospheric Administration \(noaa.gov\)](https://www.noaa.gov/oil-spills).
- National Oceanic and Atmospheric Administration (NOAA). (2024). Daily CO<sub>2</sub>, Mauna Loa Observatory, Hawaii.
- National Research Council (NRC). (2020). *Climate change: Evidence and causes: Update 2020*. National Academies Press. <https://doi.org/10.17226/25733>.
- National Research Council (NRC). (2014). *Development of unconventional hydrocarbon resources in the Appalachian Basin: Workshop summary*. National Academies Press. <https://doi.org/10.17226/18624>.
- National Research Council. (2012). *Induced seismicity potential in energy technologies (No. 13355)*. National Academies Press. [induced-seismicity-potential-in-energy-technologies](https://doi.org/10.17226/13355).

- Neff, J. M., Lee, K., & DeBlois, E. (2011). Produced water: Overview of composition, fates and effects. In J. Neff, K. Lee, and E. M. DeBlois (Eds.), *Produced water* (pp. 3–54). Springer. [https://doi.org/10.1007/978-1-4614-0046-2\\_1](https://doi.org/10.1007/978-1-4614-0046-2_1).
- New York Times. (1880). The oil wells of Alsace. *New York Times*, 23 February 1880. [PDF]
- Newcomb, W. D., & Rimstidt, J. D. (2002). Trace element distribution in United States groundwater: A probabilistic assessment using public domain data. *Applied Geochemistry*, 17, 49–57. [https://doi.org/10.1016/S0883-2927\(01\)00089-0](https://doi.org/10.1016/S0883-2927(01)00089-0).
- Ng, G. H. C., Bekins, B. A., Cozzarelli, I. M., Baedeker, M. J., Bennett, P. C., & Amos, R. T. (2014). A mass balance approach to investigating geochemical controls on secondary water quality impacts at a crude oil spill site near Bemidji, MN. *Journal of Contaminant Hydrology*, 164, 1–15. <https://doi.org/10.1016/j.jconhyd.2014.04.006>.
- Ni, Y., Liao, F., Chen, J., Yao, L., Wei, J., Sui, J., Gao, J., Coyte, R.M., Lauer, N., & Vengosh, A. (2021). Multiple geochemical and isotopic (Boron, Strontium, Carbon) indicators for reconstruction of the origin and evolution of oilfield water from Jiuquan Basin, Northwestern China. *Applied Geochemistry*, 130. <https://doi.org/10.1016/j.apgeochem.2021.104962>.
- Nicot, J. P. (2017). Decisions on hydraulic fracturing must be science based. *Groundwater*, 55, 441–442. <https://doi.org/10.1111/gwat.12528>.
- Nicot, J. P., & Scanlon, B. R. (2012). Water use for shale gas production in Texas, U.S.A. *Environmental Science & Technology*, 46, 3580–3586. <https://doi.org/10.1021/es204602>.
- Nicot, J. P., Scanlon, B. R., Reedy, R. C., & Costley, R. (2014). Source and fate of hydraulic fracturing water in the Barnett Shale: A historical perspective. *Environmental Science & Technology*, 48(4), 2464–2471. <https://doi.org/10.1021/es404050r>.
- Nicot, J. P., Larson, T., Darvari, R., Mickler, P., Sloten, M., Aldridge, J., Uhlman, K., & Costley, R. (2017a). Controls on methane occurrences in shallow aquifers overlying the Haynesville shale gas field, east Texas. *Groundwater*, 55(4), 443–454. <https://doi.org/10.1111/gwat.12500>.
- Nicot, J. P., Larson, T., Darvari, R., Mickler, P., Uhlman, K., & Costley, R. (2017b). Controls on methane occurrences in aquifers overlying the Eagle Ford shale play, south Texas. *Groundwater*, 55(4), 455–458. <https://doi.org/10.1111/gwat.12506>.
- Nicot, J. P., Mickler, P., Larson, T., Castro, M. C., Darvari, R., Uhlman, K., & Costley, R. (2017c). Methane occurrences in aquifers overlying the Barnett shale play with a focus on Parker County, Texas. *Groundwater*, 55(4), 469–481. <https://doi.org/10.1111/gwat.12508>.
- Nicot, J. P., Darvari, R., Eichhubl, P., Scanlon, B. R., Elliott, B. A., Bryndzia, L. T., Gale, J. F. W., & Fall, A. (2020). Origin of low salinity, high volume produced water in the Wolfcamp Shale (Permian), Delaware Basin, USA. *Applied Geochemistry*, 122, 104771. <https://doi.org/10.1016/j.apgeochem.2020.104771>.

- Nordbotten, J. M., Kavetski, D., Celia, M. A., & Bachu, S. (2009). Model for CO<sub>2</sub> leakage including multiple geological layers and multiple leaky wells. *Environmental Science and Technology*, 43, 743–749.
- Ohmoto, H., & Lasaga, A. C. (1982). Kinetics of reactions between aqueous sulfates and sulfides in hydrothermal systems. *Geochimica et Cosmochimica Acta*, 46, 1727–1745. [https://doi.org/10.1016/0016-7037\(82\)90113-2](https://doi.org/10.1016/0016-7037(82)90113-2).
- Oil and Gas Climate Initiative (OGCI). (2021). *OGCI progress report 2021*. <https://www.ogci.com/ogci-releases-its-2021-progress-report/>.
- Oil and Gas Journal. (1993). EPA Drafts Tougher Injection Well Rules [Editorial]. *Oil and Gas Journal*, 91.
- O'Neil, J. R., & Kharaka, Y. K. (1976). Hydrogen and oxygen isotope exchange reactions between clay minerals and water. *Geochimica et Cosmochimica Acta*, 40, 241–246. [https://doi.org/10.1016/0016-7037\(76\)90181-2](https://doi.org/10.1016/0016-7037(76)90181-2).
- Orem, W., Tatu, C., Varonka, M., Lerch, H., Bates, A., Engle, M., Crosby, L., & McIntosh, J. (2014). Organic substances in produced and formation water from unconventional natural gas extraction in coal and shale. *International Journal of Coal Geology*, 126, 20–31. <https://doi.org/10.1016/j.coal.2014.01.003>.
- Orem, W., Varonka, M., Crosby, L., Haase, K., Loftin, K., Hladik, M., Akob, D.M., Tatu, C., Mumford, A., Jaeschke, J., Bates, A., & Schell, T. (2017). Organic geochemistry and toxicology of a stream impacted by unconventional oil and gas wastewater disposal operations. *Applied Geochemistry*, 80, 155–167. <https://doi.org/10.1016/j.apgeochem.2017.02.016>.
- Ortoleva, P., Al-Shaieb, Z., & Puckette, J. (1995). Genesis and dynamics of basin compartments and seals. *American Journal of Science*, 295(4), 345–427. <https://sysbio.indiana.edu/publication/genesis-and-dynamics-of-basin-compartments-and-seals/>.
- Osborn, S. G., & McIntosh, J. C. (2010). Chemical and isotopic tracers of the contribution of microbial gas in Devonian organic-rich shales and reservoir sandstones, northern Appalachian Basin. *Applied Geochemistry*, 25, 456–471. <https://doi.org/10.1016/j.apgeochem.2010.01.001>.
- Osborn, S. G., Vengosh, A., Warner, N. R., & Jackson, R. B. (2011). Methane contamination of drinking water accompanying gas-well drilling and hydraulic fracturing. *Proceedings of the National Academy of Sciences*, 108, 8172–8176. <https://doi.org/10.1073/pnas.1100682108>.
- Otton, J. K., & Zielinski, R. A. (2003). *Produced water and hydrocarbon releases at the Osage-Skiatook petroleum environmental research studies, Osage county Oklahoma: introduction and geologic setting (Water Resources Investments Report 03-4260)* (pp. 14–41). US Geologic Survey. <https://pubs.er.usgs.gov/publication/70216506>.
- Otton, J. K., R. A. Zielinski, B. D. Smith, and M. M. Abbott. (2007). Geologic controls on movement of produced-water releases at US geological survey research Site A,

- Skiatook lake, Osage county, Oklahoma. *Applied Geochemistry*, 22, 2138–2154. <https://doi.org/10.1016/j.apgeochem.2007.04.015>.
- Overton, E. B., Sharp, W. D., & Robert, P. (1994). Toxicity of petroleum. In L. G. Cockerham, & B. S. Shane (Eds.), *Basic environmental toxicology* (pp. 133–156). CRC Press. <https://books.google.com.br/books?hl=pt-BR&lr=&id=>.
- Pačes, T.. (1987). Hydrochemical evolution of saline water from crystalline rocks of the Bohemian Massif (Czechoslovakia). In P. Fritz, & S.K. Frapé (Eds.), *Saline water and gases in crystalline rocks (Special Paper, number 33)* (pp. 1451–1456). Geological Association of Canada.
- Saunders, J. A., & Swann, C. T. (1992). Nature and origin of authigenic rhodochrosite and siderite from the Paleozoic aquifer, northeast Mississippi, U.S.A. *Applied Geochemistry*, 7, 375–387. [https://doi.org/10.1016/0883-2927\(92\)90027-Z](https://doi.org/10.1016/0883-2927(92)90027-Z).
- Taylor, S. R., & McLennan, S. M. (1985). *The continental crust: Its composition and evolution*. Blackwell Scientific.
- Palandri, J. L., & Reed, M. H. (2001). Reconstruction of in situ composition of sedimentary formation water. *Geochimica et Cosmochimica Acta*, 65, 1741–1767. [https://doi.org/10.1016/S0016-7037\(01\)00555-5](https://doi.org/10.1016/S0016-7037(01)00555-5).
- Palandri, J. L., & Kharaka, Y. K. (2005). Ferric iron-bearing sediments as a mineral trap for CO<sub>2</sub> sequestration: Iron reduction using sulfur-bearing waste gas. *Chemical Geology*, 217, 351–364. <https://doi.org/10.1016/j.chemgeo.2004.12.018>.
- Palandri, J. L., Rosenbauer, R. J. & Kharaka, Y.K. (2005). Ferric iron in sediments as a novel CO<sub>2</sub> mineral trap: CO<sub>2</sub>-SO<sub>2</sub> reaction with hematite. *Applied Geochemistry*, 20, 2038–2048. <https://doi.org/10.1016/j.apgeochem.2005.06.005>.
- Palmer, M. R., & Swihart, G. H. (1996). Boron mineralogy, petrology, and geochemistry. *Reviews in Mineralogy and Geochemistry*, 33, 709–744. [https://books.google.com/books/about/Boron.html?id=10PkjgEACAAJ&redir\\_esc=ybooks.google.com.br/books?hl=pt-BR&lr=&id=](https://books.google.com/books/about/Boron.html?id=10PkjgEACAAJ&redir_esc=ybooks.google.com.br/books?hl=pt-BR&lr=&id=).
- Pang, Z., & Reed, M. (1998). Theoretical chemical thermometry on geothermal water: Problems and methods. *Geochimica et Cosmochimica Acta*, 62, 1083–1091. [https://doi.org/10.1016/S0016-7037\(98\)00037-4](https://doi.org/10.1016/S0016-7037(98)00037-4).
- Pang, Z., Yang, F., Li, Y. H., & Duan, Z. (2010). Integrated CO<sub>2</sub> sequestration and geothermal development: Saline aquifers in Beitang depression, Tianjin, North China Basin. In P. Birkle, & I. S. Torres-Alvarado (Eds.), *Water-Rock Interaction: Proceedings of the 13th International Symposium on the Water Rock Interaction WRI-13, Guanajuato, Mexico, 16–20 August, 2010* (pp. 31–36). CRC Press.
- Parkhurst, D. L., & Appelo, C. A. J. (1999). *User's Guide to PHREEQC (version 2): A computer program for speciation, batch-reaction, one dimensional transport and inverse geochemical modeling*. United States Geological Survey Water Resources Investigation Report 99-4259. <https://doi.org/10.3133/wri994259>.

- Parkhurst, D. L., & Appelo, C. A. J. (2015). *PH REdox Equilibrium (Volume 3.3)* [Computer software]. US Geological Survey.
- Passey, Q. R. (2010). *From oil-prone source rock to gas-producing shale reservoir-Geologic and petrophysical characterization and unconventional shale-gas reservoirs (SPE 131350)*. Society of Petroleum Engineers. <https://doi.org/10.2118/131350-MS>.
- Patterson, L. A., Konschnik, K. E., Wiseman, H., Fargione, J., Maloney, K. O., Kiesecker, J., Nicot, J. P., Baruch-Mordo, S., Entekin, S., Trainor, A., & Saiers, J. E. (2017). Unconventional oil and gas spills: Risks, mitigation priorities, and state reporting Requirements. *Environmental Science & Technology*, 51(5), 2563–2573.
- Payne, R. D. (1966). Salt water pollution problems in Texas. *Journal of Petroleum Technology*, 18(11), 1401–1410. <https://doi.org/10.2118/1424-PA>.
- Peterman, Z. E., Thamke, J., & Futa, K. (2010). *Use of strontium isotopes to detect produced-water contamination in surface water and groundwater in the Williston Basin, Northeastern Montana (Search and discovery article number 90172)*. American Association of Petroleum Geologists. <https://www.researchgate.net/publication/298127743>.
- Phelps, T. J., McCallum, S. D., Cole, D. R., Kharaka, Y. K., & Hovorka, S. D. (2006, May). Monitoring geological CO<sub>2</sub> sequestration using perfluorocarbon gas tracers and isotopes. *Proceedings of the 5th Annual Conference on Carbon Capture and Sequestration, Alexandria, VA., May 8-11, 2006* (pp. 8–11). [CD-ROM].
- Phillips, F. M. (2000). Chlorine-36. In P. Cook, & A. L. Herczeg (Eds.), *Environmental tracers in subsurface hydrology* (pp. 299–348). Kluwer Academic.
- Phillips, F. M., & Castro, M. C. (2014). 5.15 Groundwater dating and residence-time measurements. In J. I. Drever (Ed.), *Treatise on Geochemistry*, 5, 451–499.
- Phillips, S. (2015). *Pennsylvania Department of Environmental Protection (DEP): Unauthorized drilling fluid contaminated Potter County aquifer. DEP's Notice of Violation regarding the Sweden Township incident*. October 1, 2015.
- Plata, D. L., Jackson R. B., Vengosh, A., Mouser, P. J. (2019). More than a decade of hydraulic fracturing and horizontal drilling research. *Environmental Science: Processes & Impacts*, 21, 193–194. <https://pubs.rsc.org/en/content/articlelanding/2019/em/c9em90004g>.
- Plummer, L. (2005). Dating of young groundwater. In P. K. Aggarwal., J. R. Gat, & K. F. Froehlich (Eds.), *Isotopes in the water cycle* (pp. 193–218). Springer. [https://doi.org/10.1007/1-4020-3023-1\\_14](https://doi.org/10.1007/1-4020-3023-1_14).
- Podgorski, D. C., Zito, P., Kellerman, A. M., Bekins, B. A., Cozzarelli, I. M., Smith, D. F., Cao, X., Schmidt-Rohr, K., Wagner, S., Stubbins, A., & Spencer, R. G. M. (2021). Hydrocarbons to carboxyl-rich alicyclic molecules: A continuum model to describe biodegradation of petroleum-derived dissolved organic matter in contaminated groundwater plumes. *Journal of Hazardous Materials*, 402, 123998. <https://doi.org/10.1016/j.jhazmat.2020.123998>.

- Pokrovsky, O. S., Sergey, V., Schott, J., & Castillo, A. (2009). Calcite, dolomite and magnesite dissolution kinetics in aqueous solutions at acid to circumneutral pH, 25 to 150.C and 1 to 55 atm pCO<sub>2</sub>: New constraints on CO<sub>2</sub> sequestration in sedimentary basins. *Chemical Geology*, 265, 20–32. <https://doi.org/10.1016/j.chemgeo.2009.01.013>↗.
- Porcelli, D., Ballentine, C. J., & Wieler, R. (Eds.) (2002). An overview of noble gas geochemistry and cosmochemistry. *Reviews in Mineralogy and Geochemistry*, 47, 1–19. <https://doi.org/10.2138/rmg.2002.47.1>↗.
- Presser, T. S., & Barnes, I. (1984). *Dissolved constituents including selenium in water in the vicinity of the Kesterson National Wildlife Refuge, Fresno and Merced counties, California (Water Resources Investigations Report 84-4122)*. US Geological Survey. <https://doi.org/10.3133/wri854220>↗.
- Purtschert, R., Yokochi, R., Jiang, W., Lu, Z. T., Mueller, P., Zappala, J., Heerdene, E. Van, Cason, E., Lau, M., Kieft, T. L., Gerber, C., Brennwald, M. S., & Onstott, T. C. (2021). Underground production of <sup>18</sup>K detected in subsurface fluids. *Geochimica et Cosmochimica Acta*, 295, 65–79. <https://pubs.usgs.gov/wri/1984/4122/report.pdf>↗.
- Quest CCS. (2022). *Quest carbon capture and storage project, Alberta, Canada. (Report)*. <https://www.hydrocarbons-technology.com/projects/quest-carbon-capture-and-storage-project-alberta/>↗.
- Ranganathan, V. & Hanor, J. S. (1987). A numerical model for the formation of saline water due to diffusion of dissolved NaCl in subsiding sedimentary basins with evaporites. *Journal of Hydrology*, 92, 97–120. [https://doi.org/10.1016/0022-1694\(87\)90091-6](https://doi.org/10.1016/0022-1694(87)90091-6)↗.
- Rapp, J. B. (1976). Amino acids and gases in some springs and an oil field in California. *Journal of Research of the US Geological Survey*, 4, 227–232.
- Reguly, T. (2019). Reguly: Ørsted's 'black-to-green transformation' shows benefits of rapid decarbonization. *The Energy Mix Climate News Network*, 29 November 2019. <https://www.theenergymix.com/2019/11/29/reguly-orsted-black-to-green-transformation-shows-benefits-of-rapid-decarbonization/>↗.
- Reilly, T. E., Dennehy, K. F., Alley, W. M., & Cunningham, W. L. (2008). *Ground-water availability in the United States (Circular, 1323)*. United States Geological Survey. <https://water.usgs.gov/watercensus/AdHocComm/Background/Ground-WaterAvailabilityintheUnitedStates.pdf>↗.
- Revil, A., Cathles, L. M., Losh, S., & Nunn, J. A. (1998). Electrical conductivity in shaly sands with geophysical applications. *Journal of Geophysical Research*, 103, 925–936. <https://doi.org/10.1029/98JB02125>↗.
- Reyes, F. R., Engle, M. A., Jin, L., Jacobs, M. A., & Konter, J. G. (2018). Hydrogeochemical controls on brackish groundwater and its suitability for use in hydraulic fracturing: The Dockum Aquifer, Midland Basin, Texas, U.S.A. *Environmental Geosciences*, 25(2), 37–63. <https://archives.datapages.com/data/deg/2018/EG022018/eg17017/eg17017.html>↗.

- Rice, C. A., Ellis, M. S., & Bullock Jr., J. H. (2000). *Water co-produced with coalbed methane in the Powder River Basin, Wyoming: Preliminary compositional data (Open-File Report 00-372)*. US Geological Survey. <https://doi.org/10.3133/ofr00372>.
- Rice, C. A., Cathcart, J. D., Zielinski, R. A., & Otton, J. K. (2003). *Characterization of soils and rock at an active oil production site: Effects of brine and hydrocarbon contamination (Water-Resources Investigations 03-4260)* (pp. 133–146). US Geological Survey.
- Richardson, C. K., & Holland, H. D. (1979). The solubility of fluorite in hydrothermal solutions, an experimental study. *Geochimica Et Cosmochimica Acta*, 1313–1325. [https://doi.org/10.1016/0016-7037\(79\)90121-2](https://doi.org/10.1016/0016-7037(79)90121-2).
- Richter, B. C., Kreitler, C. W., & Bledsoe, B. E. (Eds.) (1993). *Geochemical techniques for identifying sources of ground-water salinization*. C. K. Smoley. <https://books.google.com.br/books?hl=pt-BR&lr=&id=SF1-SDh>.
- Rider, M. (1996). *The geological interpretation of well logs* (2nd ed.). Gulf Publishing.
- Roberts, S. J., & Nunn, J. A. (1995). Episodic fluid expulsion from geopressed sediments. *Marine and Petroleum Geology*, 12, 195–204. [https://doi.org/10.1016/0264-8172\(95\)92839-O](https://doi.org/10.1016/0264-8172(95)92839-O).
- Rochon, E., Kuper, J., Bjureby, E., Johnston, P., Oakley, R., Santillo, D., & Von Goerne, G. (2008). False hope. Why carbon capture and storage won't save the climate. *Greenpeace International*, 2 May 2008. <https://www.greenpeace.org/usa/research/false-hope-why-carbon-capture/>.
- Rodriguez, A. Z., Wang, H., Hu, L., Zhang, Y., & Xu, P. (2020). Treatment of produced water in the Permian Basin for hydraulic fracturing: Comparison of different coagulation processes and innovative filter media. *Water*, 12(3), 770. <https://doi.org/10.3390/w12030770>.
- Rogelj, J., Popp, A., Calvin, K. V., Luderer, G., Emmerling, J., Gernaat, D., Fujimori, S., Strefler, J., Hasegawa, T., Marangoni, G., Krey, V., Kriegler, E., Riahi, K., van Vuuren, D. P., Doelman, J., Drouet, L., Edmonds, J., Fricko, O., Harmsen, M., Havlík, P., Humpenöder, F., Stehfest, E., & Tavoni, M. (2018). Scenarios towards limiting global mean temperature increase below 1.5 degrees C. *Nature Climate Change*, 8, 325–332. <https://www.nature.com/articles/s41558-018-0091-3>.
- Rogelj, J., Forster, P. M., Kriegler, E., Smith, C. J., & Séférian, R. (2020). Estimating and tracking the remaining carbon budget for stringent climate targets. *Nature*, 571, 335–342. <https://www.nature.com/articles/s41586-019-1368-z>.
- Rooney-Varga, J. N., Anderson, R. T., Fraga, J. L., Ringelberg, D., & Lovely, D. R. (1999). Microbial communities associated with anaerobic benzene degradation in a petroleum-contaminated aquifer. *Applied and Environmental Microbiology*, volume 65(7), 3056–3063. <https://doi.org/10.1128/AEM.65.7.3056-3063.1999>.
- Rostrom, B., & Arkadaskiy, S. (2014). Fingerprinting “stray” formation fluids associated with hydrocarbon exploration and production. *Elements*, 10, 285–290. <https://doi.org/10.2113/gselements.10.4.285>.

- Rowan, E. L., Engle, M. A., Kirby, C. S., & Kraemer, T. F. (2011). *Radium content of oil-and gas-field produced water in the northern Appalachian Basin (USA): Summary and discussion of data (Scientific Investigations Report 5135)*. US Geological Survey.  
<https://doi.org/10.3133/sir20115135>.
- Rowan, E. L., & Kraemer, T. F. (2012). *Radon-222 content of natural gas samples from Upper and Middle Devonian sandstone and shale reservoirs in Pennsylvania: Preliminary data (Open-File Report 2012-159)*. US Geological Survey.  
<https://doi.org/10.3133/ofr20121159>.
- Rowan, E. L., Engle, M. A., Kraemer, T. F., Schroeder, K. T., Hammack, R. W., & Doughten, M. W. (2015). Geochemical and isotopic evolution of water produced from Middle Devonian Marcellus shale gas wells, Appalachian basin, Pennsylvania. *American Association of Petroleum Geologists, Bulletin*, 99(2), 181–206.  
<https://doi.org/10.1306/07071413146>.
- Roychaudhuri, B., Tsotsis, T., & Jessen, K. (2011). *An experimental investigation of spontaneous imbibition in gas shales (SPE 147652)*. Society of Petroleum Engineers.  
<https://doi.org/10.1016/j.petrol.2013.10.002>.
- Rozell, D. J., & Reaven, S. J. (2012). Water pollution risk associated with natural gas extraction from the Marcellus shale. *Risk Analysis*, 32, 1382–1393.  
<https://doi.org/10.1111/j.1539-6924.2011.01757.x>.
- Rubinstein, J. L., & Mahani, A. B. (2015). Myths and facts on wastewater injection, hydraulic fracturing, enhanced oil recovery and induced seismicity. *Seismological Research Letters*, 86, 1060–1067. <https://doi.org/10.1785/0220150067>.
- Saeed, W. (2021). *Assessment of saltwater origin in the Rub' al-Khali basin and its relation to the formation of sabkha Matti* [Unpublished doctoral dissertation]. University of Waterloo.
- Salvador, A. (1991). Origin and development of the Gulf of Mexico basin. In A. Salvador (Ed.), *The Gulf of Mexico Basin* (pp. 389–444). Geological Society of America.  
<https://doi.org/10.1130/DNAG-GNA-J.389>.
- Sandstrom, M. W., & Wilde, F. D. (2014). Syringe-filter procedure for processing samples for analysis of organic compounds by DAI LC-MS/MS. In *National field manual for the collection of water-quality data techniques (Water-Resources Investigations, 9)*. US Geological Survey.
- Saunders, J. A., & Swann, C. T. (1992). Nature and origin of authigenic rhodochrosite and siderite from the Paleozoic aquifer, northeast Mississippi, U.S.A. *Applied Geochemistry*, 7, 375–387. [https://doi.org/10.1016/0883-2927\(92\)90027-Z](https://doi.org/10.1016/0883-2927(92)90027-Z).
- Savvaidis, A., Lomas, A., & Breton, C. L. (2020). Induced seismicity in the Delaware Basin, West Texas, is caused by hydraulic fracturing and wastewater disposal. *Bulletin of the Seismological Society of America*, 110(5), 2225–2241.  
<https://doi.org/10.1785/0120200087>.
- Scanlon, B. R., Weingarten, M. B., Murray, K. E., & Reedy, R. C. (2019). Managing basin-scale fluid budgets to reduce injection-induced seismicity from the recent

- United States shale oil revolution. *Seismological Research Letters*, 90(1), 171–182. <https://doi.org/10.1785/0220180223>.
- Scanlon, B. R., Ikonnikova, S., Yang, Q., & Reedy, R. C. (2020a). Will water issues constrain oil and gas production in the United States? *Environmental Science & Technology*, 54(6), 3510–3519. <https://doi.org/10.1021/acs.est.9b06390>.
- Scanlon, B. R., Reedy, R. C., Xu, P., Engle, M., Nicot, J. P., Yoxtheimer, D., Yang, Q., & Ikonnikova, S. (2020b). Can we beneficially reuse produced water from oil and gas extraction in the United States? *Science of the Total Environment*, 717, 137085. <https://doi.org/10.1016/j.scitotenv.2020.137085>.
- Scanlon, B. R., Reedy, R. C., & Wolaver, B. D. (2022). Assessing cumulative water impacts from shale oil and gas production: Permian Basin case study. *Science of the Total Environment*, 717, 521–537. <https://doi.org/10.1016/j.scitotenv.2021.152306>.
- Schenk, C. J., & Pollastro, R. M. (2001). National assessment of oil and gas fact sheet: Natural gas production in the United States. US Geological Survey. <https://www.energy.cr.usgs.gov/oilgas/noga>.
- Schenk, C. J., Cook, A. T., Charpentier, R. R., Pollastro, R. M., Klett, T. R., Tennyson, M. E., Kirschbaum, M. A., Brownfield, M. E., & Pitman, J. K. (2010). An estimate of recoverable heavy oil resources of the Orinoco oil belt, Venezuela. US Geological Survey. <https://doi.org/10.3133/fs20093028>.
- Schmidt, L. (1928). *Report of inspection trip through west Texas fields, 10 Oct. 1928, box 106, Bartlesville Records (Bureau of Mines, RG 70-4)*. NARS.
- Shock, E. L. (1995). Organic acids in hydrothermal solutions: Standard molal thermodynamic properties of carboxylic acids and estimates of dissociation constants at high temperatures and pressures. *American Journal of Science*, 295, 496–580. <https://doi.org/10.2475/ajs.295.5.496>.
- Schreiber, M., & Cozzarelli, I. M. (2021). Arsenic release to the environment from hydrocarbon production, storage, transportation, use and waste management. *Journal of Hazardous Materials*, 441, 125013. <https://doi.org/10.1016/j.jhazmat.2020.125013>.
- Schulz, H. D. (2000). Quantification of early diagenesis: dissolved constituents in marine pore water. In H. D. Schulz, & M. Zabel (Eds.), *Marine geochemistry* (pp. 85–128). Springer-Verlag.
- Seal, R. R., Alpers, C. N., & Rye, R. O. (2000). Stable isotope systematics of sulfate minerals. *Reviews in Mineralogy and Geochemistry*, 40, 541–602. <https://doi.org/10.2138/rmg.2000.40.12>.
- Seewald, J. S. (2001). Model for the origin of carboxylic acids in basinal brines. *Geochimica et Cosmochimica Acta*, 65, 3779–3789. [https://doi.org/10.1016/S0016-7037\(01\)00702-5](https://doi.org/10.1016/S0016-7037(01)00702-5).
- Selley, R. C., & Sonnenberg, S. A. (2014). *Elements of petroleum geology*. Academic Press.
- Shaheen, S. W., Wen, T., Herman, A. & Brantley, S. L. (2022). Geochemical evidence of potential groundwater contamination with human health risks where hydraulic

- fracturing overlaps with extensive legacy hydrocarbon extraction. *Environmental Science & Technology*, 56, 10010–10019. <https://doi.org/10.1021/acs.est.2c00001>↗.
- Shelton, J. L., Andrews, R. S., Akob, D. M., DeVera, C. A., Mumford, A. C., Engle, M., Plampin, M. R., & Brennan, S. T. (2020). *Compositional analysis of formation water geochemistry and microbiology of commercial and carbon dioxide-rich wells in the southwestern United States (Scientific Investigations Report 2020-5037)*. US Geological Survey. <https://doi.org/10.3133/sir20205037>↗.
- Sheppard, S. M. F. (1986). Characterization and isotopic variations in natural water. In J. W. Valley, H. P. Taylor Jr., & J. R. O'Neil (Eds.), *Stable isotopes in high-temperature geological processes. Reviews in Mineralogy and Geochemistry*, 16, 165–183.
- Sirivedhin, T., & Dallbauman, L. (2004). Organic matrix in produced water from the Osage-Skiatook Petroleum Environmental Research site, Osage County, Oklahoma. *Chemosphere*, 57, 463–469.
- Skalak, K. J., Engle, M. A., Rowan, E. L., Jolly, G. D., Conko, K. M., Benthem, A. J., & Kraemer, T. F. (2014). Surface disposal of produced water in western and southwestern Pennsylvania: Potential for accumulation of alkali-earth elements in sediments. *International Journal of Coal Geology*, 126, 162–170. <https://doi.org/10.1016/j.coal.2013.12.001>↗.
- Shouakar-Stash, O. (2008). *Evaluation of stable chlorine and bromine isotopes in sedimentary formation fluids* [Unpublished doctoral dissertation]. University of Waterloo,.
- Shouakar-Stash, O., Frape, S. K., & Wood, W. W. (2006). The role of stable chlorine and bromine stable isotopes in determining the geochemical evolution of the Abu Dhabi coastal sabkha (United Arab Emirates). *Proceedings of the Sixth International Conference on the Geology of the Middle East, United Arab Emirates, March 20–23, 2006*. <http://www.fsc.uaeu.ac.ae/Geology/c/me.htm>Ⓞ.
- Smith, B. D., Bisdorf, R. J., Horton, R. J., Otton, J. K., & Hutton, R. S. (2003). *Preliminary geophysical characterization of two oil production sites, Osage County, Oklahoma-Osage Skiatook petroleum environmental research project (Water-Resources Investigations, 03-4260, 41–55)*. US Geological Survey. <https://pubs.er.usgs.gov/publication/70216509>↗.
- Smyth, R. C., Hovorka, S. D., Lu, J., Romanak, K. D., Partin, J. W., & Wong, C. (2008). Assessing risk to fresh water resources from long term CO<sub>2</sub> injections: Laboratory and field studies. *Energy Procedia*, 1(1), 1957–1964. <https://doi.org/10.1016/j.egypro.2009.01.255>↗.
- Smyth, R. C., & Hovorka, S. D. (2018). *Best management practices for offshore transportation and sub seabed geologic storage of carbon dioxide (OCS Study BOEM 2018-004)*. US Department of the Interior, Bureau of Ocean Energy Management. [https://epis.boem.gov/final\\_percent\\_20reports/5663.pdf](https://epis.boem.gov/final_percent_20reports/5663.pdf)↗.
- Soeder, D. J. & Kent, D. B. (2018). When oil and water mix: Understanding the environmental impacts of shale development. *Geological Society of America Today*, 28(9), 4–10. <https://doi.org/10.1130/gsatg361a.1>↗.

- Sofer, Z., Gat, J. (1972). Activities and concentrations of  $^{18}\text{O}$  in concentrated aqueous salt solutions: analytical and geophysical implications. *Earth and Planetary Science Letters*, 15, 232–238. [https://doi.org/10.1016/0012-821X\(72\)90168-9](https://doi.org/10.1016/0012-821X(72)90168-9).
- Solomon, D. K. (2000).  $^4\text{He}$  in groundwater. In P. Cook, & A. L. Herczeg (Eds.), *Environmental tracers in subsurface hydrology* (pp. 425–440). Kluwer Academic.
- Solomon, S. (2021). *Benefits to safely managing orphaned oil and gas wells (Fact Sheet, April 2021)*. AAAS Center for Scientific Evidence in Public Issues (EPI Center).
- Sorkhabi, R. (2010). The king of giant fields. *GEO ExPro*, 7(4).
- Spangler, L. H., Dobeck, L. M., Repasky, K. S., Nehrir, A. R., Humphries, S. D., Barr, J. L., Keith, C. J., Shaw, J. A., Rouse, J. H., Cunningham, A. B., Benson, S. M., Oldenburg, C. M., Lewicki, J. L., Wells, A. W., Diehl, J. R., Strazisar, B. R., Fessenden, J. E., Rahn, R. A., Amonnette, J. E.,...Wielopolski, L. (2009). A shallow subsurface controlled release facility in Bozeman, Montana, USA, for testing near surface  $\text{CO}_2$  detection techniques and transport models. *Environmental Earth Sciences*, 60, 227–239. <https://doi.org/10.1007/s12665-009-0400-2>.
- Spivack A. J., Palmer, M. R. & Edmond, J. M. (1987). The sedimentary cycle of the boron isotopes. *Geochimica et Cosmochimica Acta*, 51, 1939–1949. [https://doi.org/10.1016/0016-7037\(87\)90183-9](https://doi.org/10.1016/0016-7037(87)90183-9).
- Stanton, J. S., Anning, D. W., Brown, C. J., Moore, R. B., McGuire, V. L., Qi, S. L., Harris, A. C., Dennehy, K. F., McMahon, P. B., Degnan, J. R., & Bohlke, J. K. (2017). *Brackish groundwater in the United States (Professional Paper, 1833)*. US Geological Survey. <https://doi.org/10.3133/pp1833>.
- Stelman, C. M., Klazinga, D. R., Cahill, A. G., Endres, A. L., & Parker, B. L. (2017). Monitoring the evolution and migration of a methane gas plume in an unconfined sandy aquifer using time-lapse GPR and ERT. *Journal of Contaminant Hydrology*, 205, 12–24. <https://doi.org/10.1016/j.jconhyd.2017.08.011>.
- Stenhouse, M., Arthur, R., & Zhou, W. (2009). Assessing environmental impacts from geological  $\text{CO}_2$  storage. *Energy Procedia*, 1, 1895–1902. <https://doi.org/10.1016/j.egypro.2009.01.247>.
- Stephens, M. J., Shimabukuro, D. H., Gillespie, J. M., & Chang, W. (2018). Groundwater salinity mapping using geophysical log analysis within the Fruitvale and Rosedale Ranch oil fields, Kern County, California, USA. *Hydrogeology Journal*, 27, 731–746. <https://doi.org/10.1007/s10040-018-1872-5>.
- Stewart-Gordon, T. (1992). Industry Eyes New Standards for Injection Wells. *The Oil Daily*.
- Stoessell R. K., & Carpenter, A. B. (1986). Stoichiometric saturation tests of  $\text{NaCl}_{1-x}\text{Br}_x$  and  $\text{KCl}_{1-x}\text{Br}_x$ . *Geochimica et Cosmochimica Acta*, 50, 1465–1474.
- Stringfellow W. T., Camarillo, M. K., Domen, J. K., Sandelin, W. L., Varadharajan, C., Jordan, P. D., Reagan, M. T., Cooley, H., Heberger, M. G., & Birkholzer, J. T. (2017). Identifying chemicals of concern in hydraulic fracturing fluids used for oil

- production. *Environmental Pollution*, 220, 413–420.  
<https://doi.org/10.1016/j.envpol.2016.09.082>↗.
- Striolo, A., Klaessig, F., Cole, D. R., Wilcox, J., Chase, G. G., Sondergeld, C. G., & Pasquali, M. (2012). *Identification of fundamental interfacial and transport phenomena for the sustainable deployment of hydraulic shale fracturing—Role of chemicals used* [Workshop Report: NSF Workshop on Hydraulic Fracturing, Arlington, VA. Award #CBET 1229931]. National Science Foundation, Division of Chemical, Bioengineering, Environmental and Transport Systems.
- Stueber, A. M., Saller, A. H., & Ishida, H. (1998). Origin, migration, and mixing of brines in the Permian Basin: Geochemical evidence from the eastern Central Basin platform, Texas. *American Association of Petroleum Geologists Bulletin*, 82, 1652–1672.  
<https://pubs.geoscienceworld.org/aapgbull/article-abstract/82/9/1652/39601/Origin-migration-and-mixing-of-brines-in-the?redirectedFrom=fulltext>↗.
- Stueber, A. M., & Walter, L. M. (1991). Origin and chemical evolution of formation water from Silurian–Devonian strata in the Illinois Basin, USA. *Geochimica et Cosmochimica Acta*, 55, 309–325. [https://doi.org/10.1016/0016-7037\(91\)90420-A](https://doi.org/10.1016/0016-7037(91)90420-A)↗.
- Stueber A. M., Walter, L. M., Huston, T. J., & Pushkar, P. (1993). Formation water from Mississippian–Pennsylvanian reservoirs, Illinois Basin, USA – Chemical and isotopic constraints on evolution and migration. *Geochimica et Cosmochimica Acta*, 57, 763–784.  
[https://doi.org/10.1016/0016-7037\(93\)90167-U](https://doi.org/10.1016/0016-7037(93)90167-U)↗.
- Sublette, K. L., Tapp, J. B., Fisher, J. B., Jennings, E., Duncan, K., Thoma, G., Brokaw, J. & Todd, T. (2007). Lessons learned in remediation and restoration in Oklahoma prairie: A review. *Applied Geochemistry*, 22, 2225–2239.  
<https://doi.org/10.1016/j.apgeochem.2007.04.011>↗.
- Sundquist, E. T., Ackerman, K. V., Parker, L., & Huntzinger, D. N. (2009). An Introduction to global carbon cycle. In B. J. McPherson, & E. T. Sundquist (Eds.), *Carbon sequestration and its role in global carbon cycle*. American Geophysical Union Geophysical Monograph, 183, 1–23.
- Surdam, R. C., Crossey, L. J., Hagen, E. S., & Heasler, H. P. (1989). Organic–inorganic interactions and sandstone diagenesis. *American Association of Petroleum Geologists Bulletin*, 73, 1–23.
- Sweet, W. V., Hamlington, B. D., Kopp, R. E., Weaver, C. P., Barnard, P. L., Bekaert, D., Brooks, W., Craghan, M., Dusek, G., Frederikse, T., Garner, G., Genz, A. S., Krasting, J. P., Larour, E., Marcy, D., Marra, J. J., Obeysekera, J., Osler, M., Pendleton, M., Roman, D.,...Zuzak, C. (2022). *Global and regional sea level rise scenarios for the United States: Updated mean projections and extreme water level probabilities along US coastlines* (NOAA Technical Report NOS 01). National Oceanic and Atmospheric Administration, National Ocean Service.  
<https://ambpublicoceanservice.blob.core.windows.net/oceanserviceprod/hazards/sealevelrise/noaa-nos-techrpt01-global-regional-SLR-scenarios-US.pdf>↗.

- Szalkowski, D. S., & Hanor, J. S. (2003). Spatial variations in the salinity of produced water from southwestern Louisiana. *Gulf Coast Association of Geological Societies Transactions*, 53, 798–806.  
[https://www.researchgate.net/publication/301840996\\_Spatial\\_variations\\_in\\_the\\_salinity\\_of\\_produced\\_water\\_from\\_southwestern\\_Louisiana](https://www.researchgate.net/publication/301840996_Spatial_variations_in_the_salinity_of_produced_water_from_southwestern_Louisiana).
- Tagirov, B., & Schott, J. (2001). Aluminum speciation in crustal fluids revisited. *Geochimica et Cosmochimica Acta*, 65, 3965–3992. [https://doi.org/10.1016/S0016-7037\(01\)00705-0](https://doi.org/10.1016/S0016-7037(01)00705-0).
- Tasker, T. L., Burgos, W. D., & Warner, N. R. (2020). Geochemical and isotope analysis of produced water from the Utica/Point Pleasant Shale, Appalachian Basin. *Environmental Science: Processes and Impacts*, 6, 1224–1232.
- Taylor, S. R., & McLenna, S. M. (1985). *The continental crust: Its composition and evolution*. Blackwell Scientific.  
<https://osti.gov/biblio/6582885-continental-crust-its-composition-evolutionh>.
- Teng, F. Z., Watkins, J., & Dauphas, N. (2017). Non-traditional stable isotopes. *Reviews in Mineralogy & Geochemistry*, 82. [www.minsocam.org/msa/rim/rim82.html](http://www.minsocam.org/msa/rim/rim82.html).
- Thamke, J. N., & Smith, B. D. (2014). *Delineation of brine contamination in and near the East Poplar oil field, Fort Peck Indian Reservation, northeastern Montana, 2004-09 (Scientific Investigations Report 2014-5024)*. US Geological Survey.  
<https://doi.org/10.3133/sir20145024>.
- Thordsen, J. J., Kharaka, Y. K., Kakouros, E., & Ambats, G. (2007). *The fate of inorganic and organic chemicals in produced water from the Osage-Skiatook Petroleum Environmental Research sites "A" and "B", Osage County, Oklahoma (Open-File Report, OFR 2007-1055)*. US Geological Survey.
- Thorstenson, D. C., & Parkhurst, D. L. (2004). Calculation of individual isotope equilibrium constants for geochemical reactions. *Geochimica et Cosmochimica Acta*, 68, 2449–2465. <https://doi.org/10.1016/j.gca.2003.11.027>.
- Thurman, E. M. (1985). *Organic geochemistry of natural water (Developments in Biogeochemistry, 2)*. Kluwer Academic. [Organic Geochemistry of Natural Water 1985](https://doi.org/10.1007/978-3-642-87813-8).
- Timofeeff, M. N., Lowenstein, T. K., Martins da Silva, M. A., & Harris, N. B. (2006). Secular variation in the major-ion chemistry of seawater: Evidence from fluid inclusions in Cretaceous halites. *Geochimica et Cosmochimica Acta*, 70, 1977–1994. <https://doi.org/10.1016/j.gca.2006.01.020>.
- Tissot, B. P., & Welte, D. H. (1984). *Petroleum formation and occurrence. A new approach to oil and gas exploration (2nd ed.)*. Springer-Verlag.  
<https://doi.org/10.1007/978-3-642-87813-8>.
- Trautz, R. C., Pugh, J. D., Varadharajan, C., Zheng, L. G., Bianchi, M., Nico, P. S., Spycher, N. F., Newell, D. L., Esposito, R. A., Wu, Y. X., Dafflon, B., Hubbard, S. S., & Birkholzer, J. T. (2013). Effect of dissolved CO<sub>2</sub> on a shallow groundwater system: A

- controlled release field experiment. *Environmental Science & Technology*, 47(1), 298–305. <https://doi.org/10.1021/es301280t>.
- Trost, J. J., Krall, A. L., Baedecker, M. J., Cozzarelli, I. M., Herkelrath, W. N., Jaeschke, J. B., Delin, G. N., Berg, A. M., & Bekins, B. A. (2020). *Data sets from the National Crude Oil Spill Fate and Natural Attenuation Research site near Bemidji, Minnesota, USA (Version 3.0, April 2020)* [Data set]. US Geological Survey. <https://doi.org/10.5066/P9FJ8I0P>.
- Underschultz, J., Boreham, C., Dance, T., Stalker, L., Freifeld, B., Kirste, D., & Ennis-King, J. (2011). CO<sub>2</sub> storage in a depleted gas field: An overview of the CO<sub>2</sub>CRC Otway Project and initial results. *International Journal of Greenhouse Gas Control*, 5, 922–923.
- US Department of Energy (NETL). (2005). *Heavy oil database 2005*. US Department of Energy, National Energy Technology Laboratory. <https://www.netl.doe.gov/>.
- US Department of Energy (NETL). (2009). *Storage of captured carbon dioxide beneath federal lands*. US Department of Energy, National Energy Technology Laboratory. <https://www.netl.doe.gov/>.
- US Department of Energy (NETL). (2018). *Carbon storage program*. US Department of Energy, National Energy Technology Laboratory. <https://www.netl.doe.gov/>.
- US Energy Information Administration (EIA). (2018). *Annual energy outlook 2018 with projections to 2050 (Report #AEO.2018)*. [www.eia.gov/aeo](http://www.eia.gov/aeo).
- US Energy Information Administration (EIA). (2021). *Statistical review of world energy 2021*. BP. [Statistical Review 2021](https://www.eia.gov/statistical-review-2021).
- US Environmental Protection Agency (EPA). (1986). *Method 9081: Cation-exchange capacity of soils (sodium acetate) (Technical Manual EPA-9081)*. US EPA. [www.epa.gov/sites/default/files/2015-12/documents/9081.pdf](http://www.epa.gov/sites/default/files/2015-12/documents/9081.pdf).
- US Environmental Protection Agency (EPA). (1999). *Update of ambient water quality criteria for ammonia (EPA-822-R-99-014)*. US EPA. <https://nepis.epa.gov/Exe/ZyNET.exe>.
- US Environmental Protection Agency (EPA). (2009). *National primary and national secondary drinking water regulations (EPA 816-F-09-004)*. National Research Council. <https://www.nrc.gov/docs/ML1307/ML13078A040.pdf>.
- US Environmental Protection Agency (EPA). (2011). *Plan to study the potential impacts of hydraulic fracturing on drinking water resources (EPA/600/R-11/122)*. US Environmental Protection Agency. <https://cfpub.epa.gov/ncea/hfstudy/recordisplay.cfm?deid=240888h>.
- US Environmental Protection Agency (EPA). (2015). *Assessment of the potential impacts of hydraulic fracturing for oil and gas on drinking water resources (External review draft) (EPA/600/R-15/047)*. US Environmental Protection Agency. [www.epa.gov/sites/default/files/2015-07/documents/hf\\_es\\_erd\\_jun2015.pdf](http://www.epa.gov/sites/default/files/2015-07/documents/hf_es_erd_jun2015.pdf).
- US Environmental Protection Agency (EPA). (2016). Hydraulic fracturing for oil and gas: Impacts from the hydraulic fracturing water cycle on drinking water resources in the United States (EPA-600-R-16-236F). *Federal Register*, 27 December 2016.

- <https://www.federalregister.gov/documents/2016/12/27/2016-31034/hydraulic-fracturing-for-oil-and-gas-impacts-from-the-hydraulic-fracturing-water-cycle-on-drinking>.
- US Environmental Protection Agency (EPA). (2017). Chapter 3: Water quality criteria. In *Water Quality Standards Handbook (EPA-823-B-17-001)*. EPA Office of Water, Office of Science and Technology.  
[www.epa.gov/sites/production/files/2014-10/documents/handbook-chapter3.pdf](http://www.epa.gov/sites/production/files/2014-10/documents/handbook-chapter3.pdf).
- US Environmental Protection Agency (EPA). (2019). *Study of oil and gas extraction wastewater management under the clean water act (EPA- 821-R19-001)*. US Environmental Protection Agency, Office of Water. [epa.gov/eg/study-oil-and-gas-extraction-wastewater-management](http://epa.gov/eg/study-oil-and-gas-extraction-wastewater-management).
- US Environmental Protection Agency (EPA). (2020). National Emissions Inventory (NEI) documentation. [info.chief@epa.gov](mailto:info.chief@epa.gov).
- US Environmental Protection Agency (EPA). (2021). *Underground storage tanks (USTs)*. US Environmental Protection Agency.  
[www.epa.gov/ust/frequent-questions-about-underground-storage-tanks](http://www.epa.gov/ust/frequent-questions-about-underground-storage-tanks).
- US Geological Survey (USGS). (2018). General introduction for the national field manual for the collection of water-quality data (Version 1.1). *Techniques and Methods*, 9, A0. US Geological Survey. <https://doi.org/10.3133/tm9A0>.
- US Geological Survey (USGS). (2020). Dissolved oxygen. *Techniques and Methods*, 9, A6.2). US Geological Survey. <https://doi.org/10.3133/tm9A6.2>.
- US Geological Survey (USGS). (2021). Measurement of pH. *Techniques and Methods*, 9, A6.4. US Geological Survey. <https://doi.org/10.3133/tm9A6.4>.
- US [Pipeline and Hazardous Materials Safety Administration](http://www.usa.gov/agencies/pipeline-and-hazardous-materials-safety-administration). (2021).  
<https://www.usa.gov/agencies/pipeline-and-hazardous-materials-safety-administration>.
- United Nations (UN). (2015). *Adoption of the Paris Agreement*. UN Climate Change.  
<https://unfccc.int/gcse?q=adoption%20of%20the%20paris%20agreement>.
- United Nations (UN). (2021). *Water facts*. UN Water. <https://www.unwater.org/water-facts>.
- Valder, J. F., McShane, R. R., Thamke, J. N., McDowell, J. S., Ball, G. P., Houston, N. A., & Galanter, A. E. (2021). *Estimates of water use associated with continuous oil and gas development in the Permian Basin, Texas and New Mexico, 2010–19 (Scientific Investigations Report 2021-5090)*. US Geological Survey.  
<https://doi.org/10.3133/sir20215090>.
- van Everdingen, R. O., Shakur, M. A., & Michel, F. A. (1985). Oxygen- and sulfur-isotope geochemistry of acidic groundwater discharge in British Columbia, Yukon, and District of Mackenzie, Canada. *Canadian Journal of Earth Sciences*, 22, 1689–1695.  
<https://doi.org/10.1139/e85-177>.
- Varonka, M. S., Gallegos, T., Bates, A. L., Doolan, C. A., & Orem, W. H. (2020). Organic compounds in produced water from the Bakken Formation and Three Forks

- Formation in the Williston Basin, North Dakota. *Heliyon*, 6(3).  
<https://doi.org/10.1016/j.heliyon.2020.e03590>.
- Veil, J. A. (2020). *US Produced Water Volumes and Management Practices in 2019. Report prepared for the Ground Water Research and Education Foundation*. Veil Environmental, LLC.
- Veil, J. A., Pruder, M. G., Elcock, D., & Redweik Jr., R. J. (2004), *A white paper describing produced water from production of crude oil, natural gas and coal bed methane (Report W-31-109-Eng-38)*. Argonne National Laboratory.  
<https://doi.org/10.2172/821666>.
- Vengosh, A., Warner, N. R., Darrah, T. H., Jackson, R. B., & Kondash, A. J. (2014). A critical review of the risks to water resources from unconventional shale gas development and hydraulic fracturing in the United States. *Environmental Science and Technology*, 48(15), 8334–8348. <https://doi.org/10.1021/es405118y>.
- Vengosh, A., Mitch, W. A., & McKenzie, L. M. (2017). Environmental and human impacts of unconventional energy development. *Environmental Science & Technology*, 51(18), 10271–10273. <https://doi.org/10.1021/acs.est.7b04336>.
- Vengosh, A., Davis, T. A., Landon, M. K., Tyne, R. L., Wright, M. T., Kulongoski, J. T., Hunt, A. G., Barry, P. H., Kondash, A. J., Wang, Z., & Ballentine, C. J. (2019). Occurrence and sources of radium in groundwater associated with oil fields in the southern San Joaquin Valley, California. *Environmental Science & Technology*, 53(16), 9398–9406. <https://doi.org/10.1021/acs.est.9b02395>.
- Vetshteyn, V. V., Gavish, V. K., & Gutsalo, L. K. (1981). Hydrogen and oxygen isotope composition of water in deep-seated fault zones. *International Geology Review*, 23, 302–310. <https://doi.org/10.1080/00206818109455060>.
- Vidic, R., Brantley, S., Vandenbossche, J., Yoxheimer, D., & Abad, J. (2013). Impact of shale gas development on regional water quality. *Science*, 340(6134).  
<https://www.science.org/doi/10.1126/science.1235009>.
- Villalobos, J. (2018). Water challenges in Permian Basin fracturing operations. *Water Technology*, September 27, 2018.  
<https://watertechonline.com/wastewater/article/15550696/water-challenges-in-permian-basin-fracturing-operations>.
- Wang, S., & Jaffe, P. R. (2004). Dissolution of trace metals in potable aquifers due to CO<sub>2</sub> releases from deep formations. *Energy Conversion and Management*, 45(18-19), 2833–2848. <https://doi.org/10.1016/j.enconman.2004.01.002>.
- Warner, N. R., Jackson, R. B., Darrah, T. H., Osborn, S. G., Down, A., Zhao, K., White, A., & Vengosh, A. (2012). Geochemical evidence for possible natural migration of Marcellus Formation brine to shallow aquifers in Pennsylvania. *Proceedings of the National Academy of Sciences*, 109, 11961–11966.  
<https://doi.org/10.1073/pnas.1121181109>.

- Warner, N. R., Christie, C., Jackson, R., & Vengosh, A. (2013). Impacts of shale gas wastewater disposal on water quality in western Pennsylvania. *Environmental Science and Technology*, 47(20), 11849–11857. <https://doi.org/10.1021/es402165b>.
- Warner, N. R., Darrah, T. H., Jackson, R. B., Millot, R., Kloppmann, W., Vengosh, A. (2014). New tracers identify hydraulic fracturing fluids and accidental releases from oil and gas operations. *Environmental Science & Technology*, 48(21), 12552–12560. <https://doi.org/10.1021/es5032135>.
- Warwick, P.D., E.D. Attanasi, M.S. Blondes, S.T. Brennan, M.L. Buursink, S.M. Cahan, C.A. Doolan, P.A. Freeman, C.O. Karacan, C.D. Lohr, M.D. Merrill, R.A. Olea, J.L. Shelton, E.R. Slucher, B.A. Varela (2022). National assessment of carbon dioxide enhanced oil recovery and associated carbon dioxide retention resources — Results. U. S. Geological Survey Circular 1489, 39 p., <https://doi.org/10.3133/cir1489>.
- Wells, A. W., Diehl, J. R., Bromhal, G., Strazisar, B. R., Wilson, T. H., & White, C. M. (2007). The use of tracers to assess leakage from the sequestration of CO<sub>2</sub> in a depleted oil reservoir, New Mexico. USA. *Applied Geochemistry*, 22, 996–1016. <https://doi.org/10.1016/j.apgeochem.2007.01.002>.
- Welsby, D., Price, J., Pye, S., & Ekins, P. (2021). Unextractable reserves of fossil fuels in a 1.5 °C world. *Nature*, 597(7875), 230–234. <https://pubmed.ncbi.nlm.nih.gov/34497394/>.
- White, C. M., Strazisar, B. R., Granite, E. J., Hoffman, J. S., & H. W. Pennline. (2003). Separation and capture of CO<sub>2</sub> from large stationary sources and sequestration in geological formations—coalbeds and deep saline aquifers. *Journal of the Air & Waste Management Association*, 53, 645–715. <https://doi.org/10.1080/10473289.2003.10466206>.
- White, D. E., Hem, J. D., & Waring, G. A. (1963). *Chemical composition of subsurface water (Professional paper 440F)*. US Geological Survey. <https://doi.org/10.3133/pp440F>.
- White, M. D., & Oostrom, M. (2000). *STOMP Subsurface Transport over Multiple Phases User Guide (Version 2.0, PNNL-12034)*, Pacific Northwest National Laboratory. [Simulator].
- White, S. P., Allis, R. G., & Moore, J. (2005). Simulation of reactive transport of injected CO<sub>2</sub> on the Colorado Plateau, Utah, USA. *Chemical Geology*, 217, 387–405.
- Whitfield, S. (2017). Permian, Bakken operators face produced water challenges. *Journal of Petroleum Technology*, 69, 48–51. <https://doi.org/10.2118/0617-0048-JPT>.
- Whitworth, T. M., & Fritz, S. J. (1994). Electrolyte-induced solute permeability effects in compacted smectite membranes. *Applied Geochemistry*, 9(5), 533–546. [https://doi.org/10.1016/0883-2927\(94\)90015-9](https://doi.org/10.1016/0883-2927(94)90015-9).
- Wilde, F. D. (2010). *Water-quality sampling by the US Geological Survey: Standard protocols and procedures*. US Geological Survey. <https://doi.org/10.3133/fs20103121>.
- Wilde, F. D., Sandstrom, M. W., & Skrobialowski, S. C. (2014). Selection of equipment for water sampling. In *Techniques of Water Resources Investigations*, 9, A2. US Geological Survey. <https://doi.org/10.3133/twri09A2>.

- Willey, L. M., Kharaka, Y. K., Presser, T. S., Rapp, J. B., & Barnes, I. (1975). Short-chain aliphatic acids in oil-field water of Kettleman Dome Oil Field, California. *Geochimica et Cosmochimica Acta*, 39(12), 1707–1710. [https://doi.org/10.1016/0016-7037\(75\)90092-7](https://doi.org/10.1016/0016-7037(75)90092-7).
- Willhite, G. P. (1986). *Water flooding*. Society of Petroleum Engineers.
- Williams, M. D., & Ranganathan, V. (1994). Ephemeral thermal and solute plumes formed by upwelling ground-water near salt domes. *Journal of Geophysical Research, B, Solid Earth and Planets*, 99, 15667–15681. <https://doi.org/10.1029/94JB00903>.
- Williams, L. B., Hervig, R. L., Wieser, M. E., & Hutcheon, I. (2001a). The influence of organic matter on the boron isotope geochemistry of the Gulf Coast sedimentary basin, USA. *Chemical Geology*, 174, 445–461. [https://doi.org/10.1016/S0009-2541\(00\)00289-8](https://doi.org/10.1016/S0009-2541(00)00289-8).
- Williams, L. B., Wieser, M. E., Fennell, J., Hutcheon, I., & Hervig, R. L. (2001b). Application of boron isotopes to the understanding of fluid–rock interactions in a hydrothermally stimulated oil reservoir in the Alberta Basin, Canada. *Geofluids*, 1, 229–240.
- Williamson, H. F., Andreano, R. L., Daum, A. R., & Klose, G. C. (1963). *The American petroleum industry: The age of energy, 1899–1959*. Northwestern University [The Petroleum Industry-The Age of Energy 1899-1959](#).
- Wilson, A. M., Garven, G. & Boles, J. R. (1999). Paleohydrogeology of the San Joaquin Basin, California. *Bulletin of the Geological Society of America*, 111, 432–449. [https://doi.org/10.1130/0016-7606\(1999\)111<0432:POTSJB>2.3.CO;2](https://doi.org/10.1130/0016-7606(1999)111<0432:POTSJB>2.3.CO;2).
- Wilson, A. M., & Monea, M. (Eds.). (2004). *IEA GHG Weyburn CO<sub>2</sub> Monitoring & Storage Project, Summary Report 2000–2004*. Petroleum Technology Research Centre.
- Woessner, W. W., & Poeter, E. P. (2020). *Hydrogeologic properties of earth materials and principles of groundwater flow*. The Groundwater Project. <https://gw-project.org/books/hydrogeologic-properties-of-earth-materials-and-principles-of-groundwater-flow/>.
- Wolery, T. J. (1992). EQ3/6: *A software package for geochemical modeling of aqueous systems* [Computer software]. Lawrence Livermore National Laboratory.
- Wolff-Boenisch, D., & Evans, K. (2014). Review of available fluid sampling tools and sample recovery techniques for groundwater and unconventional geothermal research as well as carbon storage in deep sedimentary aquifers. *Journal of Hydrology*, 513, 68–80. <https://doi.org/10.1016/j.jhydrol.2014.03.032>.
- Worden, R. H. (1996). Controls on halogen concentrations in sedimentary formation water. *Mineralogical Magazine*, 60, 259–279.
- Worden, R. H., Coleman, M. L., & Matray, J. M. (1999). Basin scale evolution of formation water: a diagenetic and formation water study of the Triassic Chaunoy Formation, Paris Basin. *Geochimica et Cosmochimica Acta*, 63, 2513–2528. [https://doi.org/10.1016/S0016-7037\(99\)00121-0](https://doi.org/10.1016/S0016-7037(99)00121-0).

- Workman, A. L., & Hanor, J. S. (1985). Evidence for large-scale vertical migration of dissolved fatty acids in Louisiana oil-field brines: Iberia field, south-central Louisiana. *Gulf Coast Association of Geological Societies Transactions*, 35, 293–300.
- Worrall, D. M., & Snelson, S. (1989). Evolution of the northern Gulf of Mexico, with emphasis of Cenozoic growth faulting and the role of salt. In A. W. Bally, & A. R. Palmer (Eds.), *The geology of North America; An overview* (pp. 128–156). Geological Society of America.
- Wycherley, H., Fleet, A., & Shaw, H. (1999). Observations on the origins of large volumes of carbon dioxide accumulations in sedimentary basins. *Marine and Petroleum Geology* volume 16, 489–494. [https://doi.org/10.1016/S0264-8172\(99\)00047-1](https://doi.org/10.1016/S0264-8172(99)00047-1).
- Xu, T., Kharaka, Y. K., Doughty, C., Freifeld, B. M., & Daley, T. M. (2010). Reactive transport modeling to study changes in water chemistry induced by CO<sub>2</sub> injection at the Frio-I Brine Pilot. *Chemical Geology*, 271, 153–164. <https://doi.org/10.1016/j.chemgeo.2010.01.006>.
- Yaghoubi, A., Dusseault, M. B., Leonenko, Y. (2022). Injection-induced fault slip assessment in Montney Formation in Western Canada. *Scientific Reports*, 12, 11551. <https://doi.org/10.1038/s41598-022-15363-8>.
- Yen, T. F. (1984). Characterization of heavy oil. In R. F. Meyer, J. C. Wynn, & J. C. Olson (Eds.), *The second UNITAR international conference on heavy crude and tar sands, Caracas, Venezuela* (pp. 412–423). McGraw-Hill.
- Zhang, T., Gregory, K., Hammack, R. W., & Vidic, R. D. (2014). Co-precipitation of radium with barium and strontium sulfate and its impact on the fate of radium during treatment of produced water from unconventional gas extraction. *Environmental Science & Technology*, 48, 4596–4603. <https://doi.org/10.1021/es405168b>.
- Zheng, L., Apps, J. A., Zhang, Y., Xu, T., & Birkholzer, J. T. (2009). On mobilization of lead and arsenic in groundwater in response to CO<sub>2</sub> leakage from deep geological storage. *Chemical Geology*, 268, 281–297. <https://doi.org/10.1016/j.chemgeo.2009.09.007>.
- Zheng, L., Apps, J. A., Spycher, N., Birkholzer, J., Kharaka, Y. K., Thordsen, J., Beers, S. R., Herkelrath, W. N., Kakouros, E., & Trautz, R. C. (2011). Geochemical modeling of changes in shallow groundwater chemistry observed during the MSU-ZERT CO<sub>2</sub> injection experiment. *International Journal of Greenhouse Gas Control*, 7, 202–217. <https://doi.org/10.1016/j.ijggc.2011.10.003>.
- Zhu, C., & Anderson, G. M. (2002). *Environmental applications of geochemical modeling*. Cambridge University Press.
- Zhu, C., Liu, Z. Y., Wang, C., Schaefer, A., Lu, P., Zhang, G. R., Zhang, Y. L., Georg, R. B., Rimstidt, J. D., & Yuan, H. L. (2016). Measuring silicate mineral dissolution rates using Si isotope doping. *Chemical Geology*, 445, 146–163. <https://j.chemgeo.2016.02.027>.
- Ziegler, K., & Coleman, M. L. (2001). Palaeohydrodynamics of fluids in the Brent Group (Oseberg Field, Norwegian North Sea) from chemical and isotopic compositions of

formation water. *Applied Geochemistry*, 16, 609–632. [https://doi.org/10.1016/S0883-2927\(00\)00057-3](https://doi.org/10.1016/S0883-2927(00)00057-3)↗.

Zou, C. (2017). *Unconventional petroleum geology* (2nd ed.). Elsevier.

Zou, C., Ni, Y., Li, J., Kondash, A., Coyte, R., Lauer, N., Cui, H., Liao, F., & Vengosh A. (2018). The water footprint of hydraulic fracturing in Sichuan Basin, China. *The Science of the Total Environment*, 630, 349–356. <https://doi.org/10.1016/j.scitotenv.2018.02.219>↗.

Zuddas, P. (2010). Water-rock interaction processes seen through thermodynamics. *Elements*, 6, 305–308. <https://doi.org/10.2113/gselements.6.5.305>↗.

## 15 Boxes

### Box 1 Glossary

The following terminology (terms are listed alphabetically) has been extracted mainly from Hanor (1987), Kharaka and Thordsen (1992), and Kharaka and Hanor (2014). The interested reader should also consult Sheppard (1986).

**API gravity of oil (API)** stands for the American Petroleum Institute; API gravity is key parameter used to classify oils from light (API 35 to 45 degrees) to extra heavy crude (API < 15 degrees). API gravity is calculated by using the specific gravity of oil, which is its density/density of water at 60 °F.

$$\text{API gravity} = \frac{141.5}{\text{specific gravity of the oil at } 60^{\circ}\text{F}} - 131.5$$

**Concentrations of chemical constituents** in water are given either in milligrams per liter (mg/L or mg L<sup>-1</sup>) or micrograms per liter (µg/L). Concentrations may also be given in meq/L, where meq/L = (mg/L)(valence)/(atomic mass).

**Connate water** is a term that has taken on a variety of meanings. The word *connate* (Latin for *born with*) was introduced by Lane (1908) to describe what he presumed to be seawater of unaltered chemical composition trapped in the pore spaces of a Proterozoic pillow basalt since the time of extrusion onto the seafloor. While some authors prefer to use connate in its original sense (Hanor, 1987), others have used it to refer to water that have been modified chemically and isotopically but have been out of contact with the atmosphere since their deposition, although they need not be present in the rocks with which they were deposited (Kharaka and Thordsen, 1992). Connate water may be specified as marine connate if it was deposited with marine sediments.

**Conversion factors** are provided in Table Box1-1.

**Table Box1-1 - Conversion factors**

Multiply	By	To obtain
millimeter (mm)	0.03937	inch (in.)
centimeter (cm)	0.3937	inch (in.)
meter (m)	3.281	foot (ft)
kilometer (km)	0.6214	mile (mi)
hectare (ha)	2.471	acre
cubic meter (m <sup>3</sup> )	6.290	barrel (petroleum, 1 bbl = 42 gal)
liter (L)	0.2642	gallon (gal)
cubic meter per second (m <sup>3</sup> /s)	70.07	acre-foot per day (acre-ft/d)
cubic meter per second (m <sup>3</sup> /s)	35.31	cubic foot per second (ft <sup>3</sup> /s)
liter per second (L/s)	15.85	gallon per minute (gal/min)
cubic meter per day (m <sup>3</sup> /d)	264.2	gallon per day (gal/d)
gram (g)	0.03527	ounce (oz)
kilogram (kg)	2.205	pound (lb)
kilopascal (kPa)	0.009869	atmosphere, standard (atm)
kilopascal (kPa)	0.01	bar
meter per day (m/d)	3.281	foot per day (ft/d)
meter per kilometer (m/km)	5.27983	foot per mile (ft/mi)
meter squared per day (m <sup>2</sup> /d)	10.76	foot squared per day (ft <sup>2</sup> /d)

**Formation water** is water present in the pores and fractures of rocks immediately before drilling (Case, 1955). This term is used extensively in the petroleum industry but has no genetic or age significance.

**Geogenic contaminants** are concentrations of certain compounds in some groundwater that exceed the MCL or the secondary SMCL values that are not caused by human activities but result from natural processes like the reactions of water with aquifer minerals. The main geogenic contaminants in groundwater in USA are Mn, As, Ra, Sr, and U.

**MCL and SMCL** are acronyms used to describe the contaminant limit of a chemical allowed by law in public drinking water in the USA. The limits are set by the US EPA to safeguard the public health. **MCL** is the maximum contaminant limit of a chemical. **SMCL** is the secondary maximum contamination limit for any chemical. Although it is not regulated by the US EPA, SMCL may be mandated by states.

**Meteoric water** is water derived from rain, snow, streams, and other bodies of surface water that percolates in rocks and displaces interstitial water that may have been connate, meteoric, or of any other origin. Meteoric water in sedimentary basins is generally recharged at higher elevations along the margins of the basin. The time of last contact with the atmosphere is intentionally omitted from this definition but may be specified to further define meteoric water. Thus, *recent meteoric water*, *Pleistocene meteoric water*, or *Tertiary meteoric water* would indicate the time of last contact with the atmosphere (Kharaka & Carothers, 1986).

**Produced water** is described by a number of terms including oil-field brine, produced water, basinal brine, basinal water, and formation water, have been used in the literature to describe deep aqueous fluids in sedimentary basins that are or are not associated with hydrocarbons. No satisfactory overall classification system exists because this water can be assessed by several different criteria including the salinity of the water, the concentration and origin of various dissolved constituents, and the origin of the water, which is commonly different from that of the solutes. We use the term here to denote all water produced while drilling for or producing conventional and unconventional oil and natural gas. Some limit the term to water co-produced with oil and natural gas.

**Proppant** is made up of sand and/or ceramic particles that comprise approximately 9 percent of the fracturing fluid production of oil and natural gas from shale and tight reservoirs require fracturing, this is carried out by injecting large volumes of water with added chemicals and proppant at pressures high enough to fracture the rock. The fractures are kept open by the proppant.

**Sources of energy** can be conventional or unconventional.

- **Conventional sources of energy** are a category that includes crude oil and natural gas and its condensates that are generally produced by drilling vertical wells into relatively small structural or stratigraphic traps.
- **Unconventional sources of energy** are also known as *continuous* sources of energy and include shale oil, shale natural gas, tight sandstone oil and natural gas (or light tight oil and gas), heavy oil, tar sand, and coalbed methane. Shale and tight sandstone formations are continuous, extending for 100 km or more and require hydrofracturing to produce the fluids.

**Stripper wells**, also called *marginal* wells, are oil or natural gas wells that are nearing the end of their economically useful life. However, these wells can continue to produce small volumes of oil and natural gas for long periods. Many of these wells are still operating, producing approximately 10 percent of total US oil and natural gas in 2017. There are several production levels to define a stripper well. The Interstate Oil and Gas Compact Commission defines a stripper well as a well that produces 10 bbl/d (1.58 m<sup>3</sup>/d) or less of oil or 60,000 cf/d or less of natural gas during a 12-month period. The IRS—for tax purposes—defines this type of well as one that produces 15 bbl/d (2.38 m<sup>3</sup>/d) or less of oil or 90,000 cf/d or less of natural gas over a calendar year. The Energy Information Administration (EIA) uses the IRS definition.

**Symbols used in this book include.**

B for Billion.

k for thousand.

M for million.

T for trillion.

**Total dissolved solids (TDS)** are generally reported in milligrams per liter (mg/L) as determined directly by summing all the measured organic and inorganic dissolved constituents. Also relevant is water salinity, below.

**Specific conductance** is given in milli siemens or micro siemens per centimeter at 25 degrees Celsius (mS/cm or  $\mu$ S/cm at 25 °C).

**Temperature** can be converted between degrees Celsius (°C) and degrees Fahrenheit (°F).

$$^{\circ}\text{F} = 1.8 (\text{Temperature in } ^{\circ}\text{C}) + 32$$

$$^{\circ}\text{C} = (\text{Temperature in } ^{\circ}\text{F} - 32) / 1.8$$

**USDW** are the part of an aquifer that is capable of supplying water for human consumption now or in the future. The water has a salinity of less than 10,000 mg/L TDS. Federal regulations require owners and operators of produced water and other injection wells to follow safe injection well operations to prevent the contamination of underground sources of drinking water.

**Water chlorinity** refers to the dissolved chloride concentration and is generally reported in mg/L.

**Water cut** in percent is given by:

$$100 \frac{\text{volume of produced water}}{\text{volume of oil} + \text{volume of produced water}}$$

**Water quality** refers to the chemical, physical, and biological characteristics of water based on the standards of its usage. It is most frequently used by reference to a set of standards against which compliance, generally achieved through treatment of the water, can be assessed. The most common standards used to monitor and assess water quality convey the health of ecosystems, the safety of human contact, and the condition of drinking water. Water quality has a significant impact on water supply and often determines supply options.

**Water salinity** is synonymous with total dissolved solids (TDS) and is generally reported in milligrams per liter (mg/L) as determined either (1) directly by summing all the measured dissolved constituents or by weighing solid residues after evaporation or (2) indirectly from logs, electrical conductivity, or spontaneous potential response. Based on its salinity, water is divided into four types:

- Freshwater Water: Water of salinity < 1,000 mg/L TDS;
- Brackish Water: Water of salinity 1,000 to 10,000 mg/L TDS;
- Saline Water: Water of salinity 10,000 to 35,000 mg/L DS; and
- Brine: Water of salinity higher than that of average seawater, that is > 35,000 mg/L TDS. Most oil field water is brine according to this definition, whereas only a small fraction would be classified as brine based on the definitions of Davis (1964) and Carpenter and others (1974), which place the lower salinity limit of brine at 100,000 mg/L.

**Water type** categorizes water by listing the major cations followed by the major anions in water in order of decreasing concentrations. Most produced water is Na-Cl or Na-Ca-Cl type water. The concentration, commonly in mg/L, of any ion listed must be  $\geq 5$  percent of the value of TDS. This is approximately equivalent to 10 percent of the total of cations or anions, respectively (Kharaka & Thordsen, 1992).

[Return to where text linked to Box 1↑](#)

## Box 2 USA National Primary Drinking Water Regulations

Table Box 2-1 presents the water-quality criteria, standards, or recommended limits, as well as the general significance of the physical properties and constituents discussed in this book.

**Table Box 2-1 - National Primary Drinking Water Regulations (US EPA, 2009).**

Contaminant	MCL or TT <sup>1</sup> (mg/L) <sup>2</sup>	Potential health effects from long-term <sup>3</sup> exposure above the MCL	Common sources of contaminant in drinking water	Public Health Goal (mg/L) <sup>2</sup>
 Acrylamide	TT <sup>4</sup>	Nervous system or blood problems; increased risk of cancer.	Added to water during sewage/wastewater treatment.	zero
 Alachlor	0.002	Eye, liver, kidney, or spleen problems; anemia; increased risk of cancer.	Runoff from herbicide used on row crops.	zero
 Alpha/photon emitters	15 picocuries per liter(pCi/L)	Increased risk of cancer.	Erosion of natural deposits of certain minerals that are radioactive and may emit a form of radiation known as alpha radiation.	zero
 Antimony	0.006	Increase in blood cholesterol; decrease in blood sugar.	Discharge from petroleum refineries; fire retardants; ceramics; electronics; solder.	0.006
 Arsenic	0.010	Skin damage or problems with circulatory systems; may have increased risk of cancer.	Erosion of natural deposits; runoff from orchards; runoff from glass & electronics production wastes.	0
 Asbestos (fibers >10 micrometers)	7 M fibers per liter (MFL)	Increased risk of developing benign intestinal polyps.	Decay of asbestos cement in water mains; erosion of natural deposits.	7 MFL
 Atrazine	0.003	Cardiovascular system or reproductive problems.	Runoff from herbicide used on row crops.	0.003

Contaminant	MCL or TT <sup>1</sup> (mg/L) <sup>2</sup>	Potential health effects from long-term <sup>3</sup> exposure above the MCL	Common sources of contaminant in drinking water	Public Health Goal (mg/L) <sup>2</sup>
 Barium	2	Increase in blood pressure.	Discharge of drilling wastes; discharge from metal refineries; erosion of natural deposits.	2
 Benzene	0.005	Anemia; decrease in blood platelets; increased risk of cancer.	Discharge from factories; leaching from gas storage tanks and landfills.	zero
 Benzo(a)pyrene (PAHs)	0.0002	Reproductive difficulties; increased risk of cancer.	Leaching from linings of water storage tanks and distribution lines.	zero
 Beryllium	0.004	Intestinal lesions.	Discharge from metal refineries and coal-burning factories; discharge from electrical, aerospace, and defense industries.	0.004
 Beta photon emitters	4 millirems per year	Increased risk of cancer.	Decay of natural and human-made deposits of certain minerals that are radioactive and may emit forms of radiation known as photons and beta radiation.	zero
 Bromate	0.010	Increased risk of cancer.	Byproduct of drinking water disinfection.	zero
 Cadmium	0.005	Kidney damage.	Corrosion of galvanized pipes; erosion of natural deposits; discharge from metal refineries; runoff from waste batteries and paints.	0.005
 Carbofuran	0.04	Problems with blood, nervous system, or reproductive system.	Leaching of soil fumigant used on rice and alfalfa.	0.04
 Carbon tetrachloride	0.005	Liver problems; increased risk of cancer.	Discharge from chemical plants and other industrial activities.	zero
 Chloramines (as Cl <sub>2</sub> )	MRDL=4.0 <sup>1</sup>	Eye/nose irritation; stomach discomfort; anemia.	Water additive used to control microbes.	MRDLG=4 <sup>1</sup>

Contaminant	MCL or TT <sup>1</sup> (mg/L) <sup>2</sup>	Potential health effects from long-term <sup>3</sup> exposure above the MCL	Common sources of contaminant in drinking water	Public Health Goal (mg/L) <sup>2</sup>
 Chlordane	0.002	Liver or nervous system problems; increased risk of cancer.	Residue of banned termiticide.	zero
 Chlorine (as Cl <sub>2</sub> )	MRDL=4.0 <sup>1</sup>	Eye/nose irritation; stomach discomfort.	Water additive used to control microbes.	MRDLG=4 <sup>1</sup>
 Chlorine dioxide (as ClO <sub>2</sub> )	MRDL=0.8 <sup>1</sup>	Anemia; nervous system effects among infants, young children, and fetuses of pregnant women.	Water additive used to control microbes.	MRDLG=0.8 <sup>1</sup>
 Chlorite	1.0	Anemia; nervous system effects among infants, young children, and fetuses of pregnant women.	Byproduct of drinking water disinfection.	0.8
 Chlorobenzene	0.1	Liver or kidney problems.	Discharge from chemical and agricultural chemical factories.	0.1
 Chromium (total)	0.1	Allergic dermatitis.	Discharge from steel and pulp mills; erosion of natural deposits.	0.1
 Copper	TT <sup>5</sup> ; Action Level=1.3	Short-term exposure: gastrointestinal distress. Long-term exposure: liver or kidney damage. People with Wilson's Disease should consult their personal doctor if the amount of copper in their water exceeds the action level.	Corrosion of household plumbing systems; erosion of natural deposits.	1.3
 <i>Cryptosporidium</i>	TT <sup>7</sup>	Short-term exposure: gastrointestinal illness (e.g., diarrhea, vomiting, cramps).	Human and animal fecal waste.	zero
 Cyanide (as free cyanide)	0.2	Nerve damage or thyroid problems.	Discharge from steel/metal factories; discharge from plastic and fertilizer factories.	0.2
 2,4-D	0.07	Kidney, liver, or adrenal gland problems.	Runoff from herbicide used on row crops.	0.07
 Dalapon	0.2	Minor kidney changes.	Runoff from herbicide used on rights of way.	0.2

Contaminant	MCL or TT <sup>1</sup> (mg/L) <sup>2</sup>	Potential health effects from long-term <sup>3</sup> exposure above the MCL	Common sources of contaminant in drinking water	Public Health Goal (mg/L) <sup>2</sup>
 1,2-Dibromo-3-chloropropane (DBCP)	0.0002	Reproductive difficulties; increased risk of cancer.	Runoff/leaching from soil fumigant used on soybeans, cotton, pineapples, and orchards.	zero
 o-Dichlorobenzene	0.6	Liver, kidney, or circulatory system problems.	Discharge from industrial chemical factories.	0.6
 p-Dichlorobenzene	0.075	Anemia; liver, kidney, or spleen damage; changes in blood.	Discharge from industrial chemical factories.	0.075
 1,2-Dichloroethane	0.005	Increased risk of cancer.	Discharge from industrial chemical factories.	zero
 1,1-Dichloroethylene	0.007	Liver problems.	Discharge from industrial chemical factories.	0.007
 cis-1,2-Dichloroethylene	0.07	Liver problems.	Discharge from industrial chemical factories.	0.07
 trans-1,2-Dichloroethylene	0.1	Liver problems.	Discharge from industrial chemical factories.	0.1
 Dichloromethane	0.005	Liver problems; increased risk of cancer.	Discharge from industrial chemical factories.	zero
 1,2-Dichloropropane	0.005	Increased risk of cancer.	Discharge from industrial chemical factories.	zero
 Di(2-ethylhexyl) adipate	0.4	Weight loss, liver problems, or possible reproductive difficulties.	Discharge from chemical factories.	0.4
 Di(2-ethylhexyl) phthalate	0.006	Reproductive difficulties; liver problems; increased risk of cancer.	Discharge from rubber and chemical factories.	zero
 Dinoseb	0.007	Reproductive difficulties.	Runoff from herbicide used on soybeans and vegetables.	0.007

Contaminant	MCL or TT <sup>1</sup> (mg/L) <sup>2</sup>	Potential health effects from long-term <sup>3</sup> exposure above the MCL	Common sources of contaminant in drinking water	Public Health Goal (mg/L) <sup>2</sup>
 Dioxin (2,3,7,8-TCDD)	0.00000003	Reproductive difficulties; increased risk of cancer.	Emissions from waste incineration and other combustion; discharge from chemical factories.	zero
 Diquat	0.02	Cataracts.	Runoff from herbicide use.	0.02
 Endothall	0.1	Stomach and intestinal problems.	Runoff from herbicide use.	0.1
 Endrin	0.002	Liver problems.	Residue of banned insecticide.	0.002
 Epichlorohydrin	TT <sup>4</sup>	Increased cancer risk; stomach problems.	Discharge from industrial chemical factories; an impurity of some water treatment chemicals.	zero
 Ethylbenzene	0.7	Liver or kidney problems.	Discharge from petroleum refineries.	0.7
 Ethylene dibromide	0.00005	Problems with liver, stomach, reproductive system, or kidneys; increased risk of cancer.	Discharge from petroleum refineries.	zero
 Fecal coliform and <i>E. coli</i>	MCL <sup>6</sup>	Fecal coliforms and <i>E. coli</i> are bacteria whose presence indicates the water may be contaminated with human or animal wastes. Microbes in these wastes may cause short-term effects such as diarrhea, cramps, nausea, headaches, or other symptoms. They may pose a special health risk for infants, young children, and people with severely compromised immune systems.	Human and animal fecal waste.	zero <sup>6</sup>

Contaminant	MCL or TT <sup>1</sup> (mg/L) <sup>2</sup>	Potential health effects from long-term <sup>3</sup> exposure above the MCL	Common sources of contaminant in drinking water	Public Health Goal (mg/L) <sup>2</sup>
 Fluoride	4.0	Bone disease (pain and tenderness of the bones); children may get mottled teeth.	Water additive that promotes strong teeth; erosion of natural deposits; discharge from fertilizer and aluminum factories.	4.0
 <i>Giardia lamblia</i>	TT <sup>7</sup>	Short-term exposure: gastrointestinal illness (e.g., diarrhea, vomiting, cramps).	Human and animal fecal waste.	zero
 Glyphosate	0.7	Kidney problems; reproductive difficulties.	Runoff from herbicide use.	0.7
 Haloacetic acids (HAA5)	0.060	Increased risk of cancer.	Byproduct of drinking water disinfection.	n/a <sup>9</sup>
 Heptachlor	0.0004	Liver damage; increased risk of cancer.	Residue of banned termiticide.	zero
 Heptachlor epoxide	0.0002	Liver damage; increased risk of cancer.	Breakdown of heptachlor.	zero
 Heterotrophic plate count (HPC)	TT <sup>7</sup>	HPC has no health effects; it is an analytic method used to measure the variety of bacteria that are common in water. The lower the concentration of bacteria in drinking water, the better maintained is the water system.	HPC measures a range of bacteria that are naturally present in the environment.	n/a
 Hexachlorobenzene	0.001	Liver or kidney problems; reproductive difficulties; increased risk of cancer.	Discharge from metal refineries and agricultural chemical factories.	zero
 Hexachlorocyclopentadiene	0.05	Kidney or stomach problems.	Discharge from chemical factories.	0.05
 Lead	TT <sup>5</sup> ; Action Level=0.015	Infants and children: delays in physical or mental development; children could show slight deficits in attention span and learning abilities; Adults: kidney problems, high blood pressure.	Corrosion of household plumbing systems; erosion of natural deposits.	zero

Contaminant	MCL or TT <sup>1</sup> (mg/L) <sup>2</sup>	Potential health effects from long-term <sup>3</sup> exposure above the MCL	Common sources of contaminant in drinking water	Public Health Goal (mg/L) <sup>2</sup>
 <i>Legionella</i>	TT <sup>7</sup>	Legionnaire's Disease, a type of pneumonia.	Found naturally in water; multiplies in heating Systems.	zero
 Lindane	0.0002	Liver or kidney problems.	Runoff/leaching from insecticide used on cattle, lumber, and gardens.	0.0002
 Mercury (inorganic)	0.002	Kidney damage.	Erosion of natural deposits; discharge from refineries and factories; runoff from landfills and croplands.	0.002
 Methoxychlor	0.04	Reproductive difficulties.	Runoff/leaching from insecticide used on fruits, vegetables, alfalfa, and livestock.	0.04
 Nitrate (measured as Nitrogen)	10	Infants below the age of six months who drink water containing nitrate in excess of the MCL could become seriously ill and, if untreated, may die. Symptoms include shortness of breath and blue-baby syndrome.	Runoff from fertilizer use; leaching from septic tanks, sewage; erosion of natural deposits.	10
 Nitrite (measured as Nitrogen)	1	Infants below the age of six months who drink water containing nitrite in excess of the MCL could become seriously ill and, if untreated, may die. Symptoms include shortness of breath and blue-baby syndrome.	Runoff from fertilizer use; leaching from septic tanks, sewage; erosion of natural deposits.	1
 Oxamyl (Vydate)	0.2	Slight nervous system effects.	Runoff/leaching from insecticide used on apples, potatoes, and tomatoes.	0.2
 Pentachlorophenol	0.001	Liver or kidney problems; increased cancer risk.	Discharge from wood-preserving factories.	zero
 Picloram	0.5	Liver problems.	Herbicide runoff.	0.5

Contaminant	MCL or TT <sup>1</sup> (mg/L) <sup>2</sup>	Potential health effects from long-term <sup>3</sup> exposure above the MCL	Common sources of contaminant in drinking water	Public Health Goal (mg/L) <sup>2</sup>
 Polychlorinated biphenyls (PCBs)	0.0005	Skin changes; thymus gland problems; immune deficiencies; reproductive or nervous system difficulties; increased risk of cancer.	Runoff from landfills; discharge of waste chemicals.	zero
 Radium 226 and Radium 228 (combined)	5 pCi/L	Increased risk of cancer.	Erosion of natural deposits.	zero
 Selenium	0.05	Hair or fingernail loss; numbness in fingers or toes; circulatory problems.	Discharge from petroleum and metal refineries; erosion of natural deposits; discharge from mines.	0.05
 Simazine	0.004	Problems with blood.	Herbicide runoff.	0.004
 Styrene	0.1	Liver, kidney, or circulatory system problems.	Discharge from rubber and plastic factories; leaching from landfills.	0.1
 Tetrachloroethylene	0.005	Liver problems; increased risk of cancer.	Discharge from factories and dry cleaners.	zero
 Thallium	0.002	Hair loss; changes in blood; kidney, intestine, or liver problems.	Leaching from ore-processing sites; discharge from electronics, glass, and drug factories.	0.0005
 Toluene	1	Nervous system, kidney, or liver problems.	Discharge from petroleum factories.	1
Total Coliforms	5.0 percent <sup>8</sup>	Coliforms are bacteria that indicate that other, potentially harmful bacteria may be present. See fecal coliforms and <i>General</i> .	Naturally present in the environment.	zero
 Total Trihalomethanes (TTHMs)	0.080	Liver, kidney, or central nervous system problems; increased risk of cancer.	Byproduct of drinking water disinfection.	n/a <sup>9</sup>
 Toxaphene	0.003	Kidney, liver, or thyroid problems; increased risk of cancer.	Runoff/leaching from insecticide used on cotton and cattle.	zero



Contaminant	MCL or TT <sup>1</sup> (mg/L) <sup>2</sup>	Potential health effects from long-term <sup>3</sup> exposure above the MCL	Common sources of contaminant in drinking water	Public Health Goal (mg/L) <sup>2</sup>
 2,4,5-TP (Silvex)	0.05	Liver problems.	Residue of banned herbicide.	0.05
 1,2,4-Trichlorobenzene	0.07	Changes in adrenal glands.	Discharge from textile finishing factories.	0.07
 1,1,1-Trichloroethane	0.2	Liver, nervous system, or circulatory problems.	Discharge from metal degreasing sites and other factories.	0.2
 1,1,1-Trichloroethane	0.2	Liver, nervous system, or circulatory problems.	Discharge from metal degreasing sites and other factories.	0.2
 1,1,2-Trichloroethane	0.005	Liver, kidney, or immune system problems.	Discharge from industrial chemical factories.	0.003
 Trichloroethylene	0.005	Liver problems; increased risk of cancer.	Discharge from metal degreasing sites and other factories.	zero
 Turbidity	TT <sup>7</sup>	Turbidity is a measure of the cloudiness of water. It is used to indicate water quality and filtration effectiveness (e.g., whether disease-causing organisms are present). Higher turbidity levels are often associated with higher levels of disease-causing microorganisms such as viruses, parasites, and some bacteria. These organisms can cause short-term symptoms such as nausea, cramps, diarrhea, and associated headaches.	Soil runoff.	n/a
 Uranium	30 µg/L	Increased risk of cancer, kidney toxicity.	Erosion of natural deposits.	zero
 Vinyl chloride	0.002	Increased risk of cancer.	Leaching from PVC pipes; discharge from plastic factories.	zero
 Viruses (enteric)	TT <sup>7</sup>	Short-term exposure: gastrointestinal illness (e.g., diarrhea, vomiting, cramps).	Human and animal fecal waste.	zero

Contaminant	MCL or TT <sup>1</sup> (mg/L) <sup>2</sup>	Potential health effects from long-term <sup>3</sup> exposure above the MCL	Common sources of contaminant in drinking water	Public Health Goal (mg/L) <sup>2</sup>
 Xylenes (total)	10	Nervous system damage.	Discharge from petroleum factories; discharge from chemicals factories.	10

Legend

					
Disinfectant	Disinfection Byproduct	Inorganic Chemical	Microorganism	Organic Chemical	Radionuclides

<sup>1</sup>Definitions

**Maximum Contaminant Level Goal (MCLG):** The level of a contaminant in drinking water, below which level is no known or expected risk to health. MCLGs allow for a margin of safety and are non-enforceable public health goals.

**Maximum Contaminant Level (MCL):** The highest level of a contaminant that is allowed in drinking water. MCLs are set as close to MCLGs as feasible using the best available treatment technology and taking cost into consideration. MCLs are enforceable standards.

**Maximum Residual Disinfectant Level Goal (MRDLG):** The level of a drinking water disinfectant, below which level is no known or expected risk to health. MRDLGs do not reflect the benefits of the use of disinfectants to control microbial contaminants.

**Maximum Residual Disinfectant Level (MRDL):** The highest level of a disinfectant allowed in drinking water. There is convincing evidence that addition of a disinfectant is necessary for control of microbial contaminants.

**Treatment Technique (TT):** A required process intended to reduce the level of a contaminant in drinking water.

<sup>2</sup>Units are in milligrams per liter (mg/L) unless otherwise noted. Milligrams per liter are equivalent to parts per million (ppm).

<sup>3</sup>Health effects are from long-term exposure unless specified as short-term exposure.

<sup>4</sup>Each water system must certify annually—in writing—to the state (using third-party or manufacturers certification) that when it uses acrylamide and/or epichlorohydrin to treat water, the combination (or product) of dose and monomer level does not exceed the levels specified as follows: Acrylamide = 0.05 percent dosed at 1 mg/L (or equivalent), Epichlorohydrin = 0.01 percent dosed at 20 mg/L (or equivalent).

<sup>5</sup>Lead and copper are regulated by a Treatment Technique that requires systems to control the corrosiveness of their water. If more than 10 percent of tap water samples exceed the action level, water systems must take additional steps. For copper, the action level is 1.3 mg/L; for lead, the action level is 0.015 mg/L.

<sup>6</sup>A routine sample that is fecal coliform-positive or *E. coli*-positive triggers repeat samples. If any repeat sample is total coliform-positive, the system has an acute MCL violation. A routine sample that is total coliform-positive and fecal coliform-negative or *E. coli*-negative triggers repeat samples. If any repeat sample is fecal coliform-positive or *E. coli*-positive, the system has an acute MCL violation (see also Definitions <sup>8</sup>: Total Coliforms).

<sup>7</sup>EPA's surface water treatment rules require systems using surface water or ground water under the direct influence of surface water to (1) disinfect their water and (2) filter their water or meet criteria for avoiding filtration so the following contaminants are controlled at the following level:

**Cryptosporidium:** 99 percent removal for systems that filter. Unfiltered systems are required to include *Cryptosporidium* in their existing watershed control provisions;

**Giardia lamblia:** 99.9 percent removal/inactivation;

**Viruses:** 99.9-percent removal/inactivation;

**Legionella:** No limit, but EPA believes that if *Giardia* and viruses are removed/ inactivated, according to the treatment techniques in the surface water treatment rule, *Legionella* will also be controlled;

**Turbidity:** For systems that use conventional or direct filtration, at no time can turbidity (cloudiness of water) go higher than 1 nephelometric turbidity unit (NTU); samples for turbidity must be less than or equal to 0.3 NTU in at least 95 percent of the samples in any month. Systems that use filtration other than the conventional or direct filtration must follow state limits, which must include turbidity at no time exceeding 5 NTU;

**HPC:** No more than 500 bacterial colonies per milliliter;

**Long Term 1 Enhanced Surface Water Treatment:** Surface water systems or ground water systems under the direct influence of surface water serving fewer than 10,000 people must comply with the applicable Long Term 1 Enhanced Surface Water Treatment Rule provisions (e.g., turbidity standards, individual filter monitoring, *Cryptosporidium* removal requirements, updated watershed control requirements for unfiltered systems);

**Long Term 2 Enhanced Surface Water Treatment:** This rule applies to all surface water systems or ground water systems under the direct influence of surface water. The rule targets additional *Cryptosporidium* treatment requirements for higher risk systems and includes provisions to reduce risks from uncovered finished water storages facilities and to ensure that the systems maintain microbial protection as they take steps to reduce the formation of disinfection by-products. Monitoring start dates are staggered by system size. The largest systems (serving at least 100,000 people) will begin monitoring in October 2006 and the smallest systems (serving fewer than 10,000 people) will not begin monitoring until October 2008. After completing monitoring and determining their treatment bin, systems generally have three years to comply with any additional treatment requirements.

**Filter Backwash Recycling:** The Filter Backwash Recycling Rule requires systems that recycle to return specific recycle flows through all processes of the system's existing conventional or direct filtration system or at an alternate location approved by the state.

<sup>8</sup>No more than 5.0 percent samples total coliform-positive in a month. (For water systems that collect fewer than forty routine samples per month, no more than one sample can be total coliform-positive per month.) Every sample that has total coliform must be analyzed for either fecal coliforms or *E. coli*. If two consecutive TC-positive samples, and one is also positive for *E. coli* or fecal coliforms, then the system has an acute MCL violation.

<sup>9</sup>Although there is no collective MCLG for this contaminant group, there are individual MCLGs for some of the individual contaminants:

**Haloacetic acids:** dichloroacetic acid (zero); trichloroacetic acid (0.3 mg/L).

**Trihalomethanes:** bromodichloromethane (zero); bromoform (zero); dibromochloromethane (0.06 mg/L).

[Return to where text linked to Box 2 ↑](#)

## Box 3 USA National Secondary Drinking Water Regulations

Secondary Maximum Contaminant Levels (SMCLs) were established for contaminants that can adversely affect the taste, odor, or appearance of water and may result in discontinuation of use of the water. SMCLs are non-enforceable, generally non-health-based standards that are related to the aesthetics of water use. These are listed in Table Box 3-1.

**Table Box 3-1 - US National Secondary Drinking Water Regulations (US EPA, 2009).**

<b>Contaminant</b>	<b>Secondary maximum contaminant level</b>
<b>Aluminum</b>	0.05 to 0.2 mg/L
<b>Chloride</b>	250 mg/L
<b>Color</b>	15 (color units)
<b>Copper</b>	1.0 mg/L
<b>Corrosivity</b>	Noncorrosive
<b>Fluoride</b>	2.0 mg/L
<b>Foaming Agents</b>	0.5 mg/L
<b>Iron</b>	0.3 mg/L
<b>Manganese</b>	0.05 mg/L
<b>Odor</b>	3 threshold odor number
<b>pH</b>	6.5–8.5
<b>Silver</b>	0.10 mg/L
<b>Sulfate</b>	250 mg/L
<b>Total Dissolved Solids</b>	500 mg/L
<b>Zinc</b>	5 mg/L

[Return to where text linked to Box 3](#) ↑

## 16 Exercise Solutions

### Solution Exercise 1

Global environmental impacts of using fossil fuels include (1) air pollution and (2) the interrelated global warming that results from continuous addition of large and increasing amounts of CO<sub>2</sub> to the atmosphere (40.1 billion tonnes CO<sub>2</sub> in 2019, compared with 31 billion tonnes in 2011 and 20 billion tonnes in 1991), largely from the burning of fossil fuels. Local impacts of using fossil fuels include (3) groundwater contamination from leaking USTs at homes and gas stations, which are the largest single threat to groundwater quality in the United States today. There are approximately 1.2 million USTs nationwide, many of which were installed prior to new regulations in 1988. Many USTs are a concern because older tanks corrode quickly when buried unprotected in the soil. Local impacts also include contamination of (4) groundwater and (5) soil from produce water, the largest volume of wastewater produced in the USA.

[Click to return to where text linked to Exercise 1](#) ↗

[Return to Exercise 1](#) ↗

### Solution Exercise 2

Drake's well was considered the first oil well because:

1. it was drilled, not dug by hand;
2. a steam engine was used to drill the well;
3. a company associated with it (the Seneca Oil Company with Drake as president), and;
4. it started a major oil boom, the first oil rush not only in Pennsylvania, but throughout the USA.

[Click to return to where text linked to Exercise 2](#) ↗

[Return to Exercise 2](#) ↗

### Solution Exercise 3

Four global potential adverse impacts of climate warming and rising atmospheric CO<sub>2</sub> concentrations include:

1. sea-level rise from the melting of alpine glaciers and polar ice sheets and from ocean water expansion due to warming;
2. increased frequency and intensity of wildfires, floods, droughts, and tropical storms;
3. changes in the amount, timing, and distribution of rain, snow, and runoff; and
4. increased CO<sub>2</sub> dissolved in ocean water, which increases ocean water acidity with potentially disruptive effects on coral reefs, marine plankton, and some marine ecosystems.

[Click to return to where text linked to Exercise 3 ↑](#)

[Return to Exercise 3 ↑](#)

### Solution Exercise 4

The W/O ratio in the USA is currently 10/1.

In 1965, a total of 23 million bbl/d of produced water were generated with 7.67 million bbl/d oil, for a W/O ratio of 3.0.

In 2050, the W/O ratio from depleted conventional wells may reach 25/1, but most of the oil would come from unconventional sources with much lower W/O ratio. Such that the overall ratio may be 10 to 15.

When oil production from wells in oil fields is depleted, the W/O ratio may reach a value of 50, with oil making up 2 percent or less of the total fluid produced.

[Click to return to where text linked to Exercise 4 ↑](#)

[Return to Exercise 4 ↑](#)

### Solution Exercise 5

- 1) The median volume of 94,000 bbl/well (15,000 m<sup>3</sup>/well) is needed to hydraulically fracture individual horizontal oil wells.
- 2) The fracturing fluid is comprised of approximately 90.5 percent water, 9 percent proppant, and 0.5 percent organic and inorganic chemicals. The chemicals added to improve production include potassium chloride, acids, bactericides, biocides, surfactants, friction reducers, and corrosion and scale inhibitors (Table 1).

[Click to return to where text linked to Exercise 5 ↑](#)

[Return to Exercise 5 ↑](#)

## Solution Exercise 6

Wells selected for sampling must meet four of the following criteria:

- 1) have not been affected by water flooding, acidification, or other chemical treatment;
- 2) must have been producing oil for at least 6 months to minimize contamination from drilling operations;
- 3) have a single and narrow perforation zone;
- 4) produce large amounts of water relative to oil; and
- 5) have ports for sampling close to the well head and before the fluid enters a separator.

[Click to return to where text linked to Exercise 6](#) ↑

[Return to Exercise 6](#) ↑

## Solution Exercise 7

Five additional culling criteria to create a useful data set from oil company data:

- 1) concentration of Cl or Na not reported;
- 2) concentration of Cl or Na reported as < or > a given value;
- 3) concentration of Mg  $\geq$  Ca;
- 4) pH < 5 or > 10; and
- 5) density less than 1.

Table 8 in section 6.6.1 of this book provides more culling criteria.

[Click to return to where text linked to Exercise 7](#) ↑

[Return to Exercise 7](#) ↑

## Solution Exercise 8

- 1) Modified connate seawater because the Cl/Br ratio is in the 300 range
- 2) Bittern brine, evaporated seawater because of its high salinity and high concentrations of major ions
- 3) High salinity from dissolving halite because of the high Cl/Br ratio

[Click to return to where text linked to Exercise 8](#) ↑

[Return to Exercise 8](#) ↑

## Solution Exercise 9

Reservoir temperature is an important parameter that affects water-mineral interactions and produced water compositions in the subsurface. The concentration of certain chemicals and chemical ratios (especially Li/Na, K/Na, and Rb/Na) generally increase with increasing reservoir temperature (deeper reservoirs tend to be warmer). The most useful chemical markers for increasing subsurface temperatures are the concentrations of silica, boron, and ammonia, and the Li/Mg, Li/Na, and K/Na ratios. The proportions of alkali metals alone or combined with those of alkaline-earth metals (magnesium and calcium in particular) and the concentrations of SiO<sub>2</sub> are so strongly dependent on subsurface temperature that they have been combined into several chemical geothermometers that can be used to provide a good estimate of the reservoir temperature. When temperatures calculated using chemical geothermometers are concordant with and close to those obtained by oil companies for that reservoir, the chemical analyses are more reliable. When the calculated temperatures are not concordant and vary greatly from reported values, then it is reasonable to investigate the source of the discrepancy, which may be a sampling problem, mixing with water from a leaked zone, or an analysis issue.

[Click to return to where text linked to Exercise 9](#) ↗

[Return to Exercise 9](#) ↗

## Solution Exercise 10

The concentrations of acetate and other organic acid anions in produced water may be as high as 10,000 mg/L. The values are primarily controlled by subsurface temperature and the age of the reservoir rocks. The highest concentrations of aliphatic acid anions are observed in the youngest (Tertiary age) and shallowest reservoir rocks at temperatures of 80 to 120 °C. Their concentration generally decreases with both increasing and decreasing subsurface temperatures (Figure 31) and with the age of the reservoir rocks. At temperatures < 80 °C, acetate is consumed by bacteria. The high temperature limit of decarboxylation above which no measurable acid anions are present, is estimated to be ~220 °C.

[Click to return to where text linked to Exercise 10](#) ↗

[Return to Exercise 10](#) ↗

## Solution Exercise 11

The polycyclic aromatic hydrocarbons (PAHs) are aromatic hydrocarbons with 2 to 7 fused hydrocarbon rings, which may have substituted elements like N, S, or O attached to the rings. The concentration of PAHs in produced water is low; however, PAHs are heavily concentrated ( $K_{OW}$  values in many thousands) in the crude fraction, comprising 0.2 to 7 percent of the crude, with the highest amounts in heavy crude oils. Many of the PAHs are extremely toxic, some at lower concentrations than benzene (MCL for benzo(a)pyrene is 0.2  $\mu\text{g/L}$ ). Sixteen of the PAHs are designated by the EPA as priority pollutants. Also, PAHs can persist in the environment for many years. In some cases, PAHs continue to harm organisms and the environment until all crude is removed and the site is completely remediated.

[Click to return to where text linked to Exercise 11](#) ↑

[Return to Exercise 11](#) ↑

## Solution Exercise 12

Although boron (B) is an essential element in plants, it is extremely toxic to many fruit trees and vegetable, even at relatively low concentrations of 0.5 mg/L. Toxicity occurs with the uptake of B from the soil solution. B tends to accumulate in the leaves until it becomes toxic to the leaf tissue and results in the death of the plant. The threshold concentration of B in irrigation water for grape vines, citrus trees, and other fruit trees is 0.75 mg/L. Most groundwater, with B values of 0.05 to 0.5 mg/L meets the irrigation criteria. However, produced water generally has very high B concentrations such that even diluted produced water exceeds the threshold concentration of boron in irrigation water. For example, produced water from California oil fields have B concentrations of up to 600 mg/L, which is 500 times the threshold value for B-sensitive trees and vegetables.

[Click to return to where text linked to Exercise 12](#) ↑

[Return to Exercise 12](#) ↑

## Solution Exercise 13

Five chemical parameters that, if encountered in groundwater, would suggest contamination with produced water and would prompt a detailed hydrogeological investigation to confirm the source of contamination are listed here.

- 1) In the USA, the MCL value for the salinity of drinking water is 500 mg/L (TDS) and almost all produced water have 1 to 3 orders of magnitude higher salinity that is easily measured using a conductance electrode. Thus, salinity could be the first indication of contamination by produced water.
- 2) A more definitive indicator may be obtained from the ratios of individual conservative ions such as Cl, Br, B, and Li.
- 3) Groundwater generally has low DOC values (< 1.0 mg/L) while produced water has DOC values that are 1 to 3 orders of magnitude higher.
- 4) More detailed chemical analyses (including organic acid anions, BTEX, and especially long-lived PAHs) are definitive diagnostic compounds to indicate contamination from oil or produced water.
- 5) Further confirmation using the isotopes of water, especially the more conservative  $\delta D$  values and those of many solutes (e.g., B, Li, Sr) should reveal the source of contamination.

Potential contamination of groundwater by activities of the petroleum industry may be evaluated using detailed hydrological, chemical, and isotope data. Such investigation can accurately determine or trace a particular water contaminant to its source and help in designing proper remediation protocols.

[Click to return to where text linked to Exercise 13](#) ↗

[Return to Exercise 13](#) ↗

## Solution Exercise 14

Strontium has four stable isotopes:  $^{84}\text{Sr}$  (0.56 percent),  $^{86}\text{Sr}$  (9.86 percent),  $^{87}\text{Sr}$  (7.0 percent), and  $^{88}\text{Sr}$  (82.58 percent); it also has a radiogenic  $^{87}\text{Sr}$  isotope that is produced by the decay of Rb (half-life =  $4.88 \times 10^{10}$  years). Rocks having high initial concentrations of rubidium, such as granites, are characterized by high  $^{87}\text{Sr}/^{86}\text{Sr}$  ratios. Rocks derived from materials having low rubidium concentrations (such as mantle-derived rocks) have correspondingly low  $^{87}\text{Sr}/^{86}\text{Sr}$ . Since the Precambrian, the  $^{87}\text{Sr}/^{86}\text{Sr}$  of seawater has fluctuated between  $\sim 0.7070$  and  $\sim 0.7092$  as the result of variations in the relative rates of input of  $^{87}\text{Sr}$ -enriched strontium from continental weathering and  $^{87}\text{Sr}$ -depleted strontium from mantle sources. Fluids in sedimentary basins containing Paleozoic strata typically have  $^{87}\text{Sr}/^{86}\text{Sr}$  ratios higher than current seawater values that are contemporaneous or coeval with the depositional age of the current host sediment. The enrichment is due to the release of strontium attending the alteration of silicates. Due to the significant increase of  $^{87}\text{Sr}/^{86}\text{Sr}$  in seawater since the Jurassic, some formation water in Cenozoic sedimentary basins has  $^{87}\text{Sr}/^{86}\text{Sr}$  ratios lower than those of contemporaneous seawater due to the addition of strontium dissolved from older and deeper sedimentary sources. Precipitates derived from such sources, such as barite in Holocene seafloor vents in the Gulf of Mexico, have lower  $^{87}\text{Sr}/^{86}\text{Sr}$  values than present-day seawater.

[Click to return to where text linked to Exercise 14](#) ↑

[Return to Exercise 14](#) ↑

## Solution Exercise 15

A number of radioactive isotopes produced primarily by cosmic ray interactions in the upper atmosphere—especially  $^{14}\text{C}$ ,  $^{36}\text{Cl}$ ,  $^{129}\text{I}$ ,  $^{39}\text{Ar}$ , and  $^{81}\text{K}$ , as well as total dissolved  $^4\text{He}$ —have been used in conjunction with data for the stable isotopes and calculated flow rates, to determine the residence time (age of) natural water including fluids in sedimentary basins. The 5.73 ka half-life of  $^{14}\text{C}$  is so short that it is only useful for dating basinal water younger than 40 ka.  $^{36}\text{Cl}$  ( $t_{1/2} = 0.301 \text{ Ma}$ ) is useful for dating water of up to 2 Ma in age. The ratio of  $^{129}\text{I}$  ( $t_{1/2} = 15.7 \text{ Ma}$ ) to total iodide can be used to estimate ages up to 80 Ma. The determination of even higher ages is theoretically possible by using  $^4\text{He}$  generated from the decay of uranium and thorium in rocks. However, the ages obtained carry large uncertainty because the radioactive isotopes can have several sources and are often subject to fractionation due to isotopic exchange and partitioning. In addition, the origin and age of  $\text{H}_2\text{O}$  in formation water is generally different from that of the radioactive and other isotopes used for age determination.

The ratio of  $^{129}\text{I}$  to total I, at times in combination with  $^{36}\text{Cl}/\text{Cl}$  ratios, has been successfully used to estimate the residence time of subsurface water, to trace the migration of brine, and to identify hydrocarbon sources. This method can also be used to illustrate the difficulties of dating very old formation water.

[Click to return to where text linked to Exercise 15](#) ↗

[Return to Exercise 15](#) ↗

## Solution Exercise 16

The terms *autochthonous* and *allochthonous* (literally, *same earth* and *other earth*, respectively) are used in salt tectonics to refer to salt masses such as salt beds that lie in their original stratigraphic position (autochthonous), and salt formations such as domes and sheets that have been physically displaced from their original depositional location (allochthonous). The portions of the Jurassic Louann Salt that still lie stratigraphically where they were originally deposited represent autochthonous salt. The examples of salt domes and sheets presented in Section 9 are all allochthonous.

[Click to return to where text linked to Exercise 16](#) ↗

[Return to Exercise 16](#) ↗

## Solution Exercise 17

Oil field waste water from Jurassic and Cretaceous host reservoirs will have significantly higher concentrations of dissolved calcium and bromide than water from Cenozoic reservoirs, even if partially diluted. Magnesium concentrations might provide a nondefinitive answer. Based on the information in Figure 42, the composition of basinal brine from Gulf of Mexico sediments has distinctly different than the composition of both modern and ancient seawater as well as their evaporated equivalents.

[Click to return to where text linked to Exercise 17](#) ↑

[Return to Exercise 17](#) ↑

## Solution Exercise 18

The spatial variations in salinity and chemical composition of the formation water in the sediments surrounding the allochthonous salt structures discussed in Section 9 can best be explained by dynamic fluid flow. Driving forces for fluid flow include differences in fluid density resulting from spatial variation in salinity and temperature (e.g., Bay Marchand allochthonous salt sheet, Figure 39) and fluid over-pressuring (e.g., Welsh Dome, Figure 40).

[Click to return to where text linked to Exercise 18](#) ↑

[Return to Exercise 18](#) ↑

## Solution Exercise 19

Important findings of research at the Bemidji, Minnesota, oil spill site include the following so the response should include four of the following five items.

- 1) Initial cleaning following the pipeline break in 1979 removed approximately 75 percent of the crude, but 400,000 L remained, contaminating the soil and groundwater at the site.
- 2) In 1999, the pipeline company installed a dual-pump recovery system in selected remediation wells. This system was used for five years and resulted in removal of about 115,000 liters of crude oil, representing ~40 percent of estimated crude that was present in the aquifer in 1998. Additional removal became difficult and complete remediation is impossible.
- 3) The crude oil at the spill site has undergone weathering since the time of the spill about 40 years ago; the relative contributions to weathering from volatilization, dissolution, and biodegradation vary depending on compound properties and location in the oil body. Biodegradation and dissolution have continuously produced a plume comprised of dissolved hydrocarbons, partially oxidized hydrocarbon metabolites, and hydrocarbon oxidation products. The plume extends approximately 340 m downgradient from the source to a lake.
- 4) Results of measurements show DOC concentrations measured for the nineteen sampled wells as a function of time from the center of the oil body. The concentration of DOC in the wells directly adjacent to the oil body is 31 mg/L, decreasing to 2.3 mg/L in a well located 254 m downgradient from the center of the source.
- 5) Compositional results indicated that changes in the dissolved organic compounds in the groundwater plume were gradual as relatively low molecular weight, reduced, aliphatic compounds from the oil source were selectively degraded and high molecular weight, alicyclic/aromatic compounds, including PAHs and unsaturated oxidized compounds, persisted.

[Click to return to where text linked to Exercise 19](#) ↑

[Return to Exercise 19](#) ↑

## Solution Exercise 20

Water from Skiatook Lake is suitable for human consumption as no chemical component exceeds the MCL values.

To obtain the required dilution factors, compare the components in groundwater from BE-62 with the MCL values in Table Box 2-1 or SMCL values in Table Box 3-1.

For example, in the case of the groundwater TDS of 15,700 mg/L, the SMCL from Table Box 3-1 is 500 mg/L, and the TDS of the lake water is 165 mg/L. Defining  $x$  as the fraction of groundwater and  $(1-x)$  as the amount of lake water,  $x$  is determined as follows.

$$15700 \frac{\text{mg}}{\text{L}} x + 165 \frac{\text{mg}}{\text{L}} (1 - x) = 500 \frac{\text{mg}}{\text{L}}$$

$$15700 \frac{\text{mg}}{\text{L}} x + 165 \frac{\text{mg}}{\text{L}} - 165 \frac{\text{mg}}{\text{L}} x = 500 \frac{\text{mg}}{\text{L}}$$

$$x = \frac{335 \frac{\text{mg}}{\text{L}}}{15535 \frac{\text{mg}}{\text{L}}} = 0.02$$

Thus, 0.02 parts of groundwater—always rounding down to ensure the mix will be less than the maximum allowed—and 0.98 parts lake water result in a water that meets the drinking water standard, a dilution factor of 49 to 1.

As another example, for benzene ( $\text{C}_6\text{H}_6$ ), the MCL value in Table Box 2-1 is 0.005 mg/L and its concentration in the groundwater is 0.058 mg/L, while the concentration of benzene in lake water is zero.

$$0.058 \frac{\text{mg}}{\text{L}} x + 0 \frac{\text{mg}}{\text{L}} (1 - x) = 0.005 \frac{\text{mg}}{\text{L}}$$

$$0.058 \frac{\text{mg}}{\text{L}} x = 0.005 \frac{\text{mg}}{\text{L}}$$

$$x = \frac{0.005 \frac{\text{mg}}{\text{L}}}{0.058 \frac{\text{mg}}{\text{L}}} = 0.08$$

Thus, 0.08 parts of groundwater—always rounding down to ensure the mix will be less than the maximum allowed—and 0.92 parts lake water result in a water that meets the drinking water standard, a dilution factor of 11.5 to 1.

[Click to return to where text linked to Exercise 20](#) ↑

[Return to Exercise 20](#) ↑

## Solution Exercise 21

A weir and an automated precipitation gauge were installed close to Skiatook Lake to investigate the natural overland transport of salts from this site by measuring the volume and chemical composition of surface runoff from precipitation events draining a 1.7-ha area. Results show runoff that leaches the previously precipitated surficial salts can have a relatively high salinity (up to 3,000 mg/L TDS) but that only small amounts of total salts (500 to 1,000 kg/year of salt) are removed by this process. This and other studies indicate that natural attenuation at this site will be very slow, possibly taking 100 years or more.

[Click to return to where text linked to Exercise 21](#) ↑

[Return to Exercise 21](#) ↑

## Solution Exercise 22

To investigate the source of brine in a sample obtained from a borehole below the brine pit and close to Skiatook Lake, check the TDS, chemical and isotopic composition of water from the borehole and calculate chemical ratios (e.g., Cl/Br, Li/Na, and so on) and also isotope ratios (e.g.,  $^{87}\text{S}/^{86}\text{S}$ ) for the sample and compare them with that of produced water from the brine pit and the tanks above the brine pit. Also, look for oil globules, oil odor, and high values of measured hydrocarbon gases and other VOCs. A tracer dye such as fluorescein or Rhodamine WT added to the brine pit and observed later in water from the borehole would confirm the source.

[Click to return to where text linked to Exercise 22](#) ↑

[Return to Exercise 22](#) ↑

## Solution Exercise 23

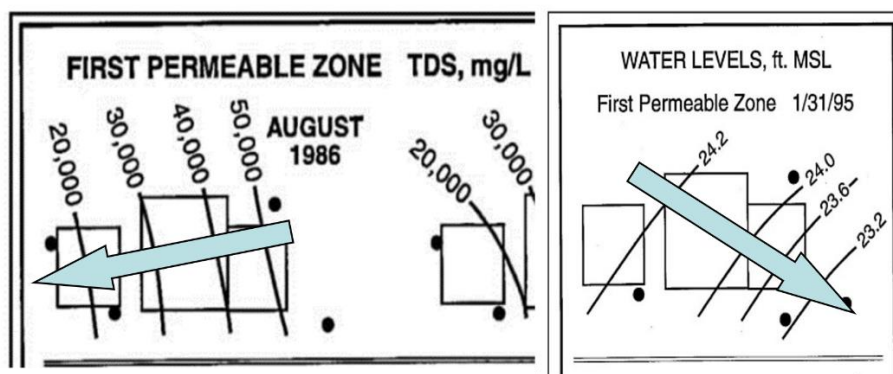
The calculated oil field wastewater composition shows increased dissolved sodium, calcium, and magnesium with increased chloride similar to Gulf of Mexico formation water, although there is much scatter in the calculated magnesium data. The relative proportions of calculated cations are  $\text{Na} > \text{Ca} > \text{Mg}$ , which is similar to the formation water. Calculated concentrations of K show a great deal of scatter and no clear trend. However, Figure 42 does not provide data for K in the formation water, so K values cannot be compared.

[Click to return to where text linked to Exercise 23](#) ↑

[Return to Exercise 23](#) ↑

## Solution Exercise 24

Arrows indicating apparent downgradient directions are shown in the image below.



The TDS (salinity) decreases from right (east) to left (west). From this sparse information alone, one might reasonably conclude there is a broad area of contamination in the east and a contaminant plume is moving from east to west. An alternative interpretation might be that flow of fresh groundwater from west to east is receiving an influx of salt from above thus becoming more contaminated as it flows to the east. In contrast, water levels in wells screened in the first permeable zone decrease in yet another direction, from northwest to southeast. If this were a fresh groundwater system, which it is not, one could reasonably conclude from the water levels that groundwater flow is in a southeasterly direction. Thus, these field data alone are insufficient to make a definitive interpretation of contaminant transport conditions at the site.

[Click to return to where text linked to Exercise 24](#) ↑

[Return to Exercise 24](#) ↑

## Solution Exercise 25

A CCUS Hub is a location where multiple industrial point sources of CO<sub>2</sub> such as power plants and natural gas fields with significant CO<sub>2</sub> concentrations, are connected to a shared transport and storage network. The location (see Table 48) has to have access to a geological feature with high capacity to store the CO<sub>2</sub> permanently and safely for hundreds of years. The project needs to be commercially viable and the hub keeps the unit cost of CO<sub>2</sub> storage low because of economies of scale. The hub's shared existing and added infrastructure likely would attract new clean industries as well as innovation and negative emissions technologies.

[Click to return to where text linked to Exercise 25](#) ↑

[Return to Exercise 25](#) ↑

## Solution Exercise 26

Field determinations at the ZERT facility showed rapid and systematic changes in pH (7.0 to 5.6), alkalinity (400 to 1,300 mg/L as  $\text{HCl}_3$ ) and electrical conductance (600 to 1,800  $\mu\text{S}/\text{cm}$ ) in response to  $\text{CO}_2$  injection. These easily monitored and sensitive chemical changes could provide early detection of  $\text{CO}_2$  leakage into shallow groundwater from deep storage operations; laboratory results could be used to confirm any such leaks.

The chemical changes observed in the ZERT groundwater are similar in trend, though much lower in concentration, to the changes observed in the Frio Brine Pilot tests discussed earlier in the same section. There are differences between Frio and ZERT with respect to pH changes. Frio pH was low (i.e., 3) and pH at ZERT declined but only to approximately 6. The differences are related to several geochemical parameters. An important reason relates to the subsurface  $\text{pCO}_2$  value for Frio of approximately 150 bar, compared with the  $\text{pCO}_2$  value measured and computed with SOLMINEQ for the ZERT samples, which ranged from 0.035 to -1 bar. The maximum amount of  $\text{CO}_2$  dissolved in water is a strong function of fluid pressure.

[Click to return to where text linked to Exercise 26](#)↑

[Return to Exercise 26](#)↑

## 17 About the Authors



**Dr. Yousif K. Kharaka** was born in Mangesh, a small town located in northern Iraq, close to the Turkish border. Dr. Kharaka is currently an emeritus hydrogeochemist with the USGS, Menlo Park, California. As a Research Scientist at the University of California (UC) Berkeley (1971–1975) and at the USGS (since 1975), he has been conducting field, laboratory, and simulation geochemical investigations in the broad areas of water-gas-rock interactions over a wide range of salinity, temperature, and pressure conditions and in a variety of natural and contaminated systems.

Dr. Kharaka has investigated numerous systems including conventional and unconventional oil and natural gas fields in sedimentary basins, agricultural areas, and hydrothermal (Yellowstone National Park) and major fault (San Andreas) systems. His recent investigations cover naturally occurring organics, organic–inorganic interactions, CO<sub>2</sub> sequestration in depleted oil reservoirs, and characterization and remediation of contaminated groundwater in active and legacy petroleum fields. Dr. Kharaka has authored or coauthored more than 120 scientific papers and book chapters and delivered more than 200 scientific presentations at universities and national and international conferences.

He received his B.Sc. (honors) in Geology from Kings College, London, in 1963, and his Ph.D. in Geology from the UC Berkeley in 1971. Dr. Kharaka was the Secretary General for the 7th International Symposium on Water–Rock Interaction (WRI-7) held in 1992 and was the Chairman of the Working Group on WRI of the International Association of GeoChemistry (IAGC) from 2001 to 2007. Dr. Kharaka has received many honors and awards, including paid scholarships by the Iraqi government to Kings College, London, and UC Berkeley. He received the US Department of Interior Meritorious Service Award (1994) and the International Working Group on WRI Leadership Award (2010). Dr. Kharaka also received the IAGC Distinguished Service Award (2009) and the Vernadsky Medal in geochemistry (2022).



**Dr. Brian Hitchon** was born in St. John, New Brunswick, Canada, in 1930 and educated in England, receiving his Ph.D. from Manchester University in 1955. After two years as a geologist with the Northern Rhodesia Geological Survey, he returned to Canada in 1957 and joined the Alberta Research Council (Edmonton, Alberta). He has held many positions at Council including Research Fellow, Vice President for Facilities, and Acting Director, and is currently emeritus. He retired in 1989 and started Hitchon Geochemical Services Ltd., a consultancy, and in 1995 branched out into publishing with Geoscience Publishing Ltd., which currently has seven titles with more planned. The fourth book, *Alberta Beneath Our Feet*, was winner of the 2006

Association of Earth Science Editors *Outstanding Publication in the Print Category*. The seventh book, *Best Practices for Validating CO<sub>2</sub> Geological Storage*, received Honorable Mention in 2012 from the Association of Earth Science Editors for *Outstanding Publication in the Book Category*.

Dr. Hitchon was active in IAGC affairs for two decades: first, as chairman of the IAGC Working Group on Water–Rock Interaction (1974–1983) and then as secretary of IAGC (1984–1992), as well as Executive Editor of the journal *Applied Geochemistry* (1986–1993). He is a Fellow of the Geological Society.

Dr. Hitchon has specialized in the geochemistry and flow of formation water in sedimentary basins with more than 86 publications, the majority in refereed journals, in addition to 27 bulletins and reports of the two organizations he has worked for and 23 consultant reports for the Alberta Research Council and Hitchon Geochemical Services Ltd. His other interests include things Japanese (gardens, architecture, food), eclectic reading (biography, medieval history, natural history, travel—especially related to Africa, and mystery novels), and travel (worldwide), gardening, classical music (especially piano), and English language and literature.

**Dr. Jeffrey S. Hanor** is an emeritus professor at Louisiana State University, where he taught



courses in environmental geology and sedimentary geochemistry in the Department of Geology and Geophysics. He received his B.A. (honors) in Geology from Carleton College in 1961, his Ph.D. in Geology from Harvard in 1967, and was a Postdoctoral Fellow at the Scripps Institution of Oceanography from 1967 to 1970 before joining LSU in 1970. Dr. Hanor has been the thesis and dissertation adviser to nearly fifty graduate and honors undergraduate students. These students have gone on to careers of their own in academia, the oil and gas industry, and environmental consulting. In addition to ongoing research dealing with fluids and rocks ranging in age from the Paleoproterozoic to the Recent, Dr. Hanor has served as an expert in numerous cases involving groundwater contamination in the Louisiana Gulf Coast. He was the 1998 Geological Society of America Hydrogeology Division Birdsall-Dreiss Distinguished Lecturer.

Please consider signing up for the GW-Project mailing list to stay informed about new book releases, events, and ways to participate in the GW-Project. When you sign up for our email list, it helps us build a global groundwater community. [Sign up](#)<sup>7</sup>.



## Modifications to Original Release

### Changes from the Original Version to Version 2

Original Version: August 18, 2023, Version 2: January 19, 2024

Page numbers refer to the original PDF.

page ii, added page requesting support of the Groundwater Project

page ii, now page iii, updated version number and date

page iii, now page iv, added “Any use of trade, firm, or product names is for descriptive purposes only and does not imply endorsement by the U.S. Government.”

page 30, third sentence of Section 4.4.3, corrected typo ( $\text{HCl}_3^-$ ) to ( $\text{HCO}_3^-$ )

page 66, deleted repeated sentence that began “There was little gas”

### Changes from the Version 2 to Version 3

Original Version: August 18, 2023, Version 3: August 31, 2024

Page numbers refer to the Version 2 PDF.

#### General changes:

minor punctuation changes were made throughout the book

minor typographical errors were corrected throughout the book

some adjustments were made to capitalizations

when referring to specific oil fields by name, all were changed from “Name oil field” to “Name Field”

when referring to specific basins by name, the word “basin” was capitalized

chemical symbols/formulae that were not in regular Cambria Math font were adjusted to be so

occurrences of “mEq” were changed to “meq”

occurrences of “waters” were changed to “water”

slight adjustments were made to the size of some figures and the width of some captions

where chemical formulae were inserted as an image, they were changed to text with Cambria Math font

where chemical formulae without superscripts or subscripts were inserted with Palatino Linotype font, they were changed to Cambria Math font

where chemical formulae with superscripts or subscripts were entered as text, they were adjusted to use MSWord Equation format to maintain consistency of appearance

when a cross reference to a figure was in bold font, it was changed to not be bold

### **Specific changes:**

page iv, updated version number with date

page v, updated number of pages

page 2, second paragraph, added: *“Detailed analyses of groundwater-levels in 170,000 monitoring wells and close to 1,700 aquifers in 40 countries by Jasechko and others (2024) showed rapid groundwater-level declines, >0.5 m per year, in the twenty first century, especially in dry regions with extensive croplands, like the Central Valley in California. They also showed that in the last four decades, groundwater-level declines accelerated in 30 percent of the world’s regional aquifers. Their results, however, also showed reversal of declines in specific cases where aquifers were carefully managed.”*

page 4, end of first sentence, added: *“Groundwater Protection Council, 2019”*

page 11, third paragraph, modified section number references. and modified and added citations

page 12, last full paragraph, deleted the word “atmospheric”

page 26, last paragraph of section 4.2, deleted minus sign after the cube in 3.65 million m<sup>3</sup>

page 30, second sentence of 4.4.3, “are” was changed to “is”

page 32, section 4.5, second to last paragraph, modified “*Contamination could only be detected if the water quality of existing freshwater wells in an area change significantly over time*” to read “*Contamination can only be detected by finding significant changes in the quality of water in existing freshwater wells in an area over time*”

Page 34, paragraph following Figure 8, end of first sentence, added: “*Groundwater Protection Council, 2019*”

page 37, end of last paragraph, changed “GWPC” to “Groundwater Protection Council, 2023; Groundwater Protection Council”

page 41, last paragraph, added “Formation” after “Wolfcamp”

page 42, only paragraph, added “Formation” after “Wolfcamp”

page 46, third paragraph, changed “GWPC” to “Groundwater Protection Council, 2019; Groundwater Protection Council”

page 49, first partial paragraph, the degree signs that followed API gravity numbers were removed

page 53, second paragraph, remove repeated word “in”

page 58, last complete paragraph, added “(“ before “strontium”

page 71, “also” was added to the third footnote of Table 7

page 73, first paragraph of section 6.6.1, second sentence, “For” was changed to “In”

page 73, first paragraph of section 6.6.1, last sentence,  $\text{CO}_3$  was changed to  $\text{CO}_3^{-2}$

page 74, Table 8, first cell of information, removed duplicate words “with either  $\text{HCO}_3$ ”

page 74, Table 10, row 5. removed “(explained in Note below table)”

page 75, third paragraph, deleted “when” from first line

page 75, third paragraph, second to last line change “,the” to “. The”

page 76, first full paragraph, changed “in the” to “of the”

page 76, second paragraph, changed “chained, aliphatic acid” to “chain, aliphatic-acid”

page 77, Table 11, moved citations from caption to beneath table; moved units of mg/L from caption to column heading; changed the heading “Sample source” to “Source”

page 77, Table 12, moved citations from caption to beneath table; moved units of mg/L from caption to column heading; changed the heading “Sample” to “Source”; changed “unconventional hydrocarbon class” to “produced water”

page 78, Table 13, changed the heading “Sample” to “Source”; corrected punctuation in citations, added “a” between “but” and “significant”

page 78, last paragraph changed “because no important precipitation reaction maintains” to “because there is no important precipitation reaction that maintains”

page 79, first partial paragraph, changed “on in” to “ion”

page 79, first full paragraph, changed “a solution” to “solution”

page 79, first full paragraph, changed “—clasts—” to “(clasts)”

page 79, first full paragraph, changed “In short” to “However ”

page 79, paragraph above Table 14, first sentence, changed “Potassium has” to “Potassium is a lithophile element with”

page 79, paragraph above Table 14, second sentence, changed “Potassium is a lithophile element with; in” to “In”

page 79, Table 14, changed the heading “Sample” to “Source”; corrected punctuation in citations, added “a” between “but” and “significant”

page 80, first line, added "it" after "thus"

page 80, Table 15, changed the heading "Sample" to "Source"; corrected punctuation in citations

page 81, first paragraph, changed "because magnesium" to "because the magnesium"

page 81, Table 16, changed the heading "Sample" to "Source"; changed emdashes to hyphens; corrected punctuation in citations

page 81, last paragraph, second sentence changed "The major factors" to "The major factor"; changed "are equilibria" to "is equilibria"

page 82, bullet list for Cl, changed first words to lower case and corrected punctuation

page 82, Table 17, changed the heading "Sample" to "Source"; corrected punctuation in citations

page 83, first sentence, changed "present natural" to "present in, effectively, all natural"

page 83, second sentence, deleted "water moves"

page 83, fourth paragraph, changed "water, With" to "water, with"

page 83, fourth paragraph, changed "salinity and temperature as the amount occurring as various chlorine-metal complexes increases slightly." to "salinity and temperature, concomitantly with slight increases of various chlorine-metal complexes."

page 84, Table 18, changed the heading "Sample" to "Source"; corrected punctuation in citations

page 84, paragraph before Table 19, changed "the pH was calculated at aquifer temperature ss shown in" to "the pH calculated at aquifer temperature is shown in"

page 84, last paragraph, changed "SOLMINEQ88" to "SOLMINEQ.88"

page 85, first paragraph, changed “and 6: for 3,” to “and 6. For 3,”

page 85, Table 20, changed the heading “Sample” to “Source”; changed emdashes to hyphens; corrected punctuation in citations

page 85, last paragraph, changed “Where anhydrites are absent,” to “Where anhydrite is absent,”

page 86, first paragraph in Lithium section, changed “Lithium is concentrated in shales in the sedimentary environment, and” to “In the sedimentary environment, lithium is concentrated in shales and”

page 86, Table 21, changed the heading “Sample” to “Source”; changed emdashes to hyphens; corrected punctuation in citations

page 86, paragraph after Table 21, changed “It is later leached and removed” to “It is then removed”

page 87, Table 22, changed the heading “Sample” to “Source”; changed emdashes to hyphens; corrected punctuation in citations

page 87, paragraph after Table 22, changed “(P05 = 5.1 to P95 = 7.4)” to “(P05 = 5.4 to P95 = 7.1)”

page 88, Table 23, changed the heading “Sample” to “Source”; changed emdashes to hyphens; corrected punctuation in citations

page 89, last paragraph, changed “data in Table 25 to simplify” to “data in Table 25. To simplify”. and deleted unbalanced “)”

page 90, Table 25, removed “(in bold)” from caption; moved citation to bottom, below the Table

page 90, paragraph before Table 26, changed “It is always univalent in nature, but—unlike the other halides” to “Like the other halides, it is univalent in nature, but—unlike them”

page 90, Table 26, changed the heading "Sample" to "Source"; moved Range from right column to left column as range; changed emdashes to hyphens; corrected punctuation in citations

page 91, second paragraph, third sentence, changed "rock" to "rocks"

page 91, third paragraph, first sentence, changed "for" to "in"

page 91, Table 27, changed the heading "Sample" to "Source"; changed emdashes to hyphens; corrected punctuation in citations

page 92, first full paragraph, first sentence, changed "(low: in the range 0.05 to 1.0 mg/L." to "low (in the range 0.05 to 1.0 mg/L)."

page 92, first paragraph under Silicon, changed

"The order in which the silicates weather is related to their relative thermodynamic stability. As a broad generalization, the order of ease of weathering is olivine > anorthite > diopside, hornblende > pyroxene, tremolite > albite, K-feldspar, micas > quartz, rutile, zircon."

to

"The relative order in which the silicates weather is related to their relative thermodynamic stability. As a broad generalization, the order of ease of weathering is as follows.

olivine = anorthite > pyroxene > amphibole > biotite = albite > K-feldspar > muscovite > quartz"

page 92, Table 28, changed the heading "Sample" to "Source"; changed emdashes to hyphens; corrected punctuation in citations

page 92, paragraph following Table 29, changed "we understand" to "hydrogeologists have come to recognize"

page 93, first paragraph, changed

"The average silica content of river water is 14 mg/L. In most unpolluted groundwater, the silica content is in the range of 5 to 50 mg/L. Carbonate brine may have high contents of silica: for example, 1,712 mg/L in groundwater from the Okavango Delta, Botswana, and 1,055 mg/L in Lake Magadi, Kenya. In thermal

water, the content of silica depends on temperature; in hotter water, it may approach 1,000 mg/L. There are few reports of silica determinations in polluted groundwater. One of the highest amounts is 259 mg/L from groundwater contaminated by coal pile leachates (Hitchon, 2023).”

to

“The average silica content of river water is 14 mg/L. In most unpolluted groundwater, the silica content ranges from 5 to 50 mg/L. Carbonate brine may have high contents of silica: for example, 1,712 mg/L in groundwater from the Okavango Delta, Botswana, and 1,055 mg/L in Lake Magadi, Kenya. In thermal water, the content of silica depends on temperature, and in hotter water may approach 1,000 mg/L. There are few reports of silica in polluted groundwater: one of the highest amounts is 259 mg/L from groundwater contaminated by coal pile leachates.”

page 93, second paragraph, first sentence, changed “that” to “and”

page 93, first paragraph under Nitrogen, changed emdashes to hyphens for negative signs

page 93, first paragraph under Nitrogen, changed

“0 (74.9 percent as N<sub>2</sub> or NH<sub>3</sub> gas), -3 (25.1 percent NH<sub>3</sub>, ammonium), and +5 (trace, as NO<sub>3</sub><sup>-</sup> nitrates).”

to

“0 (74.9 percent as N<sub>2</sub>), -3 (25.1 percent NH<sub>3</sub>, ammonium), and +5 (trace, as NO<sub>3</sub><sup>-</sup> nitrates).”

page 93, Table 29, changed the heading “Sample” to “Source”; deleted “as ammonium”;

changed emdashes to hyphens; corrected punctuation in citations

page 93, paragraph after Table 29, deleted “(+5 valence state)”

page 93, paragraph after Table 29, changed “SOLMINEQ88” to “SOLMINEQ.88”

page 95, Table 30, changed the heading “Sample” to “Source”; corrected punctuation in citations

page 95, first paragraph of Fluorine section, added (HF)

page 95, Table 31, changed the heading "Sample" to "Source"; corrected punctuation in citations

page 96, first full paragraph, changed "analyzed samples" to "analyzed formation water"

page 96, Table 32, changed the heading "Sample" to "Source"; corrected punctuation in citations

page 96, before numbered list, changed "natural water:" to "natural water, the:"

page 96, added sentence to last paragraph, "In formation water, lead occurs predominantly as chloride complexes."

page 97, deleted first sentence, that read "Lead occurs predominantly as chloride complexes, and these are the forms in which lead moves into formation water."

page 97, Table 33, changed the heading "Sample" to "Source"; corrected punctuation in citations

page 97, second to last paragraph, changed "zinc in this deeper" to "zinc in the deeper"

page 97, last paragraph, changed "Zinc is absorbed" to "Zinc is adsorbed"

page 98, Table 34, changed the heading "Sample" to "Source"; corrected punctuation in citations

page 98, second to last paragraph, changed "In several" to "Several"

page 98, second to last paragraph, changed "high concentration of iron" to "high iron content"

page 98, last paragraph, changed "compared to samples" to "compared to lower amounts in samples"

page 99, first paragraph of Manganese section, changed "It occurs" to "Manganese occurs"

page 99, first paragraph of Manganese section, changed “fugacity than those found in igneous” to “fugacity than found in igneous”

page 99, first paragraph of Manganese section, changed “environments. Examples include fine-grained” to “environments: for example, fine-grained”

page 99, Table 35, changed the heading “Sample” to “Source”; corrected punctuation in citations

page 100, first paragraph, changed “Mn<sup>2+</sup> and a large part” to “Mn<sup>2+</sup> and a large part”

page 100, second paragraph, changed “manganese will be in the ionic form” to “manganese will occur as Mn<sup>2+</sup>”

page 100, second paragraph, last sentence, changed “for groundwater” to “for most groundwater”

page 100, second paragraph, last sentence, changed “Mn<sup>2+</sup> is typically controlled by” to “Mn<sup>2+</sup> is controlled by”

page 100, third paragraph, changed “Mn to “Manganese”

page 100, third paragraph, changed “geologic” to “geological”

page 100, third paragraph, changed “Higher Mn concentration may” to “Higher manganese contents may”

page 101, Table 36, changed the heading “Sample” to “Source”; corrected punctuation in citations

page 101, paragraph beginning “In the presence”, changed “groundwater and its reduction” to “groundwater, and of the reduction”

page 102, paragraph beginning “The wealth of data”, changed “carbon” to “CO<sub>2</sub>”

page 102, Table 37, changed the heading "Sample" to "Source"; corrected punctuation in citations

page 104, Table 38, caption, changed "Analytical values for chemical" to "Chemical"; removed footnote

page 105, Table 39, removed "values" after "SI (saturation Index)"

page 106, first paragraph of section 6.7.1, changed "Salina Formation of the Michigan Basin" to "Salina Formation in the Michigan Basin"

page 106, first paragraph of section 6.7.1, changed "in general" to "generally"

page 108, Table 40, changed "Sample #" to "Sample Number"

page 109, Table 41, changed "Sample #" to "Sample Number"

page 113, paragraph beginning "It is generally", changed "Br" to "bromide"

page 116, first paragraph of 6.7.3, changed "concentration" to "content"

page 117, paragraph beginning "The generally lower magnesium concentrations", changed "Formation of ankerite becomes important at subsurface temperatures higher than ~120 °C (Boles, 1978). The concentrations of alkali metals, in the absence of evaporites, are strongly affected by temperature-dependent reactions with clays (transformation of smectite to mixed layer illite/smectite, then with increasing temperature to illite) and feldspar"

to

"Formation of ankerite (an iron-rich mineral related to dolomite) becomes important at subsurface temperatures higher than ~120 °C (Boles, 1978). In the absence of evaporites, the concentrations of alkali metals are strongly affected by temperature-dependent reactions with clays (transformation of smectite to mixed layer illite/smectite, then with increasing temperature to illite) and feldspar"

page 120, first paragraph, changed "which" to "because"

page 120, last sentence of paragraph beginning "Chloride is by far the dominant" changed "Other anionic species and weak (e.g.," to "Other weak anionic species (e.g.,"

page 121, first full paragraph, first line, deleted "is" after "brine"

page 124, last paragraph, changed "high concentration of H<sub>2</sub>S" to "high concentrations of H<sub>2</sub>S"

page 124, last paragraph, changed "reason and because" to "reason; because:"

page 126, paragraph beginning, "The solubility of PbS and ZnS", changed last sentence and first sentence of next paragraph, then joined then to read "Most formation water that has concentrations of dissolved lead and dissolved zinc"

page 126, paragraph beginning, "Thermodynamic calculations", changed "dissolved H<sub>2</sub>S by as much as 15 orders of magnitude" to "dissolved H<sub>2</sub>S, 15 orders of magnitude"

page 128, item 1., first sentence, changed "by" to "to"

page 130, first paragraph, changed "aluminum" to "aluminium"

page 130, second paragraph, last sentence, changed

"Kharaka & Hanor, 2014; Kharaka et al., 2009; Orem et al., 2017, 2014; US EPA, 2019; Varonka et al., 2020)."

to

"Kharaka et al., 2009; Kharaka & Hanor, 2014; McDevitt et al., 2022; Orem et al., 2017, 2014; Varonka et al., 2020; US EPA, 2019)."

page 135, last paragraph, first sentence, added citation, "as well as to ecosystems (McDevitt et al., 2022)."

page 136, first paragraph second to last sentence, changed

"The most common standards used to monitor and assess water quality convey the health of ecosystems, safety of human contact, and condition of drinking water."

to

“The most common standards used to monitor and assess water quality concern the health of ecosystems, the safety of human contact, and the condition of drinking water.”

page 137, first full paragraph, changed first sentence from

“The concentration of PAHs in produced water is low; however, they have high concentrates in all crude oil ( $K_{OW}$  values in many thousands, where  $K_{OW}$  is the equilibrium ratio of concentration of a chemical in n-octanol and water at a specified temperature) (Hoffman et al., 2002; Kharaka & Hanor, 2014).”

to

“The concentration of PAHs in produced water is low; however, they have high concentrates in all crude oil with  $K_{OW}$  values in the many thousands, where  $K_{OW}$  is the equilibrium ratio of concentration of a chemical in n-octanol and water at a specified temperature as discussed by Hoffman and others (2002) and Kharaka and Hanor (2014).”

page 137, second to last paragraph, last sentence, deleted “in Minnesota, USA”

page 141, paragraph beginning “Both stable and”, corrected “(H<sub>2</sub>)” to “(<sup>2</sup>H)”

page 143, first paragraph of 8.2.1, changed “indicate” to “indicates” and “vary” to “varies”

page 143, caption Figure 32, changed “\* indicates isotopic values for SMOW, the standard mean ocean water.” to “The \* indicates the isotopic value for SMOW, the standard mean ocean water.”

page 146-147, paragraph beginning “Abnormally high fluid pressures”, changed “indicate” to “show”; added “that” between “indicating upward”; changed “up dip” to “updip”

page 150, first paragraph of 8.2.5, changed “western Canada sedimentary basin.” to “Western Canada Basin.”

page 152, paragraph beginning “Under diagenetic”, changed “importance” to “significance”

page 158, first paragraph of 8.4, changed “geothermometers, tracers” to “geothermometers, and tracers”

page 158, last line, added “that” between “suggest the”

page 159, first sentence of last paragraph, added “to” between “and identify”

page 160, item 4., deleted “may occur” from end of sentence and moved to be after “sediments”

page 160, first paragraph after numbered list, added “the” between “nor travel”

page 160, last paragraph of section 8.5, added “that” between “showed the”

page 163, paragraph beginning “The original”, changed “sediments that occurred” to “sediments, occurred”

page 167, end of first paragraph, changed “on the top” to “at the top”

page 171, third bullet, changed “Ms” to “millions”

page 173, first line, changed “are” to “is”

page 173, figure 44 caption, changed

“a) Three-dimensional representation of fluid flow on the southwestern flank of the Iberia salt dome as deduced from spatial variation in formation water chemistry. Distribution of: b) VFA= volatile fatty acids; c) chloride, d) temperature; and e)  $\delta^{18}\text{O}$  (Hanor, 1987). b) Spatial variations in formation water chemistry and temperature (Workman & Hanor, 1989).”

to

“(Top) Three-dimensional representation of fluid flow on the southwestern flank of the Iberia salt dome as deduced from spatial variation in formation water chemistry and temperature in cross sections. West-east (A-A’) and north-south (B-B’) cross sections display the distribution of: a) total volatile fatty acids (VFA); b) chloride; c) temperature; and d)  $\delta^{18}\text{O}$  (Workman & Hanor, 1989).”

page 183, second paragraph, last sentence, deleted “estimated”

page 215, first paragraph, changed “Hanon” to Hanor”

page 230, first paragraph of 11.1, changed

“preindustrial times to approximately 420 ppmv as of 2022.”

to

“preindustrial times to 423 ppmv as of January 23, 2024 (National Oceanic and Atmospheric Administration, NOAA, 2024).”

page 230, added a paragraph after the first paragraph,

“Preliminary results of CO<sub>2</sub> emissions from USA sources in 2023 could indicate that global CO<sub>2</sub> levels may stabilize at a lower level than that listed above (King et al., 2024). In 2023, the US greenhouse gas emissions were 1.9 percent lower than in 2022, even while the economy expanded by 2.4 percent. The US emissions remained below pre-pandemic levels and dropped to 17.2 percent below 2005 levels. A decline in emissions in 2023 is a step in the right direction. But the deadline for the US 2030 climate target under the Paris Agreement of a 50 to 52 percent reduction in GHG emissions below 2005 levels is rapidly approaching, and achievement of that goal requires the US to average a 6.9 percent emissions reduction every year from 2024 through 2030—more than triple the 1.9 percent drop in 2023 (King et al., 2024).”

page 230, paragraph beginning “There is now a broad”, added a sentence after the first sentence, “According to new data from the Copernicus Climate Change Service, the Earth’s average temperature in 2023 was the hottest in recorded human history, reaching 1.48 °C (2.66 °F) hotter than the preindustrial average and dangerously close to a long feared warming threshold of 1.5 °C listed in the Paris Agreement of 2016 (Dance et al., 2024).”

page 230, paragraph beginning “There is now a broad”, added the year 2023 to “IPCC 2017, 2021a, 2021b, 2023;”

page 239, paragraph beginning “At the global level”, added citation to the end of the first sentence “(IES, 2022; IPCC, 2023)”

page 241, paragraph beginning “The US DOE estimates”, added a citation to the end of the last sentence, “Bump & Hovorka, 2023;”

O

page 242, first line of 11.3.2, deleted “comprehensively”

page 248, first sentence of last paragraph, added citation, “Warwick et al., 2022”

page 251, paragraph beginning “However”, changed first line from “However, uncertainties and scientific gaps exist in understanding CO<sub>2</sub>-brine-mineral interactions” to “However, there are uncertainties and scientific gaps in our understanding of CO<sub>2</sub>-brine-mineral interactions”

page 263, first paragraph of 11.6, added citation to the end of the first sentence, “Meckel et al., 2023”

page 265, first line of 11.6.2, deleted “include”

page 291, reference added, “Bump, A. P., and Hovorka, S. D., (2023)”

page 293, reference added, “Dance, S., Kaplan, S., & Penney, V. (2024)”

page 301, reference added, “Ground Water Protection Council, (2023)”

page 305, reference date corrected, “Hitchon, B. (2022)” to “Hitchon, B. (2023)”

page 308, reference added, “IPCC, (2023)”

page 308, reference added, “Jasechko, S., Seybold, H., Perrone, D. et al. (2024)”

page 315, reference added, “King, B., Gaffney, M., & Rivera, A. (2024)”

page 319, reference added, “McDevitt, B., A.M. Jubb, M.S. Varonka, M.S. Blondes, M.A. Engle, T.J. Gallegos, & J.L. Shelton (2022)”

page 320, reference added, “Meckel, J., R. H. Treviño, S. Hovorka, & Bump, A. (2023)”

page 323, reference added, “National Oceanic and Atmospheric Administration (NOAA). (2024)”

page 338, reference added, “Warwick, P.D., E.D. Attanasi, M.S. Blondes, S.T. Brennan, M.L. Buursink, S.M. Cahan, C.A. Doolan, P.A. Freeman, C.O. Karacan, C.D. Lohr, M.D. Merrill, R.A. Olea, J.L. Shelton, E.R. Slucher, B.A. Varela (2022)”

page 373, enhanced the first sentence, “**Dr. Yousif K. Kharaka** was born in Mangesh, a small town located in northern Iraq, close to the Turkish border. Dr. Kharaka is currently an emeritus hydrogeochemist with the USGS, Menlo Park, California.”

page 374, paragraph beginning “Dr. Hitchon was”, deleted from the end of the paragraph “and has been a member of the Association of Professional Engineers and Geoscientists of Alberta (as a Professional Geologist) for more than half a century”